STIC-ILL

From: Vogel, Nancy
Sent: Thursday, December 09, 2004 2:09 PM
To: STIC-ILL
Subject: refs for 10/045,116 (references from lost parent case 09/033,555)

AU 1636

Please send me the following:

Proc. Natl. Acad. Sci. USA (1 989) 86:4574-4578

EIC X Adonis
MIC X BioTech X MAIN
NO Vol NO NOS
Ck Cite Dupl Request
Call # QH.N26
12/9/04 D.C.

Virol. 1997 227:239-244

Virolo 1994 202:695-706

Virolo 1993 193:631-641

Genes and Dev. 1988 2:453-461

Nucleic Acid Research 1983 11 17 :6003-6020 .

Proc. Natl. Acad. Sci. USA 1994 91:8802-8806
J Virolo I 993 67 10 :591 1-592 1

Anticancer Res. 1997 17:1471-1505

J Immunol. 1988 141 6 :2084-2089

J Virol. 1989 63 2 :631-638

Science 1989 244:1288-1292

Chang et al. Cancer Gene therapy Using Novel Tumor specific Replication Competent Adenovirus Vectors" Cold Spring Harbor Gene Thera Meeting Sept. 1996

Nucleic Acids Res. 1996 24 12 :2318-2323

Current Protocols in Molecular Biology
Ausubel et al., eds., 1987 , Supp. 30, section 7.7.18 Table 7.7.1

Nature (1989) 337:387-388

Advances in Virus Research 1986 31: 169-228

Biochem. Biophys. Acta 1982 651:175-208

Mol. Cell. Biol. 1989 9 (9) :41 5-42

J Virol. 1997 71 (1) :548-561

EMBO J 1984 3 (12) :2917-2922

J Genetic Virolo 1977 68:937-940

1973 Virolo 52:456-467

1987 J Gen. Virol 36:59-72

Biochem. J. 1987 241:25-38

Hallenbeck, P.L. et a1., Novel Tumor Specific Replication Competent Adenoviral Vectors for Gene Therapy of Cancer" abstract no. 0-36 Cancer Gene Thera 1996) 3 (6) :S19-S20.

J. Biol. Chem. 1995 270 (8) :3602-3610 .
J Biol. Chem. 1994 269 (39) :23872-23875
Adv. Dru Delive Rev. 1995 17:279-292

Proc. Natl. Acad. Sci. USA
Vol. 86, pp. 4574–4578, June 1989
Genetics

Targeted homologous recombination at the endogenous adenine phosphoribosyltransferase locus in Chinese hamster cells

(gene targeting/transfection/targeted integration/gene conversion)

GERALD M. ADAIR†‡, RODNEY S. NAIRN†, JOHN H. WILSON§, MICHAEL M. SEIDMAN¶, KATHERINE ANN BROTHERMAN†, CHRISTY MACKINNON†, AND JULIA B. SCHEERER†

†The University of Texas M. D. Anderson Cancer Center, Science Park-Research Division, Smithville, TX 78957; §Marrs McLean Department of Biochemistry, Baylor College of Medicine, Houston, TX 77030; and ¶Otsuka Pharmaceutical Co., Ltd., Maryland Research Laboratories, 9900 Medical Center Drive, Rockville, MD 20850

Communicated by Leroy Hood, November 30, 1988

ABSTRACT **We have developed a system that permits analysis of targeted homologous recombination at an endogenous, chromosomal gene locus in cultured mammalian cells. Using a hemizygous, adenine phosphoribosyltransferase (APRT)-deficient, Chinese hamster ovary (CHO) cell mutant as a transfection recipient, we have demonstrated correction of a nonrevertible deletion mutation by targeted homologous recombination. Transfection with a plasmid carrying a fragment of the *APRT* gene yielded APRT$^+$ recombinants at a frequency of $\approx 4.1 \times 10^{-7}$. The ratio of targeted recombination to nontargeted integrations of plasmid sequences was ≈1:4000. Analysis of 31 independent APRT$^+$ recombinants revealed conversions of the endogenous *APRT* gene, targeted integration at the *APRT* locus, and a third class of events in which the plasmid donor *APRT* fragment was converted to a full-length, functional gene.**

Targeted homologous recombination is a powerful tool for genetic manipulation in yeast, permitting precise gene correction, site-specific gene modification, or targeted gene disruption at any chromosomal locus for which a cloned sequence is available (1–4). Potential applications of such techniques in mammalian cells include (*i*) site-specific gene modification or precise targeting of engineered gene sequences into their normal chromosomal environments for studying expression and structure–function relationships; (*ii*) generation of animal models for the study of heritable human diseases by targeted gene disruption or insertional mutagenesis of gene loci in mouse embryo cells; and (*iii*) precise replacement or correction of defective human genes as an approach to gene therapy. However, the paucity of good assay systems and selectable markers for studying homologous recombination at endogenous gene loci and the propensity of mammalian cells for integration of foreign DNA by illegitimate recombination events requiring little or no homology (5–7) have been major impediments to the practical application of gene targeting approaches in mammalian cells.

Most studies of targeted homologous recombination in mammalian cells have used one of two basic approaches: analysis of the production of viable viruses by recombination between defective exogenous and chromosomally integrated viral sequences (8–11) or introduction and stable integration of a defective viral or bacterial gene sequence into a mammalian cell genome to serve as an artificial chromosomal target sequence for subsequent homologous recombination events (12–16). Very few studies have used mammalian genes in their normal chromosomal environments as targets for homologous recombination (17–19).

The publication costs of this article were defrayed in part by page charge payment. This article must therefore be hereby marked "*advertisement*" in accordance with 18 U.S.C. §1734 solely to indicate this fact.

We have developed a system that permits analysis of targeted homologous recombination at an endogenous, chromosomal gene locus in cultured mammalian cells. This system utilizes a hemizygous adenine phosphoribosyltransferase (*APRT*) gene (20–24) as a target for homologous recombination. In this paper we (*i*) demonstrate targeted correction of a nonrevertible *APRT* deletion mutation by homologous recombination of a transfection-introduced plasmid *APRT* sequence with the defective chromosomal locus; (*ii*) determine the relative frequencies of targeted homologous recombination and nontargeted integration of plasmid sequences; and (*iii*) analyze 31 independent APRT$^+$ recombinants to determine the nature of the targeted recombination events.

MATERIALS AND METHODS

Cell Lines and Culture Conditions. CHO-ATS-49 is a spontaneous 8-azaadenine-resistant, APRT-deficient mutant derived from CHO-AT3-2 (20–22). ATS-49 cells are hemizygous for an *Mbo* II *APRT* restriction fragment length polymorphism that reflects loss of the exon V *Mbo* II restriction site (Fig. 1*a*). A spontaneous 6-thioguanine-resistant, hypoxanthine (guanine) phosphoribosyltransferase (HPRT)-deficient subline, ATS-49tg, was used for targeting experiments. Cells were maintained as exponentially growing monolayer cultures in alpha modified Eagle's minimal essential medium (α-MEM) supplemented with 10% fetal bovine serum, penicillin, and streptomycin (20, 21).

Plasmid DNAs. Plasmid pAG-7 (Fig. 1*b*) was constructed by replacing the 0.7-kb *Eco*RI–*Bam*HI region of pSV2gpt (25, 26) with a 2.6-kb *Eco*RI–*Bam*HI fragment derived from pHaprt-1 (23). This fragment includes only the 3′ portion of the Chinese hamster *APRT* gene (22). During the construction of pAG-7, a *Pst* I site in the bacterial ampicillin-resistance gene was removed in such a way as to leave the gene functional, making the *Pst* I site in the *APRT* gene fragment unique.

Transfections. Plasmid DNAs were introduced into ATS-49tg cells by calcium phosphate transfection (27, 28). Each 100-mm dish received 8 μg of plasmid DNA. No carrier DNA was used. After 4 hr of exposure to calcium phosphate/DNA precipitates, cells were treated for 25 min with 10% (vol/vol) dimethyl sulfoxide and maintained in α-MEM for ≈40 hr before exposure to selective media.

Selections. APRT$^+$ recombinants were selected in ALASA (25 μM alanosine/50 μM azaserine/100 μM adenine) medium (21, 28). The frequency of GPT$^+$ transformants was monitored

Abbreviations: APRT, adenine phosphoribosyltransferase; HPRT, hypoxanthine (guanine) phosphoribosyltransferase; GPT, guanine phosphoribosyltransferase; WT, wild type; ALASA, alanosine/azaserine/adenine; HAT, hypoxanthine/amethopterin/thymidine.
‡To whom reprint requests should be addressed.

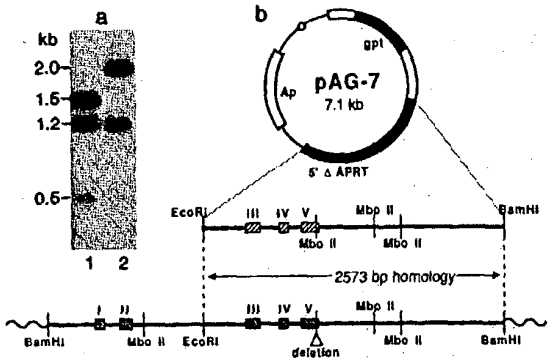

FIG. 1. Target gene and targeting vector. (*a*) *Mbo* II-digested DNAs from CHO-AT3-2 (lane 1) and CHO-ATS-49tg (lane 2) after hybridization with the 3.9-kilobase (kb) *APRT* probe, showing loss of the exon-V *Mbo* II site in ATS-49tg. Internal 1.5- and 0.5-kb fragments are generated by *Mbo* II sites in intron 2, exon V, and just downstream of the *APRT* gene; the upstream and downstream genomic flanking sequences are present on overlapping 1.2-kb *Mbo* II fragments. (*b*) Diagram showing the shared *APRT* sequence homology [2573 base pairs (bp)] between pAG-7 and the targeted ATS-49tg chromosomal *APRT* locus. The location of the ATS-49tg *APRT* deletion site is indicated. Ap, ampicillin-resistance gene; *gpt*, guanine phosphoribosyltransferase gene.

by plating a small aliquot of cells from each culture into HAT (100 μM hypoxanthine/2 μM amethopterin/50 μM thymidine) medium. One APRT$^+$ recombinant was picked from each independent transfection population for molecular analysis. Alanosine (NSC-529469) was obtained from the Drug Synthesis and Chemistry Branch of the National Cancer Institute.

DNA Isolation and Molecular Analysis. DNA was isolated either by the NaDodSO$_4$/proteinase K method (21, 27) or by a simple salting-out procedure (29). DNA samples (10–15 μg) were digested by overnight incubation with restriction enzymes in the buffers recommended by the suppliers (Boehringer Mannheim and New England Biolabs), electrophoresed for 560 V·hr in 0.8% agarose gels, and transferred to nitrocellulose membranes (21). [α-^{32}P]dCTP-labeled probes were prepared by nick-translation (21, 27) or random oligonucleotide-primed synthesis (30), using either the 3.9-kb *Bam*HI fragment derived from pHaprt-1 or a 1.3-kb *Bam*HI–*Eco*RI fragment that includes only the 5′ portion of the *APRT* gene. Hybridizations and autoradiography were carried out as described (21, 27).

RESULTS

Correction of a Nonrevertible Mutation at the Endogenous *APRT* Locus by Targeted Homologous Recombination. CHO-ATS-49tg cells are hemizygous for the *APRT* locus; they contain a single, mutationally altered copy of the *APRT* gene. A small (<20-base-pair) deletion has resulted in loss of the exon-V *Mbo* II restriction site (Fig. 1*a*). No APRT$^+$ revertants of this cell line have been obtained after screening >10^9 cells. However, targeted homologous recombination between transfection-introduced plasmid-derived *APRT* sequences and the defective chromosomal *APRT* gene in ATS-49tg should yield APRT$^+$ (ALASA^r) recombinants. To search for such recombinants, ATS-49tg cells were transfected with *Pst* I-linearized pAG-7 DNA, which shares ≈2.6 kb of *APRT* sequence homology with the target gene (Fig. 1*b*), or with *Bam*HI-linearized pSV2gpt DNA, which lacks any *APRT* gene sequences.

Results of these experiments are summarized in Table 1. The two plasmid DNAs yielded comparable frequencies of GPT$^+$ (HAT^r) transformants, reflecting nontargeted integration and expression of plasmid *gpt* sequences. No APRT$^+$ (ALASA^r) clones were obtained after transfection of ≈10^8 ATS-49tg cells with *Bam*HI-linearized pSV2gpt DNA. However, transfection of ATS-49tg cells with *Pst* I-linearized pAG-7 DNA yielded APRT$^+$ colonies (presumptive targeted recombinants) at a frequency of ≈4×10^{-7}. The ratio of the APRT$^+$ and GPT$^+$ frequencies (≈1:4000) provides a measure of the relative frequency of targeted homologous recombination versus nontargeted integration of plasmid sequences.

Southern Blot Hybridization Analysis of APRT$^+$ Recombinant Clones. To determine the nature of the targeted homologous recombination events, DNA samples from 31 independent APRT$^+$ clones were digested with *Mbo* II and seven other restriction enzymes and subjected to Southern blot hybridization analysis using full-length (3.9-kb) and 5′-end-specific (1.3-kb) *APRT* probes. APRT$^+$ clones with multiple nontargeted integrations of plasmid sequences show complex restriction fragment patterns with the full-length probe, because it detects plasmid-derived *APRT* sequences as well as the targeted chromosomal gene. Hybridization with the 1.3-kb (5′-end-specific) *APRT* probe allows selective identification of fragments containing *APRT* sequences unique to the target gene, greatly facilitating interpretation of restriction patterns and deduction of the nature of the recombinational events. Throughout this paper, restriction fragments that are hybridized by the 5′-end-specific *APRT* probe will be identified by an asterisk (*).

Restoration of the exon-V *Mbo* II site at the ATS-49tg chromosomal *APRT* locus by targeted recombination should be accompanied by the reappearance of the *1.5-kb *Mbo* II fragment characteristic of the wild-type (WT) CHO *APRT* gene. Each of the 31 APRT$^+$ clones analyzed had indeed regained this fragment (as illustrated by six cell lines in Fig. 2*a*). The majority of the APRT$^+$ clones analyzed (19/31) showed simple restriction fragment patterns after with very few (<3) or no untargeted integrations. However, 12 clones showed more complex patterns reflecting multiple nontargeted integrations of single and/or tandemly arrayed pAG-7 plasmid sequences.

Table 1. Targeted correction of the *APRT* gene in CHO-ATS-49tg cells

Plasmid vector*	Total cells transfected, no. × 10^{-8}	APRT$^+$ colonies: Frequency† No.	APRT$^+$ colonies: Frequency† × 10^7	APRT$^+$ colonies: Yield‡	GPT$^+$ colonies: Frequency† × 10^3	GPT$^+$ colonies: Yield‡	APRT$^+$/GPT$^+$ frequency ratio
pSV2gpt	0.96	0	0	0	1.3	164	—
pAG-7	1.20	33	4.1	0.05	1.6	201	1:3900

*Eight micrograms of *Bam*HI-linearized pSV2gpt DNA was added to each of 80 dishes (≈1.2×10^6 cells per dish); 8 μg of *Pst* I-linearized pAG-7 DNA was added to each of 100 dishes (≈1.2×10^6 cells per dish).

†Forty hours after treatment with calcium phosphate-precipitated DNAs, two-thirds of each transfected cell population was plated into ALASA selection medium; one-fourth of each transfected cell population was simultaneously plated into HAT selection medium. Data are expressed as the frequency of ALASA^r (APRT$^+$) or HAT^r (GPT$^+$) colonies per transfected cell.

‡Colonies per microgram of DNA per 10^6 transfected cells.

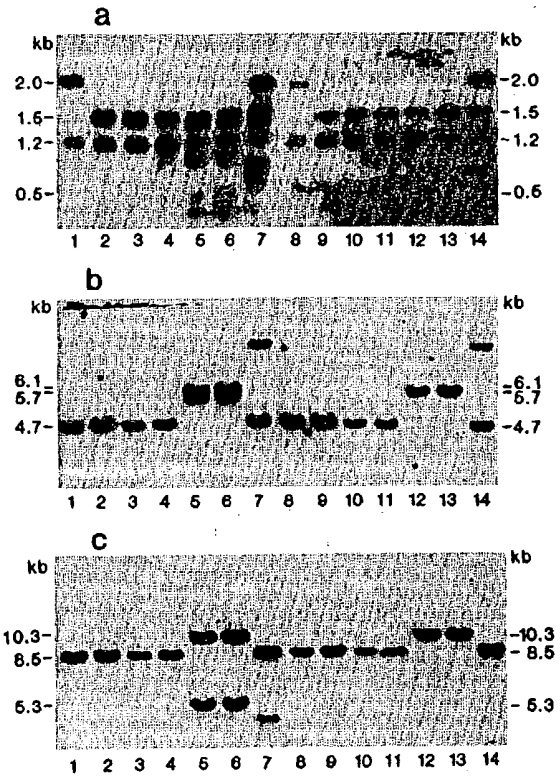

FIG. 2. Southern blot hybridization analysis of CHO-ATS-49tg and APRT$^+$ recombinant DNAs, following digestion with *Mbo* II (*a*), *Bgl* II (*b*), or *Hin*dIII (*c*). Lanes: 1 and 8, CHO-ATS-49tg; 2 and 9, clone 8-44; 3 and 10, clone 8-77; 4 and 11, clone 8-11; 5 and 12, clone 8-35; 6 and 13, clone 8-57; 7 and 14, clone 8-39. Lanes 1–7 were hybridized with the full-length 3.9-kb Chinese hamster *APRT* probe; lanes 8–14 were hybridized with a 1.3-kb probe that is specific for 5′-end, chromosomal *APRT* gene sequences.

We anticipated that APRT$^+$ recombinants might arise by at least two types of recombination events: targeted conversion of the chromosomal *APRT* gene and targeted integration into the chromosomal *APRT* locus (Fig. 3). These two classes of recombinants can be distinguished by their diagnostic restriction fragment patterns. APRT$^+$ recombinants arising by targeted conversion will have normal, WT restriction patterns for all restriction enzymes. APRT$^+$ recombinants arising by targeted integration will have diagnostic restriction fragment patterns for *Bgl* II (*6.1 and 5.7 kb), *Hin*dIII (*10.3 and 5.3 kb), *Eco*RV (*2.2, *4.6 and 15 kb), and *Sac* I (≈*21 kb). For example, since there are no *Sac* I restriction sites in pAG-7 and the genomic sites lie well outside of the *APRT* gene sequence, a targeted integration would increase the size of the WT *14-kb *Sac* I fragment to ≈21-kb, while a conversion event would leave this fragment unchanged. Both types of APRT$^+$ recombinants have been observed.

Given the nature of the pAG-7 *APRT* donor sequence (which lacks the entire 5′ portion of the *APRT* gene, including the promoter region and first two exons), we did not anticipate that it would be possible to recover recombination products in which the incoming plasmid sequence had been corrected by recombination with the targeted chromosomal gene and then integrated elsewhere in the genome. Surprisingly, this class of recombinants accounted for nearly one-third of the APRT$^+$ clones analyzed.

Targeted Conversion of the Endogenous CHO-ATS-49tg *APRT* Gene. The majority of APRT$^+$ recombinants with simple restriction patterns (15/19) appeared to have arisen by

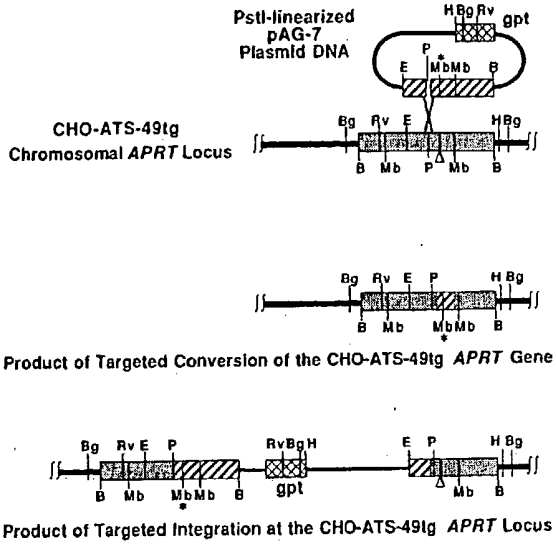

FIG. 3. Targeted homologous recombination of pAG-7 *APRT* sequences with the CHO-ATS-49tg chromosomal *APRT* locus, showing the predicted targeted conversion and integration products. Crossed lines indicate the region where recombination is initiated. Conversion and integration, as drawn, represent potential outcomes of recombination at this site. Restriction enzyme recognition sites: B, *Bam*HI; Bg, *Bgl* II; E, *Eco*RI; Rv, *Eco*RV; H, *Hin*dIII; Mb, *Mbo* II; P, *Pst* I.

targeted conversion of the ATS-49tg *APRT* locus. Thirteen of these clones showed no evidence of nontargeted integration of pAG-7 plasmid sequences. Two such recombinants, which appeared to contain only a single, WT copy of the *APRT* gene, are shown in Fig. 2 (clone 8-44 in lanes 2 and 9 and clone 8-77 in lanes 3 and 10). Both clones have a GPT$^-$ (HAT^s) phenotype. Both showed loss of the *2.0-kb ATS-49tg *Mbo* II fragment and reappearance of a WT *1.5-kb fragment (Fig. 2*a*); all other restriction fragment patterns are unchanged. Clone 8-11 (Fig. 2, lanes 4 and 11) is an example of a recombinant with a targeted conversion of the ATS-49tg *APRT* locus plus a single, nontargeted integration of pAG-7 elsewhere in its genome. The additional bands present in lane 4 in Fig. 2 *b* and *c* represent novel junction fragments produced by the nontargeted integration. Novel junction fragments were also observed after digestion with other enzymes; such fragments can be detected only with the 3.9-kb probe. Clone 8-66 (data not shown) reflected two nontargeted integrations. Both of these clones have a GPT$^+$ (HAT^r) phenotype. Curiously, of the 12 APRT$^+$ recombinants that showed multiple nontargeted integrations, only 1 (8-33) appears to have arisen by targeted conversion.

Targeted Integration at the CHO-ATS-49tg *APRT* Locus. Three APRT$^+$ clones with simple restriction fragment patterns arose by targeted integration at the *APRT* locus. Each displayed a GPT$^+$ phenotype. Two of these recombinants (clones 8-35 and 8-57; Fig. 2, lanes 5 and 12 and lanes 6 and 13, respectively) showed no evidence of untargeted integration of pAG-7 plasmid sequences. The third clone (8-52; data not shown) showed a targeted integration plus a nontargeted integration of two tandem copies of pAG-7 elsewhere in its genome. As shown in Fig. 2*b*, digestion with *Bgl* II (which does not cut within the *APRT* gene but cuts once within the pAG-7 *gpt* gene) yields a single *4.7-kb fragment for ATS-49tg or APRT$^+$ recombinants that have arisen by conversion, whereas targeted integrations generate diagnostic *6.1- and 5.7-kb recombinant fragments. Digestion with *Hin*dIII (which likewise does not cut within the *APRT* gene but cuts once within *gpt*) yields an *8.5-kb fragment for ATS-49tg or

$APRT^+$ convertants, whereas targeted integrations generate diagnostic *10.3- and 5.3-kb recombinant fragments (Fig. 2*c*). The extra bands in lanes 5 and 6 of Fig. 2*a* represent recombinant fragments defined by *Mbo* II sites within the targeted *APRT* locus together with sites in the integrated pAG-7 sequences. Addtional evidence of targeted integration in clones 8-35, 8-57, and 8-52 was provided by the observation of diagnostic *Eco*RV (*2.2-, *4.6-, and 15-kb) and *Sac* I (*21-kb) restriction fragments (data not shown). *Bgl* II, *Hin*dIII, *Eco*RV, and *Sac* I restriction fragments indicative of targeted integration were also detected in 3 of the 12 $APRT^+$ clones that showed multiple nontargeted integrations.

$APRT^+$ Recombinants That Retain an Unaltered Mutant *APRT* Gene at the Original Chromosomal Locus. Among the 19 $APRT^+$ clones with simple restriction patterns, 1 clone (8-39) did not appear to have arisen by either targeted conversion or targeted integration. As can be seen in Fig. 2*a* (lanes 7 and 14), while this clone has regained a *1.5-kb *Mbo* II fragment indicative of a reconstructed WT *APRT* gene, it has not lost the *2.0-kb *Mbo* II fragment characteristic of the ATS-49tg mutant allele. Based upon the restriction fragment patterns shown in Fig. 2, as well as information obtained from other restriction digests (not shown), it appears that clone 8-39 has retained an unaltered copy of the ATS-49tg *APRT* gene at the original chromosomal locus yet has somehow acquired a second, WT copy of the *APRT* gene, which has integrated elsewhere in the genome. Furthermore, of the 12 $APRT^+$ clones that showed complex restriction patterns with multiple nontargeted integrations of plasmid sequences, 8 resembled clone 8-39 in that they too had regained a *1.5-kb *Mbo* II fragment, characteristic of a reconstructed WT *APRT* gene, without having lost the original *2.0-kb *Mbo* II fragment. Each of these recombinants was found to contain at least two *Sac* I fragments that hybridized with the 1.3-kb (5′-end-specific) *APRT* probe; a *14-kb fragment corresponding to that of ATS-49tg and a second fragment of variable size that appeared to represent a junction fragment produced by random integration of the recombination-corrected input plasmid *APRT* sequence.

DISCUSSION

Most studies of targeted homologous recombination in mammalian cells have utilized "artificial" transfection- or electroporation-introduced, chromosomally integrated viral or bacterial gene sequences such as the herpes simplex virus thymidine kinase (*tk*) gene or the bacterial neomycin-resistance (*neo*) gene as recombinational targets (8-16). Many of the primary transfectants that have been employed in such targeting experiments have contained multiple single or tandem copies of the integrated target sequence (13, 14, 16), complicating analysis of recombinants and interpretation of the results. Such "artificial" target sequences may or may not be representative of a normal mammalian gene locus.

We have developed an experimentally adaptable system that permits analysis of targeted homologous recombination at an endogenous mammalian gene in its normal chromosomal context. Our system utilizes a hemizygous mutant CHO *APRT* gene (20–24) as a target locus. *APRT* is a constitutively expressed "housekeeping" gene that codes for a purine salvage-pathway enzyme (22). There are good forward and back selections for this locus (20–23). Hemizygous, nonrevertible *APRT* deletion mutants such as ATS-49tg are ideal for use in targeting experiments. The small size of the Chinese hamster *APRT* gene (22–24), its convenient distribution of restriction sites (22–24), and the absence of *APRT* pseudogenes in CHO cells (22) greatly facilitate molecular analysis of $APRT^+$ recombinants. Using ATS-49tg as a recipient cell line, we have demonstrated targeted correction of a nonrevertible *APRT* deletion mutation by homologous recombination of transfection-introduced plasmid *APRT* sequences with the defective chromosomal gene.

$APRT^+$ recombinants were obtained in our targeting experiments at a frequency of $\approx 4 \times 10^{-7}$, with a ratio of targeted recombination to nontargeted integration of ≈1:4000. Ratios ranging from about 1:100,000 to 1:100 have been reported in other targeting studies (12–14, 16, 19). The efficiency of targeted recombination varies at different locations in the genome and with different extents of homology in the input plasmid. Song *et al.* (16) detected targeted recombination in six out of eight transfectant cell lines with integrated *neo* target sequences. Targeted recombination frequencies varied over a 130-fold range (from 0.04 to 5.3 per microgram of plasmid DNA), with ratios of targeted recombination to nontargeted integration ranging from 1:500 to ≈1:75. In targeting experiments involving the *HPRT* locus in mouse embryo stem cells, Thomas and Capecchi (18) observed ratios of targeted recombination to nontargeted integration ranging from 1:40,000 to 1:950. They found the efficiency of targeted recombination to be strongly dependent upon the extent of shared homology between plasmid and target gene sequences, with targeting frequencies ranging from $\approx 4 \times 10^{-8}$ for a vector with 4.0 kb of target sequence homology to 4.1×10^{-7} for a vector with 9.1 kb of homology (18). In comparison, we have obtained targeted recombination at a frequency of 4.1×10^{-7} with a plasmid that carries only 2.6 kb of *APRT* sequence homology.

In general, molecular analyses of recombinants obtained from mammalian targeting experiments have painted a rather confusing picture. In experiments utilizing a defective *neo* gene as a target sequence, Thomas *et al.* (14) obtained only gene conversion events. Song *et al.* (16) obtained gene conversion and single-crossover events at approximately equal frequencies. In targeting experiments with mouse embryo stem cells, Doetschman *et al.* (19) recovered two recombinants that appeared to have arisen by a simple crossover, while three others reflected crossover accompanied by gap repair or gene conversion. In "knockout" experiments employing sequence-replacement vectors, Thomas and Capecchi (18) observed only gene conversion events; when sequence-insertion vectors were used, approximately three-fourths of the recombinants arose by targeted integration of the vector sequences at the *HPRT* locus. A mechanistic association between gene conversion and crossing over is a common feature of recombination models derived from studies of meiotic recombination (31, 32).

We have observed three types of recombination events in the $APRT^+$ recombinants obtained from our targeting experiments. Most of these recombinants had simple restriction fragment patterns, with few or no untargeted integrations of pAG-7 plasmid sequences. Of the 31 independent $APRT^+$ clones analyzed, 16 arose by targeted correction (conversion) of the endogenous *APRT* gene by homologous recombination with plasmid donor *APRT* sequences. Six recombinants appeared to be the products of single crossovers (reciprocal exchanges) that resulted in targeted integration of the plasmid sequences at the *APRT* locus. Each of the 9 remaining $APRT^+$ clones retained an unaltered copy of the ATS-49tg *APRT* gene, at the original chromosomal locus, plus a second, WT copy of the *APRT* gene, which had integrated elsewhere in the genome.

We are particularly intrigued by the third class of recombination events. Although correction and subsequent integration of a defective plasmid gene with an internal deletion have been observed in other studies (14, 16), we did not anticipate such events in our experiments because the pAG-7 plasmid *APRT* sequence lacked the entire 5′ half of the *APRT* gene. Meiotic recombination models (31, 32) require homology on both sides of a double-strand break, gap, or mutation to effect correction by homologous recombination. Since the

donor plasmid in our experiments carried a truncated, 5'-end-deleted *APRT* gene fragment that was not flanked on its 5' side by any sequences homologous to the chromosomal *APRT* target sequences, it should not be a suitable substrate for correction by recombination. Nevertheless, in nine APRT$^+$ recombinants, this truncated plasmid *APRT* gene segment appears to have been converted to a complete, functional *APRT* gene, which would require the duplication and recombinational acquisition of ≈2 kb of chromosomal 5' *APRT* sequences.

We can envision at least two mechanisms by which such recombinants could have been generated: (*i*) one-armed, 3'-OH strand invasion into the chromosomal *APRT* gene duplex by the *Pst* I-linearized plasmid *APRT* DNA sequence, followed by elongation of the invading strand using a chromosomal *APRT* strand as a template, with branch migration and lagging-strand synthesis to generate a complete *APRT* gene on the plasmid duplex; or (*ii*) homologous recombination between input plasmid *APRT* sequences and an extrachromosomal, circular-DNA copy of the ATS-49tg *APRT* gene. The first mechanism would closely resemble the "join-copy" replication pathway that has been described in phage T4, in which replication forks are initiated from recombinational intermediates (33). The second mechanism is suggested by studies that have demonstrated the ubiquitous presence of heterogeneous populations of extrachromosomal, small polydisperse circular (spc) DNAs in the cells of higher eukaryotes (34, 35). These spcDNAs are derived from chromosomal DNAs and range in size from ≈0.15 to >250 kb (34, 35). Their heterogeneity and sequence complexity suggest that they are probably generated by multiple mechanisms (34–38) and that they may represent random samples of chromosomal DNA (35, 36). Wiberg *et al.* (38) observed a 5-fold increase in the levels of spcDNA in mammalian cells after calcium phosphate-mediated transfection; the new spcDNAs appeared to be derived from cellular DNA. Additional experiments will be required to distinguish between these alternative mechanisms.

We thank Drs. Paul Berg and Richard Axel for providing pSV2gpt and pHaprt, Drs. Tom Porter and Rodney Rothstein for stimulating discussions, John Riley and Judy Ing for artwork and photography, and Carol Hildman for helping to prepare the manuscript. This work was supported by Grants CA28711 and RR5511-25 (G.M.A.), CA36361 (R.S.N.), and GM38219 (J.H.W.) from the National Institutes of Health.

1. Rothstein, R. (1983) *Methods Enzymol.* **101**, 202–211.
2. Winston, F., Chumley, F. & Fink, G. (1983) *Methods Enzymol.* **101**, 211–228.
3. Orr-Weaver, T., Szostak, J. & Rothstein, R. (1983) *Methods Enzymol.* **101**, 228–245.
4. Botstein, D. & Fink, G. (1988) *Science* **240**, 1439–1443.
5. Roth, D. & Wilson, J. (1985) *Proc. Natl. Acad. Sci. USA* **82**, 3244–3249.
6. Roth, D., Porter, T. & Wilson, J. (1985) *Mol. Cell. Biol.* **5**, 2599–2607.
7. Kato, S., Anderson, R. & Camerini-Otero, R. (1986) *Mol. Cell. Biol.* **6**, 1787–1795.
8. Shaul, Y., Laub, O., Walker, M. & Rutter, W. (1985) *Proc. Natl. Acad. Sci. USA* **82**, 3781–3784.
9. Jasin, M., de Villiers, J., Weber, F. & Schaffner, W. (1985) *Cell* **43**, 695–703.
10. Subramani, S. (1986) *Mol. Cell. Biol.* **6**, 1320–1325.
11. Rommerskirch, W., Graeber, I., Grassman, M. & Grassman, A. (1988) *Nucleic Acids Res.* **16**, 941–952.
12. Smith, A. & Berg, P. (1984) *Cold Spring Harbor Symp. Quant. Biol.* **49**, 171–181.
13. Lin, F., Sperle, K. & Sternberg, N. (1985) *Proc. Natl. Acad. Sci. USA* **82**, 1391–1395.
14. Thomas, K., Folger, K. & Capecchi, M. (1986) *Cell* **44**, 419–426.
15. Thomas, K. & Capecchi, M. (1986) *Nature (London)* **324**, 34–38.
16. Song, K.-Y., Schwartz, F., Maeda, N., Smithies, O. & Kucherlapati, R. (1987) *Proc. Natl. Acad. Sci. USA* **84**, 6820–6824.
17. Smithies, O., Gregg, R., Boggs, S., Koralewski, A. & Kucherlapati, R. (1985) *Nature (London)* **317**, 230–234.
18. Thomas, K. & Capecchi, M. (1988) *Cell* **51**, 503–512.
19. Doetschman, T., Gregg, R., Maeda, N., Hooper, M., Melton, D., Thompson, S. & Smithies, O. (1988) *Nature (London)* **330**, 576–578.
20. Adair, G., Carver, J. & Wandres, D. (1980) *Mutat. Res.* **72**, 187–205.
21. Adair, G., Stallings, R., Nairn, R. & Siciliano, M. (1983) *Proc. Natl. Acad. Sci. USA* **80**, 5961–5964.
22. Adair, G. (1987) in *Banbury Report 28: Mammalian Cell Mutagenesis*, eds. Moore, M., DeMarini, D., DeSerres, F. & Tindall, K. (Cold Spring Harbor Laboratory, Cold Spring Harbor, NY), pp. 3–13.
23. Lowy, I., Pellicer, A., Jackson, J., Sim, G., Silverstein, S. & Axel, R. (1980) *Cell* **22**, 817–823.
24. Nalbantoglu, J. & Meuth, M. (1986) *Nucleic Acids Res.* **14**, 8361–8371.
25. Mulligan, R. & Berg, P. (1980) *Science* **209**, 1422–1427.
26. Jagadeeswaran, P., Ashman, C., Roberts, S. & Langenberg, J. (1984) *Gene* **31**, 309–313.
27. Nairn, R., Adair, G. & Humphrey, R. (1982) *Mol. Gen. Genet.* **187**, 384–390.
28. Nairn, R., Humphrey, R. & Adair, G. (1988) *Int. J. Radiat. Biol.* **53**, 249–260.
29. Miller, S., Dykes, D. & Polesky, H. (1988) *Nucleic Acids Res.* **16**, 1215.
30. Feinberg, A. & Vogelstein, B. (1983) *Anal. Biochem.* **132**, 6–13.
31. Meselson, M. & Radding, C. (1975) *Proc. Natl. Acad. Sci. USA* **72**, 358–361.
32. Szostak, J., Orr-Weaver, T., Rothstein, R. & Stahl, F. (1983) *Cell* **33**, 25–35.
33. Mosig, G. (1987) *Annu. Rev. Genet.* **21**, 347–371.
34. Stanfield, S. & Helinski, D. (1984) *Mol. Cell. Biol.* **4**, 173–180.
35. Stanfield, S. & Helinski, D. (1986) *Nucleic Acids Res.* **14**, 7823–7838.
36. Schimke, R., Sherwood, S., Hill, A. & Johnston, R. (1986) *Proc. Natl. Acad. Sci. USA* **83**, 2157–2161.
37. Carroll, S., DeRose, M., Gaudray, P., Moore, C., Needham-Vandevanter, D., Von Hoff, D. & Wahl, G. (1988) *Mol. Cell. Biol.* **8**, 1525–1533.
38. Wiberg, F., Sunnerhagen, P. & Bjursell, G. (1986) *Mol. Cell. Biol.* **6**, 653–662.

STIC-ILL

From: Vogel, Nancy
Sent: Thursday, December 09, 2004 2:09 PM
To: STIC-ILL
Subject: refs for 10/045,116 (references from lost parent case 09/033,555)

Please send me the following:

Proc. Natl. Acad. Sci. USA (1 989) 86:4574-4578

Virol. 1997 227:239-244

Virolo 1994 202:695-706

Virolo 1993 193:631-641

Genes and Dev. 1988 2:453-461

Nucleic Acid Research 1983 11 17 :6003-6020 .

Proc. Natl. Acad. Sci. USA 1994 91:8802-8806
J Virolo I 993 67 10 :591 1-592 1

Anticancer Res. 1997 17:1471-1505

J Immunol. 1988 141 6 :2084-2089

J Virol. 1989 63 2 :631-638

Science 1989 244:1288-1292

Chang et al. Cancer Gene therapy Using Novel Tumor specific Replication Competent Adenovirus Vectors" Cold Spring Harbor Gene Thera Meeting Sept. 1996

Nucleic Acids Res. 1996 24 12 :2318-2323

Current Protocols in Molecular Biology
Ausubel et al., eds., 1987 , Supp. 30, section 7.7.18 Table 7.7.1

Nature (1989) 337:387-388

Advances in Virus Research 1986 31: 169-228

Biochem. Biophys. Acta 1982 651:175-208

Mol. Cell. Biol. 1989 9 (9) :41 5-42

J Virol. 1997 71 (1) :548-561

EMBO J 1984 3 (12) :2917-2922

J Genetic Virolo 1977 68:937-940

1973 Virolo 52:456-467

1987 J Gen. Virol 36:59-72

Biochem. J. 1987 241:25-38

Hallenbeck, P.L. et a1., Novel Tumor Specific Replication Competent Adenoviral Vectors for Gene Therapy of Cancer" abstract no. 0-36 Cancer Gene Thera 1996) 3 (6) :S19-S20.

J. Biol. Chem. 1995 270 (8) :3602-3610 .
J Biol. Chem. 1994 269 (39) :23872-23875
Adv. Dru Delive Rev. 1995 17:279-292

VIROLOGY 227, 239–244 (1997)
ARTICLE NO. VY968269

SHORT COMMUNICATION

Fiber Genes of Adenoviruses with Tropism for the Eye and the Genital Tract

NIKLAS ARNBERG, YA-FANG MEI, and GÖRAN WADELL[1]

Department of Virology, University of Umeå, Umeå, Sweden

Received June 24, 1996; revised September 17, 1996; accepted October 1, 1996

We have characterized the fibergenes of adenovirus type 19p (Ad19p), Ad19a, and Ad37 by sequencing. The fiber genes of Ad19a and Ad37 are identical and only five amino acids differ comparing Ad19a/Ad37 with Ad19p. Based on the translated sequences we calculated the isoelectrical points (Ips) and found that the fiber knobs of Ad19p, Ad19a, and Ad37 together with Ad8 display the highest Ips of all so far characterized. Two regions within the fiber knob with unusually basic characteristics have been identified. Sequence alignments revealed that the corresponding regions in other fiber knobs are highly antigenic in pepscan analysis and of importance for hemagglutination. Only two positions differ in the knobs comparing Ad19a/Ad37 with Ad19p. Hence, either of these or both amino acid residues should be expected to be responsible for the observed differences in hemagglutination between Ad19p and Ad19a/Ad37. Moreover, we have found two amino acids (Ala_{227} and Lys_{252}) that are unique in their respective position in Ad19p, Ad19a, Ad37, and Ad8. Three amino acids (Lys_{236}, Lys_{240}, and Asn_{251}) are unique in their respective position in Ad19a and Ad37, that manifest a tropism for the genital tract. All five amino acids colocalize within one of the two basic regions.

Subgenus D adenovirus serotypes 8, 19a, and 37 have frequently been reported as the major cause of epidemic keratoconjunctivitis (EKC) (*1–7*). Ad19a has been shown to be distinct from Ad19p (*8*). Ad19p, has not been shown to cause illness in man since its original isolation in Saudi arabia in 1955 (*9, 10*). In addition, Ad37 and Ad19a have been reported to cause sexually transmitted urogenital infections that sometimes coincide with EKC (*11–16*). Adenovirus associated conjunctivitis is primarily caused by Ad9, Ad15, Ad3, and Ad4. This infection is frequently associated with an infection in the upper respiratory tract causing pharyngoconjunctival fever (PCF) (*17–19*).

The different tropisms of these adenoviruses are reflected in their hemagglutination pattern: Ad8, Ad19a, and Ad37 agglutinates dog and guinea pig erythrocytes more efficiently than Ad9, Ad15, Ad3, and Ad4 (*7, 20, 21*).

The fiber mediates the primary contact with so far unknown cellular receptor(s) (*22–26*), while the penton base links the fiber to the virus particle (*27, 28*) and is suggested to be of importance in the second step of infection, the internalization (*29–32*).

Ad5-based vectors predominate in studies evaluating the feasibility of adenovirus vectors in gene therapy. We have demonstrated that subgenus D adenoviruses manifest affinity for the genital tract. They might consequently be used to deliver genes to the genital mucosa. To elucidate the specificity of the fibers of adenoviruses belonging to subgenus D, we have sequenced the fiber genes of Ad19p, Ad19a, and Ad37.

Virus strains GW (Ad37), 587 (Ad19p), and ME (Ad19a) were propagated in A549 cells and viral DNA was extracted from infected cells according to the method reported by Shinagawa and coworkers (*33*). Since the fiber genes of Ad37 and Ad19a are identical it is important to mention that the work with Ad37 and Ad19a, i.e., propagation of virus DNA, digestion of viral DNA by restriction enzymes revealing unique RE-patterns, PCR, and sequencing were performed 3 months apart, which minimized the risk for contamination. The genomes were digested with *Bam*HI, *Bgl*II, *Sac*I, *Sal*I, and *Sma*I (Promega and Boehringer Mannheim) and compared with previously published restriction enzyme maps to ensure the correct identity of the viral DNA (data not shown). From the genome of each type, fiber genes were amplified according to Allard and coworkers (*34*) (data not shown). Primers F1, 5′-AAGGGATGTCAAATTCC-3′, and R1, 5′-CTGGTGGTGGGAGA-3′, were based on those used by Pring-Åkerblom and Adrian (*35*).

Three Ad19p-, three Ad19a-, and three Ad37 fiber amplimers were cloned into pT7Blue vector (Novagen) with T4 DNA Ligase (New England Biolabs). Sequencing was performed according to the instructions of Pharmacia Sequencing kit and ALF equipment. Fluorescent primers were constructed from conserved regions flanking subgenus D adenovirus fibers. Both strands of three fiber amplimers from each type was sequenced in order to establish DNA sequences and avoid possible errors made by the enzyme. The sequencing data was analyzed

[1] To whom correspondence and reprint requests should be addressed. Fax: 46 90129905.

0042-6822/97 $25.00

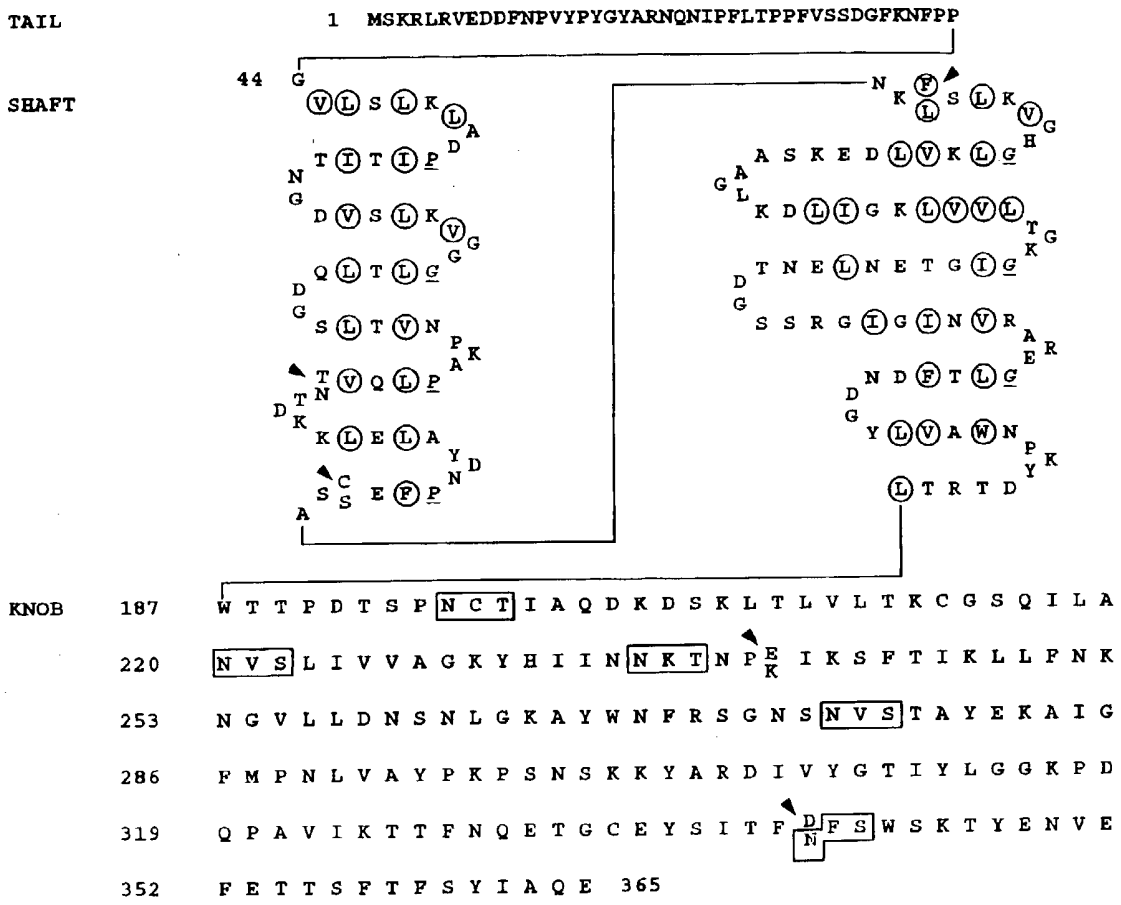

FIG. 1. Amino acid sequences of Ad19p, Ad19a, and Ad37 fiber polypeptides divided in a N-terminal tail, a shaft composed of eight repeated motifs, and a C-terminal knob. In the shaft, hydrophobic residues are indicated by circles, and the conserved prolines/glycines in position a5 (37) are underlined and written in italics. The five amino acid residues that differ between Ad19p and Ad19a/Ad37 are indicated by arrows. The upper amino acids of these five represent the Ad19p fiber, while the lower represent the Ad19a/Ad37 fiber. All potential -N-"X"-T/S-linked glycosylation sites found in the fibers are boxed.

and aligned with Lasergene software (DNASTAR), which was also used to compute the isoelectric points of the amino acid sequences.

The nucleotide sequence data reported in this paper have been submitted to the GenBank nucleotide sequence database and have been assigned Accession Nos. U69130 (Ad19p fiber), U69131 (Ad19a fiber), and U69132 (Ad37 fiber).

The length of all three fiber genes is 1098 bp while the fiber polypeptides comprise 365 amino acids (Fig. 1). The genes encoding the fibers in Ad19a and Ad37 were found to be identical. This could be the consequence of a recent recombination event. This hypothesis is supported by the epidemiology shown by these types: Ad19a was discovered in 1973 and was frequently isolated during 1973–1977 (*8*), while a new adenovirus causing EKC emerged in 1976 (*36*) and was demonstrated to be a new adenovirus type 37 (*36, 37*). However, we can neither prove that Ad37 has emerged after a recombination event nor exclude the possibility. The overall homology between the fibers of Ad19p vs Ad37/Ad19a is 98.4% at the amino acid level (Table 1). Three of the discordant amino acids are located to the shaft and two amino acids to the knob.

In conformity with other fibers, the fibers of Ad19p, Ad19a, and Ad37 could be divided into an N-terminal tail, a shaft with eight repeated motifs with a described β-sheet/β-turn model (*38*), and a C-terminal knob. Several consensus sequences in the fiber polypeptides of Ad19p, Ad19a, and Ad37 have been identified, which are consistent with data presented about other adenovirus fibers. In the tail we identified three conserved regions. -K-R-L-K- was proposed to be involved in guiding the fiber into the nucleus (*39, 40*). The intercalated region -F-N-P-V-Y-P- was suggested to be the pentonbase interaction domain (*27*), and the most C-terminal conserved domain -Y-A-R-N-Q-N-I- was suggested to be a subgenus-specific region (*35*). The tail/shaft junction -G-V-L-S-L- and the shaft/knob junction -T-L-W-T- are also conserved.

In the knob we identified the suggested inter-subgenus-specific determinant (C and D) represented by the amino acid sequence -L-T-K-C-G-S-Q- (*38*). The conserved region -A-"XX"-F-M-P-"XXX"-A-Y-P- has been suggested as a contributor to the formation of the secondary

TABLE 1

Nucleotide and Predicted Amino Acid Sequence Homologies for Subgenus D Adenovirus Fibers

	Tail		Shaft		Knob		Overall	
	DNA	Protein	DNA	Protein	DNA	Protein	DNA	Protein
Ad37 vs Ad19a	100	100	100	100	100	100	100	100
Ad37/Ad19a vs Ad19p	100	100	99.3	97.7	99.1	98.9	99.3	98.4
Ad37/Ad19a vs Ad8	93.8	90.7	54.0	47.5	80.6	82.8	71.4	70.2
Ad37/Ad19a vs Ad9	99.2	97.7	54.4	49.6	78.1	82.8	71.5	71.9
Ad37/Ad19a vs Ad15	97.7	95.3	50.7	51.4	55.4	51.1	59.3	56.0
Ad19p vs Ad8	93.8	90.7	53.7	47.5	81.5	83.8	71.8	70.2
Ad19p vs Ad9	99.2	97.7	54.0	49.6	79.1	83.8	71.7	71.9
Ad19p vs Ad15	97.7	95.3	50.5	51.4	54.6	52.0	58.8	56.0

Note. DNA- and amino acid-homologies are obtained through Lasergene software.

structure (*41*) which is compatible with the location, buried between the major receptor-facing sheet (β-sheets G, H, I, and D), and the virus-facing sheet (β-sheets J, C, B, and A) in the knob (Fig. 3). Four and five possible N-linked glycosylation sites (-N-"X"-S/T) were found in the fibers of Ad19p and Ad37/Ad19a, respectively, and all were localized to the knobs (Fig. 1).

The Ips have been derived from the amino acid-sequence of the tail, the shaft, the knob, and the whole fiber by computer analysis (Table 2). The knob of Ad8, Ad19p, Ad19a, and Ad37 display the highest Ips. The comparison of the values of the Ips in the knobs of adenoviruses with a manifested tropism for the cornea (Ad8, Ad19p, Ad19a, and Ad37; Ip = 8.5–9.1), with adenovirus regions with tropism for the conjunctiva rather than the cornea (Ad9 and Ad15; Ip = 6.6; Ad3, Ad4, Ad7, and Ad11a; Ip = 5.2–5.7), revealed significant differences.

In Ad5, the knob comprises 35% β-sheets and 65% loops and turns (*41*). The loops are less conserved and shape the outer surface of the protein, while the β-sheets maintain the secondary structure. Since the β-sheets together with the tail/shaft junction and the shaft/knob junction are conserved between the members of all subgenera, it has been proposed that the overall structure of the fibers is preserved across the genus (*41*). We have therefore adapted the structure of the sheets and loops in the knob of Ad5 to the knobs of Ad19p, Ad19a, and Ad37, in order to localize specific regions in these structures of the knobs of Ad19p, Ad19a, and Ad37, that correlate to the highly basic values of the entire knobs. In this way, we have localized two basic regions in Ad19p, Ad19a, Ad37, and Ad8, to the immediate center of the top of the trimer (region 1; Fig. 2A), and to the surface running along the side of each monomer (region 2; Fig. 2B). The regions are hereby exposed and consequently potent to interact with cellular receptors.

Subsequently we addressed the question whether a specific domain of the knob could be responsible for these differences. Two knob regions of potential interest with highly basic characteristics were found. Region one is located between the conserved amino acid triplet Ala_{292}-Tyr_{293}-Pro_{294} and a conserved Proline (Pro_{320}), and enclose 19–36 residues depending on serotype (Fig. 2A). This region is antigenic (*42*) and of importance for agglutination of monkey or rat erythrocytes (*43*). Each group with a specific HA-pattern has preserved certain residues in this region which may be involved in the hemagglutination. Among members of subgenus D, the amino acids $KKX_{(1,2)}AX_{(2,3)}IVX_{(0,1)}GX_{(2)}YLXGX_{(3)}Q$ were conserved, where X_0 symbolizes the number of inserted nonconserved amino acids. The members of subgenus C and E have the amino acids TXKXNIVXQVYX$_{(2)}$GDXK conserved, subgenus A and F adenoviruses have the amino acids $SEX_{(1,3)}QX_{(1,3)}LTYX_{(0,2)}LQGD$ conserved, while subgenus B has the amino acids EXYIXGXCXY conserved. Comparison of isoelectric points in knob region one with the hemagglutination properties of the respective virus results in distinct patterns: subgenus A, C, D, E, and F

TABLE 2

Isoelectric Points of Adenovirus Fibers and Fiber Components

Domain	Ad37	Ad19a	Ad19p	Ad8	Ad15	Ad9	Ad3	Ad4	Ad7	Ad11a
Overall	8.97	8.97	8.53	8.48	8.22	6.08	6.02	5.47	5.17	5.01
Tail	8.64	8.64	8.64	8.70	4.58	6.32	5.57	6.38	4.70	5.57
Shaft	7.15	7.15	7.08	5.69	9.21	5.80	7.98	5.29	4.93	4.85
Knob	9.08	9.08	8.50	8.95	6.59	6.56	5.31	5.70	5.61	5.23

Note. The isoelectric points are shown in log10 values and are obtained through Lasergene software.

A

Virus		Sub-genus	Alkaline/ Acidic Residues	Ip	HA-pattern Rat	HA-pattern Monkey
Ad12	AYPRPNASEA---------KSQMVSLTYLQGDTSK---P	A	3/2	8.69	+/-	-
Ad31	AYPRPNAGEA---------KSQMLSQTYLQGDTTK---P	A	3/2	8.69	+/-	-
Ad3	AYP------FVLPNAGTHNENYIFGQCYYKAS-DGALFP	B	1/2	5.41	-	+
Ad7	AYP------F--NVNSREKENYIYGTCYYTAS-DHTAFP	B	2/3	5.54	-	+
Ad16	AYP------FITYATETLNEDYIYGECYYKST-NGTLFP	B	1/4	3.83	-	+
Ad21	AYP------F--NTTTRDSENYIHGICYYMTSYDRSLVP	B	2/3	5.45	-	+
Ad11p	AYP------F--NDNSREKENYIYGTCYYTAS-DRTAFP	B	3/4	4.64	-	+
Ad11a	AYP------F--NNNSREKENYIYGTCHYTAS-DHTAFP	B	2/3	6.30	U	-
Ad34a	AYP------F--NDNSREKENYIYGTCYYTAS-DHTAFP	B	2/4	4.63	-	+
Ad35	AYP------F--NTTTRDSENYIHGICYYMTSYDRSLFP	B	2/3	5.45	-	+
Ad2	AYPKTQSQTA---------KNNIVSQVYLHGDKTK---P	C	4/1	9.74	+*	-
Ad5	AYPKSHGKTA---------KSNIVSQVYLNGDKTK---P	C	5/1	9.91	+*	-
Ad9	AYPKPTAGS------KKYARDIVYGNIYLGGKPDQ---P	D	5/2	9.60	+	+/-
Ad15	AYPKIINSTTVPENKKSSAKKTIVGNVYLEGNAGQ---P	D	5/2	9.64	+	+/-
Ad8	AYPKPTTGS------KKYARDIVYGNIYLGGKPHQ---P	D	5/1	9.83	+	+/-
Ad19p	AYPKPSN-S------KKYARDIVYGTIYLGGKPDQ---P	D	5/2	9.58	+	+/-
Ad19a	AYPKPSN-S------KKYARDIVYGTIYLGGKPDQ---P	D	5/2	9.58	+	+/-
Ad37	AYPKPSN-S------KKYARDIVYGTIYLGGKPDQ---P	D	5/2	9.58	+	+/-
Ad4	AYPKTQSSTT---------KNNIVGQVYMNGDVSK---P	E	3/1	9.46	+*	-
Ad40-1	RYP---------NEKGSEVQNMALTYTFLQGD------P	F	2/3	4.56	+/-	-
Ad40-2	VYP---------RNKTADPGNM-----LIQIS------P	F	2/1	8.86		
Ad41-1	RYP---------NQKGSEVQNMALTYTFLQGD------P	F	2/2	6.31	+/-	-
Ad41-2	VYP---------RNKTAHPGNM-----LIQIS------P	F	2/0	10.05		

B

Virus		Sub-genus	Alkaline/ Acidic Residues	Ip	HA-pattern Dog	HA-pattern Guinea Pig
Ad12	KGNLLNIQSTTTT----VGVHLVFDE	A	1/2	5.41	-	-
Ad31	KGDLLHIQPTTTT----VGLHLVFDR	A	2/2	7.32	-	-
Ad3	SDYVNTLFKNKNVS---INVELYFDA	B	2/3	4.36	-	-
Ad7	SNDFNMLTTHKNIN---FTAELFFDS	B	1/3	4.36	-	-
Ad16	SEYTNTLFKNNQVT---IDVNLAFDN	B	1/3	3.78	-	-
Ad21	SDTVNQMFTQKSAT---IQLRLYFDS	B	2/2	6.10	-	-
Ad11p	SNNFNMLTTHRNIN---FTAELFFDS	B	1/2	5.41	-	-
Ad11a	SNNFNMLTTYRNIN---FTAELFFDS	B	1/2	4.18	U	U
Ad34a	SNNFNMLTTHRNIN---FTAELFFDS	B	1/2	5.41	U	U
Ad35	SDTVNQMFTQKTAN---IQLRLYFDS	B	2/2	6.10	-	-
Ad2	-GDLSSMTGTVAS----VSIFLRFDQ	C	1/2	3.92	-	-
Ad5	-GSLAPISGTVQS----AHLIIRFDE	C	1/2	5.41	-	-
Ad9	DGKYKIINNNTQPALKGFTIKLLFDE	D	4/3	8.62	+	+/-
Ad15	KGTYATVDKNT--TNKQFSIKLLFDA	D	4/2	9.44	-	-
Ad8	AGRYKIINNNTNPALKGFTIKLLFDK	D	5/1	10.19	+	+
Ad19p	AGKYHIINNKTNPEIKSFTIKLLFNK	D	5/1	10.02	-	-
Ad19a	AGKYHIINNKTNPKIKSFTIKLLFNK	D	6/0	10.41	+	+
Ad37	AGKYHIINNKTNPKIKSFTIKLLFNK	D	6/0	10.41	+	+
Ad4	SGNLNPITGTVSS----AQVFLRFDA	E	1/1	6.01	-	-
Ad40-1	KGTLLKPTASFIS----FVMY--FYS	F	2/0	9.59	-	-
Ad40-2	KGALREMNDNALS----VKL	F	3/2	8.84		
Ad41-1	KGILLRPTASFIS----FVMY--FYS	F	2/0	9.77	-	-
Ad41-2	KGALREMHDNALS----LKL	F	3/2	8.84		

FIG. 2. Basic knob region one (A) and two (B) in Ad19p, Ad19a, and Ad37 compared to the corresponding regions in other adenovirus fiber knobs. The regions in each fiber are delineated by the N-terminal conserved -"X"-Y-P- and at a C-terminal proline (region one) and by the only two residues that are unique only within Ad8, Ad19p, Ad19a, and Ad37 (region two), from a homology alignment using the whole fiber polypeptides. These regions are then aligned a second time to obtain maximum homology. The following characteristics are presented: the subgenera, the relationship between strongly basic (L [Lys] and R [Arg]) and strongly acidic (D [Asp] and E [Glu]) amino acids, the isoelectric point (Ip) in the region represented by log values and the hemagglutination pattern (HA). "+" indicates complete HA; "+*" indicates incomplete HA; "+/−" indicates weak HA; and "−" indicates no HA at all. U indicates that the HA is unknown. The HA-pattern obtained from each subgenus F adenovirus (containing two fibergenes) is indicated after the brackets. HA data are obtained from (7, 20, 21).

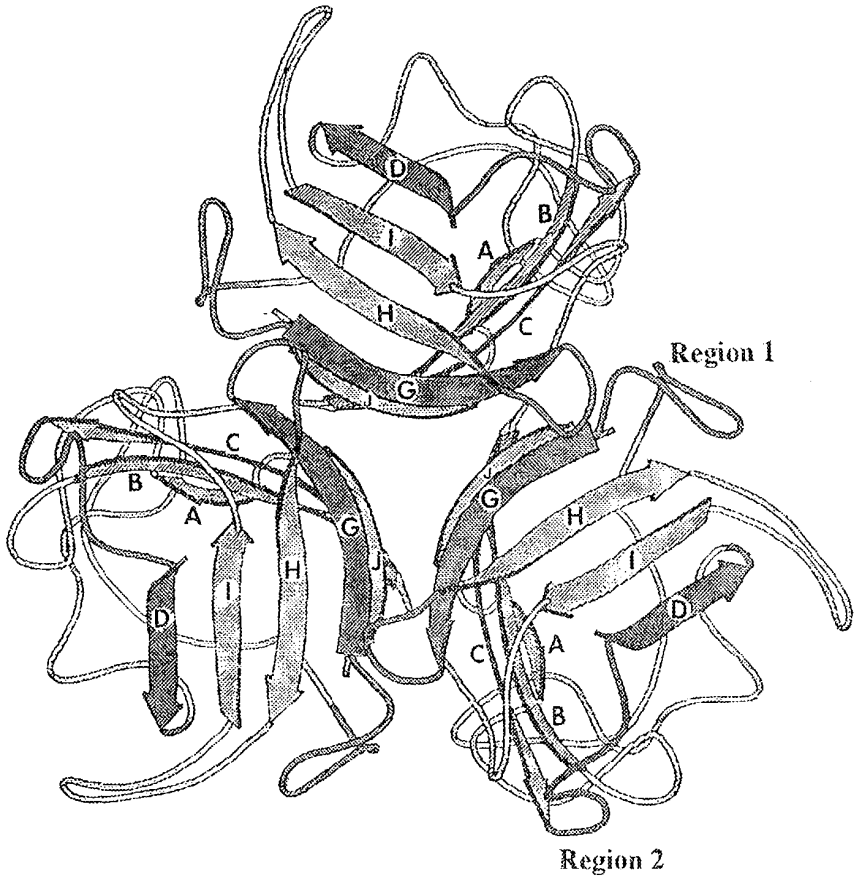

FIG. 3. Localization of the two basic regions within the stereo ribbon diagram derived from the crystal structure of the Ad5 fiber knob protein. The diagram is viewed down the threefold symmetry axis toward the virus surface. The uppercase letters are marked according to the suggestions and sequence alignment of Xia and coworkers (40).

all agglutinate rat erythrocytes but in different fashions: subgenus D displays complete agglutination, subgenus C and E display incomplete agglutination, and subgenus A and F display hardly discernable agglutination. On the other hand, subgenus B adenoviruses manifest complete agglutination of monkey erythrocytes, whereas rat erythrocytes are not agglutinated (Fig. 2A). It should be noted that Ad11a which does not display agglutination of monkey erythrocytes display the highest Ip in region one among subgenus B adenoviruses (Fig. 2A). Subgenus F adenoviruses expose two fibers, one of which is basic and the other more acidic in this domain. This leads us to suggest that the more basic fiber may serve as ligand to rat erythrocytes, mediating the hardly discernable hemagglutination of rat cells. In conclusion, even though a high Ip seems to facilitate agglutination of rat erythrocytes, it does not have to be the only requirement. In addition, a high Ip seems to impair the ability to agglutinate monkey erythrocytes, but we cannot exclude that additional factors are involved. Similarly, a low Ip seems to be a prerequisite for agglutination of monkey erythrocytes and hampers agglutination of rat erythrocytes.

The second knob region is located between residues Ala_{227}-Lys_{252} and distinctly separate subgenus D and F adenoviruses from the rest, regarding the isoelectric point of this region (Fig. 2B). Ad8, Ad19p, Ad19a, and Ad37 displayed the highest Ip of all in this region. The domain comprised 5:1 (basic vs acidic amino acids) in Ad8 and Ad19p, and 6:0 in Ad37 and Ad19a. In Ad2, knob region two has proven to be highly antigenic in pepscan analysis (*42*), using both monoclonal and polyclonal antibodies, especially the domain that covers the amino acids Asn_{251} and Lys_{252} in the knobs of Ad19p, Ad19a, and Ad37. A low Ip in knob region two coincides with a complete lack of agglutination of dog and guinea pig erythrocytes, whereas a high Ip usually coincides with an ability to agglutinate the same erythrocytes. Apparently, high Ips of the knob region is a necessary but probably not a sufficient prerequisite for agglutination of dog and guinea pig erythrocytes.

Using maximum homology alignment we were able to identify two residues in the knobs of Ad8, Ad19p, Ad19a, and Ad37 (Ala_{292} and Lys_{320}), which are unique when compared with the knob sequences of other adenoviruses (Fig. 2B). Surprisingly, these two residues localize to each side of the above described β-sheet D in region

two. Further analysis revealed five residues, nonsynonymous in the respective position, in the knobs of Ad19a and Ad37. Three of these colocalize within region two. Two of these three reside in the CD-loop (Lys_{236}, Lys_{240}; Figs. 1 and 3) and one at the immediate end of the D β-sheet (Asn_{251}). The remaining two amino acids (Ala_{265} and Asn_{275}) reside at the middle of the long DG-loop, facing the shaft rather than the environment (Fig. 3). No other amino acid residue that represents a nonsynonymous change compared to all other sequenced adenoviruses has been found. Glu/Lys_{240} (Ad19p/[Ad19a/Ad37]) in region two are together with Asp/Asn_{340} (Ad19p/[Ad19a/Ad37]; Fig. 1), the only amino acids that distinguish the knob of Ad19p from the knobs of Ad19a and Ad37 and are probably responsible for the characteristic differences in hemagglutination between these adenoviruses (Fig. 2B). Based on the basic characteristic of the knobs or specific domains of the knob, conserved nonsynonymous amino acids in region two in fiber knobs expressed by adenoviruses with a common tropism, the compatibility of the regions with hemagglutination patterns, and previously presented data proving knob region one in subgenus B2 adenoviruses to be of importance for hemagglutination (*43*), we suggest fiber knob region one and two in Ad8, Ad19p, Ad19a, and Ad37 to be of importance for hemagglutination and interaction with cellular receptor(s). To explain some of these features, we propose a model in which the charge of the fiber knob may be critical for enabling the fiber knob to approach the receptor region of the cellular receptor.

ACKNOWLEDGMENTS

This study was supported by grants from The Fund for Advanced Medical Research at the University Hospital of Northern Sweden and from the Swedish Medical Research Council, Grant 16X05688. We thank Dr. Robert D. Gerard and Dr. Johann Diesenhofer at University of Texas for allowing us to adapt our results to the three-dimensional model of the Ad5 fiber knob. We thank Dr. Alistair H. Kidd for critically reading the manuscript and Kristina Lindman for technical assistance.

REFERENCES

1. Jawetz, E., Kimura, S., Nicholas, A. N., Thygeson, P., and Hanna, L., *Science* **122,** 1190–1192 (1955).
2. Burns, R. P., and Potter, M. H., *Am. J. Ophthalmol.* **81,** 27–29 (1976).
3. Darougar, S., Quilan, M. P., Gibson, J. A., Jones, B. R., and McSwiggan, D. A., *Br. J. Ophthalmol.* **16,** 76–85 (1977).
4. Guyer, B., O'Day, M., Hierholzer, J. C., and Schaffner, W., *J. Infect. Dis.* **132,** 142–150 (1975).
5. Hierholzer, J. C., Guyer, B., O'Day, D., and Schaffner, W., *N. Engl. J. Med.* **290,** 1436 (1974).
6. Adrian, T., deJong, J. C., Wermenbol, A. G., van der Avoort, H. G. A. M., and Wigand, R., *J. Med. Virol.* **25,** 77–83 (1988).
7. Kemp, M. C., Hierholzer, J. C., Cabradilla, C. P., and Obijeski, J. F., *J. Infect. Dis.* **148,** 24–33 (1983).
8. Wadell, G., and de Jong, J. C., *Infect. Immunity* **27,** 292–296 (1980).
9. Bell, S. D., Jr., McComb, D. E., Murray, E. S., Chang, R. S-M., and Snyder, J., *Trop. Med. Hyg.* **8,** 492–500 (1959).
10. Feng, M., Chang, R. S., Smith, T. R., and Snyder, J. C., *Am. J. Trop. Med. Hyg.* **8,** 501–504 (1959).
11. Cevenini, R., Donati, M., Laudini, M. P., and LaPlaca, M., *Microbiologica* **2,** 425–427 (1979).
12. Harnett, G. D., and Newnham, W. A., *Br. J. Vener. Dis.* **57,** 55–57 (1981).
13. Harnett, G. D., Phillips, P. A., and Gollow, M. M., *Med. J. Aust.* **141,** 337–338 (1984).
14. Laverty, C. R., Russel, P., Black, N., Kappágoda, N., Ben, R. A., and Booth, N., *Acta Cytol.* **21,** 114–117 (1977).
15. Phillips, P. A., Harnett, G. B., and Gollow, M. M., *Br. J. Vener. Dis.* **58,** 131–132 (1982).
16. Swenson, P., Lowens, M. S., Celum, C. S., and Hierholzer, J. C., *J. Clin. Microbiol.* **33,** 2728–2731 (1995).
17. Aoki, K., Kawana, R., Matsumoto, I., Wadell, G., and de Jong, J. C., *Jpn. J. Ophthalmol.* **30,** 158–164 (1986).
18. Bennet, F. M., Law, B. B., Hamilton, W., and MacDonald, A., *Lancet* **2,** 670–673 (1957).
19. Murray, E., Chang, R. S., Bell, S. D., Tarizzo, M. L., and Snyder, J. C., *Am. J. Ophthalmol.* **4,** 32 (1957).
20. Hierholzer, J. C., *J. Infect. Dis.* **128,** 541–550 (1973).
21. Hierholzer, J. C., Stone, Y. O., and Broderson, J. R., *Arch. Virol.* **121,** 179–197 (1991).
22. Defer, C., Belin, M-T., Caillet-Boudin, M-L., and Boulanger, P., *J. Virol.* **64,** 3661–3673 (1990).
23. Henry, L. J., Xia, D., Wilk, M. E., Diesenhofer, J., and Gerard, R. D., *J. Virol.* **68,** 5239–5246 (1994).
24. Louis, N., Fender, P., Barge, A., Kitts, P., and Chroboczek, J., *J. Virol.* **68,** 4104–4106 (1994).
25. Philipson, L., Lonberg-Holm, K., Pettersson, U., *J. Virol.* **2,** 1064–1075 (1968).
26. Stevenson, S. C., Rollence, M., White, B., and Weaver, L., *J. Virol.* **69,** 2850–2857 (1995).
27. Caillet-Boudin, M. L., *J. Mol. Biol.* **208,** 195–198 (1989).
28. Boudin, M. L., Rigolet, M., Lemay, P., Galibert, F., and Boulanger, P., *EMBO J.* **2,** 1921–1927 (1983).
29. Bai, M., Harfe, B., and Freimuth, P., *J. Virol.* **67,** 5198–5205 (1993).
30. Bai, M., Campisi, L., and Freimuth, P., *J. Virol.* **68,** 5925–5932 (1994).
31. Mathias, P., Wickham, T. J., Moore, M., and Nemerow, G., *J. Virol.* **68,** 6811–6814 (1993).
32. Wickham, T. J., Mathias, P., Cheresh, D. A., and Nemerow, G. R., *Cell* **73,** 309–319 (1993).
33. Shinagawa, M., Matsuda, A., Ishiyama, T., Goto, H., and Sato, G., *Microbiol. Immunol.* **27,** 817–822 (1983).
34. Allard, A., Girones, R., Juto, P., and Wadell, G., *J. Clin. Microbiol.* **28,** 2659–2667 (1990).
35. Pring-Åkerblom, P., and Adrian, T., *Virology* **206,** 564–571 (1995).
36. de Jong, J. C., Wigand, R., Wadell, G., Keller, D., Muzerie, C. J., Wermenbol, A. G., and Schaap, G. J. P., *J. Med. Virol.* **7,** 105–108 (1981).
37. Wadell, G., Sundell, G., and de Jong, J. C., *J. Med. Virol.* **7,** 119–125 (1981).
38. Green, N. M., Wrigley, N. G., Russel, W. C., Martin, S. R., and McLaghlan, A. D., *EMBO J.* **2,** 1357–1365 (1983).
39. Hong, J. S., and Engler, J. A., *Virology* **185,** 758–767 (1991).
40. Hong, J. S., and Boulanger, P., *EMBO J.* **14,** 4714–4727 (1995).
41. Xia, D., Henry, L. J., Gerard, R. D., and Diesenhofer, J., *Structure* **2,** 1259–1270 (1994).
42. Fender, P., Kidd, A. H., Brebant, R., Öberg, M., Drouet, E., and Chroboczek, J., *Virology* **214,** 110–117 (1995).
43. Mei, Y-F., and Wadell, G., *J. Virol.* **70,** 3688–3697 (1996).

STIC-ILL

From: Vogel, Nancy
Sent: Thursday, December 09, 2004 2:09 PM
To: STIC-ILL
Subject: refs for 10/045,116 (references from lost parent case 09/033,555)

AU 1636

Please send me the following:

Proc. Natl. Acad. Sci. USA (1 989) 86:4574-4578

Virol. 1997 227:239-244

Virolo 1994 202:695-706

Virolo 1993 193:631-641

Genes and Dev. 1988 2:453-461

Nucleic Acid Research 1983 11 17 :6003-6020 .

Proc. Natl. Acad. Sci. USA 1994 91:8802-8806
J Virolo l 993 67 10 :591 1-592 1

Anticancer Res. 1997 17:1471-1505

J Immunol. 1988 141 6 :2084-2089

J Virol. 1989 63 2 :631-638

Science 1989 244:1288-1292

Chang et al. Cancer Gene therapy Using Novel Tumor specific Replication Competent Adenovirus Vectors" Cold Spring Harbor Gene Thera Meeting Sept. 1996

Nucleic Acids Res. 1996 24 12 :2318-2323

Current Protocols in Molecular Biology
Ausubel et al., eds., 1987 , Supp. 30, section 7.7.18 Table 7.7.1

Nature (1989) 337:387-388

Advances in Virus Research 1986 31: 169-228

Biochem. Biophys. Acta 1982 651:175-208

Mol. Cell. Biol. 1989 9 (9) :41 5-42

J Virol. 1997 71 (1) :548-561

EMBO J 1984 3 (12) :2917-2922

J Genetic Virolo 1977 68:937-940

1973 Virolo 52:456-467

1987 J Gen. Virol 36:59-72

Biochem. J. 1987 241:25-38

Hallenbeck, P.L. et a1., Novel Tumor Specific Replication Competent Adenoviral Vectors for Gene Therapy of Cancer" abstract no. 0-36 Cancer Gene Thera 1996) 3 (6) :S19-S20.

J. Biol. Chem. 1995 270 (8) :3602-3610 .
J Biol. Chem. 1994 269 (39) :23872-23875
Adv. Dru Delive Rev. 1995 17:279-292

An Efficient and Flexible System for Construction of Adenovirus Vectors with Insertions or Deletions in Early Regions 1 and 3

Andrew J. Bett; Wael Haddara; Ludvik Prevec; Frank L. Graham

Proceedings of the National Academy of Sciences of the United States of America, Vol. 91, No. 19 (Sep. 13, 1994), 8802-8806.

Proc. Natl. Acad. Sci. USA
Vol. 91, pp. 8802–8806, September 1994
Medical Sciences

An efficient and flexible system for construction of adenovirus vectors with insertions or deletions in early regions 1 and 3

ANDREW J. BETT*, WAEL HADDARA*, LUDVIK PREVEC*†, AND FRANK L. GRAHAM*†‡

Departments of *Biology and †Pathology, McMaster University, Hamilton, ON, Canada, L8S 4K1

Communicated by C. Thomas Caskey, May 17, 1994

ABSTRACT **Human adenoviruses (Ads) are attracting considerable attention because of their potential utility for gene transfer and gene therapy, for development of live viral vectored vaccines, and for protein expression in mammalian cells. Engineering Ad vectors for these applications requires a variety of reagents in the form of Ads and bacterial plasmids containing viral DNA sequences and requires different strategies for construction of vectors for different purposes. To simplify Ad vector construction and develop a procedure with maximum flexibility, efficiency, and cloning capacity, we have developed a vector system based on use of Ad5 DNA sequences cloned in bacterial plasmids. Expanded deletions in early region 1 (3180 bp) and early region 3 (2690 or 3132 bp) can be combined in a single vector that should have a capacity for inserts of up to 8.3 kb, enough to accommodate the majority of cDNAs encoding proteins with regulatory elements. Genes can be inserted into either early region 1 or 3 or both and mutations or deletions can be readily introduced elsewhere in the viral genome. To illustrate the flexibility of the system, we have introduced a wild-type early region 3 into the vectors, and to illustrate the high capacity for inserts, we have isolated a vector with two genes totaling 7.8 kb.**

Construction of adenovirus (Ad) vectors involves insertion of foreign DNA into the Ad genome, usually with compensating deletions in early region 1 (E1) or early region 3 (E3). E1 is not required for viral replication in 293 cells (1), which express the left 11% of the Ad5 genome. For viral viability, deletions in this region must not affect the inverted terminal repeat (ITR; 1–103 bp) or packaging signals (194–358 bp) (2–5). In addition, deletions should not extend into the coding sequences for protein IX, which is essential for packaging of full-length genomes into functional virions (6). Since Ad virions can package ≈105% of the wild-type (wt) genome length (7), deletions of up to 2.9 kb in E1 (8–10) permit construction of defective vectors with inserts up to 4.7–4.9 kb.

E3 is nonessential for viral replication in any normally permissive human cell and can be deleted to produce nondefective vectors (11, 12). Deletions in E3 presumably cannot extend into essential virion structural genes, pVIII and fiber, flanking this region. Several E3 deletions have been used for vector construction, the most common resulting from removal of 1.88 kb of E3 sequences between *Xba* I sites at 79.6 and 84.8 map units (mu) in the Ad5 genome (11, 12), providing a capacity for inserts of 3.7–3.9 kb.

Among current methods for generating Ad vectors (8), there is no simple procedure for generating vectors with both E1 and E3 deletions. To construct Ad5 vectors that combine E1 and E3 deletions or substitutions and to simplify Ad vector production, we have developed a methodology based on a series of bacterial plasmids (pBHG) containing most of the viral genome in circular form but lacking the DNA packaging signals. In this paper, we describe this system and its use to generate vectors with a wt E3 region or with inserts of up to 7.8 kb of foreign DNA in the E1 region.

The publication costs of this article were defrayed in part by page charge payment. This article must therefore be hereby marked "*advertisement*" in accordance with 18 U.S.C. §1734 solely to indicate this fact.

MATERIALS AND METHODS

Construction of Recombinant Plasmids. Plasmids constructed by standard protocols (13) were used to transform *Escherichia coli* DH5 (13) by electroporation (14) or *E. coli* HMS174 by using $CaCl_2$. Plasmid DNA was prepared by the alkaline lysis method (15) and purified by CsCl–ethidium bromide density gradient centrifugation.

Cells and Viruses. Cell culture media were obtained from GIBCO. Ad vectors were propagated and titered on 293 cells as described (16). Recombinant viruses were isolated by cotransfection of 293 cells with appropriate plasmids or viral DNA (17). After 8–10 days, plaques were isolated and expanded, and viral DNA was analyzed by restriction enzyme digestion as described (12, 16). [^{35}S]Methionine labeling, immunoprecipitation, and SDS/PAGE were carried out as described (16, 18). Densitometry was performed using the LKB Ultroscan XL enhanced laser densitometer.

RESULTS

Generation of the Plasmid pBHG10. In developing the strategy to be described, advantage was taken of previous observations made by ourselves (10, 12, 19–21) and other investigators (2, 11, 22–24). One key finding is the fact that Ad DNA can circularize in infected cells (19) and that this phenomenon can be exploited to generate infectious circular Ad genomes that can be propagated as bacterial plasmids (10, 20, 21). Secondly, it has been shown that the cotransfection into mammalian cells of two plasmids with overlapping sequences can generate infectious virus with good efficiency (11, 12, 21). The third finding important to this strategy is that Ads carry a cis-acting sequence in the left end of the genome that is essential for encapsidation of viral DNA (2, 22–24). When this cis-acting signal, located from bp 194 to 358 in Ad5, is deleted, viral genomes cannot be packaged but are expected to replicate their DNA in transfected cells (2–5).

These findings led us to design and execute the strategy outlined in Fig. 1. The first step involved the construction of AdBHG, a virus that contains the Ad5 genome with the deletion of E3 sequences from bp 28,133 to 30,818 and the insertion of modified pBR322 at bp 1339. AdBHG was made by cotransfection of 293 cells with purified viral DNA from Ad5PacI, digested with *Cla* I and *Xba* I, and pWH3.

The next step involved the generation of a bacterial plasmid containing the entire AdBHG genome and subsequent identification of infectious clones. Baby rat kidney (BRK) cells were infected with AdBHG under conditions that result in the generation of circular Ad5 genomes (10, 19). At 48 h after infection DNA was extracted from the infected BRK

Abbreviations: Ad, adenovirus; E1 and E3, early regions 1 and 3, respectively; wt, wild type; ITR, inverted terminal repeat; mu, map unit(s); Ap^r, ampicillin resistance; Tet^r, tetracycline resistance; Kn^r, kanamycin resistance; HCMV, human cytomegalovirus; HSV-1, herpes simplex virus type 1.

‡To whom reprint requests should be addressed.

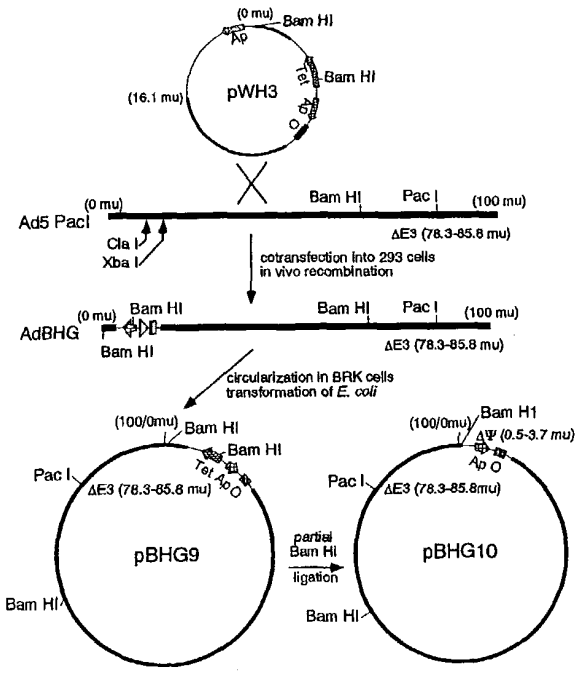

FIG. 1. Construction of pBHG10. pWH1 (not shown) was constructed from the plasmid pKH188 (25, 26) (derived by insertional mutagenesis of the E1A region in pKH101 resulting in the introduction of a *Bam*HI site at bp 188 in the Ad5 genome) by inserting pBRX (27) (a pBR322 derivative with an *Xba* I site at nt 2066) into the *Xba* I site at bp 1339 in Ad5 sequences. pWH1 was then combined with pXC38 (25) to include Ad5 sequences from 5.7 to 16.1 mu, generating pWH3. Ad5PacI [derived by cotransfection of 293 cells with pFG173 (18) and pAB14PacI, a modification of pAB14 (7) that substitutes a *Pac* I cloning site for 2.69 kb of E3] was digested with *Cla* I and *Xba* I and cotransfected into 293 cells with pWH3 to generate AdBHG. In the next step, the AdBHG genome was circularized by infecting BRK cells at multiplicity of infection of ≈20 under conditions that result in the generation of circular Ad5 genomes (10, 19). At 48 h after infection, DNA was extracted from the infected BRK cells and used to transform *E. coli* HMS174 to Ap^r and Tet^r. Small-scale plasmid preparations were made from the colonies obtained and screened by *Hin*dIII and *Bam*HI/*Sma* I digestion followed by gel electrophoresis (data not shown). Four candidates that appeared to possess a full AdBHG genome with intact junction regions were tested for infectivity and sequenced in the region of the junction. A single infectious clone was chosen, pBHG9. In the final step, the packaging signals were deleted from pBHG9 by partial *Bam*HI digestion and religation generating pBHG10. mu refers to Ad5 sequences, solid bars represent Ad5 sequences, and hatched bars represent Ap^r, Kn^r, and Tet^r segments.

cells and used to transform *E. coli* HMS174 to ampicillin and tetracycline resistance (Ap^r and Tet^r, respectively). From two experiments, plasmid DNA from a total of 104 colonies was screened by *Hin*dIII and *Bam*HI/*Sma* I digestion and gel electrophoresis (data not shown). Four candidate plasmids that appeared to posses a complete AdBHG genome were selected and all four were found to be infectious when transfected into 293 cells (data not shown). Since large palindromes, like that created by head to tail joining of the ITRs in these clones, are not compatible with plasmid replication in most strains of *E. coli* and result in rearrangements or deletions that disrupt the palindrome structure (10, 28, 29), the ITR junctions in each of the infectious clones were sequenced and analyzed. The number of nucleotides missing from the midpoint of the palindrome in each clone varied from as few as 4 bp (1 bp from the right ITR and 3 bp from the left) to as many as 19 bp (1 bp from the right ITR and 18 bp from the left). Because plasmids containing long palindromes tend to be unstable, we chose the clone missing 19 bp from the junction for further work. This plasmid was called pBHG9.

The final step involved generation of pBHG10 by deleting the packaging signals in pBHG9 by partial *Bam*HI digestion and religation (Fig. 1). Screening for pBHG10 was facilitated by the fact that removing the packaging signals also deleted the Tet^r gene. pBHG10 contains Ad5 DNA sequences from bp 19 (left genomic end) to bp 188; bp 1339–28,133 and bp 30,818–35,934 (right genomic end). The left and right termini of the Ad5 genomes are covalently joined and a segment of plasmid pBR322 is present between Ad5 bp 188 and 1339 to allow propagation of pBHG10 in *E. coli*. A *Pac* I restriction enzyme site, unique in this plasmid, is present between Ad5 bp 28,133 and bp 30,818 to permit insertion of foreign genes. Because the packaging signal is deleted, pBHG10 is noninfectious but cotransfections with plasmids that contain the left-end Ad5 sequences including the packaging signal produce infectious viral vectors with an efficiency comparable to that obtained with pJM17 (20) (unpublished data and see below).

Additional Alterations to pBHG10: Vectors with wt E3 Sequences or with an Expanded Deletion in E3. The use of plasmids such as pBHG10 allows for rapid and relatively simple manipulation of the Ad genome. Two modifications of pBHG10 are described in this section. Since for some applications it may be desirable to generate Ad vectors with intact wt Ad5 E3 sequences, we reintroduced wt E3 sequences into pBHG10 (Fig. 2). First, pBHG10 was digested with *Spe* I, which cuts only at 75.4 mu in Ad5 sequences, and ligated with pFG23K also linearized with *Spe* I, generating pBHG10A that now contains the desired wt E3 sequences in tandem with the previous E3 region containing the 2.69-kb deletion. To remove repeated sequences, pBHG10A was partially digested with *Nde* I and religated, generating pBHG10B. The kanamycin-resistance (Kn^r) segment was removed from pBHG10B by partial *Xba* I digestion and religation, generating pBHGE3. Except for the presence of a wt E3 region, pBHGE3 is identical to pBHG10 and is equally efficient for generation of Ad vectors with E1 substitution by cotransfection (unpublished).

For some applications, it may be desirable to have as large a deletion as possible within the E3 region. By utilizing a PCR and following a strategy similar to that described above for the construction of pBHGE3 (Fig. 2), we created a 3.13-kb E3 deletion and introduced it into pBHG10. The resulting plasmid pBHG11 is identical to pBHG10 except for an expanded E3 deletion that removes sequences from bp 27,865 to 30,995. Like pBHG10, pBHG11 contains a unique *Pac* I restriction enzyme site in place of the deleted E3 sequences to permit insertion of foreign genes. A detailed description of the construction of pBHG11 is available on request from the authors.

Construction of E1 Deletion Plasmids for Use in Cotransfections with pBHG Vectors. Plasmids pBHG10, pBHG11, and pBHGE3 were designed to contain all the essential Ad5 sequences required to produce infectious virus upon transfection of 293 cells except for the packaging signal (194–358 bp) needed to encapsidate viral DNA into viral particles. To generate infectious viral vectors, these plasmids or derivatives with an insert in E3 must be cotransfected into 293 cells with a second plasmid containing left end viral sequences including the packaging signal as illustrated in Fig. 3. To maximize the capacity of the BHG vector system, we required a plasmid with the largest possible E1 deletion for cotransfections with the BHG plasmids. Analysis of E1 sequences revealed that 3.2 kb could be deleted between an *Ssp* I site at 339 bp and an *Afl* II site at 3533 bp (Fig. 4). This

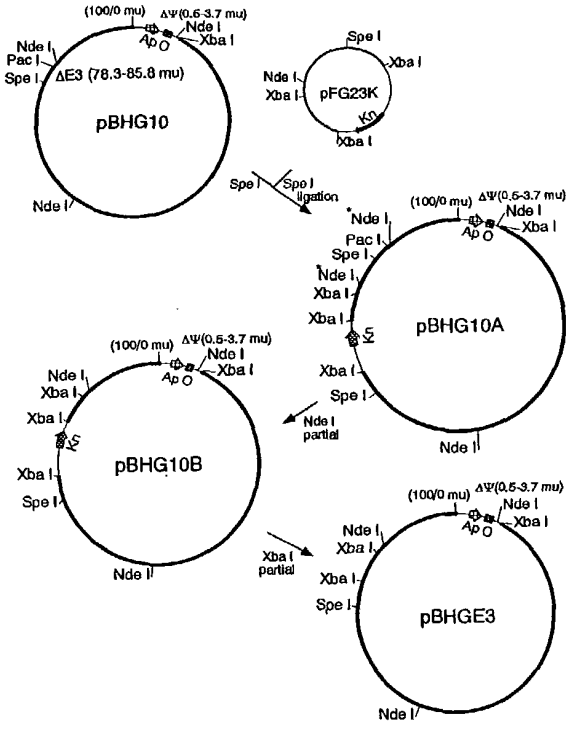

FIG. 2. Construction of pBHGE3. For insertion of wt E3 sequences, pBHG10 was digested with *Spe* I, which cuts at 75.4 mu in Ad5 sequences, and ligated with *Spe* I-digested pFG23K, generating pBHG10A. pFG23K was derived from the Ap^r plasmid pFG23 (30) (not shown), which contains Ad5 sequences from 60 to 100 mu. pFG23 was digested with *Xba* I, which cuts at bp 28,592 in Ad5 sequences (there is no cleavage at bp 30,470 due to Dam methylation in the *E. coli* strain used), and ligated with *Xba* I-digested pKN30 (31), a small Kn^r plasmid, generating pFG23AK (not shown). To remove Ad5 sequences that were not required and the Ap^r gene, pFG23AK was digested with *Afl* II and ligated, generating pFG23K. To remove the repeated sequences (shown between the asterisks), pBHG10A was partially digested with *Nde* I and religated, generating pBHG10B. In the final step, the Kn^r segment was removed from pBHG10B by partial *Xba* I digestion and religation, generating pBHGE3. mu refers to Ad5 sequences, solid bars represent Ad5 sequences, and hatched bars represent Ap^r and Kn^r segments.

deletion does not interfere with the ITR (1–103 bp), the essential core packaging signal (194–358 bp) (3–5), or coding sequences for protein IX, but does remove the Sp1 binding site (3525–3530 bp) from the protein IX promoter. Since the Sp1 binding site is thought to be essential for protein IX expression (32), it was reintroduced as a synthetic oligonucleotide that positioned the Sp1 site 1 bp closer to the protein IX TATA box (Fig. 4). To assess the effect of the 3.2-kb E1 deletion and the reintroduction of the Sp1 binding site on protein IX expression, 293 cells were infected at 10 plaque-forming units per cell with a number of different viruses. These include viruses with no deletion in E1 (wt Ad5), one with a 2.3-kb deletion extending into the protein IX gene (dl313) (33), one with the 3.2-kb deletion described above (dl70-3), and viruses with the 3.2-kb deletion containing the human cytomagalovirus (HCMV) immediate early promoter (AdHCMV) or the human β-actin promoter (AdβAct) in the E1-antiparallel orientation with or without the reintroduced Sp1 binding site. After labeling with [^{35}S]methionine, cell extracts were harvested and samples were immunoprecipitated with anti-Ad2 protein IX antibodies and analyzed by SDS/PAGE. The results (Fig. 5) indicate that variable levels

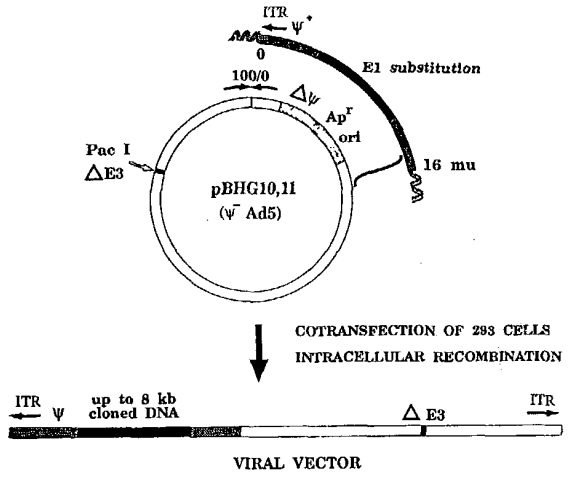

FIG. 3. Rescue using pBHG vectors. The general strategy used for generating infectious viral vectors using the BHG system is illustrated. Cotransfection of 293 cells with pBHG10, pBHG11, pBHGE3, or a pBHG derivative containing a foreign gene inserted in E3 plus a plasmid containing left-end viral sequences including the packaging signals results in the generation of infectious viral vectors by *in vivo* recombination.

of protein IX were expressed depending on the sequences upstream from the protein IX gene. With the reintroduced Sp1 site present, there was at most a 25% reduction compared to wt Ad5. The near-wt levels of protein IX expression obtained with mutant dl70-3 may be explained by sequences from left of the deletion (nt 333–338: GCGCGT, in Ad5 sequences) that fortuitously resemble and may act as an Sp1 site. The detection of reduced but significant levels of protein IX in cells infected by vectors containing only the HCMV or β-actin promoters, which have no potential Sp1 binding sites, suggests that the Sp1 binding site may not be absolutely essential for protein IX expression, in contrast to the findings of Babiss and Vales (32). Because protein IX is known to affect the heat stability of virions, we measured the infectious titers of wt Ad5 compared to dl313, dl70-3, AdHCMV2, AdβAct2, AdHCMVsp1, and AdβActsp1 after incubation at 45°C for 1 and 2 h. Of the six viral mutants tested, only dl313 differed significantly in heat lability from wt (Fig. 6). Even AdβAct2, which produces only 16% of wt levels of protein IX (Fig. 5), was as resistant to heat inactivation as was wt virus, suggesting that protein IX is likely made in excess during wt viral infection. We have also found that viruses containing the 3.2-kb E1 deletion replicate in 293 cells to the same final titers as wt Ad5 (data not shown).

Since the growth characteristics and stability of viruses with the 3.2-kb E1 deletion were not affected, this deletion was incorporated into pΔE1sp1A and pΔE1sp1B for use in cotransfections with the BHG plasmids (Fig. 4).

Testing the Efficiency and Capacity of the pBHG Vectors. To assess the ability of the BHG plasmids to generate infectious viral vectors, cotransfections with various left end plasmids were performed, and the efficiency of rescue was usually comparable to that obtained with pJM17 (20) (data not shown). Although pJM17 has been useful for rescue of E1 mutations or substitutions into infectious virus, because it is derived from dl309 (33), it has neither a wt E3 region nor a useful E3 deletion. Thus pJM17 will be superseded by the pBHG series of plasmids for most Ad5 vector constructions.

Use of pBHGE3, pBHG10, or pBHG11 combined with the 3.2-kb deletion in E1 should permit rescue of inserts of ≈5.2, ≈7.9, and ≈8.3 kb, respectively, into viral vectors. To test the capacity of the BHG system, we constructed an insert of

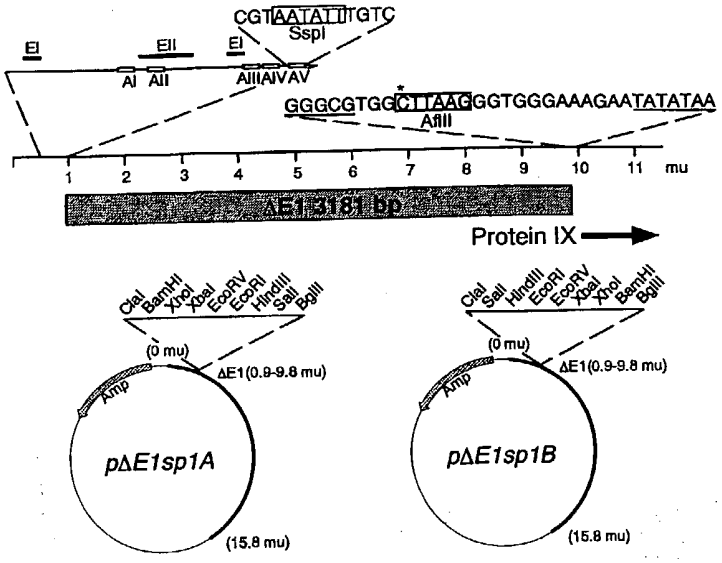

FIG. 4. Left-end shuttle plasmids with a 3.2-kb E1 deletion. The sequences removed by the 3.2-kb deletion are indicated. At the 5′ end of the deletion the region from bp 190 to bp 348 has been expanded to show the position of repeated elements (AI–AV) involved in packaging and the enhancer elements (EI and EII). At the 3′ end of the deletion, the region from bp 3525 to bp 3557 contains the protein IX promoter with the Sp1 binding site and TATA box (underlined). To create the E1 deletion, sequences were removed between the *Ssp* I (bp 339) and *Afl* II (bp 3533) restriction sites (boxed). This deletion does not interfere with the ITR (bp 1–103), the essential core packaging signal (bp 194–358), or coding sequences for protein IX, but does remove the Sp1 binding site (bp 3525–3530), which was subsequently reintroduced 1 bp closer to the protein IX TATA box. Thus the cytidine residue, indicated with the asterisk, is missing in plasmids pΔE1sp1A and pΔE1sp1B. In addition to the modified Sp1 site, plasmid pΔE1sp1A contains Ad5 DNA sequences from bp 1 to bp 341 and bp 3524 to bp 5790 with a polycloning oligonucleotide inserted between Ad5 bp 341 and bp 3524. Plasmid pΔE1sp1B is identical to pΔE1sp1A except that the restriction sites between the *Cla* I and *Bgl* II sites in the polycloning region are reversed.

7.8 kb consisting of the *lacZ* gene driven by the HCMV promoter (E1-antiparallel orientation) and the herpes simplex virus type 1 (HSV-1) *gB* gene driven by the simian virus 40 promoter (E1-parallel orientation) in the 3.2-kb E1 deletion. The 7.8-kb insert was constructed by inserting the 4.1-kb *Xba* I fragment from pgBdX17 (34) containing HSV-1 *gB* gene driven by the simian virus 40 promoter into the *Xba* I site in pHCMVsp1LacZ (35), generating pHlacZgBR (data not shown). After cotransfection of 20 60-mm dishes of 293 cells, 10 with 5 μg of pBHG10 and 5 μg of pHlacZgBR and the other half with 10 μg of each, one plaque was obtained. This plaque was isolated, expanded, analyzed by restriction digest with *Hin*dIII, and found to have the expected restriction pattern. The isolate, AdHlacZgBR, expressed both *lacZ* and HSV-1 *gB* at levels comparable to those obtained with vectors containing single inserts of these genes (data not shown).

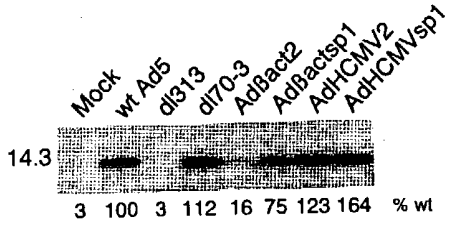

FIG. 5. Immunoprecipitation of protein IX from cells infected with viruses having a 3.2-kb E1 deletion. The levels of protein IX, a minor capsid protein required for the packaging of full-length viral genomes, were compared for wt Ad5 and viruses with a 3.2-kb E1 deletion with and without the reintroduced Sp1 binding site. The 293 cells were mock infected or infected at a multiplicity of infection of 10 with wt Ad5, dl313, dl70-3, AdβAct2, AdβActsp1, AdHCMV2, or AdHCMVsp1 and labeled with [^{35}S]methionine from 22 to 24 h after infection. Cell extracts were prepared and immunoprecipitated with anti-Ad2 protein IX antibodies, and samples were separated by SDS/PAGE. The gel was dried and bands were visualized by autoradiography. The lanes contain the samples indicated above and the molecular mass at 14.3 kDa is indicated on the left. Levels of protein IX were determined by densitometric analysis and are indicated below the samples relative to wt Ad5. dl313 contains a 2.3-kb deletion extending into the protein IX gene and, therefore, makes no protein IX; dl70-3 carries the 3.2-kb E1 deletion; AdβAct2 and AdHCMV2 contain the β-actin and HCMV promoters in the 3.2-kb E1 deletion, respectively; AdβActsp1 and AdHCMVsp1 contain the β-actin and HCMV promoters in the 3.2-kb E1 deletion with the Sp1 binding site reintroduced into the protein IX promoter. The β-actin and HCMV promoters were inserted in the E1-antiparallel orientation.

DISCUSSION

We have constructed and tested a vector system based on a series of bacterial plasmids (pBHG) that contain all the essential Ad5 sequences required to produce infectious virus upon transfection of 293 cells except for the packaging signal (bp 194–358) needed to encapsidate viral DNA. These plasmids are noninfectious in single transfections and must be cotransfected with a second plasmid containing left-end sequences including a packaging signal to generate infectious viral vectors (Fig. 3). This vector system is the most versatile system yet developed for generating Ad5 helper-independent vectors and will allow the construction of vectors with any combination of inserts, mutations, or wt sequences in both E1 and E3. Because with the pBHG system the entire viral genome is propagated as bacterial plasmids, manipulation of

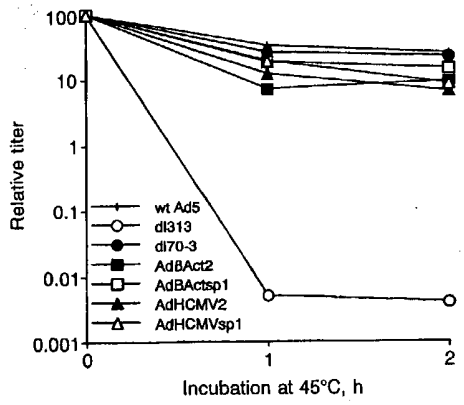

FIG. 6. Heat stability of viruses with the 3.2-kb E1 deletion. The heat stability of viruses with the 3.2-kb E1 deletion, with and without the reintroduced Sp1 binding site in the protein IX promoter, was compared to wt Ad5 and dl313. Viral stocks of wt Ad5, dl313, dl70-3, AdβAct2, AdHCMV2, AdβActsp1, and AdHCMVsp1 were titered on 293 cells prior to and after incubation for 1 and 2 h at 45°C. The structure of these viruses is explained in Fig. 5. The data presented for wt Ad5 and dl70-3 represent the average of four experiments and the data for dl313, AdβAct2, AdHCMV2, AdβActsp1, and AdHCMVsp1 represent the average of three experiments.

viral DNA sequences can be done rapidly and efficiently. To illustrate this and to generate two useful variants, we constructed pBHGE3 and pBHG11 from the original plasmid pBHG10. pBHGE3 permits construction of vectors with wt E3 sequences (Fig. 2), and pBHG11 increased the cloning capacity of resulting viral vectors. The 2.69-kb E3 deletion in pBHG10 removes the major portions of all E3 mRNAs, the first E3 3′ splice acceptor site, and the L4 polyadenylylation site but leaves the E3 promoter, the 5′ initiation site, the first E3 5′ splice donor site, and the E3b polyadenylylation site intact (36). Viruses with the 2.69-kb E3 deletion have the same growth kinetics and progeny virus yields as wt virus (7). The 3.1-kb E3 deletion in pBHG11 removes two additional elements not removed by the 2.69-kb E3 deletion: the first E3 5′ splice donor site and the E3b polyadenylylation site (36). This deletion does not interfere with the open reading frame for pVIII or any of the L5 family of mRNAs. Viruses containing the 3.1-kb deletion were found to give wt progeny yields in infected 293 cells (data not shown).

To maximize the capacity of the BHG system and to facilitate the introduction of inserts into the E1 region, we have constructed plasmids containing a 3.2-kb deletion of E1 sequences and multiple restriction sites for the insertion of foreign genes (Fig. 4*B*). This deletion leaves intact the left ITR and packaging signals and extends just past the Sp1 binding site of the protein IX promoter. The promoter for transcription of the protein IX gene is relatively simple, consisting of this Sp1 binding site and a TATA box. It has been reported that the Sp1 binding site is essential for expression of protein IX (32) and it was, therefore, reintroduced at a position 1 bp closer to the TATA box than in the wt promoter. However, neither the original 3.2-kb E1 deletion nor the deletion mutants containing the synthetic Sp1 site appeared to be significantly altered in protein IX expression (Fig. 5), heat stability (Fig. 6), or final progeny yields of viruses with this deletion. Although we did see a reduction in protein IX expression to ≈16% of wt levels for the virus containing the β-actin promoter combined with the 3.2-kb E1 deletion, even this level of expression appeared to be adequate for the formation of stable virions.

The Ad5 packaging signal, which overlaps the E1A enhancer region, has been found to consist of at least five AT-rich elements, which, by extensive mutational analysis, have been found to be functionally redundant (Fig. 4) (3–5). The E1A enhancer is composed of two functionally distinct enhancer elements, I and II (2, 37). Two repeats of enhancer element I flank element II and are responsible for regulating expression from the E1A gene (2). Enhancer element II regulates the transcription of all the early regions in the genome (37). The 3.2-kb E1 deletion does not interfere with the enhancer region but does remove the 3′ most packaging element. The removal of this element has been shown to have little or no effect on packaging (3–5) and should not, therefore, affect the packaging of recombinants that utilize the 3.2-kb E1 deletion.

One observation made when testing the BHG system was that the larger the insert being rescued in the E1 region the lower the efficiency of rescue. Although we have not systematically investigated the relationship between insert size and efficiency of recombination between cotransfected plasmids, we have observed that longer segments of foreign DNA seem to be more difficult to rescue into infectious virus than small inserts. This could be due to the inhibitory effect of heterologous sequences on recombination in agreement with the observations of Munz and Young (38).

When using pBHGE3, pBHG10, or pBHG11 in combination with the 3.2-kb deletion in E1, it should be possible to rescue inserts of up to 5.2, 7.9, and 8.3 kb, respectively, in conditional helper-independent vectors. To test the capacity of the system, we used pBHG10 to rescue a 7.8-kb insert consisting of the HSV-1 *gB* gene and *lacZ* gene in tandem, each with its own promoter. The vector obtained, AdHlacZgBR, was found to replicate efficiently and to express both *lacZ* and HSV-1 *gB* at levels comparable to that obtained with Ad vectors containing single inserts of these genes. The pBHG system has now been in use in our laboratory for ≈1 year and has facilitated the rescue of a variety of genes into E1 and E3. This vector system should have wide applications for the construction of Ad vectors for use as recombinant viral vaccines and for gene therapy transfer vectors.

We thank J. Rudy for excellent technical assistance and W. Russell for his generous donation of Ad2 protein IX antibody. This work was supported by grants from the Natural Sciences and Engineering Research Council, the Medical Research Council, and the National Cancer Institute of Canada. F.L.G. is a Terry Fox Research Scientist of the National Cancer Institute and A.J.B. was a Natural Sciences and Engineering Research Council postgraduate scholarship recipient and currently holds an Ontario Graduate Scholarship.

1. Graham, F. L., Smiley, J., Russell, W. C. & Nairn, R. (1977) *J. Gen. Virol.* **36**, 59–72.
2. Hearing, P. & Shenk, T. (1983) *Cell* **33**, 695–703.
3. Hearing, P., Samulski, R. J., Wishart, W. L. & Shenk, T. (1987) *J. Virol.* **61**, 2555–2558.
4. Grable, M. & Hearing, P. (1990) *J. Virol.* **64**, 2047–2056.
5. Grable, M. & Hearing, P. (1992) *J. Virol.* **64**, 723–731.
6. Ghosh-Choudhury, G., Haj-Ahmad, Y. & Graham, F. L. (1987) *EMBO J.* **6**, 1733–1739.
7. Bett, A. J., Prevec, L. & Graham, F. L. (1993) *J. Virol.* **67**, 5911–5921.
8. Berkner, K. L. (1992) *Curr. Top. Microbiol. Immunol.* **158**, 39–66.
9. Graham, F. L. & Prevec, L. (1992) in *Vaccines: New Approaches to Immunological Problems*, ed. Ellis, R. W. (Butterworth-Heinemann, Boston), pp. 363–390.
10. Graham, F. L. (1984) *EMBO J.* **3**, 2917–2922.
11. Berkner, K. L. & Sharp, P. A. (1983) *Nucleic Acids Res.* **11**, 6003–6020.
12. Haj-Ahmad, Y. & Graham, F. L. (1986) *J. Virol.* **57**, 267–274.
13. Sambrook, J., Fritsch, E. F. & Maniatis, T. (1989) *Molecular Cloning: A Laboratory Manual* (Cold Spring Harbor Lab. Press, Plainview, NY), 2nd Ed.
14. Dower, W. J., Miller, J. F. & Ragsdale, C. W. (1988) *Nucleic Acids Res.* **16**, 6127–6145.
15. Birnboim, H. C. & Doly, J. (1978) *Nucleic Acids Res.* **7**, 1513–1523.
16. Graham, F. L. & Prevec, L. (1991) in *Methods in Molecular Biology*, ed. Murray, E. J. (Humana, Clifton, NJ), Vol. 7, pp. 109–128.
17. Graham, F. L. & Van der Eb, A. J. (1973) *Virology* **52**, 456–467.
18. Mittal, S. K., McDermott, M. R., Johnson, D. C., Prevec, L. & Graham, F. L. (1993) *Virus Res.* **28**, 67–90.
19. Ruben, M., Bacchetti, S. & Graham, F. L. (1983) *Nature (London)* **301**, 172–174.
20. McGrory, W. J., Bautista, D. S. & Graham, F. L. (1988) *Virology* **163**, 614–617.
21. Ghosh-Choudhury, G., Haj-Ahmad, Y., Brinkley, P., Rudy, J. & Graham, F. L. (1986) *Gene* **50**, 161–171.
22. Daniell, E. (1976) *J. Virol.* **19**, 685–708.
23. Tibbetts, C. (1977) *Cell* **17**, 243–249.
24. Hammarskjold, M.-L. & Winberg, G. (1980) *Cell* **20**, 787–795.
25. Bautista, D. S., Hitt, M., McGrory, J. & Graham, F. L. (1991) *Virology* **182**, 578–596.
26. Bautista, D. S. & Graham, F. L. (1989) *Gene* **82**, 201–208.
27. Haj-Ahmad, Y. (1986) Ph.D. thesis (McMaster Univ., Hamilton, ON).
28. Lilly, D. M. J. (1981) *Nature (London)* **292**, 380–382.
29. Leach, D. R. F. & Stahl, F. W. (1983) *Nature (London)* **305**, 448–451.
30. McKinnon, R. D., Bacchetti, S. & Graham, F. L. (1982) *Gene* **19**, 33–42.
31. Lee, F. (1989) Ph.D. thesis (McMaster Univ., Hamilton, ON).
32. Babiss, L. E. & Vales, L. D. (1991) *J. Virol.* **65**, 598–605.
33. Jones, N. & Shenk, T. (1979) *Cell* **17**, 683–689.
34. Johnson, D. C., Ghosh-Choudhury, G., Smiley, J. R., Fallis, L. & Graham, F. L. (1988) *Virology* **164**, 1–14.
35. Morsey, M. A., Alford, E. L., Bett, A., Graham, F. L. & Caskey, C. T. (1993) *J. Clin. Invest.* **92**, 1580–1586.
36. Cladaras, C. & Wold, W. S. M. (1985) *Virology* **140**, 28–43.
37. Hearing, P. & Shenk, T. (1986) *Cell* **45**, 229–236.
38. Munz, P. L. & Young, C. S. H. (1984) *Virology* **135**, 503–514.

STIC-ILL

From: Vogel, Nancy
Sent: Thursday, December 09, 2004 2:09 PM
To: STIC-ILL
Subject: refs for 10/045,116 (references from lost parent case 09/033,555)

Please send me the following:

Proc. Natl. Acad. Sci. USA (1 989) 86:4574-4578

Virol. 1997 227:239-244

Virolo 1994 202:695-706

Virolo 1993 193:631-641

Genes and Dev. 1988 2:453-461

Nucleic Acid Research 1983 11 17 :6003-6020 .

Proc. Natl. Acad. Sci. USA 1994 91:8802-8806
J Virolo l 993 67 10 :591 1-592 1

Anticancer Res. 1997 17:1471-1505

J Immunol. 1988 141 6 :2084-2089

J Virol. 1989 63 2 :631-638

Science 1989 244:1288-1292

Chang et al. Cancer Gene therapy Using Novel Tumor specific Replication Competent Adenovirus Vectors" Cold Spring Harbor Gene Thera Meeting Sept. 1996

Nucleic Acids Res. 1996 24 12 :2318-2323

Current Protocols in Molecular Biology
Ausubel et al., eds., 1987 , Supp. 30, section 7.7.18 Table 7.7.1

Nature (1989) 337:387-388

Advances in Virus Research 1986 31: 169-228

Biochem. Biophys. Acta 1982 651:175-208

Mol. Cell. Biol. 1989 9 (9) :41 5-42

J Virol. 1997 71 (1) :548-561

EMBO J 1984 3 (12) :2917-2922

J Genetic Virolo 1977 68:937-940

1973 Virolo 52:456-467

1987 J Gen. Virol 36:59-72

Biochem. J. 1987 241:25-38

Hallenbeck, P.L. et a1., Novel Tumor Specific Replication Competent Adenoviral Vectors for Gene Therapy of Cancer" abstract no. 0-36 Cancer Gene Thera 1996) 3 (6) :S19-S20.

J. Biol. Chem. 1995 270 (8) :3602-3610 .
J Biol. Chem. 1994 269 (39) :23872-23875
Adv. Dru Delive Rev. 1995 17:279-292

2318–2323 Nucleic Acids Research, 1996, Vol. 24, No. 12

Stabilization of triple-stranded oligonucleotide complexes: use of probes containing alternating phosphodiester and stereo-uniform cationic phosphoramidate linkages

Surendra Chaturvedi+, Thomas Horn[1] and Robert L. Letsinger*

Department of Chemistry, Northwestern University, Evanston, IL 60208, USA and [1]Nucleic Acids Systems, Chiron Corporation, Emeryville, CA 94608, USA

Received March 4, 1996; Revised and Accepted April 30, 1996

ABSTRACT

Pyrimidine oligonucleotides containing alternating anionic and stereo-uniform cationic *N*-(dimethylaminopropyl)phosphoramidate linkages [e.g. d(T+T–)$_7$T, d(T+T–)$_2$(T+C–)$_5$T and (U′+U′–)$_7$dT, where U′ is 2′-*O*-methyluridine)] are shown to bind to complementary double-stranded DNA segments in 0.1 M NaCl at pH 7 to form triple-stranded complexes with the pyrimidine.purine.pyrimidine motif. For each of the sequences investigated, one stereoisomer bound with higher affinity, and the other stereoisomer with lower affinity, than the corresponding all-phosphodiester oligonucleotide. The stereoisomer of d(T+T–)$_7$T that interacted weakly with a dT.dA target in 0.1 M NaCl formed a novel dA.dA.dT triple-stranded complex with poly(dA) or d(A$_{15}$C$_4$A$_{15}$) in 1 M NaCl; in contrast, the stereoisomer that bound strongly to the dT.dA target failed to form a dA.dA.dT triple-stranded complex.

INTRODUCTION

Current research on triple-stranded polynucleotides has been stimulated by a general interest in molecular recognition and by the potential applications for triple-stranded complexes in processing DNA chemically (1) and in modulating biological processes dependent on DNA (2). Two major structural motifs for these complexes have been recognized. One, designated pyr.pur.pyr, involves binding a pyrimidine oligonucleotide to a duplex segment, with the added pyrimidine strand oriented parallel to the purine strand of the duplex (3,4). In the other motif, pur.pur.pyr (5), a purine oligonucleotide binds to a duplex such that the two purine strands are antiparallel (6–8). Since formation of a triplex brings three polyanionic strands into proximity, the stability of these complexes is very dependent on salt concentration. High salt concentrations (e.g. 1.0 M NaCl) favor triplex formation. In 0.1 M NaCl at pH 7 triplexes containing a moderate size oligonucleotide (e.g. 15mer) have low stability.

Recently we reported that an oligonucleotide containing alternating phosphodiester and stereo-uniform cationic *N*-(dimethylaminopropyl)phosphoramidate linkages, d(T+T–)$_7$T, binds to poly(dA) and poly(A) targets with unusually high affinity in low salt solutions (9). Under the same conditions, the binding affinity of the stereoisomer with opposite chirality at the phosphoramidate linkages is very low. These findings suggest that a zwitterionic oligonucleotide with appropriate stereochemistry at the P–N internucleoside linkages might serve as a superior probe for double-stranded DNA sequences in solutions of low ionic strength, as in biological media. We report here the results of a study to test this possibility. The zwitterionic probes and the targets investigated are listed in Chart 1, where '**a**' represents the stereoisomer with the upfield, and '**b**' the isomer with the downfield, signal in the ^{31}P NMR spectrum for the phosphoramidate groups. The symbol '+' signifies a protonated [3′-OP(O)(NHCH$_2$CH$_2$CH$_2$NMe$_2$)-O-5′] internucleoside link; '–', a phosphodiester link; and U′, a 2′-*O*-methyluridine unit in an oligonucleotide. For comparison, the all-phosphodiester probes dT$_{15}$, U′$_{14}$dT and d[T$_4$(TC)$_5$T] were also prepared.

Probes		Targets	
d(T+T–)$_7$T	(U′+U′–)$_7$dT	d(T$_{15}$C$_4$A$_{15}$),	d(A$_{15}$C$_4$A$_{15}$), Poly(dA)
1a and **1b**	**2a** and **2b**	**4**	**5**
d(T+T–)$_2$(T+C–)$_5$T		d[A$_5$(GA)$_5$T$_4$(TC)$_5$T$_5$]	
3a and **3b**		**6**	

Chart 1.

MATERIALS AND METHODS

General methods

Reagents grade chemicals were used throughout. Pyridine, DMF and CH$_3$CN were dried over calcium hydride. THF was freshly distilled over sodium/benzophenone prior to use. 5′-*O*-Dimethoxytritylthymidine (5′-O-DMT-dT) was purchased from Chem Impex, IL, and 5′-*O*-dimethoxytrityl-2′-*O*-methyluridine was purchased from Monomer Sciences (Huntsville, AL). Column chromatography was performed on silica gel (70–230 mesh, 60 A; Aldrich). Reversed phase (RP) HPLC was carried out on a Supelco LC-18 column (25 cm × 4.6 mm) with a 0–50% gradient (2%/min) of CH$_3$CN in 5% CH$_3$CN in 0.1 M TEAA buffer, pH

*To whom correspondence should be addressed

+Present address: Chemsyn Science Laboratory, Lenexa, KS 66215-1297, USA

7.5; flow rate 1 ml/min or on a Dionex chromatograph with a Hewlett Packard Hypersil ODS-5 column (4.6 × 200 mm) using a 1%/min gradient of CH_3CN in 30 mM triethylammonium acetate buffer at pH 7.0 with a flow rate of 1 ml/min. A Dionex DX 500 chromatograph system equipped with a P40 gradient pump, an AD 20 absorbance detector, and a NucleoPack PA-100 column (4 × 250 mm) was used for ion-exchange (IE) chromatography. The eluant was 10 mM aqueous NaOH, and a 2%/min gradient of 1.0 M NaCl in 10 mM NaOH was used with a flow rate of 1.5 ml/min. TLC was performed using Whatman analytical silica gel plates (60 Å) or Merck Silica Gel 60 F_{254} precoated TLC aluminum plates. The TLC plates were prerun in 8% CH_3OH/2%TEA/CH_2Cl_2, then spotted and developed in the same system.

Circular dichroism (CD) measurements were carried out on a Hitachi Joel 500 instrument. Temperature was controlled with a refrigerated water bath, and nitrogen was continuously circulated through the cuvette compartments. Melting curves were determined using either a Varian Cary 3E UV-Visible spectrophotometer or a Perkin Elmer Lambda 2 UV spectrophotometer equipped with a Peltier 2 temperature programmer for automatically increasing the temperature at the rate of 0.5°C/min. Unless stated otherwise, dissociation curves and CD spectra were obtained in a 0.1 M NaCl, 10 mM phosphate buffer at pH 7.0 with each oligomer 3.3 μM for the T_m measurements and 1.7 μM for the CD spectra. Concentrations were calculated using ε = 8.1 and 8.4 A_{260} U/μmol of residue for dT_{15} and poly(dA), respectively. The extinction coefficients for the mixed oligomers were calculated using a formula based on nearest neighbors (18). The ^{31}P NMR spectra were run in CH_3CN (dimer blocks) or D_2O (oligomers) with d_6 DMSO for a lock and aq. 85% H_3PO_4 as an external reference. Ion-spray MS (ESI) measurements were run by Dr Frank Masiarz at Chiron on a Perkin-Elmer PE SCIEX API III electrospray quadrupole instrument. LSI MS were obtained by Dr Doris Hung at Northwestern University on a VG 70SE instrument.

Protected dinucleotide derivatives

3′-*O*-*t*-Butyldimethylsilylthymidine, dT(TBDMS), (10.4 mmol) was treated with 5′-*O*-dimethoxytritylthymidine-3′-*O*-(methyl *N,N*-diisopropylphosphoramidite) (10 mmol) in 50 ml dry CH_3CN containing 20 mmol tetrazole. The reaction was complete after stirring for 5 min at room temperature, as indicated by TLC (silica gel; 5% MeOH and 1% Et_3N in CH_2Cl_2); the triester product migrated slightly faster than dT(3′-*O*-TBDMS). The reaction mixture was diluted with CH_2Cl_2 and extracted with 400 ml 5% aq. $NaHCO_3$/NaCl. The organic layer was dried (Na_2SO_4) and concentrated under reduced pressure. After coevaporation of the residue with several portions of dry toluene, the triester was dissolved in 100 ml dry CH_3CN and treated with 3-dimethylaminopropylamine (10 ml, 16 mmol), followed by dropwise addition of iodine (2.53 g, 10 mmol) in 50 ml dry CH_3CN (11). After 30 min, the reaction mixture was poured into 300 ml 5% aqueous sodium bisulfite and extracted with CH_2Cl_2. The organic layer was washed repeatedly with 5% aq. $NaHCO_3$ and sat. NaCl, then dried (Na_2SO_4) and concentrated under reduced pressure. The resulting diastereomers of d(DMT)T+T(TBDMS) (7.7 g, 7.4 mmol) were separated by silica gel chromatography as the 'fast' and the 'slow' eluting isomers using a 2–6% MeOH gradient in 2% Et_3N in CH_2Cl_2: 'fast isomer', **a**, 2.9 g (29%), Rf 0.62, ^{31}P NMR 10.4 p.p.m., ESI MS, MW calcd for $C_{52}H_{71}N_6O_{13}PSi$ 1047.2, found 1046.6; 'slow isomer', **b**, 3.1 g (30%), Rf 0.40, ^{31}P NMR 10.6 p.p.m., ESI MS, MW calcd 1047.2, found 1046.9. The middle fraction containing both isomers amounted to 1.7 g (16%). Efforts to separate the two isomers after, rather than before, desilylation were unsuccessful.

The amidate dinucleotide block d(DMT)T+C^{Bz}(TBDMS) was prepared from 5′-*O*-dimethoxytritythymidine-3′-*O*-(methyl *N,N*-diisopropylphosphoramidite) and dC^{Bz}(3′-*O*-TBDMS) on a 20 mmol scale essentially as described above for the preparation of (DMT)T+T(TBDMS). Separation of the stereoisomers by silica gel chromatography yielded, **a**, 1.78 g (8%), Rf 0.75, ^{31}P NMR 10.4 p.p.m., and **b**, 1.94 g (8.5%), Rf 0.60, ^{31}P NMR 10.6 p.p.m. The 2′-*O*-methyluridine derivatives, (DMT)U′+U′ (TBDMS), were obtained in the same way: **a**, 1.66 g (16%), Rf 0.50, ^{31}P NMR 10.6 p.p.m., ESI MS, MW calcd for $C_{52}H_{71}N_6O_{15}PSi$ 1079.2, found 1078.6; **b**, 1.94 (19%), Rf 0.39, ^{31}P NMR 11.1 p.p.m.; ESI MS calcd MW 1079.2, found 1078.6.

Desilylation of dimer derivatives

Desilylation of the 'fast isomer', **a**, of d(DMT)T+T(TBDMS) (0.7 mmol) was effected by treatment with tetrabutylammonium fluoride (3.5 mmol) in dry CH_3CN (20 ml) for 3 h. After dilution with CH_2Cl_2 and washing with water (2 × 200 ml), the organic layer was dried (Na_2SO_4) and evaporated under reduced pressure. Purification by silica gel chromatography using a 0–18% gradient of MeOH in 2% Et_3N in CH_2Cl_2 afforded d(DMT)T+T (isomer **a**) as a white solid: 0.57 g (80%), ^{31}P NMR 10.4 p.p.m., ESI MS, MW calcd for $C_{46}H_{57}N_6O_{13}P$ 933.0, found 933.3. Desilylation of the 'slow isomer' was achieved in a similar fashion and gave a comparable yield of the diastereomeric dimer block, **b**: ^{31}P NMR 10.6 p.p.m., ESI MS, MW calcd. 933.0, found 933.5.

The other dimer blocks were desilylated in the same way. The % yield and ^{31}P NMR shifts for the products were: d(DMT)T+C^{Bz}, isomer **a**, 77%, 10.4 p.p.m.; isomer **b**, 75%, 10.6 p.p.m.; (DMT)U′+U′ isomer **a**, 82%, 10.6 p.p.m.; isomer **b**, 56%, 11.1 p.p.m.

Phosphoramidites of dinucleotide derivatives

(DMT)T+T isomer **a** (0.61 g, 0.57 mmol) in 5 ml dry of CH_2Cl_2 and 0.75 ml (6.5 mmol) of diisopropylethylamine was treated with 1.5 eq. of 2-cyanoethyl *N,N*-diisopropylchlorophosphoramidite (Cl-BCE) at room temperature. The reaction was complete in 3 h as indicated by TLC (8% MeOH in 2% Et_3N in CH_2Cl_2). After dilution with CH_2Cl_2 (200 ml), the organic layer was washed successively with 250 ml 5% aq. $NaHCO_3$ and 250 ml sat. NaCl. The organic layer was dried (Na_2SO_4) and concentrated under reduced pressure. Chromatography on silica gel afforded the phosphoramidite derivative as a white solid: 0.52 g (79%); ^{31}P NMR, 150.0 and 149.7 p.p.m. (stereoisomeric phosphoramidite groups) and 10.4 p.p.m. (internucleoside phosphoramidate group) (the ratio of the integrated areas for the phosphoramidite/phosphoramidate peaks was 1/1); LSI MS, MW calcd 1133.2, found 1133. Isomer **b** was prepared similarly: ^{31}P NMR, 150.0, 149.7 and 10.6 p.p.m. (phosphoramidite/phosphoramidate, 1/1).

The other phosphoramidite dinucleotide blocks were prepared in the same manner, except that for the 2′-*O*-methyluridine derivatives 2.2 equiv. of 2-cyanoethyl *N,N*,-diisopropylphosphoramidite was used and the phosphitilation reaction was allowed to proceed for 18 h. Each exhibited signals for phosphoramidite and phosphoramidate in a 1/1 ratio. The yields (%) and ^{31}P

signals (p.p.m.) were: DMT(T+C^{Bz})BCE **a**, 68% and 150.1, 149.7, 10.56, 10.47 p.p.m.; **b**, 68% and 150.1, 149.7, 10.86, 10.80 p.p.m.; DMT(U′+U′)BCE **a**, 95% and 151.9, 151.5, 10.7, 10.6 p.p.m.; **b**, 95% and 151.8, 151.3, 11.1 p.p.m.

Zwitterionic oligonucleotides

Dimer blocks were used to synthesize pentadecanucleotide derivatives by conventional phosphoramidite chemistry using cyanoethyl phosphoramidite reagents as previously described (9). The RP-HPLC elution times in minutes for oligomers with the DMT group 'on', and the DMT group 'off', were, respectively: **1a**, 19.8, 11.6; **1b**, 19.3, 11.4; **2a**, 19.0, 11.2; **2b**, 18.3, 10.8; **3a**, 19.0, 9.6; **3b**, 18.3, 9.4. The ^{31}P NMR (D_2O solvent, DMT 'off') δ values in p.p.m. were: **1a**, 9.0 (phosphoramidate) and –2.2 (phosphodiester), area ratio, 1/1; **1b**, 9.35, –2.2 (plus a minor peak at –2.0), phosphoramidate/phosphodiester, 1/1. The spectra of the other oligomers were similar (solvent, 1:5 H_2O/D_2O): **2a**, 8.95 and –2.4 (ratio, 1/1); **2b**, 9.8 and –2.4 (ratio 1/1); **3a**, 8.95 and –2.3 (ratio 1/1); **3b**, 9.2 and –2.3 (ratio 1/1).

RESULTS

The stereo-uniform zwitterionic oligomers, **1a**, **1b**, **2a**, **2b**, **3a** and **3b**, were prepared by a general procedure outlined previously (9) which utilized sequential coupling of stereo-uniform dimer blocks on a solid support. The key intermediates were the fully protected dinucleotide phosphoramidate derivatives blocks represented by formula I. These compounds were separated into the component stereoisomers by chromatography on silica gel. Subsequent removal of the silyl protecting group and phosphitilation afforded the phosphoramidite reagents employed in the polymer synthesis. Comparison of properties of **1a,b**, **2a,b** and **3a,b** to properties of oligonucleotide analogues containing aminoethylphosphonate (12), uncharged phosphormorpholidate (13–15) and methyl phosphonate (16,17) linkages suggests that, for a given pair of stereoisomers in our series, the compound exhibiting the greater upfield shift in the ^{31}P NMR spectrum for the amidate P, and designated here as '**a**', probably has the R configuration. In each case the compounds in the '**a**' series came from the stereoisomer of the fully protected dimer block that eluted first on silica gel chromatography.

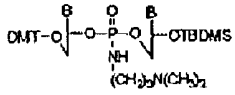

Pyr·Pur·Pyr triple strands

We used d($T_{15}C_4A_{15}$), **4**, to test for hybridization of thymidine and 2′-*O*-methyluridine zwitterionic derivatives to a duplex target. In absence of other oligomers, **4** forms a self-complementary structure with a dT.dA stem of high stability (T_m 62°C in 0.1 M NaCl and 78°C in 1 M NaCl). We found that the affinities of the oligothymidylate derivatives for this target depend strongly on the charge and stereochemistry of the probe and the ionic strength of the solution (Table 1). Of special interest was the observation that *one of the zwitterionic isomers, 1a, formed a relatively stable triple-stranded complex with target 4 even in 0.1 M NaCl.* The melting curve for an equimolar mixture of **1a** and **4** showed a transition (T_m 24°C) for dissociation of the zwitterionic strand from the duplex segment, as well as a transition (T_m 68°C) for

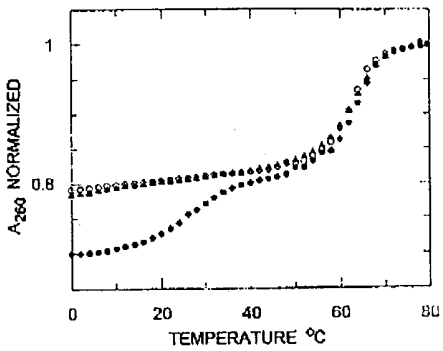

Figure 1. Normalized melting curves for d($T_{15}C_4A_{15}$) (3.3 μM) with: **1a** (●), or **1b** (▲) or dT_{15} (○); 3.3 μM each, in 0.1 M NaCl, pH 7.0.

denaturation of **4** (Fig. 1); and a plot of A_{260} *versus* titrant for titration of **1a** with **4** at 0°C displayed a break at equimolar concentrations of the two oligomers (data not shown), in accord for a complex with the dT.dA.dT motif. Under the same conditions, neither dT_{15} nor the zwitterionic isomeric oligomer (**1b**) interacted significantly with **4** (Fig. 1). In a high salt solution (1.0 M NaCl) dT_{15} did bind to **4** (T_m 30°C). The stability of the complex formed by **1a** also increased with an increase in the salt concentration (T_m 32°C in 1.0 M NaCl); however, the rise in T_m was less than in the case of the all anionic probe. Oligomer **1b** did not bind significantly to **4** even in 1 M NaCl.

Table 1. T_m values (°C) for dissociation of triple-stranded complexes formed from single-stranded probes and target **4**, d($T_{15}C_4A_{15}$), 3.3 μM each at pH 7.0

Probe	0.1 M NaCl	1.0 M
d(T+T–)$_7$T, **1a**	24	32
d(T+T–)$_7$T, **1b**	<0	<5
dT_{15}	<0	30
(U′+U′–)$_7$dT, **2a**	35	42
(U′+U–)$_7$dT, **2b**	–	<10
U′$_{14}$dT	<5	40
d(T+T–)$_2$(T+C–)$_5$T, **3a**	<0	<5

It has been shown that replacement of thymidine by 2′-*O*-methyluridine in a phosphodiester oligonucleotide probe enhances stability of triple-stranded complexes formed with the probe (18). The stereoisomeric oligomers **2a** and **2b** were prepared to test the effect of this substitution on binding of *zwitterionic* oligonucleotides to double-stranded targets. We found that one of the 2′-*O*-methyluridine analogues, **2a**, indeed bound to **4** more effectively (T_m 35°C, 0.1 M NaCl) than the thymidine analogue, **1a**, (T_m 24°C, 0.1 M NaCl). Neither the isomeric oligomer, **2b**, nor the corresponding phosphodiester control, U′$_{14}$dT, interacted significantly with **4** under these conditions. In contrast to the results for the triple-stranded complexes, the 2′-*O*-methyluridine derivative, **2a**, was found to bind less effectively than the thymidine analogue, **1a**, to an equivalent of poly(dA). The T_m values for formation of the double-stranded complex in 0, 0.1 and 1.0 M NaCl solutions were, respectively: 35, 36 and 41°C for **2a**;

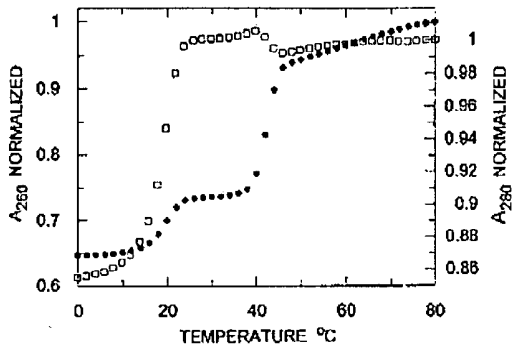

Figure 2. Melting curves for poly(dA) with **1b** at equivalent nucleotide concentrations (50 μM in dT and 50 μM in dA), 1.0 M NaCl, pH 7.0, followed at 260 nm (●) (left ordinate) or at 280 nm (□) (right ordinate).

and 58, 58 and 58°C for **1a** (see reference 9 for experiments with the dT oligonucleotides).

Data for the mixed dT,dC oligomers (**3a** and **3b**) are presented in Table 2. Target **6**, $d[A_5(GA)_5T_4(TC)_5T_5]$, self-associates under the conditions employed (T_m 68°C at pH 7.0 and 67°C at pH 6.0; 0.1 M NaCl). The dT,dC pentadecamers bound to **6** with higher affinity than the dT or dU' pentadecamers bound to **4**, and, as expected for triple-stranded structures containing dC (5), the affinity was greater at pH 6 than at pH 7. A striking feature was the thermal stability of the triple-stranded complex formed by one of the zwitterionic probes, **3a**, and target **6** in a low salt solution (0.1 M NaCl) at pH 7. The T_m value was 23°C higher than that for the complex formed by the corresponding all-phosphodiester probe. That the high affinity of the zwitterionic oligonucleotides depends on sequence as well as ionic charge and stereochemistry at phosphorus was demonstrated by experiments in which **1a** was paired with a mismatched target, **6**, and **3a** was similarly paired with **4**. Neither of these systems afforded stable-triple stranded complexes (Tables 1 and 2).

Table 2. T_m values (°C) for dissociation of triple-stranded complexes formed from single-stranded probes and target **6**, $d[A_5(GA)_5T_4(TC)_5T_5]$, each 5 μM in 0.1 M NaCl

Probe	pH 7.0	pH 6.0
$d(T+T-)_2(T+C-)_5T$, **3a**	42	52
$d(T+T-)_2(T+C-)_5T$, **3b**	11	37
$dT_5(CT)_5$	19	45
$d(T+T-)_7T$, **1a**	<0[a]	

[a]Also <0°C in 1.0 M NaCl.

dA.dA.dT triple strands

We previously noted an unusual feature in the melting curve obtained at 260 nm for a 1/1 dT/dA mixture of **1b** and poly(dA) in 1 M NaCl solution (9). The melting curve showed two transitions, differing in T_m by ~20°C. On the basis of further work we now propose that the first transition stems from a reversible disproportionation of two **1b**.poly(dA) duplex segments to give a triplex with the dA.dA.dT motif plus a strand of **1b**, and that the second transition represents reversible dissociation of the triplex to give free poly(dA) and **1b**. Several lines of evidence support this conclusion. (i) Melting curves for this system are given in Figure 2. Two transitions appear in the curve measured at 280 nm as well as the one at 260 nm. An unusual feature, however, is that the higher temperature transition in the 280 nm curve is hypochromic. Characteristically, transitions for dissociation of dT.dA duplexes and dT.dA.dT triplexes are hyperchromic at this wavelengths. This results points to dissociation of a complex with a novel structure. (ii) Melting curves obtained in low salt solutions (0–0.1 M NaCl) showed a single transition (~T_m 22°C) that was independent of the salt concentration. As the salt concentration was increased incrementally, a second transition appeared at progressively higher temperatures. The salt dependence for the second transition is consistent with expectations for dissociation of a triple-stranded complex containing a zwitterionic and two anionic strands. (iii) Association curves obtained by cooling solutions of the oligomers slowly from 80 to 0°C demonstrated that the transitions are fully reversible. As a further test, a 1dT/1dA mixture of **1b** and poly(dA) in 1 M NaCl was allowed to cool from 80 to 25°C and held at the lower temperature for 2 h to permit a slow equilibration to take place. No change in absorbance occurred during the 2 h, indicating that the system was stable at this temperature. When the temperature was then further reduced through the range for the lower transition to 18°C, the absorbance at 260 nm dropped rapidly and equilibrium was reached within 2 min. (iv) A single transition (T_m 42°C; 1 M NaCl) was observed on heating a mixture of **1b** and poly(dA) at a 1dT/2dA nucleotide ratio from 0 to 80°C, demonstrating that the triple-stranded complex was stable at 0°C in absence of excess **1b**. (v) In agreement with these results, titration of **1b** in 1 M NaCl (pH 7.0) with poly(dA) consumed twice as much poly(dA) at 30°C as at 0°C, and the breaks corresponded to formation of a 1dT/2dA complex at 30°C and a 1dT/1dA complex at 0°C. As controls, dT_{15} was also titrated with poly(dA) under the same conditions. These experiments showed breaks corresponding to 2dT/1dA, 1dT/1dA and 1dT/1dA, as expected, for titrations at 0°C in 1.0 M NaCl, 30°C in 1.0 M NaCl and 0°C in 0.1 M NaCl, respectively. Also, titration of **1b** at 0°C in 0.1 M NaCl gave a 1dT/1dA ratio. (vi) A single transition (T_m 26°C) was found on heating a mixture of **1b** with either one or two equivalents of $d(CCA_{15}CC)$ in 1.0 M NaCl. This result suggested that appearance of the second transition in the case of poly(dA) might be related to the fact poly(dA) could fold to a hairpin structure that would stabilize a dA.dA.dT triple-stranded complex. We therefore examined hybridization of **1b** with a shorter, well defined oligomer, $d(A_{15}C_4A_{15})$, which also could fold to a hairpin structure. This target indeed simulated poly(dA) in behavior, although the complexes formed were somewhat less stable (T_m ~ 17°C for the disproportionation reaction and ~32°C for dissociation of the triplex in 1.0 M NaCl; see Fig. 3). A comparison with the heating curve for $d(A_{15}C_4A_{15})$ alone (curve B in Fig. 3) shows that these breaks indeed reflect interaction of **1b** with this target oligonucleotide. As in the case with poly(dA), the transitions were reversible.

Formation of two distinct complexes from **1b** and poly(dA) is further supported by CD spectral data. The spectrum for a mixture of **1b** and poly(dA) containing equivalent concentrations of dT and dA units in 1 M NaCl at 5°C is given in Figure 4, curve A. It is very similar to the CD spectrum for the same combination of

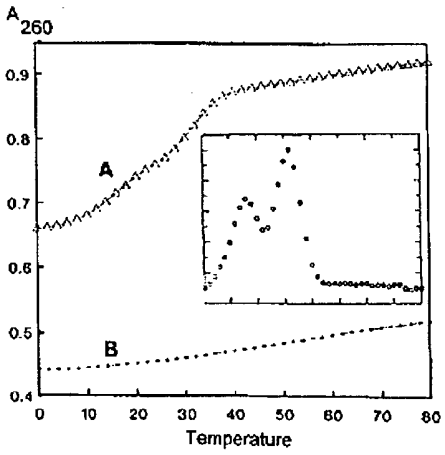

Figure 3. (**A**) Melting curve for $d(A_{15}C_4A_{15})$ (3.3 μM) with **1b** (3.3 μM), 1.0 M NaCl, pH 7.0; inset, the derivative curve. (**B**) Melting curve for $d(A_{15}C_4A_{15})$ (3.3 μM) alone under the same conditions.

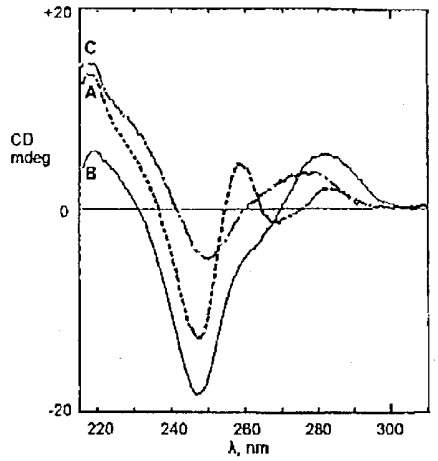

Figure 4. CD spectra for poly(dA) with **1b** at equivalent nucleotide concentrations in 1.0 M NaCl at pH 7.0: curve A, at 0°C (—), and curve B, at 27 °C (—). Curve C is the sum of the spectra of separate samples of poly(dA) and **1b** at 27°C (— - —).

1b and poly(dA) in 0.1 M NaCl and for the spectra of poly(dT).poly(dA) in 0.1 M and in 1 M NaCl. The two peaks and the trough in the 255–300 nm region are distinctive (19) and serve as a signature for the poly(dT).poly(dA) duplex. The similarity in the spectra for all these systems indicates that the base stacking is much the same in all cases. These data therefore point to a conventional duplex structure for the complex derived from **1b** and poly(dA) in 1 M NaCl at 5°C. A very different spectrum (Fig. 4, curve B) was obtained when the solution of **1b** and poly(dA) was warmed to 27°C. The trough at 247 nm deepened, the peak at 259 nm fell, the trough at 268 nm disappeared, and the peak at 282 nm increased. When the solution was then cooled, spectrum B readily reverted to spectrum A. These changes correlate well with the UV absorbance changes observed on heating and cooling the solution. Furthermore, spectrum B is quite different from the spectrum expected for a mixture of free **1b** and poly(dA) (Fig. 4, curve C). We attribute spectrum B to the presence of a dA.dA.dT triple stranded complex derived from poly(dA) and **1b**. This assignment leads to the prediction that the CD spectrum of a 2dA/1dT ratio of poly(dA) and **1b** in 1 M NaCl at 27°C would be similar to spectrum B and that it would remain unchanged on cooling to 5°C. These results were indeed observed.

The CD spectrum for a 1dT/1dA mixture of oligomer **1a** and poly(dA) in 1 M NaCl at 27°C is very similar to the spectrum of the poly(dT).poly(dA) duplex (data not shown). In contrast to the case with **1b**, no evidence for formation of a dA.dA.dT triplex was found. The CD spectrum was virtually unchanged on cooling to 5°C and was not altered significantly by addition of a second equivalent of poly(dA). These results buttress data from the melting curves indicating that **1a** forms a duplex, but not a dA.dA.dT triplex, with poly(dA).

DISCUSSION

Pyr.Pur.Pyr triple strands

Three pairs of stereoisomeric zwitterionic 15mers were prepared for this study. Pair **1** was derived from thymidine, pair **2** from 2′-*O*-methyluridine and pair **3** from thymidine and deoxycytidine. In each case, all phosphoramidate linkages in a given oligomer had the same configuration. Thermal denaturation experiments showed that participation of these alternating cationic–anionic oligonucleotides in formation of triple-stranded complexes is highly dependent on chirality at the modified phosphate linkages.

The most significant finding with respect to potential applications is that in each case one of the stereoisomeric probes, designated as the '**a**' isomer, binds more effectively to a complementary double-stranded DNA target than the corresponding all phosphodiester probe does. In 0.1 M aqueous NaCl at pH 7, the enhancement in T_m is of the order of 20°C for the dT and the dT,dC zwitterionic 15mers (**1a** and **3a**) and ~35°C for the 2′-*O*-methyluridine derivative (**2a**). The enhancement in T_m in 1 M NaCl solutions is less, but still significant. It is noteworthy that the affinity of **3a** is relatively high at pH 7, even though the probe contains several dC units. Strong binding of this unsymmetrical, mixed base probe to the double-stranded target is consistent with a structure in which the third strand is oriented parallel to the purine strand, as in other triple-stranded complexes derived from two pyrimidine and one purine strand.

In contrast to the results with the '**a**' stereoisomeric oligomers, the phosphoramidate oligomers with the opposite configuration at phosphorus ('**b**') exhibited very low affinity for the double-stranded targets. Since the absolute configuration of the isomers has not yet been definitively assigned, and structural information on the geometry of the triple strand complex is limited, speculation on the reasons for these differences is premature. It is interesting, however, that the configuration at the phosphoramidate links that favors binding of an oligonucleotide probe to double-stranded DNA is the same that favors binding to a single-stranded target to give a double-stranded complex (9).

Gryaznov *et al.* have shown that oligodeoxyribonucleotide N3′–P5′ phosphoramidate derivatives bind to DNA duplexes to give unusually stable pyr.pur.pyr and pur.pur.pyr complexes (20,21), and Nielsen *et al.* have found that 'peptide nucleic acids' (PNAs) interact with appropriate DNA sequences by strand

invasion to give PNA.pur.PNA triple-stranded segments (22–24). The stereo-uniform cationic phosphoramidate derivatives comprise another family of oligonucleotide analogues that bind strongly to double-stranded DNA targets. Since these three families differ from one another in physical and chemical properties and, no doubt, in behavior in biological systems as well, they offer the chemist rich opportunities for tailoring DNA binding agents for specific applications.

dA.dA.dT triple strands

A surprising set of equilibria was found for systems containing $d(T+T-)_7T$ isomer **1b** and poly(dA) or $d(A_{15}C_4A_{15})$ in 1 M NaCl solution. A model consistent with the data is indicated schematically in Chart 2 for a system containing **1b** and poly(dA) in a 1dT/1dA ratio. According to this, at 0°C the components form a double-stranded complex; at 30°C they exist as a dA.dA.dT triple-stranded complex and an equivalent of free **1b**; and at 50°C the complex is fully dissociated. The transitions between the states are relatively sharp (T_m 22 and 42°C) and equilibrium is established rapidly both on heating and cooling the solution. The system involving $d(A_{15}C_4A_{15})$ fits the same scheme, but with a dC_4 strand serving as the linker to facilitate alignment of two dA_{15} segments. The importance of the configuration of the phosphoramidate linkages is shown by the fact that oligomer **1a**, in contrast to **1b**, did not form triple stranded complexes of this type.

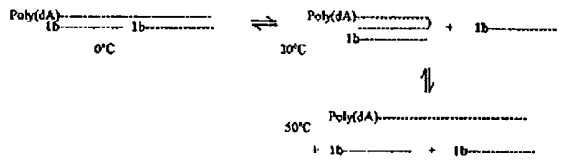

Chart 2.

Two features in these equations are unusual, though not without some related precedents: (i) formation of a stable triple-stranded complex containing exclusively dA.dA.dT triads, and (ii) formation of a triple-stranded complex by a thermally induced disproportionation of a double-stranded complex. Although a number of examples of pur.pur.pyr triplexes have been reported (see 5–8 for representative cases), the stable complexes containing dA.dA.dT triads that have been described have also contained dG units in one of the purine strands. Pilch *et al.* have noted that "...the presence of guanine residues appears to be crucial for stabilization of short pur.pur.pyr triplexes" (8). For the ribonucleotide family, however, Broitman *et al.* have described a triple-stranded complex, poly(A).poly(A).poly(U), which can form when the degree of polymerization of poly(A) falls in the range of ~28–150 (25), and Lauceri *et al.* (26) have shown that cationic porphyrins in low concentration induce formation of poly(A).poly(A).poly(U) triple-stranded complexes from high molecular weight poly(A) (>400 bp). With respect to thermally induced disproportions, examples affording pyr.pur.pyr complexes have been reported for both ribonucleotide, [poly(A).poly(U)] (27,28,25), and deoxyribonucleotide polymers, [poly(dTdC).poly(dGdA)] (29–31).

We conclude that the unusual stability of the dA.dA.dT complexes containing oligonucleotide **1b**, and the disproportionation reaction leading to their formation, must reflect the presence of the stereo-uniform side chains in the probe. The properties of zwitterionic oligomers with this chirality may prove useful in designing novel self-assembly systems based on oligonucleotide hybridization.

ACKNOWLEDGMENTS

The research at Northwestern University was supported by a research grant from the Chiron Corp. We thank Dr Paul Loach for use of the CD spectrophotometer.

REFERENCES

1 Moser,H.E. and Dervan,P.B. (1987) *Science*, **238**, 645–650.
2 Maher,L.J., Wold,B. and Dervan,P.B. (1989) *Science*, **245**, 725–745.
3 Felsenfeld,G., Davies,D.R. and Rich,A. (1957) *J. Am. Chem. Soc.* **79**, 2023.
4 Arnott,S. and Selsing,E. (1974) *J. Mol. Biol.* **88**, 509–521.
5 Lipsett,M.N. (1964) *J. Biol. Chem.* **239**, 1256–1260.
6 Cooney,M., Czernuszewicz,G., Postel,E.H., Flint,J. and Hogan,M.E. (1989) *Science*, **241**, 456–459.
7 Beal,P.A. and Dervan,P.B. (1992) *Nucleic Acids Res.* **20**, 2773–2776.
8 Pilch,D.S., Levenson,C. and Shafer,R.H. (1991) *Biochemistry*, **30**, 6081–6087.
9 Horn,T., Chaturvedi,S., Balasubramaniam,T.N. and Letsinger,R.L. (1996) *Tetrahedron Lett.*, **37**, 743–746.
10 Fasman,G. (ed.) (1975) *Handbook of Biochemistry and Molecular Biology, 3rd Ed.*, CRC Press, Cleveland, OH, p. 589.
11 Jäger,A., Levy,M.J. and Hecht,S.M. (1988) *Biochemistry*, **27**, 7237–7246.
12 Fathi,R., Huang,Q., Coppola,G., Delaney,W., Teasdale,S., Krieg,A.M. and Cook,A.F. (1994) *Nucleic Acids Res.*, **22**, 55416–55424.
13 Ozaki,H., Yamana,K. and Shimidzu,T. (1989) *Tetrahedron Lett.* 30, 5899–5902.
14 Ozaki,H., Masanori,K., Yamana,K., Murakami,A. and Shimidzu,T. (1990) *Bull. Chem. Soc. Jpn*, **63**, 1929–1926.
15 Wilk,A., Uznanski,B. and Stec,W.J. (1991) *Nucleosides Nucleotides*, **10**, 319–322.
16 Loschner,T. and Engels,J.W. (1990) *Nucleic Acids Res.*, **18**, 5083–5088.
17 Seela,F. and Kretchmer,U. (1991) *J. Org. Chem.*, **56**, 3861–3868.
18 Escude,C., Sun,J.-S., Rougee,M., Garestier,T. and Hélène,C. (1992) *C.R. Acad. Sci. Paris III*, **315**, 521–525.
19 Wells,R.D., Larson,J.E., Grant,R.C., Shortle,B.E. and Cantor,C.R. (1970) *J. Mol. Biol.* **54**, 465–497.
20 Gryaznov,S. and Chen,J.-K. (1994) *J. Am. Chem. Soc.* **116**, 3143–3144.
21 Gryaznov,S.M., Lloyd,D.H., Chen, J.-K., Schultz,R.G., DeDionisio,L.A., Ratmeyer,L. and Wilson,W.D. (1995) *Proc. Natl. Acad. Sci. USA*, **92**, 5798–5802.
22 Nielsen,P.E., Egholm,M.; Berg,R.H. and Buchardt,O. (1991) *Science*, **254**, 1497–1500.
23 Chemy,D.Y., Belotserkovskii,B.P., Frank-Kamenetskii, MD., Egholm,M., Buchardt,O., Berg, R.H. and Nielsen,P.E. (1993) *Proc. Natl. Acad. Sci. USA*, **90**, 1667–1670.
24 Nielsen,P.E., Egholm,M., Berg,R.H. and Buchardt,O. (1993) *Nucleic Acids Res.*, **21**, 197–200.
25 Broitman,S.L., Im,D.D. and Fresco,J.R. (1987) *Proc. Natl. Acad. Sci. USA*, **84**, 5120–5124.
26 Lauceri,R., Campagna,T., Contino,A. and Purrello,R. (1996) *Angew. Chem. Int. Ed. Engl.*, **35**, 215–216.
27 Miles,H.T. and Frazier,J. *Biochem. Biophys. Res. Comm.* (1964) **14**, 129–136.
28 Stevens,C.L. and Felsenfeld,G. (1964) *Biopolymers*, **2**, 293–314.
29 Lee,J.S., Johnson,D.A. and Morgan,A.R. (1979) *Nucleic Acids Res.* **6**, 3073–3091.
30 Lee,J.S., Woodsworth,M.L., Latimer,L.J.P. and Morgan,A.R. (1984) *Nucleic Acids Res.* **12**, 6603–6613.
31 Hampel,K.J., Crosson,P. and Lee,J.S. (1991) *Biochemistry*, **30**, 4455–4459.

STIC-ILL

From: Vogel, Nancy
Sent: Thursday, December 09, 2004 2:09 PM
To: STIC-ILL
Subject: refs for 10/045,116 (references from lost parent case 09/033,555)

Please send me the following:

Proc. Natl. Acad. Sci. USA (1 989) 86:4574-4578

Virol. 1997 227:239-244

Virolo 1994 202:695-706

Virolo 1993 193:631-641

Genes and Dev. 1988 2:453-461

Nucleic Acid Research 1983 11 17 :6003-6020 .

Proc. Natl. Acad. Sci. USA 1994 91:8802-8806
J Virolo I 993 67 10 :591 1-592 1

Anticancer Res. 1997 17:1471-1505

J Immunol. 1988 141 6 :2084-2089

J Virol. 1989 63 2 :631-638

Science 1989 244:1288-1292

Chang et al. Cancer Gene therapy Using Novel Tumor specific Replication Competent Adenovirus Vectors" Cold Spring Harbor Gene Thera Meeting Sept. 1996

Nucleic Acids Res. 1996 24 12 :2318-2323

Current Protocols in Molecular Biology
Ausubel et al., eds., 1987 , Supp. 30, section 7.7.18 Table 7.7.1

Nature (1989) 337:387-388

Advances in Virus Research 1986 31: 169-228

Biochem. Biophys. Acta 1982 651:175-208

Mol. Cell. Biol. 1989 9 (9) :41 5-42

J Virol. 1997 71 (1) :548-561

EMBO J 1984 3 (12) :2917-2922

J Genetic Virolo 1977 68:937-940

1973 Virolo 52:456-467

1987 J Gen. Virol 36:59-72

Biochem. J. 1987 241:25-38

Hallenbeck, P.L. et a1., Novel Tumor Specific Replication Competent Adenoviral Vectors for Gene Therapy of Cancer" abstract no. 0-36 Cancer Gene Thera 1996) 3 (6) :S19-S20.

J. Biol. Chem. 1995 270 (8) :3602-3610 .
J Biol. Chem. 1994 269 (39) :23872-23875
Adv. Dru Delive Rev. 1995 17:279-292

JOURNAL OF VIROLOGY, Jan. 1997, p. 548–561
0022-538X/97/$04.00+0

Vol. 71, No. 1

The Early Region 1B 55-Kilodalton Oncoprotein of Adenovirus Relieves Growth Restrictions Imposed on Viral Replication by the Cell Cycle

FELICIA D. GOODRUM[1] AND DAVID A. ORNELLES[1,2]*

Molecular Genetics Program[1] and Department of Microbiology and Immunology,[2] Bowman Gray School of Medicine, Wake Forest University, Winston-Salem, North Carolina 27157-1064

Received 23 July 1996/Accepted 20 September 1996

The E1B 55-kDa oncoprotein of adenovirus enables the virus to overcome restrictions imposed on viral replication by the cell cycle. Approximately 20% of HeLa cells infected with an E1B 55-kDa mutant adenovirus produced virus when evaluated by electron microscopy or by assays for infectious centers. By contrast, all HeLa cells infected with a wild-type adenovirus produced virus. The yield of E1B mutant virus from randomly cycling HeLa cells correlated with the fraction of cells in S phase at the time of infection. In synchronously growing HeLa cells, approximately 75% of the cells infected during S phase with the E1B mutant virus produced virus, whereas only 10% of the cells infected during G_1 produced virus. The yield of E1B mutant virus from HeLa cells infected during S phase was sevenfold greater than that of cells infected during G_1 and threefold greater than that of cells infected during asynchronous growth. Cells infected during S phase with the E1B mutant virus exhibited severe cytopathic effects, whereas cells infected with the E1B mutant virus during G_1 exhibited a mild cytopathic effect. Viral DNA synthesis appeared independent of the cell cycle because equivalent amounts of viral DNA were synthesized in cells infected with either wild-type or E1B mutant virus. The inability of the E1B mutant virus to replicate was not mediated by the status of p53. These results define a novel property of the large tumor antigen of adenovirus in relieving growth restrictions imposed on viral replication by the cell cycle.

Adenovirus (Ad) encodes proteins that deregulate normal cellular growth to the advantage of viral replication (reviewed in references 7 and 67). The oncoproteins of Ad are encoded within the early regions 1A (the E1A 12S and 13S proteins) and 1B (the E1B 55-kDa and 19-kDa proteins). The E1A proteins have been shown to deregulate the cell cycle and induce cellular DNA synthesis by binding cellular regulatory proteins such as pRb and p300 (reviewed in reference 17). Less is known about the function of the large tumor antigen of Ad, the E1B 55-kDa protein, during the lytic infection and during cellular transformation or how these functions are linked (61, 69).

During the late stage of a lytic infection, the E1B 55-kDa protein, in complex with the E4 34-kDa protein, preferentially facilitates the transport of viral mRNA while impeding the transport of cellular mRNA (4, 8, 23, 36, 45). Consequently, Ad mutants that fail to express the E1B 55-kDa protein are defective for expression of viral late proteins. The defect in mRNA transport lies at an intranuclear step after mRNA synthesis but before translocation through the nuclear pore complex (36, 45). The E1B 55-kDa protein has also been demonstrated to directly inhibit host protein synthesis by mechanisms unrelated to the inhibition of mRNA transport (3).

Alone, the E1B 55-kDa protein has no transforming activity (64). However, the E1B 55-kDa and E1B 19-kDa proteins cooperate with the E1A proteins to fully transform nonpermissive cells (6, 18, 20, 54). The E1B 55-kDa protein contributes to transformation by inactivating the cellular tumor suppressor p53 (73). This inhibition of p53-mediated transactivation is required for transformation by both the weakly oncogenic group C and highly oncogenic group A Ad (30, 72, 74, 75). In addition, the E1B gene products have been shown to cooperate with E1A proteins to down regulate p53-driven expression of cyclin D1, which is required for cells to progress through the G_1 phase of the cell cycle (60). Also in cooperation with E1A proteins, the E1B 55-kDa protein stimulates cellular DNA synthesis in nonpermissive cells (50). Thus, in cooperation with other viral proteins, the E1B 55-kDa protein appears to promote a favorable cellular environment for the transformation of nonpermissive cells.

A potential role for the E1B 55-kDa protein in deregulating the cell cycle during the lytic infection has been examined in the work presented here. Ad mutants that fail to express the E1B 55-kDa protein replicated poorly, producing approximately 35-fold fewer progeny virions than a wild-type virus. Although each HeLa cell was infected, only 20% of the cells in an infected population produced progeny E1B mutant virus. However, as many as 75% of the HeLa cells infected with the E1B 55-kDa mutant virus during S phase produced virus, whereas only 10% of cells infected with the same virus during G_1 produced virus. Cell populations infected during S phase also produced higher titers of the E1B 55-kDa mutant virus than cells infected during G_1. These results suggest that the E1B 55-kDa protein functions directly in overcoming the growth restrictions imposed on viral replication by the cell cycle.

MATERIALS AND METHODS

Cell culture. Cell culture media, cell culture supplements, and serum were obtained from Life Technologies (Gibco/BRL, Gaithersburg, Md.) through the Tissue Culture Core Laboratory of the Comprehensive Cancer Center of Wake Forest University. HeLa (ATCC CCL 2, Rockville, Md.), A549 (ATCC CCL 185), and 293 (ATCC CRL 1573) cells were maintained as monolayers in Dulbecco-modified Eagle's minimal essential medium (DMEM) supplemented with 10% newborn calf serum (CS), 100 U of penicillin, and 100 μg of streptomycin per ml. Saos-2 (ATCC HTB 85) cells were maintained as monolayers in DMEM supplemented with 5% fetal bovine serum (FBS), 100 U of penicillin, and 100 μg

* Corresponding author. Mailing address: Department of Microbiology and Immunology, Bowman Gray School of Medicine of Wake Forest University, Winston-Salem, NC 27157-1064. Phone: (910) 716-9332. Fax: (910) 716-9928. E-mail: ornelles@mgrp.bgsm.edu.

of streptomycin per ml. NCI-H460 (ATCC HTB 117) and NCI-H358 (ATCC CTL 5807) were purchased from the American Type Culture Collection (Rockville, Md.) and maintained in antibiotic-free RPMI 1640 supplemented with 10% FBS and essential amino acids. Cells were maintained in subconfluent adherent cultures in a 5% CO_2 atmosphere at 37°C by passing twice weekly at a 1:10 dilution. Cells were preserved in liquid nitrogen in 93% FBS and 7% dimethyl sulfoxide.

Synchronization of the HeLa cell cycle was achieved by a combination of mitotic detachment and hydroxyurea block modified from previously described methods (11). HeLa cells were passaged 1:5 into 75-cm^2 flasks for synchronization 16 to 24 h prior to the mitotic detachment. All but 5 ml of growth media was removed, and the flasks were tapped sharply five times on each of the three flat sides. The detached cells were resuspended in DMEM + 10% CS + 2 mM hydroxyurea (Sigma, St. Louis, Mo.), replated at 2×10^5 cells per ml, and incubated at 37°C in a 5% CO_2 atmosphere. After 1 h, the medium and nonadherent cells were replaced with fresh DMEM + 10% CS + 2 mM hydroxyurea and incubated for 11 h at 37°C in a 5% CO_2 atmosphere. At the completion of the incubation with hydroxyurea, the cells were washed twice with warm phosphate-buffered saline (PBS) (137 mM NaCl, 3 mM KCl, 1.76 mM KH_2PO_4, 10 mM $NaHPO_4$) and the last wash was replaced with normal growth medium to release the G1/S block.

Viruses. The phenotypically wild-type Ad type 5, *dl*309 (26), used in these studies served as the parent virus to the mutant viruses containing a large deletion in the gene encoding the E1B 55-kDa protein, *dl*338 (45), or the E1B 19-kDa protein, *dl*337 (44). The E1B 55-kDa mutant virus, *dl*1520D, has been described previously (6). The propagation of these viruses has been described elsewhere (26). In brief, virus stocks were prepared by infecting 293 cells at a multiplicity of infection of 1 to 3. Virus was harvested 3 days after infection from a concentrated freeze-thaw lysate by sequential centrifugation in discontinuous and equilibrium cesium chloride gradients (25). The gradient-purified virus was supplemented with 5 volumes of 12 mM HEPES (pH 7.4), 120 mM NaCl, 0.1 mg of bovine serum albumin (fraction V; Life Technologies Inc.) per ml, 50% glycerol (Fisher Scientific, Pittsburgh, Pa.) and stored at −20°C. The titers of *dl*309 (8×10^9 PFU per ml) and *dl*338 (2.5×10^9 PFU per ml) were determined by plaque assays using 293 cells as previously described (25).

For infection with Ad, cells were passaged 16 to 24 h prior to infection to achieve approximately 40% confluence at the time of infection. Cells were washed twice with PBS, and the final wash was replaced with virus (5 to 10 PFU per cell) in Ad infection medium (PBS supplemented with 0.2 mM $CaCl_2$, 0.2 mM $MgCl_2$, 2% CS, 100 U of penicillin, and 100 μg of streptomycin per ml). The virus was added at one-fourth the normal culture volume, and the cells were gently rocked for 60 to 90 min at 37°C. The virus suspension was then replaced with normal growth medium, and the infected cells were returned to 37°C.

Electron microscopy. HeLa cells were fixed for transmission electron microscopy with 2.5% glutaraldehyde in PBS + 1.5 mM $MgCl_2$ at 20 h postinfection. The fixed cell pellet was postfixed with osmium tetroxide in phosphate buffer and dehydrated in a graded series in alcohol. Specimens were infiltrated with Spurr's resin-propylene oxide and cut into approximately 100-nm-thick sections with a diamond knife. Sections were collected on copper grids and stained with uranyl acetate and lead citrate and analyzed at 80 keV with a Philips 400 transmission electron microscope. Specimens were embedded and sectioned by MicroMed, the Electron Microscopy Core Laboratory of the Comprehensive Cancer Center of Wake Forest University.

Indirect immunofluorescence. Indirect immunofluorescence and photomicroscopy of whole cells was performed as described previously (43). For staining the Ad E2A 72-kDa DNA-binding protein, the E2A 72-kDa-specific monoclonal antibody (clone B6-8) (51) was used as hybridoma cell medium diluted 1:2 in Tris-buffered saline (137 mM NaCl, 3 mM KCl, 25 mM Tris-Cl [pH 8.0], 1.5 mM $MgCl_2$, 0.5% bovine serum albumin, 0.1% glycine, 0.05% Tween 20, 0.02% sodium azide). The primary antibody was visualized with fluorescein-conjugated goat antibodies specific for mouse immunoglobulin G (Jackson Immunoresearch, West Grove, Pa.). Cells were examined and photographed by epifluorescence with a Leitz Dialux 20 EB microscope.

Plaque assay for infectious centers. The percentage of cells producing virus was determined by a modified plaque assay for infectious centers (34, 58). Either asynchronous or synchronized HeLa cells were passed to 2×10^5 cells per ml 16 to 24 h prior to infection. HeLa cells were infected with 5 to 10 PFU per cell of either the wild-type (*dl*309) or the E1B 55-kDa mutant (*dl*338) virus. The infected cells were incubated with virus for 2 h at 37°C to allow viral attachment and penetration. The virus was removed, and cells were washed twice with PBS. The cells were collected, and the extracellular virus was inactivated by incubation with 0.25% trypsin-EDTA for 10 min at 37°C. The trypsin was neutralized with DMEM + 10% CS. The infected cells were diluted to various cell densities (4,000, 2,000, 1,000, 500, and 250 cells per ml) in DMEM + 10% CS, and 0.1 ml of each cell dilution was added to 0.1 ml of 2.8% agarose type VII (Sigma) in DMEM with 0.6% sodium bicarbonate at 42°C. The cells were gently overlaid onto subconfluent 293 cells plated in 65-mm-diameter dishes. Once the initial agar overlay solidified, cells were overlaid with 0.7% SeaKem ME agarose (FMC, Rockland, Maine) in DMEM with 0.75% sodium bicarbonate and 4% CS. The infected cells were scored as plaques by staining with neutral red on day 9 after infection. The data were analyzed by plotting the number of infectious centers (plaques) obtained versus the number of infected cells plated.

$TCID_{50}$ assay for infectious centers. The percentage of HeLa cells producing virus was statistically determined from a modification of the 50% tissue culture infectious dose ($TCID_{50}$) assay (15). Asynchronous or synchronized HeLa cells were passaged, infected, and harvested 2 h postinfection as previously described for the plaque assay for infectious centers. The infected cells were diluted in growth medium to 1,000, 250, 64, 16, 4, 1, and 0.24 cells per ml, and mock-infected HeLa cells were diluted to 1,000 cells per ml. One-tenth milliliter of each dilution was added to each of 12 wells of a 96-well culture dish, and the infected HeLa cell culture was returned to growth conditions. At 48 h postinfection, the infected HeLa cells were lysed in the 96-well dish by freezing and thawing three times. The entire HeLa cell lysate containing any released progeny virus was transferred onto subconfluent monolayers of 293 cells grown in a 96-well dish. The plate was scored for infected wells 5 days later by evaluating the 293 cell monolayer at low power through an inverted microscope for cytopathic effect. The fraction of infected wells was expressed as a function of the number of infected HeLa cells added to each well, and the data were fit to equation 1:

$$f = \frac{1}{1 + (a/n)^b}$$

where f is the fraction of infected wells and n is the number of cells added per well. The parameters a and b were determined by the method of nonlinear, least squares analysis using MacCurvefit (Kevin Raner Software, Waverley, Australia). When b is fixed at 1, a is the $TCID_{50}$. By assuming a Poisson distribution for the number of infected cells and setting $b = 1$, the number of cells required to obtain an infectious center (virus-producing cell) was determined by solving equation 1 for n when $f = 1/e = 0.632$. The error associated with b after b was forced to 1 was typically ±0.15 and did not exceed ±0.35 for any values presented in Table 1.

Flow cytometry. HeLa cells were detached with trypsin and fixed in 70% ethanol for 1 h to overnight. The ethanol was removed, and the cells were resuspended to approximately 10^6 cells per ml in propidium iodide buffer (100 mM NaCl, 36 mM sodium citrate, 50 μg of propidium iodide per ml, 0.6% Nonidet P-40) supplemented with 0.04 mg of RNase (Sigma) per ml and Nonidet P-40. The cells were filtered through nylon mesh and passed through a 27.5-gauge needle to achieve a single-cell suspension. The DNA content of individual cells was measured by fluorescence-activated cell sorting (FACS) using a Coulter Epics XL flow cytometer (Coulter Corp, Miami, Fla.) with an argon laser as the excitement source (488 nm). The emitted light was analyzed for forward and 90° scatter, pulse width (to discriminate doublets), and red fluorescence (>630 nM) of propidium iodide to determine the DNA content per nucleus. In most cases, 40,000 events were measured in each analysis. The resulting data were acquired in list mode for discriminatory analysis such as the use of standard gating procedures to define distinct populations of cells, doublets, and debris. All flow cytometric analyses were conducted by the Steroid Receptor Laboratory in cooperation with the Hematology Flow Cytometry Laboratory of North Carolina Baptist Hospital.

Plaque assays. Detailed methods for Ad plaque assays have been described elsewhere (25). In brief, virus was harvested from HeLa cells in culture medium 48 to 72 h postinfection by multiple cycles of freezing and thawing. The cell lysates were clarified by centrifugation and serially diluted in infection medium for infection of 293 cells for plaque assays. After incubation with lysates for 1 h, the 293 cells were overlaid with 0.7% SeaKem ME agarose (FMC) in DMEM supplemented with 0.75% sodium bicarbonate and 4% CS. The cells were fed with additional overlays every third day for 7 days. The plaques were visualized by staining with neutral red in an agarose overlay.

DNA slot blot. The DNA slot blotting procedure has been described previously (2, 29) and is briefly described here. Total cellular DNA was isolated from infected HeLa cells. HeLa cells were collected, pelleted, and resuspended in 10 mM Tris, pH 8.0. An equal volume of lysis buffer was added (400 mM Tris-HCl [pH 8.0], 100 mM EDTA, 1% sodium dodecyl sulfate, and 200 μg of proteinase K per ml), and the cells were kept at 50°C for 1 h. DNA was extracted with phenol-chloroform, precipitated, and quantified by spectrophotometry (A_{260}). Equivalent amounts of total cellular DNA were blotted onto Nytran nylon membranes (Schleicher & Schuell, Inc., Keene, N.H.) using a manifold device (Life Technologies, Gaithersburg, Md.) and vacuum. The immobilized DNA was denatured, neutralized, and cross-linked to the matrix with UV light (Stratalinker; Stratgene, La Jolla, Calif.). The DNA was then hybridized with an excess of [α-^{32}P]dATP-labeled (ICN, Costa Mesa, Calif.) DNA probe generated by random-primed synthesis of wild-type Ad DNA (2). Hybridized probe was quantified with the use of a Molecular Dynamics PhosphorImager and ImageQuant analysis software (Molecular Dynamics, Sunnyvale, Calif.).

RESULTS

The E1B 55-kDa mutant Ad produces virions in a subpopulation of infected HeLa cells. Previous work demonstrated that HeLa cells infected with the E1B 55-kDa mutant Ad *dl*338 produce nearly 2 orders of magnitude fewer progeny virus than cells infected with the wild-type Ad, *dl*309 (45). However, not

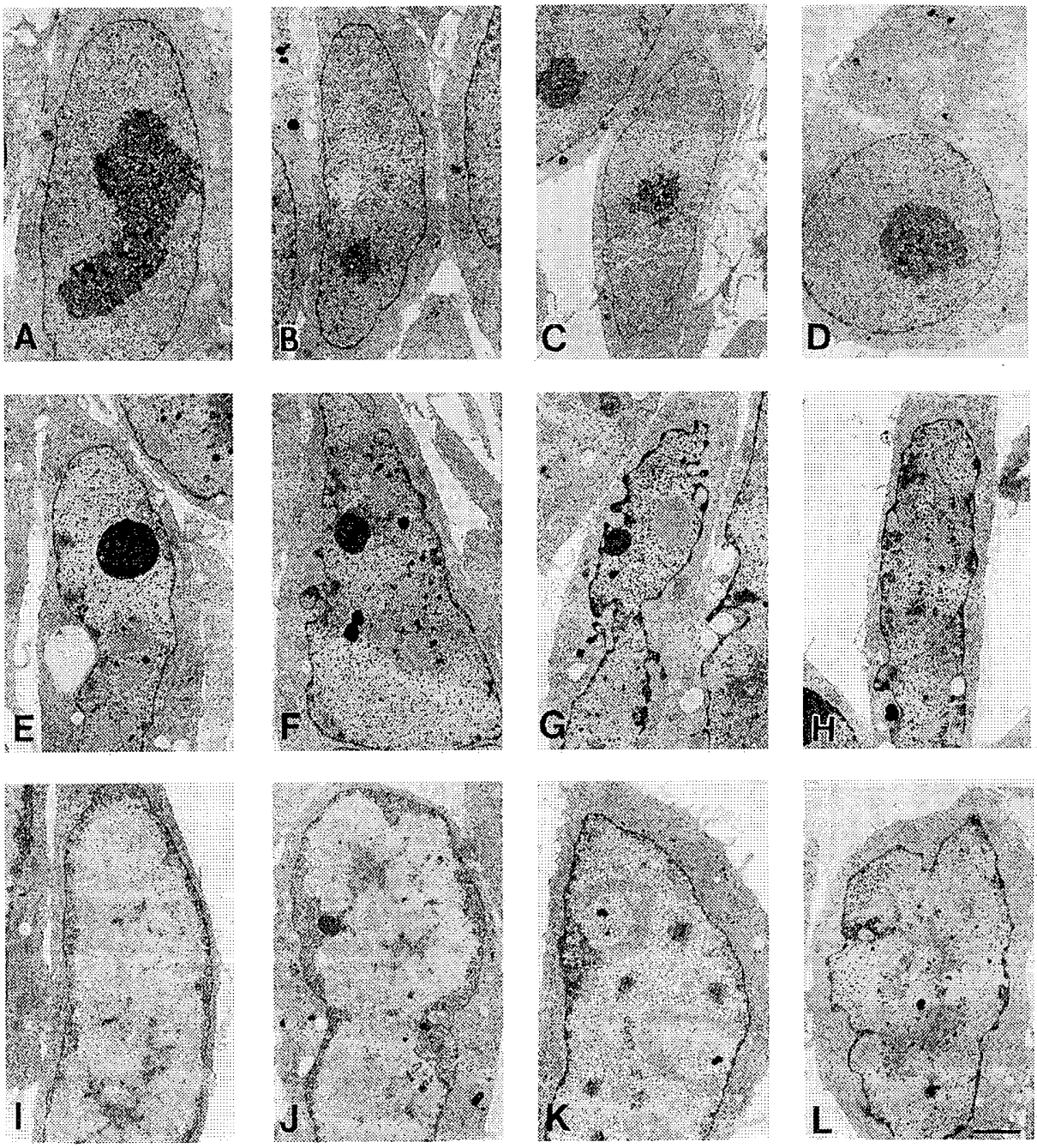

FIG. 1. Only 20% of HeLa cells infected with an E1B 55-kDa mutant virus contain viral particles, whereas all cells infected with a wild-type virus contain viral particles. Monolayers of HeLa cell were mock infected (A to D) or infected with either the wild-type virus, *dl*309 (E to H), or the E1B 55-kDa mutant virus, *dl*338 (I to L), at a multiplicity of 10 PFU per cell. At 20 h postinfection, cells were fixed in 2.5% glutaraldehyde, embedded, and sectioned for transmission electron microscopy. Nearly all (>97%) cells infected with wild-type virus contained electron-dense viral particles in the nucleus by 20 h postinfection. Four representative wild-type virus-infected cells are shown in panels E through H. Of the four representative cells infected with the E1B mutant virus (I to L), only the cell in panel L displays viral particles in the nucleus. All cells shown are representative of each infected population. Bar, 2 μm.

all cells infected with the E1B 55-kDa mutant virus contained progeny viral particles when evaluated by electron microscopy, as shown in Fig. 1. HeLa cells were mock infected or infected with either wild-type or E1B 55-kDa mutant Ad and processed for transmission electron microscopy 20 h after infection. The nuclear structures evident in the mock-infected cells seen in Fig. 1A to D include the nucleolus, cellular chromatin, and granules of chromatin or ribonucleoprotein. In cells infected with wild-type virus, the nuclear membrane has become crenulated, the nucleolus has changed in appearance, and cellular

chromatin has condensed at the periphery of the nucleus. In addition, virus-specific inclusions and virus particles were evident in the nuclei of nearly all cells infected with the wild-type virus (Fig. 1E to H). At the magnification of Fig. 1, the virus particles appear as small, densely stained particles. At higher magnification, the Ad particles are icosahedral in symmetry and are uniform in size and shape (Fig. 2B, inset).

Strikingly, the majority of cells infected with the E1B 55-kDa mutant virus failed to produce any intranuclear viral particles, although all cells contained the characteristic viral nuclear inclusions and displayed crenulated nuclear membranes (Fig. 1I to L). In more than 400 infected cells evaluated by transmission electron microscopy, approximately 20% of the E1B mutant virus-infected population contained virus. Of the four representative cells infected with the E1B 55-kDa mutant virus in Fig. 1I to L, only the cell in panel L contained progeny virus particles. In addition, those E1B 55-kDa mutant virus-infected cells that contained progeny virus particles appeared to contain fewer progeny virions than any wild-type-infected cell examined. Thus, although 20% of the population of E1B mutant virus-infected cells appeared to permit replication of the mutant virus, these cells produced less than a wild-type yield of virus. This result is to be expected because if 20% of the cells (1 in 5) produced E1B mutant virus, each cell would have to produce approximately 20-fold fewer virus particles than those seen in a wild-type virus-infected cell to account for the 100-fold reduced yield compared with cells infected with the wild-type virus.

The cells in Fig. 1K and L, are shown at higher magnification in Fig. 2A and B, respectively. The cell shown in Fig. 2A failed to produce intracellular virus and represents approximately 80% of the E1B 55-kDa mutant virus-infected cell population. The cell seen in Fig. 2B contains intracellular virus that can be seen in the enlarged inset of a representative region of the nucleus. This cell is typical of 20% of the HeLa cells infected with the E1B mutant virus. Except for the paucity of virus particles in the nucleus, the ultrastructural morphology of cells infected with the E1B 55-kDa mutant virus was similar to that of cells infected with the wild-type virus.

Among cells infected with either the E1B 55-kDa mutant or the wild-type virus, all cells appeared to be infected as determined by electron microscopy. During the late phase of infection, the nucleus becomes occupied by clear fibrillar inclusions, referred to here as viral inclusions (Fig. 2, VI). The viral inclusions seen in the electron micrographs indicated a successful infection by either the wild-type or E1B 55-kDa mutant Ad infection. These inclusions were apparent in all infected cells that were examined and can be recognized in the low magnification images of Fig. 1E to L. Mock-infected cell nuclei were devoid of structures resembling viral inclusions (Fig. 1A to D). Viral inclusions have been shown to be the centers of viral DNA synthesis and accumulation (9, 38, 40, 47, 48, 66) and late viral RNA synthesis and processing (38, 40, 46, 49, 70).

An alternative assay using indirect immunofluorescent staining for the Ad E2A 72-kDa DNA-binding protein confirmed that essentially all cells (>99%) were infected with either wild-type or E1B 55-kDa mutant virus under the conditions used in this study. HeLa cells were infected with either the wild-type or the E1B 55-kDa mutant virus at 10 PFU per cell and processed for indirect immunofluorescence at 14 h postinfection. Cell nuclei were visualized by staining with 4,6-diamidino-2-phenylindole (DAPI, Sigma) a nonspecific DNA-binding stain (Fig. 3A and C). The cells were also stained with a monoclonal antibody (B6-8) against the Ad DNA-binding protein that localizes to the viral inclusions late in infection (51). Viral inclusions were visualized as discrete points of fluorescence in the infected cell nucleus. The representative fields of wild-type virus- and E1B mutant virus-infected cells shown in Fig. 3 demonstrate that all cells were infected (compare Fig. 3A with B and C with D). Taken together, the electron microscopic and immunofluorescent analysis indicated that all cells were infected, although not all cells in the E1B 55-kDa mutant virus-infected populations contained intracellular virus.

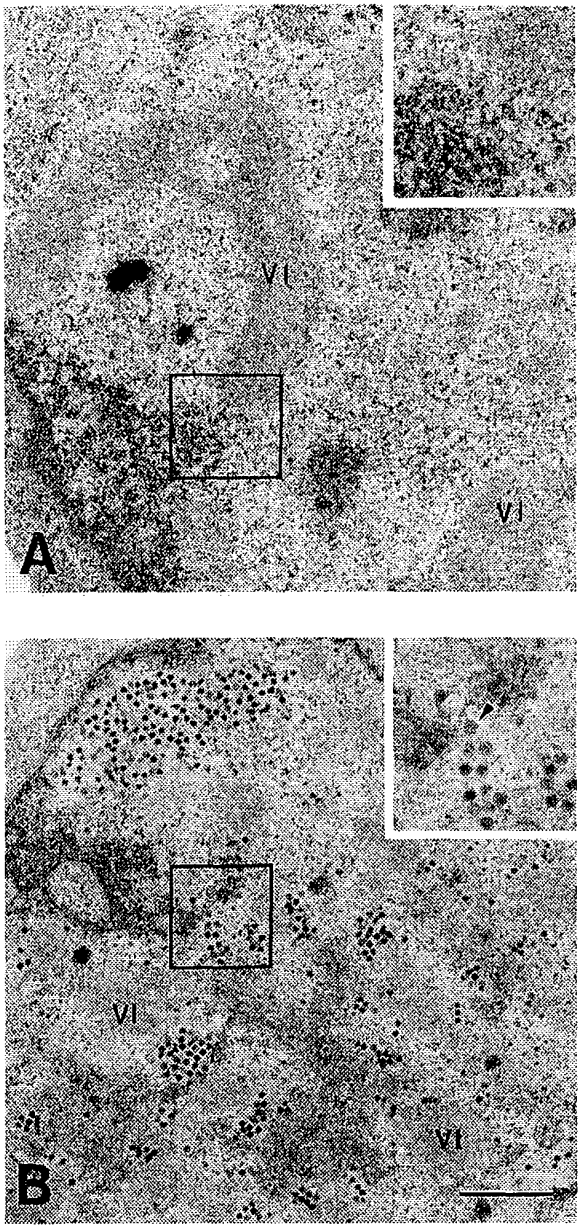

FIG. 2. The E1B 55-kDa mutant virus appears to replicate in only 20% of the infected HeLa cells. The E1B 55-kDa mutant virus-infected cells in panels K and L of Fig. 1 are shown at higher magnification in panels A and B of this figure, respectively. The cell in panel A is representative of approximately 80% of the cells in an E1B 55-kDa mutant virus-infected population. The cell in panel B is representative of 20% of the E1B 55-kDa mutant virus-infected cells. The insets are threefold enlargements of the boxed regions of the nucleus. Adenovirus particles are clearly evident (arrowhead) in the enlarged inset of panel B, whereas no virus particles are apparent in panel A. The presence of viral inclusions (VI) in nearly all cells examined indicates that all cells were infected. Bar, 1 μm.

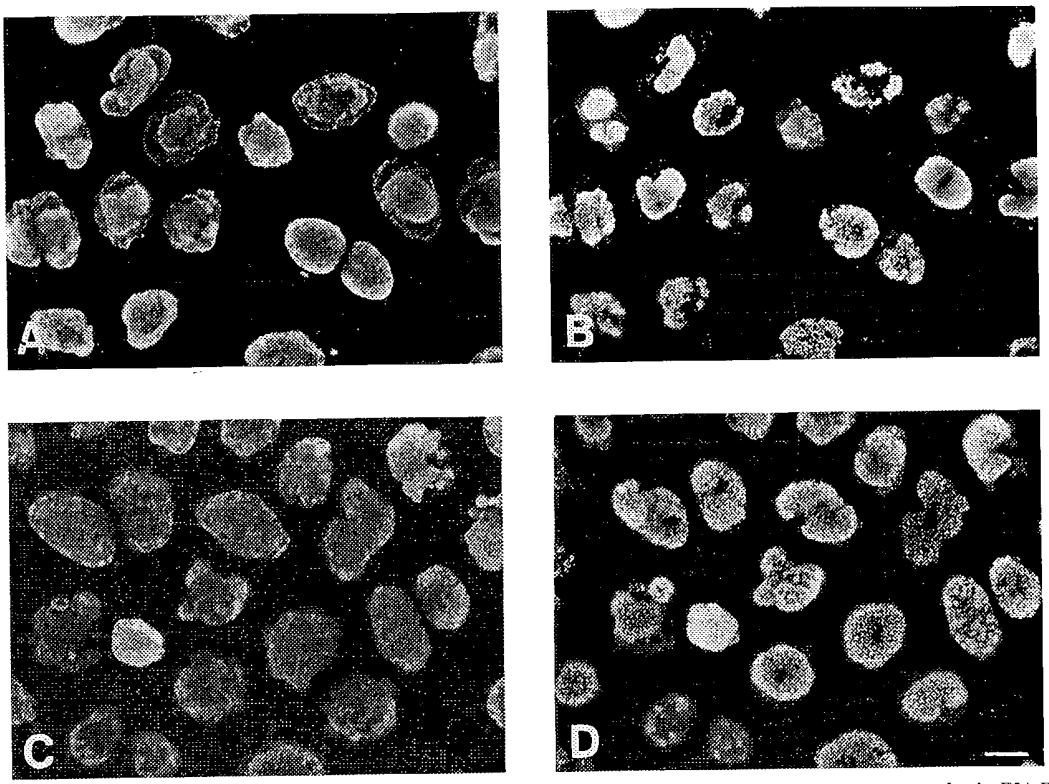

FIG. 3. All cells infected with the wild-type or E1B 55-kDa mutant virus are infected, as determined by an immunofluorescent assay for the E2A DNA-binding protein. HeLa cells were infected with either the wild-type virus, *dl*309, or the E1B 55-kDa mutant virus, *dl*338, at a multiplicity of 10 PFU per cell. The cells were processed for indirect immunofluorescence at 16 h postinfection. All cells in the field are visualized by DAPI staining as seen in panels A and C. The E2A 72-kDa DNA-binding protein was visualized by indirect immunofluorescence in cells infected with the wild-type virus in panel B and in cells infected with the E1B 55-kDa mutant virus in panel D. Typically, greater than 99% of the cells visualized with DAPI also demonstrated DNA-binding protein-specific fluorescence. Bar, 20 μm.

The failure of the cells infected with *dl*338 to produce virus in most infected cells is a property shared by another E1B 55-kDa mutant virus, *dl*1520. The large deletion and premature termination codon in the E1B 55-kDa coding region of *dl*1520 precludes expression of any E1B 55-kDa-related protein (6), whereas the deletion present in the *dl*338 genome could allow expression of a truncated (17-kDa) E1B 55-kDa protein. HeLa cells were infected with the E1B 55-kDa mutant virus, *dl*1520D, or the E1B 19-kDa mutant virus, *dl*337, at 10 PFU per cell. At 20 h postinfection, the infected cells were processed for transmission electron microscopy. In an identical manner to HeLa cells infected with *dl*338, only 20% of the cells infected with *dl*1520 produced progeny virions (data not shown). By contrast, all cells infected with the E1B 19-kDa mutant virus, *dl*337, produced progeny virus (data not shown). These results suggest that the inability to replicate in all infected cells is a property of viruses containing mutations that specifically inactivate or delete the E1B 55-kDa coding region and is not common to all mutations within the early region 1B.

The results obtained by electron microscopy suggest that only 20% of the HeLa cells infected with the E1B 55-kDa mutant virus produce particles that appear to be progeny virions. These morphological data were confirmed by a plaque assay modified to measure virus-producing cells or infectious centers. For this assay, HeLa cells were infected with either the wild-type or the E1B 55-kDa mutant virus at 10 PFU per cell for 90 min. The extracellular virus was inactivated by incubating the cells with a mixture of trypsin and EDTA for 10 min. Various numbers of infected HeLa cells in molten agar were overlaid onto a monolayer of 293 cells. 293 cells express the early region 1 products of Ad5 and are permissive for the replication of all Ad E1 mutants (21). Plaques were formed when an infected HeLa cell in the agar overlay successfully replicated the virus and lysed and infected 293 cells below the agar overlay. The number of plaques obtained was plotted on the abscissa as a function of the number of infected cells plated. In the representative experiment shown in Fig. 4, the line corresponding to cells infected with the wild-type virus (circles) has a slope of 0.24 ± 0.05 infectious centers per cell, whereas the slope of the line corresponding to cells infected with the E1B mutant virus (squares) is 0.060 ± 0.003. The ratio of these values (0.06/0.24) is 0.25, indicating that cells infected with mutant virus produce infectious centers at 25% of the frequency of cells infected with the wild-type virus. From six independent experiments, an average of 22 ± 4% of cells infected with the E1B 55-kDa mutant virus produced infectious progeny virus compared to cells infected with the wild-type virus. These results precisely agree with the results obtained by electron microscopy.

Replication of the E1B 55-kDa mutant Ad is dependent on cell density. Because not all HeLa cells in an infected population replicate the E1B 55-kDa mutant virus, it seems likely that differences in the physiological state among individual cells dictate permissivity for replication of an Ad mutant that fails to express the E1B 55-kDa protein. Because the physiological state of the cells, including the specific stage of the cell cycle at

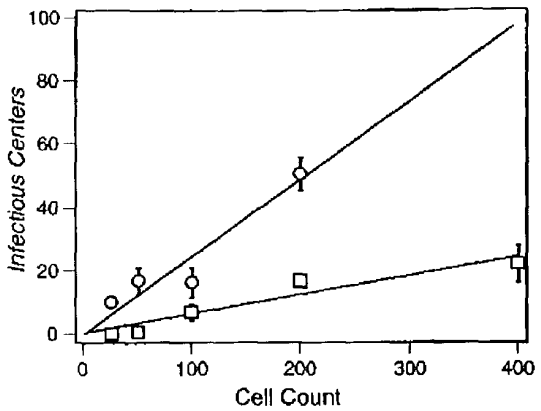

FIG. 4. A plaque assay for infectious centers indicates that fewer HeLa cells infected with the E1B 55-kDa mutant virus replicate the virus than cells infected with the wild-type virus. HeLa cells were infected with either the wild-type virus, *dl*309, or the E1B 55-kDa mutant virus, *dl*338, at a multiplicity of 5 to 10 PFU per cell. The virus was inactivated, and the infected HeLa cells were harvested 90 min postinfection and diluted in molten agar. Various numbers of infected cells in agar were overlaid onto a monolayer of 293 cells. Plaques were formed when an infected HeLa cell in the agar overlay successfully replicated the virus and lysed and infected 293 cells below the agar overlay. The number of plaques obtained was plotted on the abscissa as a function of the number of infected cells plated (ordinate). A representative experiment is shown with results obtained from HeLa cells infected with the wild-type virus (○) and HeLa cells infected with the E1B mutant virus (□). The standard error associated with the dependent variable (infectious centers) is plotted for each datum. The error associated with the value in the ordinate (cell number) was not determined.

the time of infection, is sensitive to cell density, this relationship was systematically investigated (Fig. 5). For this experiment, HeLa cells were plated at various densities prior to infection. The cells were infected with the wild-type or the E1B mutant virus at 10 PFU per cell, and the virus yield was measured by a plaque assay. Identically treated cells were harvested at the time of infection and analyzed by FACS to determine if the cell cycle distribution in the population of cells varied with cell density. The results shown in Fig. 5A demonstrate that wild-type Ad replication is largely independent of cell density. By contrast, the yield of the E1B 55-kDa mutant virus showed an inverse dependence on cell density (Fig. 5B). In two independent experiments, HeLa cells infected at increasing cell densities produced lower yields of E1B mutant virus per cell. Furthermore, as the HeLa cell density increased, the percentage of cells in S phase decreased (Fig. 5C) and the percentage of cells in G_1 increased (not shown). These results agree with previous findings suggesting that as HeLa cells grow to increased density, they partially arrest in G_1 (32, 71). Indirect immunofluorescent staining for the Ad DNA-binding protein demonstrated that the lower virus yields associated with increasing cell density were not the result of decreased infectivity. All cells in each wild-type or mutant virus-infected population expressed the viral DNA-binding protein, irrespective of cell density (data not shown). The dependence of the E1B 55-kDa mutant virus on cell density for replication coupled with the observation that only ≈20% of HeLa cells infected with the E1B 55-kDa mutant virus replicate the virus suggests that, in contrast to the wild-type virus, the E1B 55-kDa mutant virus requires cells to be in S phase for viral replication.

The E1B 55-kDa mutant virus produces virus in a greater percentage of cells infected during S phase than cells infected during G_1. To determine if the stage of the cell cycle at the time of infection impacts replication of the E1B 55-kDa mutant virus, HeLa cells were synchronized and infected at various points throughout the cell cycle. For all experiments using synchronized cells, a parallel set of cells was analyzed by FACS. The DNA content of each cell was measured, and this value was used to determine the stage of the cell cycle for each cell. The results of a typical synchronization procedure are shown in Fig. 6. Asynchronously growing HeLa cells (Fig. 6A) were found to contain 65% cells in G_1 (or G_0), 11% in G_2 or

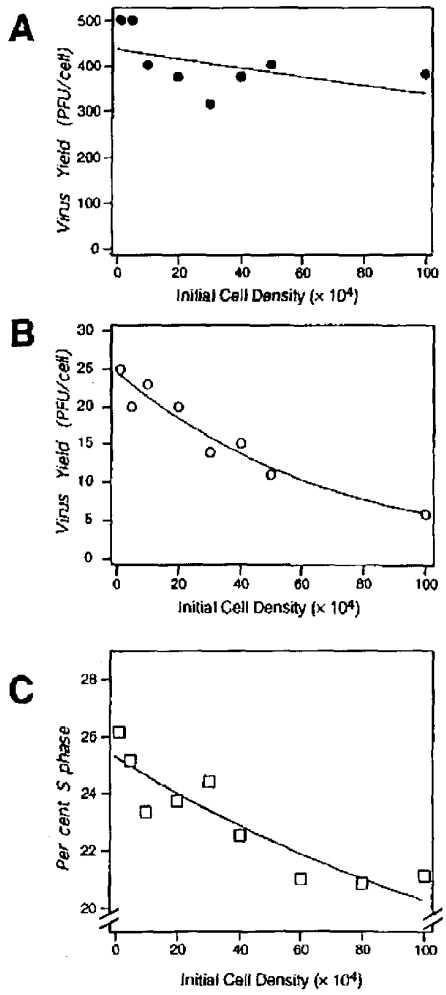

FIG. 5. Replication of the E1B 55-kDa mutant virus depends on cell density. HeLa cells were passed to various cell densities and infected 24 h after attachment with either the wild-type virus, *dl*309, or the E1B 55-kDa mutant virus, *dl*338, at a multiplicity of 10 PFU per cell. Virus yields were measured by plaque assay using 293 cells and are expressed as PFU per cell on the abscissa versus the initial cell density on the ordinate. (A) Replication of the wild-type virus is poorly correlated with the density of the cells at the time of infection (●). The exponential curve shown fits the data with a correlation coefficient of 0.247. The data also fit a horizontal line (not shown) with a correlation coefficient of 0.243. (B) Replication of the E1B 55-kDa mutant virus demonstrated an inverse relationship to cell density (○). The data are shown fit to an exponentially decaying curve with a coefficient of correlation equal to 0.93. (C) The percentage of HeLa cells in S phase was also inversely related to cell density (□). The data in panel C were obtained by plating HeLa cells at the indicated densities and harvesting the cells 24 h after attachment. After staining with propidium iodide, the DNA content of the cells was measured by FACS and used to determine the number of cells in S phase. The data fit an exponentially decaying curve that asymptotically approaches 15%, with a correlation coefficient equal to 0.94.

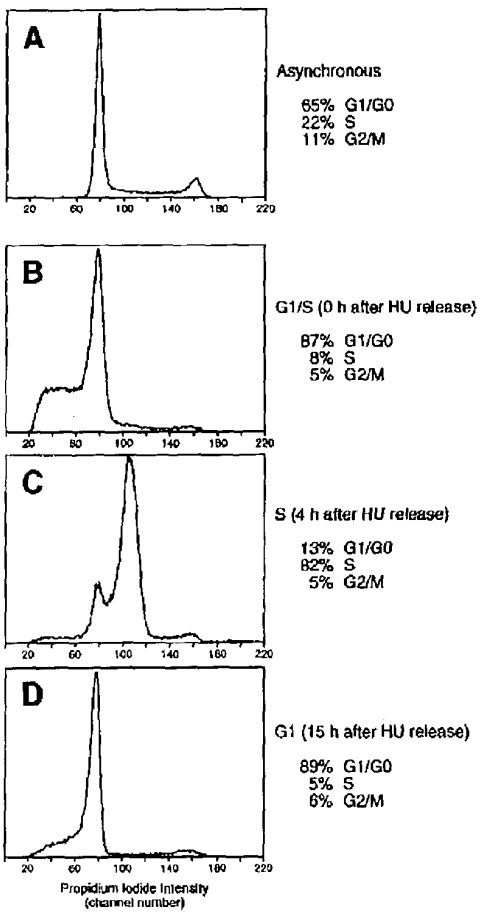

FIG. 6. HeLa cells were synchronized to achieve a high degree of synchrony as determined by FACS analysis. HeLa cells were synchronized by a combination of mitotic detachment and a hydroxyurea block. The hydroxyurea block was released with normal growth medium, and the HeLa cells were allowed to enter S phase synchronously. Asynchronously growing cells as well as synchronized cells obtained 0, 4, and 15 h after release of the hydroxyurea block were fixed and stained with propidium iodide. The intensity of the propidium iodide fluorescence in individual cells was measured by FACS to determine DNA content. The distribution of cells between G_1/G_0, S, and G_2/M phases of the cell cycle was determined by standard means as described in Materials and Methods. The histograms display the number of cells counted at the indicated fluorescence intensity; these values were scaled to accommodate the maximum value for each panel. Typically 40,000 cells were analyzed for each sample. Panel A shows the cell cycle distribution of cells in an asynchronous population. Panel B shows the distribution of cells immediately after the release of the hydroxyurea block in which 87% of the cells occur at the G_1-S boundary. The shoulder in the curve appearing between channel numbers 20 and 68 was infrequently observed in synchronized cell populations. These values most likely are due to dead or apoptotic cells and were not included in the analysis. Panel C shows the synchronous shift of 82% of the HeLa cells into S phase 4 h after release of the hydroxyurea. Panel D shows that 89% of the cells were found in G_1 (or G_0) phase 15 h after hydroxyurea release.

M, and 22% in S phase. HeLa cells were synchronized by a combination of mitotic detachment and hydroxyurea block (11). Hydroxyurea is selectively cytotoxic to cells in S phase and blocks progression through the cell cycle at the G_1/S boundary. Removal of the hydroxyurea block permitted the HeLa cell populations to enter S phase synchronously. An effect of the hydroxyurea treatment can be seen in the histograms of cell number versus DNA content in Fig. 6B. The shoulder preceding the G_1 peak represents cell debris resulting from apoptosis of S phase cells collected by mitotic detachment and treated with hydroxyurea (63). As the synchronized cells progressed through the cell cycle (Fig. 6C and D), this shoulder decreased as apoptotic cells detached from the plates and were washed away. For each experiment a high degree of synchrony was achieved as populations of cells shifted to approximately 87% G_1/S phase (Fig. 6B), 82% S phase (Fig. 6C), or 89% G_1 phase (Fig. 6D).

HeLa cells were synchronized and infected with the wild-type and E1B mutant virus both during early S phase (corresponding to the cells analyzed in Fig. 6B) and during G_1 (corresponding to cells analyzed in Fig. 6D). The infected cells were analyzed by transmission electron microscopy 20 h postinfection. HeLa cells infected with the wild-type virus both during S phase (Fig. 7A) and during G_1 (Fig. 7B) contained progeny viral particles as expected. Viral particles from a representative portion of the nucleus are shown in the insets. No ultrastructural differences were noted between HeLa cells infected with the wild-type virus at S phase or G_1. By contrast, cells infected with the E1B 55-kDa mutant virus during S phase (Fig. 7C) appeared more permissive for replication of the mutant virus than cells infected during G_1 (Fig. 7D) or cells infected as asynchronous populations (Fig. 1 and 2). Greater than 75% of the S phase cells infected with the E1B 55-kDa mutant virus produced intracellular virus particles, as determined by electron microscopy. The percentage of S phase cells that failed to produce mutant virus may be partially accounted for by cells that were not in S phase (≈18%) or were in late S phase at the time of infection due to incomplete synchrony. Only 10% of cells infected with the E1B mutant virus during G_1 produced progeny virus particles (Fig. 7D). The majority of the cells infected with the E1B 55-kDa mutant virus during G_1 were devoid of any particles resembling virions. The small percentage of cells in a G_1 population that produced E1B mutant virions may result from the presence of cells that were in other phases of the cell cycle (S) at the time of infection due to incomplete synchronization. The cells depicted in the micrographs are representative of the majority of each infected population. The presence of viral inclusions in the nuclei of all the cells in each population indicated that all cells were infected (Fig. 7). The results of this electron microscopy study suggest that the replication of an Ad mutant that fails to express the E1B 55-kDa protein depends on a transient environment present in S phase cells at the time of infection.

An endpoint or $TCID_{50}$ assay for infectious centers confirmed that a greater percentage of cells infected with the E1B 55-kDa mutant virus during S phase were permissive for replication of the mutant virus (Table 1) than cells infected in G_1. The $TCID_{50}$ assay for infectious centers was developed for these experiments because the efficiency of detection of infectious centers was greater than that of the plaque assay for infectious centers. HeLa cells infected in an asynchronous state of growth as well as synchronized HeLa cells infected in early S phase or G_1 were compared using this assay. For these experiments, HeLa cells were infected and harvested as for the plaque assay for infectious centers. The infected HeLa cells were replated at various cell numbers (100, 25, 6.4, 1.6, 0.4, 0.1, and 0.024 cells per well) in a 96-well tissue culture dish. After 2 days of incubation to allow virus growth, the infected HeLa cells were lysed in situ to ensure the quantitative release and recovery of progeny virions. The HeLa cell lysates were assayed for the presence of infectious centers by using the lysate to infect a monolayer of 293 cells in a new 96-well tissue culture dish.

The data obtained were fit to equation 1 to determine the

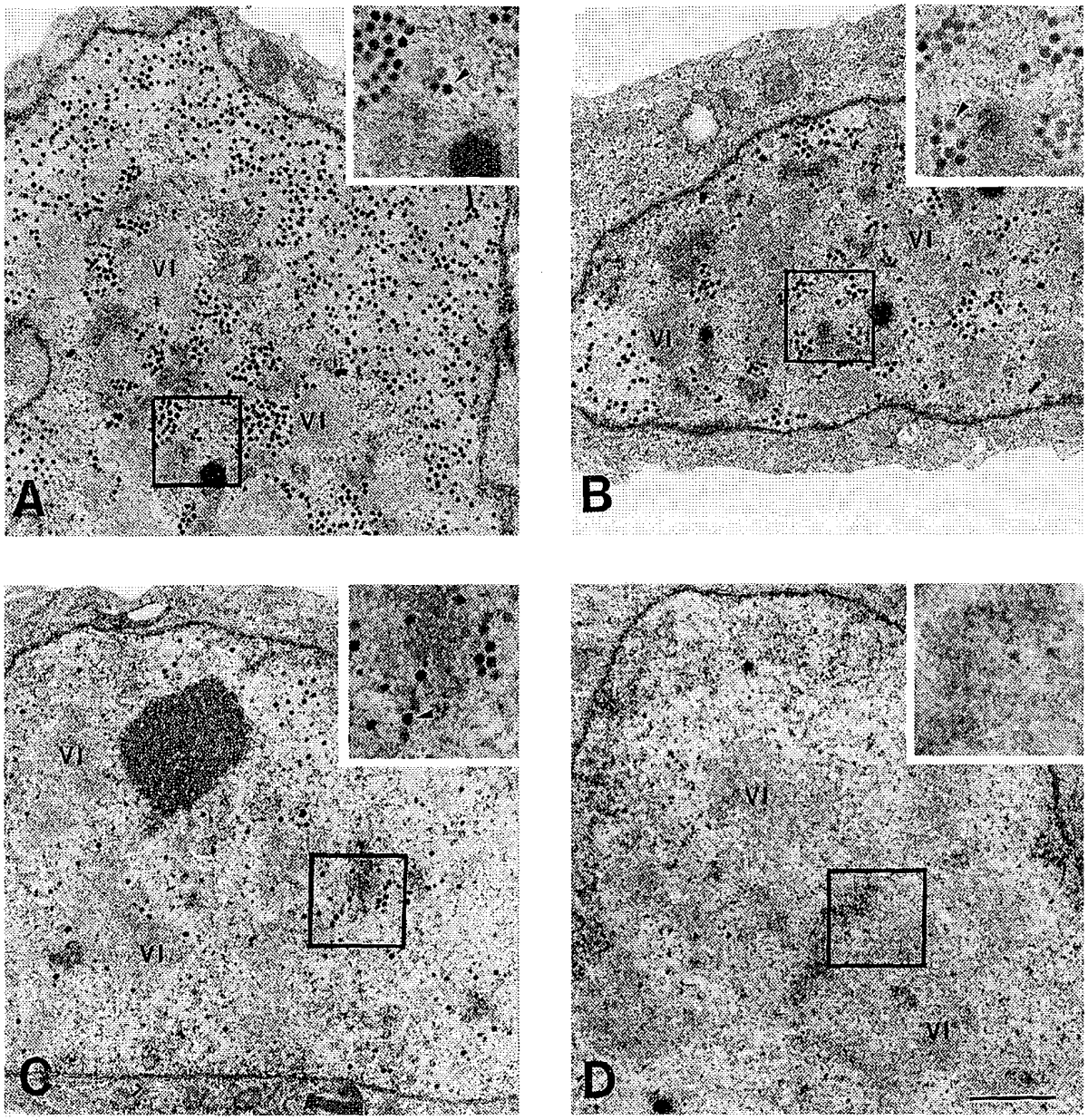

FIG. 7. HeLa cells infected during S phase appear permissive for replication of the E1B 55-kDa mutant virus, whereas cells infected during G_1 do not. HeLa cells were infected at specific points during the cell cycle with either (A and B) the wild-type virus, *dl*309, or (C and D) the E1B 55-kDa mutant virus, *dl*338, at a multiplicity of 10 PFU per cell. The cells in panels A and C were synchronized to S phase at the time of infection. The cells in panels B and D were synchronized to G_1 at the time of infection. At 20 h postinfection, the cells were prepared for transmission electron microscopy. The cells infected with the wild-type virus in panels A and B are representative of the typical wild-type virus-infected cell. The cell seen in panel C is representative of greater than 75% of the cells infected during S phase with the E1B mutant virus. The cell shown in panel D is representative of greater than 85% of the cells infected during G_1 phase with the E1B mutant virus. The insets are threefold enlargements of the boxed regions of the nucleus. Virus particles (arrowheads) are evident in the insets (A, B, and C but not D). All cells were infected as determined by the presence of viral inclusions (VI). Bar, 1 μm.

number of infected cells producing virus. These results indicate that essentially each HeLa cell infected with the wild-type virus was an infectious center regardless of stage of the cell cycle at the time of infection (Table 1). This result is consistent with the results obtained by electron microscopic analysis of HeLa cells infected with the wild-type virus. In addition, this result suggests that the $TCID_{50}$-based assay was more efficient than the plaque-based assay for the detection of infectious centers. The reason for this difference is not known but may be due to inefficient cell lysis and release of progeny virus from cells embedded in the agar in the plaque-based assay. Cells infected during G_1 appeared slightly better able to replicate the wild-type virus compared to a randomly cycling population or S phase population of cells (1 in 0.8 cells versus 1 in 1.4 cells). By

TABLE 1. Infectious centers from asynchronously growing and synchronized HeLa cells infected with wild-type or E1B mutant virus

Virus	Cell cycle[a]	Frequency of infectious centers		
		Replicate values[b]	Avg	Fraction wild type (%)[c]
Wild type	Asynch	1.3 ± 0.2		
		1.6 ± 0.3	1.4 ± 0.15	100 ± 11
		1.1 ± 0.3		
	G_1	0.72 ± 0.1		
		0.85 ± 0.3	0.8 ± 0.12	175 ± 26
		0.80 ± 0.2		
	S	1.2 ± 0.4		
		1.3 ± 0.4	1.4 ± 0.23	100 ± 16
		1.7 ± 0.4		
E1B mutant	Asynch	6.7 ± 1.8		
		5.0 ± 2.5	5.4 ± 1.0	26 ± 5
		4.5 ± 1.0		
	G_1	7.8 ± 2.0		
		8.6 ± 3.8	9.1 ± 1.9	15 ± 3
		10.8 ± 4.1		
	S	4.3 ± 1.5		
		3.2 ± 0.7	3.8 ± 0.65	37 ± 6
		3.9 ± 1.2		

[a] The cells were infected at the stage of the cell cycle indicated. Asynch, cells infected as a randomly cycling population.

[b] The number of cells required to obtain an infectious center ± standard error was determined with the use of equation 1 in three independent replicates.

[c] The fraction of infectious centers (1/number of cells required to obtain an infectious center) ± standard error is expressed as a percentage of the fraction of infectious centers for asynchronously growing cells infected with the wild-type virus.

contrast, only a fraction of the HeLa cells infected with the E1B mutant virus produced virus. Only 1 in 5.4 cells in a randomly cycling population of HeLa cells infected with the E1B mutant virus was productive. Normalized to the number of wild-type virus-infected cells that produce virus (1 in 1.4), this assay would suggest that 26 ± 5% of the E1B mutant-infected cells were productive. This value agrees closely with the value of 20% estimated by electron microscopy (Fig. 1) and the value of 22% estimated by the infectious centers assay by plaque formation (Fig. 4). Also in accord with the electron microscopic analysis, the results in Table 1 reveal that HeLa cells infected in S phase were better able to support replication of the E1B mutant virus than cells infected in G_1. Approximately 2.5-fold more HeLa cells infected in S phase produced the E1B mutant virus than HeLa cells infected in G_1 (1 in 3.8 versus 1 in 9.1). Nonetheless, the normalized fraction of cells infected with the E1B mutant virus during S phase that yielded infectious centers (37 ± 6%) was less than the value of 75% estimated by electron microscopy. The reason for this difference is not understood. Because the infectious centers assay measures infectious virus and electron microscopy visualizes physical particles, it remains possible that some of the cells observed to contain intranuclear viral particles contained noninfectious virions. Finally, the fraction of cells that produced E1B mutant virus after being infected in G_1 (15 ± 3%) is close to the value estimated by electron microscopic analysis. The differences between these two assays could partially be due to variations in the number of non-G_1 cells in the synchronized population arising from incomplete synchronization and a loss of synchrony after progression through one complete cell cycle.

Cells infected during S phase with the E1B 55-kDa mutant virus produce greater yields of progeny virus than do cells infected during G_1. The total yield of virus from cells infected at S and G_1 phase was measured and compared to the yield from asynchronously growing populations of cells. Asynchronous populations of cells infected with the E1B 55-kDa mutant virus produced approximately 35-fold less virus than the wild-type infection (Fig. 8). Infection of synchronized cells with the wild-type virus demonstrated that all cells were permissive for replication of the wild-type virus irrespective of the stage of the cell cycle at the time of infection. However, cells infected with the wild-type virus during G_1 produced threefold more virus than cells infected during S phase. By contrast, the E1B 55-kDa mutant virus replicated most successfully in cells infected during S phase, producing approximately sevenfold more progeny virus than cells infected during G_1 and threefold more virus than asynchronous populations of cells. These results, taken together with the previous infectious center data obtained from synchronized cells, indicate that G_1 cells are better suited for the replication of wild-type virus whereas S phase cells are better suited for the replication of the E1B mutant virus.

Although HeLa cells infected during S phase were better suited for replication of the E1B 55-kDa mutant virus than G_1 cells or asynchronously growing cells, S phase did not entirely complement the defect in viral replication. S phase cells infected with the E1B mutant virus produced ninefold less virus than did wild-type infection. Nonetheless, the data presented thus far indicate that S phase cells are the primary cells permissive for replication of the E1B 55-kDa mutant virus. Ad mutants that fail to express the E1B 55-kDa protein have acquired a dependence on S phase to produce progeny virus. Therefore, the E1B 55-kDa protein appears to overcome restrictions imposed on viral replication by the cell cycle.

HeLa cells infected during different stages of the cell cycle exhibited differing degrees of cytopathic effect, as seen by cell rounding. HeLa cells were infected as an asynchronous population or synchronized and infected in S phase or G_1. The cells were analyzed by phase-contrast microscopy between 24 and 48 h after infection. During this time, mock-infected cells grew

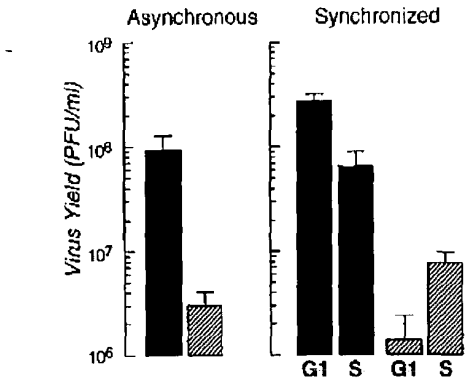

FIG. 8. HeLa cells infected during S phase produce more E1B mutant virus than do asynchronously growing HeLa cells or HeLa cells infected during G_1. Asynchronously and synchronously growing monolayers of HeLa cells were infected with either the wild-type virus, *dl*309, or the E1B 55-kDa mutant virus, *dl*338, at a multiplicity of 10 PFU per cell. The phase of the cell cycle at the time of infection is indicated below the appropriate bar. Cells were lysed 48 h postinfection, and virus yield was measured by plaque assay using 293 cells. The yield (PFU per milliliter) and upper range of the standard error are shown. ■, wild-type virus; ▨, E1B mutant virus.

to confluence and only mitotic cells (<5%) exhibited cell rounding (Fig. 9A). The cytopathic effect induced by the wild-type Ad consisted of severe cell rounding of approximately 70% of the asynchronous infected population by 48 h after infection (Fig. 9B). Asynchronously growing HeLa cells infected with the E1B 55-kDa mutant virus contained approximately 10 to 20% rounded cells (Fig. 9C). All HeLa cells infected with the wild-type Ad during either S phase or G_1 exhibited a cytopathic effect similar to that seen in asynchronous cells (Fig. 9D and F, respectively). However, HeLa cells infected during S phase with the E1B 55-kDa mutant virus showed markedly more severe cytopathic effect than did asynchronous cells or cells infected during G_1 (Fig. 9 compare E with G). Mock-infected synchronized cells exhibited cell rounding only during mitosis at 11 and 33 h after removal of the hydroxyurea block (data not shown). The cell rounding seen in cells infected during either S phase or G_1 was not coincident with the anticipated time of mitosis. This observation indicates that the cell rounding exhibited by cells infected during either S phase or G_1 was due to virus-induced cytopathic effect and not cell division. Although an increased cytopathic effect does not necessarily correlate with virus production, HeLa cells infected in S phase with the E1B 55-kDa mutant virus showed both an increased cytopathic effect and produced more virus than cells infected in G_1. These results lead to the hypothesis that cells infected with the E1B 55-kDa mutant Ad during S phase support an infection that more closely resembles the wild-type virus infection.

Cells infected with the E1B 55-kDa mutant virus synthesize viral DNA to levels of the wild-type virus infection. The failure of G_1 cells to allow replication of the E1B 55-kDa mutant virus could reflect a dependence of the E1B 55-kDa mutant virus on S phase and the cellular program of DNA synthesis in order to synthesize viral DNA. However, the presence of viral centers in the nuclei of all cells in an infected population indicated that viral DNA was synthesized in all cells whether or not they produce progeny virions. In addition, hybridization analysis of total DNA isolated from asynchronous populations of HeLa cells infected with either the wild-type virus or the E1B 55-kDa mutant virus demonstrated that E1B 55-kDa mutant virus-infected cells synthesized viral DNA to levels equivalent to those of wild-type virus-infected cells (Fig. 10). In two independent experiments, the amount of viral DNA synthesized in E1B mutant virus-infected cells either equaled or exceeded the amount of viral DNA synthesized in wild-type virus-infected cells. These data indicate that, in HeLa cells, the E1B 55-kDa mutant virus successfully completes the early phase of viral replication and synthesizes viral DNA to levels equivalent to those of the wild-type infection. Therefore, the lesion of the E1B 55-kDa mutant virus, and presumably the role of the E1B 55-kDa protein, appears to reside in the late phase of viral replication.

The wild-type and E1B 55-kDa mutant viruses not only synthesized equivalent amounts of viral DNA during the course of an infection but also induced the synthesis of viral DNA at the same time in infection. Incorporation of bromodeoxyuridine (BrdU) into mock-infected, wild-type-infected or E1B mutant-infected HeLa cells at various times postinfection demonstrated that both the wild-type virus- and the E1B 55-kDa mutant virus-infected cells induced viral DNA synthesis at approximately 9 h after infection (data not shown). Prior to 9 h after infection, approximately 25 to 30% of both mock-infected and Ad-infected populations of cells incorporated BrdU. By 9 h after infection, 85 to 90% of the cells in both wild-type-infected and E1B 55-kDa mutant virus-infected cultures stained positively for incorporation of BrdU. These results indicate that both the wild-type and E1B mutant Ad initiate viral DNA synthesis at the same time in infection.

The failure of the E1B 55-kDa mutant virus to replicate in all infected cells is not mediated by p53. The experiments discussed above were conducted with HeLa cells that contain a wild-type p53 gene. Normally, the HeLa p53 protein is inactivated by the human papillomavirus early protein E6 (56, 68). However, Ad infection of HeLa cells has been shown to elevate levels of p53, which could hinder viral replication by inducing a G_1 growth arrest and inhibiting viral DNA synthesis (13, 22). During an Ad infection, the E1B 55-kDa protein binds and inactivates p53 (55, 72, 75). Thus, the failure to inactivate p53 may account for the inability of the E1B 55-kDa mutant virus to replicate in all infected cells. To address this hypothesis, two wild-type p53 cell lines, H460 and A549 (10, 35), and two p53-null cell lines, H358 and Saos-2 (39, 62), were analyzed for the ability to allow replication of the E1B mutant virus. If the failure of the E1B 55-kDa mutant virus to replicate was mediated by p53, we would expect that the mutant virus would replicate to levels approaching those of the wild-type virus in a p53-null cell line and replicate poorly in cells containing a wild-type p53. As can be seen in virus yields in Table 2, this effect was not observed.

The E1B 55-kDa mutant virus replicated to the highest titer in H460 and A549 cells expressing the wild-type p53 protein. In addition, both the greatest (18-fold) and least (1.9-fold) difference between replication of the wild-type and E1B mutant virus was observed in the cell lines reported to contain a wild-type p53 gene. Finally, to within 1 log unit, the wild-type virus replicated to the same extent in all cell lines. These results suggest that although replication of the E1B 55-kDa mutant virus is dependent on the cell type, these differences may not be mediated by p53. Taken with the previous results, these findings suggested that the E1B 55-kDa protein relieves growth restrictions by a p53-independent mechanism, perhaps by interacting with other unidentified cellular growth regulatory proteins.

DISCUSSION

The Ad E1B 55-kDa tumor antigen relieves restrictions imposed on viral growth by the cell cycle. Mutant viruses (*dl*338 and *dl*1520) that failed to express the E1B 55-kDa protein produced progeny virions in only 20% of the infected cells as determined by electron microscopy (Fig. 1 and 2 and data not shown). Similarly, assays for infectious centers showed that only 20 to 25% of the cells infected with the E1B 55-kDa mutant virus allowed replication of the mutant virus compared to 100% of the cells infected with the wild-type virus (Fig. 4 and Table 1). The fraction of cells that support growth of the E1B mutant virus is the same as the fraction of cells in S phase in an asynchronously growing culture of HeLa cells (Fig. 5C). The contribution of the cell cycle to growth of the E1B mutant virus was determined by infecting HeLa cells synchronized to S phase or G_1. Compared to cells infected in G_1, cells infected in S phase with the E1B mutant virus had a greater number of infectious centers (Fig. 7 and Table 1), produced higher levels of virus progeny (Fig. 8), and demonstrated a near wild-type cytopathic effect (Fig. 9). These data demonstrate that Ad mutants that fail to express the E1B 55-kDa protein have acquired a dependence on the cell cycle for virus production.

When infected during S phase, HeLa cells support efficient replication of Ads that fail to express the E1B 55-kDa protein. It is not known whether the environment that complements the defect in virus production exists at the time of infection or develops during the course of the infection. Because cells in-

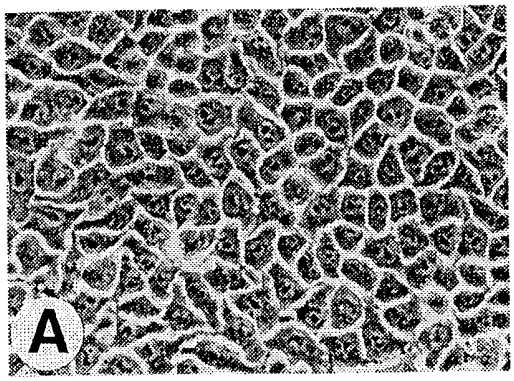
A

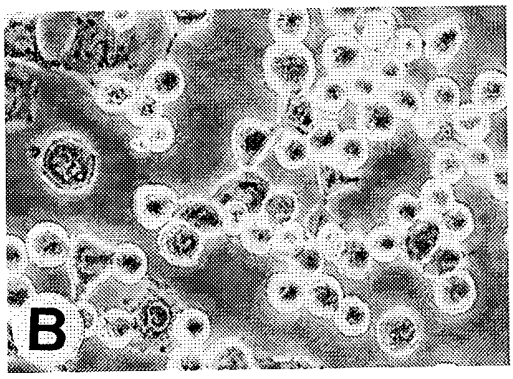
B

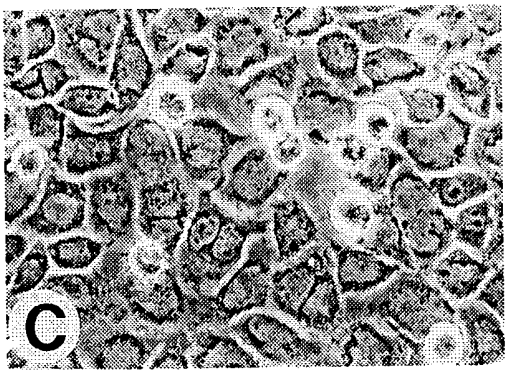
C

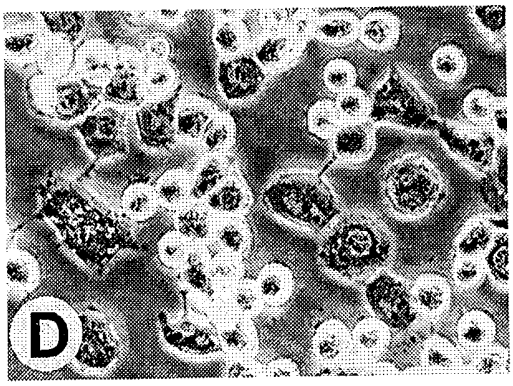
D

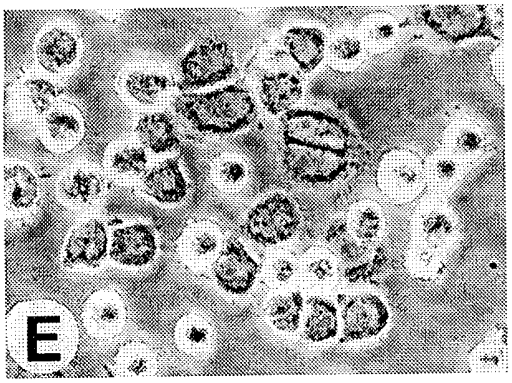
E

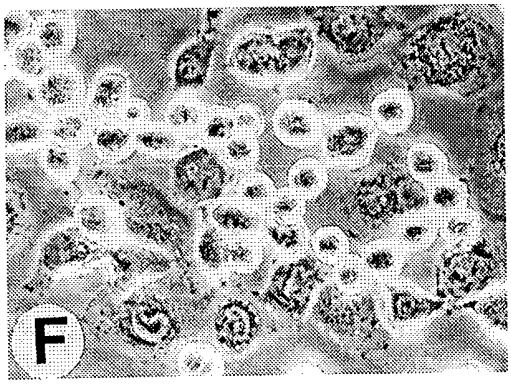
F

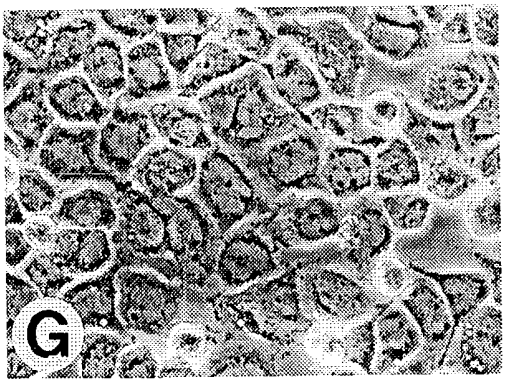
G

FIG. 9. HeLa cells infected with the E1B 55-kDa mutant virus during S phase exhibit a more severe virus-induced cytopathic effect than asynchronous cells or cells infected during G_1. Asynchronously growing HeLa cells (A to C), HeLa cells in S phase (D and E), or HeLa cells in G_1 phase (F and G) were either mock infected (A) or infected with the wild-type virus (B, D, and F) or the E1B 55-kDa mutant virus (C, E, and G) at 10 PFU per cell. At 48 h postinfection, cells were analyzed by phase-contrast microscopy. The Ad-induced cytopathic effect is characterized by cell rounding, as evidenced by the light-refractive bodies.

fected with either wild-type or E1B mutant virus fail to enter mitosis (data not shown), we favor the hypothesis that Ad infection halts normal progression of the cell cycle. Clearly the very definition of the cell cycle following infection remains uncertain. Although cells infected in S phase with the E1B mutant virus produced more virus than asynchronous or G_1 cells, they produced ninefold less virus than S phase cells infected with the wild-type virus (Fig. 8). Furthermore, by electron microscopy it appeared that each E1B 55-kDa mutant virus-infected cell containing viral particles produced fewer particles than any cell infected with the wild-type virus (compare Fig. 7A or B to C). Moreover, when applied to synchronized HeLa cells infected in S phase, both the $TCID_{50}$ assay for infectious centers (Table 1) and the plaque assay for infectious centers (data not shown) determined that between 24 to 37% of the S phase cells produced infectious E1B mutant virus; this range of values is significantly less than the 75% estimated by electron microscopy. Perhaps some of the productive cells identified by morphological means contain noninfectious particles. If so, it seems likely that the ratio of particles to PFU for virus obtained from synchronized cells infected in S phase is higher than that for virus obtained from cells infected at other stages of the cell cycle. Nonetheless, a property of S phase enables production of the E1B mutant virus although it cannot fully restore viral replication to wild-type levels.

Other viruses such as the parvoviruses, depend on S phase and the normal progression of the cell cycle for their replication. Replication of the bovine gammaherpesvirus 4 (BHV-4) DNA was shown to depend on transition through S phase. In this study, the number of cells expressing late proteins and synthesizing viral DNA among BHV-4-infected cells was inversely correlated with cell density (65). We identified only one other report of a mutant virus that acquired a dependence on the cell cycle for replication. The herpes simplex virus type 1 Vmw65 (VP16) insertion mutant was shown to depend on cells infected during S phase for early protein synthesis and replication (14). However, any relationship between the Vmw65 mutant herpesvirus and the E1B 55-kDa mutant Ad is unclear.

By contrast to synchronized cells infected with the E1B 55-kDa mutant virus, cells infected with the wild-type virus during G_1 appear slightly better suited for replication of the wild-type virus than cells infected during S phase. G_1-infected cells produced threefold more wild-type virus than S phase-infected cells. Similarly, the results in Table 1 indicate that more cells infected in G_1 produced wild-type virus than cells infected during S phase. Similar results were obtained with a plaque assay for infectious centers (data not shown). These observations suggest that infection of cells in G_1 permits the wild-type virus to more effectively establish a program of virus replication. During an Ad infection, the E1A gene products relieve growth suppression and elicit unscheduled cellular DNA synthesis by inactivating growth suppressors associated with G_1 (5, 33, 41). Therefore, it may be suggested that the E1 region of Ad is poised to promote progression from G_1 into S. When cells are infected during S phase, a cellular program of DNA synthesis has already been established, and the virus may be forced to compete with the cell for limiting factors, such as free nucleotides, that are essential for DNA and RNA synthesis. Support for this possibility can be derived from the findings of Hodge and Scharff (24) who showed that when Ad DNA synthesis began prior to initiation of cellular DNA synthesis (S phase), the subsequent initiation at the next S phase was prevented. However, when viral DNA synthesis began after the onset of cellular DNA synthesis, cellular DNA synthesis was not completely inhibited (24). Together, these findings offer an hypothesis as to why G_1 phase cells better replicate the wild-type virus than S phase cells.

In contrast to the well-established role played by the E1A proteins in deregulating the cell cycle during lytic growth, (reviewed in references 17 and 67), the E1B 55-kDa protein has not been shown to function directly in deregulating the cell cycle during virus replication. It has, however, been hypothesized that the E1B 55-kDa protein permits E1A-induced DNA synthesis by preventing p53-mediated G_1 growth arrest or apoptosis (50, 59). Such a response by p53 to viral challenge would severely hinder if not shut down the ability of the virus

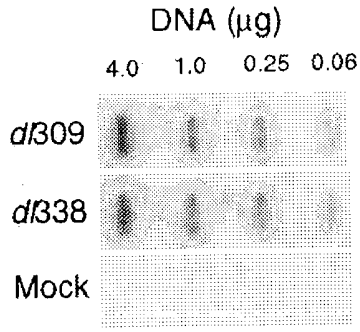

FIG. 10. E1B 55-kDa mutant virus-infected cells synthesize viral DNA at the same level as wild-type virus infection. HeLa cells were infected with either the wild-type virus, *dl*309, or the E1B 55-kDa mutant virus, *dl*338, at a multiplicity of 10 PFU per cell. Total cellular DNA was isolated from equal numbers of Ad-infected HeLa cells 20 h postinfection. Total DNA in the amount indicated above each lane was transferred to a nylon membrane, denatured, and hybridized with radioactive Ad-specific DNA probes generated by random-primed synthesis. Hybridized probe was quantified by densitometry, and mock-infected background was subtracted. Identical amounts of viral DNA were measured in E1B 55-kDa mutant virus-infected cells and wild-type virus-infected cells.

TABLE 2. Virus yield following infection of wild-type p53 and p53-null cell lines[a]

Cell line	p53 status	Virus yield (10^6 PFU per ml)[b]		
		E1B mutant	Wild type	Fold difference[c]
H460	Wild type	6.6 (4.5, 10)	120 (40, 230)	18
A549		44 (33, 58)	84 (46, 99)	1.9
H358	Null	2.9 (1.3, 4.7)	19 (7, 41)	6.4
Saos-2		1.1 (0.5, 2.2)	14 (7, 24)	13

[a] A total of 8×10^5 of the indicated cells in 4 ml were infected with 5 PFU per cell of either the wild-type virus, *dl*309, or the E1B mutant virus, *dl*338. The cells were lysed in a volume of 4 ml 2 days postinfection, and the titer of the progeny virus was determined by plaque assay with 293 cells.

[b] The virus yield was obtained by averaging the results of 6 to 10 independent measurements. The results are presented as the average (minimum/maximum).

[c] The fold difference is the ratio of wild-type virus yield to E1B mutant virus yield in the indicated cell line.

to transform cells or synthesize viral DNA and establish a lytic infection (16, 37, 69). However, replication of the E1B 55-kDa mutant virus was not related to the status of p53 in the five cell lines examined in this study (Fig. 8 and Table 2). Thus, these data suggest that the E1B 55-kDa protein relieves growth constraints of the cell cycle by mechanisms independent of p53. Other interactions between the E1B 55-kDa protein and cellular regulatory factors may exist to permit virus production in the wild-type Ad infection. Such positively acting regulatory factors may be made available or negatively acting factors may be absent when cells are infected during the S phase of the cell cycle.

Based on the known functions of the E1B 55-kDa protein in lytic infection, the inability of the E1B mutant virus to produce progeny virions in all infected cells may be linked to the defect in viral mRNA transport. The E1B 55-kDa mutant virus appears able to enter the late phase of viral replication. However, although late genes are transcribed, the transcripts never reach the cytoplasm (45). S phase cells may provide a property or factor that partially compensates for the E1B 55-kDa protein in promoting transport of viral mRNA. Work is in progress to determine if a correlation exists between the cell cycle-dependent replication and the mRNA transport defect of the E1B 55-kDa mutant virus. For example, if cell cycle-dependent viral replication and the mRNA transport defect are linked, the E4 34-kDa mutant virus may also depend on the cell cycle for virus production. As previously suggested, the E1B 55-kDa–E4 34-kDa protein complex may interact with and recruit a limiting cellular factor to the sites of viral RNA processing to aid in the transport of viral mRNA (43). Perhaps this factor is abundant in cells infected in S phase and can promote the transport of viral RNA in the absence of the E1B 55-kDa–E4 34-kDa complex. If such a factor exists, our previous work suggests that the cellular factor may be unique to primate cells (19). Several cellular proteins have been shown to function in cell cycle regulation and mRNA transport such that these two regulatory processes may be linked to some extent. For example, Ran/TC4 (31, 52, 53, 57) and the regulator of chromatin condensation-1, RCC1 (1, 12, 27, 28, 42), are cellular proteins involved in mediating both RNA transport and cell cycle progression. These or similar proteins would be potential targets of the E1B 55-kDa protein.

ACKNOWLEDGMENTS

This work was supported in part by Public Health Service grant AI35589 from the National Institute of Allergy and Infectious Disease to D.A.O. and grant CA12197 from the National Cancer Institute to the Comprehensive Cancer Center of Wake Forest University. Tissue culture reagents and services were provided by the Tissue Culture Core Laboratory of the Comprehensive Cancer Center of Wake Forest University supported in part by NIH grant CA12197.

We gratefully acknowledge Tom Shenk (Princeton University) for the *dl*309 and *dl*338 viruses, Arnie Berk (U.C.L.A.) for the *dl*1520D virus, and Arnie Levine (Princeton University) for the B6-8 hybridoma cell line. We thank Doug Lyles and Griff Parks (Wake Forest University) for critically reading the manuscript and for scientific discussions. We also thank Ken Grant and Nora Zbieranski of Wake Forest University for invaluable assistance with electron microscopy and FACS analysis, respectively.

ADDENDUM IN PROOF

After this article was accepted, Bischoff et al. (J. R. Bischoff, D. H. Kirn, A. Williams, C. Heise, S. Horn, M. Muna, L. Ng, J. A. Nye, A. Sampson-Johannes, A. Fattaey, and F. McCormick, Science **274**:373–376, 1996) reported that the E1B mutant virus *dl*1520 selectively replicates in and kills p53-deficient human tumor cells. These authors also reported that *dl*1520 fails to replicate in and kill human tumor cells expressing wild-type p53. In contrast to the findings of these investigators, we found that replication of the E1B mutant virus *dl*338 was not necessarily blocked by the presence of wild-type p53. Our findings, which include an analysis of the replication of *dl*1520 in HeLa cells, suggest that the fraction of cells in S phase at the time of viral challenge, rather than the status of p53, is prognostic for a productive infection by an E1B mutant virus. This hypothesis, if substantiated, would suggest that the range of human tumor cells that can be killed by the E1B mutant virus extends beyond p53-deficient cells.

REFERENCES

1. **Amberg, D. C., M. Fleischmann, I. Stagljar, C. N. Cole, and M. Aebi.** 1993. Nuclear PRP20 protein is required for mRNA export. EMBO J. **12**:233–241.
2. **Ausubel, F. M., R. Brent, R. E. Kingston, D. D. Moore, J. G. Seidman, J. A. Smith, and K. S. Struhl (ed.).** 1993. Current protocols in molecular biology, vol. 2. Greene Publishing Associates and John Wiley and Sons, Inc., New York, N.Y.
3. **Babich, A., L. T. Feldman, J. R. Nevins, J. E. Darnell, and C. Weinberger.** 1983. Effect of adenovirus on metabolism of specific host mRNAs: transport control and specific translational discrimination. Mol. Cell. Biol. **3**:1212–1221.
4. **Babiss, L. E., H. S. Ginsberg, and J. E. Darnell.** 1985. Adenovirus E1B proteins are required for accumulation of late viral mRNA and for effects on cellular mRNA translation and transport. Mol. Cell. Biol. **5**:2552–2558.
5. **Bagchi, S., P. Raychaudhuri, and J. R. Nevins.** 1990. Adenovirus E1A proteins can dissociate heterodimeric complexes involving the E2F transcription factor: a novel mechanism for E1A trans-activation. Cell **62**:659–669.
6. **Barker, D. D., and A. J. Berk.** 1987. Adenovirus proteins from both E1B reading frames are required for transformation of rodent cells by viral infection and DNA transfection. Virology **156**:107–121.
7. **Boulanger, P. A., and G. E. Blair.** 1991. Expression and interactions of human adenovirus oncoproteins. Biochem. J. **275**:281–299.
8. **Bridge, E., and G. Ketner.** 1990. Interaction of adenoviral E4 and E1B products in late gene expression. Virology **174**:345–353.
9. **Brigati, D. J., D. Myerson, J. J. Leary, B. Spalholz, S. Z. Travis, C. K. Y. Fong, G. D. Hsiung, and D. C. Ward.** 1983. Detection of viral genomes in cultured cells and paraffin-embedded tissue sections using biotin-labeled hybridization probes. Virology **126**:32–50.
10. **Brower, M., D. N. Carney, H. K. Oie, A. F. Gazdar, and J. D. Minna.** 1986. Growth of cell lines and clinical specimens of human non-small cell lung cancer in a serum-free defined medium. Cancer Res. **46**:798–806.
11. **Cao, G., L.-M. Liu, and S. F. Cleary.** 1991. Modified method of mammalian cell synchronization improves yield and degree of synchrony. Exp. Cell Res. **193**:405–410.
12. **Cheng, Y., J. E. Dahlberg, and E. Lund.** 1995. Diverse effects of the guanine nucleotide exchange factor RCC1 on RNA transport. Science **267**:1807–1810.
13. **Chiou, S.-K., C.-C. Tseng, L. Rao, and E. White.** 1994. Functional complementation of the adenovirus E1B 19-kilodalton protein with Bcl-2 in the inhibition of apoptosis in infected cells. J. Virol. **68**:6553–6566.
14. **Daksis, J. I., and C. M. Preston.** 1992. Herpes simplex virus immediate early gene expression in the absence of transinduction by Vmw65 varies during the cell cycle. Virology **189**:196–202.
15. **Davis, B. D., R. Dulbecco, H. N. Eisen, and H. S. Ginsberg.** 1990. Microbiology, 4th ed. J. B. Lippincott Co., Philadelphia, Pa.
16. **Debbas, M., and E. White.** 1993. Wild-type p53 mediates apoptosis by E1A, which is inhibited by E1B. Genes Dev. **7**:546–554.
17. **Dyson, N., and E. Harlow.** 1992. Adenovirus E1A targets key regulators of cell proliferation. Cancer Surv. **12**:161–195.
18. **Gallimore, P. H., P. A. Sharp, and J. Sambrook.** 1974. Viral DNA in transformed cells. II. A study of the sequences of adenovirus 2 DNA in nine lines of transformed rat cells using specific fragments of the viral genome. J. Mol. Biol. **89**:49–72.
19. **Goodrum, F. D., T. Shenk, and D. A. Ornelles.** 1996. Adenovirus early region 4 34-kilodalton protein directs the nuclear localization of the early region 1B 55-kilodalton protein in primate cells. J. Virol. **70**:6323–6335.
20. **Graham, F. L., P. J. Abrahams, C. Mulder, H. L. Heijneker, S. O. Warnaar, A. J. de Vries, W. Fiers, and A. J. van der Eb.** 1974. Studies on in vitro transformation by DNA and DNA fragments of human adenoviruses and simian virus 40. Cold Spring Harbor Symp. Quant. Biol. **39**:637–650.
21. **Graham, F. L., J. Smiley, W. C. Russell, and R. Nairn.** 1977. Characteristics of a human cell line transformed by DNA from human adenovirus type 5. J. Gen. Virol. **36**:59–72.
22. **Grand, R. J. A., M. L. Grant, and P. H. Gallimore.** 1994. Enhanced expression of p53 in human cells infected with mutant adenoviruses. Virology **203**:229–240.

23. **Halbert, D. N., J. R. Cutt, and T. Shenk.** 1985. Adenovirus early region 4 encodes functions required for efficient DNA replication, late gene expression, and host cell shutoff. J. Virol. **56**:250–257.
24. **Hodge, L. D., and M. D. Scharff.** 1969. Effect of adenovirus on host cell DNA synthesis in synchronized cells. Virology **37**:554–564.
25. **Jones, N., and T. Shenk.** 1978. Isolation of deletion and substitution mutants of adenovirus type 5. Cell **13**:181–186.
26. **Jones, N., and T. Shenk.** 1979. Isolation of Ad5 host range deletion mutants defective in transformation of rat embryo cells. Cell **17**:683–689.
27. **Kadowaki, T., D. Goldfarb, L. M. Spitz, A. M. Tartakoff, and M. Ohno.** 1993. Regulation of RNA processing and transport by a nuclear guanine release protein and members of the Ras superfamily. EMBO J. **12**:2929–2937.
28. **Kadowaki, T. D., Y. Zhao, and A. M. Tartakoff.** 1992. A conditional yeast mutant deficient in mRNA transport from nucleus to cytoplasm. Proc. Natl. Acad. Sci. USA **89**:2312–2316.
29. **Kafotos, F. C., C. W. Jones, and A. Efstratiadis.** 1979. Determination of nucleic acid sequence homologies and relative concentrations by a dot hybridization procedure. Nucleic Acids Res. **7**:1541–1552.
30. **Kao, C. C., P. R. Yew, and A. J. Berk.** 1990. Domains required for in vitro association between the cellular p53 and the adenovirus 2 E1B 55kD proteins. Virology **179**:806–814.
31. **Kornbluth, S., M. Dasso, and J. Newport.** 1994. Evidence for a dual role for TC4 protein in regulating nuclear structure and cell cycle progression. J. Cell Biol. **125**:705–719.
32. **Koza, R. A., and E. J. Herbst.** 1992. Deficiencies in DNA replication and cell cycle progression in polyamine-depleted HeLa cells. Biochem. J. **281**:87–93.
33. **La Thangue, N. B.** 1994. DP and E2F proteins: components of a heterodimeric transcription factor implicated in cell cycle control. Curr. Opin. Cell. Biol. **6**:443–450.
34. **Ledinko, N.** 1966. Changes in metabolic and enzymatic activities of monkey kidney cells after infection with adenovirus 2. Virology **28**:679–692.
35. **Lehman, T. A., W. P. Bennett, R. A. Metcalf, J. A. Welsh, J. Ecker, R. V. Modali, S. Ullrich, J. W. Romano, E. Appella, J. R. Testa, B. I. Gerwin, and C. C. Harris.** 1991. p53 mutations, ras mutations, and p53-heat shock protein complexes in human lung carcinoma cell lines. Cancer Res. **51**:4090–4096.
36. **Leppard, K. N., and T. Shenk.** 1989. The adenovirus E1B-55 kD protein influences mRNA transport via an intranuclear effect on RNA metabolism. EMBO J. **8**:2329–2336.
37. **Lowe, S. W., and H. E. Ruley.** 1993. Stabilization of the p53 tumor suppressor is induced by adenovirus 5 E1A and accompanies apoptosis. Genes Dev. **7**:535–545.
38. **Martinez-Palomo, A.** 1968. Ultrastructural study of the replication of human adenovirus type 12 in cultured cells. Pathol. Microbiol. **31**:147–164.
39. **Masuda, H., C. Miller, H. P. Koeffler, H. Battifora, and M. J. Cline.** 1987. Rearrangement of the p53 gene in human osteogenic sarcomas. Proc. Natl. Acad. Sci. USA **84**:7716–7719.
40. **Moyne, G., E. Pichard, and W. Bernhard.** 1978. Localization of simian adenovirus 7 (SA 7) transcription and replication in lytic infection. An ultracytochemical and autoradiographical study. J. Gen. Virol. **40**:77–92.
41. **Nevins, J. R.** 1992. E2F: a link between the Rb tumor suppressor protein and viral oncoproteins. Science **258**:424–429.
42. **Nishimoto, T., E. Eilen, and C. Basilico.** 1978. Premature chromatin condensation in a ts DNA-mutant of BHK cells. Cell **15**:475–483.
43. **Ornelles, D. A., and T. Shenk.** 1991. Localization of the adenovirus early region 1B 55-kilodalton protein during lytic infection: association with nuclear viral inclusions requires the early region 4 34-kilodalton protein. J. Virol. **65**:424–439.
44. **Pilder, S., J. Logan, and T. Shenk.** 1984. Deletion of the gene encoding the adenovirus 5 early region 1B 21,000-molecular-weight polypeptide leads to degradation of viral and host cell DNA. J. Virol. **52**:664–671.
45. **Pilder, S., M. Moore, J. Logan, and T. Shenk.** 1986. The adenovirus E1B-55K transforming polypeptide modulates transport or cytoplasmic stabilization of viral and host cell mRNAs. Mol. Cell. Biol. **6**:470–476.
46. **Puvion-Dutilleul, F., J.-P. Bachellerie, N. Visa, and E. Puvion.** 1994. Rearrangements of intranuclear structures involved in RNA processing in response to adenovirus infection. J. Cell Sci. **107**:1457–1468.
47. **Puvion-Dutilleul, F., and E. Puvion.** 1990. Analysis by in situ hybridization and autoradiography of sites of replication and storage of single- and double-stranded adenovirus type 5 DNA in lytically infected HeLa cells. J. Struct. Biol. **103**:280–289.
48. **Puvion-Dutilleul, F., and E. Puvion.** 1990. Replicating single-stranded adenovirus type 5 DNA molecules accumulate within well-defined intranuclear areas of lytically infected HeLa cells. Eur. J. Cell Biol. **52**:379–388.
49. **Puvion-Dutilleul, F., R. Roussev, and E. Puvion.** 1992. Distribution of viral RNA molecules during the adenovirus type 5 infectious cycle in HeLa cells. J. Struct. Biol. **108**:209–220.
50. **Quinlan, M. P.** 1994. Enhanced proliferation, growth factor induction and immortalization by adenovirus E1A 12S in the absence of E1B. Oncogene **9**:2639–2647.
51. **Reich, N. C., P. Sarnow, E. Duprey, and A. J. Levine.** 1983. Monoclonal antibodies which recognize native and denatured forms of the adenovirus DNA-binding protein. Virology **128**:480–484.
52. **Ren, M., E. Coutavas, P. D'Eustachio, and M. G. Rush.** 1994. Effects of mutant Ran/TC4 proteins on cell cycle progression. Mol. Cell. Biol. **14**:4216–4224.
53. **Ren, M., G. Drivas, P. D'Eustachio, and M. G. Rush.** 1993. Ran/TC4: a small nuclear GTP-binding protein that regulates DNA synthesis. J. Cell Biol. **120**:313–323.
54. **Ruley, H. E.** 1983. Adenovirus early region 1A enables viral and cellular transforming genes to transform primary cells in culture. Nature (London) **304**:602–606.
55. **Sarnow, P., C. A. Sullivan, and A. J. Levine.** 1982. A monoclonal antibody detecting the adenovirus type 5 E1b-58kD tumor antigen: characterization of the E1b-58kD tumor antigen in adenovirus-infected and -transformed cells. Virology **120**:510–517.
56. **Scheffner, M., B. A. Werness, J. M. Huibregtse, A. J. Levine, and P. M. Howley.** 1990. The E6 oncoprotein encoded by human papillomavirus types 16 and 18 promotes the degradation of p53. Cell **63**:1129–1136.
57. **Schlenstedt, G., C. Saaverda, D. J. Loeb, C. N. Cole, and P. A. Silver.** 1995. The GTP-bound form of the yeast Ran/TC4 homologue blocks nuclear protein import and the appearance of poly (A)+ RNA in the cytoplasm. Proc. Natl. Acad. Sci. USA **92**:225–229.
58. **Schmidt, M. R., and R. T. Woodland.** 1990. Virus-lymphocyte interactions: inductive signals necessary to render B lymphocytes susceptible to vesicular stomatitis virus infection. J. Virol. **64**:3289–3296.
59. **Shepherd, S. E., J. A. Howe, J. S. Mymryk, and S. T. Bayley.** 1993. Induction of the cell cycle in baby rat kidney cells by adenovirus type 5 E1A in the absence of E1B and a possible influence of p53. J. Virol. **67**:2944–2949.
60. **Spitkovsky, D., P. Steiner, R. V. Gopalkrishnan, M. Eilers, and P. Jansen-Durr.** 1995. The role of p53 in coordinated regulation of cyclin D1 and p21 gene expression by the adenovirus E1A and E1B oncogenes. Oncogene **10**:2421–2425.
61. **Stillman, B.** 1986. Functions of the adenovirus E1B tumor antigens. Cancer Surv. **5**:389–404.
62. **Takahashi, T., M. M. Nau, I. Chiba, M. J. Birrer, R. K. Rosenberg, M. Vinocour, M. Levitt, H. Pass, A. F. Gazdar, and J. D. Minna.** 1989. p53: a frequent target for genetic abnormalities in lung cancer. Science **246**:491–494.
63. **Urbani, L., S. W. Sherwood, and R. T. Schimke.** 1995. Dissociation of nuclear and cytoplasmic cell cycle progression by drugs employed in cell synchronization. Exp. Cell Res. **219**:159–168.
64. **van den Elsen, P. J., A. Houweling, and A. J. van der Eb.** 1983. Morphological transformation of human adenoviruses is determined to a large extent by gene products of region E1A. Virology **131**:242–246.
65. **Vanderplasschen, A., M. Goltz, J. Lyaku, C. Benarafa, H.-J. Buhk, E. Thiry, and P.-P. Pastoret.** 1995. The replication in vitro of the gammaherpesvirus bovine herpesvirus 4 is restricted by its DNA synthesis dependence on the S phase of the cell cycle. Virology **213**:328–340.
66. **Voelkerding, K., and D. F. Klessig.** 1986. Identification of two nuclear subclasses of the adenovirus type 5-encoded DNA binding protein. J. Virol. **60**:353–362.
67. **Vousden, K. H.** 1995. Regulation of the cell cycle by viral oncoproteins. Semin. Cancer Biol. **6**:109–116.
68. **Werness, B. A., A. J. Levine, and P. M. Howley.** 1990. Association of human papilloma virus types 16 and 18 E6 proteins with p53. Science **248**:76–79.
69. **White, E.** 1994. Function of the adenovirus E1B oncogene in infected and transformed cells. Semin. Virol. **5**:341–348.
70. **Wolgemuth, D. J., and M.-T. Hsu.** 1981. Visualization of nascent RNA transcripts and simultaneous transcription and replication in viral nucleoprotein complexes from adenovirus 2-infected HeLa cells. J. Mol. Biol. **147**:247–268.
71. **Yamaguchi, H., K. Hosokawa, Z.-L. Jiang, A. Takahashi, T. Ikehara, and H. Miyamoto.** 1993. Arrest of cell cycle progression in HeLa cells in the early G1 phase in K+-depleted conditions and its recovery upon addition of insulin and LDL. J. Cell. Biochem. **53**:13–20.
72. **Yew, P. R., and A. J. Berk.** 1992. Inhibition of p53 transactivation required for transformation by adenovirus early 1B protein. Nature (London) **357**:82.
73. **Yew, R. P., X. Lui, and A. J. Berk.** 1994. Adenovirus E1B oncoprotein tethers a transcriptional repression domain to p53. Genes Dev. **8**:190–202.
74. **Zantema, A., J. A. M. Fransen, A. Davis-Oliver, F. C. S. Ramaekers, G. P. Vooijs, B. DeLeys, and A. J. van der Eb.** 1985. Localization of the E1B proteins of adenovirus type 5 in transformed cells as revealed by interaction with monoclonal antibodies. Virology **142**:44–58.
75. **Zantema, A., P. I. Schrier, A. Davis-Oliver, T. van Laar, R. T. M. J. Vaessen, and A. J. van der Eb.** 1985. Adenovirus serotype determines association and localization of the large E1B tumor antigen and cellular tumor antigen p53 in transformed cells. Mol. Cell. Biol. **5**:3084–3091.

Nat. Gent. 1992 1:372-378
Science 1989 245:1234-1236

Eur. J Biochem. 1985 148:265-270

Mol. Immunol 1995 32:1057-1064

Science 1993 259:988-990

Nature 1988 336:348-352

J Clin. Invest. 1993 91:225-234

Mol. Cell. Biol. 1987 7:1576-1579

Gene 1982 19:33-42

Neuron 1992 8:507-520

Adv. Virus Res. 1989 37:35-83

1994 Cancer Res. 54:5258-5261

Cell 1987 50:435-443

Nucleic Acids Res. (1996) 24(10):1841-1848

J Biol. Chem. 1988 263 10 :4837-4843

Proc. Natl. Acad. Sci. USA 1992 89:2581-2584

1993 Nature 361:647-650

DNA Seq. 1993 4:185-196

Human Gene Ther. 1995 6:881-893

Science 1991 252:431-434

Cell 1992 68:143-155

Mol. Cell. Biol. 1990 10 6 :2738-2748

Nucleic Acids Res. 1996 24 15 :2966-2973

Human Gene Thera 1990 1:241-256

J Clin. Invest 1992 . 90:626-630

Curr. Topics in Micro. and Imm. 1995 199 part 3 :177-194

Lancet 1981 11:832-834

Cancer Res. 1996 56:1341-1345

J Virol. 1992 66 (6) :3633-3642

J Virol. 1996 70 (4) :2296-2306

Nature (1997) 389:239-242

J Virol. 1984 51 (3) : 822-831

Adv. Ex . Med. Biol. 1991 3098:61-66

Proc. Natl. Acad. Sci. 1983 80:5383-5386

Genomics 1990 8:492-500

Gastroenter. 1990 98:470-477 .

N. Vogel
Au 1636
12/9
10045116

JOURNAL OF VIROLOGY, Apr. 1996, p. 2296–2306
0022-538X/96/$04.00+0

Vol. 70, No. 4

The Adenovirus Death Protein (E3-11.6K) Is Required at Very Late Stages of Infection for Efficient Cell Lysis and Release of Adenovirus from Infected Cells

ANN E. TOLLEFSON,[1] ABRAHAM SCARIA,[1]† TERRY W. HERMISTON,[1] JAN S. RYERSE,[2] LORA J. WOLD,[1] AND WILLIAM S. M. WOLD[1]*

Department of Molecular Microbiology and Immunology[1] and Department of Pathology,[2] St. Louis University School of Medicine, St. Louis, Missouri 63104

Received 21 November 1995/Accepted 5 January 1996

Adenovirus (Ad) infection is concluded by assembly of virions in the cell nucleus followed by lysis of cells by an unknown mechanism. We have described an Ad nuclear membrane glycoprotein of 11,600 kDa (E3-11.6K) which is encoded by the E3 transcription unit and which is synthesized in small amounts from the E3 promoter at early stages of infection but in large amounts from the major late promoter at very late stages of infection. We now report that E3-11.6K is required for the efficient lysis (death) of Ad-infected cells, and we propose that the function of E3-11.6K is to mediate the release of Ad progeny from infected cells. We have renamed E3-11.6K the Ad death protein (ADP). Virus mutants that lack ADP replicated as well as *adp*$^+$ Ad, but the cells lysed more slowly, virus release from the cell was retarded, and the plaques were small and developed slowly. Cells infected with *adp*$^+$ viruses began to lyse at 2 or 3 days postinfection (p.i.) and were completely lysed by 5 or 6 days p.i. In contrast, cells infected with *adp* mutants did not begin significant lysis until 5 or 6 days p.i. Cell lysis and viability were determined by plaque size, extracellular virus, cell morphology, release of lactate dehydrogenase, trypan blue exclusion, the 3-(4,5-dimethylthiazol-2-yl)-2,5-diphenyl-2H-tetrazolium bromide (MTT) assay for mitochondrial activity, RNA degradation, and DNA degradation as determined by agarose gel electrophoresis and the terminal deoxynucleotidyltransferase end labeling assay. Protein synthesis was almost nonexistent at 3 days p.i. in cells infected with *adp*$^+$ Ads, but it was still increasing in cells infected with *adp* mutants. Host cell protein synthesis was undetectable at 1 day p.i. in cells infected with *adp*$^+$ Ads or *adp* mutants. Cells infected with *adp* mutants showed Ad cytopathic effect at 1 or 2 days p.i. in that they rounded up and detached, but the cells remained metabolically active and intact for >5 days p.i. When examined by electron microscopy, the nuclei were extremely swollen and full of virus, and the nuclear membrane appeared to be intact. ADP is unrelated in sequence to other known cell death-promoting proteins.

Human adenoviruses (Ads) consist of a nonenveloped icosahedral capsid (reviewed in reference 45). The linear duplex DNA genome within the capsid is tightly associated with Ad-encoded core proteins. Infection of cultured cells is initiated via binding of the Ad fiber capsid protein to an unknown cellular receptor. This is followed by endosome-mediated internalization of the virion via interaction between the penton capsid protein and $\alpha_v\beta_3$ and $\alpha_v\beta_5$ integrins (63). The virion is sequentially disassembled and extruded from the acidified endosome (20), and then the DNA-protein core enters the nucleus.

In the nucleus, the immediate-early E1A proteins are expressed initially, and then they induce transcription of the delayed-early genes in the E1B, E2, E3, E4, and L1 (early) transcription units (reviewed in references 2 and 34). About 25 early proteins function to usurp the cell, convert it into an efficient factory for virus replication, carry out viral DNA replication, and counteract host antiviral defenses (reviewed in reference 27). Viral DNA replication begins at about 7 h postinfection (p.i.), and then the infection moves into the late phase. Late proteins are primarily virion proteins and proteins required for assembly of infectious virions. Synthesis of cellular DNA, mRNA, and proteins is inhibited at late stages. Virions begin to assemble in the cell nucleus at about 1 day p.i. (reviewed in reference 12) and continue to increase in abundance until 2 or 3 days p.i.

The fate of Ad virions at the termination of productive infection is unclear and has not been investigated in detail. Most Ad researchers prepare Ad stocks by extracting virions from infected cells at 2 or 3 days p.i., a time when there is much less virus in the culture supernatant than within the cells. It is not known whether cells eventually lyse and release free infectious virions or whether Ad remains associated with cells or cellular remnants. If the cells do lyse, is it a nonspecific process, or is there a specific mechanism?

An 11,600-kDa protein (E3-11.6K) that is encoded by the E3 transcription unit has been described previously (64). E3-11.6K is an integral membrane glycoprotein that contains O-linked and complex N-linked oligosaccharides (41). E3-11.6K initially localizes to the endoplasmic reticulum and Golgi apparatus and then ultimately to the Golgi apparatus and nuclear membrane (41). Interestingly, although E3-11.6K is encoded within the early E3 transcription unit, it is synthesized in only very small amounts from the E3 promoter at early stages of infection (52). Rather, E3-11.6K is synthesized very abundantly from the Ad major late promoter beginning at about 20 to 25 h p.i. (52). In fact, E3-11.6K primarily is a late protein, and it represents the sixth family of major late proteins (52).

In this communication, we report that E3-11.6K is required for the efficient lysis of Ad-infected cells beginning at 2 or 3

* Corresponding author. Mailing address: Department of Molecular Microbiology and Immunology, St. Louis University School of Medicine, 1402 S. Grand Blvd., St. Louis, MO 63104. Phone: (314) 577-8435. Fax: (314) 773-3403.

† Present address: Genzyme Corporation, Framingham, MA 01701.

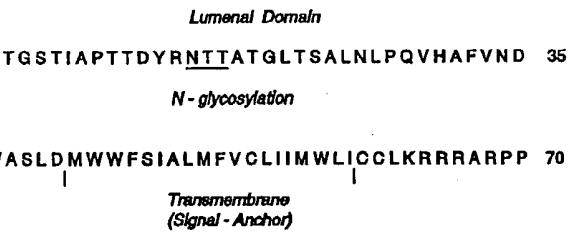

FIG. 1. Amino acid sequence of ADP from Ad2 (64). The *adp* gene is located at nucleotides 29468 to 29771 in the Ad2 genome. Shown are the single Asn-linked glycosylation site, the predicted signal-anchor transmembrane domain, and the predicted N_{lumen}-C_{exo} orientation in the membrane (41). ADP localizes primarily to the nuclear membrane at >30 h p.i., but it is not known whether localization is to the inner or outer nuclear membrane (41).

days p.i. We propose that the function of E3-11.6K is to mediate the release of virus from the infected cell. Considering that E3-11.6K is required for efficient cell lysis (death), we have renamed it the Ad death protein (ADP).

MATERIALS AND METHODS

Cells and viruses. Human A549 cells were grown in Dulbecco's modified Eagle's medium (DMEM) containing 10% fetal bovine serum (FBS). Virus stocks were prepared in suspension cultures of human KB cells and banded in CsCl, and the titers of virus were determined using A549 cells as described previously (21). Plaques were counted at 2- or 3-day intervals until ca. 4 weeks p.i.

The viruses used in this study are Ad type 5 (Ad5) (wild type), Ad2 (wild type), and *rec*700 (wild type). *rec*700 is an Ad5-Ad2-Ad5 recombinant consisting of the Ad5 *Eco*RI A (map positions 0 to 76), Ad2 *Eco*RI D (map positions 76 to 83), and Ad5 *Eco*RI B (map positions 83 to 100) fragments (65). *rec*700 is the parental virus for *dl*712 (11), which lacks the entire *adp* gene, and for *pm*734.1 (with ADP residues 1 to 48 deleted [Δ1-48]), which has Met-1 and Met-41 in ADP mutated to Ser so that the 101-residue ADP (Fig. 1) initiates at Met-49. Construction of *pm*734.1 will be described elsewhere. *pm*734.1 does not express ADP sequences that are detectable by immunoprecipitation (53). H5*dl*309 (28), which has the genes for the E3 10.4K, 14.5K, and 14.7K proteins deleted (3), expresses ADP (53). H5*dl*327, which is isogenic with H5*dl*324 (50), has all E3 genes except the gene for the 12.5K protein deleted. H2*dl*801 (5) has all E3 genes except those for the 12.5K and 14.7K proteins deleted (24, 57).

Virus growth curves. For assay of virus growth, A549 cells (2.9×10^6 cells per 60-mm-diameter dish) were infected at 20 PFU per cell in 2 ml of serum-free DMEM. At the end of 1.5 h, the medium was removed and the cells were washed with DMEM (10% FBS), then 5 ml of DMEM (2% FBS) was added, and the cells were incubated at 37°C. At the times indicated in the figures, the supernatant was removed and centrifuged to collect cells; the cells were returned to the dish in 2 ml of DMEM (2% FBS). Monolayers were freeze-thawed three times in the dishes and then collected. Supernatant and monolayer samples were assayed by plaque assay to determine the virus titer.

LDH release assay. A549 cells (1.5×10^6 per 60-mm-diameter dish) were infected at 20 PFU per cell. At 6 h p.i., the cells were trypsinized and 1.0×10^4 cells (100-μl aliquots) were plated per well in 96-well plates in 8% FBS–DMEM. Twenty-microliter samples were removed at the times indicated in the figures and assayed for lactate dehydrogenase (LDH) release with the Cytotox 96 assay (Promega Biotec Corp., Madison, Wis.). Samples were assayed in triplicate, and results were read on a EL340 Microplate reader (BioTec Instruments, Inc.) at 490 nm.

MTT assay. A549 cells were infected at 20 PFU per cell, and 2.3×10^4 cells were plated per well in 96-well plates at 6 h p.i. At times p.i., 20 μl of 3-(4,5-dimethylthiazol-2-yl)-2,5-diphenyl-2H-tetrazolium bromide (MTT) (Sigma Chemical Co., St. Louis, Mo.) in phosphate-buffered saline (PBS) (5 mg/ml) was added to each well. After 2 h, lysis buffer (20% sodium dodecyl sulfate [SDS] in 50:50 dimethyl formamide–double-distilled water, pH 4.7) was added to each well, and the plates were incubated overnight at 37°C. Results were read on a microplate reader at 570 nm; samples were processed in triplicate.

Trypan blue exclusion assay. A549 cells were infected at 100 PFU per cell (1.3×10^6 cells per 60-mm-diameter dish) in 1 ml of serum-free DMEM; at 1 h p.i., 4 ml of DMEM (10% FBS) was added to each dish. At the times indicated in the figures, the supernatant was removed and cells were trypsinized. The supernatants and cells were combined, and trypan blue (GibcoBRL, Gaithersburg, Md.) was added to a final concentration of 0.02%. Cells were counted with a hemacytometer (a total of 600 to 1,000 cells were counted per time point). Similar results were obtained when cells were infected with 20 PFU of virus per cell.

Protein synthesis. A549 cells were mock infected or infected with 20 PFU of *rec*700 or *dl*712 per cell, metabolically labeled for 2 h with 25 μCi of Expre^{35}S^{35}S (NEN Dupont Research Products, Boston, Mass.) at different periods p.i., and then proteins were analyzed by SDS-polyacrylamide gel electrophoresis (SDS-PAGE) (52). All gels were 15% polyacrylamide. Some samples were treated with 20 μg of 1-β-D-arabinofuranosylcytosine (araC) per ml; araC inhibits viral DNA replication and prevents the transition from early to late stages of infection.

DNA and RNA degradation assay by agarose gel electrophoresis. A549 cells (1.8×10^6 cells per 60-mm-diameter dish) were infected at 25 PFU per cell. The cells were trypsinized at 4 h p.i. and then replated at 3.6×10^5 cells per 35-mm-diameter dish. On subsequent days, Hirt supernatants were prepared (65), treated with RNase, electrophoresed on a 1.5% agarose gel, stained with ethidium bromide, and visualized under UV light. RNA was analyzed in the same manner but without treatment with RNase.

DNA degradation assay by the terminal deoxynucleotidyltransferase end labeling (TUNEL) method. A549 cells were plated on no. 1 coverslips 1 day prior to infection. The cells were infected at 50 PFU per cell in 1 ml of serum-free DMEM; at 1 h p.i., 1 ml of DMEM (10% FBS) was added and the cells were incubated at 37°C. At 58 h p.i., the cells were rinsed with PBS, then fixed with paraformaldehyde (3.7% in PBS) for 10 min at room temperature, and treated with methanol for 6 min at −20°C. DNA was stained with 4′,6-diamidino-2-phenylindole (DAPI) (2 μg/ml) in methanol at room temperature for 2 min and then rinsed with methanol and then with 70% ethanol. Cells on coverslips were processed to detect DNA fragmentation by the addition of dUTP-digoxigenin by terminal deoxynucleotidyltransferase and detection of digoxigenin by fluorescein isothiocyanate-conjugated antibody (ApopTag in situ apoptosis detection kit; Oncor, Inc., Gaithersburg, Md.).

Light microscope cytology. A549 cells were infected at 20 PFU per cell. At daily intervals, the cells were gently trypsinized and pelleted for 1 min at 5,000 rpm in a microcentrifuge. After the supernatant was discarded, the cell pellets were fixed overnight at 4°C in 2.5% glutaraldehyde in 0.1 M sodium cacodylate buffer (pH 7.3) containing 2% sucrose and 1 mM calcium chloride. The tissue was washed several times in cold cacodylate buffer containing 5% sucrose and postfixed for 3 h at 4°C with 1% osmium tetroxide in cacodylate buffer containing 2% sucrose. The tissue was washed twice at room temperature with distilled water, stained en bloc for 1 h with 2.5% aqueous uranyl acetate, dehydrated through graded ethanols and propylene oxide, and infiltrated overnight with a 1:1 mixture of propylene oxide and Polybed resin (Polysciences, Inc., Warrington, Pa.). The tissue was then infiltrated for 6 h with 100% Polybed resin and embedded in fresh resin in BEEM capsules and polymerized overnight at 70°C. Sections (0.5 μm thick) were cut from the trimmed tissue blocks with a Reichert Ultracut E ultramicrotome and glass knives, dried onto glass microscope slides, stained with toluidine blue, and photographed on a Zeiss research light microscope with Kodak T-max 100 film. The film was developed with Kodak HC110 developer, dilution B, and printed on Kodak paper.

Electron microscopy. Cells at 4 days p.i. were prepared as described above. Silver-gray thin sections were cut from the trimmed tissue blocks with a Reichert Ultracut E ultramicrotome by using a diamond knife and were collected on 200-mesh copper grids. The sections were stained with uranyl acetate and lead citrate and viewed and photographed with a JEOL 100 CX electron microscope at 60 kV.

RESULTS

Cells infected with *adp* mutants have small plaques that are slow to develop. The first clue to the function of ADP as a cell death-promoting agent came from studies of the plaque morphology of virus mutants that lack the *adp* gene. Ad5, H5*dl*309, Ad2, and *rec*700 form large, distinct plaques (Fig. 2). These viruses all express ADP. In contrast, H5*dl*327, H2*dl*801, and *dl*712 have much smaller plaques (Fig. 2). These viruses all lack the *adp* gene, and *dl*712 lacks only the *adp* gene.

The difference in plaque sizes among *adp* mutants can be quantitated by observing the rate at which the plaques develop. Figure 3 illustrates the rate of plaque development for the experiment whose results are shown in Fig. 2. The data are presented as the number of plaques observed on any given day of the plaque assay as a percentage of the final number of plaques that were observed at the end of the plaque assay (on the *y* axis) versus the number of days of the plaque assay (on the *x* axis). At 10 days p.i., 10% of the final number of plaques were observed with H5*dl*327, which lacks ADP, versus 90 to 95% of the final plaques with Ad5 and H5*dl*309, which express

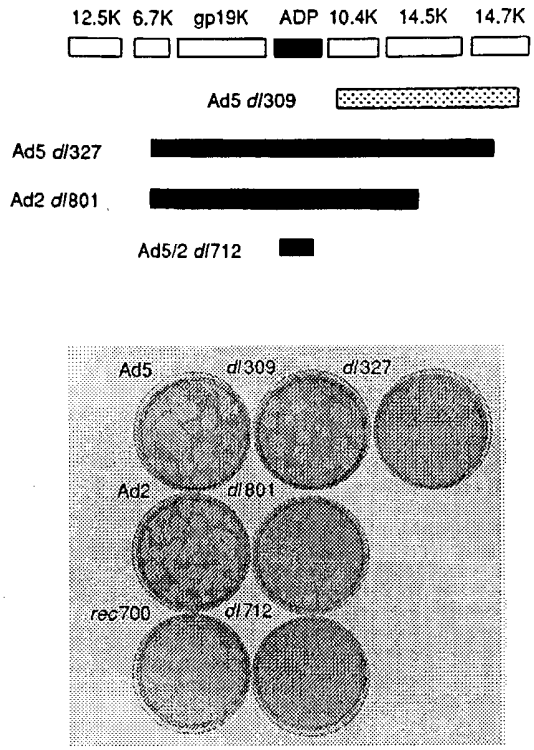

FIG. 2. Plaque morphology of wild-type Ads and Ads that have deletions in the E3 transcription unit. The plaques are on human A549 cells at 14 days p.i. *rec*700 is an Ad5-Ad2-Ad5 recombinant that, in common with Ad5 and Ad2, has a wild-type phenotype with respect to the properties of ADP. *rec*700 has the Ad2 version of ADP. The genes deleted in the mutants H5*dl*309, H5*dl*327, H2*dl*801, and *dl*712 are indicated in the schematic. All mutants that lack the *adp* gene have much smaller plaques than do the Ads that retain the *adp* gene, as shown below the diagram.

ADP (Fig. 3A). With H2*dl*801, which lacks ADP, 25% of the final plaques were observed at 10 days versus 90% for Ad2 (Fig. 3B). With *dl*712, in which the ADP gene is the only E3 gene deleted, 8% of the final plaques were observed at 10 days compared with 75% with *rec*700 (Fig. 3C). The deletion in *dl*712 changes the splicing of the E3 mRNAs at early stages of infection, and therefore the relative abundance of the E3 proteins at early stages is affected (11). The *dl*712 deletion does not have a marked effect on the E3 mRNAs at late stages of infection (data not shown), the period when ADP is synthesized abundantly. Nevertheless, we constructed *pm*734.1 (Δ1-48), a double missense mutant which does not express detectable ADP (53). With *pm*734.1 and *dl*712, 10% of the final plaques were observed at 10 days p.i. versus 85% with *rec*700 (Fig. 3D). Thus, *pm*734.1 is as defective as *dl*712 in promoting cell death, not only in the plaque development assay (Fig. 3D) but also in all other assays of cell viability (e.g., see Fig. 5).

We conclude that mutants that do not express functional ADP have small plaques that are slow to develop. (We note that in order to obtain an accurate titer for *adp* mutants, it is necessary to keep the A549 cell monolayer alive for 20 to 30 days.) The small-plaque phenotype is specific to the *adp* gene, as indicated by plaque morphology and development studies of virus mutants with individual deletions of the E3 genes (data not shown).

Mutants with alterations in the *adp* gene could have small plaques because they do not grow as well as wild-type Ad or because progeny virions are released more slowly from cells than wild-type virions. If the virions are released more slowly, then it will take longer for the virus to spread from cell to cell and form a plaque. To address these two possibilities, monolayers of A549 cells were infected with *rec*700 (wild type) or *dl*712 (ADP negative [ADP$^-$]); then the virions present in the cells and released into the culture supernatant were quantitated by plaque assay. The amounts of virus within cells increased rapidly until about 2 days p.i. with both *rec*700 and *dl*712 and then declined slightly for *rec*700 but remained stable for *dl*712 (Fig. 4). It is clear that *dl*712 grows as well as *rec*700. This is consistent with many experiments in which CsCl-banded virus stocks of wild-type Ad and *adp* mutants had similar titers (e.g., Fig. 3). When the culture supernatant was examined, a dramatic difference was seen between *rec*700 and *dl*712: from 2 to 4 days p.i., there were 10^{10} to 10^{11} *rec*700 infectious particles but only 10^7 to 10^8 *dl*712 infectious particles per ml (Fig. 4). Thus, *adp* mutant virions are released more slowly from cells than are wild-type virions. (It is unclear why 10^5 to 10^7 infectious virions were found in the culture supernatants at 12 to 30 h p.i., prior to progeny virus assembly [12 h] or cell lysis [30 h; see below], but this was a reproducible observation. Possibly, these are virions that remained adsorbed to cells during the infection and subsequent washings before addition of media. Also, 6×10^7 PFU of virus was added to each dish; if 1 to 3% of cells undergo spontaneous lysis in the period immediately following infection and these cells release virus, this could account for the background levels of virus observed in the experiment.)

Cells infected with *adp* mutants stay alive much longer than cells infected with *adp*$^+$ Ad. The data in Fig. 2 to 4 raise the possibility that cells infected with *rec*700 (wild type) are lysed more rapidly than are cells infected with *dl*712 (ADP$^-$), so several cell viability assays were employed. With *rec*700, A549 cell lysis assayed by the release of LDH began at 2 days p.i. and increased until 7 days p.i. (Fig. 5A). In marked contrast, with two *adp* mutants, *dl*712 and *pm*734.1 (Δ1-48), the cells did not release LDH until 6 days p.i.

Trypan blue exclusion was also used to assay cell viability. With *rec*700, 60% of A549 cells were dead by 3 days p.i. and 90% were dead by 5 days p.i. (Fig. 5B). With *pm*734.1 (Δ1-48) and *dl*7001 (which lacks all E3 genes, including *adp*), 90% of cells were alive at 5 days and cell death began only at 6 days p.i. The *pm*734.1-infected cells died with the same kinetics as cells infected with *dl*7001, indicating that none of the E3 genes except *adp* plays a major role in promoting cell death.

The MTT assay was carried out to monitor the mitochondrial activity in infected cells. Cells infected with *rec*700 and *dl*712 were similar until 2 days p.i., but then cells infected with *rec*700 began to lose mitochondrial activity, and all cells were dead by 5 days (Fig. 5C). Cells infected with *dl*712 retained 90% of mitochondrial activity at 5 days p.i. Human A549 cells were used in the experiment whose results are shown in Fig. 5C; similar results were obtained with monolayers of human KB cells and A431 cells (data not shown).

These results indicate that cells infected with *adp* mutants remain viable much longer than cells infected with wild-type Ad.

As another indicator of cell viability, we examined protein synthesis. Cells were labeled with [^{35}S]Met-Cys for 2 h at different periods p.i., and then proteins were resolved by SDS-PAGE. With *rec*700, Ad late protein synthesis was readily apparent at 25 and 29 h p.i. (Fig. 6A; compare the protein bands in lanes d and e with those of mock-infected cells [lane a] and mock- and Ad-infected cells treated with araC [lanes b and c]). Protein synthesis began to decline at 45 h p.i. (Fig. 6A,

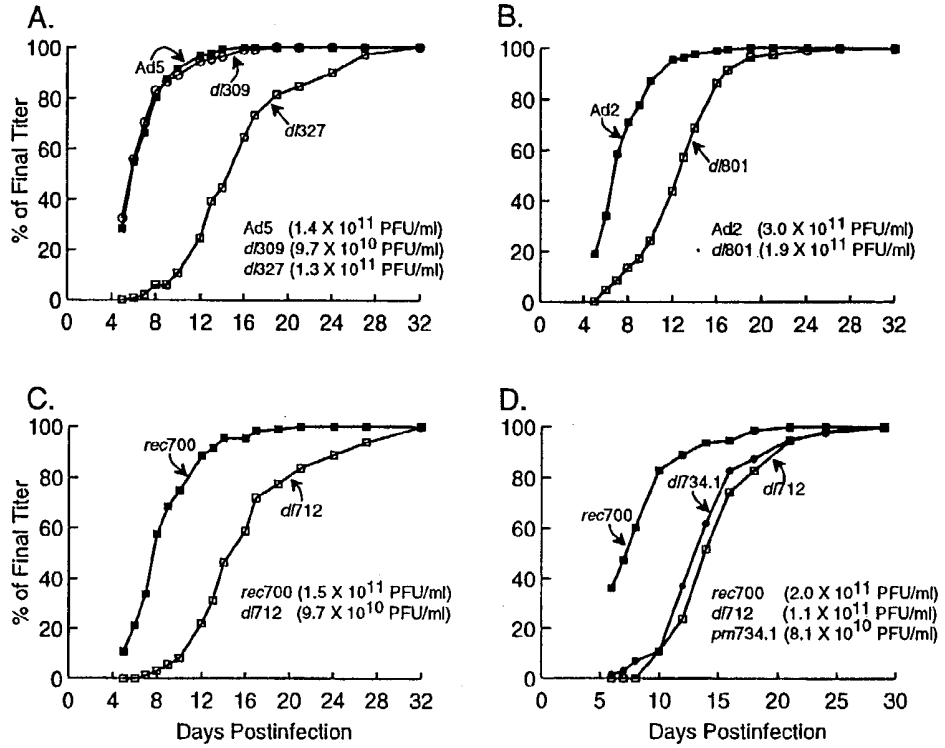

FIG. 3. Plaque development assay for mutants with alterations in ADP. Panels A to C are from the experiment whose results are shown in Fig. 2; panel D is from a separate experiment. The *y* axis shows the number of plaques observed on any given day of the plaque assay (the *x* axis), as a percentage of the number of plaques observed on the final day (day 32 or 30, as indicated) of the plaque assay. Each panel shows the final titer of the CsCl-banded virus stock that was assayed. A549 cells were used. The plaques of mutants that lack ADP (*dl*327, *dl*801, *dl*712, and *pm*734.1) developed much more slowly than *adp*$^+$ viruses, but the final titers obtained for all virus stocks were similar.

lane f) and was barely detectable at 71 h p.i. (lane h). In marked contrast, with *dl*712, the rate of protein synthesis was still increasing at 71 h p.i. (Fig. 6A, lanes j to n). In a separate experiment, protein synthesis was examined up to 6 days p.i., and this was correlated with cell viability as determined by trypan blue exclusion. The gel was overexposed in order to detect protein synthesis at very late times. With *rec*700, Ad late proteins were synthesized actively at 2 days p.i., a time when

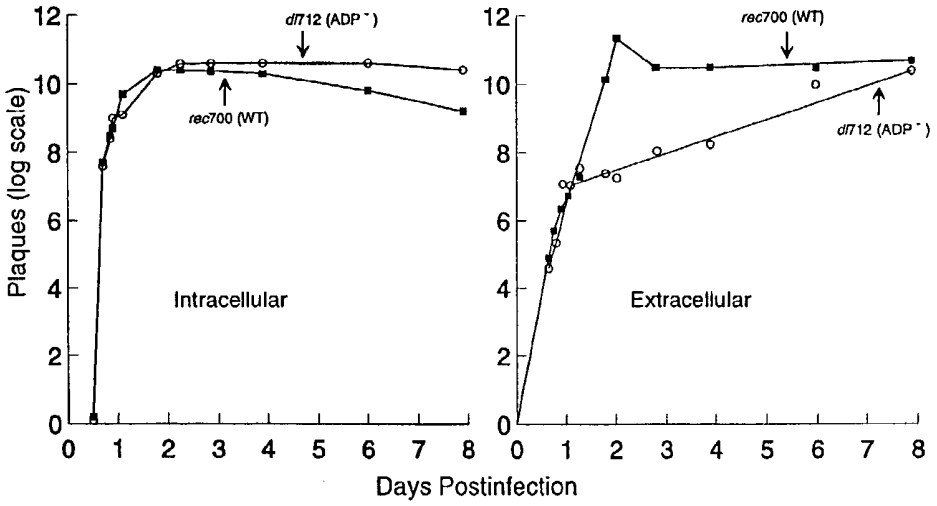

FIG. 4. Assay for the accumulation of *rec*700 (wild-type [WT]) and *dl*712 virions inside cells and in the extracellular medium. Monolayers of A549 cells were infected, and the virus present within the cells (left panel) and in the culture supernatant (right panel) was quantitated by plaque assay. The data show that the *adp* mutant grows as well as the wild-type virus within the cells but that the mutant virions are released much more slowly from the infected cells than are wild-type virions.

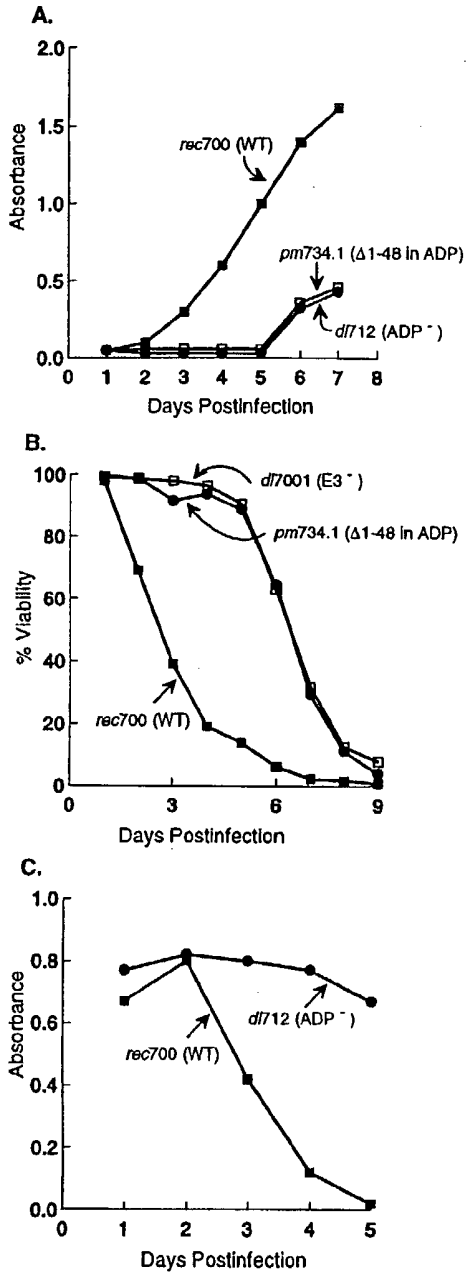

FIG. 5. Cell viability assays for A549 cells infected with *rec*700 (wild type [WT]) or mutants that lack a functional *adp* gene. *dl*712 lacks the entire *adp* gene, *pm*734.1 (Δ1-48) synthesizes only residues 49 to 101 of ADP, and *dl*7001 lack all the genes in the E3 transcription unit. (A) Cells were infected and cell lysis was measured by release of LDH into the culture medium. Cells infected with *rec*700 died (i.e., released LDH) much more rapidly than did cells infected with the two *adp* mutants. (B) Cells were infected, and the percentage of viable cells was determined on the basis of exclusion of trypan blue from the cells. Cells infected with *rec*700 died much more rapidly than did cells infected with *dl*7001 or *pm*734.1. (C) Cells were infected and cell viability was assayed (MTT assay) on the basis of mitochondrial activity within the cells. Cells infected with *dl*712 remained metabolically active much longer than cells infected with *rec*700.

66% of the cells were viable (Fig. 6B, lane c). Protein synthesis declined dramatically at 3 days and was undetectable at 5 days, when 48 and 16%, respectively, of the cells were viable (Fig. 6B, lanes d to f). With *pm*734.1 (Δ1-48), the rate of protein synthesis increased until 3 days, declined slightly at 4 days, and declined dramatically at 5 days p.i. (Fig. 6B, lanes j to m). On days 2 to 5, from 95 to 84% of the cells were viable. Thus, active protein synthesis continued for at least 2 days longer in cells infected with the two *adp* mutants than in those infected with wild-type Ad.

With *pm*734.1 (Fig. 6B, lane m) and *dl*712 (data not shown), it is interesting that protein synthesis had nearly ceased even though most of the cells were still viable (i.e., still intact, as indicated by trypan blue exclusion). This was also the case for *rec*700 (Fig. 6A, lanes f to h).

Another noteworthy result is that *rec*700 and the two *adp* mutants were equally effective in suppressing the synthesis of host cell proteins (Fig. 6). Thus, the prolonged synthesis of Ad proteins in cells infected with *adp* mutants is not due to the inability of the mutants to block host protein synthesis (e.g., it is unlikely that the host cell synthesizes antiapoptosis proteins in *adp* mutant-infected cells and not in wild-type-infected cells).

As still another indication of cell viability, cellular RNA and DNA were examined. When total cellular RNA was analyzed by agarose gel electrophoresis, the RNA was degraded by 3 days p.i. with *rec*700, but it was intact at 5 or 6 days p.i. in cells infected with *dl*712 (Fig. 7). The DNA from cells infected with *rec*700 or *dl*712 was intact at 2 days p.i., but at 3 to 5 days p.i. the DNA from *rec*700 was much more degraded than the DNA from *dl*712 (Fig. 8). A DNA ladder characteristic of apoptosis was not observed, even though DNA from cells undergoing apoptosis (dying thymocytes) yielded such a ladder on a comparable gel (data not shown). The TUNEL assay was also used to monitor DNA integrity. This assay uses a fluorescein isothiocyanate-coupled monoclonal antibody to digoxigenin to detect digoxigenin-labeled nicked DNA in fixed cells. With mock-infected cells, two nuclei contained nicked DNA (Fig. 9; compare the fields in which the DNA was stained with DAPI with the fields stained with the ApopTag kit). With *rec*700, most of the nuclei had nicked DNA, whereas with *dl*712 virtually none of them did (Fig. 9). Thus, DNA is degraded much sooner in cells infected with *rec*700 than in those infected with *dl*712.

When cells were examined by microscopy at 4 days p.i., the majority of *rec*700-infected cells were lysed, whereas nearly all *pm*734.1 (Δ1-48)-infected cells were intact (Fig. 10). The nuclei in the *pm*734.1-infected cells were extremely swollen, occupying nearly the entire cell; this is shown clearly in the electron micrograph in Fig. 11A. The nucleus was full of virus; in fact, a crystal array of virus is apparent. The nuclear membrane appeared to be intact. Figure 11B shows a *rec*700-infected cell; the cell is totally lysed. Note that the cell does not have features typical of apoptosis, i.e., condensed chromatin, cell shrinkage, membrane blebbing, and membrane-bound apoptotic bodies.

We conclude from all these data that ADP is required for the efficient lysis (death) of Ad-infected cells at very late stages of infection.

ADP is not required for Ad CPE. Although it is clear that cells infected with *adp* mutants remain viable for several days longer than those infected with *adp*$^+$ Ads, monolayer cells show typical Ad cytopathic effect (CPE). For both the wild type and *adp* mutants, CPE was observed between 1 and 2 days p.i. and was very pronounced by 3 days p.i. An example of such cells at 4 days p.i. is shown in Fig. 12. Cells infected with *rec*700

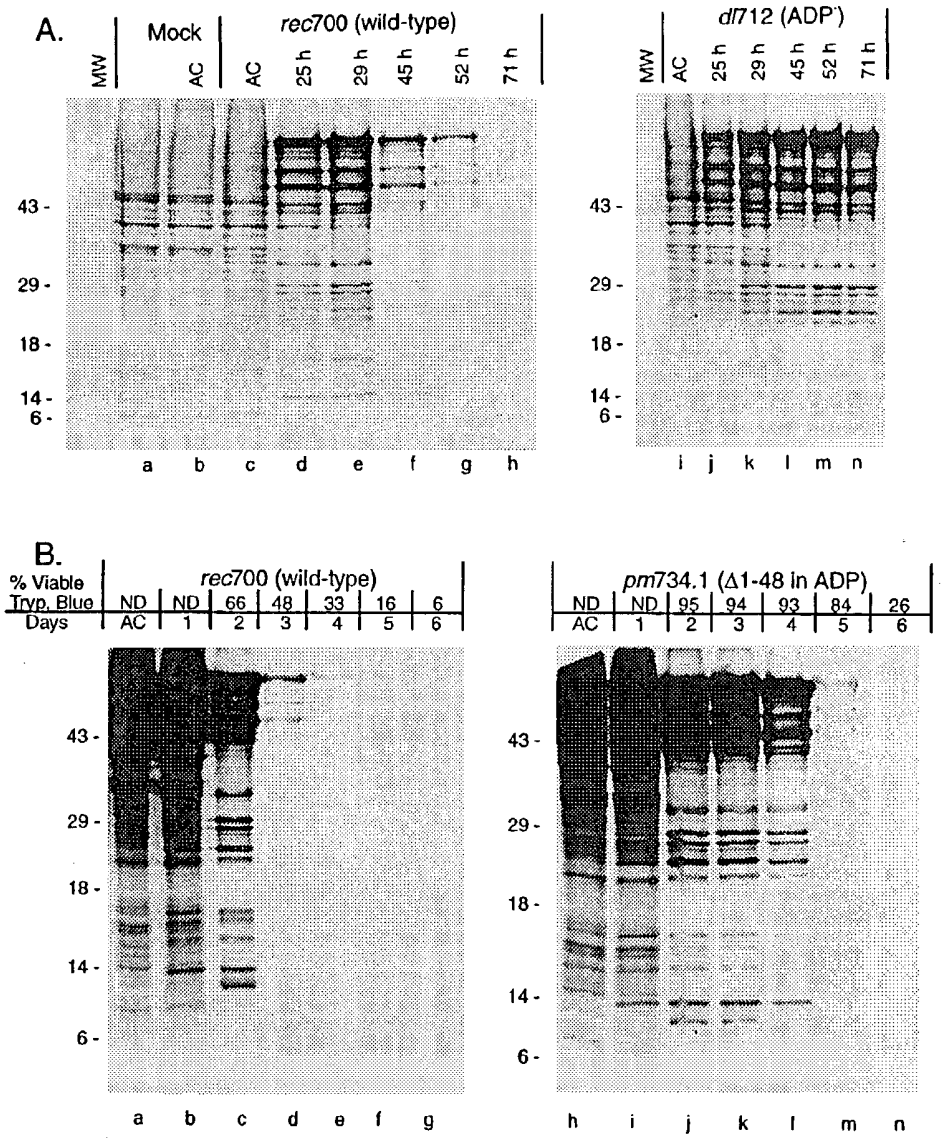

FIG. 6. Protein synthesis in cells infected with *rec*700, *dl*712, or *pm*734.1. A549 cells were mock infected or infected with *rec*700, *dl*712, or *pm*734.1 and metabolically labeled for 2 h with 25 μCi of Expre^{35}S^{35}S (NEN Dupont) at the indicated times p.i., and then proteins were analyzed by SDS-PAGE. Panels A and B are results of separate experiments. In panel B, cell viability was determined by trypan blue exclusion in parallel with labeling of the proteins. araC (AC) inhibits viral DNA replication and prevents the transition from early to late stages of infection. ND, not done; MW, molecular weight markers (weights are shown to the left of the gels, in thousands). At 25 h p.i., Ad late proteins are readily apparent, and host cell protein synthesis is curtailed.

had rounded up and detached from the plastic dishes into individual floating cells, many of which showed ballooning of the plasma membrane as if the cells had lost the ability to control osmotic pressure. On the basis of our measurements of cell viability and macromolecular synthesis and integrity, most of these cells were probably dead. With *pm*734.1 (Δ1-48), the cells had rounded up and detached into grape-like clusters. The cells were highly refractile and intact. As judged by our viability studies, most of these cells should be viable. These cells were metabolically active as indicated by the acidity (pH) of the medium (data not shown). By day 6, when many of the *adp* mutant-infected cells were dead, the grape-like clusters had dispersed into single floating cells (data not shown) in the manner of *rec*700-infected cells at day 4. That is, most of the

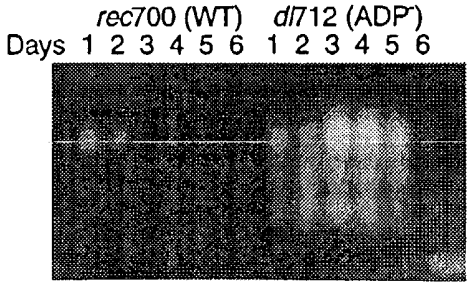

FIG. 7. Agarose gel assay for total cellular RNA in cells infected with *rec*700 (wild type [WT]) or *dl*712 at days 1 to 6 p.i.

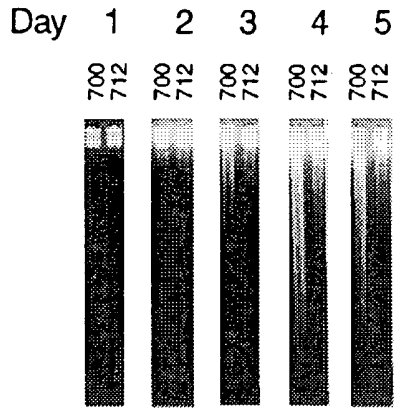

FIG. 8. Agarose gel DNA degradation assay for cells infected with *rec*700 (wild type) (lanes 700) and *dl*712 (ADP$^-$) (lanes 712). The DNA from cells infected with *rec*700 was degraded more rapidly than the DNA from cells infected with *dl*712.

clumped cells were alive, whereas most of the individual cells were dead.

We conclude that although ADP is required for efficient cell lysis, it is not required for most of the features of Ad CPE.

DISCUSSION

This study was prompted by our observation that Ad mutants that lack the *adp* gene have small plaques that are slow to develop. We then showed that mutants in the *adp* gene replicate as well as wild-type Ad, but the mutant virions are released more slowly from cells. Thus, mutant viruses spread more slowly from cell to cell, and the plaques are small.

Further studies showed that ADP is required for the efficient lysis (death) of Ad-infected cells at very late stages of infection. Cell death was demonstrated by LDH release, trypan blue exclusion, the MTT assay for mitochondrial activity, protein synthesis, DNA and RNA degradation, and cell morphology. Monolayers of permissive human cells infected with *adp*$^+$ Ad begin to die at 2 to 3 days p.i., and all the cells are typically dead by 5 to 7 days. Cells infected with *adp* mutants do not begin to die until about 6 days p.i. The cells stay intact, nuclear DNA can be readily stained with DAPI, and the cells remain metabolically active. Prior to death, cells infected with *adp* mutants have swollen nuclei that are full of virus. In recent experiments in which the medium was changed every 2 days, cells infected with wild-type Ad died with normal kinetics, but the survival of cells infected with *dl*712 (ADP$^-$) was significantly enhanced so that about 20% of the cells were still viable after 14 days p.i. (data not shown).

Our studies establish that ADP is necessary for efficient cell death, but they do not address whether ADP is sufficient for cell death. This will require experiments in which ADP is expressed autonomously.

Although Ad is one of the most prolific models in molecular biology and has been intensively studied for four decades, the mechanism by which Ad is released from cells is not understood. ADP begins to be synthesized abundantly at 1 day p.i., when virions begin to assemble in the cell nucleus, and both ADP (52) and virions (Fig. 4) continue to increase in abundance. As mentioned, cells begin to die at 2 to 3 days p.i. We propose that the function of ADP is to promote cellular lysis and the release of virus from the infected cell. To our knowledge, ADP is the first protein encoded by a mammalian DNA virus to have such a function.

Viruses encode a variety of proteins that either induce or inhibit cell death (reviewed in reference 42). Ad has several such proteins (reviewed in references 42, 58, 60, and 66 to 68). The E1A proteins induce apoptosis (59, 62), presumably by deregulating the cell cycle (10, 32, 58, 59). The E1B-19K (8, 10, 38, 40, 46, 47, 49) and E1B-55K (38, 69) proteins inhibit E1A-induced apoptosis. The E1A proteins also render cells susceptible to lysis by tumor necrosis factor (6, 13, 43), an inflammatory cytokine that is secreted by activated macrophages. Tumor necrosis factor-induced cytolysis is inhibited independently by the Ad E1B-19K protein (16, 62), the E3-14.7K protein (17, 19, 26, 37, 56), and the E3-10.4K–14.5K complex of proteins (18). These proteins presumably maintain cell viability so that virus replication can occur. ADP appears to have the opposite function: it promotes cell death so that Ad can be released from the infected cell.

In studies related to Ad-induced CPE, Chen et al. (7) observed that the Ad L3-encoded protease cleaves cytokeratin 18 and thereby disrupts the cytokeratin network of HeLa cells. Since disruption of keratin filaments renders epithelial cells more susceptible to lysis by mild mechanical stress (9, 55), Chen et al. (7) proposed that disruption of the cytoskeletal system might promote host cell lysis and release of progeny virions. Zhang and Schneider (70) extended this concept, reporting that disruption of the cytoskeletal network by the Ad protease, together with inhibition of host protein synthesis (to prevent repair of the cytokeratin network by newly synthesized keratin), is necessary for marked Ad CPE and for facilitation of lysis of infected cells and the release of mature virus particles.

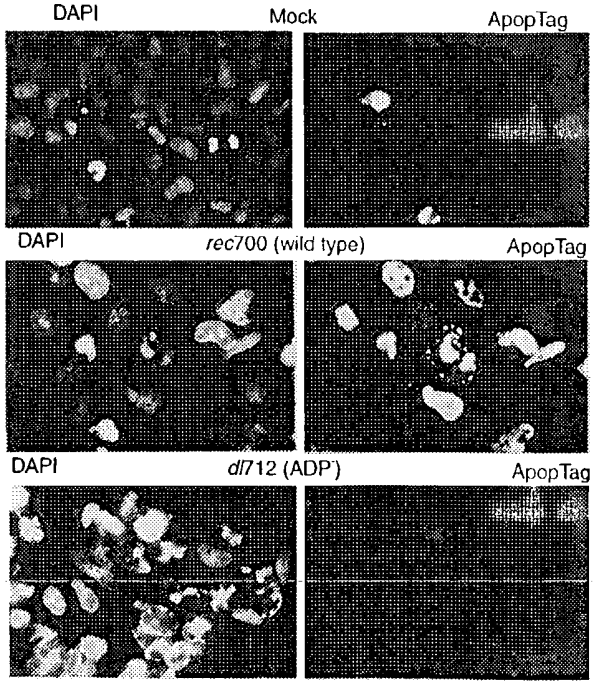

FIG. 9. TUNEL assay for nicked DNA in mock-infected A549 cells and in cells infected with *rec*700 (wild type) or *dl*712 (ADP$^-$). The cells are at 58 h p.i. DNA is stained with DAPI; fragmented DNA in the same field is labeled with ApopTag.

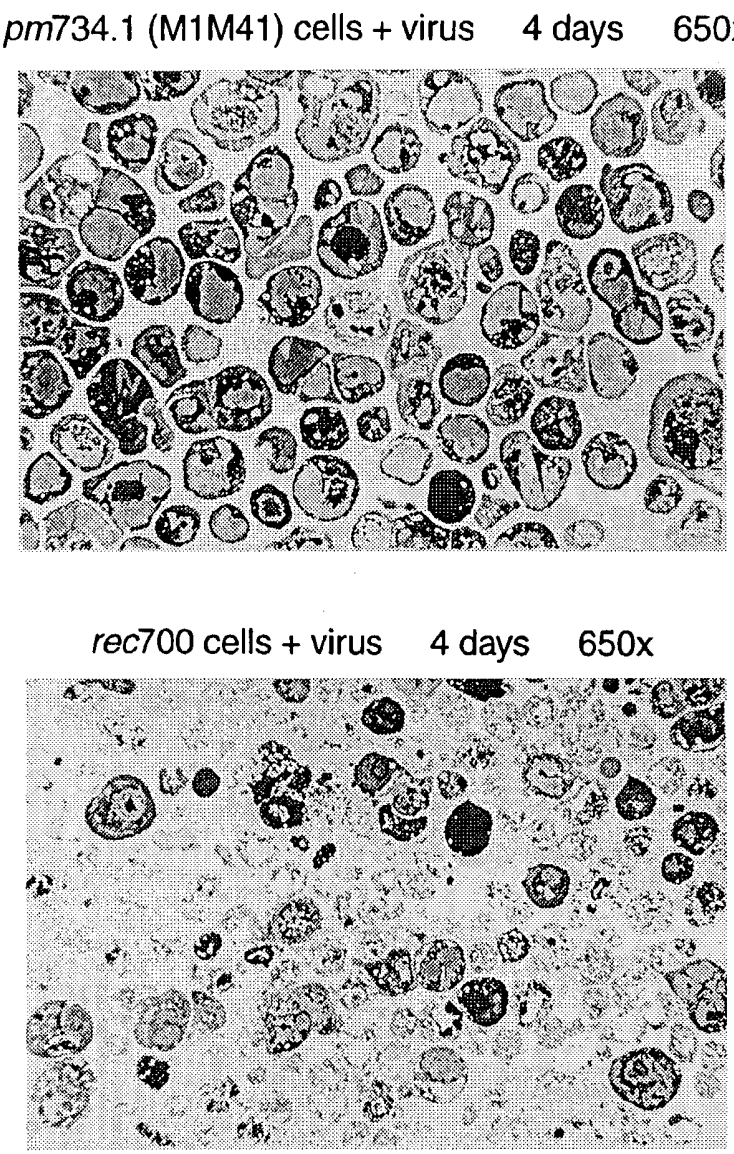

FIG. 10. Morphology at 4 days p.i. of cells infected with *rec*700 (wild type) or *pm*734.1 (lacks functional ADP). M1M41 refers to the fact that *pm*734.1 has missense mutations in Met-1 and Met-41 in ADP; thus, ADP initiates at Met-49. Most cells infected with *rec*700 are lysed, whereas most cells infected with *pm*734.1 are intact.

In our studies, cells infected with *adp* mutants showed Ad CPE in that the cells rounded up and detached from plastic dishes. Although we did not examine the Ad protease directly, it must be active in cells infected with *adp* mutants, because the protease is necessary for the production of mature infectious Ad, and deletion of the *adp* gene does not affect virus replication (Fig. 4). Also, in our studies, cellular protein synthesis was inhibited equally efficiently in cells infected with wild-type Ad or *adp* mutants (Fig. 6). Thus, the cytokeratin network was presumably equally disrupted in the infected cells. Nevertheless, our data show that *adp* is required for efficient cell lysis and progeny release. It would not be surprising if disruption of the cytokeratin network by the Ad protease and inhibition of cellular protein synthesis contribute to the fragility of infected cells, but our data show clearly that *adp* is the major determinant of cellular integrity.

At very late stages of infection, e.g., 30 to 40 h p.i., ADP becomes localized exclusively in the Golgi apparatus and nuclear membrane in A549 cells (41) and also in HeLa, A431, Hep3B, and 293 cells (53). Most likely, the site of action of ADP in promoting cell death is the nuclear membrane. Bcl-2 (15, 31) and E1B-19K (61), proteins that inhibit apoptosis, localize to the nuclear membrane. This is also true for Nip1, Nip2, and Nip3, cellular proteins that interact with Bcl-2 and E1B-19K (4). Perhaps ADP promotes cell death by directly or indirectly interacting in the nuclear membrane with these proteins and abrogating their ability to inhibit cell death. Other possibilities are that ADP forms a channel for, e.g., Ca^{2+} ions or that ADP disrupts the nuclear membrane. Whatever the mechanism of action, it is likely that ADP functions in a stoichiometric rather than catalytic manner, because the protein is made in very large amounts (52).

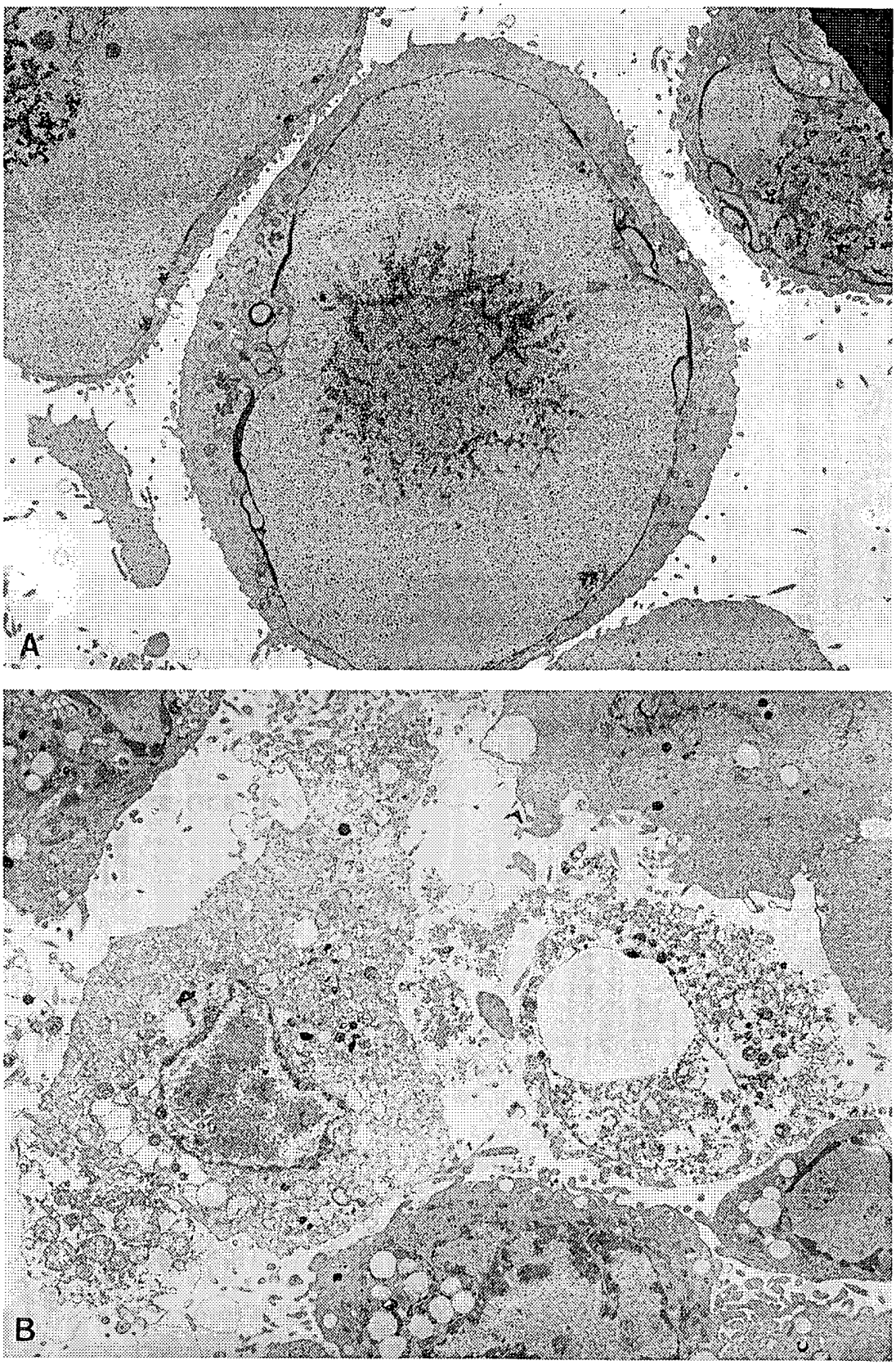

FIG. 11. Electron micrographs of typical A549 cells at 4 days p.i. with *pm*734.1 (Δ1-48) (A) or *rec*700 (wild type) (B).

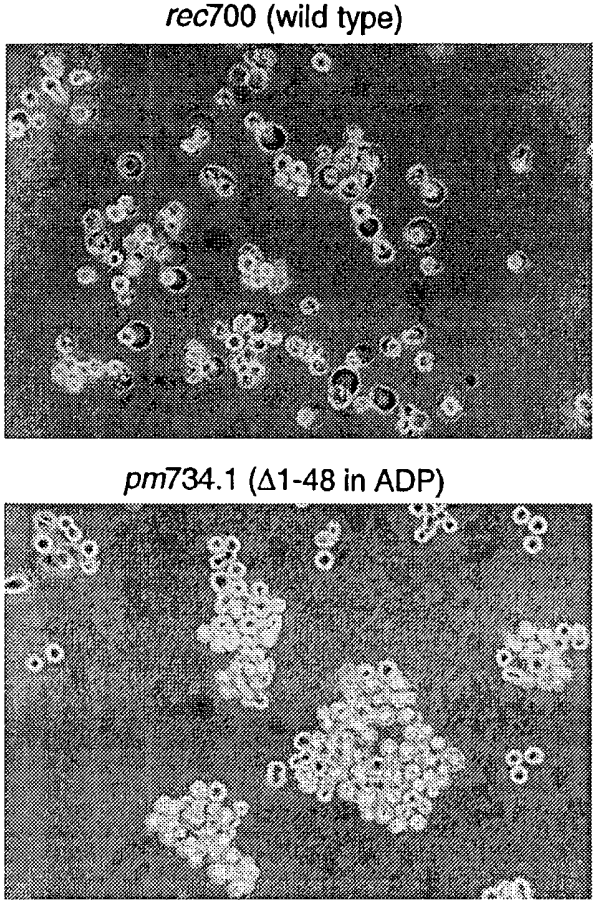

FIG. 12. Phase-contrast microscopy of A549 cells infected with *rec*700 or *pm*734.1 at 4 days p.i. With *rec*700, the cells are round, detached from the plastic dish, and dispersed, many are lysed, and many have the plasma membrane ballooned out. With *pm*734.1, the cells are round and detached into grape-like clusters, but most are intact.

There are other proteins that promote cell death (reviewed in references 30, 33, 36, 39, 44, and 51). ADP is not related to any of these proteins, including p53, c-Myc, ICE and ICE family members, Ced4, Bax, Bad, Bcl-X_S, Fas, tumor necrosis factor receptor, TRADD, MORT1, MyD118, and Reaper (14). Thus, ADP represents a new class of proteins that promote cell death. It will be interesting to determine whether ADP functions in the same pathway(s) as these other death-inducing proteins or in a novel cell death pathway. Regardless, ADP should be a useful tool for studying cell death.

Cells dying by apoptosis display distinct morphological characteristics and usually a ladder of DNA nicked between the nucleosomes. In our studies, the cells did not have the morphological characteristics of apoptosis, nor did the degraded DNA form a ladder on agarose gels. Thus, ADP may induce atypical apoptosis. It seems unlikely that the cells are dying by nonspecific necrosis, as this would not be expected to be mediated by a specific protein. Cell death in the Ad system appears to be different from the apoptosis reported to be induced by human immunodeficiency virus type 1 (1, 22), chicken anemia virus (35), Sindbis virus (54), and influenza virus (25, 48).

There is a great deal of interest in the use of Ad vectors for somatic cell gene therapy (23). Most vectors have the E3 region deleted because it is not required for virus replication in cultured cells. However, some workers are developing vectors that retain E3 in the anticipation that E3 proteins may counteract the inflammatory response to the vector. We suggest that such vectors should not contain the *adp* gene, because ADP may promote the death of the transduced cells.

Ad transcription units tend to have genes with similar functions. We have postulated that the E3 transcription unit is a cassette of genes that counteracts immunosurveillance (66–68). The cell death-promoting function of ADP is in accord with this proposal. That is, the quicker the virus is released from the infected cell, the less chance the virus has of being killed in the cell by cytotoxic T lymphocytes, NK cells, and phagocytic cells and the greater chance it has to infect another cell. Also, if the cell death induced by ADP is a form of apoptosis, then there may not be an inflammatory response, because cell fragments produced during apoptosis are rapidly phagocytosed and do not induce inflammation (29).

ACKNOWLEDGMENTS

This work was supported by grant CA24710 from the National Institutes of Health.

We thank Gary Ketner for H2*dl*801 and Tom Shenk for H5*dl*309 and H5*dl*327.

REFERENCES

1. **Banda, N. K., J. Bernier, D. K. Kurahara, R. Kurrle, N. Haigwood, R. P. Sekaly, and T. H. Finkel.** 1992. Crosslinking CD4 by human immunodeficiency virus gp120 primes T cells for activation-induced apoptosis. J. Exp. Med. **176**:1099–1106.
2. **Bayley, S. T., and J. S. Mymryk.** 1994. Adenovirus E1A proteins and transformation. Int. J. Oncol. 5:425–444.
3. **Bett, A. J., V. Krougliak, and F. L. Graham.** 1995. DNA sequence of the deletion/insertion in early region 3 of Ad5 dl309. Virus Res. 39:75–82.
4. **Boyd, J. M., S. Malstrom, T. Subramanian, L. K. Venkatesh, U. Schaeper, B. Elangovan, C. D'Sa-Eipper, and G. Chinnadurai.** 1994. Adenovirus E1B 19 kDa and Bcl-2 proteins interact with a common set of cellular proteins. Cell **79**:341–351.
5. **Challberg, S. S., and G. Ketner.** 1981. Deletion mutants of adenovirus 2: isolation and initial characterization of virus carrying mutations near the right end of the viral genome. Virology **114**:196–209.
6. **Chen, M. J., B. Holskin, J. Strickler, J. Gorniak, M. A. Clark, P. J. Johnson, M. Mitcho, and D. Shalloway.** 1987. Induction by E1A oncogene expression of cellular susceptibility to lysis by TNF. Nature (London) **330**:581–583.
7. **Chen, P. H., D. A. Ornelles, and T. Shenk.** 1993. The adenovirus L3 23-kilodalton proteinase cleaves the amino-terminal head domain from cytokeratin 18 and disrupts the cytokeratin network of HeLa cells. J. Virol. **67**: 3507–3514.
8. **Chiou, S. K., C. C. Tseng, L. Rao, and E. White.** 1994. Functional complementation of the adenovirus E1B 19-kilodalton protein with Bcl-2 in the inhibition of apoptosis in infected cells. J. Virol. **68**:6553–6566.
9. **Coulombe, P. A., M. E. Hutton, R. Vassar, and E. Fuchs.** 1991. A function for keratins and a common thread among different types of epidermolysis bullosa simplex diseases. J. Cell Biol. **115**:1661–1674.
10. **Debbas, M., and E. White.** 1993. Wild-type p53 mediates apoptosis by E1A, which is inhibited by E1B. Genes Dev. **7**:546–554.
11. **Deutscher, S. L., B. M. Bhat, M. H. Pursley, C. Cladaras, and W. S. M. Wold.** 1985. Novel deletion mutants that enhance a distant upstream 5′ splice in the E3 transcription unit of adenovirus 2. Nucleic Acids Res. **13**:5771–5788.
12. **D'Halluin, J.-C.** 1995. Virus assembly, p. 47–66. *In* W. Doerfler and P. Bohm (ed.), The molecular repertoire of adenoviruses. Springer-Verlag, Heidelberg, Germany.
13. **Duerksen-Hughes, P. J., T. W. Hermiston, W. S. M. Wold, and L. R. Gooding.** 1991. The amino-terminal portion of CD1 of the adenovirus E1A proteins is required to induce susceptibility to tumor necrosis factor cytolysis in adenovirus-infected mouse cells. J. Virol. **65**:1236–1244.
14. **Feinstein, E., A. Kimchi, D. Wallach, M. Boldin, and E. Varfolomeev.** 1995. The death domain: a module shared by proteins with diverse cellular functions. Trends Biochem. Sci. **20**:342–344.
15. **Givol, I., I. Tsarfaty, J. Resau, S. Rulong, P. P. da Silva, G. Nasioulas, J. DuHadaway, S. H. Hughes, and D. L. Ewert.** 1994. Bcl-2 expressed using a retroviral vector is localized primarily in the nuclear membrane and the endoplasmic reticulum of chicken embryo fibroblasts. Cell Growth Differ. 5: 419–429.
16. **Gooding, L. R., L. Aquino, P. J. Duerksen-Hughes, D. Day, T. M. Horton, S. P. Yei, and W. S. M. Wold.** 1991. The E1B 19,000-molecular-weight

protein of group C adenoviruses prevents tumor necrosis factor cytolysis of human cells but not of mouse cells. J. Virol. 65:3083–3094.
17. **Gooding, L. R., L. W. Elmore, A. E. Tollefson, H. A. Brady, and W. S. M. Wold.** 1988. A 14,700 MW protein from the E3 region of adenovirus inhibits cytolysis by tumor necrosis factor. Cell 53:341–346.
18. **Gooding, L. R., T. S. Ranheim, A. E. Tollefson, L. Aquino, P. Duerksen-Hughes, T. M. Horton, and W. S. M. Wold.** 1991. The 10,400- and 14,500-dalton proteins encoded by region E3 of adenovirus function together to protect many but not all mouse cell lines against lysis by tumor necrosis factor. J. Virol. 65:4114–4123.
19. **Gooding, L. R., I. O. Sofola, A. E. Tollefson, P. Duerksen-Hughes, and W. S. M. Wold.** 1990. The adenovirus E3-14.7K protein is a general inhibitor of tumor necrosis factor-mediated cytolysis. J. Immunol. 145:3080–3086.
20. **Greber, U. F., M. Willetts, P. Webster, and A. Helenius.** 1993. Stepwise dismantling of adenovirus 2 during entry into cells. Cell 75:477–486.
21. **Green, M., and W. S. M. Wold.** 1979. Human adenoviruses: growth, purification, and transfection assay. Methods Enzymol. 58:425–435.
22. **Groux, H., G. Torpier, D. Monte, Y. Mouton, A. Capron, and J. C. Ameisen.** 1992. Activation-induced death by apoptosis in $CD4^+$ T cells from human immunodeficiency virus-infected asymptomatic individuals. J. Exp. Med. 175:331–340.
23. **Grunhaus, A., and M. S. Horwitz.** 1992. Adenoviruses as cloning vectors. Semin. Virol. 3:237–252.
24. **Hawkins, L. K., and W. S. M. Wold.** 1992. A 12,500 MW protein is coded by region E3 of adenovirus. Virology 188:486–494.
25. **Hinshaw, V. S., C. W. Olsen, N. Dybdahl-Sissoko, and D. Evans.** 1994. Apoptosis: a mechanism of cell killing by influenza A and B viruses. J. Virol. 68:3667–3673.
26. **Horton, T. M., T. S. Ranheim, L. Aquino, D. I. Kusher, S. K. Saha, C. F. Ware, W. S. M. Wold, and L. R. Gooding.** 1991. Adenovirus E3 14.7K protein functions in the absence of other adenovirus proteins to protect transfected cells from tumor necrosis factor cytolysis. J. Virol. 65:2629–2639.
27. **Horwitz, M. S.** 1990. Adenoviridae and their replication, p. 1679–1712. *In* B. N. Fields and D. M. Knipe (ed.), Virology. Raven Press, New York.
28. **Jones, N., and T. Shenk.** 1979. Isolation of adenovirus type 5 host range deletion mutants defective for transformation of rat embryo cells. Cell 17: 683–689.
29. **Kerr, J. F., A. H. Wyllie, and A. R. Currie.** 1972. Apoptosis: a basic biological phenomenon with wide-ranging implications in tissue kinetics. Br. J. Cancer 26:239–257.
30. **Kumar, S.** 1995. ICE-like proteases in apoptosis. Trends Biochem. Sci. 20: 198–202.
31. **Lithgow, T., R. van Driel, J. F. Bertram, and A. Strasser.** 1994. The protein product of the oncogene bcl-2 is a component of the nuclear envelope, the endoplasmic reticulum, and the outer mitochondrial membrane. Cell Growth Differ. 5:411–417.
32. **Lowe, S. W., and H. E. Ruley.** 1993. Stabilization of the p53 tumor suppressor is induced by adenovirus 5 E1A and accompanies apoptosis. Genes Dev. 7: 535–545.
33. **Martin, S. J., and D. R. Green.** 1995. Protease activation during apoptosis: death by a thousand cuts? Cell 82:349–352.
34. **Moran, E.** 1994. Mammalian cell growth controls reflected through protein interactions with the adenovirus E1A gene products. Semin. Virol. 5:327–340.
35. **Noteborn, M. H. M., D. Todd, C. A. J. Verschueren, H. W. F. M. de Gauw, W. L. Curran, S. Veldkamp, A. J. Douglas, M. S. McNulty, A. J. van der Eb, and G. Koch.** 1994. A single chicken anemia virus protein induces apoptosis. J. Virol. 68:346–351.
36. **Oltvai, Z. N., and S. J. Korsmeyer.** 1994. Checkpoints of dueling dimers foil death wishes. Cell 79:189–192.
37. **Ranheim, T. S., J. Shisler, T. M. Horton, L. J. Wold, L. R. Gooding, and W. S. M. Wold.** 1993. Characterization of mutants within the gene for the adenovirus E3 14.7-kilodalton protein which prevents cytolysis by tumor necrosis factor. J. Virol. 67:2159–2167.
38. **Rao, L., M. Debbas, P. Sabbatini, D. Hockenbery, S. Korsmeyer, and E. White.** 1992. The adenovirus E1A proteins induce apoptosis, which is inhibited by the E1B 19-kDa and Bcl-2 proteins. Proc. Natl. Acad. Sci. USA 89: 7742–7746.
39. **Reed, J. C.** 1994. Bcl-2 and the regulation of programmed cell death. J. Cell Biol. 124:1–6.
40. **Sabbatini, P., S. K. Chiou, L. Rao, and E. White.** 1995. Modulation of p53-mediated transcriptional repression and apoptosis by the adenovirus E1B 19K protein. Mol. Cell. Biol. 15:1060–1070.
41. **Scaria, A., A. E. Tollefson, S. K. Saha, and W. S. M. Wold.** 1992. The E3-11.6K protein of adenovirus is an Asn-glycosylated integral membrane protein that localizes to the nuclear membrane. Virology 191:743–753.
42. **Shen, Y., and T. E. Shenk.** 1995. Viruses and apoptosis. Curr. Opin. Genet. Dev. 5:105–111.
43. **Shisler, J., P. Duerksen-Hughes, T. W. Hermiston, W. S. M. Wold, and L. R. Gooding.** 1996. Induction of susceptibility to tumor necrosis factor by adenovirus E1A is dependent on binding to either p300 or p105-Rb and induction of DNA synthesis. J. Virol. 70:68–77.
44. **Steller, H.** 1995. Mechanisms and genes of cellular suicide. Science 267: 1445–1449.
45. **Stewart, P. L., and R. M. Burnett.** 1995. Adenovirus structure by x-ray crystallography and electron microscopy, p. 25–38. *In* W. Doerfler and P. Bohm (ed.), The molecular repertoire of adenoviruses. Springer-Verlag, Heidelberg, Germany.
46. **Subramanian, T., J. M. Boyd, and G. Chinnadurai.** 1995. Functional substitution identifies a cell survival promoting domain common to adenovirus E1B 19 kDa and Bcl-2 proteins. Oncogene 11:2403–2409.
47. **Subramanian, T., B. Tarodi, R. Govindarajan, J. M. Boyd, K. Yoshida, and G. Chinnadurai.** 1993. Mutational analysis of the transforming and apoptosis suppression activities of the adenovirus E1B 175R protein. Gene 124:173–181.
48. **Takizawa, T., S. Matsukawa, Y. Higuchi, S. Nakamura, Y. Nakanishi, and R. Fukuda.** 1993. Induction of programmed cell death (apoptosis) by influenza virus infection in tissue culture cells. J. Gen. Virol. 74:2347–2355.
49. **Tarodi, B., T. Subramanian, and G. Chinnadurai.** 1993. Functional similarity between adenovirus E1B 19K gene and Bcl2 oncogene: mutant complementation and suppression of cell death induced by DNA damaging agents. Int. J. Oncol. 3:467–472.
50. **Thimmappaya, B., C. Weinberger, R. J. Schneider, and T. Shenk.** 1982. Adenovirus VAI RNA is required for efficient translation of viral mRNAs at late times after infection. Cell 31:543–551.
51. **Thompson, C. B.** 1995. Apoptosis in the pathogenesis and treatment of disease. Science 267:1456–1462.
52. **Tollefson, A. E., A. Scaria, S. K. Saha, and W. S. M. Wold.** 1992. The 11,600-M_w protein encoded by region E3 of adenovirus is expressed early but is greatly amplified at late stages of infection. J. Virol. 66:3633–3642.
53. **Tollefson, A. E., A. Scaria, and W. S. M. Wold.** Unpublished results.
54. **Ubol, S., P. C. Tucker, D. E. Griffin, and J. M. Hardwick.** 1994. Neurovirulent strains of Alphavirus induce apoptosis in bcl-2-expressing cells: role of a single amino acid change in the E2 glycoprotein. Proc. Natl. Acad. Sci. USA 91:5202–5206.
55. **Vassar, R., P. A. Coulombe, L. Degenstein, K. Albers, and E. Fuchs.** 1991. Mutant keratin expression in transgenic mice causes marked abnormalities resembling a human genetic skin disease. Cell 64:365–380.
56. **Voelkel-Johnson, C., A. J. Entingh, W. S. M. Wold, L. R. Gooding, and S. M. Laster.** 1995. Activation of intracellular proteases is an early event in TNF-induced apoptosis. J. Immunol. 154:1707–1716.
57. **Wang, E. W., M. O. Scott, and R. P. Ricciardi.** 1988. An adenovirus mRNA which encodes a 14,700-M_r protein that maps to the last open reading frame of region E3 is expressed during infection. J. Virol. 62:1456–1459.
58. **White, E.** 1994. Function of the adenovirus E1B oncogene in infected and transformed cells. Semin. Virol. 5:341–348.
59. **White, E., R. Cipriani, P. Sabbatini, and A. Denton.** 1991. Adenovirus E1B 19-kilodalton protein overcomes the cytotoxicity of E1A proteins. J. Virol. 65:2968–2978.
60. **White, E., and L. R. Gooding.** 1994. Regulation of apoptosis by human adenoviruses, p. 111–142. *In* L. D. Tomei and F. O. Cope (ed.), Apoptosis II: the molecular basis of apoptosis in disease. Cold Spring Harbor Laboratory Press, Cold Spring Harbor, N.Y.
61. **White, E., T. Grodzicker, and B. W. Stillman.** 1984. Mutations in the gene encoding the adenovirus early region 1B 19,000-molecular-weight tumor antigen cause the degradation of chromosomal DNA. J. Virol. 52:410–419.
62. **White, E., P. Sabbatini, M. Debbas, W. S. M. Wold, D. I. Kusher, and L. R. Gooding.** 1992. The 19-kilodalton adenovirus E1B transforming protein inhibits programmed cell death and prevents cytolysis by tumor necrosis factor alpha. Mol. Cell. Biol. 12:2570–2580.
63. **Wickham, T. J., P. Mathias, D. A. Cheresh, and G. R. Nemerow.** 1993. Integrins $\alpha_v\beta_3$ and $\alpha_v\beta_5$ promote adenovirus internalization but not virus attachment. Cell 73:309–319.
64. **Wold, W. S. M., C. Cladaras, S. C. Magie, and N. Yacoub.** 1984. Mapping a new gene that encodes an 11,600-molecular-weight protein in the E3 transcription unit of adenovirus 2. J. Virol. 52:307–313.
65. **Wold, W. S. M., S. L. Deutscher, N. Takemori, B. M. Bhat, and S. C. Magie.** 1986. Evidence that AGUAUAUGA and CCAAGAUGA initiate translation in the same mRNA region E3 of adenovirus. Virology 148:168–180.
66. **Wold, W. S. M., and L. R. Gooding.** 1991. Region E3 of adenovirus: a cassette of genes involved in host immunosurveillance and virus-cell interactions. Virology 184:1–8.
67. **Wold, W. S. M., A. E. Tollefson, and T. W. Hermiston.** 1994. Adenovirus proteins that subvert host defenses. Trends Microbiol. 2:437–443.
68. **Wold, W. S. M., A. E. Tollefson, and T. W. Hermiston.** 1995. Strategies of immune modulation by adenoviruses, p. 145–183. *In* G. McFadden (ed.), Viroreceptors, virokines, and related mechanisms of immune modulation by DNA viruses. R. G. Landes Co., Austin, Tex.
69. **Yew, P. R., and A. J. Berk.** 1992. Inhibition of p53 transactivation required for transformation by adenovirus early 1B protein. Nature (London) 357: 82–85.
70. **Zhang, Y., and R. J. Schneider.** 1994. Adenovirus inhibition of cell translation facilitates release of virus particles and enhances degradation of the cytokeratin network. J. Virol. 68:2544–2555.

Nat. Gent. 1992 1:372-378
Science 1989 245:1234-1236

Eur. J Biochem. 1985 148:265-270

Mol. Immunol 1995 32:1057-1064

Science 1993 259:988-990

Nature 1988 336:348-352

J Clin. Invest. 1993 91:225-234

Mol. Cell. Biol. 1987 7:1576-1579

Gene 1982 19:33-42

Neuron 1992 8:507-520

Adv. Virus Res. 1989 37:35-83

1994 Cancer Res. 54:5258-5261

Cell 1987 50:435-443

Nucleic Acids Res. (1996) 24(10):1841-1848

J Biol. Chem. 1988 263 10 :4837-4843

Proc. Natl. Acad. Sci. USA 1992 89:2581-2584

1993 Nature 361:647-650

DNA Seq. 1993 4:185-196

Human Gene Ther. 1995 6:881-893

Science 1991 252:431-434

Cell 1992 68:143-155

Mol. Cell. Biol. 1990 10 6 :2738-2748

Nucleic Acids Res. 1996 24 15 :2966-2973

Human Gene Thera 1990 1:241-256

J Clin. Invest 1992 . 90:626-630

Curr. Topics in Micro. and Imm. 1995 199 part 3 :177-194

Lancet 1981 11:832-834

Cancer Res. 1996 56:1341-1345

J Virol. 1992 66 (6) :3633-3642

J Virol. 1996 70 (4) :2296-2306

Nature (1997) 389:239-242

J Virol. 1984 51 (3) : 822-831

Adv. Ex . Med. Biol. 1991 3098:61-66

Proc. Natl. Acad. Sci. 1983 80:5383-5386

Genomics 1990 8:492-500

Gastroenter. 1990 98:470-477 .

N. Vogel
AU 1636
12/9
10045116

Gene therapy — promises, problems and prospects

Inder M. Verma and Nikunj Somia

In principle, gene therapy is simple: putting corrective genetic material into cells alleviates the symptoms of disease. In practice, considerable obstacles have emerged. But, thanks to better delivery systems, there is hope that the technique will succeed.

In 1990, the first clinical trials for gene-therapy approaches to combat disease were carried out. Conceptually, the technique involves identifying appropriate DNA sequences and cell types, then developing suitable ways in which to get enough of the DNA into these cells. With efficient delivery, the therapeutic prospects range from tackling genetic diseases and slowing the progression of tumours, to fighting viral infections and stopping neurodegenerative diseases. But the problems — such as the lack of efficient delivery systems, lack of sustained expression, and host immune reactions — remain formidable challenges.

Although more than 200 clinical trials are currently underway worldwide, with hundreds of patients enrolled, there is still no single outcome that we can point to as a success story. To explore why this is the case, we will use our own experience and other examples to look at the many technical, logistical and, in some cases, conceptual hurdles that need to be overcome before gene therapy becomes routine practice in medicine.

At present, gene therapy is being contemplated only on somatic (essentially, non-reproductive) cells. Although many somatic tissues can receive therapeutic DNA, the choice of cell usually depends on the nature of the disease. Sometimes a clear definition of the target cell is needed. For example, the gene that is defective in cystic fibrosis has been identified, and clinical trials to deliver DNA as an aerosol into the lung have already begun[1]. Although cystic fibrosis is manifest in this organ, it is still not clear that delivery of a correcting gene by this method will reach the right type of cell. On the other hand, to correct blood-clotting disorders such as haemophilia, all that is needed is a therapeutic level of clotting protein in the plasma[2]. This protein may be supplied by muscle or liver cells, fibroblasts, or even blood cells[3–5]. The choice of tissue in which to express the therapeutic protein will also ultimately depend on considerations such as the efficiency of gene delivery, protein modifications, immunological status, accessibility and economics.

We also need to consider how much of the therapeutic protein should be delivered. In haemophilia B, which is caused by a deficiency of a blood-clotting protein called factor IX, giving patients just 5% of the normal circulating levels of this protein can substantially improve their quality of life[2]. Most people have about 5 μg of factor IX per millilitre of plasma, produced by the 10^{13} cells that make up the liver. So we need to deliver a correcting gene to 5×10^{11} cells — that is, 5% of liver cells. Alternatively, fewer liver cells would need to be modified if more factor IX could be produced per cell, without being deleterious. In the brain, however, gene transfer to just a few hundred cells could considerably benefit patients with neurological disease. And finally, we can consider the transfer of genes to a handful of stem (or progenitor) cells, which grow and divide to generate millions of progeny. The range in the number of cells that this technology has to cover is vast.

The Achilles heel of gene therapy is gene delivery, and this is the aspect that we will concentrate on here. Thus far, the problem has been an inability to deliver genes efficiently and to obtain sustained expression. There are two categories of delivery vehicle ('vector'). The first comprises the non-viral vectors, ranging from direct injection of DNA to mixing the DNA with polylysine or cationic lipids that allow the gene to cross the cell membrane. Most of these approaches suffer from poor efficiency of delivery and transient expression of the gene[6]. Although there are reagents that increase the efficiency of delivery, transient expression of the transgene is a conceptual hurdle that needs to be addressed.

Most of the current gene-therapy approaches make use of the second category — viral vectors. Importantly, the viruses used have all been disabled of any pathogenic effects. The use of viruses is a powerful technique, because many of them have evolved a specific machinery to deliver DNA to cells. However, humans have an immune system to fight off the virus, and our attempts to deliver genes in viral vectors have been confronted by these host responses. ▶

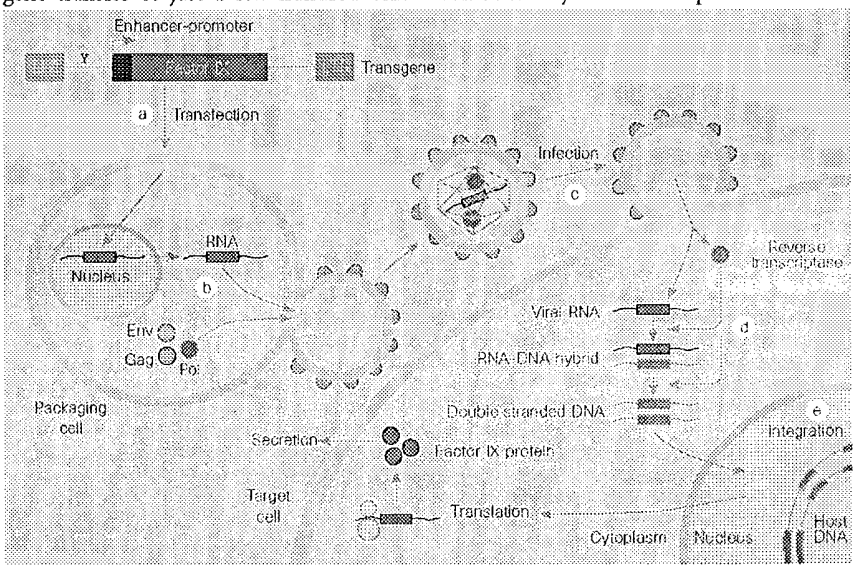

Figure 1 To create the retroviral vectors that are used in gene therapy, the life-cycles of their naturally occurring counterparts are exploited. a, The transgene (in this case, the gene for factor IX) in a vector backbone is put into a packaging cell, which expresses the genes that are required for viral integration (*gag*, *pol* and *env*). b, The transgene is incorporated into the nucleus, where it is transcribed to make vector RNA. This is then packaged into the retroviral vector, which is shed from the packaging cell. c, The vector is delivered to the target cell by infection. The membrane of the viral vector fuses with the target cell, allowing the vector RNA to enter. d, The virally encoded enzyme reverse transcriptase converts the vector RNA into an RNA–DNA hybrid, and then into double-stranded DNA. e, The vector DNA is integrated into the host genome, then the host-cell machinery will transcribe and translate it to make RNA and, in this case, factor IX protein. LTR, long terminal repeat; ψ, packaging sequence.

Retroviral vectors

Retroviruses are a group of viruses whose RNA genome is converted to DNA in the infected cell. The genome comprises three genes termed *gag*, *pol* and *env*, which are flanked by elements called long terminal repeats (LTRs). These are required for integration into the host genome, and they define the beginning and end of the viral genome. The LTRs also serve as enhancer–promoter sequences — that is, they control expression of the viral genes. The final element of the genome, called the packaging sequence (ψ), allows the viral RNA to be distinguished from other RNAs in the cell (Fig. 1)[7].

By manipulating the viral genome, viral genes can be replaced with transgenes — such as the gene for factor IX (Table 1). Transcription of the transgene may be under the control of viral LTRs or, alternatively, enhancer–promoter elements can be engineered in with the transgene. The chimaeric genome is then introduced into a packaging cell, which produces all of the viral proteins (such as the products of the *gag*, *pol* and *env* genes), but these have been separated from the LTRs and the packaging sequence. So, only the chimaeric viral genomes are assembled to generate a retroviral vector. The culture medium in which these packaging cells have been grown is then applied to the target cells, resulting in transfer of the transgene. Typically, a million target cells on a culture dish can be infected with one millilitre of the viral soup.

A critical limitation of retroviral vectors is their inability to infect non-dividing cells[8], such as those that make up muscle, brain, lung and liver tissue. So, when possible, the cells from the target tissue are removed, grown *in vitro*, and infected with the recombinant retroviral vector. The target cells producing the foreign protein are then transplanted back into the animal. This procedure has been termed '*ex vivo* gene therapy' and our group has used it to infect mouse primary fibroblasts or myoblasts (connective-tissue and muscle precursors, respectively) with retroviral vectors producing the factor IX protein. But within five to seven days of transplanting the infected cells back into mice, expression of factor IX is shut off[3,5,9]. This transcriptional shut-off has even been observed in mice lacking a functional immune system (nude mice), and it cannot be due to cell loss or gene deletion[5] because the transplanted cells can be recovered.

What is the mechanism of this unexpected but intriguing problem? We do not yet know, but the exceptions may provide some clues. To obtain sustained expression in mouse muscle following the transplantation of infected myoblasts, we used the muscle creatine kinase enhancer–promoter to control transcription of the transgene. Unfortunately, this is a weak promoter, and only low levels of protein were produced. So, we generated a chimaeric vector in which the muscle creatine kinase enhancer was linked to a strong promoter from cytomegalovirus. Using this vector, sustained and high levels of factor IX were expressed when the infected myoblasts were transplanted back into mice. Remarkably, these expression levels remained unchanged for more than two years (the life of the animal). So we can override the 'off switch' and achieve higher levels of expression by using an appropriate enhancer–promoter combination. But the search for such combinations is a case of trial and error for a given type of cell.

Another formidable challenge to the *ex vivo* approach is the efficiency of transplantation of the infected cells. Attempts to repeat the long-term myoblast transplantation in haemophiliac dogs led to only short-term expression, because the infected dog myoblasts could not fuse with the muscle fibres. So perhaps successful animal models will prove inadequate when the same protocols are extended to humans. Moreover, these models are based on inbred animals — the outbred human population, with individual variation, will add yet another degree of complexity. The haematopoietic (blood-producing) system may offer an advantage for *ex vivo* gene therapy because resting stem cells can be stimulated to divide *in vitro* using growth factors and the transplantation technology is well established. But there is still a lack of good enhancer–promoter combinations that allow sustained production of high levels of protein in these cells.

Another problem is the possibility of random integration of vector DNA into the host chromosome. This could lead to activation of oncogenes or inactivation of tumour-suppressor genes. Although the theoretical probability of such an event is quite low, it is of some concern (see section on clinical trials).

Table 1 **Candidate diseases for gene therapy**

Disease	*Defect*	*Incidence*	*Target cells*
Genetic			
Severe combined immunodeficiency (SCID/ADA)	Adenosine deaminase (ADA) in ~25% of SCID patients	Rare	Bone marrow cells or T lymphocytes
Haemophilia A	Factor VIII deficiency	1:10,000 males	Liver, muscle, fibroblasts or bone marrow cells
Haemophilia B	Factor IX deficiency	1:30,000 males	
Familial hypercholesterolaemia	Deficiency of low-density lipoprotein (LDL) receptor	1:1 million	Liver
Cystic fibrosis	Faulty transport of salt in lung epithelium. Loss of *CFTR* gene	1:3,000 Caucasians	Airways in the lungs
Haemoglobinopathies: thalassaemias/ sickle-cell anaemia	Structural defects in α- or β-globin gene	1:600 in certain ethnic groups	Bone marrow cells, giving rise to red blood cells
Gaucher's disease	Defect in the enzyme glucocerebrosidase	1:450 in Ashkenazi Jews	Bone marrow cells, macrophages
α_1-antitrypsin deficiency: inherited emphysema	Lack of α_1-antitrypsin	1:3,500	Lung or liver cells
Acquired			
Cancer	Many causes, including genetic and environmental	1 million/year in USA	Variety of cancer cell types: liver, brain, pancreas, breast, kidney
Neurological diseases	Parkinson's, Alzheimer's, spinal-cord injury	1 million Parkinson's and 4 million Alzheimer's patients in USA	Direct injection in the brain, neurons, glial cells, Schwann cells
Cardiovascular	Restinosis, arteriosclerosis	13 million in USA	Arteries, vascular endothelial cells
Infectious diseases	AIDS, hepatitis B	Increasing numbers	T cells, liver, macrophages

Lentiviral vectors

Lentiviruses also belong to the retrovirus family, but they can infect both dividing and non-dividing cells[10]. The best-known lentivirus is the human immunodeficiency virus (HIV), which has been disabled and developed as a vector for *in vivo* gene delivery. Like the simple retroviruses, HIV has the three *gag*, *pol* and *env* genes, but it also carries genes for six accessory proteins termed *tat*, *rev*, *vpr*, *vpu*, *nef* and *vif*[11].

Using the retrovirus vectors as a model, lentivirus vectors have been made, with the transgene enclosed between the LTRs and a packaging sequence[12]. Some of the accessory proteins can be eliminated without affecting production of the vector or efficiency of infection. The *env* gene product would restrict HIV-based vectors to infecting only cells that express a protein called $CD4^+$ so, in the vectors, this gene is substituted with *env* sequences from other RNA viruses that have a broader infection spectrum (such as glycoprotein from the vesicular stomatitis virus). These vectors can be produced — albeit on a small scale at the moment — at concentrations of $>10^9$ virus particles per ml (ref. 12).

When lentivirus vectors are injected into rodent brain, liver, muscle, eye or pancreatic-islet cells, they give sustained expression for over six months — the longest time tested so far[13,14]. Unlike the prototypical retroviral vectors, the expression is not subject to 'shut off'. Little is known about the possible immune problems associated with lentiviral vectors, but injection of 10^7 infectious units

does not elicit the cellular immune response at the site of injection. Furthermore, there seems to be no potent antibody response. So, at present, lentiviral vectors seem to offer an excellent opportunity for *in vivo* gene delivery with sustained expression.

Adenoviral vectors

The adenoviruses are a family of DNA viruses that can infect both dividing and non-dividing cells, causing benign respiratory-tract infections in humans[11]. Their genomes contain over a dozen genes, and they do not usually integrate into the host DNA. Instead, they are replicated as episomal (extrachromosomal) elements in the nucleus of the host cell. Replication-deficient adenovirus vectors can be generated by replacing the *E1* gene — which is essential for viral replication — with the gene of interest (for example, that for factor IX) and an enhancer–promoter element. The recombinant vectors are then replicated in cells that express the products of the *E1* gene, and they can be generated in very high concentrations ($>10^{11}$–10^{12} adenovirus particles per ml)[15].

Cells infected with recombinant adenovirus can express the therapeutic gene but, because essential genes for viral replication are deleted, the vector should not replicate. These vectors can infect cells *in vivo*, causing them to express very high levels of the transgene. Unfortunately, this expression lasts for only a short time (5–10 days post-infection). In contrast to the retroviral vectors, long-term expression can be achieved if the recombinant adenoviral vectors are introduced into nude mice, or into mice that are given both the adenoviral vector and immunosuppressing agents[16]. This indicates that the immune system is behind the short-term expression that is usually obtained from adenoviral vectors.

The immune reaction is potent, eliciting both the cell-killing 'cellular' response and the antibody-producing 'humoral' response. In the cellular response, virally infected cells are killed by cytotoxic T lymphocytes[16,17]. The humoral response results in the generation of antibodies to adenoviral proteins, and it will prevent any subsequent infection if the animal is given a second injection of the recombinant adenovirus. Unfortunately for gene therapy, most of the human population will probably have antibodies to adenovirus from previous infection with the naturally occurring virus.

It is possible that the target cell contains factors that might trigger the synthesis of adenoviral proteins, leading to an immune response. To try to get around this problem, second-generation adenoviral vectors were developed, in which additional genes that are implicated in viral replication were deleted. These vectors showed longer-term expression, but a decline after 20–40 days was still apparent[18]. This idea has now been taken further with the generation of 'gut-less' vectors — all of the viral genes are deleted, leaving only the elements that define the beginning and the end of the genome, and the viral packaging sequence. The transgenes carried by these viruses were expressed for 84 days[19].

There are considerable immunological problems to be overcome before adenoviral vectors can be used to deliver genes and produce sustained expression. The incoming adenoviral proteins that package DNA can be transported to the cytoplasm where they are processed and presented on the cell surface, tagging the cell as infected for destruction by cytotoxic T cells. So adenoviral vectors are extremely useful if expression of the transgene is required for short periods of time. One promising approach is to deliver large numbers of adenoviral vectors containing genes for enzymes that can activate cell killing, or immunomodulatory genes, to cancer cells. In this case, the cellular immune response against the viral proteins will augment tumour killing. Finally, although immunosuppressive drugs can extend the duration of expression, our goal should be to manipulate the vector and not the patient.

Adeno-associated viral vectors

A relative newcomer to the field, adeno-associated virus (AAV) is a simple, non-pathogenic, single-stranded DNA virus. Its two genes (*cap* and *rep*) are sandwiched between inverted terminal repeats that define the beginning and the end of the virus, and contain the packaging sequence[20]. The *cap* gene encodes viral capsid (coat) proteins, and the *rep* gene product is involved in viral replication and integration. AAV needs additional genes to replicate, and these are provided by a helper virus (usually adenovirus or herpes simplex virus).

The virus can infect a variety of cell types, and — in the presence of the *rep* gene product — the viral DNA can integrate preferentially[20] into human chromosome 19. To produce an AAV vector, the *rep* and *cap* genes are replaced with a transgene. Up to 10^{11}–10^{12} viral particles can be produced per ml, but only one in 100–1,000 particles is infectious. Moreover, preparation of the vector is laborious and, due to the toxic nature of the *rep* gene product and some of the adenoviral helper proteins, we currently have no packaging cells in which all of the proteins can be stably provided. Vector preparations must also be carefully separated from any contaminating adenovirus, and AAV vectors can accommodate only 3.5–4.0 kilobases of foreign DNA — this will exclude larger genes. Finally, we need more information about the immunogenicity of the viral proteins, especially given that 80% of the adult population have circulating antibodies to AAV. These considerations notwithstanding, AAV vectors containing human factor IX complementary DNA have been used to infect liver and muscle cells in immunocompetent mice. The mice produced therapeutic amounts of factor IX protein in their blood for over six months[21,22], confirming the promise of AAV as an *in vivo* gene-therapy vector.

Other vectors

Among the other viruses being considered and developed, is herpes simplex virus, which infects cells of the nervous system[23]. The virus contains more than 80 genes, one of which (*IE3*) can be replaced to create the vector. Around 10^8–10^9 viral particles are produced per ml, but the residual proteins are toxic to the target cell. Additional genes can be deleted, allowing more than one transgene to be included. But if essentially all of the viral proteins are deleted (gut-less vectors), only around 10^6 viral particles are produced per ml. And, again, many people have an immunity to components of herpes simplex virus, having already been infected at some time.

Vaccinia-virus-based vectors have also

What makes an ideal vector?

All of the current methods of gene delivery – whether viral or non-viral – have some limitation. So, the choice of vector will often be dictated by the need. If expression of the gene is required for only a short time (for example, expression of a toxic gene-product in cancer cells), then the adenoviral vectors are ideal. But if sustained expression is needed (such as for most genetic diseases), then an integrating vector without attendant immunological problems is more desirable. An ideal vector may have to borrow properties from both viral and synthetic systems, and it should have:

- High concentration ($>10^9$ viral particles per ml), allowing many cells to be infected;
- Convenience and reproducibility of production;
- Ability to integrate in a site-specific location in the host chromosome, or to be successfully maintained as a stable episome;
- A transcriptional unit that can respond to manipulation of its regulatory elements;
- Ability to target the desired type of cell;
- No components that elicit an immune response.

Although no such vector is currently available, all of these properties exist, individually, in disparate delivery systems.

been explored, largely for generating vaccines[24]. The Sindbis and Semliki Forest virus is being exploited as a possible cytoplasmic vector[25] which does not integrate into the nucleus. Although most of these systems produce the foreign protein only transiently, they add diversity to the available systems of gene transfer (Table 2).

Clinical trials

Over half of the 200 clinical trials that have been launched in the United States involve therapeutic approaches to cancer. Nearly 30 of them involve correction of monogenic diseases (Table 1) such as cystic fibrosis, α_1-antitrypsin deficiency and severe combined immunodeficiency (SCID). Most of the trials are phase I (safety) studies and, by and large, the existing delivery systems have no major toxicity problems. Moreover, lessons can be learned from previous clinical trials[26,27]. For example, seven years ago two patients were enrolled in a trial to correct deficiencies in adenosine deaminase (ADA, which leads to severe immunodeficiency). One of the patients improved, and makes 25% of normal ADA in her T cells, five years after the last infusion of infected T cells (although she is still treated with PEG–ADA; bovine adenosine deaminase mixed with polyethylene glycol). But in the other patient, the infected T cells could not produce enough of the deficient enzyme.

The efficacy of gene therapy cannot be evaluated until patients are completely taken off alternative treatments (in the above example, PEG–ADA). In another trial[28], weaning a patient away from PEG–ADA reduced the ability of the T cells to respond *in vitro* to a challenge by pathogens. Clearly, in these cases the retroviral vectors were not optimal, and the number of infected blood-progenitor cells was extremely low. However, these trials did help to establish the technology for generating clinical-grade recombinant retroviral particles, the procedures for infection and transplantation, and the protocols for monitoring patients and analysing data. The disappointing outcome probably lies in the inefficient gene-delivery system. We need a system in which the vector — containing the ADA gene — is efficiently delivered to progenitor cells, leading to sustained expression of high levels of the ADA protein. But, encouragingly, despite being repeatedly injected with highly concentrated recombinant viruses, the patients have suffered no untoward effects to date.

Future prospects

We now need a renewed emphasis on the basic science behind gene therapy — particularly the three intertwined fields of vectors, immunology and cell biology.

All of the available viral vectors arose from understanding the basic biology of the structure and replication of viruses. Clearly, existing vectors need to be streamlined further (see box on page 241), and vectors that target specific types of cell are being developed. The use of antibody fragments, ligands to cell-specific receptors, or chemical modifications to the vector need to be explored systematically. And advances such as the report — published only last week[29] — of the three-dimensional structure of the Env protein from mouse leukaemia virus (a commonly used vector), will facilitate the design of targeted vectors. A better understanding of gene transcription will allow us to design regulatory elements that permit promoter activity to be modulated, and development of tissue-specific enhancer–promoter elements should be vigorously pursued. Finally, we need to begin merging some of the qualities of viral vectors with non-viral vectors, to generate a safe and efficient gene-delivery system.

With respect to immunology, viruses still have many secrets to be unravelled. Viral systems that have evolved to escape immune surveillance can be incorporated into viral vectors. Some of these are being characterized; for example, the adenoviral E3 protein, the herpes simplex ICP47 protein and the cytomegalovirus US11 protein[30]. Systems from other pathogens may also be borrowed and incorporated into vectors. In some cases, the correcting protein will be sensed as foreign, eliciting an immune response. Animal models should help us to understand this and, where necessary, to develop strategies for tolerance.

Cell biology is involved because, in many cases, the goal of gene therapy is to correct differentiated cells, such as epithelial cells in cystic fibrosis and lymphoid cells in ADA deficiency. However, because these cells are continuously replaced there has to be either continued therapy or an attempt to target the stem cells. We first need to develop further the technologies for identifying and isolating these cells, to understand their regulation, and to target infection to them *in vivo*.

So how far have we come since clinical trials began? The promises are still great, and the problems have been identified (and they are surmountable). But what of the prospects? Our view is that, in the not too distant future, gene therapy will become as routine a practice as heart transplants are today. □

Inder M. Verma and Nikunj Somia are in the Laboratory of Genetics, The Salk Institute for Biological Studies, La Jolla, California 92037, USA.

Table 2 **Comparison of properties of various vector systems**

Features	*Retroviral*	*Lentiviral*	*Adenoviral*	*AAV*	*Naked/ lipid DNA*
Maximum insert size	7–7.5 kb	7–7.5 kb	~30 kb	3.5–4.0 kb	Unlimited size
Concentrations (viral particles per ml)	$>10^8$	$>10^9$	$>10^{11}$	$>10^{12}$	No limitation
Route of gene delivery	*Ex vivo*	*Ex/In vivo*	*Ex/In vivo*	*Ex/In vivo*	*Ex/In vivo*
Integration	Yes	Yes	No	Yes/No	Very poor
Duration of expression *in vivo*	Short	Long	Short	Long	Short
Stability	Good	Not tested	Good	Good	Very good
Ease of preparation (scale up)	Pilot scale up, up to 20–50 l	Not known	Easy to scale up	Difficult to purify, difficult to scale up	Easy to scale up
Immunological problems	Few	Few	Extensive	Not known	None
Pre-existing host immunity	Unlikely	Unlikely, except maybe AIDS patients	Yes	Yes	No
Safety problems	Insertional mutagenesis?	Insertional mutagenesis?	Inflammatory response, toxicity	Inflammatory response, toxicity	None

1. Crystal, R. G. *Science* 270, 404–410 (1995).
2. Scriver, C. R. S., Beaudet, A. L., Sly, W. S. & Valle, D. V. *The Metabolic Basis of Inherited Disease* (McGraw-Hill, New York, 1989).
3. Dai, Y., Roman, M., Naviaux, R. K. & Verma, I. M. *Proc. Natl Acad. Sci. USA* 89, 10892–10895 (1992).
4. Kay, M. A. *et al. Science* 262, 117–119 (1993).
5. St Louis, D. & Verma, I. M. *Proc. Natl Acad. Sci. USA* 85, 3150–3154 (1988).
6. Felgner, P. L. *Sci. Am.* 276, 102–106 (1997).
7. Verma, I. M. *Sci. Am.* 263, 68–72 (1990).
8. Miller, D. G., Adam, M. A. & Miller, A. D. *Mol. Cell. Biol.* 10, 4239–4242 (1990).
9. Palmer, T. D., Rosman, G. J., Osborne, W. R. & Miller, A. D. *Proc. Natl Acad. Sci. USA* 88, 1330–1334 (1991).
10. Lewis, P., Hensel, M. & Emerman, M. *EMBO J.* 11, 3053–3058 (1992).
11. Field, B. N., Knipe, D. M. & Howley, P. M. (eds) *Virology* (Lippincott-Raven, Philadelphia, PA, 1996).
12. Naldini, L. *et al. Science* 272, 263–267 (1996).
13. Miyoshi, H., Takahashi, M., Gage, F. H. & Verma, I. M. *Proc. Natl Acad. Sci. USA* 94, 10319–10323 (1997).
14. Blömer, U. *et al. J. Virol.* 71, 6641–6649 (1997).
15. Yeh, P. & Perricaudet, M. *FASEB J.* 11, 615–623 (1997).
16. Dai, Y. *et al. Proc. Natl Acad. Sci. USA* 92, 1401–1405 (1995).
17. Yang, Y., Ertl, H. C. & Wilson, J. M. *Immunity* 1, 433–442 (1994).
18. Engelhardt, J. F., Ye, X., Doranz, B. & Wilson, J. M. *Proc. Natl Acad. Sci. USA* 91, 6196–6200 (1994).
19. Chen, H. H. *et al. Proc. Natl Acad. Sci. USA* 94, 1645–1650 (1997).
20. Muzyczka, N. *Curr. Top. Microbiol. Immunol.* 158, 97–127 (1992).
21. Snyder, R. O. *et al. Nature Genet.* 16, 270–276 (1997).
22. Herzog, R. W. *et al. Proc. Natl Acad. Sci. USA* 94, 5804–5809 (1997).
23. Fink, D. J., DeLuca, N. A., Goins, W. F. & Glorioso, J. C. *Annu. Rev. Neurosci.* 19, 265–287 (1996).
24. Moss, B. *Proc. Natl Acad. Sci. USA* 93, 11341–11348 (1996).
25. Berglund, P. *et al. Biotechnology (NY)* 11, 916–920 (1993).
26. Blaese, R. M. *et al. Science* 270, 475–480 (1995).
27. Bordignon, C. *et al. Science* 270, 470–475 (1995).
28. Kohn, D. B. *et al. Nature Med.* 1, 1017–1023 (1995).
29. Fass, D. *et al. Science* 277, 1662–1665 (1997).
30. Wiertz, E. J. *et al. Cell* 84, 769–779 (1996)

STIC-ILL

From: Vogel, Nancy
Sent: Thursday, December 09, 2004 2:09 PM
To: STIC-ILL
Subject: refs for 10/045,116 (references from lost parent case 09/033,555)

1636

Please send me the following:

NPL ✓ Adonis
MIC BioTech MAIN
NO Vol NO NOS
Ck Cite Dupl Request
Call #

Proc. Natl. Acad. Sci. USA (1 989) 86:4574-4578

Virol. 1997 227:239-244

Virolo 1994 202:695-706

Virolo 1993 193:631-641

Genes and Dev. 1988 2:453-461

Nucleic Acid Research 1983 11 17 :6003-6020 .

Proc. Natl. Acad. Sci. USA 1994 91:8802-8806
J Virolo I 993 67 10 :591 1-592 1

Anticancer Res. 1997 17:1471-1505

J Immunol. 1988 141 6 :2084-2089

J Virol. 1989 63 2 :631-638

Science 1989 244:1288-1292

Chang et al. Cancer Gene therapy Using Novel Tumor specific Replication Competent Adenovirus Vectors" Cold Spring Harbor Gene Thera Meeting Sept. 1996

Nucleic Acids Res. 1996 24 12 :2318-2323

Current Protocols in Molecular Biology
Ausubel et al., eds., 1987 , Supp. 30, section 7.7.18 Table 7.7.1

Nature (1989) 337:387-388

Advances in Virus Research 1986 31: 169-228

Biochem. Biophys. Acta 1982 651:175-208

Mol. Cell. Biol. 1989 9 (9) :41 5-42

J Virol. 1997 71 (1) :548-561

EMBO J 1984 3 (12) :2917-2922

J Genetic Virolo 1977 68:937-940

1973 Virolo 52:456-467

1987 J Gen. Virol 36:59-72

Biochem. J. 1987 241:25-38

Hallenbeck, P.L. et a1., Novel Tumor Specific Replication Competent Adenoviral Vectors for Gene Therapy of Cancer" abstract no. 0-36 Cancer Gene Thera 1996) 3 (6) :S19-S20.

J. Biol. Chem. 1995 270 (8) :3602-3610 .
J Biol. Chem. 1994 269 (39) :23872-23875
Adv. Dru Delive Rev. 1995 17:279-292

THE JOURNAL OF BIOLOGICAL CHEMISTRY
© 1995 by The American Society for Biochemistry and Molecular Biology, Inc.

Vol. 270, No. 8, Issue of February 24, pp. 3602–3610, 1995
Printed in U.S.A.

Transcriptional Regulation of the Carcinoembryonic Antigen Gene

IDENTIFICATION OF REGULATORY ELEMENTS AND MULTIPLE NUCLEAR FACTORS*

(Received for publication, August 10, 1994, and in revised form, December 1, 1994)

Wendy Hauck and Clifford P. Stanners‡

From the Department of Biochemistry and McGill Cancer Centre, McGill University, Montreal, Quebec H3G 1Y6, Canada

Human carcinoembryonic antigen (CEA) belongs to a family of membrane glycoproteins that are overexpressed in many carcinomas; CEA functions *in vitro* as a homotypic intercellular adhesion molecule and can inhibit differentiation when expressed ectopically in myoblasts. The regulation of expression of CEA is therefore of considerable interest. The CEA gene promoter region between −403 and −124 base pairs upstream of the translation initiation site directed high levels of expression in CEA-expressing SW403 cells and was 3 times more active in differentiated than in undifferentiated Caco-2 cells, correlating exactly with the 3-fold increase in CEA mRNA seen in differentiated Caco-2 cells. Inclusion of additional upstream sequences between −1098 and −403 base pairs repressed all activity. By *in vitro* footprinting and deletion analyses, four *cis*-acting elements were mapped within the positive regulatory region, and one element within the silencing region. Several nuclear factors binding to these domains were identified: USF, Sp1, and an Sp1-like factor. By co-transfection, USF directly activated the CEA gene promoter *in vivo* in both SW403 and Caco-2 cells. In addition, the levels of factors binding to each positively acting element increased dramatically with differentiation in Caco-2 cells. Thus the transcriptional control of the CEA gene depends on the interaction of several regulatory elements that bind multiple specific factors.

CEA,[1] a membrane glycoprotein first observed in human fetal colon and colorectal cancer (1), is a widely used clinical tumor marker. CEA has been shown to function *in vitro* as a homotypic intercellular adhesion molecule (2, 3) and could thus play an important role during development. A model for a possible carcinogenic role of CEA overproduction in the colon has been suggested (2, 4). In support of this model, we have recently shown that the ectopic expression of CEA on the surface of rat L6 myoblasts can completely block terminal differentiation and the normal loss of proliferative capacity (5). These attributes make CEA an important candidate for studies on control of gene expression.

CEA is a member of the immunoglobulin supergene family and is the prototype for its own subfamily of closely related molecules that vary in domain composition and tissue distribution (for a review, see Ref. 6). This subfamily consists of 29 closely linked genes on chromosome 19, including those coding for CEA itself, nonspecific cross-reacting antigen (NCA), biliary glycoprotein (BGP), CEA gene family member 6 (CGM6), and a number of other genes with yet undetermined products (hsCGMs) (6, 7). As with CEA, NCA and BGP have been shown to function *in vitro* as intercellular adhesion molecules (2, 3, 6).

Cloned cDNAs for CEA, NCA, and BGP have been used as probes to study their expression in normal and tumor tissue (6). Whereas CEA mRNA is present at low levels in normal adult colon and is usually overexpressed in malignant colon and other cancers of epithelial cell origin, NCA mRNA is found in normal colon, lung, and granulocytes and is elevated by a greater factor in tumors of the colon, breast, and lung (6). Several forms of BGP have been isolated from bile ducts, gallbladder mucosa, and various tumors (6). In contrast to CEA and NCA mRNAs, the expression of two BGP mRNAs have been shown to be down-regulated in colorectal carcinomas in comparison to normal adjacent mucosa (8). The increased levels of CEA have been shown not to be due to gene rearrangements or amplification (9) but, instead, to hypomethylation of upstream regions (9–11) and/or factor changes leading to altered rates of transcription; post-transcriptional changes have also been implicated (9, 12).

CEA and NCA mRNA levels have also been investigated in the differentiating Caco-2 cell system (12). When cultured *in vitro*, between 4 and 11 days after reaching confluence, this human colon adenocarcinoma cell line differentiates and becomes highly polarized, with tight junctions between individual cells and a brush border membrane containing enzymes characteristic of a fully differentiated intestinal epithelium (13, 14). We found that CEA transcript levels were 3-fold higher in fully differentiated Caco-2 cells than in undifferentiated monolayers (12). In the present study, we have used the differentiation control of the *CEA* gene in Caco-2 cells to check the biological validity of the *CEA* promoter analysis.

To carry out this analysis, we characterized the upstream noncoding region of the CEA gene. A 424-bp 5′ flanking sequence has been reported to confer cell-type specific expression on a reporter gene (15). Numerous purine-rich sites were postulated to play a role in transcriptional control (11), but the exact regulatory elements involved remained unknown. We now demonstrate that both positive and negative elements reside within 1098 bp upstream of the translational start site and that a 403-bp upstream sequence confers cell type-specific and differentiation-dependent expression on the luciferase reporter gene. We identify five nuclear factor binding sites and three of the multiple *trans*-acting factors (USF, Sp1, and Sp1-like) interacting with the stimulatory domain. In addition, we present direct evidence that USF activates CEA gene transcription *in vivo*.

* This work was supported by grants from the Medical Research Council of Canada and the National Cancer Institute of Canada. The costs of publication of this article were defrayed in part by the payment of page charges. This article must therefore be hereby marked "*advertisement*" in accordance with 18 U.S.C. Section 1734 solely to indicate this fact.

‡ To whom correspondence should be addressed: McGill Cancer Centre, McGill University, 3655 Drummond St., Rm. 701, Montreal, Quebec H3G 1Y6, Canada. Tel.: 514-398-7279; Fax: 514-398-6769.

[1] The abbreviations used are: CEA, carcinoembryonic antigen; bp, base pair(s); LUC, luciferase; RSV, Rous sarcoma virus; FP, footprint; NCA, nonspecific cross-reacting antigen; BGP, biliary glycoprotein; CGM6, CEA gene family member 6; USF, upstream stimulatory factor; HNF-4, hepatic nuclear factor 4; PSG, pregnancy-specific glycoprotein.

MATERIALS AND METHODS

Plasmid Constructions—Upon probing a human epithelial genomic EMBL3 phage library (gift from N. Laskin, Cold Spring Harbor Laboratory, Cold Spring Harbor, NY) with the 5′ untranslated and leader region of human CEA cDNA (16), a 17.7-kilobase pair genomic clone was found to contain sequence identical to that of the CEA coding region. In addition, 2.3 kilobase pairs of upstream sequence were found to be virtually identical to the *CEA* gene (COSCEA01) sequence already published (15); only five dispersed single base differences were found in 1098 bp of sequenced DNA immediately upstream of the initiation codon. The −3500 to +1 (translational start site of the CEA gene) upstream region of this genomic clone was used for promoter analyses.

5′ deletion mutants of the CEA gene promoter lacked the CEA translation initiation codon and were fused immediately 5′ to the firefly luciferase (LUC) reporter gene (17) at the *Sma*I site of the pXP2 vector (18). The resulting plasmids were named according to the sizes of their respective CEA promoter restriction fragments as shown in Fig. 1. Internal deletion mutants of the CEA gene promoter, p1098Δ279LUC and p1098aΔ279LUC, were constructed as follows: the *Avr*II^{-1098} to *Ava*I^{-403} fragment was blunt-ended and inserted in the sense and antisense (a) orientation into the blunt-ended *Avr*II site in p124LUC, thus preserving the transcriptional initiation site at its proper position. p1098+279LUC contains the 974-bp *Avr*II fragment, spanning from −124 to −1098, inserted into the *Avr*II site of p403LUC. pRSVLUC (18), containing the RSV long terminal repeat fused to the LUC gene in pXP2, was obtained from Dr. M. Featherstone (McGill Cancer Centre, Montreal); pRSVZβ-gal was obtained from Dr. E. Shoubridge (Montreal Neurological Institute, Montreal) and contains the β-galactosidase gene driven by the RSV long terminal repeat.

Cells and DNA Transfections—Four human cultured cell lines, SW403 (CCL 230, human colon adenocarcinoma), HT29 (HTB 38, human colon adenocarcinoma), Caco-2 (HTB 37, human colon adenocarcinoma), and HepG2 (HB 8065, human hepatocellular carcinoma) were obtained from ATCC (Rockville, MD) and maintained in Dulbecco's modified Eagle's medium supplemented with 10% fetal bovine serum and penicillin/streptomycin (Life Technologies, Inc.). The LR-73 (Chinese hamster ovary cell-derived) (19) and HeLa R19 (human epithelial cervical carcinoma) (20) cell lines were grown in α-minimal essential medium (21), supplemented with 10% fetal bovine serum and penicillin/streptomycin.

Cells were plated at a density of 1×10^6 cells/100-mm plastic Petri dish 24 h before transfection. 10 μg of pRSVLUC or equimolar amounts of the promoter-LUC gene constructs were cotransfected with 5 μg of pRSVZβ-gal and 10 μg of calf thymus carrier DNA by calcium phosphate-DNA coprecipitation as described previously (22). The precipitate was removed after 15 h, and the cultures were incubated for another 72 h in normal growth medium. Undifferentiated Caco-2 monolayers were transfected at 2 days before confluence; fully differentiated Caco-2 cells were transfected at 11 days after confluence. Their state of differentiation was confirmed by the presence of domes and the development of a brush border membrane (12). γ-Interferon (Collaborative Research Inc., Bedford, MA) was applied to Caco-2 cells at 2000 units/ml as described previously (12) immediately following transfection, with a fresh medium change. LUC activity was measured as described by DeWet *et al.* (17). β-Galactosidase activity (23) in these same extracts was measured to correct for variations in transfection efficiency. Relative luciferase activity was calculated as the ratio between LUC and β-galactosidase activities for each transfection and then reported as -fold above background (considered as activity of the parental promoterless vector, pXP2). Each plasmid was tested in duplicate plates and in three to five different transfection experiments.

To assess the effect of USF on CEA promoter activity *in vivo*, 10 μg of p403LUC and either 5 or 15 μg of pRSV.USF (as indicated in Table II) were coprecipitated with calcium phosphate and transiently transfected into the SW403 or Caco-2 cell line. pRSV.USF was constructed by inserting human USF cDNA (24, 25) into a pUC18-derived expression vector driven by the RSV long terminal repeat (18). Rat HNF-4 cDNA in the pSG5 expression vector (26) was generously provided by Dr. F. M. Sladek (University of California, Riverside, CA).

Nuclear Extracts and DNase I Footprinting Assays—Nuclear extracts were prepared as described by Therrien *et al.* (27). All buffers contained leupeptin, pepstatin A, and aprotinin at concentrations of 1 μg/ml, and phenylmethylsulfonyl fluoride at 1 mM. Extracts were assayed for protein content by the Bio-Rad protein assay and stored at −75 °C.

DNase I footprinting assays were performed essentially as described by LeFèvre *et al.* (28) with modifications as by Howell *et al.* (29). Briefly, 1–2 fmol (10,000 cpm) of DNA probes, labeled at only one end, were incubated with 0–160 μg of nuclear extracts for 15 min on ice; restriction enzyme-grade bovine serum albumin (Boehringer Mannheim) was added so that equal total amounts (160 μg) of protein were present in each reaction. Freshly diluted DNase I (Life Technologies, Inc.) at 20 ng/30 μl reaction volume was added for 3 min on ice. Reactions were stopped, and the DNA was digested with proteinase K, phenol-extracted, and precipitated. The dried DNAs were suspended in formamide loading dye, and equal counts/min were loaded on an 8% polyacrylamide, 8 M urea sequencing gel. Sequencing reactions (23) were run alongside as size markers. The dried gels were autoradiographed at −75 °C with Cronex Quanta III intensifying screens (E. I. du Pont de Nemours & Co.).

Gel Mobility Shift Assays—Probes used for gel mobility shift assays corresponded to the protected sequences in the DNase I footprinting experiments, including a few nucleotides on either side. Their sequences and that of other competitor oligonucleotides used are shown in Table I. The double-stranded oligonucleotides were synthesized (Sheldon Biotechnology Centre, McGill University), purified by gel electrophoresis, phosphorylated with T4 polynucleotide kinase (Pharmacia Biotech Inc.) in the presence of [γ-^{32}P]ATP (Amersham Corp.), and purified from unincorporated radioactivity by passage through NICK columns (Pharmacia). About 2 fmol (15,000 cpm) of 5′-end-labeled, double-stranded oligonucleotides were then incubated with 20–60 μg of various nuclear extracts and 4 μg of poly(dI-dC) in binding buffer (29) at 23 °C for 15 min. For competition experiments, the competitor oligonucleotides and extracts were mixed together for 15 min at 23 °C, then probe was added for an additional 15-min incubation. All samples were subjected to electrophoresis on 5% nondenaturing polyacrylamide gels buffered with 1 × TGE (Tris/glycine/EDTA) (23). The gels were autoradiographed at −75 °C with an intensifying screen. Purified human AP-2 (30) and Sp1 (31) transcription factors were obtained from Promega Corp. (Madison, WI); rabbit polyclonal IgG specific to the human p95 and p106 Sp1 proteins was obtained from Santa Cruz Biotechnology, Inc. (Santa Cruz, CA). Human USF cDNA (24, 25) in a T7-driven plasmid and a USF-specific antibody were gifts of Dr. R. G. Roeder (The Rockefeller University, New York, NY). USF protein was obtained directly from USF cDNA by T7 RNA polymerase (New England Biolabs) transcription *in vitro*, followed by translation *in vitro* using rabbit reticulocyte lysate (Promega).

To determine equivalent amounts of nuclear extracts from Caco-2 cells in their undifferentiated and differentiated states, oligonucleotides binding to ubiquitous factors such as Sp1 (31) or AP1 (32) could not be used since the levels of these factors have been observed to change with differentiation (Ref. 33 and data not shown). Thus equal concentrations of isolated nuclei were used to normalize the extracts. Using this approach, with the preparations shown in Fig. 6, 20 μg of undifferentiated Caco-2 nuclear extract was equivalent to 18 μg of differentiated Caco-2 nuclear extract. The data shown in Fig. 6 are representative of several independent experiments using independent nuclear extracts.

RESULTS

Functional Analysis Reveals Negative and Positive Cell-specific Regulatory Elements—A genomic *CEA* clone containing 3.5 kilobase pairs of sequence upstream of the initiation codon was isolated from a normal human epithelial cell library and was found to be virtually identical in the 5′ noncoding sequence reported by Schrewe *et al.* (15) for the *CEA* gene. In the present report, we specifically localize the regulatory elements in the CEA upstream region by various 5′ deletion constructs in several CEA-producing and non-producing cell lines. A very high CEA-producing human colon carcinoma cell line, SW403, showed high levels of luciferase expression when driven by a 403-bp upstream region of the CEA gene (the p403LUC construct in Fig. 1): 91-fold above background relative to only 2-fold and 5.5-fold above background in CEA-non-expressing rodent LR-73 and human HeLa R19 cells, respectively. In a low CEA-expressing human hepatocarcinoma cell line, HepG2, the 403-bp minimal promoter gave 7.7-fold above background activity, whereas in HT29 cells, a medium CEA-expressing human colon carcinoma cell line, it was surprisingly not active (1.8-fold above background) This was perhaps due to the inher-

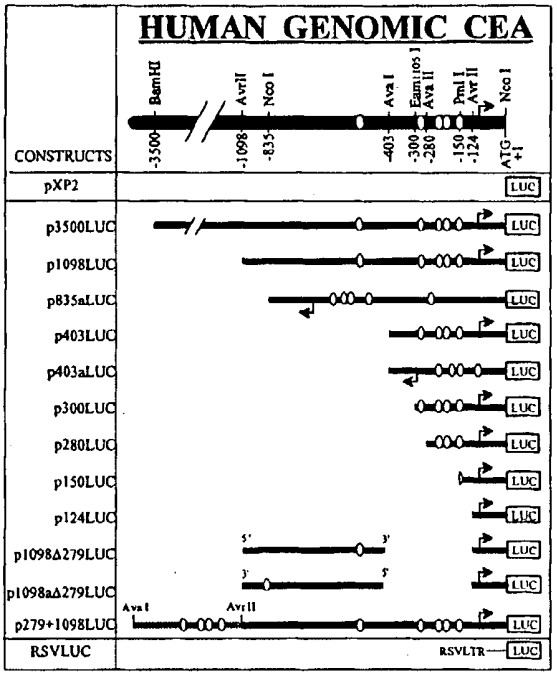

RELATIVE LUCIFERASE ACTIVITY

(fold above background)

CONSTRUCTS	SW403	LR-73	HepG2	HeLa R19	HT29	Caco-2	
						UNDIFF	DIFF
pXP2	1	1	1	1	1	1	1
p3500LUC	1	1	1	1	1	1	1
p1098LUC	14 ± 2	1.0 ± 2	2.2 ± 0.3	1.0 ± 1	1.0 ± 0.5	2.0 ± 1	4.0 ± 1
p835aLUC	2.0 ± 1	1.0 ± 1	1.3 ± 0.5	1.2 ± 0.5	1.0 ± 0.5	1.0 ± 0.8	1.7 ± 0.4
p403LUC	91 ± 9	2.0 ± 1	7.7 ± 1	5.5 ± 0.7	1.8 ± 0.2	57 ± 11	165 ± 23
p403aLUC	29 ± 1	1.5 ± 1	4.0 ± 0.9	2.5 ± 0.5	0.7 ± 0.2	10 ± 2	8.4 ± 2
p300LUC	70 ± 11	1.5 ± 0.5	6.9 ± 1.1	4.2 ± 0.4	1.8 ± 0.3	94 ± 20	238 ± 35
p280LUC	38 ± 8	1.0 ± 0.6	5.5 ± 1.2	1.0 ± 0.8	1.5 ± 0.1	48 ± 5	96 ± 14
p150LUC	1.0 ± 0.3	1.0 ± 0.5	1.0 ± 0.7	1.0 ± 0.3	0.8 ± 0.2	1.0 ± 0.8	1.1 ± 0.9
p124LUC	1.0 ± 0.8	1.0 ± 0.8	0.9 ± 0.5	0.7 ± 0.2	0.7 ± 0.5	1.0 ± 1	1.0 ± 0.3
p1098Δ279LUC	1.0 ± 0.5	1.0 ± 0.5	1.7 ± 0.8	1.5 ± 0.5	1.0 ± 0.8	1.0 ± 1	1.5 ± 0.5
p1098aΔ279LUC	1.0 ± 0.6	1.0 ± 0.2	1.0 ± 0.4	0.8 ± 0.6	1.0 ± 0.6	1.0 ± 0.5	1.0 ± 0.8
p279+1098LUC	110 ± 29	2.0 ± 1	62 ± 9	47 ± 12	2.7 ± 0.4	155 ± 31	N.D.
RSVLUC	360 ± 78	94 ± 10	54 ± 9	4.0 ± 0.5	210 ± 48	219 ± 43	188 ± 17

FIG. 1. **Localization of the elements determining CEA gene promoter activity.** CEA promoter activity in various cell lines is shown. The activity of each construct in each of the cell lines is presented relative to the activity of the promoterless vector, pXP2. In all cases, CEA sequences from −2 to −124, including the 5′ untranslated region and transcription initiation site, are present in plasmid constructs. The translational start site is at position +1. *Ovals* represent regions protected in DNase I footprinting assays. Names of constructs correspond to the sizes of the fragments tested. Sites used to create constructs are shown on the restriction map, with precise positions shown in Table I. The data represent the mean ± S.D. of three to four independent experiments, each performed in duplicate, and corrected for protein concentration and for transfection efficiency by the activity of the internal RSVZβ-gal control plasmid. *N.D.*, not determined.

ently low transfection efficiency for HT29 cells, despite corrections for efficiency.

Deletion of the −403 to −124 sequence, leaving only the transcription initiation site and 5′ untranslated region intact (p124LUC construct), abolished all promoter activity (Fig. 1). Thus regulatory elements responsible for the control of cell-specific expression of the *CEA* gene reside within this 279-bp upstream region. Inversion of the 403-bp minimal promoter in the p403aLUC antisense construct strongly reduced but did not abolish activity, suggesting that the elements within the minimal promoter may use cryptic signals on either strand for transcriptional initiation (no TATA box can be found in the upstream sequence of the *CEA* gene). Inclusion of further upstream sequences (−1098 to −403) in conjunction with the minimal promoter, as seen with the p1098LUC construct, repressed promoter activity markedly in SW403 cells (Fig. 1). The −1098 to −403 region alone, placed in either orientation before the fragment containing the transcription initiation site, showed no activity whatsoever (constructs p1098Δ279LUC and p1098aΔ279LUC). Hence, a silencer region, which can down-regulate *CEA* gene transcription, must lie within the −1098 to −403 bp sequence. This silencer can nevertheless be completely overcome by the upstream placement of a second 279-bp (from −403 to −124) region at −1098 bp (construct p279+1098LUC) (Fig. 1).

Differentiation Dependence of Regulatory Elements—To determine whether the transcriptional control of CEA expression seen previously with the differentiation of Caco-2 cells (12) could be accounted for by the *CEA* gene upstream regulatory region, all promoter constructs were transiently transfected into undifferentiated, subconfluent Caco-2 cells and into fully differentiated Caco-2 cells. The last two columns in Fig. 1 summarize the results. The 403-bp minimal promoter was found to be 3 times more active in differentiated than in undifferentiated Caco-2 cells, thus correlating exactly with the 3-fold increase seen in CEA mRNA in differentiated monolayers (12). CEA regulatory elements found within this 403-bp region could therefore be responsible for differentiation-dependent CEA expression in Caco-2 cells.

As seen with the SW403 cell line, the inclusion of additional upstream (−1098 to −403) sequence also repressed promoter activity in Caco-2 cells, and further deletions of the minimal promoter past position 403 generally decreased activity. Only in Caco-2 cells does the p300LUC construct give higher activity than the p403LUC construct, however. It is thus possible that a second silencing element, recognized by factors only in Caco-2 nuclear extracts, is present in the −403 to −300 region.

Since γ-interferon increases levels of CEA mRNA quite dramatically in the Caco-2 cell line (12), this cytokine was applied for 3 days to examine changes in promoter activity. However, no effects on promoter activity were seen (data not shown), despite the presence of several possible γ-interferon activation sites and γ-interferon-stimulated response elements in the upstream promoter region (−835 to −1650).

DNase I Footprinting—To localize the regulatory elements responsible for the activities seen with the luciferase constructs in Fig. 1, we performed DNase I protection experiments using end-labeled fragments as probes incubated with nuclear extracts from various CEA-expressing and non-expressing cell lines. In all cases, any observed footprints were considered valid only if demonstrated on both strands in repeated experiments. Within the −403 to −124 upstream region, the deletion of which abolished all promoter activity (Fig. 1; p124LUC construct), we identified four sites protected from DNase I digestion by various CEA-expressing cell line nuclear extracts but not by CEA non-expressing LR-73 extracts (Fig. 2, *B* and *C*).

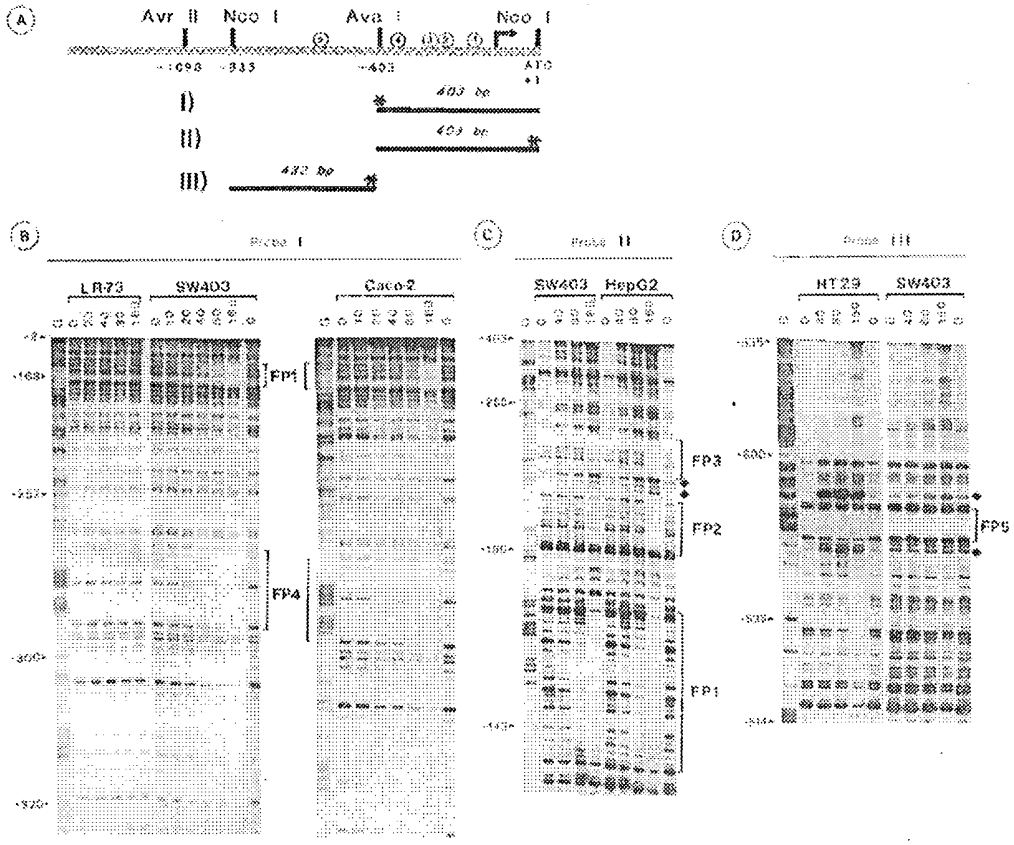

FIG. 2. **Localization of binding sites for nuclear proteins within the CEA promoter using DNase I footprinting.** *A*, restriction enzyme map of the CEA promoter showing sites used to generate the probes used in the footprinting experiments. Probes I–III were labeled as indicated by *asterisks* at either the 5′ or 3′ end. The *circled numbers* show the positions of the footprints detected. *B*, localization of sites within the −2 to −403 region. 5′-end-labeled probe I was incubated as described under "Materials and Methods," with nuclear extracts from LR-73, SW403, and Caco-2 (undifferentiated monolayers) as indicated. *G* refers to the G sequencing track; *lanes 0* contained 160 μg of bovine serum albumin only, and *lanes 10–160* show results for 10–160 μg of the indicated nuclear protein extracts. The positions of the various footprints are indicated on the *right* by *bars* and labels, their precise sequences are listed in Table III. The positions of some guanine residues are shown on the *left* for orientation purposes. Footprints were numbered according to their proximity to the transcription initiation site. *C*, localization of binding sites with a 3′-end-labeled −403 to −2 probe (Probe II). Footprints FP2 and FP3 are revealed using HepG2 nuclear extract. This probe is also shown using SW403 nuclear extract for comparison. DNase I hypersensitive sites (◆) produced by binding of nuclear proteins to the FP2 and FP3 elements are visible. *D*, localization of binding sites in the silencer region with a 5′-end-labeled −835 to −402 probe (Probe III). In addition to SW403 nuclear extract, a nuclear extract prepared from HT29 cells was assayed for comparison. Both extracts reveal DNase I hypersensitive sites (◆) flanking the FP5 element.

Footprints (FP) FP1 and FP4 were clearly visible with nuclear extracts from most of the CEA-expressing lines; their positions in the upstream sequence are shown in Fig. 2*A* and in Fig. 1 (*ovals*). Comparison of the luciferase activities of p800LUC with p280LUC, containing and lacking the FP4 element, respectively, indicates an approximately 2-fold contribution of this element to the minimal promoter activity.

Two additional footprints, labeled FP2 and FP3, were revealed using nuclear extract from HepG2 cells and were also present, although less apparent, with extracts from SW403 cells (Fig. 2*C*). Two DNase I-hypersensitive sites are visible between FP2 and FP3.

In Fig. 2*D*, the −835 to −403 silencing region was used as an end-labeled probe in DNase I footprinting experiments; only one protected region could be detected in repeated experiments. This footprint, labeled FP5, was more apparent in HT29 nuclear extract and was flanked by two DNase I-hypersensitive sites. Deletion of the −1098 to −403 region containing this element led to an increase in promoter activity in all cell lines tested (Fig. 1, p1098LUC *versus* p403LUC constructs).

USF Binds to the CEA FP1 Element—Comparison of the protected sequence in FP1 to a transcription factor data base identified several candidate binding factors. These included the upstream stimulatory factor (USF) (34) and hepatic nuclear factor 4 (HNF-4) (26), also known as liver-specific factor A1 (LF-A1) (35). Two complexes with labeled FP1 oligonucleotide (Table I), C1 and C2, were visible by band-shift assays using SW403 (Fig. 3*A*) or HepG2 (Fig. 3*C*) nuclear extracts. Formation of both complexes were competed effectively by 5- and 10-fold molar excesses of either unlabeled FP1 oligonucleotide (Fig. 3*A*, *lanes 2–4*) or of GAL2 oligonucleotide, whose sequence represents a USF-binding element in the GAL2 gene (36) (Fig.

TABLE I
Oligonucleotides used in gel mobility shift assays

Name	Sequence	Source
FP1	5′-CACACCCATGACCCACGTGATGCTG-3′	
GAL2	5′-AATGGGTCACGTGATCTATAT-3′	(36)
α1-AT	5′-CAGCCAGTGGACTTAGCCCCTGTTTGCT-3′	(35)
FP2	5′-AGAAATGAGAGGGGAGGGGACAGA-3′	
FP3	5′-AAAAAAGAGGAGGGAGAAAAGA-3′	
SP1	5′-ATTCGATCGGGGCGGGGCGAG-3′	(38)
AP1	5′-CGCTTGATGACTCAGCCGGAA-3′	(37)
PY	5′-TCGAGCAGGAAGTTCGA-3′	(39)

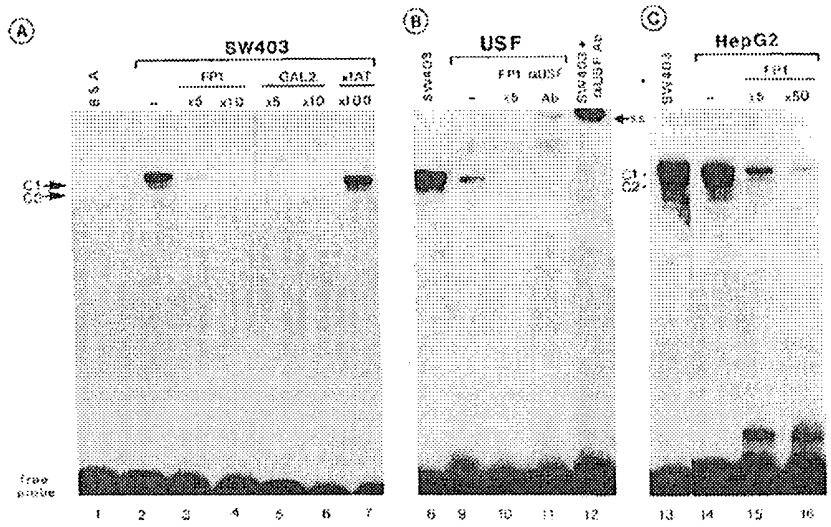

FIG. 3. **Gel mobility shift assay reveals that the USF transcription factor binds to the FP1 regulatory element.** *A*, synthetic, double-stranded oligonucleotide representing FP1 (Table I) was end-labeled, incubated with 60 μg of SW403 nuclear extract and electrophoresed, showing two complexes (C1 and C2). 5-, 10-, or 100-fold molar excesses of competing oligonucleotides were added as indicated. *B*, USF synthesized *in vitro* (see "Materials and Methods") was added to the FP1 probe in *lanes 9–11*; a 5-fold molar excess of unlabeled FP1 DNA was added in *lane 10*; *lanes 11* and *12*, USF specific antibody was first added to USF protein or SW403 nuclear extract, respectively, for 15 min at 0 °C, after which the FP1 probe was added and incubated for another 15 min on ice. The supershifted (s.s.) complex is indicated by an *arrow* on the *right*. *C*, for comparison, 40 μg of HepG2 nuclear extract was analyzed for binding under the same conditions as that with SW403 extract. 5- and 50-fold molar excesses of unlabeled, double-stranded FP1 oligonucleotide were used as competitor DNAs.

3A, *lanes 5* and *6*). The two complexes were not affected by an excess of an oligonucleotide representing the HNF-4/LF-A1 motif taken from the α1-antitrypsin gene (35) (α1-AT, Fig. 3A, *lane 7*), however, suggesting that the FP1 element is not an HNF-4/LF-A1 site. This corroborates our studies in which 10 μg of p403LUC and up to 20 μg of functional HNF-4 cDNA were co-transfected into SW403, Caco-2, HepG2, and LR-73 cells. Activation of the CEA promoter in p403LUC by HNF-4 could not be detected (data not shown), even though USF was capable of activating p403LUC in the same experiment (see below).

Since the GAL2 USF oligonucleotide competed effectively for complex formation, we tested whether purified USF transcription factor would recognize the FP1 element. The complex formed (Fig. 3*B*, *lanes 9* and *10*) comigrated with C1 from SW403 extract (Fig. 3*B*, *lane 8*). As expected, specific anti-USF antibody supershifted the DNA/USF complex (Fig. 3*B*, *lane 11*) but also supershifted the C1 complex from SW403 nuclear extract (Fig. 3*B*, *lane 12*). Thus colon carcinoma cell lines clearly contain USF, which can bind to the FP1 element in the CEA gene promoter. The presence of two complexes in HepG2 nuclear extracts comigrating with those obtained with SW403 extract (Fig. 3*C*) suggests that USF is also present in this hepatoma-derived cell line.

USF Activation of the CEA Gene Promoter in Vivo—To test directly whether USF could modulate CEA gene promoter activity *in vivo*, an expression plasmid carrying USF cDNA, pRSV.USF, together with the CEA minimal promoter construct, p403LUC, were co-transfected into various cells. Co-transfection with 15 μg of pRSV.USF produced 2.6-fold greater LUC activity in SW403 cells and 3.1-fold greater activity in undifferentiated Caco-2 cells than the level produced by co-transfection with 15 μg of pUC, the parental vector of pRSV.USF, lacking USF cDNA; in addition, the effect of pRSV.USF was concentration-dependent (Table II). In contrast, the activity of the basic luciferase vector, pXP2, was not influenced by co-transfected pRSV.USF (data not shown), indicating that USF-mediated transactivation was not due to sequences within the luciferase vector. In addition, as mentioned above, co-transfection with functional HNF-4 cDNA also had no effect on the activity of p403LUC. Thus it seems likely that CEA promoter activity is partially controlled by the level of USF in differentiated Caco-2 cells and colon tumors. However, USF is a ubiquitously expressed factor and CEA shows a much more restricted tissue-specific expression pattern. Therefore, other elements and *trans*-acting factors of the CEA gene promoter must interact to achieve tissue-specific expression.

TABLE II
USF activation of the CEA gene promoter in vivo

pUC or pRSV.USF were cotransfected with the p403LUC construct into the SW403 and Caco-2 (undifferentiated) colon carcinoma cell lines. LUC activities as shown in the two columns on the right represent the mean ± S.D. of two separate experiments, performed in duplicate.

Cotransfected constructs	LUC activity relative to p403LUC + pUC in:	
	SW403	Caco-2
	%	%
p403LUC + 15 μg of pUC	100	100
p403LUC + 5 μg of pRSV.USF	173 ± 36	231 ± 58
p403LUC + 15 μg of pRSV.USF	257 ± 41	310 ± 98

Sp1, Sp1-like, and an Unknown Nuclear Factor Bind the CEA FP2 and FP3 Elements—Gel mobility shift assays with oligonucleotides representing the FP2 and FP3 regions are shown in Figs. 4 and 5, respectively. Three retarded complexes, C1, C2, and C3, were seen with the FP2 probe (Fig. 4*A*). Two of these, C1 and C2, comigrated with the two retarded complexes seen with the FP3 probe (Fig. 5*A*). FP2 and FP3 compete with each other for the formation of C1 and C2 (Figs. 4*A* and 5*A*), as would be expected from the high sequence homology between these two adjacent sites. The C3 complex appears to be due to an unrelated factor specifically recognizing the FP2 element, since excess FP2 oligonucleotide, but not FP3 oligonucleotide, competes for its formation (Fig. 4*A*, *lanes 4* and *6*). The FP2 sequence exhibited some homology to the AP1 consensus recognition site, but molar excesses of an oligonucleotide representing an AP1 site did not compete with the FP2 probe (Fig. 4*A*, *lanes 9* and *10*) or with the FP3 probe (Fig. 5*A*, *lanes 9* and

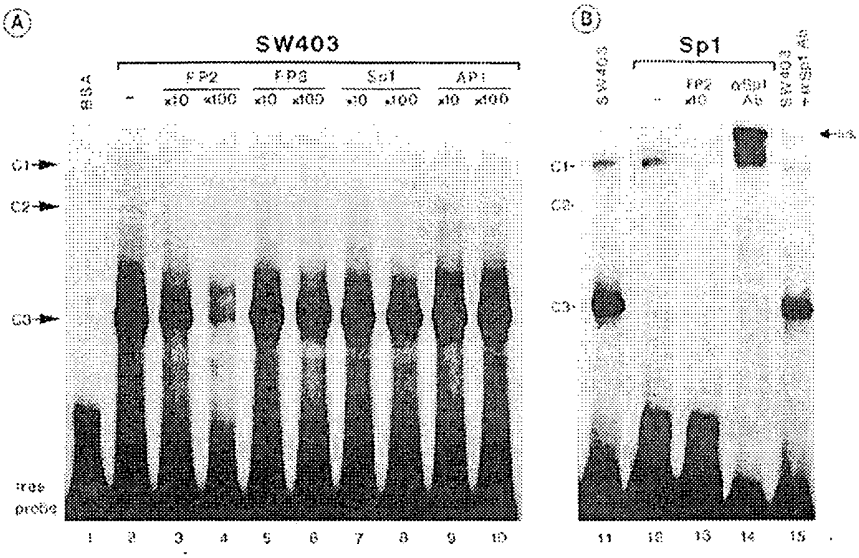

FIG. 4. **Element FP2 is recognized by Sp1 and another novel transcription factor.** *A*, end-labeled, double-stranded FP2 oligonucleotide (Table I) was incubated with 40 μg of SW403 nuclear extract and subjected to electrophoretic analysis. Three complexes (C1–C3) were revealed. Unlabeled, double-stranded FP2, FP3, Sp1, and AP1 oligonucleotides (Table I; 10- and 100-fold molar excesses) were used as competitor DNAs. *B*, 3.5 ng of purified Sp1 protein was incubated with FP2 probe in *lanes 12* and *13* under the same binding conditions. Antibody specific to Sp1 was preincubated with 14 ng of Sp1 protein (*lane 14*) and 40 μg of SW403 nuclear extract (*lane 15*). The Sp1 supershifted (*s.s.*) complex is indicated by an *arrow* on the *right*.

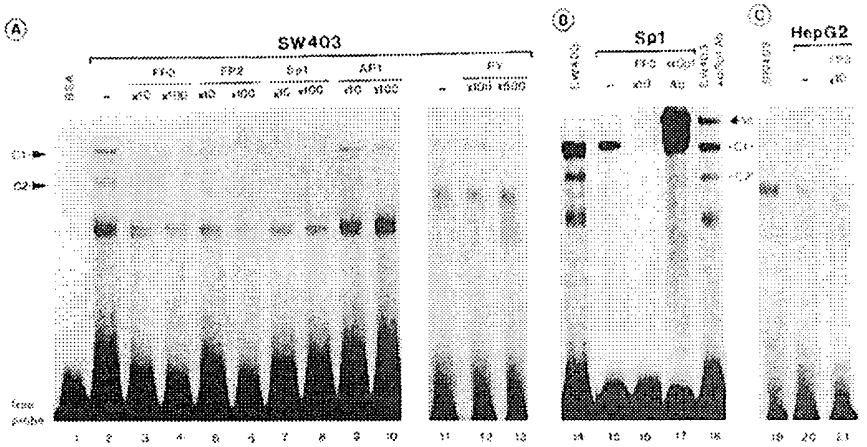

FIG. 5. **Element FP3 is bound by Sp1.** *A*, electrophoretic analysis of end-labeled, double-stranded FP3 oligonucleotide (Table I) incubated with 40 μg SW403 nuclear extract shows two specific complexes (C1 and C2). Unlabeled, double-stranded FP3, FP2, Sp1, AP1, and PY oligonucleotides (Table I; molar excesses as shown) were used as competitor DNAs. *B*, in *lanes 15* and *16*, FP3 probe and 3.5 ng of purified Sp1 protein were incubated as described in Fig. 4. Sp1-specific antibody was preincubated with 14 ng of Sp1 protein (*lane 17*) and 40 μg of SW403 nuclear extract (*lane 18*). The Sp1 supershifted (*s.s.*) complex is indicated by an *arrow* on the *right*. *C*, 20 μg of HepG2 nuclear extract was incubated with FP3 probe under the same binding conditions for comparison purposes.

10). The FP3 sequence showed some homology to a PEA3 site (32, 37), but an excess of an oligonucleotide with the PEA3 sequence from the polyoma enhancer (PY) did not inhibit complex formation with either the FP3 probe (Fig. 5, *lanes 11–13*) or the FP2 probe (data not shown). Positive competition by an oligonucleotide representing an Sp1 binding site (38) with both FP2 and FP3 as probes (Figs. 4*A* and 5*A*, *lanes 7* and *8*), however, indicated that this factor may be responsible for complexes C1 and C2, but not C3. Although the FP2 and FP3 sites are remarkably GA-rich, rather than the typical GC-rich Sp1 site sequence (38), purified Sp1 protein did form complexes with both the FP2 and FP3 probes, which comigrated with the C1 complex in SW403 extract (Fig. 4*B*, *lanes 11* and *12*; Fig. 5*B*, *lanes 14* and *15*). Antibody specific to Sp1 supershifted the Sp1 C1 complexes formed with the FP2 and FP3 elements, as expected, but also the FP2 and FP3 C1 complexes formed with SW403 nuclear extracts (Fig. 4*B*, *lanes 14* and *15*; Fig. 5*B*, *lanes 17* and *18*). The C2 and C3 complexes remained unaffected. Since Sp1 protein did not produce a band comigrating with the C2 complex and the latter was not affected by an Sp1-specific antibody, but Sp1 oligonucleotide did compete for the formation of the C2 complex, we can only surmise that the second complex is due to a Sp1-like factor, and not Sp1 itself. Thus, the FP2 and FP3 regulatory elements bind Sp1 as well as a Sp1-related factor. In addition, another unknown factor binds exclusively to the FP2 site to produce the C3 complex. Similar complexes were obtained with Caco-2 extracts (Fig. 6).

Levels of Nuclear Factors in Differentiating Caco-2 Cells—Caco-2 cells show increased levels of CEA mRNA (12) and increased transcriptional activity of transfected CEA promoter-luciferase constructs (Fig. 1) with differentiation. Equivalent amounts of undifferentiated and differentiated Caco-2 nuclear extracts (based on equivalent numbers of nuclei that differed by only 10% in the concentration of total nuclear proteins; see "Materials and Methods") were examined for the levels of transcription factors by gel mobility shift assays using labeled oligonucleotides representing three of the five CEA *cis*-acting regulatory elements identified above (Fig. 6).

Probes FP1, FP2, and FP3 each produced several complexes (Fig. 6, *lanes 1–12*), similar to those seen with SW403 extracts (Figs. 3–5). The levels of the complexes obtained were dramatically higher using differentiated (*D*) than undifferentiated (*U*) Caco-2 nuclear extracts (Fig. 6). Thus, the levels of USF, Sp1, the Sp1-like, and the unknown factor responsible for the C3 complex with the CEA FP2 element all appear to increase with differentiation in Caco-2 cells. The higher levels support our contention that an increase in the abundance of positive factors interacting with the regulatory elements in the minimal promoter are partially responsible for the rise in CEA transcription observed in this differentiating system.

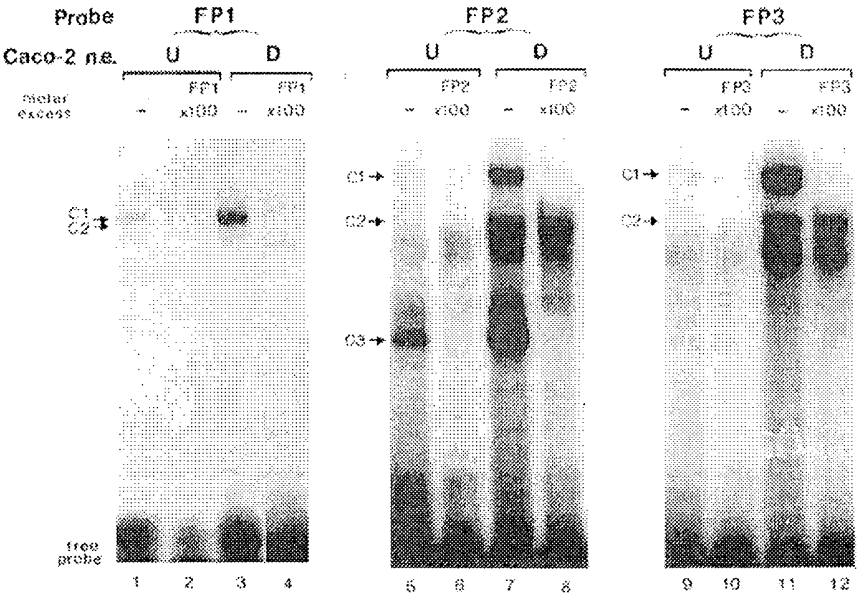

FIG. 6. **Analysis of Caco-2 nuclear proteins binding to CEA regulatory elements *versus* differentiation.** Oligonucleotides containing the DNA sequence of three of the CEA regulatory elements were used as probes to reveal Caco-2 nuclear proteins which specifically recognized them and to indicate the relative abundance of these factors in equivalent amounts of nuclear extracts prepared from undifferentiated (*U*) and differentiated (*D*) Caco-2 cells. By using equal concentrations of isolated nuclei before the elution of nuclear proteins, 20 μg of undifferentiated Caco-2 nuclear extract was found to be equivalent to 18 μg of differentiated Caco-2 nuclear extract in the experiment shown here. The indicated unlabeled oligonucleotides used as competing DNAs assessed the specificity of the complexes formed. *Arrows* point to the specific complexes.

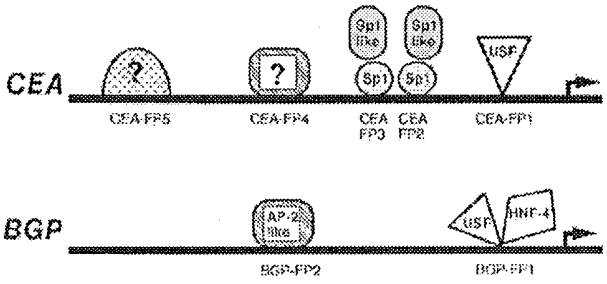

FIG. 7. **Schematic representation of the various nuclear proteins binding the regulatory elements of the CEA promoter.** These factors that have been identified are indicated. Factors binding to the BGP promoter are also shown to allow comparison of transcription factor complexes specific to the CEA gene promoter. The *arrow* signifies the major transcriptional start site. Sequences and positions are compared in Table III.

DISCUSSION

In this study, we have delineated the basic organization of the CEA gene promoter (summarized in Fig. 7 and Table III), which is the first to be determined for genes of the CEA subgroup of this human tumor marker family. Functional assays using various 5′ flanking sequences of the CEA promoter linked to the luciferase reporter gene transfected into CEA-producing cells coupled with DNase footprint assays revealed that the 5′ upstream region contains four positive (FP1–FP4) and one negative regulatory element (FP5). The upstream stimulatory factor (USF) (34), also known as the adenovirus major late transcription factor (MLTF), was shown to bind to the FP1 element; the positive control of CEA transcription by USF was confirmed directly by the demonstration of specific stimulation of the CEA promoter *in vivo* by a co-transfected USF-producing plasmid. The Sp1 (38) and an Sp1-like transcription factor were found to bind to both the FP2 and the FP3 element. Through computer sequence analyses, FP4 was found to resemble an AP-2 transcription factor site (30, 39), and preliminary experiments (data not shown) confirmed this possibility; oligonucleotides containing AP-2 binding sites competed with the FP4 site for nuclear factor binding and purified AP-2 protein was capable of forming a complex with the FP4 element. Other factors binding to the FP4 site, a third factor binding to the FP2 site and factors recognizing the FP5 silencer element remain to be identified.

The biological significance of these element and factor assignments was further tested using the Caco-2 colonocyte system, which shows an increase in CEA mRNA with differentiation into polarized epithelium. Since the positively acting factor levels increased dramatically, it is thus possible that the transcription factors identified here could also control the expression of CEA in normal colonic epithelial cells, which show an increase in CEA mRNA (40) and protein (41) production during their differentiation in transit from the bottom to the top of a crypt. The basis for transcriptional changes seen for CEA and other CEA family members in tumors remains to be investigated.

Sequence comparisons of the CEA gene regulatory elements with the upstream noncoding sequences of other CEA gene family members are shown in Table III. The control of expression of this family is of particular interest because of the unusually close alignment of the nucleotide sequences of its members (often over 90%). PSG5 and PSG11 are members of the pregnancy-specific glycoprotein (PSG) subgroup of the CEA gene family whose upstream sequences showed homology to the CEA FP2 and FP3 elements only. We have also analyzed the control of transcription of a second CEA family member, BGP (42) which, unlike CEA (6), can show decreased transcript levels in colon carcinomas relative to adjacent normal tissue (8). Comparison of the CEA and BGP gene promoters (see Fig. 7 for summary) revealed differences that could explain their differential regulation. Only two of the corresponding BGP gene elements could be shown to bind nuclear factors: thus the Sp1, the Sp1-like (recognizing FP2 and FP3 in CEA), and the silencer factors (recognizing FP5 in CEA) do not bind to the BGP promoter, while a second factor, HNF-4 (26), as well as USF, binds to the USF site (42). Experiments are in progress to determine whether the different changes in transcription of the CEA and BGP genes seen with colon carcinogenesis can be rationalized by changes in these factors.

Although the Sp1 transcription factor has long been characterized (31), only recently have dramatically increased levels of this ubiquitously expressed factor been correlated with differentiation (33). Genes regulated by Sp1 include the following: fibronectin, which shows greatly inhibited expression upon neoplastic transformation (43); E-cadherin, which is generally

TABLE III
Sequence comparisons of the CEA regulatory elements

Genetic element	Sequence[a]	Position[b]	Source
CEA FP1	CACACCCATGACCCACGTGATGCTG	−165 to −141	
NCA aligned	.G.....CC..	−167 to −143	(54)
BGP-FP1	CG..CCAG.A...A....CAGA	−158 to −137	(42)
hsCGM1 aligned	TT.....TG.AA.GTGCT	−156 to −132	(15)
GAL2 gene (USF site)	AA...GGT.....CTAT	299 to 280	(36)
USF consensus	CACGTG		(34)
CEA FP2	AGAAATGACAGGGGAGGGGACAGA	−207 to −184	
NCA aligned	.....T...	−209 to −186	(54)
BGP aligned	..G.....A....AA.....	−199 to −176	(42)
hsCGM1 aligned	.A..C.....	−199 to −174	(15)
PSG5 aligned	..G.C.....A.....	171 to 194	(55)
PSG11 aligned	..G.C.....A.A.....	412 to 435	(20)
SV40 (Sp1 site)	.TTC..TC....C....CG..		(38)
Sp1 consensus	GGGGCGGGGC TA TAAT		(38)
CEA FP3	AAAAAAGAGGAGGGACAAAAGA	−232 to −211	
NCA aligned	G..G.G.....	−234 to −213	(54)
BGP aligned	...G.GA.A.TAA.GAC...	−222 to −203	(42)
hsCGM1 aligned	CCC..G..A..A.AGA...T..	−224 to −203	(15)
PSG5 aligned	....C...A.GA.....GGAG	147 to 168	(55)
PSG11 aligned	....C...A.GA..GAC..GG.	388 to 408	(56)
SV40 (Sp1 site)	TCG.TC.G..C...G.G.G		(38)
Sp1 consensus	GGGGCGGGGC TA TAAT		(38)
CEA FP4	TCCACAGGGGATGGGGGTCCATCC	−299 to −276	
NCA aligned	.GTTAT..AACA....TC.A.A.A	−307 to −284	(54)
BGP-FP2	TCCTCC..TG.T....CA.A....TCAT.A	−305 to −273	(42)
hsCGM1 aligned	.GTTAT.AAACA...ATC.A.GTA	−299 to −276	(15)
CEA FP5	TCCATCCCT	−568 to −560	
NCA aligned	...CAGGAA	−609 to −601	(15)
BGP aligned	..TG.....	−590 to −582	(42)
hsCGM1 aligned	...CAGGAA	−598 to −590	(15)

[a] Matches to the CEA element sequences are indicated by dots.
[b] Relative to the translational initiation site at +1 for CEA family members: CEA, NCA, BGP, and hsCGM1.

down-regulated in tumors (44); and the human papillomavirus type 18 E6-E7 oncogene, which also has an unusual Sp1 site (45). Specific recognition of the DNA sequence is provided for by the three zinc finger domains of Sp1 (46). Although the core sequence is a typical GC box, substitutions are tolerated as long as certain G residues are present for contact with the "fingers" (46). These contact points exist in the FP2 and FP3 elements of the CEA gene, within the aligned homologous sequences of the NCA gene, and within the CGM1 sequence aligned to the CEA FP2 element (see Table III).

The USF gene has recently been cloned and is now known to code for a ubiquitous factor with a helix-loop-helix repeat domain and a leucine zipper (34). Its protein-binding interface is similar to that of Myc and Max (47). All Myc family members recognize an identical core DNA target sequence of CACGTG and appear to bind to DNA as homo- or heterodimers, dependent on specificities contained within the leucine zipper (34, 48, 49). Since we have directly demonstrated that USF activates the CEA promoter *in vivo*, any factors interacting with and modulating this nuclear factor should also modulate CEA gene expression. Although purified Myc protein did not bind to the CEA FP1 site (data not shown), it remains possible that the heterodimer c-Myc/Max could bind to this element or to USF itself. Both Myc/Max and USF have also been shown to bend DNA toward the minor groove to the same angle and orientation (50). Pognonec *et al.* (51) have also demonstrated that the DNA-binding activity of USF is regulated via a redox dependent mechanism. The activity of the CEA promoter could therefore be partially controlled by a complex balance between the binding of various other b-HLH proteins to form heterodimers with USF, the redox mechanism, and competition for DNA binding by other factors, such as HNF-4 as shown for the BGP promoter (42). As previously mentioned, CEA mRNA levels are up-regulated in colon carcinomas. About 70% of colon carcinomas overexpress the c-Myc gene as well as other members of the Myc gene family (52, 53), although the status of USF expression is presently unknown.

This study has identified many of the *cis*-acting elements involved in the transcriptional control of the CEA gene and some of the *trans*-acting factors which interact with them. USF, in particular, is involved in both CEA and BGP control and may play an important part in the overall control system of the CEA gene family. These assignments, coupled with further studies on other family members, should lead to the rationalization of the observed tissue-specific, differentiation-dependent expression of the family. The possible deregulation of these *trans*-acting transcriptional factors in colon carcinogenesis could represent the basis for changes in the expression of CEA and other family members seen in tumors, changes that could be instrumental in the carcinogenetic process (2). Ectopic expression of CEA, for example, has been shown recently to block myogenic differentiation and leave cells with division potential (5). It will now be of interest to determine whether the CEA regulatory elements identified here are targets for the action of oncogenes and tumor suppressor genes.

Acknowledgments—We are indebted to Drs. P. Pognonec, T. Gutjahr, and R. Roeder (Rockefeller University, New York) for USF cDNA and anti-USF antibody, and to Dr. F. M. Sladek (University of California, Riverside, CA) for HNF-4 cDNA. We also thank Dr. N. Beauchemin for stimulating discussions and critical advice and Drs. M. Chamberlin and J. Chou (National Institutes of Health, Bethesda, MD) for helpful discussions of unpublished work.

REFERENCES

1. Gold, P., and Freedman, S. O. (1965) *J. Exp. Med.* **121**, 439–462
2. Benchimol, S., Fuks, A., Jothy, S., Beauchemin, N., Shirota, K., and Stanners, C. P. (1989) *Cell* **57**, 327–334
3. Oikawa, S., Inuzuka, C., Kuroki, M., Matsuoka, Y., Kosaki, G., and Nakazato,

H. (1989) *Biochem. Biophys. Res. Commun.* **164**, 39–45
4. Jessup, J. M., and Thomas, P. (1989) *Cancer Metastasis Rev.* **8**, 263–280
5. Eidelman, F. J., Fuks, A., DeMarte, L., Taheri, M., and Stanners, C. P. (1993) *J. Cell Biol.* **123**, 467–475
6. Thompson, J. A., Grunert, F., and Zimmermann, W. (1991) *J. Clin. Lab. Anal.* **5**, 344–366
7. Barnett, T. R., Drake, L., and Pickle, W., II (1993) *Mol. Cell. Biol.* **13**, 1273–1282
8. Neumaier, M., Paululat, S., Chan, A., Matthaes, P., and Wagener, C. (1993) *Proc. Natl. Acad. Sci. U. S. A.* **90**, 10744–10748
9. Boucher, D., Cournoyer, D., Stanners, C. P., and Fuks, A. (1989) *Cancer Res.* **49**, 847–852
10. Tran, R., Kashmiri, S. V. S., Kantor, J., Greiner, J. W., Pestka, S., Shively, J. E., and Schlom, J. (1988) *Cancer Res.* **48**, 5674–5679
11. Willcocks, T. C., and Craig, I. W. (1990) *Genomics* **8**, 492–500
12. Hauck, W., and Stanners, C. P. (1991) *Cancer Res.* **51**, 3526–3533
13. Pinto, M., Robine-Leon, S., Appay, M.-D., Kedinger, M., Triadou, N., Dussaulx, E., Lacroix, B., Simon-Assmann, P., Haffen, K., Fogh, J., and Zweibaum, A. (1983) *Biol. Cell* **47**, 323–330
14. Rousset, M. (1986) *Biochimie (Paris)* **68**, 1035–1040
15. Schrewe, H., Thompson, J. A., Bona, M., Hefta, L. J., Maruya, A., Hassauer, M., Shively, J. E., von Kleist, S., and Zimmermann, W. (1990) *Mol. Cell. Biol.* **10**, 2738–2748
16. Beauchemin, N., Benchimol, S., Cournoyer, D., Fuks, A., and Stanners, C. P. (1987) *Mol. Cell. Biol.* **7**, 3221–3230
17. De Wet, J. R., Wood, K. V., DeLuca, M., Helinski, D. R., and Subramani, S. (1987) *Mol. Cell. Biol.* **7**, 725–737
18. Nordeen, S. K. (1983) *BioTechniques* **6**, 454–456
19. Pollard, J. W., and Stanners, C. P. (1979) *J. Cell. Physiol.* **98**, 571–586
20. Abraham, G., and Colonno, R. J. (1984) *J. Virol.* **51**, 340–345
21. Stanners, C. P., Elicieri, G. L., and Green, H. (1971) *Nature* **230**, 52–54
22. Baserga, R., Croce, C., and Rovera, G. (1980) *Introduction of Macromolecules into Viable Mammalian Cells*, Vol. 1, Wistar Symposium Series, Alan R. Liss, New York
23. Sambrook, J., Fritsch, E. F., and Maniatis, T. (1989) *Molecular Cloning: A Laboratory Manual*, 2nd Ed., Cold Spring Harbor Laboratory, Cold Spring Harbor, NY
24. Sawadogo, M. (1988) *J. Biol. Chem.* **263**, 11994–12001
25. Sawadogo, M., Van Dyke, M. W., Gregor, P. D., and Roeder, R. G. (1988) *J. Biol. Chem.* **263**, 11985–11993
26. Sladek, F. M., Zhong, W., Lai, E., and Darnell, J. E., Jr. (1990) *Genes & Dev.* **4**, 2353–2365
27. Therrien, M., and Drouin, J. (1991) *Mol. Cell. Biol.* **11**, 3492–3503
28. LeFèvre, C., Imagawa, M., Dana, S., Grindlay, J., Bodner, M., and Karin, M. (1987) *EMBO J.* **6**, 871–981
29. Howell, B. W., Lagacé, M., and Shore, G. C. (1989) *Mol. Cell. Biol.* **9**, 2928–2933
30. Williams, T., and Tjian, R. (1991) *Genes & Dev.* **5**, 670–682
31. Briggs, M. R., Kadonaga, J. T., Bell, S. P., and Tjian, R. (1986) *Science* **234**, 47–52
32. Wasylyk, C., Wasylyk, B., Heidecker, G., Huleihel, M., and Rapp, U. R. (1989) *Mol. Cell. Biol.* **9**, 2247–2250
33. Saffer, J. D., Jackson, S. P., and Annarella, M. B. (1991) *Mol. Cell. Biol.* **11**, 2189–2199
34. Gregor, P. D., Sawadogo, M., and Roeder, R. G. (1990) *Genes & Dev.* **4**, 1730–1740
35. Ramji, D. P., Tadros, M. H., Hardon, E. M., and Cortese, R. (1991) *Nucleic Acids Res.* **19**, 1139–1146
36. Bram, R. J., and Kornberg, R. D. (1987) *Mol. Cell. Biol.* **7**, 403–409
37. Wasylyk, B., Wasylyk, C., Flores, P., Begue, A., Leprince, D., and Stehelin, D. (1990) *Nature* **346**, 191–193
38. Kadonaga, J. T., Carner, K. R., Masiarz, F. R., and Tjian, R. (1987) *Cell* **51**, 1079–1090
39. Williams, T., Admon, A., Lüscher, B., and Tjian, R. (1988) *Genes & Dev.* **2**, 1557–1569
40. Jothy, S., Yuan, S.-Y., and Shirota, K. (1993) *Am. J. Pathol.* **143**, 250–257
41. Ahnen, D. J., Nakane, P. K., and Brown, W. R. (1982) *Cancer* **49**, 2077–2090
42. Hauck, W., Nédellec, P., Turbide, C., Stanners, C. P., Barnett, T. R., and Beauchemin, N. (1994) *Eur. J. Biochem.* **223**, 529–541
43. Dean, D. C., Bowlus, C. L., and Bourgeois, S. (1987) *Proc. Natl. Acad. Sci. U. S. A.* **84**, 1876–1880
44. Behrens, J., Löwrick, O., Klein-Hitpass, L., and Birchmeier, W. (1991) *Proc. Natl. Acad. Sci. U. S. A.* **88**, 11495–11499
45. Hoppe-Seyler, F., and Butz, K. (1992) *Nucleic Acids Res.* **20**, 6701–6706
46. Kriwacki, R. W., Schultz, S. C., Steitz, T. A., and Caradonna, J. P. (1992) *Proc. Natl. Acad. Sci. U. S. A.* **89**, 9759–9763
47. Blackwood, E. M., and Eisenman, R. N. (1991) *Science* **251**, 1211–1217
48. Beckmann, H., Su, L.-K., and Kadesch, T. (1990) *Genes & Dev.* **4**, 167–179
49. Fisher, D. E., Carr, C. S., Parent, L. A., and Sharp, P. A. (1991) *Genes & Dev.* **5**, 2342–2352
50. Fisher, D. E., Parent, L. A., and Sharp, P. A. (1992) *Proc. Natl. Acad. Sci. U. S. A.* **89**, 11779–11783
51. Pognonec, P., Kato, H., and Roeder, R. G. (1992) *J. Biol. Chem.* **267**, 24563–24567
52. Finley, G. G., Schulz, N. T., Hill, S. A., Geiser, J. R., Pipas, J. M., and Meisler, A. I. (1989) *Oncogene* **4**, 963–971
53. Melhem, M. F., Meisler, A. I., Finley, G. G., Bryce, W. H., Jones, M. O., Tribby, I. I, Pipas, J. M., and Koski, R. A. (1992) *Cancer Res.* **52**, 5853–5864
54. Oikawa, S., Kosaki, G., and Nakazato, H. (1987) *Biochem. Biophys. Res. Commun.* **146**, 464–469
55. Thompson, J. A., Koumari, R., Wagner, K., Barnert, S., Schleussner, C., Schrewe, H., Zimmermann, W. A., Müller, G., Schempp, W., Zaninetta, D., Ammaturo, D., and Hardman, N. (1990) *Biochem. Biophys. Res. Commun.* **167**, 848–859
56. Brophy, B. K., MacDonald, R. E., McLenachan, P. A., Beggs, K. T., and Mansfield, B. (1992) *Biochim. Biophys. Acta* **1131**, 119–121

STIC-ILL

From: Vogel, Nancy
Sent: Thursday, December 09, 2004 2:09 PM
To: STIC-ILL
Subject: refs for 10/045,116 (references from lost parent case 09/033,555)

1636

Please send me the following:

Proc. Natl. Acad. Sci. USA (1 989) 86:4574-4578

Virol. 1997 227:239-244

Virolo 1994 202:695-706

Virolo 1993 193:631-641

Genes and Dev. 1988 2:453-461

Nucleic Acid Research 1983 11 17 :6003-6020 .

Proc. Natl. Acad. Sci. USA 1994 91:8802-8806
J Virolo I 993 67 10 :591 1-592 1

Anticancer Res. 1997 17:1471-1505

J Immunol. 1988 141 6 :2084-2089

J Virol. 1989 63 2 :631-638

Science 1989 244:1288-1292

Chang et al. Cancer Gene therapy Using Novel Tumor specific Replication Competent Adenovirus Vectors" Cold Spring Harbor Gene Thera Meeting Sept. 1996

Nucleic Acids Res. 1996 24 12 :2318-2323

Current Protocols in Molecular Biology
Ausubel et al., eds., 1987 , Supp. 30, section 7.7.18 Table 7.7.1

Nature (1989) 337:387-388

Advances in Virus Research 1986 31: 169-228

Biochem. Biophys. Acta 1982 651:175-208

Mol. Cell. Biol. 1989 9 (9) :41 5-42

J Virol. 1997 71 (1) :548-561

EMBO J 1984 3 (12) :2917-2922

J Genetic Virolo 1977 68:937-940

1973 Virolo 52:456-467

1987 J Gen. Virol 36:59-72

Biochem. J. 1987 241:25-38

Hallenbeck, P.L. et a1., Novel Tumor Specific Replication Competent Adenoviral Vectors for Gene Therapy of Cancer" abstract no. 0-36 Cancer Gene Thera 1996) 3 (6) :S19-S20.

J. Biol. Chem. 1995 270 (8) :3602-3610
J Biol. Chem. 1994 269 (39) :23872-23875
Adv. Dru Delive Rev. 1995 17:279-292

Communication

THE JOURNAL OF BIOLOGICAL CHEMISTRY
Vol. 269, No. 39, Issue of September 30, pp. 23872–23875, 1994

Expression of a Thyroid Hormone-responsive Recombinant Gene Introduced into Adult Mice Livers by Replication-defective Adenovirus Can Be Regulated by Endogenous Thyroid Hormone Receptor*

(Received for publication, July 8, 1994)

Yoshitaka Hayashi‡, Alexander M. DePaoli‡, Charles F. Burant‡, and Samuel Refetoff‡§¶‖

From the Departments of ‡Medicine and §Pediatrics and the ¶J. P. Kennedy Jr. Mental Retardation Research Center, University of Chicago, Chicago, Illinois 60637

We constructed a recombinant adenovirus carrying the firefly luciferase gene driven by the thymidine kinase promoter and controlled by the palindromic thyroid hormone/retinoic acid-responsive element. The same adenovirus vector without the hormone-responsive element was used as control. Regulation of the luciferase gene expression was tested in pituitary-derived GH cells and hepatoma-derived HepG2 cells infected with the recombinant adenoviruses. Administration of triiodothyronine to GH cells and all-*trans*-retinoic acid to HepG2 cells resulted in 8.0 ± 0.3-fold and 4.6 ± 0.5-fold induction of luciferase activity, respectively. No significant increase was observed with the control adenovirus. Hormonal regulation was also examined in adult mice. Mice depleted of thyroid hormone were injected intravenously with the recombinant adenoviruses and given 4 times the replacement dose of triiodothyronine or vehicle only for 4 days. Hormone administration resulted in 4.2-fold increase of luciferase activity in liver homogenates. No significant effect was observed in animals injected with the control adenovirus. This recombinant adenovirus provides a new experimental system in the study of thyroid hormone and retinoic acid action and offers the potential to regulate by physiological means the expression of genes transferred for the purpose of therapy.

The replication-defective adenovirus is an efficient vehicle for the transfer of foreign genes to a broad spectrum of eukaryotic cells. Since adenovirus can infect non-proliferating cells, it can be efficiently incorporated into a variety of organs in the whole animal with rare integration of the viral genome into chromosomes (1, 2). These characteristics make the adenovirus suitable for use in gene therapy, and a number of studies in animals and in man have been pursued in recent years with the purpose of treating cystic fibrosis (3, 4), familial hypercholesterolemia (5), hemophilia B (6), Duchenne muscular dystrophy (7), and α_1-antitrypsin deficiency (8). In all instances expression of the therapeutic genes has been insured by the inclusion of a strong constitutive promoter and the level of expression determined by the infection dose. The utility of the system would be greatly improved if the expression levels of the transferred gene could be modulated by the administration of a regulatory substance. To address this possibility, we constructed a recombinant adenovirus in which the firefly luciferase gene is driven by a promoter responsive to both thyroid hormone and retinoic acid. The level of expression of this reporter gene, when transferred into adult mice, could be regulated by varying the thyroid hormone concentration within the broad physiological range.

EXPERIMENTAL PROCEDURES

Construction of Recombinant Adenovirus—The herpes simplex virus thymidine kinase promoter (tk) and 3 copies of palindromic thyroid hormone/retinoic acid-responsive element (TREpal: AGGTCA-TGACCT)[1] separated by 10 base pairs, were excised from the plasmid TREpalx3-CAT (9) and placed upstream of firefly luciferase (Luc) gene in pGL2Basic (Promega, Madison, WI) to construct tk-TREpalx3-Luc. The Luc expression cassette (tk-TREpalx3-Luc-SV40poly(A)) was then inserted into the multiple cloning site of the pAC plasmid resulting in pAC-tk-TREpalx3-Luc. A pAC plasmid carrying the Luc expression cassette without TREpal (pAC-tk-Luc) was also constructed to serve as a control. The human embryo kidney epithelial cell line, transformed with the adenovirus E1 region (293 cells) (10), was propagated in 60-mm dishes and co-transfected with 8 μg of pJM17 (11) and 2 μg of either of the two pAC plasmids by the calcium phosphate co-precipitation method (12). After overnight incubation, cells were overlaid with minimum essential medium containing 1% fetal bovine serum (FBS) and 0.75% Bacto-agar. Overlay was repeated on days 3 and 6. On day 9, minimum essential medium/FBS/Bacto-agar containing 0.01% neutral red was added to visualize the plaques, which were picked up on day 10. The recombinant adenoviruses (Ad5-tk-TREpalx3-Luc and Ad5-tk-Luc) were further propagated in 293 cells and integrity of the constructs verified by Southern blot analysis.

Preparation of Adenoviruses for Infection—293 cells were infected at a multiplicity of infection (m.o.i.) of 5. Forty-eight hours later, cells were harvested and suspended in hypotonic buffer (10 mM Tris-Cl, pH 8.0, 1 mM $MgCl_2$). After three cycles of freezing and thawing (dry ice/ethanol and 37 °C water bath), cell debris were removed by centrifugation at 2000 × *g* for 5 min. The supernatant was further purified by ultracentrifugation in cesium chloride gradient (12) and dialyzed against isotonic saline (135 mM NaCl, 5 mM KCl, 1 mM $MgCl_2$, 10 mM Tris-Cl, pH 7.4). The concentration of adenovirus particles was determined by optical density at 260 nm (10^{12} particles = 1 OD_{260}) and by the plaque-forming assay (100 particles = 1 plaque-forming unit (pfu)).

Cell Culture Procedure—The human hepatoblastoma (HepG2) cell line and rat anterior pituitary tumor (GH) cell line were grown in Dulbecco's modified Eagle's medium supplemented with 10% FBS. Twenty-four hours before infection, medium was changed to Dulbecco's modified Eagle's medium containing 10% hormone-deficient (charcoal-stripped) FBS. Cells were infected at a m.o.i. of 0.5–5 by exposure to the adenovirus overnight. Cells were then trypsinized and distributed into 12-well plates, and 24 h later, various concentrations of 3,3',5-triiodo-

* This work was supported by Grant DK15070 from the National Institutes of Health. Portions of this work were presented at the 107th Annual Meeting of the Association of American Physicians, April 30, 1994, Baltimore, MD. The costs of publication of this article were defrayed in part by the payment of page charges. This article must therefore be hereby marked "*advertisement*" in accordance with 18 U.S.C. Section 1734 solely to indicate this fact.

‖ To whom correspondence should be addressed: University of Chicago, MC3090, 5841 S. Maryland Ave., Chicago, IL 60637. Tel.: 312-702-6939; Fax: 312-702-6940.

[1] The abbreviations used are: TRE pal, palindromic thyroid hormone/retinoic acid-responsive element; Luc, luciferase; FBS, fetal bovine serum; m.o.i., multiplicity of infection; T_3, 3,3',5-triiodothyronine; RA, all-*trans*-retinoic acid; pfu, plaque-forming unit(s); m.u., map unit(s); tk, thymidine kinase.

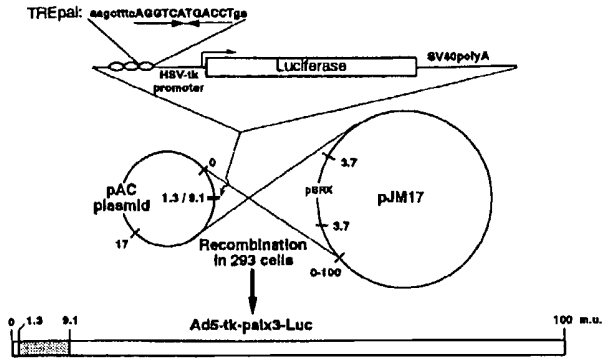

FIG. 1. **General outline of a chimeric adenovirus construction.** Co-transfection of pAC plasmid containing the Luciferase expression cassette and pJM17 into 293 cells results in the formation of the replication-defective Ad5-tk-palx3-Luc by homologous recombination. The *shaded area* in Ad5-tk-palx3-Luc represents the Luc expression cassette, which is shown at *top* of the figure. One hundred m.u. (36 kilobase pairs) is the whole length of Ad5. For details, see "Experimental Procedures."

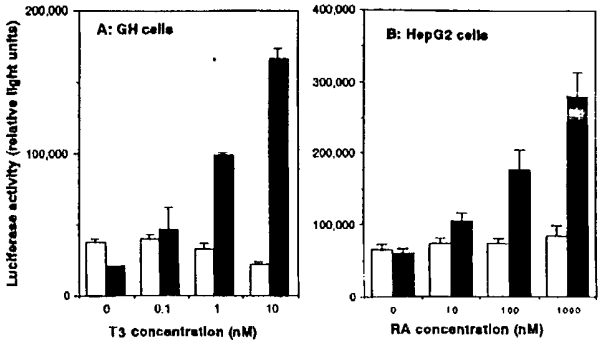

FIG. 2. **Hormonal regulation of Luc gene expression in tissue culture.** *A*, effect of T_3 on Luc gene expression in GH cells. *B*, effect of RA on Luc gene expression in HepG2 cells. Both cell lines were infected with Ad5-tk-palx3-Luc (*filled bars*) or Ad5-tk-Luc (*open bars*) at a m.o.i. of 5 and then incubated for 24 h in the absence or presence of different concentrations of the hormones. Results are expressed as mean ± S.D. Physiological concentrations of T_3 and RA in the presence of 10% FBS are 0.2 and 10 nM, respectively.

thyronine (T_3) or all-*trans*-retinoic acid (RA) were added to the medium. Cells were incubated for an additional 24 h and then lysed in 100 µl of lysis solution (25 mM Tris phosphate, pH 7.8, 2 mM dithiothreitol, 2 mM 1,2-diaminocyclohexane-*N,N,N',N'*-tetraacetic acid, 10% glycerol, 1% Triton X-100; Promega)/well. Twenty µl of lysate was used for Luc assay using reagents supplied by Promega and a Luminometer 2010 (Analytical Luminescence Laboratories, San Diego, CA).

Animal Procedures—To induce hypothyroidism, 8-week-old male mice of the CD-1 strain (body weight 30 g) were fed *ad libitum* a diet containing no iodine and supplemented with 0.15% propylthiouracil (Harland Teklad Co., Madison, WI). Ten days later, 6 mice were given tail vein injections of 2×10^9 pfu of Ad5-tk-palx3-Luc and 6 mice were injected with the same amount of the control adenovirus, Ad5-tk-Luc. Half of the mice infected with each of the two adenovirus constructs were given 4 times the replacement dose (1.5 µg/100 g of body weight) of T_3 by intraperitoneal injection every 24 h for 4 days ($+T_3$ group). The $-T_3$ group of mice were injected with the same volume of the vehicle (saline with 0.002% bovine serum albumin). Twelve hours after the fourth injection, mice were killed by cardiac puncture under light methoxyflurane anesthesia. Serum was analyzed for T_3 and thyroxine content by standard radioimmunoassays. Pieces of liver, kidney, and lung were removed and homogenized in four volumes/weight of lysis solution. After removal of cell debris by centrifugation, Luc activity was measured in 20-µl aliquots of the supernatant (4 mg of tissue).

RESULTS

Recombinant Adenovirus—The construction of the recombinant adenovirus is depicted in Fig. 1, and details are given under "Experimental Procedures." Briefly, the Luc expression cassette, tk-TREpalx3-Luc-SV40poly(A), was cloned into the pAC plasmid (13, 14). The latter contains 0–17 map units (m.u.) of the adenovirus with deleted E1 region (1.3–9.1 m.u.). The resulting plasmid was transfected into 293 cells (10) together with the plasmid pJM17 (11), which contains the entire adenovirus sequence interrupted by the pBRX sequences at 3.7 m.u. This insertion increases the size of pJM17 to 40 kilobase pairs, exceeding the packaging limit of the adenoviral particle. Homologous recombination of the two plasmids produces the recombinant adenovirus, Ad5-tk-palx3-Luc (approximately 36 kilobase pairs in length), in which the E1 region is replaced by the Luc expression cassette. Deletion of E1 region preserves the ability to infect but not to replicate, so that propagation can occur only in 293 cells that provide the E1 region. The same recombinant adenovirus without the TREpal sequences (Ad5-tk-Luc) was also constructed.

Characterization of the Recombinant Adenoviruses in Cell Culture—The rat pituitary tumor (GH) cell line, which is abundant in thyroid hormone receptors, was infected with Ad5-tk-palx3-Luc at a m.o.i. of 5. As shown in Fig. 2*A*, Luc gene expression was down-regulated by 2-fold in the absence of T_3 compared to the level of expression in the presence of 0.1 nM T_3, which is slightly less than the normal physiologic T_3 concentration of 0.2 nM. A 2-fold increase was achieved with 1 nM T_3, 5-fold the normal physiological concentration. The overall increase of Luc expression over the range of T_3 added to the medium was 8.0 ± 0.3-fold (mean ± S.D.). Infection with the control adenovirus Ad5-tk-Luc showed a small degree of suppression with 10 nM T_3. This indicates that the promoter element of Ad5-tk-palx3-Luc can be regulated by the endogenous thyroid hormone receptors. A similarly infected human hepatoblastoma (HepG2) cell line was down-regulated by approximately 2-fold in the absence of RA as compared to the expression observed with the physiological concentration of RA of 10 nM (Fig. 2*B*). Up-regulation was achieved with increasing concentrations of RA with an overall response of 4.6 ± 0.5-fold induction of Luc activity over the span of 0–1.0 µM RA. No significant change of Luc activity was observed when Ad5-tk-Luc-infected cells were treated with RA. These results indicate that Ad5-tk-palx3-Luc can be also regulated by the endogenous RA receptors, which are present in large numbers in HepG2 cells. In CV-I cells, which are relatively poor in thyroid hormone and RA receptors, both hormones increased Luc activity by only 50% (data not shown). Since a broad spectrum of cells can be infected with the adenovirus, our recombinant adenovirus could provide a means to analyze the function of endogenous thyroid hormone receptors or RA receptor in various experimental systems.

In Vivo Regulation of Ad5-tk-palx3-Luc—Adenovirus injected intravenously into mice is incorporated principally into liver (15). Normal, untreated mice were injected with 2×10^9 pfu of Ad5-tk-palx3-Luc, and various organs were harvested 4 days later and then assayed for Luc activity. Liver demonstrated the highest Luc activity, which was greater than 5,000 relative light units/mg of tissue. Other organs such as lung or kidney were also tested, but Luc activity was on the average 174 and 97 relative light units/mg with a background of 30. Immunohistochemistry of liver sections from a mouse injected with Ad5-tk-palx3-Luc showed a relatively homogeneous distribution of Luc primarily in liver parenchymal cells (data not shown).

To determine whether hormonal modulation of reporter gene expression could be achieved *in vivo*, the level of thyroid hor-

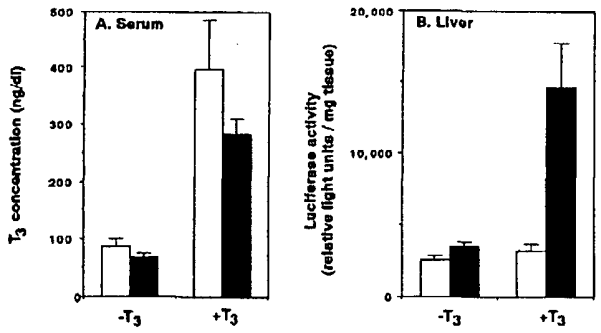

FIG. 3. **Effect of T_3 on Luc activity in liver of mice infected with Ad5-tk-palx3-Luc.** Hypothyroid mice were injected intravenously with 2×10^8 pfu of Ad5-tk-palx3-Luc (*filled bars*) or the control adenovirus, Ad5-tk-Luc (*open bars*). Half of the animals infected with each adenovirus vector were then injected for 4 days with 0.45 μg of T_3 daily, while the other half were injected with the vehicle alone. T_3 concentrations in serum (*A*) and luciferase activities in liver homogenates (*B*) are expressed as mean ± S.D.

mone was reduced in mice by feeding a low iodine, propylthiouracil-containing diet for 10 days. The animals were subsequently injected intravenously with Ad5-tk-Luc or Ad5-tk-palx3-Luc. Thereafter half of the mice from each group were injected intraperitoneally with 4-fold the maintenance dose of T_3 for 4 days (+T_3), while the other received the vehicle only (-T_3). The resulting serum T_3 levels were approximately 50–60% lower in -T_3 group and 2–3-fold higher in +T_3 group, respectively, when compared to the mean value of 135 ng/dl in untreated mice (Fig. 3*A*). As shown in Fig. 3*B*, T_3 administration resulted in the 4.2-fold stimulation of Luc gene expression in mice infected with Ad5-tk-palx3-Luc ($p < 0.005$). In contrast, T_3 administration had no significant effect on Luc gene expression in mice infected with the control adenovirus, Ad5-tk-Luc (Fig. 3*B*). These results indicate that expression of artificial gene introduced by recombinant adenovirus can be regulated by T_3 via the endogenous thyroid hormone receptor in mouse liver and that a thyroid hormone-responsive element is required to mediate the T_3 action.

DISCUSSION

The replication-defective adenovirus provides an effective mean to transfer genes into non-proliferating cells *in vitro* and *in vivo*. Recent efforts to exploit the adenovirus as a vehicle for gene therapy have focused on the achievement of high levels of gene expression through inclusion of a strong promoter and by the delivery of a high infection dose. However, as the spectrum of potential therapeutic substances expands, overexpression of some genes may prove to be as harmful as the ineffectiveness of underexpression. Thus, an effective method to control the level of expression of transferred genes could have a practical application.

In this study, we tested whether the expression level of an *in vivo* transferred gene can be regulated by simple physiological means. Since a large portion of intravenously injected adenovirus is incorporated into liver and because liver is an important target organ for thyroid hormone action, we tested whether a recombinant adenovirus containing a thyroid hormone-responsive promoter could be regulated by endogenous thyroid hormone receptors in liver and within the a reasonable range of T_3 concentrations that can be achieved *in vivo*. Indeed, thyroid hormone in concentrations overlapping the physiological range could regulate the expression of a transferred gene in adult mouse liver (Fig. 3). The current experiment provides a model for controlled expression of transferred gene by adenovirus. It is expected that T_3 would have the same effect in other tissue; however, because of the low level of infection, as well as lower levels of endogenous thyroid hormone receptors, this could not be tested. Tissue-specific regulatory element might be advantageously exploited if expression of a delivered gene could be limited to a particular tissue. Another possibility is the co-infection of regulator gene together with cognitive responsive promoter. Such a system is expected to provide a wider range of control for the expression of a therapeutic gene.

The recombinant adenovirus containing a thyroid hormone/retinoic acid response element can be also used to analyze the action of thyroid hormone and retinoic acid. Both hormones play an important role in development and differentiation. The studies on the action of these hormones has been limited by the complexity of natural responses. To overcome this problem, recent studies have utilized reconstituted systems in which these hormone receptors are overexpressed by co-transfection with a reporter gene (16–19). While reconstituted systems allow a more detailed analysis of hormone receptor function, they give a distorted view of the physiology of hormone action. The uniform adenovirus-mediated delivery of reporter genes allows examination of tissue responses mediated by their endogenous receptors under physiological conditions. Recent reports suggest that such systems can be effectively exploited. De Luze *et al.* (20) were successful in demonstrating the effect of thyroid hormone on gene transcription during regression of the *Xenopus* tadpole tail by direct injection of reporter plasmids into muscle. Others (21, 22), utilized the adenovirus to transfer androgen-responsive reporter genes into skin fibroblasts in culture. Our demonstration that a reporter gene can be introduced efficiently by simple means into adult animal tissues and that it responds to physiological concentrations of hormones provides the opportunity to study thyroid hormone and retinoic acid action in various experimental systems. This system would be of particular value in the *in vivo* study of tissue responses in animals with receptor gene knockouts (23) or in transgenic mice expressing mutant receptors (24), which exert dominant negative effect on endogenous receptors.

Acknowledgments—We thank Bert O'Malley for the provision of the TREpalx3-CAT plasmid, F. L. Graham for pJM17, and R. D. Gerard for the pAC plasmids. We are also indebted to Dr. Bernard Roizman for instructions in the propagation of the adenovirus and for the use of his virus culture facility.

REFERENCES

1. Berkner, K. L. (1988) *BioTechniques* **6**, 616–629
2. Mulligan, R. C. (1993) *Science* **260**, 926–932
3. Zabner, J., Couture, L. A., Gregory, R. J., Graham, S. M., Smith, A. E., and Welsh, M. J. (1993) *Cell* **75**, 207–216
4. Yang, Y., Raper, S. E., Cohn, J. A., Engelhardt, J. F., and Wilson, J. M. (1993) *Proc. Natl. Acad. Sci. U. S. A.* **90**, 4601–4605
5. Ishibashi, S., Brown, M. S., Goldstein, J. L., Gerard, R. D., Hammer, R. E., and Herz, J. (1993) *J. Clin. Invest.* **92**, 883–893
6. Smith, T. A. G., Mehaffey, M. G., Kayda, D. B., Saunders, J. M., Yei, S., Trapnell, B. C., McClelland, A., and Kaleko, M. (1993) *Nature Genet.* **5**, 397–402
7. Ragot, T., Vincent, N., Chafey, P., Vigne, E., Gilgenkrantz, H., Couton, D., Cartaud, J., Briand, P., Kaplan, J.-C., Perricaudet, M., and Kahn, A. (1993) *Nature* **361**, 647–650
8. Rosenfeld, M. A., Siegfried, W., Yoshimura, K., Yoneyama, K., Fukayama, M., Stier, L. E., Paakko, P. K., Gilardi, P., Stratford-Perricaudet, L. D., Perricaudet, M., Jallat, S., Pavirani, A., Lecocq, J.-P., and Crystal, R. G. (1991) *Science* **252**, 431–434
9. Baniahmad, A., Steiner, C., Kohne, A. C., and Renkawitz, R. (1990) *Cell* **61**, 505–514
10. Graham, F. L., Smiley, J., Russell, W. C., and Nairn, R. (1977) *J. Gen. Virol.* **36**, 59–72
11. McGrory, W. J. (1988) *Virology* **163**, 614–617
12. Graham, F. L., and Van Der Eb, A. J. (1973) *Virology* **52**, 456–467
13. Gluzman, Y., Reichi, H., and Solnick, D. (1982) in *Eukaryotic Viral Vectors* (Gluzman, Y., ed) pp. 187–192, Cold Spring Harbor Laboratory, Cold Spring Harbor, NY
14. Gómez-Foix, A. M., Coats, W. S., Baqué, S., Alam, T., Gerard, R. D., and Newgard, C. B. (1992) *J. Biol. Chem.* **267**, 25129–25134
15. Herz, J., and Gerard, R. D. (1993) *Proc. Natl. Acad. Sci. U. S. A.* **90**, 2812–2816
16. Graupner, G., Willis, K. N., Tzukerman, M., Zhang, X.-k., and Pfahl, M. (1989) *Nature* **340**, 635–656

17. Glass, C. K., Lipkin, S. M., Devary, O. V., and Rosenfeld, M. G. (1989) *Cell* **59**, 697–708
18. Rentoumis, A., Chatterjee, V. K. K., Madison, L. D., Datta, S., Gallagher, G. D., DeGroot, L. J., and Jameson, J. L. (1990) *Mol. Endocrinol.* **4**, 1522–1531
19. Hallenbeck, P. L., Phyillaier, M., and Nikodem, V. M. (1992) *J. Biol. Chem.* **268**, 3825–2828
20. De Luze, A. D., Sachs, L., and Demeneix, B. (1993) *Proc. Natl. Acad. Sci. U. S. A.* **90**, 7322–7326
21. Shih, W., Mears, T., Bradley, D. J., Parandoosh, Z., and Weinberger, C. (1991) *Mol. Endocrinol.* **5**, 300–309
22. McPhaul, M. J., Deslypere, J.-P., Allman, D. R., and Gerard, R. D. (1993) *J. Biol. Chem.* **268**, 26063–26066
23. Lohnes, D., Kastner, P., Dierich, A., Mark, M., LeMeur, M., and Chambon, P. (1993) *Cell* **73**, 643–658
24. Damm, K., Heyman, R. A., Umesono, K., and Evans, R. M. (1993) *Proc. Natl. Acad. U. S. A.* **90**, 2989–2993

STIC-ILL

From: Vogel, Nancy
Sent: Thursday, December 09, 2004 2:09 PM
To: STIC-ILL
Subject: refs for 10/045,116 (references from lost parent case 09/033,555)

Please send me the following:

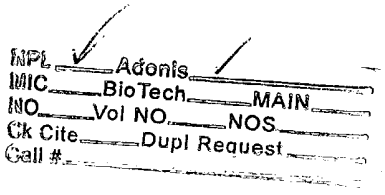

Proc. Natl. Acad. Sci. USA (1 989) 86:4574-4578

Virol. 1997 227:239-244

Virolo 1994 202:695-706

Virolo 1993 193:631-641

Genes and Dev. 1988 2:453-461

Nucleic Acid Research 1983 11 17 :6003-6020 .

Proc. Natl. Acad. Sci. USA 1994 91:8802-8806
J Virolo I 993 67 10 :591 1-592 1

Anticancer Res. 1997 17:1471-1505

J Immunol. 1988 141 6 :2084-2089

J Virol. 1989 63 2 :631-638

Science 1989 244:1288-1292

Chang et al. Cancer Gene therapy Using Novel Tumor specific Replication Competent Adenovirus Vectors" Cold Spring Harbor Gene Thera Meeting Sept. 1996

Nucleic Acids Res. 1996 24 12 :2318-2323

Current Protocols in Molecular Biology
Ausubel et al., eds., 1987 , Supp. 30, section 7.7.18 Table 7.7.1

Nature (1989) 337:387-388

Advances in Virus Research 1986 31: 169-228

Biochem. Biophys. Acta 1982 651:175-208

Mol. Cell. Biol. 1989 9 (9) :41 5-42

J Virol. 1997 71 (1) :548-561

EMBO J 1984 3 (12) :2917-2922

J Genetic Virolo 1977 68:937-940

1973 Virolo 52:456-467

1987 J Gen. Virol 36:59-72

Biochem. J. 1987 241:25-38

Hallenbeck, P.L. et a1., Novel Tumor Specific Replication Competent Adenoviral Vectors for Gene Therapy of Cancer" abstract no. 0-36 Cancer Gene Thera 1996) 3 (6) :S19-S20.

J. Biol. Chem. 1995 270 (8) :3602-3610 .
J Biol. Chem. 1994 269 (39) :23872-23875
Adv. Dru Delive Rev. 1995 17:279-292

ELSEVIER

Advanced Drug Delivery Reviews 17 (1995) 279–292

advanced
drug delivery
reviews

VDEPT: An enzyme/prodrug gene therapy approach for the treatment of metastatic colorectal cancer

Brian E. Huber*, Cynthia A. Richards, Elizabeth A. Austin

Division of Cell Biology Wellcome Research Laboratories, Research Triangle Park, NC 27709, USA

Accepted June 1995

Abstract

Colorectal carcinoma (CRC) remains a significant medical challenge with an expected 350000 new cases per year. Although the primary cancer can be successfully controlled by surgical resection, metastatic disease to the liver is the most common demise of the CRC patient. New innovative approaches must be developed for the treatment of CRC hepatic metastasis if the overall 2- and 5-year survival rates and quality of life assessments are to improved. We now describe an innovative gene therapy approach for the treatment of metastatic CRC, an approach called VDEPT. In this approach, an artificial chimeric gene is created which consists of two components: (1) the transcriptional regulatory sequence (TRS) of the human carcinoembryonic antigen gene (CEA); and (2) the protein coding domain of the nonmammlian cytosine deaminase gene (CD). This artificial gene will express CD only in cells which naturally express CEA. Expression of CD in CEA-positive cells is, by itself, nontoxic. However, CD can convert the nontoxic prodrug, 5-fluorocytosine (5-FCyt), to the toxic anabolite, 5-fluorouracil (5-FUra). Hence, the toxic compound, 5-FUra, will be selectively produced in cells which express CD. Since expression of CD is restricted to CEA-positive cells, 5-FUra will be selectively produced in CEA-positive cells. Hence, tumor-specific expression of CD permits the tumor-specific production of 5-FUra at high concentrations for extended periods of time directly at the tumor site. The artificial, chimeric gene can be delivered to CEA-positive tumors via a replication-defective retroviral vector. Chimeric genes composed of the human CEA promoter and the coding sequence of CD were created and engineered into a retroviral gene delivery vector. These chimeric genes selectively expressed CD in CEA-positive cells which resulted in the selective conversion of 5-FCyt to 5-FUra in the CEA-positive tumor cells. Human tumor xenografts demonstrated that expression of CD in solid tumors can generate complete cures if only 4% of the solid tumor cell mass expressed this enzyme. In vivo gene transfer has indicated that retroviral vectors can delivery and express CD chimeric genes in liver tumors at this 4% level.

Contents

* Corresponding author.

Abbreviations: AFP, *a*-fetoprotein protein; CD, cytosine deaminase; CEA, carcinoembryonic antigen; CRC, colorectal carcinoma; 5-FCyt, 5-fluorocytosine; 5-FUra, 5-fluorouracil; LTR, long terminal repeat; TRS, transcriptional regulatory sequence(s) [This pertains to the cis-acting elements which control the *transcription* of genes. These sequences are defined as the promoter and enhancer elements.]; VDEPT, virus-directed enzyme prodrug therapy.

SSDI 0169-409X(95)00062-3

1. Introduction

1.1. Background

Colorectal carcinoma (CRC) is the second most common cancer in the US, with an estimated 160000 new cases per year (120000, colon; 40000, rectum) (for reviews of CRC and current treatment modalities, see Refs. [1–6]). For the combined populations of the USA, UK, Japan, France, Germany, Italy, and Spain, 340000 new cases per year are expected. In 1992, it was estimated that there were 768000 prevalent cases of CRC in the US. To treat this disease, $1.1 billion dollars was allocated in 1992 which is estimated to grow to 2.3 billion by the year 2007. Standard staging of the disease is by the Dukes' classification system which assess the penetration into the bowel wall, regional lymph node involvement and the presence of overt metastatic disease. Surgical resection of the primary tumor is a curative procedure for patients diagnosed with very early disease. However, most patients are diagnosed with Dukes Stage B and C disease where there may be penetration into the bowel wall and regional lymph node involvement indicating the presence of metastatic disease. Due to regional blood flow, the liver is the most common site for distant metastasis and, in approximately 30% of patients, the sole site of tumor recurrence after successful resection of the primary colon tumor.

The single most active agent against metastatic CRC is 5-FUra, even though the response rates are usually less than 20%. Combination therapy with leucovorin or levamisole, and hepatic arterial infusion of drugs have increased response rates, and in some instances, have increased the 2-year survival rate. Due to the late-stage diagnosis of the disease (at Dukes Stage B and C) and the general lack of efficacy of conventional chemotherapeutic treatment, hepatic metastasis are the most common cause of death in the colorectal cancer patient. New innovative approaches must be developed for the treatment of CRC hepatic metastasis if the overall 2- and 5-year survival rates and quality of life assessments are to improve.

We now describe an innovative approach for the treatment of hepatic metastasis of CRC called *Virus-Directed Enzyme Prodrug Therapy (VDEPT).*

1.2. Rationale of VDEPT

We have been developing a gene therapy approach for the treatment of solid tumors that exploits the transcriptional differences between

normal and tumor cells (for summaries see Refs. [7–12]). This approach, which we call VDEPT, links the transcriptional regulatory sequences (TRS) of a tumor-associated marker gene, such as carcinoembryonic antigen (CEA), to the coding sequence of a nonmammalian enzyme, such as cytosine deaminase (CD), to create an artificial chimeric gene that is selectively expressed in cancer cells. This selective expression creates a qualitative biochemical difference between normal and neoplastic cells that can be exploited to locally activate prodrugs to toxic metabolites directly at the tumor site.

For the application of VDEPT to metastatic CRC, the artificial, chimeric gene is composed of the CEA TRS linked to the coding sequence of the CD gene (Fig. 1). This chimeric gene will result in the tumor-specific expression of CD which can subsequently convert the nontoxic prodrug, 5-FCyt, to the toxic anabolite, 5-FUra. The chimeric gene will be delivered to the metastatic tumors via a viral vector through a hepatic arterial infusion. This approach may be significantly better than the direct administration of 5-FUra since VDEPT allows extremely high concentrations of 5-FUra to be maintained for extended periods of time ($C \times T$) selectively at the tumor site.

1.3. Features and selectivity of VDEPT for metastatic CRC

The attractive features of this novel treatment approach summarized as follows:

1.3.1. 5-FCyt

The prodrug, 5-FCyt, is an approved drug with an excellent pharmacokinetic profile. 5-FCyt (4-amino-5-fluoro-2-pyrimidone;) was approved in 1972 for the treatment of *Candida* and *Cryptococcus* and is marketed under the trade names Ancobon (US), Ancotil (Europe; Canada) and Alcobon (UK). The following is a summary of 5-FCyt pharmacokinetic data in man:

Rapidly and almost completely absorbed following oral administration (80–90% bioavailability);
Negligible binding to serum proteins, extensively distributed in tissues, penetrates the blood brain barrier, and is excreted via the kidneys by means of glomerular filtration without significant tubular reabsorption;
Not significantly metabolized with greater than 92% of intact drug being recovered in the urine; $T_{1/2}$ is approximately 4.2 h in normal subjects. The $T_{1/2}$ is significantly prolonged in the pres-

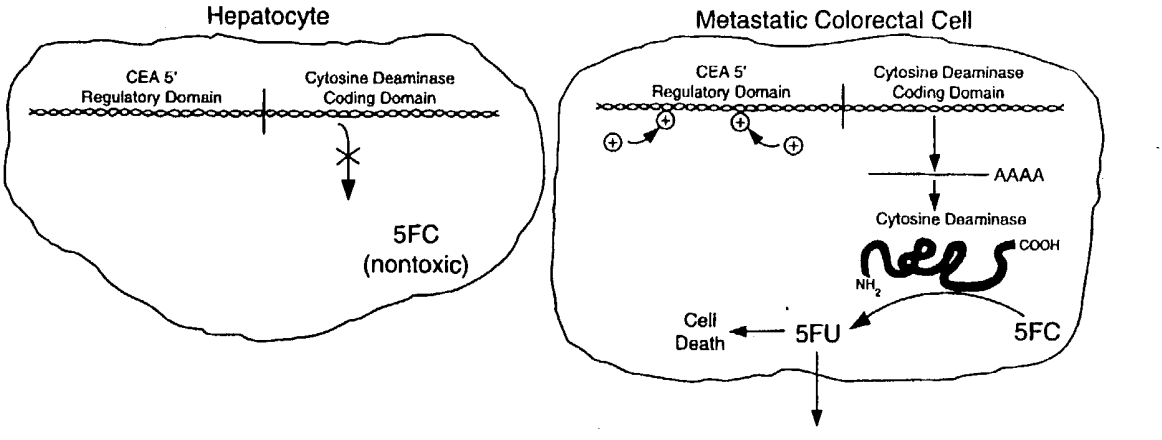

Fig. 1. Schematic representation of selective expression of the chimeric CEA/CD gene in metastatic CRC cells. After expression of the chimeric gene, treatment with 5-FCyt leads to cell death as the result of metabolism of 5-FCyt to 5-FUra by CD.

ence of renal insufficiency (average $T_{1/2}$ in anuric patients is 85 h). The mean blood concentration is approximately 80 μg/ml (630 μM) at 1–2 h in patients who received a 6 week regimen of 5-FCyt (150 mg/kg per day);
Usual dosage is 50–200 mg/kg/day up to 8 weeks. No adverse effects were observed in Cebus monkeys given 400 mg/kg per day for 13 weeks. In man, hematological toxicity can occur when blood concentrations are maintained above 110 μg/ml, presumably due to the deamination of 5-FCyt to 5-FUra by entrobacilli of the gut flora. Toxicity may be lessened and controlled by assessment of microflora composition and pre-treatment with antibiotics.

1.3.2. 5-FUra

The toxic anabolite, 5-FUra, is the drug of choice for CRC [1–6]. 5-FUra can readily diffuse by nonfacilitated diffusion into neighboring cells [13]. The levels of 5-FUra can potentially be modulated by uracil reductase inhibitors [14].

1.3.3. CEA expression

CEA is expressed in an overwhelming majority of CRC, with higher expression in metastatic tumors. There is little heterogeneity in CEA expression among metastatic CRC tumor cells (for reviews, see Refs. [15–18]).

1.3.4. Selectivity

Selectivity is achieved by:

(1) *Selective perfusion*: Since primary and metastatic tumors in the liver receive a significant portion of their blood supply via the hepatic artery, the gene delivery vector containing the chimeric gene will be infused into the liver via the hepatic artery;
(2) *Selective infection*: Initial clinical studies will use replication-defective retroviral vectors as the gene delivery vehicle. Since retroviral vector integration and expression is predominately limited to dividing cells, the retroviral delivery vector will integrate the chimeric gene selectively in the dividing tumor cells rather than the nondividing normal hepatocytes;
(3) *Selective expression*: The chimeric gene will only be expressed in the CEA-positive CRC tumor cells.

2. Results and discussion

2.1. Cytosine deaminase cloning, sequencing and analysis

The gene encoding cytosine deaminase (CD) was cloned from *E. coli*. (Fig. 2). DNA sequencing identified the exact location of the open reading frame encoding the entire 427 amino acids of the CD enzyme. This DNA sequence was confirmed by purifying the CD enzyme and determining the amino acid sequence. The purified enzyme was also used for production of polyclonal antibodies to CD, and kinetic studies. The K_m of CD for Cyt and 5-FCyt is 220 and 1700 μM, respectively.

Site-directed mutagenesis was used to change the start codon of the CD gene from GTG to

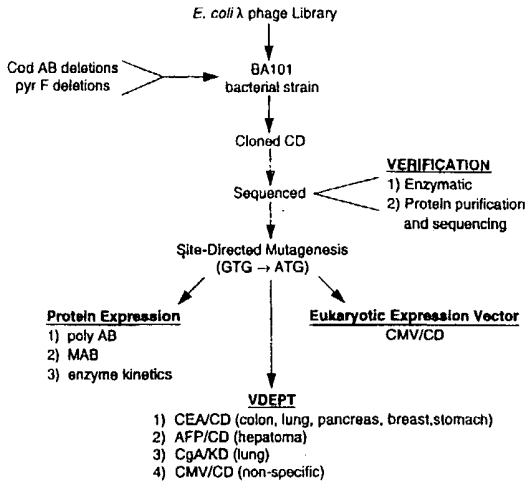

Fig. 2. Cloning and use of the cytosine deaminase gene. Bacterial strain B1010 was created to clone the gene encoding cytosine deaminase (CD). Once cloned the gene was entirely sequenced to locate the open reading frame encoding the CD protein. The gene was confirmed by enzymatic activity and protein sequencing. Site-directed mutagenesis was performed to enhance expression in mammalian cells. The CD protein was utilized to produce poly and mono clonal antibodies and enzymatic studies. The CD gene was placed into a eukaryotic expression vector for efficacy studies. For VDEPT Clinical Studies, the CD gene is expressed from tumor-specific promoters (CEA, AFP).

ATG for enhanced expression in mammalian cells (for review, see Ref. [7]).

2.2. In vitro cytotoxicity of CD/5-FCyt

The CD gene was placed into a eukaryotic expression vector to determine its utility in VDEPT. The average IC_{50} to 5-FCyt in 8 different human tumor cell lines in vitro was approximately 13000 μM. When CD was expressed in these cells, the average IC_{50} to 5-FCyt shifted approximately 600-fold to 22 μM (Fig. 3A–C). Expression of CD, by itself, did not change the growth characteristics of the human tumor cells if the prodrug was not administered.

2.3. CEA promoter and CEA/CD chimeric genes

To achieve tumor specific expression of the CD gene, the human carcinoembryonic antigen (CEA) gene was cloned and the transcriptional regulatory sequence (TRS) identified. The human CEA gene was cloned and 14500 bp of the 5′ region sequenced in both 5′ and 3′ directions. To identify the important cis-acting transcription regulatory sequences (TRS) contained in the 14500 bp, approximately 60 different regions were linked to a reporter gene and transfected into two CEA-positive cell lines and two CEA-negative cell lines (see Fig. 4). This analysis identified three important TRS regions which regulate CEA expression. The best combinations of these three regions resulted in reporter gene expression which was:

Selective – 80–120-fold higher expression in human CEA-positive cell lines compared to a human CEA-negative liver cell line;
Robust – 2–4-fold higher expression than an SV 40 TRS and equal to a CMV TRS (for review, see Ref. [12]).

Using combinations of the three important CEA TRS, 12 different CEA/CD chimeric genes were made and stably transfected into 4–6 different cell lines (Table 1). CEA/CD chimeric genes were identified which gave the highest and most selective expression of CD from the different

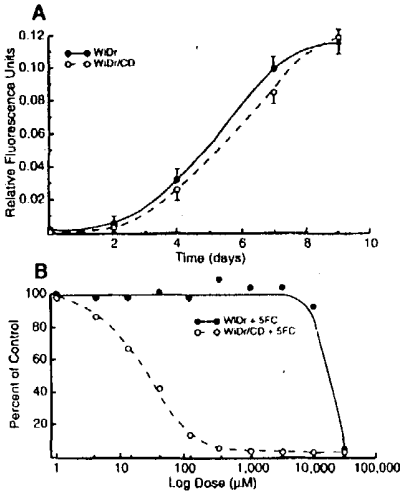

C

Human Cell Lines	Type	Parental Cells	CD Expression
WiDr	Colon	13,000 μM	22 μM
NCIH 508	Colon		
LoVo	Colon		
SW1463	Colon		
LS174	Colon		
HEP3B	Liver		
HuH7	Liver		
HEPG2	Liver		

Fig. 3. (A) CD Expression does not intrinsically affect cell growth. (B) Log dose-response curve showing increasing sensitivity to 5-FCyt if the cells express CD. (C) Six human colon tumor cell liens and three human liver tumor cells are relatively insensitive to 5-FCyt. If CD is expressed in these cells, then the IC_{50} shifts approximately 500-fold.

CEA promoters. This analysis identified 4 CEA/CD chimeric genes which are ideally suited for therapeutic purposes. These four different CEA/CD chimeric genes produced high levels of CD enzymatic activity and shift in IC_{50} selectively in human CEA-positive colorectal cells compared to human CEA-negative liver cells (NB: greater than 1000-fold shift IC_{50}; Table 2). The nomenclature for these four CEA/CD chimeric genes are: 113, 145, 165, and 176. The #145 CEA/CD chimeric gene was further quantitated for selective expression of CD and selective activation of 5FCyt (Table 3).

2.4. Retroviral gene delivery vectors

Three CEA/CD chimeric genes (113, 145, 165) were engineered into a retroviral shuttle vector system, called the pLN vector system

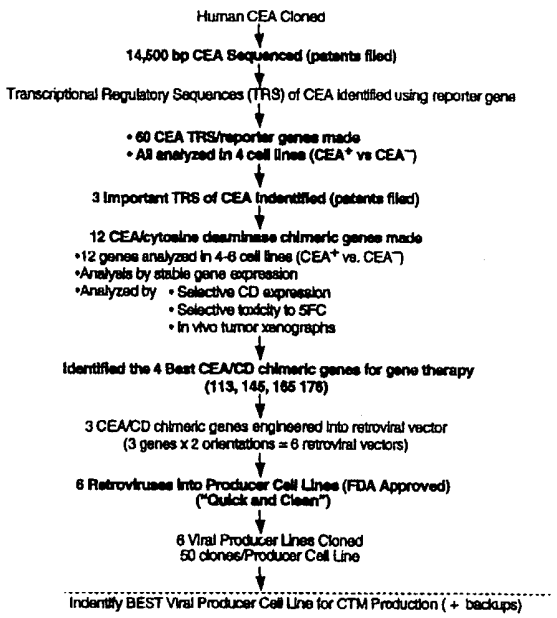

Fig. 4.

(provided by A.D. Miller, Fred Hutchinson Cancer Research Center; Fig. 5). These three genes were engineered into the pLN vector system in two different orientations so that 6 retroviral shuttle vectors were made. "Reverse orientation" produced the most selective expression. Based upon selective expression of the chimeric gene, 668W95UA is the retroviral vector in which all subsequent work was performed. These vectors were transfected into the retrovirus producer cell line PA317 (kindly provided by A.D. Miller, Fred Hutchinson Cancer Research Center). Virus producer cell lines were then single cell cloned (50 clones per vector) and the best clones identified (based on viral titer and CD gene expression). Titers of 1×10^6 were used in all subsequent experiments.

2.5. In vivo antitumor efficacy of CD/5-FCyt

WiDr cells are a well differentiated human colon tumor cell line. WiDr cells or WiDr cells expressing CD (WiDr/CD) were injected s.c. into nude mice to generate human colon tumor xenographs. When the tumors reached 1% of body weight (extrapolates to 750 g tumor burden in man), mice were treated with either 5FUra or 5-FCyt. Despite the fact that WiDr cells are sensitive to 5-FUra in vitro (IC_{50} 1uM), there were no antitumor effects observed when 5-FUra was administered from 5 mg/kg (nontoxic) to 30 mg/kg (LD90) for 10 consecutive days. However, when 5-FCyt was administered for 10 consecutive days, there was 100% regressions and 35% cures in WiDr/CD tumors with no observable animal toxicity or weight loss (Fig. 6). In subsequent experiments, cure rates of 100% were observed in WiDr/CD tumors if 5-FCyt dosing was extended (see below).

Table 1
IC_{50} to 5FC to stably transfected cells

	IC_{50} 5FC (μM) Bulk populations pCEA/CD−												
	Parental[a]	113	105	148	136	145	177	176	167	165	171	172	168
Hep 3B	13604 ± 2112	10883	9732	3078	10257	13643	12523	14284	10436	12063	14362	15490	11727
HuH7	14576 ± 2498	313	101	2119	423	3372	918	719	1621	3674	6802	6239	7073
WiDr	13660 ± 2882	223	na[b]	2498	na	461	na	na	na	1122	1470	711	893
LoVo	8675 ± 2731	123	na	5042	7544	281	7912	776	3106	5315	1281	113	6781
SW1463	4927 ± 2563	27	30	40	na	15	na	na	na	3123	332	1940	3123
NCI H508	812 ± 182	2.7	7.9	775	5.8	<2	8.9	4.5	5.6	39	20	12	40

[a] Average standard error in all experiments.
[b] na, cell line not available.

Table 2
IC_{50} to 5-FCYT (μM)

Cells	CEA level	CEA/CD genes				Average
		113	154	165	176	
HEP 3B	–	10883	13643	12063	14284	12718
HClH508	+	2.7	<2	39	4.5	12

CD activity (pmol/min per mg)

Cells	CEA level	CEA/CD genes			
		113	145	165	176
HEP 3B	–	35	6	15	BT
HClH508	+	900	19600	1690	7100

BT, below threshold.

Table 3
IC_{50} and CD enzymatic activities of parental and pCEA/CD-145 stable cell liens

	CEA (ng/mg) protein per 7 days) Parental	IC_{50} 5FU (μM) Parental	CD (pmol/min per mg protein)		IC_{50} 5FC (μM)		Ratio IC_{50} 5FC Parental/ pCEA/CD-145
			Parental	pCEA/CD-145	Parental[b]	pCEA/CD-145	
HEP 3B	BT[a]	1.2	BT	20	14336	13643	1
HuH7	BT	2.5	BT	660	13079	3372	4
WiDR	50	0.8	BT	540	12509	461	27
LoVo	745	0.2	BT	1580	7510	281	27
SW1463	640	0.2	BT	1620	2364	15	158
NCl H508	4556	0.1	BT	23980	516	<2	>258

[a] BT, below threshold, not detectable.
[b] Value obtained in experiment with pCEA/CD-145.

2.6. Mechanism of action of CD/5-FCyt

The mechanism of action was determined for the antitumor effects of the CD/5-FCyt enzyme/prodrug combination (Fig. 7).

1. *Dose response effect of 5-FCyt*: Nude mice growing WiDr/CD-derived tumors were treated with various doses of 5-FCyt. A dose response was observed with antitumor activity demonstrable down to 15 mg/kg (Fig. 8).
2. *Conversion of 5-FCyt to 5-FUra*: WiDr/CD cells growing in vitro or as tumors in nude mice converted 5-[6-^{3}H]FCyt into 5-FUra and subsequent 5-FUra anabolites. Importantly, the 5-FUra that was produced intracellular diffused out of the cells (Fig. 9).
3. *Inhibition of thymidylate synthase*: 5-FCyt caused a dose dependent inhibition of thymidylate synthase in WiDr/CD tumors. Inhibition was proportional to the IC_{50} (Fig. 10).
4. *Incorporation into RNA*: WiDr/CD tumors in nude mice showed significant incorporation of radioactivity into RNA when mice were dosed with 5-[6-^{3}H]FCyt. No significant incorporation was found in 6 internal organs.

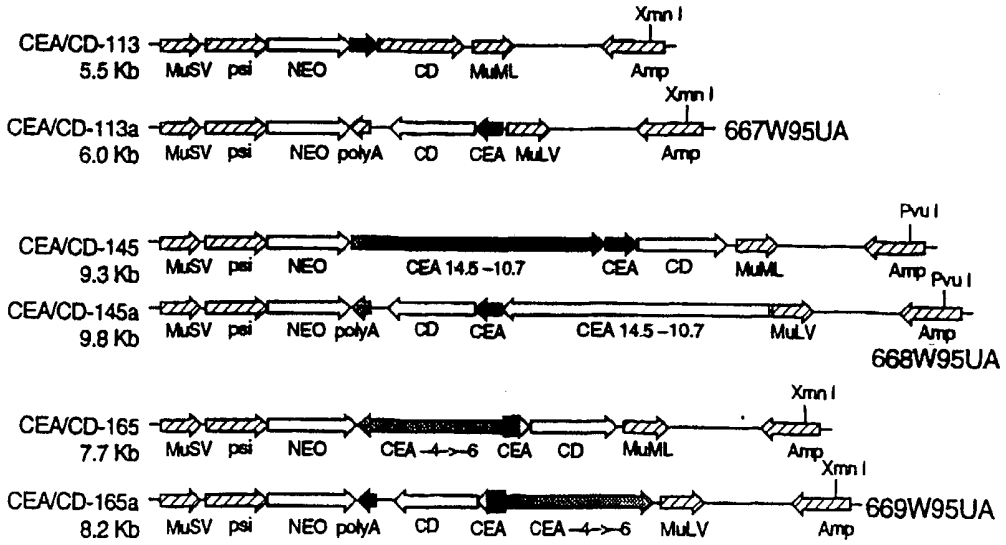

Fig. 5. Retroviral vectors containing CEA/CD chimeric genes.

5. *Concentration × time (C × T)*: The reason that the VDEPT CD/5-FCyt combination is significantly more effective than administering 5-FUra directly (see Fig. 6) is due to the fact that with VDEPT, very high concentrations of 5-FUra can be selectively produced at the tumor site and maintained for extended periods of time. In the WiDr/CD tumor model described above, greater than 500uM 5-FUra is selectively produced in the tumor cells and this high level can be maintained for at least 2 hrs (Fig. 11). This high level of 5-FUra will diffuse by nonfacilitated diffusion into adjacent tumor cells to kill them and become inactivated in normal hepatocytes by the high uracil reductase levels in the liver cells.

2.7. Required gene transfer efficiency – the bystander effect

It is recognized that for all gene transfer systems for in vivo gene delivery, only a small percentage of tumor cells will actually take up and express the artificial, chimeric gene. Due to the very high concentrations of 5-FUra produced selectively at the tumor site, and the nonfacilitated diffusion properties of 5-FUra, we hypothesized that only a very small percentage of tumor cells need express the CD gene for significant antitumor effects.

WiDr/CD cells incubated with 5-[6-^{3}H]FCyt liberated 5-FUra into the media indicating that 5-FUra produced in the tumor cells can readily diffuse by nonfacillitated diffusion. The diffusable 5-FUra killed neighboring cells which did not express the CD gene.

WiDr and WiDr/CD tumor cells were mixed together in different ratios and injected s.c. into nude mice. Hence, tumors that arose contained a specific percentage of tumor cells expressing the CD gene. Performing CD enzymatic assays on these tumors confirmed that the tumors were comprised of cells which were reflective of the original injected mixture. 5-FCyt treatment resulted in 100% tumor regressions if the tumors contained only 2% of the tumor cells expressing the CD gene. 100% regressions and a 66% cure rate was observed if the tumors contained only 4% of the tumor cells expressing the CD gene (Fig. 12).

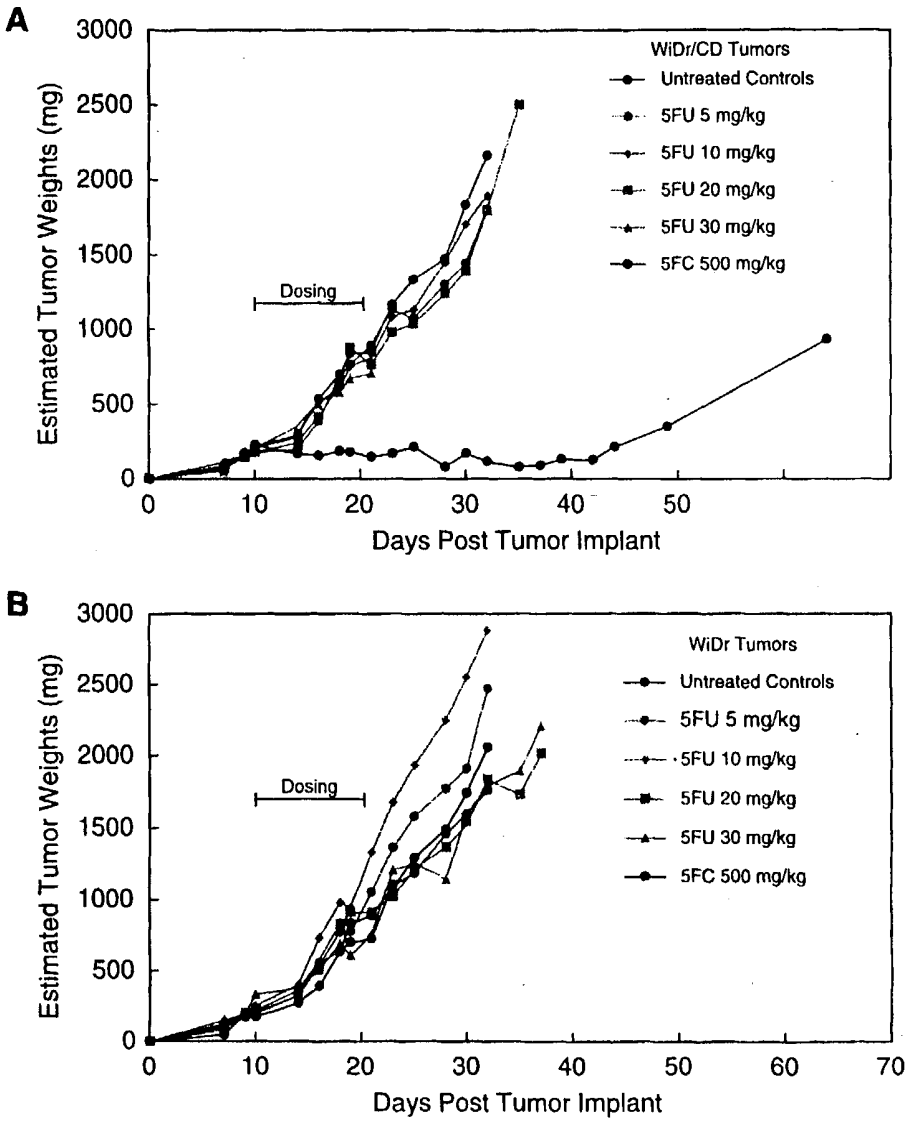

Fig. 6. Comparison of FUra and FCyt antitumor activity in WiDr- and WiDr/CD derived tumors in nude mice.

2.8. Comparison to HSV TK/ganciclovir

The HSV TK/ganciclovir enzyme prodrug combination has received considerable attention and is being used in clinical trials. Direct comparison to the CD/5-FCyt combination has shown that HSV TK/ganciclovir combination:

has less of a therapeutic window between toxicity of the prodrug (ganciclovir) and toxic metabolite compared to the CD/5-FCyt combination;
is less efficacious at producing a neighboring killing effect than the CD/5-FCyt combination (i.e. 50% of the tumor had to express HSV TK to achieve tumor regressions comparable to

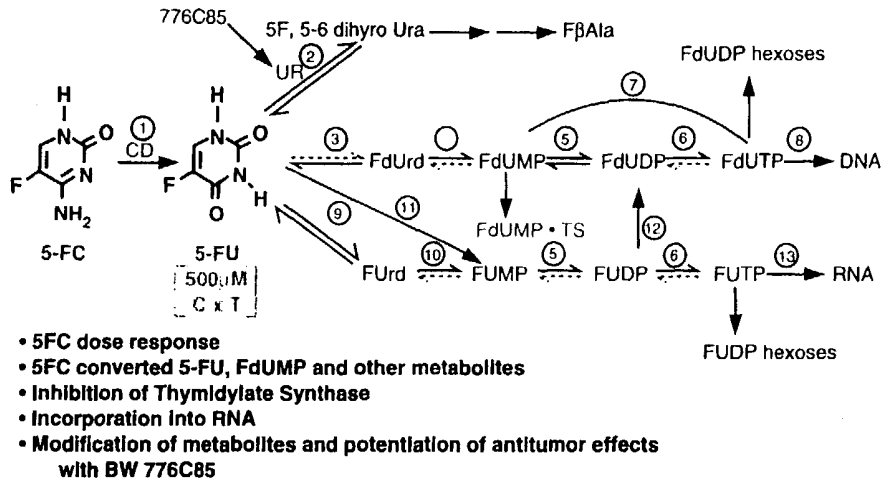

Fig. 7. Mechanism of action.

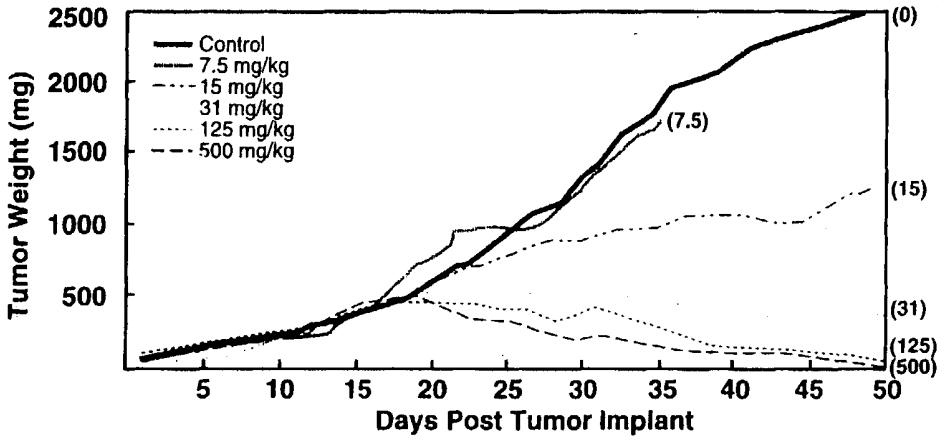

Fig. 8. 5-FC antitumor effects. Nude mice with WiDr/CD derived tumors were treated with various doses of 5-FC as indicated (Mol. Pharmacol. 43, 380–387 (1993)).

regressions observed when only 4% of tumor expressed CD).

2.9. Interactions with 5-ethynyluracil

5-Ethynyluracil (5-EU, 776C85) is a potent inactivator of uracil reductase. Uracil reductase catabolizes 5-FUra to 5,6,dihyrouracil which ultimately generates fluoro-β-alanine, a potentially neurotoxic catabolite (see Fig. 7). 776C85 dramatically increased the levels of uracil, 5-FUra, and eliminated the levels of fluoro-β-alanine when WiDr/CD cells were incubated in the presence of 5-FCyt. 776C85 potentiated the antitumor effects of 5-FCyt when WiDr/CD tumor bearing animals were treated with both 776C85 and 5-FCyt.

2.10. Retroviral gene delivery to tumors in situ

Central to the clinical success of this VDEPT approach is the ability of retroviral

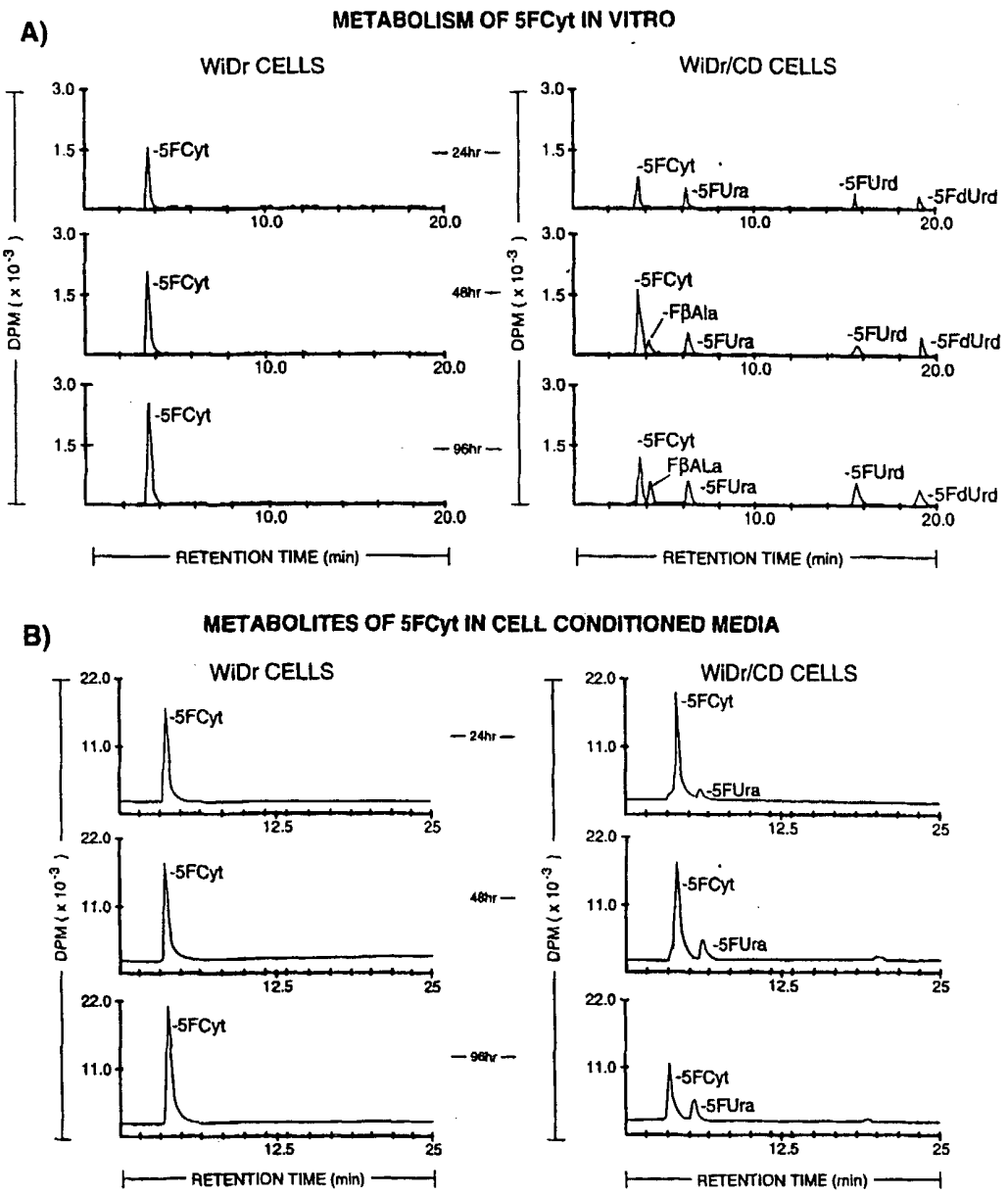

Fig. 9. Metabolism of 5-[6-^{3}H]FCyt in WiDr and WiDr/CD cells. (A) In cell extracts. (B) In cell conditioned media.

vectors to deliver the CEA/CD chimeric gene to approximately 1–5% of the tumor mass. Data indicates that this efficiency is achievable. Direct intralesional injections into liver tumors of retroviral vectors containing a CD chimeric gene indicated that gene transfer efficiency was at least 5% of the tumor mass. Direct hepatic infusion of retroviral vectors via the hepatic artery strongly suggested that uptake and expression in liver tumors was at least 5% of the tumor cells while expression in normal hepatocytes was undetectable. These studies are being expanded in rodents and woodchucks to more

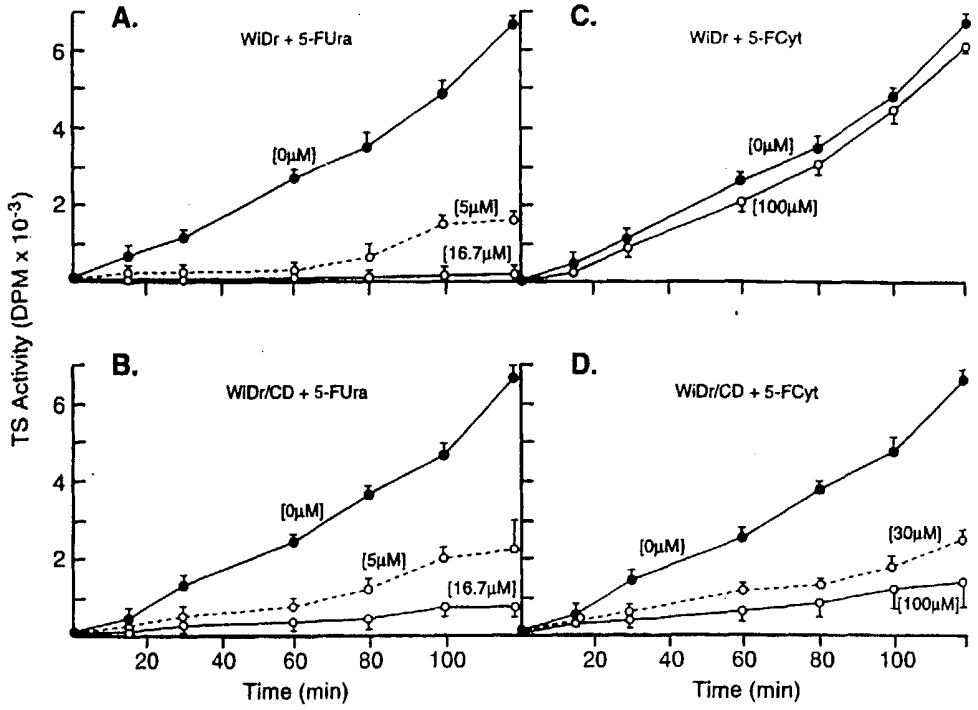

Fig. 10. TS activity in WiDr and WiDr/CD cells treated with 5-FUra or 5-FCyt.

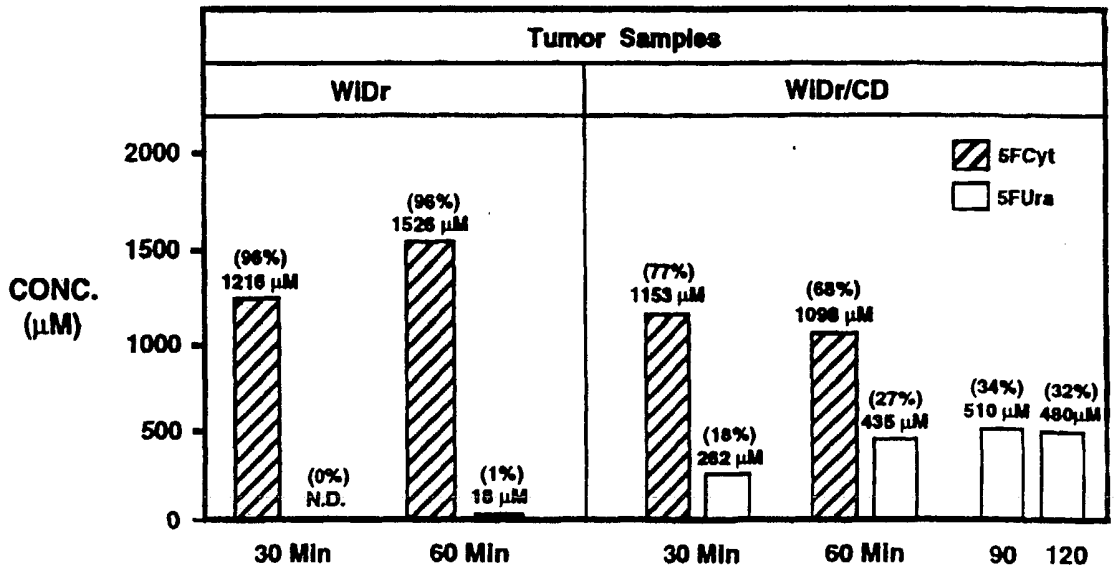

Fig. 11. Conversion of 5FCyt to 5FUra in tumor samples. 5-FCyt and 5-FUra detected in tumor extracts in mice treated with 5-FCyt. Mice contained either WiDr-derived or WiDr/CD derived tumors. At 30, 60, 90, or 120 min after 5-FCyt treatment, tumors were removed and tumor levels of 5-FCyt and 5-FUra were determined.

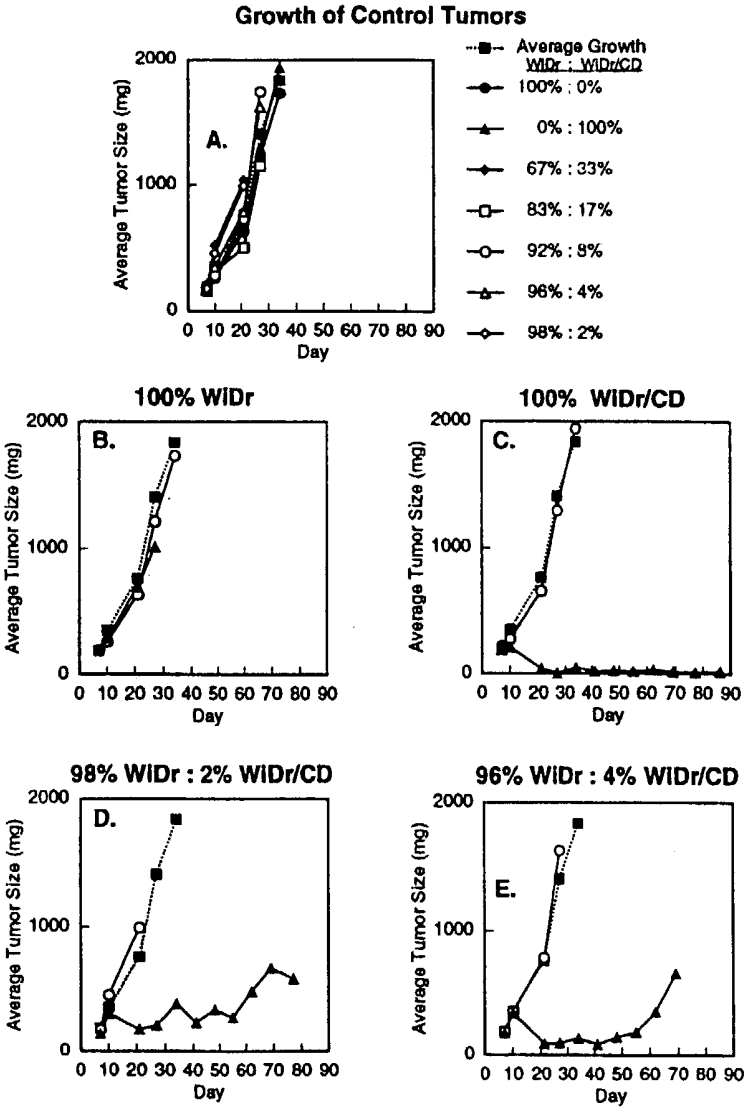

Fig. 12. WiDr and WiDr/CD cells were mixed together at the indicated ratios and injected S.C. into nude mice. (A) Tumor weights in untreated animals. (B–E) Growth rates for tumors composed of the indicated ratios. (○) Untreated animals. (▲) 5-FCyt treated animals. (■) Average tumor growth rate for all the tumor mixtures in untreated animals.

accurately address the MOI to achieve a 5% tumor cell expression rate.

References

[1] Kemeny, N. (1994) Current approaches to metastatic colorectal cancer. Semin. Oncol. 21, 67–75.

[2] Kemeny, N., Lokich, J.J., Anderson, N. and Ahlgren, J.D. (1993) Recent advances in the treatment of advanced colorectal cancer. Cancer 71, 9–18.

[3] Abbruzzese, J.L. and Levin, B. (1989) Treatment of advanced colorectal cancer. Hemat. Oncol. Clin. North Am. 3, 135–153.

[4] Cortesi, E., Padovani, A., Aloe, A., Picece, V., Pellegrini, P. and Pellegrini, A. (1991) Advanced colorectal cancer: Impact of chemotherapy on survival. J. Surg. Oncol. (Suppl. 2), 112–115.

[5] Hunt, T.M. and Taylor, I. (1989) The role of chemo-

therapy in the treatment and prohylaxis of colorectal liver metastases. Cancer Surv. 8, 89–103.

[6] Gunderson, L.L., Beart, R.W. and O'Connell, M.J. (1987) Current issues in the treatment of colorectal cancer. CRC Crit. Rev. Oncol. Hematol. 6, 223–260.

[7] Austin, E.A. and Huber, B.E. (1993) A first step in the development of gene therapy for colorectal carcinoma: cloning, sequencing and expression of *Escherichia coli* cytosine deaminase. Mol. Pharmacol. 43, 380–387.

[8] Huber, B.E., Austin, E.A., Good, S.S., Knick, V.C., Tibbles, S. and Richards, C.A. (1993) In vivo antitumor activity of 5-fluorocytosine on human colorectal carcinoma cells genetically modified to express cytosine deaminase. Can. Res. 53, 4619–4626.

[9] Huber, B.E., Austin, E.A., Richards, C.A., Davis, S.T. and Good, S.S. (1994) Metabolism of 5-fluorocytosine to 5-fluorouracil in human colorectal tumor cells transduced with the cytosine deaminase gene: Significant antitumor effects when only a small percentage of tumor cells express cytosine deaminase. Proc. Natl. Acad. Sci. USA 91, 8302–8306.

[10] Huber, B.E., Richards, C.A. and Austin, E.A. (1994) Virus-directed enzyme/prodrug therapy (VDEPT) selectively engineering drug sensitivity into tumors. In B.E. Huber and Lazo, J.S. (Eds), Gene Therapy for Neoplastic Diseases, NY Acad. Sci., New York, NY, pp. 104–114.

[11] Huber, B.E., Richards, C.A. and Krenitsky, T.A. (1991) Retroviral-mediated gene therapy for the treatment of hepatocellular carcinoma: an innovative approach for cancer therapy. Proc. Natl. Acad. Sci. USA 88, 8039–8043.

[12] Richards, C.A., Austin, E.A. and Huber, B.E. (1995) Transcriptional regulatory sequences of carcinoembryonic antigen: Identification and use with cytosine deaminase for tumor-specific gene therapy. Hum. Gene Ther. 6, 881–893.

[13] Domin, B.A., Mahony, W.B. and Zimmerman, T.P. J. Biol. Chem. 268, 20085–20090 (1993).

[14] Spector, T., Cao, S., Rustum, Y.M., Harrington, J.A. and Porter, D.J.T. (1995) Attenuation of the antitumor activity of 5-fluorouracil by (*R*)-5-fluoro-5,6-dihydrouracil. Cancer Res. 15, 1239–1241.

[15] Abbasi, A.M., Chester, K.A., Macpherson, A.J.S., Boxer, G.M., Begent, R.H. and Malcolm, A.D.B. (1992) Locaization of CEA messenger RNA by in situ hybridization in normal colonic mucosa and colorectal adenocarcinomas. J. Pathol. 168, 405–411.

[16] Jothy, S., Yuan, S.-Y. and Shirota, K. (1993) Transcription of carcinoembryonic antigen in normal colon and colon carcinoma. Am. J. Pathol. 143, 250–257.

[17] Robbins, P.F., Eggensperger, D., Qi, C.-F. and Schlom, J. (1993) Definition of expression of the human carcinoembryonic antigen and non-specific cross-reacting antigen in human breast and lung carcinomas. Int. J. Cancer 53, 892–897.

[18] Chung, J.-K., Jang, J.-J., Lee, D.-S., Lee, M.-C. and Koh, C.-S. (1994) Tumor concentration and distribution of carcinoembryonic antigen measured by in vitro quantitative autoradiography. J. Nucl. Med. 35, 1499–1505.

Nat. Gent. 1992 1:372-378

Science 1989 245:1234-1236

Eur. J Biochem. 1985 148:265-270

Mol. Immunol 1995 32:1057-1064

Science 1993 259:988-990

Nature 1988 336:348-352

J Clin. Invest. 1993 91:225-234

Mol. Cell. Biol. 1987 7:1576-1579

Gene 1982 19:33-42

Neuron 1992 8:507-520

Adv. Virus Res. 1989 37:35-83

1994 Cancer Res. 54:5258-5261

Cell 1987 50:435-443

Nucleic Acids Res. (1996) 24(10):1841-1848

J Biol. Chem. 1988 263 10 :4837-4843

Proc. Natl. Acad. Sci. USA 1992 89:2581-2584

1993 Nature 361:647-650

DNA Seq. 1993 4:185-196

Human Gene Ther. 1995 6:881-893

Science 1991 252:431-434

Cell 1992 68:143-155

Mol. Cell. Biol. 1990 10 6 :2738-2748

Nucleic Acids Res. 1996 24 15 :2966-2973

Human Gene Thera 1990 1:241-256

J Clin. Invest 1992 . 90:626-630

Curr. Topics in Micro. and Imm. 1995 199 part 3 :177-194

Lancet 1981 11:832-834

Cancer Res. 1996 56:1341-1345

J Virol. 1992 66 (6) :3633-3642

J Virol. 1996 70 (4) :2296-2306

Nature (1997) 389:239-242

J Virol. 1984 51 (3) : 822-831

Adv. Ex . Med. Biol. 1991 3098:61-66

Proc. Natl. Acad. Sci. 1983 80:5383-5386

Genomics 1990 8:492-500

Gastroenter. 1990 98:470-477 .

N. Vogel
Au 1636
12/9
10045116

Targeting of Nonexpressed Genes in Embryonic Stem Cells Via Homologous Recombination

RANDALL S. JOHNSON, MORGAN SHENG, MICHAEL E. GREENBERG, RICHARD D. KOLODNER, VIRGINIA E. PAPAIOANNOU, BRUCE M. SPIEGELMAN*

Gene targeting via homologous recombination-mediated disruption in murine embryonic stem (ES) cells has been described for a number of different genes expressed in these cells; it has not been reported for any nonexpressed genes. Pluripotent stem cell lines were isolated with homologously recombined insertions at three different loci: c-*fos*, which is expressed at a low level in ES cells, and two genes, adipsin and adipocyte P2 (aP2), which are transcribed specifically in adipose cells and are not expressed at detectable levels in ES cells. The frequencies at which homologous recombination events occurred did not correlate with levels of expression of the targeted genes, but did occur at rates comparable to those previously reported for genes that are actively expressed in ES cells. Injection of successfully targeted cells into mouse blastocysts resulted in the formation of chimeric mice. These studies demonstrate the feasibility of altering genes in ES cells that are expressed in a tissue-specific manner in the mouse, in order to study their function at later developmental stages.

GENE TARGETING IN ES CELLS HAS been envisioned as a method for studying the effects of specific mutations in the mouse (*1–4*). Genes of interest would be altered by homologous recombination-mediated disruption after DNA transfection of ES cells. These ES cell lines containing altered genes would then be used to create chimeric mice, through injection of the cells into blastocysts. If the germ line is colonized by ES cells in chimeric mice, subsequent breeding would allow the generation of mouse strains that are heterozygous or homozygous for the altered gene. This protocol appears feasible because of two advances: the development of techniques that allow the growth and maintenance of blastocyst-derived cells (ES cells) in a pluripotent state (*5–7*) and the ability to select for homologous recombination-mediated gene replacement in mammalian cell culture (*1, 8–10*).

There have been suggestions that the frequency of a homologous recombination event may depend on the transcription rate of the gene concerned (*3, 9*), although experiments with a human bladder carcinoma cell line indicated that homologous recombination at a nonexpressed locus was possible (*10*). If rates of homologous recombination in ES cells are strongly correlated with rates of expression, it might restrict gene targeting to those genes that are expressed ubiquitously or are active in early development. We report here that two genes expressed in adult mouse adipose tissue, but not detectably expressed in ES cells, can be readily disrupted by homologous recombination.

The adipsin and aP2 genes are both transcriptionally activated during adipocyte differentiation (*11–14*) and the mRNAs encoding the proteins are expressed predominantly in adipose tissue in the mouse (*15–17*). To determine the relative expression of these mRNAs in ES cells, we performed Northern blotting with the ES parent cell line CC1.2 (*5*) and several subclones. No mRNA encoded by either of these genes could be detected, even on prolonged exposures of the autoradiographs (Fig. 1, B and C). In contrast, c-*fos* is expressed in these cells, albeit at a low level compared to the nerve growth factor (NGF)–induced PC-12 cells (*18*) used as a control (Fig. 1A).

Gene targeting vectors (Fig. 2) were constructed to permit the selection of gene replacement events by a procedure similar to that outlined by Mansour *et al.* (*9*). Vectors contained the thymidine kinase (TK) gene of herpes simplex virus (HSV)–1 (*19*). The entire vector sequence is expected to be retained after random integration into the genome, making the cell sensitive to nucleoside analogs, such as gancyclovir (*20*), through the action of the HSV-TK gene product. Homologous recombination with an endogenous sequence is expected to result in the loss of nonhomologous sequences, allowing the cells to retain their native resistance to gancyclovir (*9, 20*). Thus one can use gancyclovir to select against the presence of the TK gene product and in so doing select against random integrants and enrich for homologous recombinants.

Neomycin-resistance gene (*neo*^{r}) cassettes (*1*) were inserted into genomic clones so as to disrupt transcription or translation, or both, and render the genes dysfunctional. The neomycin-resistance marker also allows a positive genetic selection for cells that have stably incorporated the vector into the genome, through resistance to the drug G418. The vectors were linearized and transfected into ES cells by electroporation. After selection with G418 and gancyclovir, colonies resistant to both drugs were clonally expanded, and DNA was isolated for

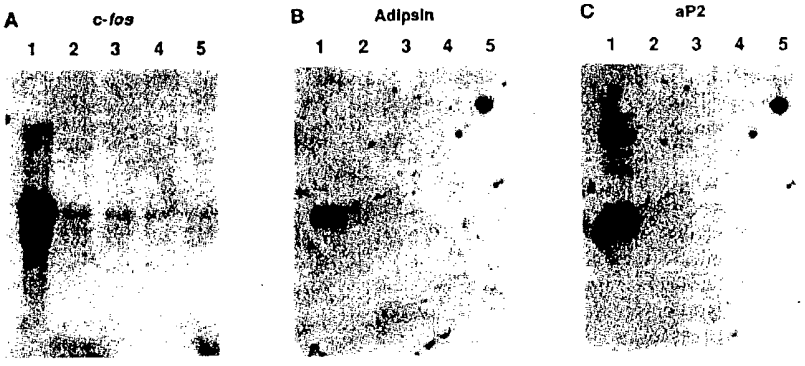

Fig. 1. Expression of c-*fos*, adipsin, and aP2 mRNA in ES cells. Blots were probed with (A) c-*fos*–, (B) adipsin (*25*)–, and (C) aP2 (*25*)–labeled cDNAs. RNA was isolated as described (*25*) and 10 μg of total cytoplasmic RNA was loaded per lane. Electrophoresis, blotting, and probing was performed as previously described (*25*). Adipsin and aP2 blots were overexposed to show the lack of a signal from ES cell lines. (**A**) Lane 1, PC-12 cells stimulated by NGF for 30 min (positive control for c-*fos* expression) (*18*); lane 2, CC1.2, parent ES cell line; lane 3, c-*fos* homologous recombinant f-16; lane 4, adipsin homologous recombinant a-16; and lane 5, aP2 homologous recombinant 8-3. (**B**) Lane 1, differentiated 3T3-F442A adipocytes; lane 2, CC1.2; lane 3, f-16; lane 4, a-16; and lane 5, 8-3. (**C**) Lanes were the same as in (B).

R. S. Johnson, R. D. Kolodner, B. M. Spiegelman, Dana-Farber Cancer Institute and the Department of Biological Chemistry and Molecular Pharmacology, Harvard Medical School, Boston, MA 02115.
M. Sheng and M. E. Greenberg, Department of Microbiology and Molecular Genetics, Harvard Medical School, Boston, MA 02115.
V. E. Papaioannou, Department of Pathology, Tufts University Schools of Medicine and of Veterinary Medicine, Boston, MA 02111.

*To whom correspondence should be addressed.

Southern blotting (Fig. 3).

G418-resistant cells occurred at a relatively constant frequency among the different DNA constructs transfected (approximately 0.1% of the transfected cells) (Table 1). The number of homologous recombinants, as determined by Southern blotting of genomic DNA, was between 5 to 10% of the colonies resistant to both G418 and gancyclovir, although the total number of doubly resistant colonies varied somewhat among constructs. Rates of homologous recombination, expressed as the number of homologous recombinants over the number of stably transfected (G418-resistant) cells, were 5×10^{-5} for c-*fos*, 4×10^{-5} for adipsin, and 3×10^{-4} for aP2. Although these rates are based on a relatively small number of recombinants (15 in all), they are all comparable to those for an expressed gene [that is, 10^{-3} to 2.5×10^{-5} for hypoxanthine-guanine phosphoribosyl-transferase (HPRT)] (*1*).

The ES cell lines with genes targeted by homologous recombination were analyzed for expression of adipsin, aP2, and c-*fos* mRNAs to ensure that the selection process did not enrich for cells with aberrant patterns of expression for those genes. The targeted cell lines and the parent cell line have very similar patterns of expression for the three genes, with no evidence of adipsin or aP2 mRNA (Fig. 1, lanes 2 to 5). Although the possibility cannot be ruled out that aP2 and adipsin are transcribed at very low levels (*21*), they appear to be good examples of genes for which no expression is anticipated or detected in ES cells. There is no reason to suspect that targeting these loci is any more or less difficult than targeting other loci not detectably expressed in these cells. This belief is supported by two observations: (i) the rates of homologous recombination for aP2 and adipsin are comparable to reported rates of recombination for other, expressed genes (*1, 9, 22, 23*), and (ii) we see no obvious relation between expression and targeting rates for a transcribed gene (c-*fos*) and for two genes not detectably expressed in our experiments.

Chimeric mice have been derived in outbred (CD1) or inbred (C57BL/6J, AG/CamPa) mouse strains, or both, with separate ES cell lines containing disrupted aP2, adipsin, and c-*fos* genes; the parent cell line and the clones used to make these mice were karyotyped to ascertain stable, diploid chromosome numbers. The mice are now being bred to ascertain germ line transmission of the altered genes (*5*). The ability of the cells to contribute to tissue formation in chimeric mice indicates that the cells have retained pluripotency during the selection process (*5–7*).

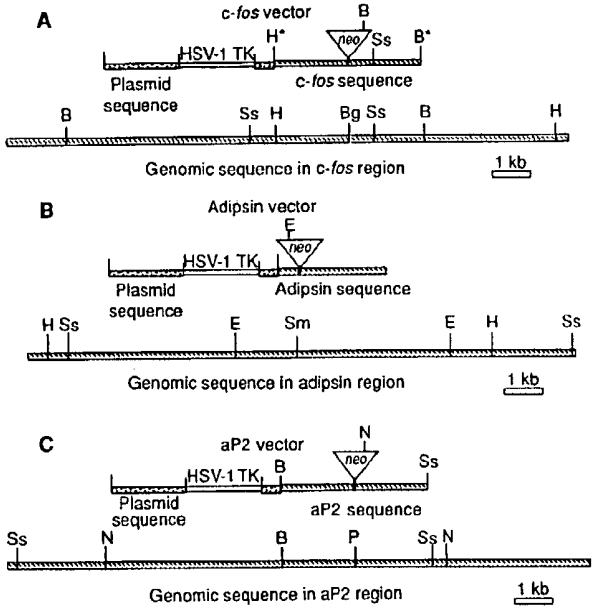

Fig. 2 Transfection vectors containing the disrupted c-*fos*, adipsin, and aP2 gene sequences. (**A**) The parent plasmid vector used to construct all of the above vectors contained the Bam HI 3.4-kb fragment of HSV-1 and its TK gene cloned into the Nae I site of the pBluescript SK(+) plasmid. The genomic sequences described above were cloned into the polylinker of this plasmid. The *neo*^{r} used for gene disruption was derived from the Xho I–Sal I fragment of pMCIneo/polyA+ (*1*). B, Bam HI; Bg, Bgl I; E, Eco RI; H, Hind III; N, Nco I; P, Pst I; Sm, Sma I; and Ss, Sst I. The c-*fos* vector was derived from Hind III–Bam HI genomic fragment containing c-*fos*. The asterisk indicates the genomic sites that were lost during cloning into the plasmid vector. The c-*fos* gene was interrupted by insertion of the *neo*^{r} cassette at a Bgl I site in the first exon. Before transfection the vector was linearized at a unique Not I site in the plasmid polylinker, with linearization giving the orientation shown at the top of the figure. (**B**) The adipsin vector was derived by Bal 31 digestion of an Eco RI genomic fragment. The adipsin gene was interrupted in the third exon at a unique Sma I site and linearized and transfected as above. (**C**) The aP2 vector was derived from a 4.5-kb Bam HI–Sst I genomic fragment. The aP2 gene was interrupted after the transcription start site and before a translation start site at a Pst I site.

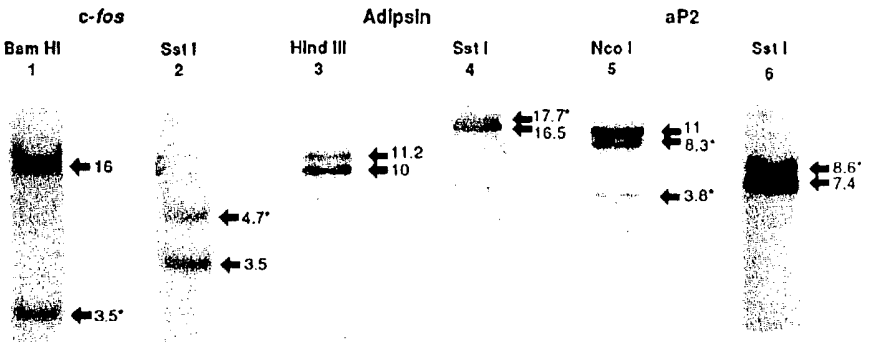

Fig. 3. Identification of ES clones with homologously recombined insertions by DNA blotting. ES cell lines resistant to both G418 and gancyclovir were selected as described in Table 1. DNA from cell lines was isolated, digested with restriction enzymes, blotted, and probed as described (*25*). The asterisk indicates bands generated by homologous recombination events. Numbers refer to kilobase pairs of DNA. Lanes 1 and 2, DNA from the c-*fos* homologous recombinant f-16 probed with the c-*fos* genomic sequence between the Bgl I site in the first exon and the Sph I site in the third intron. Lane 1, Bam HI digestion. Lane 2, Sst I digestion. Lane 1 shows the 16-kb fragment resulting from the hybridization of the probe with the unaltered copy of the gene and the 3.5-kb fragment resulting from the cleavage within the gene as a result of a site in the *neo*^{r}. Lane 2 shows the unaltered fragment at 3.5-kb as well as the 1.2-kb larger fragment at 4.7 kb engendered by the *neo*^{r} cassette. Lanes 3 and 4, DNA from the adipsin homologous recombinant clone a-16 probed with adipsin cDNA (*25*). Lane 3, digested with Hind III. Lane 4, digested with Sst I. In both lanes the lower band corresponds to the remaining copy of the endogenous gene; the upper band is the same fragment plus the 1.2-kb *neo*^{r} insertion. In lane 3 the unaltered fragment is at 10 kb and the gene plus the *neo*^{r} insertion is 11.2 kb. In lane 4 the unaltered gene is at 16.5 kb and the gene plus insertion is at 17.7 kb. Lanes 5 and 6, DNA from the aP2 homologous recombinant clone 8-3 probed with aP2 cDNA (*25*). Lane 5, digested with Nco I. Lane 6, digested with Sst I. The Nco I fragment is split because of an Nco I site in *neo*^{r}, giving the 3.8-kb and 8.3-kb fragments. The 11-kb fragment corresponds to the remaining unaltered copy of the gene. Lane 6 shows the endogenous Sst I fragment at 7.4 kb plus a 1.2-kb larger fragment at 8.6 kb containing the *neo*^{r} insertion. Blots were also probed with the *neo*^{r} sequence to confirm that the homologous recombinant bands contained *neo*^{r} cassette insertions (data not shown).

The three genes we have targeted in these experiments are likely to be important in mouse development and physiology, but their functions remain undefined genetically. The adipsin gene encodes a serine protease with complement factor D activity and has links to systemic energy balance and obesity (*15, 24*); the aP2 gene product is an adipocyte-specific fatty acid binding protein (*25–27*) whose precise role in physiology is unknown. The c-*fos* proto-oncogene is involved in the regulation of gene transcription (*28, 29*), and disruption of this gene may have numerous effects on cell function. The analysis of the phenotypic effect of disruption of these three genes should lead to a greater understanding of their function in the organism.

It is probable that many factors are involved in determining the frequency at which detectable homologous recombination occurs at a given genetic locus (*2, 3*). Our data, however, demonstrate that it is feasible to target genes not expressed in ES cells in order to study their function in mouse development and physiology.

Table 1. Rates of homologous recombination after double drug selection. Electroporations were performed with the linearized vector described in Fig. 2. The data are pooled from several transfections. ES cells were grown in Dulbecco's modified Eagle's medium (DMEM) with 15% fetal bovine serum (FBS) and 0.1 m*M* 2-mercaptoethanol on gamma-irradiated (4000 rads) Sto feeder layers made G418-resistant by transfection with the vector pSV2neo. Cells (2×10^7) in 1 ml of medium were electroporated at 750 V/cm in DMEM and FBS with vector DNA at 1 n*M*. These cells were plated out on G418-resistant feeder layers. The number of viable cells 24 hours after electroporation was always between 40 to 60%. At 36 hours after transfection, G418 (100 μg/ml) and gancyclovir (2 μ*M*) were added. After selection for 10 days, drug-resistant colonies were picked and expanded on Sto feeder layers without further drug selection. The asterisk indicates that one control plate for each transfection was selected with G418 alone and was plated at 1/20 the density of doubly selected plates (5×10^5 cells on a 150-cm^2 plate versus 2×10^7 cells on a 150-cm^2 plate), and the number of G418-resistant colonies for the entire transfection was extrapolated from this number. Clones listed as homologous recombinants were confirmed as such by digestion with two or more restriction enzymes and Southern blotting, as shown for the representative clones in Fig. 3.

DNA transfected	Cells electroporated	No. G418* resistant	No. G418 and gancyclovir resistant	Homologous recombinants
c-*fos* vector	4×10^7	2×10^4	16	1
Adipsin vector	10^8	5×10^4	22	2
aP2 vector	8×10^7	4×10^4	142	12

REFERENCES AND NOTES

1. K. R. Thomas and M. R. Capecchi, *Cell* **51**, 503 (1987).
2. M. R. Capecchi, *Science* **244**, 1288 (1989).
3. M. Frohman and G. Martin, *Cell* **56**, 145 (1989).
4. V. E. Papaioannou *et al.*, *J. Embryol. Exp. Morphol.* **44**, 93 (1978).
5. A. Bradley *et al.*, *Nature* **309**, 255 (1984).
6. M. J. Evans and M. H. Kaufman, *ibid.* **292**, 154 (1981).
7. G. R. Martin, *Proc. Natl. Acad. Sci. U.S.A* **78**, 7634 (1981).
8. K. R. Thomas *et al.*, *Cell* **44**, 419 (1986).
9. S. L. Mansour *et al.*, *Nature* **336**, 348 (1988).
10. O. Smithies *et al.*, *ibid.* **317**, 230 (1985).
11. K. S. Cook, C. R. Hunt, B. M. Spiegelman, *J. Cell. Biol.* **100**, 514 (1985).
12. D. A. Bernlohr, M. A. Bolanowski, T. J. Kelly, Jr., M. D. Lane, *J. Biol. Chem.* **260**, 5563 (1985).
13. P. Djian, M. Phillips, H. Green, *J. Cell. Physiol.* **124**, 554 (1985).
14. A. Doglio, C. Davi, P. Grimaldi, G. Ailhaud, *Biochem. J.* **238**, 123 (1986).
15. K. S. Cook, D. L. Groves, H. Y. Min, B. M. Spiegelman, *Proc. Natl. Acad. Sci. U.S.A.* **82**, 6480 (1985).
16. K. M. Zezulak and H. Green, *Mol. Cell. Biol.* **5**, 419 (1985).
17. D. A. Bernlohr *et al.*, *Biochem. Biophys. Res. Commun.* **132**, 850 (1985).
18. M. Sheng *et al.*, *Mol. Cell. Biol.* **8**, 2787 (1988).
19. S. McKnight, *Nucleic Acids Res.* **8**, 5949 (1980).
20. M. H. St. Clair, C. U. Lambe, P. A. Furman, *Antimicrob. Agents Chemother.* **31**, 844 (1987).
21. G. Sarkar and S. S. Sommer, *Science* **244**, 331 (1989).
22. T. Doetschman, N. Maeda, O. Smithies, *Proc. Natl. Acad. Sci. U.S.A.* **85**, 8583 (1988).
23. A. Joyner *et al.*, *Nature* **338**, 153 (1989).
24. B. S. Rosen *et al.*, *Science* **244**, 1483 (1989).
25. B. M. Spiegelman, M. Frank, H. Green, *J. Biol. Chem.* **258**, 10083 (1983).
26. V. Matarese and D. Bernlohr, *ibid.* **263**, 14544 (1988).
27. R. C. Hresko *et al.*, *Proc. Natl. Acad. Sci. U.S.A.* **85**, 8835 (1988).
28. R. J. Distel *et al.*, *Cell* **49**, 835 (1987).
29. T. Curran and B. R. Franza, *ibid.* **55**, 395 (1988).

30. We thank A. Bradley for the CC1.2 ES cell line; J. Spencer for technical assistance; and B. Satterberg, M. Mercola, M. Musacchio, L. Michalowsky, L. Reid, B. Koller, O. Smithies, J. Rossant, R. Kucherlapati, D. Coen, and E. Robertson for helpful discussions. Supported by a grant from NIH (DK 31405). R.J. and M.S. were supported by Lucille P. Markey predoctoral fellowships. B.S. is an Established Investigator of the American Heart Association.

3 July 1989; accepted 2 August 1989

Foregut Fermentation in the Hoatzin, a Neotropical Leaf-Eating Bird

ALEJANDRO GRAJAL, STUART D. STRAHL, RODRIGO PARRA, MARIA GLORIA DOMINGUEZ, ALFREDO NEHER

The only known case of an avian digestive system with active foregut fermentation is reported for the hoatzin (*Opisthocomus hoazin*), one of the world's few obligate folivorous (leaf-eating) birds. Hoatzins are one of the smallest endotherms with this form of digestion. Foregut fermentation in a flying bird may be explained by increased digestive efficiency by selection of highly fermentable and extremely patchy resources, coupled with microbial nutritional products and secondary compound detoxification. This unexpected digestive system gives a new perspective to the understanding of size limitations of vertebrate herbivores and to the evolution of foregut fermentation.

FOREGUT MICROBIAL FERMENTATION as a means of digesting fibrous plant matter has been reported in mammals such as ruminants, monkeys, sloths, and macropodid marsupials (*1*). Although a few bird species display hindgut fermentation (*2*), there are no documented cases of extensive foregut fermentation structures or associated digestive physiology in the entire class Aves. We now report a well-developed ruminant-like digestive system in a neotropical folivorous bird, the hoatzin, *Opisthocomus hoazin*. This is the first report of this digestive system outside the mammals, and opens new insights into the evolution of foregut fermentation.

The hoatzin is a 750-g cuculiform bird that ranges from the Guianas to Brazil and inhabits riverine swamps, gallery forests, and oxbow lakes (*3, 4*). Early descriptions suggested that the crop of this species has replaced the gizzard and proventriculus as the primary site of digestion (*5*). None of these authors documented or suggested foregut fermentation, although some noted that the characteristic odor of the bird was similar to fresh cow manure (*6*).

At our study site (*7*), more than 80% of the hoatzin's diet is composed of green leaves. Although the birds fed on the leaves of 52 species of plants in 25 families, 90% of the diet is composed of only 17 plant spe-

A. Grajal, Department of Zoology, University of Florida, Gainesville, FL 32611.
S. D. Strahl, Wildlife Conservation International, New York Zoological Society, Bronx, NY 10460.
R. Parra and A. Neher, Instituto de Producción Animal, Universidad Central de Venezuela, Facultad de Agronomía, Maracay, Estado Aragua, Venezuela.
M. G. Dominguez, Rowett Research Institute, Bucksburn, Aberdeen, Scotland, United Kingdom.

Nat. Gent. 1992 1:372-378
Science 1989 245:1234-1236
Eur. J Biochem. 1985 148:265-270
Mol. Immunol 1995 32:1057-1064
Science 1993 259:988-990
Nature 1988 336:348-352
J Clin. Invest. 1993 91:225-234
Mol. Cell. Biol. 1987 7:1576-1579
Gene 1982 19:33-42
Neuron 1992 8:507-520
Adv. Virus Res. 1989 37:35-83
1994 Cancer Res. 54:5258-5261
Cell 1987 50:435-443
Nucleic Acids Res. (1996) 24(10):1841-1848
J Biol. Chem. 1988 263 10 :4837-4843
Proc. Natl. Acad. Sci. USA 1992 89:2581-2584
1993 Nature 361:647-650
DNA Seq. 1993 4:185-196
Human Gene Ther. 1995 6:881-893
Science 1991 252:431-434
Cell 1992 68:143-155
Mol. Cell. Biol. 1990 10 6 :2738-2748
Nucleic Acids Res. 1996 24 15 :2966-2973
Human Gene Thera 1990 1:241-256
J Clin. Invest 1992 . 90:626-630
Curr. Topics in Micro. and Imm. 1995 199 part 3 :177-194
Lancet 1981 11:832-834
Cancer Res. 1996 56:1341-1345
J Virol. 1992 66 (6) :3633-3642
J Virol. 1996 70 (4) :2296-2306
Nature (1997) 389:239-242
J Virol. 1984 51 (3) : 822-831
Adv. Ex . Med. Biol. 1991 3098:61-66
Proc. Natl. Acad. Sci. 1983 80:5383-5386
Genomics 1990 8:492-500
Gastroenter. 1990 98:470-477 .

M. Vogel
Au 1636
12/9
10045116

Eur. J. Biochem. 148, 265–270 (1985)

Nucleotide sequence of cloned cDNA coding for preproricin

F. Ian LAMB, Lynne M. ROBERTS and J. Michael LORD

Department of Biological Sciences, University of Warwick, Coventry

(Received September 3/December 3, 1984) – EJB 84 0966

The primary structure of a precursor protein that contains the toxic (A) and galactose-binding (B) chains of the castor bean lectin, ricin, has been deduced from the nucleotide sequence of cloned DNA complementary to preproricin mRNA. A cDNA library was constructed using maturing castor bean endosperm poly(A)-rich RNA enriched for lectin precursor mRNA by size fractionation. Clones containing lectin mRNA sequences were isolated by hybridization using as a probe a mixture of synthetic oligonucleotides representing all possible sequences for a peptide of the ricin B chain. The entire coding sequence of preproricin was deduced from two overlapping cDNA clones having inserts of 1614 and 1049 base pairs. The coding region (1695 base pairs) consists of a 24-amino-acid N-terminal signal sequence (molecular mass 2836 Da) preceding the A chain (267 amino acids, molecular mass 29399 Da), which is joined to the B chain (262 amino acids, molecular mass 28517) by a 12-amino-acid linking region (molecular mass 1385 Da).

Ricin, the toxic lectin of *Ricinus communis* seeds, is a heterodimer whose subunits (designated the A and B chains) are joined by a disulphide bond [1]. The amino acid sequence of both subunits has been determined [2–4]. The molecular mass of the A polypeptide is 30522 Da and it contains one N-linked oligosaccharide (on asparagine residue 10), while the B chain, molecular mass 29082 Da, contains two oligosaccharide chains (asparagine residues 93 and 133). The B chain also contains two galactose-binding sites [5]. Interaction of these binding sites with exposed galactose residues on cell surface components leads to the translocation of the toxic A chain into the cytoplasm, where it irreversibly inactivates 60S ribosomal subunits [1].

We have recently shown that the A and B chains of ricin are synthesized, both *in vivo* and *in vitro*, in the form of a single precursor polypeptide tentatively assumed to contain one copy of each subunit [6]. This assumption has been confirmed in the present study by cloning and sequencing cDNAs encoding a ricin precursor.

MATERIALS AND METHODS

Materials

Restriction endonucleases and isotopes were obtained from Amersham International (England), DNA polymerase and T4 polynucleotide kinase from Boehringer (Mannheim, FRG) and S1 nuclease and calf thymus terminal deoxynucleotidyltransferase from Miles (Elkhart, IN, USA). Avian myeloblastosis virus reverse transcriptase was provided by Dr J. W. Beard (Life Sciences Inc., St Petersburg, FL, USA) and the synthetic oligonucleotide was kindly provided by Celltech Ltd (Slough, England).

Correspondence to J. M. Lord, Department of Biological Sciences, University of Warwick, Coventry, West Midlands, England CV4 7AL

Isolation of mRNA

Total RNA was isolated from maturing castor bean (*Ricinus communis*) seeds taken from greenhouse-grown plants [7]. Poly(A)-rich RNA was purified by chromatography on oligo(dT)-cellulose [8] and was fractionated on the basis of size by sucrose density gradient centrifugation [9]. mRNA was translated in the nuclease-treated rabbit reticulocyte lysate system [10].

cDNA synthesis

3.0 μg of poly(A)-rich RNA, enriched in ricin precursor mRNA, was used as a template for oligo(dT)-primed synthesis of cDNA using avian myeloblastosis virus reverse transcriptase followed by second-strand synthesis with DNA polymerase according to published procedures [11]. After treatment of the double-stranded cDNA with *Aspergillus oryzae* S1 nuclease, homopolymeric poly(dC) tails were added to the 3′ ends using calf thymus terminal deoxynucleotidyltransferase [12].

cDNA cloning and library screening

Poly(dC)-tailed cDNA was fractionated by sucrose density gradient centrifugation and cDNAs with lengths greater than 1000 base pairs were annealed to *Pst*1-linearized, poly(dG)-tailed plasmid pBR322. The recombinant plasmids were used to transform competent *E. coli* DH1 cells. Transformants were selected on the basis of their differential antibiotic sensitivity. Recombinant cDNA clones were screened *in situ* on nitrocellulose filters with a synthetic 20-mer oligonucleotide mixture. This probe represented all possible DNA sequences predicted from a stretch of seven amino acids located in the C-terminal region of the ricin B chain [2–4]. Its structure is illustrated in Fig. 1. The probe was 5′-labelled with T4 polynucleotide kinase and [γ-^{32}P]ATP. Hybridization was carried out in triplicate at 42 °C in 6 × NaCl/Cit and the filters

were finally washed at three different temperatures determined from the base composition and degree of mismatch of the probe [13]. Hybridization was predicted at two of the wash temperatures (52 °C and 56 °C) but not at a third (60 °C).

DNA sequence analysis

One of the positive clones (designated pRCL6, which contained a 1614-base-pair insert) was cloned into the M13 phage vectors mp8 and mp9 [14] and sequenced using the chain termination technique [15].

In addition, the pRCL6 insert was sequenced by the procedure of Maxam and Gilbert [16]; sequences at the ends of the insert being obtained after recloning into the *Pst*I site of plasmid pUC8 by ligation [7]. A comparison of the amino acid sequence deduced from pRCL6 revealed that this insert was a copy of preproricin mRNA, which was incomplete at the 3′ end. From restriction patterns of other positive clones an overlapping 3′ end sequence was obtained from clone pRCL17. The insert of pRCL17 was recloned into pUC8 and fragments were end-labelled and sequenced according to Maxam and Gilbert [16]. Restriction endonuclease digestions were performed using commercial enzymes according to the supplier's instructions.

Peptide -Trp-Met-Phe-Lys-Asn-Asp-Gly-

mRNA TGGATGTT$^{T}_{C}$AA$^{G}_{A}$AA$^{T}_{C}$GA$^{T}_{C}$GG

Oligo ACCTACAA$^{A}_{G}$TT$^{C}_{T}$TT$^{A}_{G}$CT$^{A}_{G}$CC

Fig. 1. *Region of the ricin B chain selected for the synthesis of an oligonucleotide probe.* All potential mRNA sequences (presented as the corresponding strand of the DNA) are shown together with the complementary oligonucleotide probe sequences

RESULTS

A library of cDNA clones was derived from poly(A)-rich RNA isolated from maturing castor bean endosperm tissue. The cDNA library was screened by hybridization to a mixture of 16 synthetic oligonucleotides (Fig. 1) representing all possible DNA sequences predicted from a stretch of 7 amino acids previously shown by protein sequencing to be close to the C terminus of the ricin B chain [2, 3]. From a total of 1600 tetracycline-resistant transformants, 80 colonies gave strong hybridization signals after washing the filters at 52 °C and 56 °C but not, as predicted [13], after washing at 60 °C. The nucleotide sequences of cloned cDNAs were determined by a combination of the Sanger 'dideoxy' method [15] and the procedure of Maxam and Gilbert [17] according to the strategy outlined in Fig. 2. Both strands were sequenced.

The primary structure of the mRNA encoding the ricin precursor was deduced from the two overlapping cDNA sequences (Fig. 3). The sequenced inserts of pRCL6 and pRCL17 exhibit no differences in the overlapping region. Amino acids 1 – 265 of the A chain and 1 – 260 of the B chain, previously determined by protein sequencing [2, 3], are encoded by, and contained within, nucleotide residues 1 – 801 and 838 – 1623 of the mRNA. Differences between the derived primary structure and the published amino acid sequences are shown in Fig. 3. The derived A chain sequence is almost identical to the published sequence [3] except for two extra

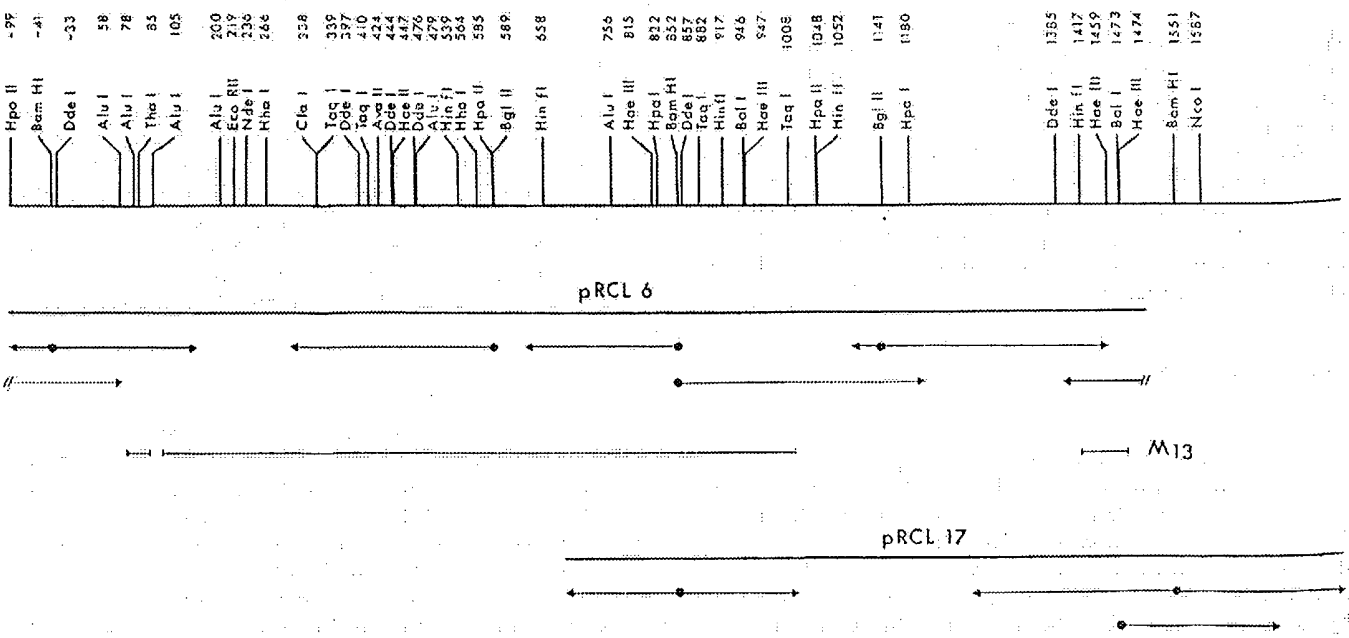

Fig. 2. *Restriction endonuclease map of ricin precursor cDNA clones pRCL6 and pRCL17 and strategy of sequencing.* The direction and extent of sequence determinations are shown by horizontal arrows. When sequencing was carried out by the procedure of Maxam and Gilbert the sites of 3′-end labelling are indicated by closed circles at the end of the arrows. The double slash marks indicate that the site of end labelling was located on the vector DNA. *Alu*1, *Sau*3AI and *Hae*III fragments of the pRCL6 insert were randomly ligated into M13 mp8 and sequenced in both directions by the chain termination technique. The 72 overlapping sequences obtained are represented by the horizontal lines labelled M13

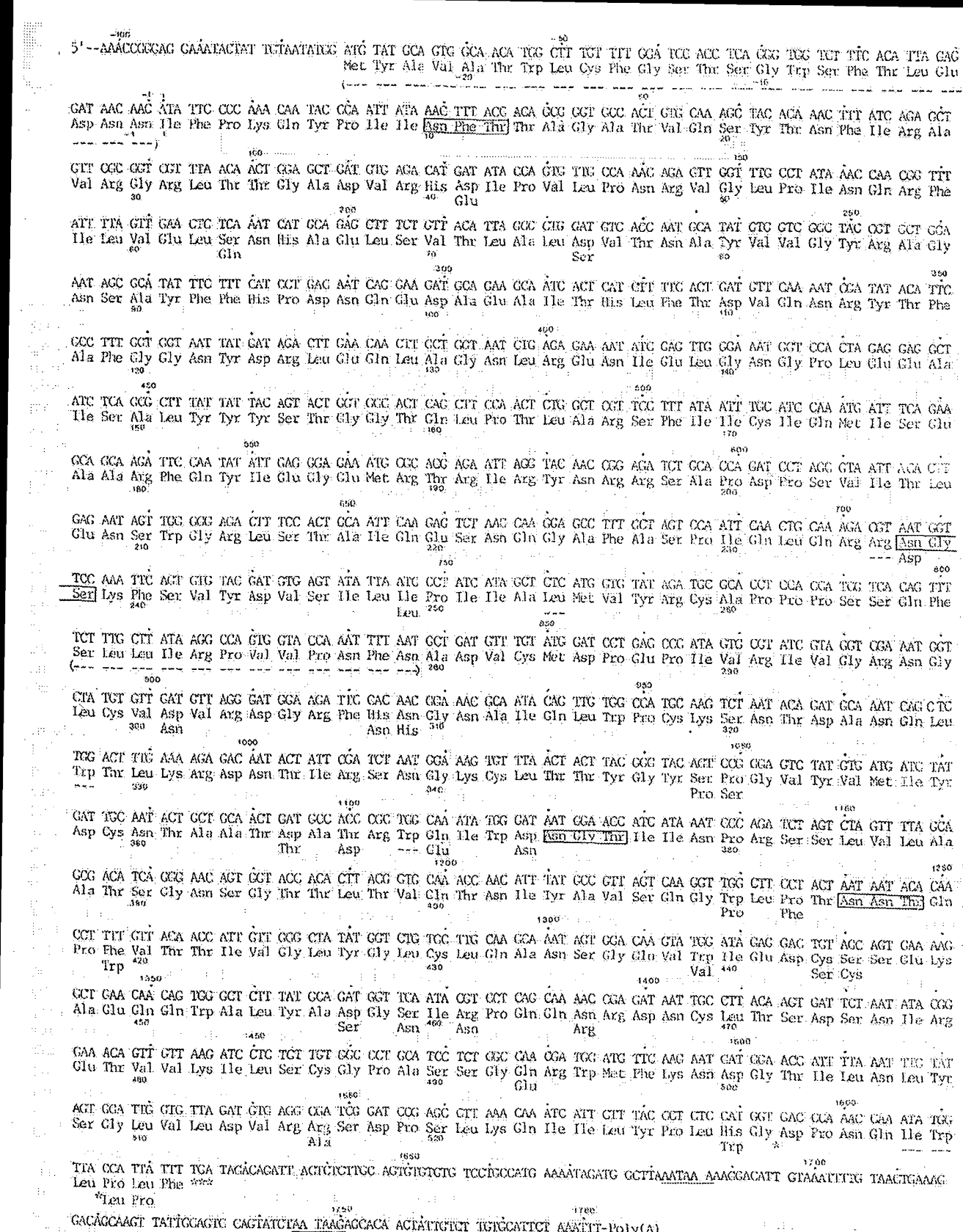

Fig. 3. *Primary structure of the mRNA encoding a ricin precursor.* Nucleotide residues (shown as the corresponding DNA strand) are numbered in the 5′ to 3′ direction with the first residue of the codon specifying the aminoterminal residue of mature A chain numbered 1 and the nucleotides on the 5′ side of residue 1 indicated by negative numbers. The 5′-terminal sequences does not extend to the 5′ end of the mRNA (see text) whereas the 3′-terminal sequence shown is followed by a poly(dA) tract 27 residues long, thus representing the complete sequence of this region. The predicted amino acid sequence is given below the nucleotide sequence and differences with the published amino acid sequence are indicated beneath. Residues absent from the published amino acid sequences [2, 3] are underlined with a dashed line and the position of amino acids present in the published sequences but absent from the derived sequence presented here are indicated by an asterisk. The dashed line beneath the 12-amino-acid sequence linking the C terminus of the A chain and the N terminus of the B chain is bracketed. Amino acids are numbered from the aminoterminal residue of the mature A chain and the preceding residues are indicated by negative numbers. Potential sites for asparagine-linked *N*-glycosylation are boxed and potential poly(A) signals are underlined

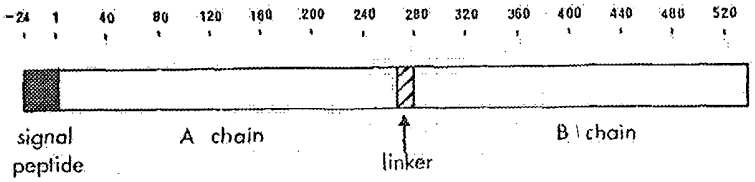

Fig. 4. *Schematic representation of the structure of preproricin.* Numbers refer to amino acid residues

amino acids at positions 235 and 254, and amino acid replacements at positions 41, 63, 75, 236 and 249. The derived A chain sequence contains 267 amino acid rather than 265 previously demonstrated by protein sequencing. The most significant amino acid replacement is that at position 236 where the nucleotide sequence predicts asparagine, thus generating a potential *N*-glycosylation site.

The derived B chain sequence was again two amino acid residues longer (262 residues) than the published primary sequence [2, 3]. In this case the degree of homology between the derived and published B chain sequence was less than that found for the corresponding A chains. Adjacent amino acids at positions 308–309, 349–350, 365–367, 443–444 and 539–540 were in reverse order, although a published partial amino acid sequence, corresponding to B chain residues 355–373 (Fig. 3), confirmed a tryptophan residue at position 369 and agrees with the derived sequence around positions 365–367 [4]. The differences observed here may be due in part to ricin heterogeneity between different seed varieties [1], or due to the two or more forms of ricin, which may be present in each seed [18].

The translation initiation site was assigned to the methionine codon d(ATG) represented by nucleotide residues −72 to −70. Although this is not the 5′-proximal d(ATG) triplet (which is found four bases upstream) it is the only one from which the nucleotide sequence yields a single, large open-reading frame that can encode a protein corresponding both in size to the prepropeptide and in amino acid sequence to the authentic subunits of ricin. Although initiation from this site cannot be reconciled with the scanning model of eukaryotic initiation [19, 20], several other examples of plant genes which apparently do not utilize the 5′-proximal d(ATG) as the initiation codon have been reported [21–23].

The derived sequence predicts an N-terminal extension of 24 amino acid for the signal peptide, which allows translocation of the ricin precursor across the endoplasmic reticulum [7]. The orientation of the preproprotein is signal–A-chain–B-chain. The A and B chain sequences are separated by a 12-amino-acid linking region as illustrated schematically in Fig. 4.

DISCUSSION

From the nucleotide sequence of cloned DNA complementary to ricin precursor mRNA we conclude that this precursor is a preproprotein containing 565 amino acids, of which 267 comprise the A chain and 262 comprise the B chain. The ricin A chain sequence is preceded by a putative signal peptide of 24 amino acids, and the mature A and B chain sequences are separated by a short linker region. In the posttranslational cleavage of proricin this 12-amino-acid linker region must be removed. One cleavage must occur on the amino-acid-terminal side of the serine residue at position 268 while the other cleavage occurs on the carboxyl side of the asparagine residue at position 279. The removal of linker regions in the processing of pea seed lectin [24] and the plant storage proteins soybean glycinin [25] and pea legumin [26] also involves a specific proteolytic cleavage on the carboxyl side of asparagine. An acid endopeptidase, which cleaves proricin into authentic A and B chains, has recently been isolated from castor bean protein bodies (unpublished data); the protein body being the ultimate destination of ricin in the castor bean endosperm cell [27, 28].

The ricin precursor contains four potential sites for asparagine-linked glycosylation at residues 10 and 236 in the A chain sequence and residues 374 and 414 in the B chain. The amino acid sequences of Yoshitake et al. [3] indicate an aspartate residue 236, where our nucleotide sequence predicts asparagine. Other partially sequenced cDNA clones (not shown) also predict this asparagine. A recent analysis has indicated that a variant or 'heavy' form of ricin A chain does indeed contain two N-linked oligosaccharide chains (B. Foxwell, personal communication).

Codon utilization for preproricin mRNA is non-random, generally reflecting a preference for dA or dT in the third position of the corresponding DNA sequence. The codon specifying phenylalanine at position 541 is followed by the translation termination codon, d(TGA). The 3′-untranslated region of the mRNA is 156 nucleotides long and contains a polyadenylation signal between nucleotides 1682–1687, 55 nucleotides downstream from the stop codon and 95 nucleotides upstream from the polyA tract.

It has been suggested that the ricin B chain may be a product of gene duplication [5]. Several areas of amino acid homology exist between the N-terminal and the C-terminal halves of the B chain when the two disulphide bridges in each half are aligned. In all, 26 identical amino acids were found in corresponding positions in each half [5]. We have now extended this analysis to the B chain nucleotide sequence. Our findings strengthen the contention that both halves of the ricin B chain may have arisen from a common ancestor. The two halves show 28.6% amino acid homology with 41 residues conserved (Fig. 5). There remain, however, numerous differences between codon sequences defining the conserved amino acids in the two halves (71.7% DNA homology).

At present there is considerable interest in the potential use of ricin-containing immunotoxins in cancer chemotherapy [29–32]. The inclusion of whole ricin in these constructs is complicated by the presence of the B chain galactose-binding sites, which override the specificity conferred by the antibody molecules [33]. The presence of the B chain seems to be necessary, however, to ensure efficient delivery of the A chain into the cytoplasm [33, 34]. Site-specific mutation of cDNA clones, affecting amino acids involved in B chain galactose binding, may ultimately lead to a modified ricin and an increased specificity of ricin-based immunotoxins.

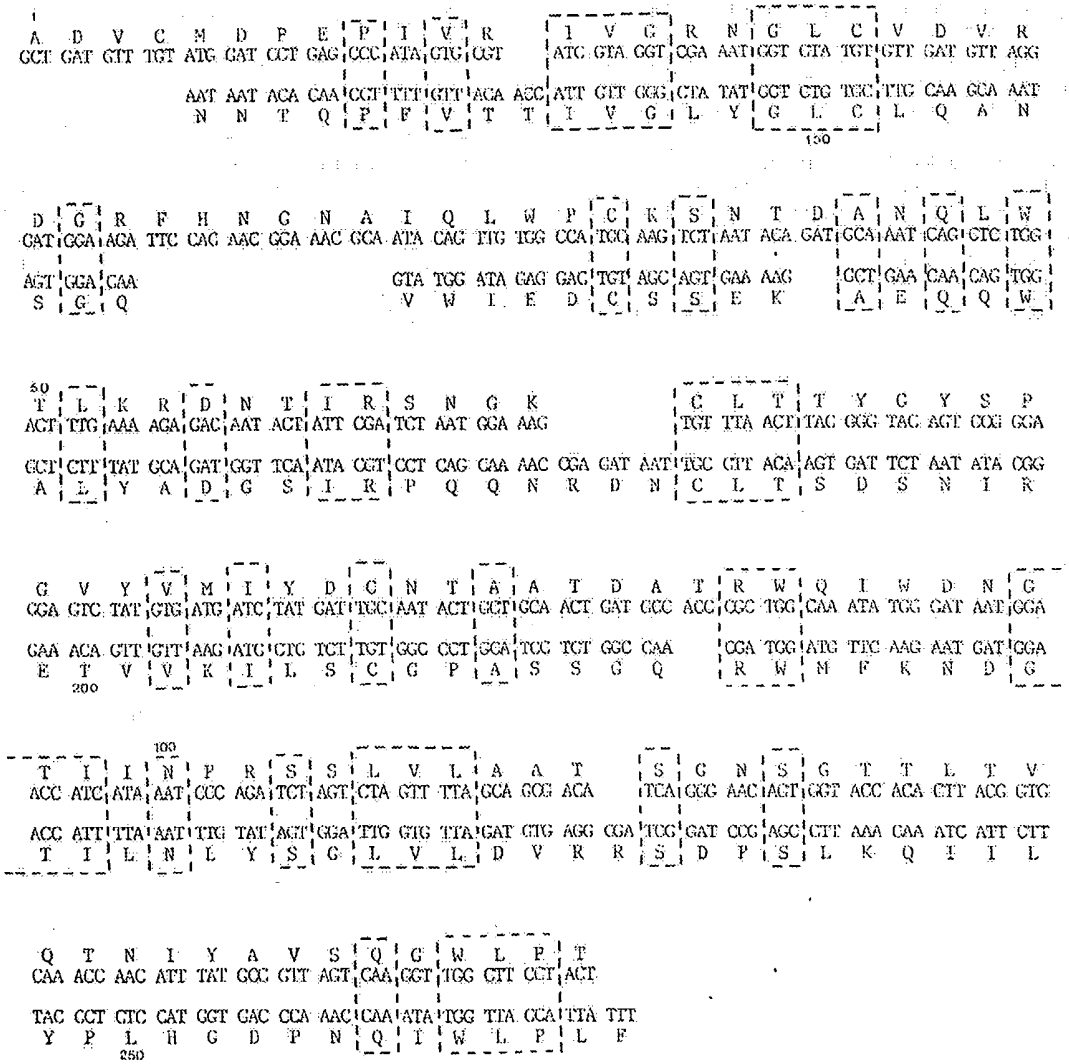

Fig. 5. *Comparison of the two halves of the ricin B chain and their cDNA sequences.* The upper line shows the N-terminal first 134 residues, which are compared with the 128 C-terminal residues (lower line), aligning the disulphide bridges in each half. Identical amino acids are enclosed in boxes

We thank Celltech (Slough) for kindly providing the oligonucleotide probe; Croda Premier Oils (Hull) for the *Ricinus communis* seeds; and Tim Harris and Mark Bodmer for assistance and advice on DNA sequencing. The work was supported by grant GR/C 66442 from the UK Science and Engineering Research Council and by grant AG 88/33 from the UK Agricultural and Food Research Council.

REFERENCES

1. Olsnes, S. & Pihl, A. (1982) in *Molecular actions of toxins and viruses* (Cohen, P. & Van Heyningen, S., eds) pp. 51–105, Elsevier Biomedical Press, Amsterdam.
2. Funatsu, G., Kimura, M. & Funatsu, M. (1979) *Agric. Biol. Chem. 43*, 2221–2224.
3. Yoshitake, S., Funatsu, G. & Funatsu, M. (1978) *Agric. Biol. Chem. 42*, 1267–1274.
4. Bull, H., Li, S. S.-L., Fowler, E. & Lin, T. T.-S. (1980) *Int. J. Peptide Protein Res. 16*, 208–218.
5. Villafranca, J. E. & Robertus, J. (1981) *J. Biol. Chem. 256*, 554–556.
6. Butterworth, A. G. & Lord, J. M. (1983) *Eur. J. Biochem. 137*, 57–65.
7. Roberts, L. M. & Lord, J. M. (1981) *Eur. J. Biochem. 119*, 31–41.
8. Aviv, H. & Leder, P. (1972) *Proc. Natl Acad. Sci. USA 69*, 1408–1412.
9. Fujii-Kuriyama, Y., Taniguchi, T., Mizukami, Y., Sakai, M., Tashiro, Y. & Muramatsu, M. (1981) *J. Biochem. (Tokyo) 89*, 1869–1879.
10. Pelham, H. R. B. & Jackson, R. J. (1976) *Eur. J. Biochem. 67*, 247–256.
11. Lehrach, H., Frischauf, A. M., Hanahan, D., Wozney, J., Fuller, F. & Boedtker, H. (1979) *Biochemistry 18*, 3146–3152.
12. Nelson, T. & Brutlag, D. (1979) *Methods Enzymol. 68*, 41–50.
13. Singer-Sam, J., Simmer, R. L., Keith, D. H., Shively, L., Teplitz, M., Itakura, K., Garther, S. M. & Riggs, A. D. (1983) *Proc. Natl Acad. Sci. USA 80*, 802–806.
14. Messing, J. & Vieira, J. (1982) *Gene 19*, 269–276.
15. Sanger, F., Nicklen, S. & Coulson, A. R. (1977) *Proc. Natl Acad. Sci. USA 74*, 5463–5467.
16. Maxam, A. M. & Gilbert, W. (1980) *Methods Enzymol. 65*, 499–560.
17. Vieira, J. & Messing, J. (1982) *Gene 19*, 257–268.
18. Lin, T. T.-S. & Li, S. S.-L. (1980) *Eur. J. Biochem. 105*, 453–459.
19. Kozak, M. (1984) *Nucleic Acids Res. 12*, 857–872.
20. Kozak, M. (1978) *Cell 15*, 1109–1123.

21. Hoffman, L. M., Ma, Y. & Barker, R. F. (1982) *Nucleic Acids Res. 10*, 7819–7828.
22. Shah, D. M., Hightower, R. C. & Meagher, R. B. (1982) *Proc. Natl Acad. Sci. USA 79*, 1022–1026.
23. Heidecker, G. & Messing, J. (1983) *Nucleic Acids. Res. 11*, 4891–4906.
24. Higgins, T. J. V., Chandler, P. M., Zurawski, G., Button, S. C. & Spencer, D. (1983) *J. Biol. Chem. 258*, 9544–9549.
25. Nielsen, N. C. (1984) *Philos. Trans. Soc. Lond. B. Biol. Sci. 304*, 287–296.
26. Boulter, D. (1984) *Phil. Trans. Roy. Soc. Lond. B. Biol. Sci. 304*, 323–332.
27. Tulley, R. E. & Beevers, H. (1976) *Plant Physiol. 58*, 710–716.
28. Youle, R. J. & Huang, A. H. C. (1976) *Plant Physiol. 58*, 703–709.
29. Raso, V. (1982) *Immunol. Rev. 62*, 93–118.
30. Thorpe, P. E. & Ross, W. C. J. (1982) *Immunol. Rev. 62*, 119–158.
31. Neville, D. M. & Youle, R. J. (1982) *Immunol. Rev. 62*, 75–91.
32. Vitetta, E., Krolick, K. A., Miyama-Inaba, M., Cushley, W. & Uhr, J. W. (1983) *Science (Wash. DC) 219*, 644–650.
33. Vitetta, E. S., Cushley, W. & Uhr, J. W. (1983) *Proc. Natl Acad. Sci. USA 80*, 6332–6335.
34. McIntosh, D. P., Edwards, D. C., Cumber, A. J., Parnell, G. D., Dean, C. J., Ross, W. C. J. & Forrester, J. A. (1983) *FEBS Lett. 164*, 17–20.

Nat. Gent. 1992 1:372-378
Science 1989 245:1234-1236

Eur. J-Biochem. 1985 148:265-270

Mol. Immunol 1995 32:1057-1064

Science 1993 259:988-990

Nature 1988 336:348-352

J Clin. Invest. 1993 91:225-234

Mol. Cell. Biol. 1987 7:1576-1579

Gene 1982 19:33-42

Neuron 1992 8:507-520

Adv. Virus Res. 1989 37:35-83

1994 Cancer Res. 54:5258-5261

Cell 1987 50:435-443

Nucleic Acids Res. (1996) 24(10):1841-1848

J Biol. Chem. 1988 263 10 :4837-4843

Proc. Natl. Acad. Sci. USA 1992 89:2581-2584

1993 Nature 361:647-650

DNA Seq. 1993 4:185-196

Human Gene Ther. 1995 6:881-893

Science 1991 252:431-434

Cell 1992 68:143-155

Mol. Cell. Biol. 1990 10 6 :2738-2748

Nucleic Acids Res. 1996 24 15 :2966-2973

Human Gene Thera 1990 1:241-256

J Clin. Invest 1992 . 90:626-630

Curr. Topics in Micro. and Imm. 1995 199 part 3 :177-194

Lancet 1981 11:832-834

Cancer Res. 1996 56:1341-1345

J Virol. 1992 66 (6) :3633-3642

J Virol. 1996 70 (4) :2296-2306

Nature (1997) 389:239-242

J Virol. 1984 51 (3) : 822-831

Adv. Ex . Med. Biol. 1991 3098:61-66

Proc. Natl. Acad. Sci. 1983 80:5383-5386

Genomics 1990 8:492-500

Gastroenter. 1990 98:470-477 .

N. Vogel
AU 1636
12/9
10045116

Pergamon

0161-5890(95)00086-0

Molecular Immunology, Vol. 32, No. 14/15, pp. 1057–1064, 1995

0161-5890/95 $9.50 + 0.00

SPECIFICITY OF MONOCLONAL ANTIBODIES PRODUCED AGAINST PHOSPHOROTHIOATE AND RIBO MODIFIED DNAs

LAURA J. P. LATIMER, YEHENEW M. AGAZIE, RALPH P. BRAUN, KEN J. HAMPEL and JEREMY S. LEE*

Department of Biochemistry, University of Saskatchewan, Saskatoon, Saskatchewan, S7N OWO Canada

(*First received* 26 *January* 1995; *accepted in revised form* 23 *May* 1995)

Abstract—A large number of phosphorothioate DNAs and mixed ribo/deoxyribo duplexes were prepared and their immunogenicity was studied in mice. Only those polymers which were nuclease-resistant were immunogenic and in these cases monoclonal antibodies were prepared. The specificity of the antibodies was measured by direct and competitive Solid Phase Radioimmune Assay (SPRIA) and on this basis four types of antibody could be identified. Type I antibodies are specific for the immunizing polymer and show very limited crossreactivity. For example, Jel 384 binds only to poly(dsA)·poly(dT); Jel 453 and 462 bind only to poly(dsG)·poly(dC)and poly(dsG)·poly(dm^{5}C). Type II antibodies bind to most polymers containing the appropriate modification but will not bind to unmodified DNAs. For example, Jel 343 binds to most thio DNAs regardless of sequence; Jel 346 binds well to most ribose-containing polymers and may be a useful reagent for the detection of the 'A' family of conformations. Type III antibodies bind to most nucleic acids whether modified or not. Their specificities are similar to autoimmune antibodies. Type IV antibodies are single strand-specific such as Jel 383 which binds to poly(dT). There were no examples of antibodies which bound specifically to the immunizing DNA and the unmodified polymer. Thus, modified DNAs cannot be used to prepare sequence-specific reagents. Also, the immunogenicity of modified nucleic acids may limit their usefulness in antisense technologies.

Key words: DNA-binding antibodies, immunogenicity, nuclease resistance.

INTRODUCTION

Nucleic acids with backbone modifications are widely used as antisense oligonucleotides (Wagner, 1994). This technology is a general method for influencing gene expression or viral replication by adding exogenous oligonucleotides which bind to a target sequence (Maher, 1992). For therapeutic applications the antisense oligonucleotide must be capable of penetrating the plasma membrane as well as being resistant to nucleases. Since most naturally-occurring DNA and RNA is rapidly degraded by intra-and extracellular nucleases, it is not suitable for antisense therapy (Eckstein, 1985). For this reason oligonucleotides have been prepared with backbone modifications which render them nuclease-resistant. These modifications include α-nucleotides, methyl phosphonates, peptide linkages and phosphorothioate (POS) groups (Gish and Eckstein, 1989; Nielsen *et al.*, 1991; Cros *et al.*, 1994; Xodo *et al.*, 1994). However, unlike DNA and RNA, modified nucleic acids are immunogenic, probably for the very reason that they are nuclease-resistant and thus survive long enough to be recognized by the immune system (Braun and Lee, 1988). Therefore, lack of immunogenicity may have to be sacrificed to achieve nuclease resistance.

A second reason for studying the immunology of modified nucleic acids is that the resultant antibodies may cross react with the unmodified form. In this way, sequence and structure-specific reagents could be prepared against antigens which are not normally immunogenic. For example, antibodies to Z DNA, triplexes or DNA/RNA hybrids have proved to be very useful for the detection and analysis of these unusual structures but, in general, sequence-specific antibodies are not available (Anderson *et al.*, 1988; Stollar, 1991; Stollar, 1994). Previously, we prepared a series of POS DNAs and mixed ribo/deoxyribo duplexes (Latimer *et al.*, 1989; Braun and Lee, 1988). Some of these modified nucleic acids, particularly those with high GC content, were nuclease-resistant and immunogenic. Also, serum antibodies from mice immunized with poly[d(GsC)], for example, showed some binding to the unmodified poly[d(GC)]. Thus, by immunizing with poly[d(GsC)] it might be possible to prepare monoclonal antibodies which bound only to poly[d(GsC)] and poly[d(GC)].

For these reasons, mice have been immunized with a large number of POS DNAs and mixed ribo/deoxyribo duplexes. In those cases where the polymers were immu-

*Author to whom correspondence should be addressed.

nogenic, monoclonal antibodies were developed and their specificities were analysed in detail.

MATERIALS AND METHODS

Nucleic acids

All homopolymer single-stranded nucleic acids, poly[d(GC)], poly(rG)·poly(dC) and poly[d(IC)], were purchased from Pharmacia (Baie d'Urbé, Québec). Calf thymus (CT) DNA was purchased from Sigma (St. Louis, MO) and rRNA was obtained from Boehringer Mannheim (Laval, Québec). Poly(rI)·poly(rC), poly(rI)·poly(dC) and poly(rA)·poly(dT) were generated by mixing equimolar amounts of the appropriate single-stranded molecules in T/E buffer (10 mM Tris-HCl, 0.1 mM EDTA, pH 8.0) and 100 mM NaCl and heating at 60 C for 15 min. The remainder of the nucleic acids were synthesized in reactions with a polymerase, a template and the appropriate nucleoside triphosphates (Evans *et al.*, 1982). Synthesis was followed by an ethidium bromide fluorescence assay (Morgan *et al.*, 1979). Duplex DNAs containing phosphorothioate groups were generated in a potassium phosphate buffer system (pH 7.2) with *E. coli* DNA polymerase and the appropriate modified nucleoside triphosphates (Pharmacia). Poly(rGdC), poly(rGdm^{5}C) and poly(rGdsC) were generated in a bicine buffer system at pH 8.9 with *E. coli* DNA polymerase (Jayasena and Behe, 1987), whereas poly(dArU), poly(rAdT), poly(dGrC), poly[r(GC)], poly[r(AU)] and poly[r(IC)] were synthesized in the pH 8.9 buffer system with *E. coli* RNA polymerase (Hall *et al.*, 1985). All of the resultant nucleic acids were purified and characterized by their melting temperature and by fluorescence upon binding of ethidium bromide (Evans *et al.*, 1982). Concentrations were calculated from absorbance measurements at 260 nm assuming an extinction coefficient of 6600 M^{-1} except for poly(rGdC) and analogues (7440 M^{-1}) (Hardin *et al.*, 1987).

Hybridomas

The immunization of the C57 Bl/6 mice and analysis of the serum antibodies have been described elsewhere (Braun and Lee, 1988). Spleen cells from immunized mice were fused with the myeloma cell line, MOPC 315.43 and the positive hybridomas were identified by SPRIA and cloned by limiting dilution (Lee *et al.*, 1982, 1985).

Solid phase radioimmune assay (SPRIA)

The procedure for the SPRIA has been described previously (Lee *et al.*, 1982, 1985). Briefly, either polyvinyl chloride (PVC) or polystyrene (Dynatech Labs, Chantilly, VA) wells were coated with the desired nucleic acid by incubating 50 μl of a 2 μg/ml sample in phosphate buffered saline (PBS, 207 mM KCl, 137 mM NaCl, 10 mM Na_2HPO_4, 1.4 mM KH_2PO_4, pH 7.2) overnight at 4°C. In some cases the wells were precoated with poly-L-lysine also by incubating 50 μl of a 2 μg/ml sample in PBS at 4°C. Precoating the plates was found to be essential for the detection of significant binding to poly(rGdm^{5}C), poly(rGdsC) and poly[r(GC)]. The reason for this is unclear, especially since detection of antibody binding to poly(rGdC) occurs readily without precoating with poly-L-lysine. To perform the assay, the wells were washed three times with PBS and 0.5% Tween 20, the antibody sample (see below) was added and incubated 1–3 hr at room temperature. The wells were washed as above and 50 μl of labelled second antibody (sheep ^{125}I-labelled anti-mouse IgG (Amersham, Oakville, Ontario) were added (50,000 cpm/well). After incubating for 2 hr at room temperature, the wells were washed as above and counted in a LKB 1271 RIAGAMMA gamma counter. The resultant cpm was a measure of the ability of the original antibody solution to bind to the nucleic acid immobilized on the wells. In all cases the background was less than 200 cpm.

Competitive SPRIA were used to obtain an accurate description of the specificities of some of the antibodies. In these experiments, a "competitor" nucleic acid is added in solution before the addition of the MoAb (Latimer *et al.*, 1989; Braun and Lee, 1988).

The antibodies were derived either from mouse serum or hybridoma supernatants and diluted in PBS. For specificity tests, the hybridoma supernatant was first titred against the immunogen to determine the highest dilution which gave maximum counts. This dilution was then used in all subsequent direct or competitive SPRIA.

RESULTS

Immunogenicity

Not all modified polymers could be produced in sufficient quantities for detailed studies. For example, DNAs such as poly[d(sTsG)]·poly[d(sCsA)] in which every residue is phosphorothioate, replicated very slowly and yields were poor. One family in which all thio polymers could be produced in good yields was poly[d(AT)]. After injecting C57/bl mice three times, serum antibodies were measured by SPRIA after serial two-fold dilutions (Fig. 1). Poly[d(sAsT)] gave a good immune response

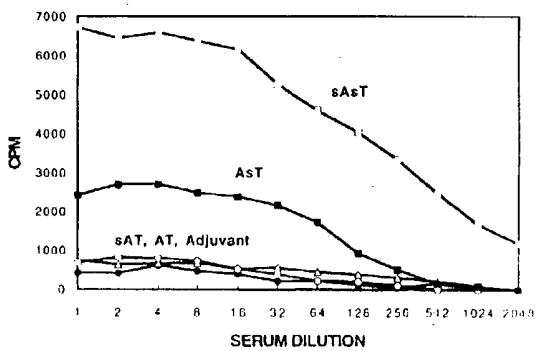

Fig. 1. Immunogenicity of poly[d(AT)] and phosphorothioate derivatives. After three injections, serum was collected and the amount of binding to the immunizing DNA was measured by SPRIA. □, poly[d(sAsT)]; ■, poly[d(AsT)]; ○, poly[d(sAsT)]; △, poly[d(sAsT)]; ●, adjuvant alone.

with a titre of 2^8 (defined as the dilution at which the cpm was half maximum). The response to poly[d(AsT)] was much weaker with a titre of 2^6, whereas poly[d(sAT)] and poly[d(AT)] were not immunogenic since the cpm was not significantly different from that of adjuvant alone. The response of BALB/c mice injected with these polymers gave the same pattern (data not shown). In contrast, it was shown previously that all thio members of the poly[d(GC)] family were immunogenic (Braun and Lee, 1988).

Poly[dTsC)]·poly[d(sGA)], poly[d(sTG)]·poly[d(sCA)] and poly[d(TC)]·poly[d(GrA)] poly[d(TG)]·poly[d(CrA)] were all tested and found to be non-immunogenic. Further experiments were concentrated on simple homopolymers which in general were easier to replicate. In addition, it seemed likely that polymers with the fewest modifications were more likely to produce antibodies which would crossreact with the unmodified nucleic acid. All the nucleic acids described below were immunogenic and at least one monoclonal antibody was recovered in each case.

Poly[d(AsT)] and poly(dsA)·poly(dT)

Two monoclonal antibodies, Jel 371 and 372, were recovered from a BALB/c immunized with poly[d(AsT)]. As judged from SPRIA (see Table 1), both antibodies bind to thio DNAs but also to poly[d(AT)], calf thymus and heat-denatured calf thymus DNA. Therefore, they are neither structure- nor sequence-specific. Although competition experiments were attempted, no inhibition of binding was observed even at the highest concentrations of DNA which were available (about 300 μM) (see Discussion).

Three types of antibodies were prepared from several fusions with mice immunized with poly(dsA)·poly(dT). As shown in Table 2, Jel 383 will only bind to DNAs containing poly(dT) and thus this single-stranded DNA presumably forms the epitope. Since the Tm of poly (dsA)·poly(dT) is lower than most duplexes, it is expected to melt easily exposing the single strands (Latimer *et al.*, 1989). This would account for the binding of Jel 383 to poly(dsA)·poly(dT) during the SPRIA and also explain how a duplex DNA can give rise to a single strand-specific antibody. The second type of antibody is exemplified by Jel 384 which binds to poly(dsA)·poly(dT) but not the unmodified duplex or poly(dT). It is therefore specific for the immunizing DNA. On the other hand, Jel 385 shows little preference and binds to duplexes, thio and single-stranded DNAs.

Table 1. Direct SPRIA for antibodies from mice immunized with poly(d[AsT)]

	% Maximum binding	
Nucleic acid	Jel 371	Jel 372
Poly[d(AT)]	22	34
Poly[d(sAT)]	91	43
Poly[d(AsT)]	78	62
Poly[d(sAsT)]	100	100
Calf thymus DNA	36	19
hd calf thymus	21	32

Table 2. Direct SPRIA for antibodies from mice immunized with poly(dsA)·poly(dT)

	% Maximum binding		
Nucleic acid	Jel 383	Jel 384	Jel 385
Poly(dsA)·poly(dT)	100	100	100
Poly(dA)·poly(dsT)	< 10	< 10	42
Poly(dA)·poly(dT)	79	< 10	81
Poly(dT)	84	< 10	63
Calf thymus DNA	< 10	< 10	44
thd calf thymus	< 10	< 10	46

Poly(rGdC) and poly[r(GC)]

Both of these ribose modified polymers are immunogenic and it was shown previously that mice immunized with poly(rGdC) produced serum antibodies that crossreacted with poly[d(GC)] (Braun and Lee, 1988). Two monoclonal antibodies, Jel 332 and 334, were produced against poly(rGdC) and one, Jel 346 against poly[r(GC)]. Direct SPRIA (see Table 3) shows that Jel 332 only binds to the immunogen and poly(rGdm^{5}C) and poly(rGdsC). Jel 334 also shows weak binding to poly[r(GC)] and poly[r(AU)], but in both cases, the highest counts are to the thio substituted poly(rGdsC). On the other hand, Jel 346 binds to all ribose-containing polymers.

Because these antibodies appeared to have considerable specificity, relative binding constants were esti-

Table 3. Direct SPRIA for antibodies from mice immunized with poly(rGdC) and poly[r(GC)]

	% Maximum binding		
Nucleic acid	Jel 332	Jel 334	Jel 346
Poly[d(GC)]	< 10	< 10	< 10
Poly[d(IC)]	< 10	< 10	< 10
Poly(rGdC)	86	96	100
Poly(rGdm^{5}C)	32	83	61
Poly(rGdsC)	100	100	25
Poly(dGrC)	< 10	< 10	< 10
Poly[r(GC)]	< 10	14	88
Poly[r(AU)]	< 10	19	76
Poly[r(IC)]	< 10	< 10	33
Poly(rI)·poly(rC)	< 10	< 10	77
Poly(rG)·poly(dC)	< 10	< 10	89
Poly(rI)·poly(dC)	< 10	< 10	78
Poly(rA)·poly(dT)	< 10	< 10	32
rRNA	< 10	< 10	11
Calf thymus DNA	< 10	< 10	< 10
hd calf thymus DNA	< 10	< 10	< 10

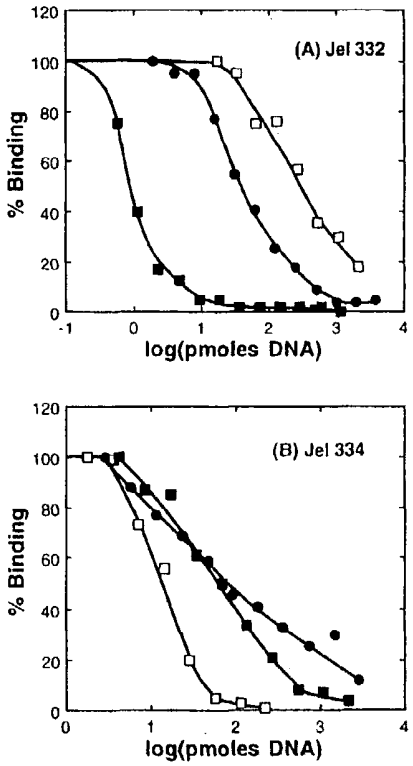

Fig. 2. Competitive SPRIA for (A) Jel 332 and (B) Jel 334. The level of binding was measured as a function of the amount of nucleic acid added as a competitor. The concentration of competitor required to reach 50% binding is inversely proportional to the binding constant. The plate was coated with poly(rGdC) and the competitors were: •, poly(rGdC); □, poly(rGdm^{5}C); ■, poly(rGdsC).

mated from competition experiments (Figs 2 and 3). The concentration of competitor required to reach 50% binding is inversely proportional to the binding constant. As can be seen in Fig. 2 for Jel 332, about 50-fold less poly(rGdsC) is required to give the same competion as poly(rGdC). Jel 334 on the other hand, had a binding constant six-fold higher to poly(rGdm^{5}C) than the immu-

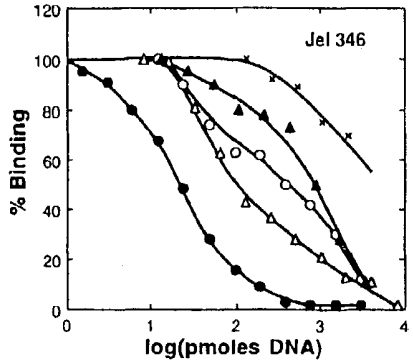

Fig. 3. Competitive SPRIA for Jel 346. The plate was coated with poly[r(GC)] and the competitors were: △, poly[r(GC)]; •, poly(rG)·poly(dC); ○, poly(rGdC); ▲, poly[r(AU)]; ×, poly(rGdsC). For clarity, not all the competitors are shown but the relative binding constants are listed in Table 4.

Table 4. Relative binding constants estimated from competitive SPRIA

	Relative binding constant		
Nucleic acid	Jel 332	Jel 334	Jel 346
Poly[d(GC)]	nc [a]	nc	nc
Poly[d(IC)]	nc	nc	nc
Poly(rGdC)	1.0	1.0	0.22
Poly(rGdm^{5}C)	0.12	5.8	0.02
Poly(rGdsC)	50	1.3	0.02
Poly[r(GC)]	nc	nc	1.0
Poly[r(AU)]	nc	nc	0.13
Poly[r(IC)]	nc	nc	nc
Poly(rI)·poly(rC)	nc	nc	1.0
Poly(rG)·poly(dC)	nc	nc	5.8
Poly(rI)·poly(dC)	nc	nc	5.2
rRNA	nc	nc	nc

[a] nc, no competition was observed at the highest concentration tested. Therefore, the relative binding constant is <0.001.

nizing polymer and thio substitution had little effect. The relative binding constants are summarized in Table 4 which also includes those for Jel 346. As shown in Fig. 3, Jel 346 has a wider range of specificity but was only competed weakly with by poly(rGdsC); rRNA and poly [r(IC)] to which binding could be detected by direct SPRIA were ineffective as competitors. It can be estimated that the binding constant to these polymers must be at least 1000-fold lower than to poly(rGdC). Thus, one problem with direct SPRIA is that the apparent level of binding is influenced by the amount of polymer bound to the PVC plate and even very weak binding may still be detected.

Poly[d(sGC)] and poly[d(GsC)]

As described previously, both these thio DNAs are strongly immunogenic (Braun and Lee, 1988). A total of eight monoclonal antibodies were produced from poly[d(sGC)] and as judged by SPRIA none of them bound to poly[d(GC)].Two of these were chosen for further study; Jel 339 because it showed weak but consistent binding to poly[d(IC)] and calf thymus DNA and Jel 343 because it bound to heat-denatured calf thymus DNA and single-stranded poly(dC) and poly(dG) (see Table 5). In general, however, both Jel 339 and 343 bound well to thio DNAs and not the unmodified forms.

Relative binding constants were measured by competitive SPRIA (Table 6). Jel 339 binds well to the immunogen, poly[d(sGC)] and poly[d(sGsC)], but not to poly[d(GsC)]. The binding constant to poly[d(sAT)] is about 12-fold lower, whereas binding to the isomer poly-[d(AsT)] could not be detected. There was no detectable competition with the unmodified duplexes poly[d(GC)] and poly[d(IC)] and the binding constant to these polymers must be at least 1000-fold lower than to poly[d(sGC)]. Thus, Jel 339 prefers a phosphorothioate 5′ to a purine with a preference for guanine. On the other

Table 5. Direct SPRIA for antibodies from mice immunized with poly[d(sGC)] and poly[d(GsC)]

Nucleic acid	% Maximum binding		
	Jel 339	Jel 343	Jel 347
Poly[d(GC)]	< 10	< 10	< 10
Poly[d(IC)]	15	< 10	< 10
Poly(dG)·poly(dC)	< 10	< 10	< 10
Poly[d(sGC)]	91	55	27
Poly[d(GsC)]	35	79	100
Poly[d(sGsC)]	100	100	64
Poly[d(AT)]	< 10	< 10	< 10
Poly[d(sAT)]	37	36	47
Poly[d(AsT)]	20	65	41
Poly[d(sAsT)]	29	81	66
Poly(dC)	20	60	84
Poly(rG)	23	79	84
Poly(dT)	< 10	< 10	60
Calf thymus DNA	12	< 10	< 10
hd calf thymus DNA	< 10	16	< 10

hand, Jel 343 is competed for by all thio DNAs and does not distinguish between a phosphorothioate 5′ to a purine or 5′ to a pyrimidine. A double substitution is preferred since both poly[d(sGsC)] and poly[d(sAsT)] have the highest binding constants. Jel 343 will also bind to poly(rGdsC) but not the unmodified duplexes.

Jel 347, produced from poly[d(GsC)], showed the highest binding to the immunogen but also bound to a variety of DNAs and RNAs as well as poly(dT) (see Table 5). Preliminary competition experiments (data not shown) demonstrated good binding to poly(dT) and other single-stranded DNAs so this antibody was not investigated further. The origin of such antibodies will be discussed below.

Table 6. Relative binding constants for antibodies from mice immunized with poly[d(sGC)]

Nucleic acid	Relative binding constant	
	Jel 339	Jel 343
Poly[d(GC)]	nc [a]	nc
Poly[d(IC)]	nc	nc
Poly[d(sGC)]	1.0	1.0
Poly[d(GsC)]	nc	1.2
Poly[d(sGsC)]	1.2	2.3
Poly(rGdsC)	nc	0.16
Poly[d(AT)]	nc	nc
Poly[d(sAT)]	0.08	0.51
Poly[d(AsT)]	nc	0.30
Poly[d(sAsT)]	nc	1.4
Poly(dC)	nc	nc
Poly(rG)	nc	nc
Poly(dT)	nc	nc
Calf thymus DNA	nc	nc
hd calf thymus DNA	nc	nc

[a] nc, no competition was observed at the highest concentration tested. Therefore, the relative binding constant is <0.001.

Poly(dsG)·poly(dC), poly(dsG)·poly(dm^{5}C), poly(dG)·poly(dm^{5}C) and poly[d(Tm^{5}C)]·poly[d(sGsA)].

These DNAs were of additional interest because they can dismutate to triplexes which are stable under physiological conditions (Latimer *et al.*, 1989). poly(dG)-poly(dm^{5}C) was also included because even though it lacks a backbone modification it was shown previously to be immunogenic (Lee *et al.*, 1984). Several antibodies were recovered from fusions with poly(dsG)·poly(dC) which had specificities exemplified by Jel 375 and Jel 453 (see Table 7). Both antibodies show very restricted binding; Jel 453 will also bind poly(dsG)·poly(dm^{5}C) while Jel 375 recognises poly(dG)·poly(dC). This apparently represents the first example of an antibody produced with a thio DNA which also bound specifically to the unmodified form. Competition experiments, however, were disappointing (Fig. 4). Whereas poly (dsG)·poly(dC) competes well, no competition could be detected with poly(dG)·poly(dC). Thus the binding constant to poly(dG)·poly(dC) is at least three orders of magnitude less than to the thio DNA.

Two types of antibody were produced after immunizing with poly(dsG)·poly(dm^{5}C). By direct SPRIA, Jel 414 bound to all the DNAs tested and thus was non-specific. On the other hand, Jel 462 will only bind to a thio DNA within the context of a homopolymer G and C sequence. By comparison, Jel 458 is representative of three antibodies with similar specificities produced from mice immunized with unmodified poly(dG)·poly(dm^{5}C). In contrast to Jel 462, Jel 458 binds to all members of the poly(dG)·poly(dC) family whether modified or not. In this case, the m^{5}C appears to be a more important determinant than the thio modification. This was confirmed by competition experiments, and the relative binding constants are shown in Table 7 (in square brackets). Thus, Jel 458 has a specificity similar to Jel 68 which was described previously (Lee *et al.*, 1984)

Finally, poly[d(Tm^{5}C)]·poly[d(sGsA)] was highly immunogenic and three monoclonal antibodies were produced from one fusion (see Table 8). Both Jel 424 and 425 bind only to thio DNA but within this group there are considerable sequence preferences. Since there is detectable interaction with poly[d(sTG)]·poly[d(sCA)] and poly[d(sAsT)] (which cannot form a triplex) but not with poly[d(Tm^{5}C)]·poly[d(GA)], it is apparent that the antibodies are not recognizing a triplex conformation. In contrast, Jel 426 has a preference for single-stranded poly[d(Tm^{5}C)] with some binding to poly(dC) and heat-denatured calf thymus DNA. Presumably, the immunogen poly[d(Tm^{5}C)]·poly[d(sGsA)] upon dismutating to a triplex produces single-stranded regions which produces a corresponding immune response.

DISCUSSION

It was proposed previously that immunogenic nucleic acids were nuclease-resistant (Braun and Lee, 1988). The

Table 7. Direct SPRIA for antibodies derived from poly(dsG)·poly(dC) and analogues

Nucleic acid	% Maximum binding				
	Jel 375	Jel 453	Jel 414	Jel 462	Jel 458
Poly(dsG)·poly(dC)	100	100	56	77	45 [0.2] [a]
Poly(dsG)·poly(dm^{5}C)	< 10	70	100	100	70 [1]
Poly(dG)·poly(dm^{5}C)	< 10	< 10	25	< 10	100 [0.8]
Poly(dG)·poly(dC)	48	< 10	19	< 10	77 [0.01]
Poly[d(sGC)]	< 10	< 10	71	< 10	< 10
Poly[d(GsC)]	< 10	< 10	66	< 10	< 10
Poly(dC)	< 10	< 10	55	< 10	< 10
Poly(dT)	< 10	< 10	40	< 10	< 10
Poly[d(Tm^{5}C)]·poly[d(GA)]	< 10	< 10	49	< 10	< 10
Calf thymus DNA	< 10	< 10	77	< 10	< 10
hd calf thymus DNA	< 10	< 10	57	< 10	< 10

[a] The relative binding constants for Jel 458 are shown in square brackets.

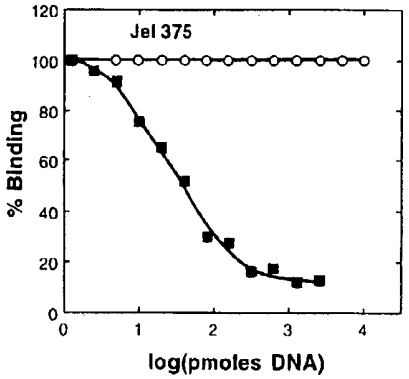

Fig. 4. Competitive SPRIA for Jel 375. The plate was coated with poly(dG)·poly(dC) and the competitors were: ○, poly(dG)·poly(dC); ■, poly(dsG)·poly(dC).

results described above support this conclusion. Poly [d(sAsT)] is completely resistant to DNase I, and poly [d(AsT)] is partially resistant, whereas poly[d(sAT)] is rapidly degraded (Latimer *et al.*, 1989). As shown in Fig. 1, there is a perfect correspondence between the degree of immunogenicity and the level of nuclease resistance. Also, poly[dTsC)]·poly[d(sGA)], poly[d(sTG)]·poly [d(sCA)], poly[d(TC)] poly[d(GrA)] and poly[d(TG)]·poly [d(CrA)] are all nuclease-sensitive (data not shown) and non-immunogenic. The apparent tolerance of animals to unmodified duplex DNA may, therefore, simply be due to rapid breakdown of the antigen.

The monoclonal antibodies produced from the immunogenic nucleic acids can be assigned to four different categories. The first type is specific for the antigen and shows limited crossreactivity. For example, Jel 384 is specific for poly(dsA)·poly(dT), Jel 453 and 462 for

Table 8. Direct SPRIA for antibodies from mice immunized with poly[d(Tm^{5}C)]·poly[d(sGsA)]

Nucleic acid	% Maximum binding		
	Jel 424	Jel 425	Jel 426
Poly[d(Tm^{5}C)]·poly[d(sGsA)]	100	60	59
Poly[d(Tm^{5}C)]·poly[d(GA)]	< 10	< 10	< 10
Poly[d(TC)]·poly[d(sGsA)]	45	31	< 10
Poly[d(TC)]·poly[d(GA)]	< 10	< 10	< 10
Poly[d(TsG)]·poly[d(CA)]	14	< 10	< 10
Poly[d(sTG)]·poly[d(sCA)]	25	7	< 10
Poly[d(Tm^{5}C)]	< 10	< 10	100
Poly(dC)	< 10	< 10	39
Poly(dT)	< 10	< 10	< 10
Poly(dsG)·poly(dC)	16	< 10	< 10
Poly(dsG)·poly(dm^{5}C)	18	< 10	< 10
Poly(dsA)·poly(dT)	82	40	< 10
Poly(dA)·poly(dT)	< 10	< 10	< 10
Poly[d(sAsT)]	43	100	< 10
Calf thymus DNA	< 10	< 10	< 10
hd calf thymus DNA	< 10	< 10	62

poly(dsG)·poly(dC) and poly(dsG)·poly(dm^{5}C), and Jel 332 and 334 for poly(rGdC) and related family members. It is interesting that neither Jel 332 nor 334 will bind to poly(dGrC). This can be explained by the fact that mixed polymers can adopt a number of unique conformations depending on whether the purine or pyrimidine is 5′ to the ribose or deoxyribose (Hung *et al.*, 1994). Also included in this group would be Jel 339 which requires a purine 5′ to a phosphorothioate. In general, these antibodies must recognize sequence and/or conformation.

The second type binds to most modified duplexes but will not bind to unmodified nucleic acids. For example, Jel 343 binds to many thio DNAs regardless of whether the phosphorothioate is 5′ to a purine or pyrimidine. Similarly, Jel 424 binds to thio DNAs containing alternating pyrimidine/purine as well as homopolymer pyrimidine·purine sequences. Jel 346 binds well to most ribose-containing polymers and, therefore, may be a useful reagent for the detection of the 'A' family of conformations.

In the third category must be included those antibodies which bind to most nucleic acids whether modified or not. This includes Jel 371, 372, 385 and 414. Since they recognize neither structure nor sequence, they must bind nucleic acids through ionic interactions with the phosphodiester backbone. From this point of view they are reminiscent of many autoimmune antibodies which also tend to show little specificity (Stollar, 1991, 1994).

The fourth type is single strand-specific and is exemplified by Jel 383 which is poly(dT) specific and Jel 426 which binds to poly(dTm^{5}C). As mentioned above, they may arise from melting or dismutation of the duplex to single strands. Similarly, immunization with poly(dI)·poly(dC) gave rise to poly(dI)-specific and poly(dC)-specific antibodies but not to duplex specific antibodies (Braun *et al.*, 1986). On the other hand, antibodies which bind to poly(dT) are a major component of autoimmune serum and low levels are found in unimmunized mice (Stollar *et al.*, 1962; Sibley *et al.*, 1986 and unpublished observations). Thus, this type of antibody may not necessarily arise from stimulation by the immunogen. For example, Jel 347 was produced from a mouse which apparently had been immunized with poly[d(sGC)] yet it bound well to poly(dT). Again these antibodies appear to be closely related to those found in autoimmune diseases.

The fifth type of antibody, namely one which was sequence-specific and bound to the unmodified form, was not found. Jel 375 was tantalizing because it bound to both poly(dsG)·poly(dC) and poly(dG)·poly(dC) by direct SPRIA but was competed against only by poly(dsG)·poly(dC). This result shows quite clearly that the direct SPRIA is exquisitely sensitive and can detect very weak binding. Since antibody/DNA binding is likely to be dominated by ionic interactions with the phosphodiester backbone, weak or non-specific binding to related structures may be inevitable. Alternatively, poly(dG)·poly(dC) may adopt a different conformation when bound to the PVC plate and it is to this conformation that Jel 375 binds well. Changes in nucleic acid conformation may also explain why no competition was observed for other antibodies such as Jel 371 and 372 (Table 1) for which binding could be detected by direct SPRIA. At present, there is no suitable technique to investigate this phenomenon.

An antibody which bound to the unmodified polymer was anticipated because serum antibodies from mice immunized with a modified DNA bound to the unmodified form (Braun and Lee, 1988). There are several possible reasons for the failure to produce this type of monoclonal antibody. First, the serum could contain antibodies like Jel 375 which binds very weakly to the unmodified DNA. Second, the serum could contain antibodies like type III above which show little overall specificity. Finally, the antibodies we were seeking may be a very small subset of the immune response and thus by chance none was detected. Since more than 50 monoclonal antibodies were investigated in this study, their frequency must be very low. Overall it is clear that immunization with modified DNAs is not a viable method for the production of sequence specific antibodies which crossreact with the unmodified form.

The type I and II antibodies which only bind to thio DNAs are of considerable interest because it is not clear how this degree of specificity is achieved. Positive recognition of a POS compared to a PO_2 group is difficult to envisage because the charge density is expected to be similar, i.e. $^{1/2-}O\text{–}P\text{–}S^{1/2-}$ (Suggs and Taylor, 1985; Frey and Sammons, 1985). Also, the Van der Waals radius of S is 1.85 Å compared to 1.40 Å for O (Cotton and Wilkinson, 1966). Therefore, a pocket in the antibody which can fit a POS should also be able to accept a PO_2 group. On this basis, it seems likely that the specificity for thio DNAs is based on conformational changes in the sugar–phosphorothioate backbone. On the other hand, autoimmune antibodies bind well to thio DNAs; for example, Jel 242 shows little preference for poly[d(GC)] compared to poly[d(sGsC)] and Jel 241 cannot distinguish between poly[d(AT)] and poly[d(sAsT)] (Braun and Lee, 1988; Latimer *et al.*, 1989). Others produced by immunization such as Jel 332, 334 and 458, described above, even appear to prefer thio DNAs. For example, Jel 332 raised against poly(rGdC) binds 53-fold better to poly(rGdsC) than the immunizing polymer. Thus in these cases, even though there are some changes in binding constant, the POS is not excluded from the PO_2-binding site. A better understanding of this puzzling molecular recognition will have to await structural studies on a thio-specific antibody.

From the perspective of antisense oligonucleotides, the implication is clear; the longer the lifetime of an oligonucleotide in serum, the more likely it is to produce an immune response. Also, the antibodies which are produced will be of several types. Types I and II will bind to the oligonucleotide, reducing its effective concentration. Types III and IV may crossreact with unmodified DNA and behave like autoimmune antibodies. These problems may seriously limit the therapeutic usefulness of antisense technology.

Acknowledgement –Supported by MRC Canada by grants to J.S.L.

REFERENCES

Anderson W. F., Cygler M., Braun R. P. and Lee J. S. (1988) Antibodies to DNA. *BioEssays* **8,** 69–74.

Braun R. P. and Lee J. S. (1988) Immunogenic nucleic acids are nuclease resistant. *J. Immun.* **141,** 2084–2089.

Braun R. P., Woodsworth M. L. and Lee J. S. (1986) The immunogenic properties of poly(dI)·poly(dC) and poly(rI)·poly(dC). Analysis of monoclonal antibodies. *Molec. Immun.* **23,** 685–691.

Cotton F. A. and Wilkinson G. (1966) In *Advanced Inorganic Chemistry*. Interscience, John Wiley and Sons, New York.

Cros P., Kurfurst R., Allibert P., Battail N., Piga N., Roig V., Thuong N. T., Mandrand B. and Helene C. (1994) Monoclonal antibodies targeted to α-oligonucleotides. Characterization and application in nucleic acid detection. *Nucleic Acids Res.* **22,** 2951–2957.

Eckstein F. (1985) Nucleoside phosphorothioates. *A. Rev. Biochem.* **54,** 367–402.

Evans D. H., Lee J. S., Morgan A. R. and Olsen R. K. (1982) A method for the sequence specific inhibition of poly[d(AT)] synthesis using the AT-specific quinoxaline antibiotic TANDEM. *Can. J. Biochem.* **60,** 131–136.

Frey P. and Sammons R. D. (1985) Bond order and charge localization in nucleoside phosphorothioates. *Science* **228,** 541–545.

Gish G. and Eckstein F. (1989) Phosphorothioates in molecular biology. *Trends Biochem. Sci.* **14,** 97–100.

Hall K., Cruz P. and Chamberlin M. J. (1985) Extensive synthesis of poly[r(GC)] using *E. coli* RNA polymerase. *Arch. Biochem. Biophys.* **236,** 47–51.

Hardin C. C., Zarling D. A., Ruglisi J. D., Frulson M. O., Davis P. W. and Tinoco I. (1987) Stabilization of Z-RNA and its recognition by anti Z-DNA antibodies. *Biochemistry* **26,** 5191–5199.

Hung S.-H., Yu Q., Gray D. M. and Ratliff R. L. (1994) Evidence from CD spectra that d(purine)·r(pyrimidine) and r(purine)·d(pyrimidine) are in different structural classes. *Nucleic Acids Res.* **22,** 4326–4334.

Jayasena S. D. and Behe M. J. (1987) Influence of tetraalkyl ammonium ions on the structure of poly(rGdC). *Nucleic Acids Res.* **15,** 3907–3916.

Latimer L. J. P., Hampel K. J. and Lee J. S. (1989) Synthetic repeating sequence DNAs containing phosphorothioates: nuclease senstivity and triplex formation. *Nucleic Acids Res.* **17,** 1549–1561.

Lee J. S., Dombroski D. F. and Mosmann T. R. (1982) Specificity of monoclonal Fab fragments binding to single-stranded DNA. *Biochemistry* **21,** 4940–4950.

Lee J. S., Latimer L. J. P. and Woodsworth M. L. (1985) A monoclonal antibody specific for the duplex DNA poly[d(TC)] poly[d(GA)]. *FEBS Lett.* **190,** 120–124.

Lee J. S., Woodsworth M. L. and Latimer L. J. P. (1984) Monoclonal antibodies specific for poly(dG)·poly(dC) and poly(dG)·poly(dm^{5}C). *Biochemistry* **23,** 3277–3281.

Maher L. J. (1992) DNA triple helix formation: an approach to artificaial gene repressors. *BioEssays* **14,** 807–815.

Morgan A. R., Lee J. S., Pulleyblank D. E., Murray N. L. and Evans D. H. (1979) Ethidium fluorescence assays, Part I. *Nucleic Acids Res.* **7,** 547–570.

Nielsen P. E., Egholm M., Berg R. H. and Buchardt O. (1991) Sequence-specific recognition of DNA by strand displacement with a thymine-substituted polyamide. *Science* **254,** 1497–1500.

Sibley J. T., Braun R. P. and Lee J. S. (1986) The production of antibodies to DNA in normal mice following immunization with poly(ADP-ribose). *Clin. exp. Immun.* **64,** 563–569.

Stollar B. D. (1991) Autoantibodies and autoantigens: a conserved system that may shape a primary immunoglobulin gene pool. *Molec. Immun.* **28,** 1399–1412.

Stollar B. D. (1994) Molecular analysis of anti-DNA antibodies. *FASEB J.* **8,** 337–342.

Stollar B. D., Levine L., Lehre H. I. and Van Vunakis H. (1962) Antibodies to denatured DNA in lupus erythematosus serum. *Proc. natn. Acad. Sci. U.S.A.* **48,** 874–880.

Suggs J. W. and Taylor D. A. (1985) Evidence for sequence specific conformational changes in DNA from the melting temperatures of DNA phosphorothioate derivatives. *Nucleic Acids Res.* **13,** 5707–5716.

Wagner R. W. (1994) Gene inhibition using antisense oligodeoxynucleotides. *Nature* **372,** 333–335.

Xodo L., Alunni-Fabroni M., Manzini G. and Quadrifoglio F. (1994) Pyrimidine phosphorothioate oligonucleotides form triple-stranded helices and promote transcription inhibition. *Nucleic Acids Res.* **22,** 3322–3330.

Nat. Gent. 1992 1:372-378
Science 1989 245:1234-1236

Eur. J Biochem. 1985 148:265-270

Mol. Immunol 1995 32:1057-1064

Science 1993 259:988-990

Nature 1988 336:348-352

J Clin. Invest. 1993 91:225-234

Mol. Cell. Biol. 1987 7:1576-1579

Gene 1982 19:33-42

Neuron 1992 8:507-520

Adv. Virus Res. 1989 37:35-83

1994 Cancer Res. 54:5258-5261

Cell 1987 50:435-443

Nucleic Acids Res. (1996) 24(10):1841-1848

J Biol. Chem. 1988 263 10 :4837-4843

Proc. Natl. Acad. Sci. USA 1992 89:2581-2584

1993 Nature 361:647-650

DNA Seq. 1993 4:185-196

Human Gene Ther. 1995 6:881-893

Science 1991 252:431-434

Cell 1992 68:143-155

Mol. Cell. Biol. 1990 10 6 :2738-2748

Nucleic Acids Res. 1996 24 15 :2966-2973

Human Gene Thera 1990 1:241-256

J Clin. Invest 1992 . 90:626-630

Curr. Topics in Micro. and Imm. 1995 199 part 3 :177-194

Lancet 1981 11:832-834

Cancer Res. 1996 56:1341-1345

J Virol. 1992 66 (6) :3633-3642

J Virol. 1996 70 (4) :2296-2306

Nature (1997) 389:239-242

J Virol. 1984 51 (3) : 822-831

Adv. Ex . Med. Biol. 1991 3098:61-66

Proc. Natl. Acad. Sci. 1983 80:5383-5386

Genomics 1990 8:492-500

Gastroenter. 1990 98:470-477 .

N. Vogel
Au 1636
12/9
10045116

An Adenovirus Vector for Gene Transfer into Neurons and Glia in the Brain

G. Le Gal La Salle, J. J. Robert, S. Berrard, V. Ridoux, L. D. Stratford-Perricaudet, M. Perricaudet, J. Mallet*

The efficient introduction of genetic material into quiescent nerve cells is important in the study of brain function and for gene therapy of neurological disorders. A replication-deficient adenoviral vector that contained a reporter gene encoding β-galactosidase infected rat nerve cells in vitro and in vivo. β-Galactosidase was expressed in almost all sympathetic neurons and astrocytes in culture. After stereotactic inoculations into the rat hippocampus and the substantia nigra, β-galactosidase activity was detected for 2 months. Infected cells were identified as microglial cells, astrocytes, or neurons with anatomical, morphological, and immunohistochemical criteria. No obvious cytopathic effect was observed.

The ability to deliver foreign genes and promoter elements directly to terminally differentiated cells of the nervous system, which no longer proliferate, would be desirable for the study of the function and regulation of cloned genes as well as for gene therapy. Although a possibility is offered by defective herpes simplex virus vectors (*1*), their usefulness has been limited by their poor efficiency of infection and their pathogenicity. Here, we show that adenovirus, whose natural target is not the nervous system but the respiratory epithelium (*2*), has the ability to infect nerve cells. The gene transfer and expression of adenovirus are highly efficient both in vitro and in the intact rat brain.

In addition to nonreplicative infection, adenovirus has several assets (*3*). Its genome can accommodate foreign genes of up to 7.5 kb. It has a large host range and low pathogenicity in humans, and high titers of the virus can be obtained (*4*). We used a replication-defective adenovirus, Ad.RSV-βgal, which expressed a nuclearly targeted β-galactosidase (β-gal) cDNA under control of the Rous sarcoma virus long terminal repeat (RSV LTR) promoter (*5*). We tested the ability of this vector to infect primary cultures of sympathetic neurons of superior cervical ganglia (SCG). These cells, cultured in the presence of an antimitotic agent, provided a pure and homogeneous preparation of neurons (*6*). After inoculation of the virus, virtually all cells were positive for β-gal activity (*7*), with no apparent toxic effects or morphological changes (Fig. 1, A and B). Labeled cells were not detected when the staining reaction was performed on a parallel, noninoculated culture (Fig. 1C). We also tested the ability of adenovirus to infect primary cultures of rat hippocampal tissue that were enriched in astrocytes (*8*). Inoculation resulted in a blue nuclear staining in about two-thirds of the cells (Fig. 1D). The identification of stained cells as astrocytes was confirmed by additional staining with an antibody against glial fibrillary acidic protein (GFAP) (Fig. 1E).

We next evaluated the ability of adenovirus to infect cells of the brain in vivo in two regions, the hippocampus and the substantia nigra (*9*). All injected animals expressed β-gal activity and β-gal protein, which were detected as early as 24 hours after inoculation and also in animals analyzed after 2 months. The diffusion of the virus was greater in the hippocampus than in the substantia nigra. Infected cells were found throughout the entire dorsal region of the hippocampus (Fig. 2), whereas in the substantia nigra the overall pattern of infection was restricted mainly to a medial-lateral orientation (Fig. 3D). This difference may reflect the propensity of the virus to spread through tissues that adhere loosely, such as the hippocampal fissure.

The extent of the infected area was correlated to the volume of viral solution administered. For instance, in rats killed 3 to 7 days after hippocampal inoculation, the infected area was 1 to 4 mm^3 for 3 to 5 μl of virus injected [10^{10} plaque-forming units (PFU) per milliliter]. Only minor differences in the distribution of the labeling were noted within the first week after inoculation (Fig. 2, A and B). At a longer time, however, the extent of the infected area was more restricted and the labeling was confined to the granule cell layer (Fig. 2C).

No cytotoxic effects in the infected animals were apparent. All recovered from the inoculation procedure without behavioral abnormalities. Examination of the virus-infected brains revealed no enlargement of the lateral ventricle or disruption of the normal anatomy of the structures. The only noticeable alteration was local tissue necrosis and reactive gliosis that were restricted to the injected sites. This phenomenon was largely a result of injection trauma because a similar alteration was observed in animals that had been injected with saline. Finally, analysis of hippocampal cells with Nissl staining showed no cell loss or evidence of cytolysis within the pyramidal or granule cell layers.

We then characterized the infected cell types. At early times (1 to 7 days), many of the β-gal–stained cells exhibited a morphology characteristic of microglial cells in both regions. These small cells had fine, highly branched processes extending radially from the cell body (Fig. 3, A to C). Their identification as microglial cells was confirmed by additional labeling with the antibody OX42, which is directed against type 3 complement receptors (*10*), and with B4-isolectin (*11*). Some of the infected cells were astrocytes, as demonstrated by double staining with the X-gal substrate and an antibody directed against GFAP.

We next determined whether neurons also were infected in both cerebral regions. In the substantia nigra, double-labeling experiments demonstrated coexpression of β-gal and immunoreactivity for tyrosine hydroxylase (TH), a classical marker of catecholaminergic neurons (Fig. 3D). About 50% of the β-gal–positive cells within the infected dopaminergic cell area were marked

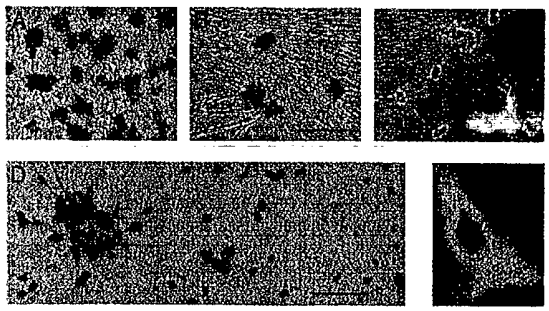

Fig. 1. Expression of β-gal in primary cultured cells after inoculation by adenovirus Ad.RSVβgal. (**A** and **B**) Virtually all the SCG neurons (*13*) expressed β-gal. (**C**) In the absence of the virus, no labeling was observed. (**D**) In enriched astroglial cultures (*14*), about two-thirds of the cells were labeled. (**E**) Additional staining with GFAP (Dakopatts, Glostrup, Denmark, 1:500 dilution, fluorescein-conjugated secondary antibody) confirms that the cells are astrocytes. Scale bars, 200 μm.

G. Le Gal La Salle and V. Ridoux, Institut Alfred Fessard, Unité Propre de Recherche 2212, Centre National de la Recherche Scientifique (CNRS), 91198 Gif sur Yvette, France.
J. J. Robert, S. Berrard, J. Mallet, Laboratoire de génétique moléculaire de la neurotransmission et des processus dégénératifs, C 9923, CNRS, 91198 Gif sur Yvette, France.
L. D. Stratford-Perricaudet and M. Perricaudet, Institut Gustave Roussy, CNRS Unité Associée 1301, 94805 Villejuif Cedex, France.
*To whom correspondence should be addressed.

with a TH antibody, which thereby demonstrates that dopaminergic neurons were infected (Fig. 3, E to G). In the hippocampus, which is composed of segregated and laminated cellular subgroups, numerous β-gal–stained cells were unambiguously identified as neurons on the basis of morphological and anatomical characteristics (Fig. 3, H to J). Recognition of the cellular type was further facilitated because a few cells revealed a Golgi-like profile as a result of the diffusion of β-gal enzyme. These positively stained cells could be identified as pyramidal neurons, granule cells, and hilar interneurons in the pyramidal cell layer CA1, the granule cell layer, and the hilus of the dentate gyrus, respectively (Fig. 3, H to J).

In rats killed 1 and 2 months after inoculation, the distribution of β-gal–positive cells was more restricted than what had been observed at earlier times. Although microglial cells represented a large number of β-gal–expressing cells up to 1 week after injection into the hippocampus, their number decreased at longer post-infection times. Most of the labeled cells at 1 month were neurons of the stratum granulosum (Fig. 4). As determined in sections counterstained with cresyl violet, β-gal–positive cells were restricted to the granular layer, and no positive cells were seen in the innermost part of the layer that includes most of the basket cells and a few glial cells. The same pattern was also obtained at 2 months. This restriction in the pattern may reflect a change in the RSV LTR promoter activity; the activity of the RSV LTR promoter may be more

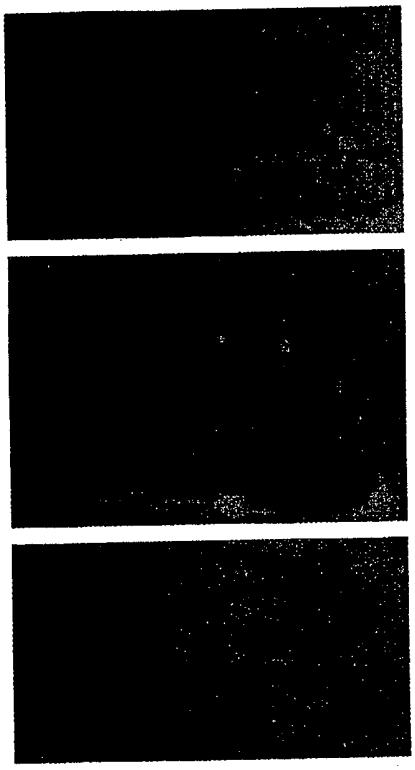

Fig. 2. General patterns of β-gal expression after unilateral intrahippocampal inoculation of the virus Ad.RSVβgal. (**A**) Staining with X-gal and fushin (Gurr, England) in a 40-μm-thick frontal section of the brain of a rat killed 24 hours after injection. (**B**) Immunohistochemical detection of β-gal 1 week after injection. The primary antibody was an affinity-purified rabbit immunoglobulin G fraction to β-gal (Cappel, Organon, West Chester, Pennsylvania, 1:800 dilution) that was then bound with a streptavidin-biotinylated peroxidase complex (Amersham) with diaminobenzidine as a chromogen, reinforced with nickel. (**C**) Distribution of β-gal–positive blue cells in the dentate gyrus of the hippocampus 1 month after injection. Counterstaining is shown in neutral red. Scale bar, 300 μm; h, hilus; hf, hippocampal fissure; ml, molecular layer; sg, stratum granulosum.

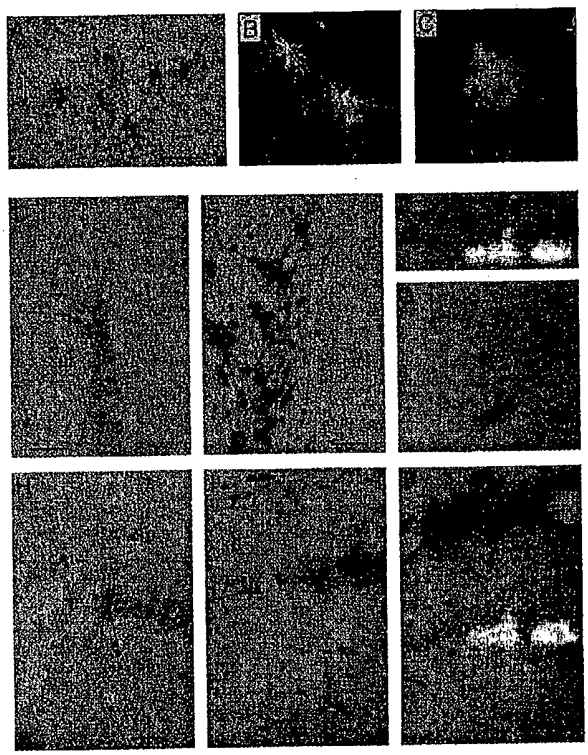

Fig. 3. Characterization of glial and neuronal cell types infected by direct in vivo inoculation of the adenovirus Ad.RSVβgal. (**A** to **C**) Immunohistochemical detection of β-gal expression in microglial cells 5 days after the injection into the hippocampus. Immunological reaction was processed with peroxidase reinforced with nickel (A) and with fluorescein-conjugated secondary antibody (B and C). (**D** to **G**) Sections across the substantia nigra. Three days after intranigral inoculation, a dense blue β-gal staining was detectable in a great number of nigral cells (D), most of which were also shown to be double-labeled with TH monoclonal antibodies (E to G) (Boehringer Mannheim, 1:200 dilution). Panel (E) is a higher magnification of the area with the highest density of β-gal–positive cells in (D). Arrows in (F) and (G) indicate cells double-stained for β-gal and TH. (**H** to **J**) Sections across the hippocampus. Pyramidal cells in CA1 (H and I) and granule cells in the dentate gyrus (J) are labeled. β-gal activity was revealed by immunohistochemistry as in (A). The cells in (D) to (G) were processed with histochemistry; in addition, the cells in (D) to (J) were labeled with antibodies. Scale bars: 30 μm in (A), 300 μm in (D), and 100 μm in (E) and (H). Abbreviations are as in Fig. 2 except for snc, substantia nigra pars compacta; snr, substantia nigra pars reticulata; sp, stratum pyramidale; so, stratum oriens; and sr, stratum radiatum.

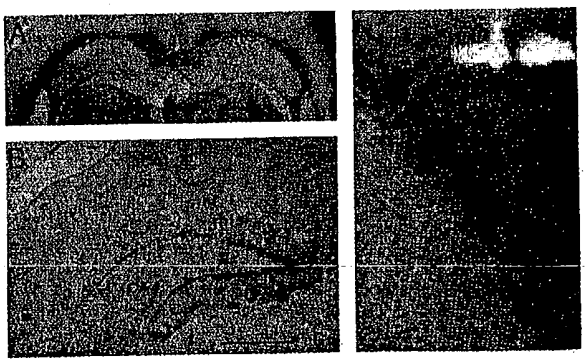

Fig. 4. Distribution of β-gal–positive cells in the dentate gyrus 1 month after Ad.RSVβgal inoculation. (**A**) Photomicrograph stained for β-gal expression with X-gal histochemistry. The cells that are stained blue were observed in the dentate gyrus of the injected left hippocampus. Scale bar, 1 mm. (**B**) Dentate localization of infected cells was confirmed by immunohistochemical β-gal detection (staining with peroxidase plus nickel). Scale bar, 300 μm. (**C**) High magnification view showing the large number of densely packed, β-gal–labeled cell nuclei in the granule cell layer of the dentate gyrus. Abbreviations are as in Fig. 3.

stable in neurons than in glial cells. Another possibility is that the virus may be transferred from one cell type to another, as has been described for rabies and herpes viruses (*12*).

The use of adenovirus vectors provides a method to study the function of cloned genes, which is complementary to that of transgenic animals. For instance, infection of the hippocampus would be useful for the study of integrated phenomena such as long-term potentiation. The possibility of selecting the time at which a particular gene is to be expressed is important when the expression of a transgene in early development is deleterious to the animal. In the context of degenerative diseases, it may also be possible to express neurotransmitters or growth factors locally as an alternative to the grafting of fetal cells.

REFERENCES AND NOTES

1. A. I. Geller and X. O. Breakefield, *Science* 241, 1667 (1988); A. I. Geller and A. Freese, *Proc. Natl. Acad. Sci. U.S.A.* 87, 1149 (1990); E. A. Chiocca *et al.*, *New Biol.* 2, 739 (1990); A. T. Dobson, T. P. Margolis, F. Sedarati, J. G. Stevens, L. T. Feldman, *Neuron* 5, 353 (1990); D. J. Fink *et al.*, *Hum. Gene Ther.* 3, 11 (1992).
2. M. A. Rosenfeld *et al.*, *Cell* 68, 143 (1992); M. A. Rosenfeld *et al.*, *Science* 252, 431 (1991).
3. L. D. Stratford-Perricaudet and M. Perricaudet, in *Human Gene Transfer*, O. Cohen-Haguenauer, M. Boiron, J. Libbey, Eds. (Eurotext Ltd., London, 1991), pp. 51–61.
4. L. D. Stratford-Perricaudet, M. Levrero, J. F. Chasse, M. Perricaudet, P. Briand, *Hum. Gene Ther.* 1, 241 (1990); B. Quantin, L. D. Perricaudet, S. Tajbakhsh, J. L. Mandel, *Proc. Natl. Acad. Sci. U.S.A.* 89, 2581 (1992).
5. L. D. Stratford-Perricaudet, I. Makeh, M. Perricaudet, P. Briand, *J. Clin. Invest.* 90, 626 (1992).
6. E. Hawrot and P. H. Patterson, *Methods Enzymol.* 58, 574 (1979).
7. Histochemical staining was performed with the chromogenic substrate 5-bromo-4-chloro-3-indolyl-β-D-galactoside (X-gal) as described [J. R. Sanes, J. L. Rubenstein, J. F. Nicolas, *EMBO J.* 5, 3133 (1986)].
8. K. D. McCarthy and J. De Vellis, *J. Cell Biol.* 85, 890 (1980).
9. Seventeen male Wistar rats (10 weeks old) were stereotactically injected under deep anesthesia with 1 to 5 μl of media that contained highly purified virus (10^{10} PFU/ml) into either the hippocampus or the substantia nigra. Animals were killed 1, 2, 3, 5, 7, 30, and 60 days after inoculation. We detected β-gal activity in positive cells histochemically by using both the X-gal substrate and an antibody directed against the protein. The latter method is more sensitive and in some instances revealed fine cytoplasmic processes.
10. A. P. Robinson, T. M. White, D. W. Mason, *Immunology* 57, 239 (1986).
11. C. E. Hayes and I. J. Goldstein, *J. Biol. Chem.* 249, 1904 (1974).
12. F. Lafay *et al.*, *Virology* 183, 320 (1991); K. Kristensson, B. Ghetti, H. M. Wisniewski, *Brain Res.* 69, 189 (1974); X. Martin and M. Dolivo, *ibid.* 273, 253 (1983).
13. The SCG were removed from 2-day-old Wistar rats, dissociated, plated on 16-mm collagen-coated dishes, and cultured as described (*7*). Cytosine arabinofuranoside (10 μM) was added during the first week of culture to prevent proliferation of ganglionic non-neuronal cells. After 6 days in culture, the cells were inoculated with 10^6 PFU of Ad.RSVβgal in culture medium or, as a control, exposed only to culture medium. Twenty-four hours later, the virus was removed, and the cells were maintained for 2 days in culture medium. After washing and paraformaldehyde fixation, β-gal–expressing cells were characterized with X-gal histochemistry.
14. Cells were plated in 35-mm-diameter plastic dishes and grown in supplemented Dulbecco's modified Eagle's medium for 5 days. The cells in each dish were then inoculated with 2 μl of the adenoviral solution (titer, 10^8 PFU/ml) for 24 hours. Histochemical staining was processed as in (*13*).
15. The first two authors contributed equally to this paper. We thank N. Faucon Biguet for helpful discussions, A. Hicks and C. Menini for critically reading this manuscript, and M. Synguelakis and S. Mirman for technical assistance. Supported by grants from CNRS, the Association pour la Recherche contre le Cancer, the Association Française contre la Myopathie, the Institut de Recherche sur la Moelle Epinière, and the Bioavenir Program (Rhône-Poulenc Rorer, Ministère de la Recherche et de l'Espace, and Ministère de l'Industrie et du Commerce Extérieur). J.J.R. received a fellowship from the Institut de Formation Supérieure Biomédicale.

4 September 1992; accepted 18 December 1992

CD40 Ligand Gene Defects Responsible for X-Linked Hyper-IgM Syndrome

R. Cutler Allen, Richard J. Armitage, Mary Ellen Conley, Howard Rosenblatt, Nancy A. Jenkins, Neal G. Copeland, Mary A. Bedell, Susanne Edelhoff, Christine M. Disteche, Denise K. Simoneaux, William C. Fanslow, John Belmont, Melanie K. Spriggs*

The ligand for CD40 (CD40L) is a membrane glycoprotein on activated T cells that induces B cell proliferation and immunoglobulin secretion. Abnormalities in the CD40L gene were associated with an X-linked immunodeficiency in humans [hyper-IgM (immunoglobulin M) syndrome]. This disease is characterized by elevated concentrations of serum IgM and decreased amounts of all other isotypes. CD40L complementary DNAs from three of four patients with this syndrome contained distinct point mutations. Recombinant expression of two of the mutant CD40L complementary DNAs resulted in proteins incapable of binding to CD40 and unable to induce proliferation or IgE secretion from normal B cells. Activated T cells from the four affected patients failed to express wild-type CD40L, although their B cells responded normally to wild-type CD40L. Thus, these CD40L defects lead to a T cell abnormality that results in the failure of patient B cells to undergo immunoglobulin class switching.

Human hyper-IgM immunodeficiency is a rare disorder characterized by normal or elevated serum concentrations of polyclonal IgM and markedly decreased concentrations of IgA, IgE, and IgG (*1*, *2*). Reports of X-linked, autosomal recessive, autosomal dominant, and acquired forms of the disorder indicate genetic heterogeneity and that several different pathologic mechanisms may be responsible (*2*, *3*). In the X-linked form of hyper-IgM syndrome, affected males usually experience the onset of recurrent infections in the first year of life. Affected males have normal numbers of circulating B and T lymphocytes, although lymph node hyperplasia with an absence of germinal centers is common (*1*, *2*). This condition is lethal in the absence of medical intervention; however, patients typically respond well to a maintenance therapy consisting of intravenous treatment with γ globulin.

The cellular abnormalities that underlie the various forms of hyper-IgM syndrome are unclear. Studies of patterns of X chromosome inactivation in obligate carrier females indicate a randomized pattern of X chromosome usage in either B or T lineage cells, which suggests that the defect does not alter maturation of these cells by cell autonomous mechanisms (*4*). Some studies have suggested that the affected phenotype is likely a result of B cell dysfunction insofar as patient B cells treated with polyclonal B cell activators, such as pokeweed mitogen, could not be induced to switch to IgG or IgA production (*5*). Other reports suggest that the

R. C. Allen, D. K. Simoneaux, J. Belmont, Howard Hughes Medical Institute, Institute for Molecular Genetics, Baylor College of Medicine, Houston, TX 77030.
R. J. Armitage and W. C. Fanslow, Department of Immunology, Immunex Research and Development Corporation, Seattle, WA 98101.
M. E. Conley, Department of Pediatrics, University of Tennessee, College of Medicine and Department of Immunology, St. Jude Children's Research Hospital, Memphis, TN 38105.
H. Rosenblatt, Department of Pediatrics, Baylor College of Medicine, Houston, TX 77030.
N. A. Jenkins, N. G. Copeland, M. A. Bedell, Mammalian Genetics Laboratory, ABL–Basic Research Program, National Cancer Institute, Frederick Cancer Research and Development Center, Frederick, MD 21702.
S. Edelhoff and C. M. Disteche, Department of Pathology, University of Washington, Seattle, WA 98195.
M. K. Spriggs, Department of Molecular Biology, Immunex Research and Development Corporation, Seattle, WA 98101.
*To whom correspondence should be addressed.

Nat. Gent. 1992 1:372-378
Science 1989 245:1234-1236

Eur. J Biochem. 1985 148:265-270

Mol. Immunol 1995 32:1057-1064

Science 1993 259:988-990

Nature 1988 336:348-352

J Clin. Invest. 1993 91:225-234

Mol. Cell. Biol. 1987 7:1576-1579

Gene 1982 19:33-42

Neuron 1992 8:507-520

Adv. Virus Res. 1989 37:35-83

1994 Cancer Res. 54:5258-5261

Cell 1987 50:435-443

Nucleic Acids Res. (1996) 24(10):1841-1848

J Biol. Chem. 1988 263 10 :4837-4843

Proc. Natl. Acad. Sci. USA 1992 89:2581-2584

1993 Nature 361:647-650

DNA Seq. 1993 4:185-196

Human Gene Ther. 1995 6:881-893

Science 1991 252:431-434

Cell 1992 68:143-155

Mol. Cell. Biol. 1990 10 6 :2738-2748

Nucleic Acids Res. 1996 24 15 :2966-2973

Human Gene Thera 1990 1:241-256

J Clin. Invest 1992 . 90:626-630

Curr. Topics in Micro. and Imm. 1995 199 part 3 :177-194

Lancet 1981 11:832-834

Cancer Res. 1996 56:1341-1345

J Virol. 1992 66 (6) :3633-3642

J Virol. 1996 70 (4) :2296-2306

Nature (1997) 389:239-242

J Virol. 1984 51 (3) : 822-831

Adv. Ex . Med. Biol. 1991 3098:61-66

Proc. Natl. Acad. Sci. 1983 80:5383-5386

Genomics 1990 8:492-500

Gastroenter. 1990 98:470-477 .

N. Vogel
Au 1636
12/9
10045116

Nucleic Acids Research, 1996, Vol. 24, No. 10 1841–1848

Oligodeoxynucleoside phosphoramidates (P-NH_2): synthesis and thermal stability of duplexes with DNA and RNA targets

Suzanne Peyrottes, Jean-Jacques Vasseur*, Jean-Louis Imbach and Bernard Rayner

Laboratoire de Chimie Bio-Organique, UMR 5625 du CNRS, CC 008, Université Montpellier II, Place Eugène Bataillon, 34095 Montpellier Cedex 5, France

Received February 16, 1996; Revised and Accepted April 1, 1996

ABSTRACT

Syntheses of non ionic oligodeoxynucleoside phosphoramidates (P-NH_2) and mixed phosphoramidate–phosphodiester oligomers were accomplished on automated solid supported DNA synthesizer using both H-phosphonate and phosphoramidite chemistries, in combination with *t*-butylphenoxyacetyl for N-protection of nucleoside bases, an oxalyl anchored solid support and a final treatment with methanolic ammonia. Thermal stabilities of the hybrids formed between these new analogues and their DNA and RNA complementary strands were determined and compared with those of the corresponding unmodified oligonucleotides, as well as of the phosphorothioate and methylphosphonate derivatives. Dodecathymidines containing P-NH_2 links form less stable duplexes with DNA targets, d($C_2A_{12}C_2$) (ΔTm/modification –1.4°C) and poly dA (ΔTm/modification –1.1°C) than the corresponding phosphodiester and methylphosphonate analogues, but the hybrids are slightly more stable than the one obtained with phosphorothioate derivative. The destabilization is more pronounced with poly rA as the target (ΔTm/modification –3°C) and could be compared with that found with the dodecathymidine methylphosphonate. The modification is less destabilizing in an heteropolymer–RNA duplex (ΔTm/modification –2°C). As expected, the P-NH_2 modifications are highly resistant towards the action of various nucleases. It is also demonstrated that an all P-NH_2 oligothymidine does not elicit *Escherichia coli* RNase H hydrolysis of the poly rA target but that the modification may be exploited in chimeric oligonucleotides combining P-NH_2 sections with a central phosphodiester section.

INTRODUCTION

The use of natural oligonucleotides as therapeutic agents in an antisense approach in which the target is RNA or DNA, suffers from drawbacks such as their inherent instability towards degradation by extra and intra-cellular nucleases and their relatively poor cellular uptake (1). Attempts to produce nuclease resistant oligonucleotides and to improve their cellular uptake while keeping the specificity of binding to their targets, has resulted in the preparation of several phosphodiester backbone modified analogues (2,3). Of these, phosphorothioates (4) are the most widely applied derivatives of oligodeoxynucleotides for an antisense approach, but they remain somewhat susceptible to degradation by nucleases (5), are taken up by cells more slowly than phosphodiesters and present a strong tendency to bind with numerous proteins (6). Replacement of the negatively charged oxygen atom in the phosphodiester backbone by uncharged groups to produce non-ionic oligonucleotide analogues such as methylphosphonates (7) or phosphoramidates (8) would allow them to enter cells by an alternative mechanism and confer increased nuclease resistance. However, methylphosphonates suffer from the disadvantage of being relatively insoluble in water, aqueous buffers and biological media (9). Furthermore, these modifications induce chirality and the binding properties of the resulting diastereoisomers to a complementary target are clearly dependent on the orientation of the substituted groups around the phosphorus atom (9–11). Despite the effort directed towards the stereocontrolled synthesis of phosphorothioates (12) and methylphosphonates (13), mixtures of heterogeneous oligomers are largely used which lower the binding to the target (14). To bypass the chirality problem, a number of non-phosphate, neutral and achiral linkages have been prepared (15,16). However, the syntheses of such backbones are in general difficult and versatile. Reported preparations are not particularly suitable for automated synthesizers to the level at which all linkages are modified. The most frequently used strategy is to prepare a modified nucleoside dimer, to convert it in a phosphoramidite synthon and to incorporate it into an oligonucleotide sequence where modified linkages are alternated with normal phosphodiesters (18). In such oligomers, the polyanionic character is reduced, but not suppressed and these modifications do not necessarily provide increased cellular uptake as well as a total nuclease resistance. For that reason and although the automatic synthesis of non-ionic phosphoro oligonucleosides cannot be rendered stereospecific for the time being, these phosphoro analogues stay attractive because they can be prepared in a relatively

* To whom correspondence should be addressed

straightforward manner by minor modifications to the existing automated DNA synthetic methods.

If it has been clearly demonstrated that the negative impact of stereoisomerism on hybridization is enhanced with bulky substituents (8). It is assumed that the influence of a modification on the stabilities of duplexes also results from the disturbance of the spin of hydration around the modified phosphate groups (8,17). The amides of phosphorus acid are known to have good solvating properties (18). Furthermore, in phosphoramidates (P-NH_2), the fact that the NH_2 group is small, uncharged in aqueous solution and forms hydrogen bonds readily (19), gives them favourable solubility characteristics required for hydration, with a minimum steric hindrance around the phosphorus atom, and makes them attractive potential candidates for non-anionic analogues of oligonucleotides. The syntheses of *N*-alkyl (8,20) and *N*-alkoxy (21) phosphoramidate derivatives of DNA have been described and their biophysical properties studied. Unfortunately, due to the reported decomposition of dithymidine phosphoramidate under the base conditions necessary for removal of the common heterocyclic *N*-acyl protecting groups and release of an oligonucleotide from the regular succinyl anchored solid support (20) (concentrated ammonia, 55°C, 5–16 h), syntheses of phosphoramidate (P-NH_2) oligonucleotides have been limited to a dimer level (19,20,22). However, recent developments in oligonucleotide chemistry on a more labile oxalyl anchored solid support (23) combined with the use of monomers possessing highly labile protecting groups (24), of mild and rapid deprotection conditions (25) have enabled us to synthesise these base-sensitive oligonucleotides. In this regard, the use of pent-4-enoyl (26) as nucleobase protective group (27) appears very promising, and recently allowed the synthesis of various dinucleosides containing a P-NH_2 linkage (28). We would like to report here, the first synthesis of partially or fully modified oligonucleotide phosphoramidates (P-NH_2) of length sufficient to explore the antisense potential of these analogues. The nuclease resistance properties of the modified oligonucleotides and the thermal stabilities of duplexes formed with their DNA or RNA complements have been evaluated and compared with those of unmodified oligonucleotide, as well as those of the phosphorothioate and methylphosphonate analogues.

MATERIALS AND METHODS

Oligonucleotide synthesis

Syntheses of the oligodeoxynucleotide analogues were carried out on 1 µmol scale using a 381A Applied Biosystems DNA-synthesizer. First, nucleoside was linked to LCAA-CPG (500 Å, from Sigma) by means of an oxalyl linker (23). Analogues combining phosphodiester and phosphoramidate internucleoside links were prepared by using both phosphoramidite and hydrogen phosphonate chemistries. After each coupling step using commercially available nucleoside-cyanoethyl phosphoramidites and appropriate reagents (from Millipore), the intermediate phosphite triesters were oxidized by a 1 min treatment with a 1.1 M solution of *t*-butylhydroperoxide in dichloromethane. H-phosphonate couplings were carried out using deoxynucleoside H-phosphonate derivatives (24) and standard reagents from Glen Research. At the end of the chain elongation, oxidative amidation was performed manually by treating CPG linked oligonucleotide with a saturated solution of ammonia in carbon tetrachloride/dioxan (4/1, v/v) for 30 min at 0°C (20). After filtration, the oligomers were released from the solid support and deprotected with a treatment with saturated methanolic ammonia at 20°C over 2 h for phosphodiester/phosphoramidate oligomers **1**, **2**, **3** and **7**, and 5 min for the fully modified P-NH_2 oligomers **4** and **6** (Table 1).

HPLC methods

HPLC was performed on a Waters-Millipore instrument equipped with two M510 solvent delivery systems, a M680 solvent programmer, a U6K injector and a M990 diode array UV detector. Oligonucleotides were purified by reverse-phase HPLC on a Delta-pack preparative column (7.8 × 300 mm, C18, 5 µm, Millipore) using a gradient of acetonitrile from 10 to 25% in 0.05 M triethylammonium acetate buffer (pH 7) in 40 min at a flow rate of 2 ml/min. The desired fractions were combined, evaporated, dissolved in water and lyophilised. Purity of the samples was checked by HPLC at 260 nm on a Nucleosil analytical column (4.6 × 150 mm, C18, 5 µm, Macherey-Nagel) using a gradient of acetonitrile from 0 to 30% in 0.05 M triethylammonium acetate buffer (pH 7) in 30 min at a flow rate of 1 ml/min. Using this procedure, 7–20 A_{260} units of purified oligomers were isolated in each case.

Mass spectrometry

Mass spectra were recorded on a SSQ 7000 quadrupole mass spectrometer (Finnigan MAT, San Jose, USA) fitted with an electrospray interface. Samples (final concentration 30 µM) were dissolved in water–methanol (v/v, 1:1) containing triethylamine (1.5%) and introduced into the mass spectrometer at a 10 µl/min flow-rate with a Harvard Apparatus 22 pump model. The negative ion electrospray mass spectra were transformed into real mass spectra, using the DEC-Finnigan software.

NMR measurements

^{31}P-NMR spectra were recorded on a Brüker AC 250 spectrometer at 100 MHz. Samples were dissolved in D_2O. Chemical shifts values are in p.p.m. relative to external 85% H_3PO_4.

Formic acid mediated degradation of d(ACACCCAATTCT) analogues (29)

One A_{260} unit of oligonucleotide was dissolved in 90% aqueous formic acid (1 ml) and the resulting solution was heated at 120°C for 12 h. After cooling, the solution was evaporated to dryness under reduced pressure, and the residue was dissolved in 0.1 M triethylammonium acetate buffer, pH 7 (0.2 ml) for HPLC analysis (Nucleosil analytical column, 4.6× 150 mm, C18, 5 µm, Macherey-Nagel, eluent: 0.05 M triethylammonium acetate, pH 6.9, flow rate of 1 ml/min). The base composition of the oligonucleotides **6**, **7** and **8** was confirmed after applying this degradation, which cleanly liberated the purine and pyrimidine bases (Cyt, 3.03 min; Thy, 7.59 min; Ade, 17.63 min) and quantification of the peak areas at 260 nm, using an equimolar mixture of the three bases as standard.

Melting temperatures

Melting curves were recorded on a UVIKON 931 spectrophotometer (Kontron). The temperature control was through a HUBER PD 415 temperature programmer connected to a refrigerated water bath (Huber Ministat). Typical experiments were carried out with

equimolar ratio of modified oligomers and their targets in a 10 mM sodium cacodylate buffer (pH 7 or pH 5.45) containing 10 mM, 100 mM or 1 M sodium chloride. The samples were preheated at 75°C, and the change in absorbance at 260 nm as a function of the temperature was recorded. The cooling or heating rate was 0.5°C/min. The cell compartment was continuously flushed with dry nitrogen for temperatures below room temperature. Tm values were determined from the maxima of the first derivative plots of absorbance versus temperature.

Enzymatic hydrolysis experiments

Snake venom phosphodiesterase (SVPDE) (*Crotalus durissus*), Nuclease S1 (*Aspergillus oryzae*) and Calf spleen Phosphodiesterase II (CSPDE) were purchased from Boehringer. The oligothymidines (2 A_{260} U) were incubated at 37°C in either: 10 µl 50 mM sodium acetate buffer (pH 4.5), 300 mM sodium chloride, 100 mM zinc acetate added with 70 µl of water containing 2 U nuclease S1; 100 µl of 100 mM Tris–HCl buffer (pH 9), 10 mM magnesium chloride added with 2 µl of the commercial solution of SVPDE (3 U/ml); or 80 µl of 125 mM ammonium acetate buffer (pH 6.8), 2.5 mM EDTA containing 2 µl of the commercial solution of CSPDE (0.5 U/ml). Aliquots were analysed using the analytical conditions described in HPLC methods.

RNase H digestion of poly rA/oligothymidine analogues duplexes

Escherichia coli RNase H was purchased from Pharmacia. These experiments were performed with oligothymidylate analogues and poly rA (240 µM in nucleotide concentration for each strand) in 10 mM Tris–HCl buffer (pH 7), 10 mM magnesium chloride and 100 mM sodium chloride (500 µl). The samples were preheated at 70°C, allowed to slowly cool down to 0°C, then the temperature was stabilised at 20°C before adding the enzyme (5 U). Digestion curves were obtained by plotting the absorbance at 260 nm as a function of time.

RESULTS AND DISCUSSION

Preparation of oligonucleosides containing phosphoramidate (P-NH_2) linkages

Standard synthesis of oligonucleotides anchored by a succinyl linker to controlled pore glass (CPG) support, requires an ultimate chemical step with concentrated ammonium hydroxide at 55°C for 5–16 h to release the oligonucleotides from the solid support and completely remove nucleobase and phosphodiester protecting groups. Although a number of *N*-alkylphosphoramidate oligonucleotide derivatives (8) have been prepared using this current methodology, the synthesis of less hindered P-NH_2 analogues has been limited to the preparation of dinucleotides (19,20,22) or trinucleotide (28). This is due to the fact that the P-NH_2 linkage could not survive the drastic ammonia treatment. Indeed, it has been shown that a dithymidine phosphoramidate (P-NH_2) was rapidly hydrolysed under such alkaline treatment ($t_{1/2}$ 15 min) (20) affording a mixture of thymidine and corresponding 3′- and 5′-phosphoramidic acid monoesters (22,30). Fortunately, we found that a treatment with saturated methanolic ammonia gave appreciably less degradation of this dimer ($t_{1/2}$ 3.8 days). This mild treatment has been used to deprotect base-sensitive oligonucleotides such as RNA and methylphosphonates (24) as well as oligonucleoside *N*-alkoxyphosphoramidates (21). Under these conditions, the release of an oligonucleotide from an oxalyl anchored solid support is quantitative after 5 min at room temperature (23), and the complete removal of cyanoethyl phosphate protecting groups is achieved within 2 h at room temperature (21,24). We estimated that <1.5% of a P-NH_2 linkage will be degraded (after 2 h treatment with methanolic ammonia) on an oligonucleotide containing both P-NH_2 and P-O^- (initially protected with cyanoethyl) linkages, which is quite acceptable.

To examine the effect of the modification on binding capacities, several analogues of dodecathymidylate **5** were prepared (Table 1). Oligomer **1** was synthesized with one modification placed in the middle of the sequence. In compound **2**, modified linkages were alternated with normal phosphodiesters, in such a way that the oligomer had six phosphoramidate and five phosphodiester internucleoside bonds. In the oligothymidine **3**, an internal part of five adjacent phosphodiesters was surrounded by two terminal sections of three contiguous phosphoramidates. In dodecathymidine **4**, natural phosphodiester linkages were completely replaced by phosphoramidate ones. In addition, two analogues of the mixed-base dodecanucleoside **8** complementary to the splice acceptor site of mRNA coding for HIV-1 tat protein (31) were synthesized (Table 1). In the oligomer **7**, as for compound **3**, an internal part of five adjacent phosphodiesters was surrounded by two terminal sections of three contiguous phosphoramidates. Finally, oligonucleotide **6** was fully modified. In order to obtain phosphodiester and phosphoramidate linkages in the same oligomer, cyanoethyl phosphoramidite and H-phosphonate chemistries were respectively employed. As it has been demonstrated that *t*-butylhydroperoxide is able to selectively oxidize phosphite triester intermediates into phosphate triesters without affecting H-phosphonate linkages (32), this reagent was used instead of the common iodine treatment after each phosphoramidite coupling step. Then, the H-phosphonate diesters were oxidized into phosphoramidate linkages, by treatment with a saturated solution of ammonia in dioxan/CCl_4 (20). As classical amino protecting groups are routinely removed under drastic conditions (concentrated aqueous ammonia, 5–16 h at 55°C), *N*-*t*-butylphenoxyacetyl protected nucleoside phosphoramidites and H-phosphonates (24) were employed during the synthesis of heteropolymers **6** and **7**, in combination with *t*-butylphenoxyacetic anhydride as capping reagent. In our hands and in contrast to what has been reported in the literature (24), the coupling efficiency of the H-phosphonate salts of deoxyadenosine and deoxycytidine was much lower (<90%) than the one of the corresponding phosphoramidites (>98%) and may account for the low yields of purified compounds (Table 2). Finally, the oligonucleotides were deprotected and removed from the solid support by treatment with saturated methanolic ammonia at room temperature (2 h for oligomers **1**, **2**, **3** and **7**; 5 min for compounds **4** and **6**).

The chromatograms of **3** and **4** (Fig. 1A) are representative analyses of the products released from the solid support after the ammonia treatment. The oligonucleotides were purified by reverse phase HPLC. Figure 1B depicts the chromatograms of compounds **3** and **4** obtained after purification. Owing to the absence of charge on phosphoramidate linkages, retention times of those analogues on reverse phase HPLC increase with the number of modifications (Table 2).

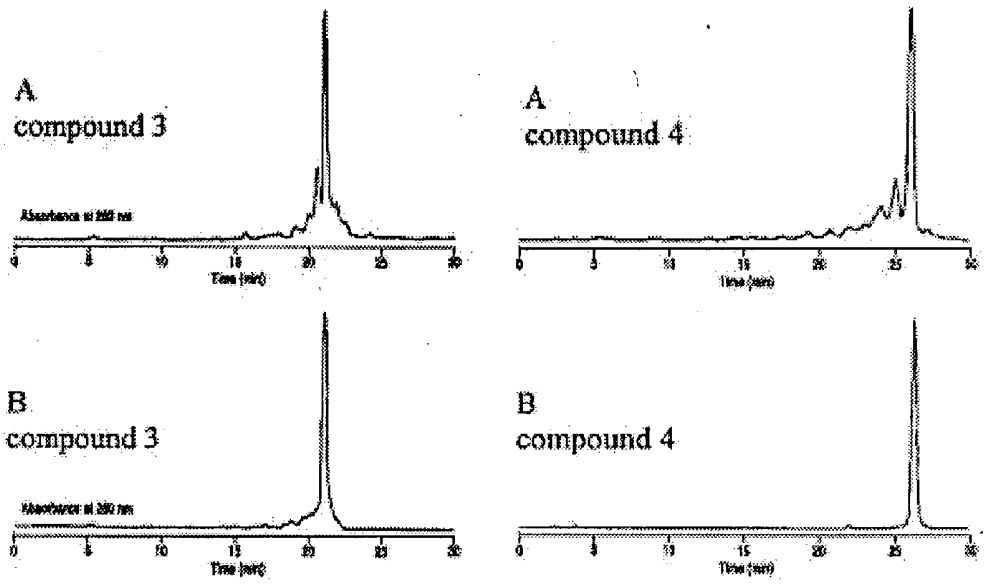

Figure 1. HPLC profiles at 260 nm of **3** and **4**. (**A**) Crude product mixtures recovered from solid support. (**B**) After purification of products obtained from (A).

Table 1. Oligonucleotides synthesized

Oligonucleotide sequences	
1	$(dTp)_5dTpn(dTp)_5dT$
2	$(dTpndTp)_5dTpndT$
3	$(dTpn)_3(dTp)_5(dTpn)_3dT$
4	$(dTpn)_{11}dT$
5	$(dTp)_{11}dT$
6	d-ApnCpnApnCpnCpnCpnApnApnTpnTpnCpnT
7	d-ApnCpnApnCpCpCpApApTpnTpnCpnT
8	d-ApCpApCpCpCpApApTpTpCpT
Targets	
9	d-CpCpApApApApApApApApApApApApCpC
	d-ApGpApApTpTpGpGpGpTpGpT
	r-ApGpApApUpUpGpGpGpUpGpU

p refers to a phosphodiester internucleoside link, and pn to a phosphoramidate linkage.

^{31}P-NMR spectroscopy was used for the characterization of the modified oligonucleotides (Table 2). The spectrum of the alternating oligomer **2** (Fig. 2) consists of two sets of peaks in a ~5:6 ratio; one set due to the phosphodiester resonances at –0.5 p.p.m. and a downfield set at 12.7 p.p.m. in agreement with the literature data concerning the phosphoramidate resonances (22,30). Similar ^{31}P-NMR spectra were obtained for **1**, **3** and **7**, with the ratio of the integration for peaks at –0.5 and 12.7 p.p.m. varying according to the expected ratio of P-O^- to P-NH_2 internucleoside bonds and in agreement with electrospray mass spectrometry data (Table 2). NMR resonances at 12.7 p.p.m. were observed for compounds **4** and **6**. These spectra provide evidence that the phosphoramidate P-NH_2 linkages survived ultimate treatment (saturated methanolic ammonia at room temperature for 2 h). In order to further confirm the integrity of the phosphoramidate linkages, dodecathymidine analogues **1**, **2**, **3** and **4** were quantitatively hydrolysed to phosphodiesters by a formic acid treatment at 90°C for 5 min (8) giving rise to $(dTp)_{11}dT$, as ascertained by HPLC in comparison with an authentic sample (Table 2). The base composition of the oligonucleotides **6**, **7** and **8** was established by a formic acid degradation (29), which cleanly released adenine, thymine and cytosine in a 4:3:5 ratio as determined by HPLC.

Table 2. Oligonucleoside phosphoramidates physical data[a]

Oligomer	R_T, min	δ^{31}P-NMR, p.p.m.	Calculated mass	Observed mass	Isolated yield[b]
5	17.51				
1	18.29	12.65, –0.27	3587.4	3587.6	60%
2	21.18	12.67, –0.53			18%
3	21.91	12.64, –0.46	3582.5	3582.0	12%
4	26.24	12.66			19%
8	22.90				
7	24.74	12.73, –0.53			6%
6	28.84	12.73			5%

[a]See Materials and Methods.
[b]Calculated from support bound nucleoside.

Base-pairing of oligonucleotide analogues with DNA and RNA complementary strands

Interactions between dodecathymidylate analogues with **9**, poly dA and poly rA were investigated by both thermal denaturation

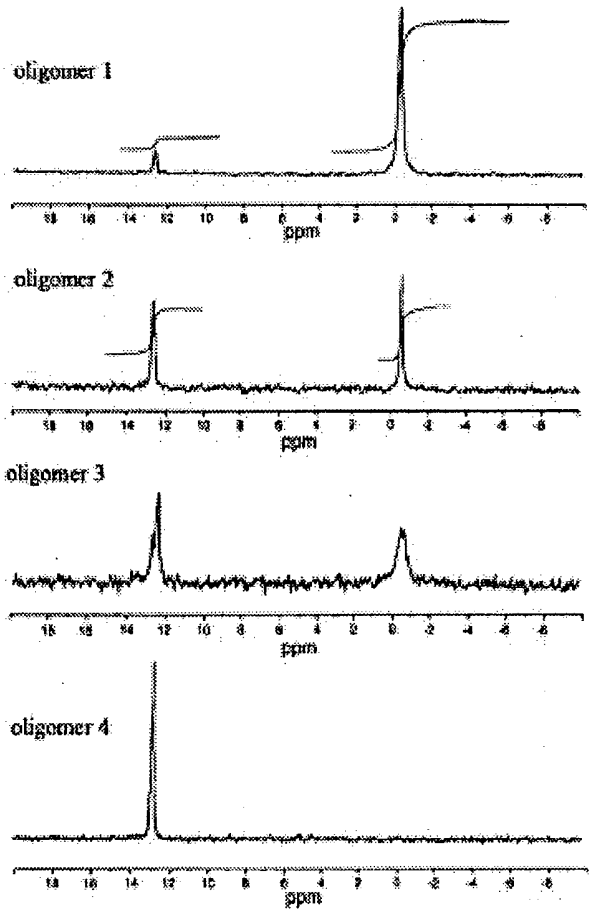

Figure 2. ^{31}P-NMR spectra of oligomers **1**, **2**, **3** and **4** in D_2O.

and renaturation analyses using changes in absorbance at 260 nm versus temperature. The experiments were carried out at an equal nucleotide concentration (60 μM) of the thymidylate analogues and the target compounds. At the end of the experiment, a sample was examined by HPLC to confirm that no significant degradation of the modified oligonucleotide had occurred. Melting temperatures are presented in Table 3. No differences were observed between thermal association and dissociation curves. It can be seen from these results that the introduction of phosphoramidate internucleoside linkages into the dodecathymidylate affects the thermal stability of the duplexes formed with either DNA or RNA complementary strands. Thus, incorporation of one, six and eleven modifications leads to a progressive decrease in the melting temperature of the complexes compared to the 'parent' unmodified duplexes. Tm value is almost a linear function of the number of modifications. The average destabilisation is 1.4°C and 1.1°C per modification in duplexes obtained with **9** and poly dA, respectively. As generally observed for oligo (dT) and its analogues (32), the affinity for duplex formation with poly rA is lower than that observed with poly dA. However, in this case, the difference of stability between the oligothymidine–poly dA and the oligothymidine–poly rA hybrids is enhanced (1.8°C) when compared with natural complexes (0.2°C). Moreover, the average decrease in Tm of ~2.9°C/modification compared with $(dTp)_{11}dT$–poly rA hybrid, did not allow us to observe the binding of the uniformly modified $(dTpn)_{11}dT$ with poly rA, indicating an appreciable distortion of the structure of the modified oligothymidine–RNA duplex compared with the 'parent' duplex. Nevertheless, at a four times higher nucleotide concentration (240 μM), Tm values of 16°C and of 38°C were observed for the modified, **4**, and the natural hybrids (ΔTm/mod = –2°C), respectively. So, even if the modification is really destabilizing, one can admit that it does not compromise Watson–Crick base pairing with a ribonucleotide complementary strand. Furthermore, the Tm value (13.3°C) of the duplex formed between oligonucleotide **3** and poly rA supports this conclusion. Indeed, this Tm value cannot be attributed only to the binding with poly rA of the internal non-modified section $(dTp)_5dT$ of the oligomer **3** under the same conditions, no transition above 0°C was observed with $(dTp)_5dT$ and poly rA.

Table 3. Thermal stabilities (°C) of duplexes formed by oligonucleoside phosphoramidates[a]

Oligomer	Complementary strand					
	9		poly dA		poly rA	
	Tm	ΔTm/mod	Tm	ΔTm/mod	Tm	ΔTm/mod
5	27.0	–	31.5	–	29.5	–
1	25.2	–1.8		nd	26.4	–3.1
2	17.7	–1.6	24.2	–1.2	11.3	–3.0
3	18.9	–1.4		nd	13.3[b]	–2.7
4	13.0	–1.3	20.5	–1.0	<0[c]	<–2.7
average ΔTm/mod		–1.4		–1.1		–2.9

[a]Experiments were carried out in a buffer (pH 7) containing 10 mM sodium cacodylate, 0.1 M sodium chloride, at 60 μM nucleotide concentration in each strand.

[b]In the same experimental conditions, no transition was observed for $(dTp)_5dT$ with poly rA (Tm <0°C).

[c]In 10 mM Tris–HCl, 10 mM $MgCl_2$, 0.1 M NaCl buffer solution (pH 7) at a nucleotide concentration of 240 μM, a Tm value of 16°C was observed for fully modified oligomer **4** with poly rA target and a Tm value of 38°C was found for the natural duplex.

Experiments at different NaCl concentrations (Table 4) show that the Tm value for the hybrid involving the fully modified oligonucleotide $d(Tpn)_{11}dT$ **4** and **9** is weakly modified by changes in the ionic strength of the medium either at pH 7 or 5.45. This behaviour most likely reflects the absence of charge repulsion between a non-ionic oligonucleotide and the negatively charged phosphodiester backbone of the target strand as observed for other neutral backbone analogues (8). Consequently, the modification P-NH_2 is not protonated between pH 5.45 and 7. This result is in accord with the known low basicity of phosphoric amide diesters (18,33,34). In contrast, the stability of the 'parent' duplex $d(Tp)_{11}dT$-**9** increases with increasing NaCl concentration as expected. Thus, under low salt conditions (10 mM NaCl), the modified duplex is as stable as the 'parent' one (Table 4).

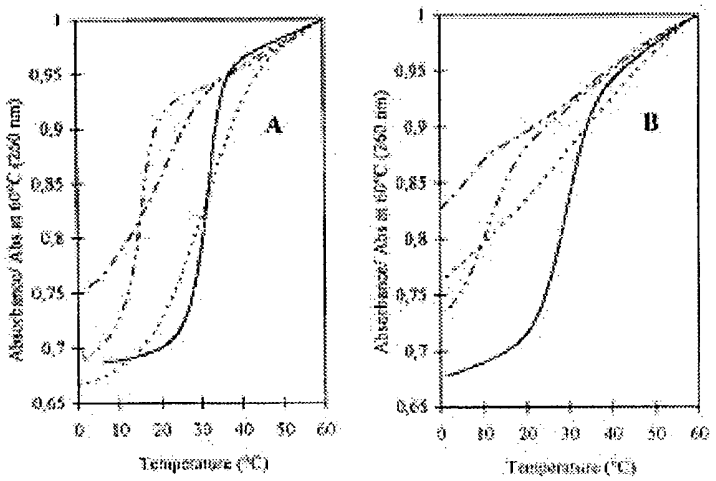

Figure 3. Thermal dissocation curves of the hybrids formed with uniformly modified dodecathymidylate analogues and (**A**) poly dA, (**B**) poly rA. (——), all phosphodiester; (.....), all methylphosphonate; (· ·—· ·), all phosphorothioate; (·—·—), all phosphoramidate. Experimental conditions, as in Table 5.

Table 4. Salt concentration dependence of the Tm (°C) of the fully modified phosphoramidate oligomer with **9** compared with the natural duplex

Oligomer		NaCl concentration		
		0.01 M	0.1 M	1 M
5	pH 7	15	27	42
4	pH 7	13	13	16
4	pH 5.45	14	14	16

Experiments were carried out in a 10 mM sodium cacodylate buffer, at 60 µM nucleotide concentration for each strand.

The affinity of the phosphoramidate oligomer **4** was also compared with that of two other backbone modified dodecathymidines: a phosphorothioate and a methylphosphonate analogues. Data on the interactions with DNA and RNA targets are reported in Table 5 and some typical dissociation curves are shown in Figure 3. It appears, when considering duplexes formed with single stranded DNA, that phosphoramidate linkage is slightly less destabilizing (ΔTm/mod = –1.3°C with **9** and –1°C with poly dA) than the phosphorothioate modification (ΔTm/mod = –1.5°C). Comparatively, the introduction of methylphosphonate linkages into the oligodeoxyribonucleotide does not perturb its ability to bind to the DNA target. However, Figure 3 clearly shows broader melting transitions for neutral methylphosphonate and phosphoramidate analogues than for ionic phosphorothioate and phosphodiester oligomers. These broad curves are most likely due to significant differences in the binding properties of the diastereoisomers within these oligomers (3). In contrast to the behaviour of the neutral phosphoramidate and methylphosphonate oligomers with DNA targets, duplex formation between these oligonucleotides and the RNA target was not detected under the conditions used for these experiments (Fig. 3). Only the upper portion of an apparent melting transition was observed with the phosphoramidate analogue, and the transition with the methylphosphonate compound was so broad that it was not possible to ascertain unambiguously that the oligomer hybridized to the poly rA target. Finally, the ionic phosphorothioate modification was the less destabilizing of the studied modifications (ΔTm/mod = –1.7°C) when considering duplexes formed with the ribonucleotide target.

Table 5. Comparison of hybridization properties[a] of several uniformly modified dodecathymidylates with **9**, poly dA and poly rA

Modification at phosphorus	Complementary strand					
	9		poly dA		poly rA	
	Tm	ΔTm/mod	Tm	ΔTm/mod	Tm	ΔTm/mod
phosphodiester **5**	27	–	31.5	–	29.5	–
phosphorothioate	10.6	–1.5	15.6	1.5	10.4	–1.7
methylphosphonate	27	0	30.5	–0.1	<0[b]	<–2.7
phosphoramidate **4**	13	–1.3	20.5	–1.0	<0	<–2.7

[a]Experiments were carried out in a buffer (pH 7) containing 10 mM sodium cacodylate and 0.1 M sodium chloride, at 60µM nucleotide concentration for each strand.

[b]No evidence for hybridization from the melting curve data (Fig. 3).

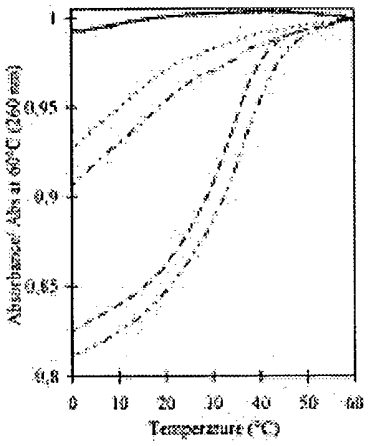

Figure 4. Thermal dissociation curves of the hybrids formed with modified heteropolymers **6** and **7** with DNA or RNA complementary strands. (——), **6** alone; (.....), **6** with ribonucleotide target; (·—·—), **6** with deoxyribonucleotide target; (– – –), **7** with ribonucleotide target; (· ·—· ·), **7** with deoxyribonucleotide target.

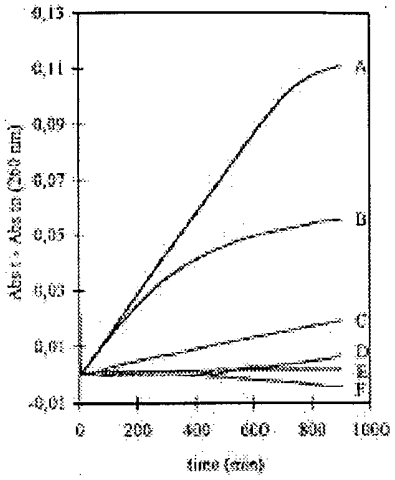

Figure 5. RNase H digestion of poly rA–dodecathymidylate duplexes. Plotted are normalized absorbance at 260 nm versus time. Experiments were carried out at 20°C in a 10 mM Tris–HCl buffer (pH 7) containing 10 mM $MgCl_2$, 0.1 M NaCl, at a 240 μM nucleotide concentration for each strand. (**A**) **5**–poly rA, (**B**) **3**–poly rA, (**C**) **2**–poly rA, (**D**) poly rA alone, (**E**) α$(dTp)_{11}$dT–poly rA, (**F**) **4**–poly rA. All samples were preheated at 70°C, then allowed to slowly cool down and stabilized at 20°C before RNase H was added.

Although the results on the hybridization of the oligothymidine phosphoramidate with poly rA seem disappointing, they deserve comment. First, we have shown that even if the modified oligomer does not form detectable duplexes with the RNA target at 60 μM nucleotide concentration for each strand, it does at higher concentration. In addition, it had been shown recently (35) that a methylphosphonate oligomer linked to a psoralen moiety, which was not able to bind to its target under melting experiment conditions, was effective in cross linking the same target at higher concentration. Secondly, the observed behaviour of the oligonucleotide analogues results from the AT base pairing and could be different with more favourable GC base pairs, as was demonstrated with phosphorothioate analogues (36). Nevertheless, Tm experiments performed with the heteropolymers **6** and **7** (Fig. 4) showed that only the oligomer **7** containing a central section of phosphodiesters was able to hybridize above 0°C with its DNA (36.5°C) or RNA (34°C) complementary strand. Tm values were however ~10°C lower than those of the phosphodiester parent duplexes (47.6 and 46.1°C, respectively, with DNA and RNA targets) (31). From this experiment, it can be pointed out that the difference in stability between duplexes with a deoxyribonucleotide and a ribonucleotide targets is less pronounced with a modified dodecamer of mixed-base sequence (ΔTm/mod = –2°C in both cases) than it was for dodecathymidine analogues. With the fully modified oligonucleoside **6**, only the upper portions of the melting transitions were observed with both DNA and RNA targets. The low binding affinity of these analogues for their RNA target may be exploited in antisense technology. Indeed, it has been shown that chimeric oligonucleotides combining methylphosphonate (37,38) or phosphoramidate (39,40) portions with a central phosphodiester section considerably reduce undesired RNase H cleavage at RNA sites of partial complementary without significantly disturbing activity at the targeted site.

Substrate activity of duplexes formed between phosphoramidate oligomers **2**, **3** or **4** and poly rA for *E.coli* RNase H was evaluated by measuring the UV absorption at 260 nm as a function of time (Fig. 5) as described by Stein *et al.* (36). Duplexes of poly rA with the 'parent diester' $(dTp)_{11}$dT and with its α-anomeric analogue (41) as well as poly rA alone were used respectively as positive and negative controls. It was shown that the chimeric oligonucleotide **3** with a central phosphodiester section was able to elicit RNase H hydrolysis of poly rA, as well as the natural phosphodiester (Fig. 5). This result is in accord with the described behaviour of chimeric oligonucleotides constituted of a central section of phosphodiester surrounded by modified sections (37,38). The fully modified oligonucleotide **4** does not elicit RNase H activity (in the conditions used we obtained a Tm for this duplex at 16°C). Surprisingly, the oligonucleotide **2** with alternated phosphodiester and phosphoramidate internucleoside linkages, is able to induce RNase H cleavage of poly rA, despite the fact that only 50% of the hybrid was present under the conditions used in this experiment. This hydrolysis, however, proceeds far more slowly than with the oligomer **3**.

Enzymatic degradation of oligonucleoside phosphoramidates

Stability of phosphodiester links present in oligonucleotide analogues **2** and **3** was investigated in comparison with that of unmodified $(dTp)_{11}$dT towards the action of purified S1 nuclease, calf spleen phosphodiesterase (CSPDE) or snake venom phosphodiesterase (SVPDE). Table 6 summarises the half-lives of the oligomers. As can be seen, the rate of hydrolysis by nuclease S1 of the alternated oligonucleotide **2** ($t_{1/2}$ = 20.7 h) is greatly reduced compared with that of unmodified **5** ($t_{1/2}$ = 7 min). In contrast, the phosphodiester 'window' of the oligomer **3** is not protected by P-NH_2 sections present at 3′- and 5′-ends. Towards the action of the 5′-exonuclease CSPDE, one modification at the 5′-end of the oligomer **2** prevents vicinal phosphodiester link from the degradation ($t_{1/2} \cong$ 26 h). The stabilizing effect of three

consecutive phosphoramidate modifications at the 5′-end on a neighbouring phosphodiester bond (oligomer **3**, $t_{1/2}$ = 12 days) is more pronounced. When **2** or **3** was incubated with 3′-exonuclease SVPDE, hydrolysis of the phosphodiester bonds was lower when compared with those obtained with **5** ($t_{1/2}$ = 14 min). No significant difference was observed between the two modified oligomers ($t_{1/2}$ = 9 h for compound **2**, and 8.5 h for compound **3**). This could result, at least in part, from the chemical instability of the phosphoramidate link in base medium (pH 9) used in these experiments ($t_{1/2}$ of ~20 h for **2** and **3**). Data reported in Table 6 clearly indicate a pH dependence for the hydrolysis of the phosphoramidate links with a maximum of stability ~pH 7.

Table 6. Half-lives of oligonucleotide analogues in the presence of purified enzymes

	$(dTp)_{11}dT$ (5)	$(dTpndTp)_5dTpndT$ (2)	$(dTpn)_3(dTp)_5(dTpn)_3dT$ (3)
S1 nuclease[a]	7 min	20.7 h (11 days)	7 min (14 days)
CSPDE[b]	22 min	26 h (19 days)	12 days (20 days)
SVPDE[c]	14 min	9 h (23 h)	8.5 h (20 h)

Half-lives were determined by measuring the disappearance of starting oligonucleotide. Reactions were performed at 37°C in:
[a]50 mM sodium acetate buffer (pH 4.5) containing 300 mM sodium chloride and 100 mM zinc acetate;
[b]125 mM ammonium acetate buffer (pH 6.8) containing 2.5 mM EDTA;
[c]100 mM Tris–HCl buffer (pH 9) containing 10 mM magnesium chloride.
Values indicated in brackets refer to half-lives in absence of nuclease.

Phosphoramidate (P-NH_2) represents an interesting oligonucleotide backbone modification because the NH_2 group is small, uncharged in aqueous solution and has favourable solubility characteristics. We have shown that the combination of H-phosphonate and phosphoramidate chemistries, with the use of the easily cleaved oxalyl anchor, labile exocyclic amino protecting groups, and a final deprotection with methanol saturated with ammonia had enabled us to synthesize partially or totally modified dodecadeoxynucleotides. These compounds are able to form hybrids with complementary DNA or RNA strands. The resulting duplexes are significantly less stable than those of the 'wild-type' species, especially with RNA targets. We demonstrated that a modified oligomer combining an internal phosphodiester section surrounded by phosphoramidate sections at 5′- and 3′-ends was resistant to exonuclease hydrolysis and able to elicit RNase H cleavage of the RNA target. These properties make the modification attractive for constructing potential candidates for the antisense approach.

ACKNOWLEDGEMENTS

This work was supported by ANRS (Agence Nationale de Recherche sur le Sida) and ARC (Association pour la Recherche contre le Cancer. One of us (S.P.) thanks the Ministère de l'Enseignement Supérieur et de la Recherche for the award of a research studentship. The authors are grateful to Dr W. Douglas for careful reading of the manuscript.

REFERENCES

1 Uhlmann, E. and Peyman, A. (1990) *Chem. Rev.* **90**, 543–584.
2 Milligan, J. F., Matteucci, M. D. and Martin, J. C. (1993) *J. Med. Chem.* **36**, 1923–1937.
3 Varma, R. S. (1993) *Synlett* **621**, 621–637.
4 Cohen, J. S. (1993) In S. T. Crooke and B. Lebleu (ed.), *Antisense Research and Applications*; CRC Press: Boca Raton (Florida); pp 205–221.
5 Stein, C. A., Tonkinson, J. L. and Yakubov, L. (1991) *Pharmac. Ther.* **52**, 365–384.
6 Crooke, R. M. (1993) In S. T. Crooke and B. Lebleu (ed.), *Antisense Research and Applications*; CRC Press: Boca Raton (Florida); pp 427–449.
7 Miller, P. S. (1989) In J. S. Cohen (ed.), *Oligodeoxynucleotides. Antisense Inhibitors of Gene Expression*, MacMillan Press, London, pp 79–95.
8 Froehler, B. C. and Matteucci, M. D. (1988) *Nucleic Acids Res.* **16**, 4831–4839.
9 Fathi, R., Huang, Q., Syi, J. L., Delaney, W. and Cook, A. F. (1994) *Bioconjugate Chem.* **5**, 47–57.
10 Ozaki, H., Kitamura, M., Yamana, K., Murakami, A. and Shimidzu, T. (1990) *Bull. Chem. Soc. Jpn* **63**, 1929–1936.
11 Durand, M., Maurizot, J. C., Asseline, U., Barbier, C., Thuong, N. T. and Helene, C. (1989) *Nucleic Acids Res.* **17**, 1823–1837.
12 Stec, W. J. and Wilk, A. (1994) *Angew. Chem.* **33**, 709–722.
13 Vyazovkina, E. V., Savchenko, E. V., Lokhov, S. G., Engels, J. W., Wickstrom, E. and Lebedev, A. V. (1994) *Nucleic Acids Res.* **22**, 2404–2409.
14 Nielsen, P., Kirpekar, F. and Wengel, J. (1994) *Nucleic Acids Res.* **22**, 703–710.
15 Sanghvi, Y. S. and Cook, P. D. (1993) In C. K. Chu and Baker D.C. (ed.), *Nucleosides and Nucleotides as Antitumor and Antiviral Agents*, Plenum Press: New York; pp 311–323.
16 Milligan, J. F., Matteucci, M. D. and Martin, J. C. (1993) *J. Med. Chem.* **36**, 1923–1937.
17 Goodchild, J. (1990) *Bioconjugate Chem.* **2**, 165–187.
18 Matrosov, E. I., Kryuchkov, A. A., Nifantyev, E. E., Kozachenko, A. G. and Kabachnik, M. I. (1982) *Phosphorus Sulfur* **13**, 69–78.
19 Letsinger, R. L., Bach, S. A. and Eadie, J. S. (1986) *Nucleic Acids Res.* **14**, 3487–3499.
20 Froehler, B. C. (1986) *Tetrahedron Lett.* **27**, 5575–5578.
21 Peyrottes, S., Vasseur, J. J., Imbach, J. L. and Rayner, B. (1994) *Nucleosides Nucleotides* **13**, 2135–2149.
22 Tomasz, J. (1983) *Nucleosides Nucleotides* **2**, 51–61.
23 Alul, R. H., Singman, C. N., Zhang, G. and Letsinger, R. L. (1991) *Nucleic Acids Res.* **19**, 1527–1532.
24 Sinha, N. D., Davis, P., Usman, N., Perez, J., Hodge, R., Kremsky, J. and Casale, R. (1993) *Biochimie* **75**, 13–23.
25 Polushin, N. N., Morocho, A. M., Chen, B. and Cohen, J. S. (1994) *Nucleic Acids Res.* **22**, 639–645.
26 Madsen, R., Roberts, C. and Fraser-Reid, B. (1995) *J. Org. Chem.* **60**, 7920–7926.
27 Iyer, R. P., Devlin, T., Habus, I., Ho, N. H., Yu, D. and Agrawal, S. (1996) *Tetrahedron Lett.* **37**, 1539–1542.
28 Iyer, R. P., Devlin, T., Habus, I., Yu, D., Johnson, S. and Agrawal, S. (1996) *Tetrahedron Lett.* **37**, 1543–1546.
29 Stec, W. J., Zon, G., Egan, W., Byrd, R. A., Philips, L. R. and Gallo, K. A. (1985) *J. Org. Chem.* **50**, 3908–3913.
30 Tomasz, J. and Simoncsits, A. (1981) *Tetrahedron Lett.* **22**, 3905–3908.
31 Morvan, F., Porumb, H., Degols, G., Lefebvre, I., Pompon, A., Sproat, B. S., Rayner, B., Malvy, C., Lebleu, B. and Imbach, J. L. (1993) *J. Med. Chem.* **36**, 280–287.
32 Jung, P. M., Histand, G. and Letsinger, R. L. (1994) *Nucleosides Nucleotides* **13**, 1597–1605.
33 Oney, I. and Caplow, M. (1967) *J. Am. Chem. Soc.* **89**, 6972–6980.
34 Bollinger, J. C., Faure, R. and Yvernault, T. (1983) *Canad. J. Chem.* **61**, 328–333.
35 Kean, J. M., Cushman, C. D., Kang, H. M., Leonard, T. E. and Miller, P. S. (1994) *Nucleic Acids Res.* **22**, 4497–4503.
36 Stein, C. A., Subasinghe, C., Shinozuka, K. and Cohen, J. S. (1988) *Nucleic Acids Res.* **16**, 3209–3221.
37 Giles, R. V. and Tidd, D. M. (1992) *Anti-Cancer Drug Des.* **7**, 37–48.
38 Giles, R. V. and Tidd, D. M. (1992) *Nucleic Acids Res.* **20**, 763–770.
39 Dagle, J. M., Walder, J. A. and Weeks, D. L. (1990) *Nucleic Acids Res.* **18**, 4751–4757.
40 Potts, J. D., Dagle, J. M., Walder, J. A., Weeks, D. L. and Runyan, R. B. (1991) *Proc. Natl. Acad. Sci. USA* **88**, 1516–1520.
41 Bloch, E., Lavignon, M., Bertrand, J. R., Pognan, F., Morvan, F., Malvy, C., Rayner, B., Imbach, J. L. and Paoletti, C. (1988) *Gene* **72**, 349–360.

Nat. Gent. 1992 1:372-378
Science 1989 245:1234-1236

Eur. J Biochem. 1985 148:265-270

Mol. Immunol 1995 32:1057-1064

Science 1993 259:988-990

Nature 1988 336:348-352

J Clin. Invest. 1993 91:225-234

Mol. Cell. Biol. 1987 7:1576-1579

Gene 1982 19:33-42

Neuron 1992 8:507-520

Adv. Virus Res. 1989 37:35-83

1994 Cancer Res. 54:5258-5261

Cell 1987 50:435-443

Nucleic Acids Res. (1996) 24(10):1841-1848

J Biol. Chem. 1988 263 10 :4837-4843

Proc. Natl. Acad. Sci. USA 1992 89:2581-2584

1993 Nature 361:647-650

DNA Seq. 1993 4:185-196

Human Gene Ther. 1995 6:881-893

Science 1991 252:431-434

Cell 1992 68:143-155

Mol. Cell. Biol. 1990 10 6 :2738-2748

Nucleic Acids Res. 1996 24 15 :2966-2973

Human Gene Thera 1990 1:241-256

J Clin. Invest 1992 . 90:626-630

Curr. Topics in Micro. and Imm. 1995 199 part 3 :177-194

Lancet 1981 11:832-834

Cancer Res. 1996 56:1341-1345

J Virol. 1992 66 (6) :3633-3642

J Virol. 1996 70 (4) :2296-2306

Nature (1997) 389:239-242

J Virol. 1984 51 (3) : 822-831

Adv. Ex . Med. Biol. 1991 3098:61-66

Proc. Natl. Acad. Sci. 1983 80:5383-5386

Genomics 1990 8:492-500

Gastroenter. 1990 98:470-477 .

N. Vogel
AU 1636
12/9
10045116

THE JOURNAL OF BIOLOGICAL CHEMISTRY
Vol. 263, No. 10, Issue of April 5, pp. 4837-4843, 1988
Printed in U.S.A.

Expression of Soluble and Fully Functional Ricin A Chain in *Escherichia coli* Is Temperature-sensitive*

(Received for publication, August 18, 1987)

Michael Piatak, Julie A. Lane, Walter Laird, Michael J. Bjorn, Alice Wang, and Mark Williams
From the Cetus Corporation, Emeryville, California 94608

Linkage of ricin A chain (RA) to a cell surface binding antibody or other ligand can result in a potent cytotoxic agent. We expressed the primary sequence for RA in *Escherichia coli* to facilitate production and to obtain protein free of naturally occurring contaminants, *i.e.* ricin B chain. Differences in the level of expression and in the characteristics of the expressed protein were noted when several different host/vector systems were tested. Recombinant RA (rRA) was expressed directly under control of the phage λ major leftward promoter (P_L) and the *E. coli trp* promoter. It was also expressed fused to *E. coli* alkaline phosphatase sequences, both in the same reading frame for secretion and out-of-reading frame for expression in a cistron-like arrangement. Expression in the P_L promoter system, which is temperature-regulated, was achieved at 37 °C as well as at 42 °C. The protein expressed at these different temperatures had grossly different properties. Whereas rRA expressed at 37 °C was soluble and fully active, that produced at 42 °C was aggregated, insoluble, and reduced in activity. Soluble rRA could be converted to the insoluble form by incubation at 42 °C *in vivo*, but not *in vitro*. Hence, this difference in properties does not simply reflect an inherent thermal instability of the protein. Conditions present *in vivo*, including the possible association with other proteins, are apparently required for this effect on rRA.

The A subunit of ricin, ricin A chain (RA),[1] has been a commonly used effector molecule for the synthesis of selectively targeted cytotoxic reagents such as immunotoxins (for reviews, see Refs. 1–3). Upon internalization, RA catalytically inactivates the large subunit of eukaryotic ribosomes, thereby causing cell death (for reviews on ricin, see Refs. 1–4). RA is a potent agent as it is able to inactivate approximately 1500 ribosomes/min. Recently, Endo *et al.* (5, 6) reported that the action of RA and related proteins on ribosomes is to cleave the *N*-glycosidic bond in the A4324 residue of 28 S rRNA, releasing adenine and exposing phosphodiester linkages to hydrolysis.

Purification of native RA from whole toxin can be difficult, involving its efficient separation from ricin B chain (RB) which binds cell surface galactose-containing structures and enhances entry of RA into the cytoplasm (7, 47). Preparations of RA and its conjugates must be rigorously controlled to avoid even trace amounts of contaminating toxin or RB that might obscure the target selectiveness of the hybrid toxin and increase general toxicity. In addition, working with large quantities of castor beans and ricin poses a health risk (8). To avoid these problems and to more economically obtain large quantities of RA for therapeutic development, we opted to express the gene for RA in *Escherichia coli*. Another potential advantage of this is that proteins expressed in *E. coli* are not glycosylated. There is evidence suggesting that the general toxicity of native glycosylated RA and its conjugates may be related to mannose-dependent uptake by the liver (9).

The cDNA and genomic sequences for ricin have been reported (10, 11). RA is synthesized with RB in a preproricin molecule. The coding order is a secretory signal, RA, a 12-amino acid junction peptide, and RB. We cloned cDNA coding specifically for RA and modified it to allow for its independent expression in several different vectors of *E. coli*. We found that under different induction conditions and also in different fusions to *E. coli* alkaline phosphatase signal peptide sequences, soluble fully active rRA was produced, although expression levels varied. We also observed that insoluble less active product was expressed at 42 °C, a condition typical for induction of promoters regulated by temperature-sensitive repressors, in this case the phage λ major leftward promoter (P_L). Expression from this promoter could be induced at lower temperatures, however, enabling us to study the effects on the expressed product of temperature manipulation during expression. The effects observed and the results mentioned above are reported here.

EXPERIMENTAL PROCEDURES AND RESULTS AND DISCUSSION[2]

Secretion and Translation-coupled Expression—As discussed in the Miniprint, rRA expressed in an insoluble aggregate form is not suited to the production of active hybrid toxins. Obviously, expression of rRA in a soluble form is preferred. One approach to express soluble rRA in *E. coli* is to secrete the protein to the periplasmic space. As RA is normally part of a secreted protein, it is possible that secretion from *E. coli* and the cooperative transport from the intracellular reducing environment to the oxidizing environment of

* The costs of publication of this article were defrayed in part by the payment of page charges. This article must therefore be hereby marked "*advertisement*" in accordance with 18 U.S.C. Section 1734 solely to indicate this fact.

The nucleotide sequence(s) reported in this paper has been submitted to the GenBank™/EMBL Data Bank with accession number(s) J03184.

[1] The abbreviations used are: RA, ricin A chain; rRA, recombinant ricin A chain; RB, ricin B chain; DEPC, diethylpyrocarbonate; SDS, sodium dodecyl sulfate; CTAB, cetyltrimethylammonium bromide; PBS, standard phosphate-buffered saline; PAGE, polyacrylamide gel electrophoresis.

[2] Portions of this paper (including "Experimental Procedures," part of "Results and Discussion," Figs. 1 and 2, and Tables I and II) are presented in miniprint at the end of this paper. Miniprint is easily read with the aid of a standard magnifying glass. Full size photocopies are included in the microfilm edition of the Journal that is available from Waverly Press.

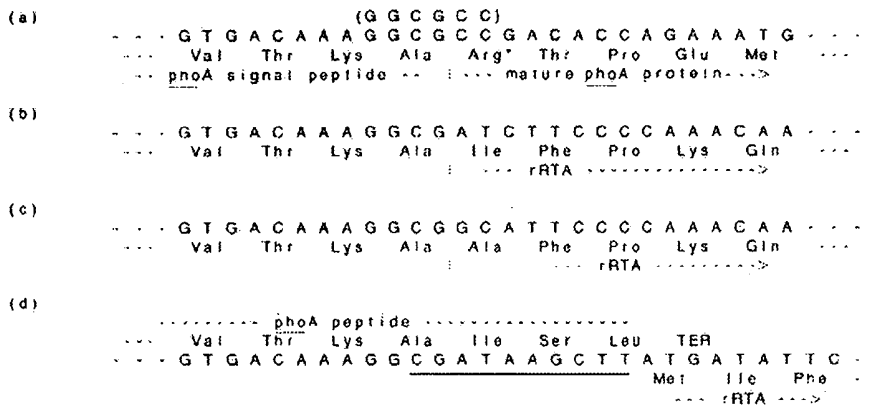

FIG. 3. **Alkaline phosphatase/rRA fusion sequences.** The DNA coding strand sequences and deduced amino acid sequences of the actual or predicted processing sites for signal peptidase are shown. *a*, *E. coli* alkaline phosphatase (*pho*A) sequence. *b*, fusion sequence in pRAP2210. *c*, fusion sequence in pRAP218. *d*, fusion sequence in pRAP229. The *Nar*I site introduced in the *pho*A sequence to facilitate fusion is shown in *parentheses* above the sequence in *a*. The sequence in the pRAP229 fusion derived from the vector portion of pRAT1 is *underlined* in *d*. *, the native arginine codon is changed to one for proline due to the introduction of the *Nar*I site.

the periplasm might effect proper folding and solubility. The coding sequence for rRA was modified by primer-directed mutagenesis to introduce restriction sites (Fig. 1) that would allow for fusion to a modified sequence encoding the *E. coli* alkaline phosphatase (*pho*A) signal peptide. Two types of such fusions were produced (Fig. 3, *b* and *c*) differing in the potential processing sequence for signal peptidase. Cleavage of the precursor to alkaline phosphatase occurs after the sequence Thr-Lys-Ala and releases mature phosphatase having an arginine at the N terminus (Fig. 3*a*). The fusion contained in pRAP2210 (Fig. 3*b*) was designed for cleavage after the same sequence at the end of the *pho*A peptide and for release of a mature rRA protein having the native isoleucine at its N terminus. The fusion contained in pRAP218 (Fig. 3*c*), however, was designed to be homologous to a *pho*A-human growth hormone fusion which had been found to be efficiently processed and resulted in secretion of human growth hormone to the periplasm.[3] In that fusion, cleavage occurs after the second alanine in the sequence Thy-Lys-Ala-Ala-Phe-Pro. In the pRAP218 fusion, then, the isoleucine normally found at the beginning of the mature RA sequence was changed to alanine, thereby generating the same sequence recognized for processing noted above.

In addition to these constructions designed for protein secretion, a third type of fusion was generated for intracellular accumulation of rRA. This fusion, shown in Fig. 3*d* and contained in pRAP229, links the rRA sequence to the *pho*A signal peptide in a cistron-like arrangement. A potential start codon for rRA is placed out-of-frame to, but overlapping, a termination codon for a *pho*A peptide. The overlap sequence, ATGA, where ATG is the start codon for the one reading frame and TGA is the termination codon for the other, is found most notably in the N region of phage λ (35). The expression of this fusion and the two *pho*A-rRA fusions described above is directed by the *pho*A promoter and ribosome binding site contained in the cloned *pho*A fragment.

Secretion of rRA product to the periplasm was tested by osmotic shock treatment (31). In addition, whole cell extracts were prepared by sonication in the absence of detergents to assess the solubility of the products. A Western blot analysis on different cellular fractions for pRAP218- and pRAP229-expressed products shows the results obtained (Fig. 4). (The

[3] S. Chang, personal communication.

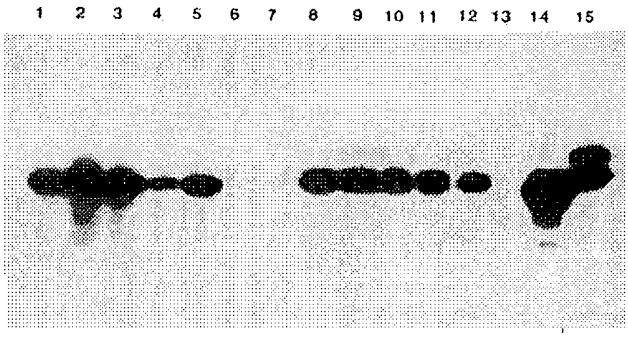

FIG. 4. **Western blot analysis of pRAP229- and pRAP218-expressed rRAs.** Cells carrying pRAP229 and pRAP218 were appropriately induced for expression of rRA and fractionated as noted under "Experimental Procedures." Samples equivalent to that derived from 0.2–0.4 A_{550} units or cells were loaded per lane. *Lanes 1–6* show pRAP229 samples; *lanes 8–13* show pRAP218 samples. The sample order in each case is: total sonicate in the presence of 1% SDS to release total material; 100,000 × *g* supernatant fraction after sonication without SDS; 12,000 × *g* supernatant fraction after sonication without SDS; 12,000 × *g* pellet fraction after sonication without SDS; cell pellet after osmotic shock; supernatant from osmotic shock. *Lane 7* shows a total sonicate with SDS of uninduced pRAP218 as a control. *Lane 14* shows about 3 μg of pRAL6 rRA. *Lane 15* shows about 3 μg of native RA.

results obtained for pRAP2210 are identical to those for pRAP218). Both types of fusions lead to production of rRA products. The pRAP218 (and pRAP2210) secretion construct expressed two major immunoreactive products in the M_r 28,000–30,000 range (a doublet is apparent in Fig. 4, *lanes 8–12*). The pRAP229 fusion construct expressed a single predominant immunoreactive product of about M_r 28,000 (Fig. 4, *lanes 1–5*).

Potentially, the slower migrating product from pRAP218 cells could be unprocessed *pho*A-rRA precursor whereas the faster migrating product could be the processed form. However, osmotic shock treatment did not separate the two forms as would be expected if one were secreted to the periplasm; both forms remained associated with the intact cells (Fig. 4, *lane 12 versus 13*). A gel run in parallel and stained with Coomassie showed that several *E. coli* proteins were selectively released by the osmotic shock treatment. Also, in an

analogous experiment, spheroplasts were generated with lysozyme; again, all rRA products remained associated with the intact cells and, additionally, were noted to be resistant to protease degradation (data not shown). The faster migrating product from pRAP218 also runs slightly slower than the rRA produced by pRAL6 or by pRAP229, either of which should represent the mature RA primary sequence with, at most, an additional methionine at its N terminus. The N terminus for the pRAP229 product has been sequenced and was found to be 60% Ile-Phe- and 40% Met-Ile-Phe- (36). Compare, for example, *lanes 5* and *14* to *lane 12* in Fig. 4. These data suggest that both of the pRAP218-expressed rRA products were intracellularly compartmentalized and that the smaller product was not derived from the larger one by the expected signal peptidase cleavage. It is possible that the smaller product was derived from the larger by alternative proteolytic cleavage, however, near either the N terminus or the C terminus of the protein. Another possibility is that the smaller product resulted from a second translation start at a GUG signal four codons upstream of the beginning of the rRA coding sequence. A GUG start codon is the signal utilized for translation of the *pho*A gene (37), and alternative mRNA secondary structures could allow for alternative starts (38). We have not pursued these possibilities.

Analyses of cell sonicate fractions to assess the solubility of the pRAP218 and pRAP229 rRA products showed surprising results, however. The distribution of rRAs among a 12,000 × *g* pellet, a 12,000 × *g* supernatant, and a 100,000 × *g* supernatant was examined. The results are shown in Fig. 4, *lanes 1–4* for pRAP229 and *lanes 8–11* for pRAP218. It is clear that rRA products distributed in both the pellet and the supernatant fractions for both constructs, but cell disruption was incomplete. Importantly, however, rRA products from both pRAP229 and pRAP218 cells remained in the 100,000 × *g* supernatant, a good criterion for solubility. It is interesting that both pRAP218 rRA products were soluble, suggesting that the *pho*A-rRA proteins did not associate with the bacterial membrane and were never candidates for secretion. The apparent solubility of the larger putative complete precursor form was particularly surprising because of the hydrophobic character of the signal peptide.

We observed that the proportion of the larger to the smaller rRA species from pRAP218 varied with each experiment. However, the combined expression level of these rRA products was reproducibly 1–2% of total cell protein. In contrast, the single pRAP229 rRA product was expressed at 6–8% of total cell protein. The reasons for this difference in expression levels from similar constructs are not clear and are likely to be complex and interactive. Their study is best the concern of a separate report. For our purposes here, though, the pRAP229 clone was subsequently selected for scale-up production of soluble rRA. The partial characterization and activity profile of this protein are described in a later section.

Temperature Effects on Expression of Soluble rRA—To summarize our results to this point, we had observed expression of freely soluble rRA at up to 8% of total cell protein from a vector/host system in which the RA sequence was linked to a *pho*A peptide, transcription and protein expression was induced by phosphate depletion and regulated by the *pho*A promoter, and the template copy number remained relatively low throughout. In addition, we had observed expression of insoluble aggregated rRA at up to 6% of total cell protein from a vector/host system in which the RA sequence was translated independently; transcription and protein expression were regulated by the phage λ P_L promoter and were rapidly induced by thermal inactivation of a repressor protein and augmented by a concurrent rapid increase in template copy number (Miniprint). Because there are several differences between the two systems, it was at first difficult to focus on a particular characteristic which could offer an explanation as to how insoluble *versus* soluble rRA was expressed. Consequently, we decided to re-examine the expression of rRA from the existing pRAT1 vector/host system to gain a third perspective on the process.

Again, pRAT1 carries the rRA sequence under control of the *E. coli trp* promoter. Our results (data not shown) indicated that rRA expressed from pRAT1 behaved similarly to that from pRAP229 in that it was found in the supernatant of cell sonicates. We did note that the detectable level of expression of rRA varied from experiment to experiment but that levels higher than initially observed, *i.e.* 6–8% of total cell protein, could be obtained. Different host isolates and extreme measures to reduce intracellular tryptophan levels were important. In particular, the highest levels of expression on a percent basis were observed if the host strain, KB2, was used. KB2 is a transductant of MM294 carrying the mutation, *trp*A46*pr*9 (39), which leads to a deficiency in tryptophan synthesis. These cells grew poorly, however, and total cell mass was typically reduced, resulting in an overall lower yield of product.

The expression of soluble rRA, then, is not dependent on linkage to *pho*A coding or regulatory sequences. In addition, there is no obvious correlation to plasmid copy number as pRAT1, a pBR322-based plasmid, is 5–10-fold more abundant per cell than pRAP229, a pACYC184-based plasmid. Given that two separate systems expressed soluble rRA under very different conditions, we thought it more relevant to ask what contributes to the production of insoluble rRA in the pRAL6 system. In this, there was one obvious difference in the manner of inducing expression from pRAL6 *versus* the other plasmids that warranted further study, *i.e.* temperature. As described under "Experimental Procedures," expression regulated by P_L is easily and commonly induced when the host cell carries a temperature-sensitive repressor for the promoter. In this case, pRAL6 was propagated in a host strain lysogenic for the λ prophage, $\lambda N_7 N_{53} cI_{857} SusP80$. There are three important features of this system regarding the practical induction of P_L. 1) Direct inactivation of the temperature-sensitive cI_{857} repressor occurs at 40–42 °C. 2) Inactivation of the cI_{857} repressor allows for expression of the *cro* gene product which is also carried in the prophage and which then represses further synthesis of the cI_{857} repressor, leading to "autoinactivation" of the repressor (40). 3) The copy number of the plasmid, pRAL6, is highest at 42 °C, 30–40-fold higher than that at 30 °C or about 300–500 copies/cell, but is also increased at 37 °C, the extent to which is dependent on the length of time at that temperature.[4] It follows that a high copy number of the operator sequence carried on pRAL6 could titrate available repressor to a point at which *cro* is activated, thereby leading to complete induction of the P_L promoter. Induction of rRA expression, then, need not depend on continued incubation at 42 °C and may be achieved by incubation at lower temperatures, *e.g.* 37 °C.

The following set of experiments was performed to test for expression of soluble and insoluble rRA from pRAL6. Cultures of pRAL6/DG95λ were propagated at 30 °C to an A_{550} of about 0.6. Several conditions were then tested for induction of rRA expression involving shifting the temperature of the cultures between 37 and 42 °C. Cells were harvested and disrupted by sonication, and aliquots of total sonicated material, material remaining in solution after centrifugation at

[4] D. Gelfand, personal communication.

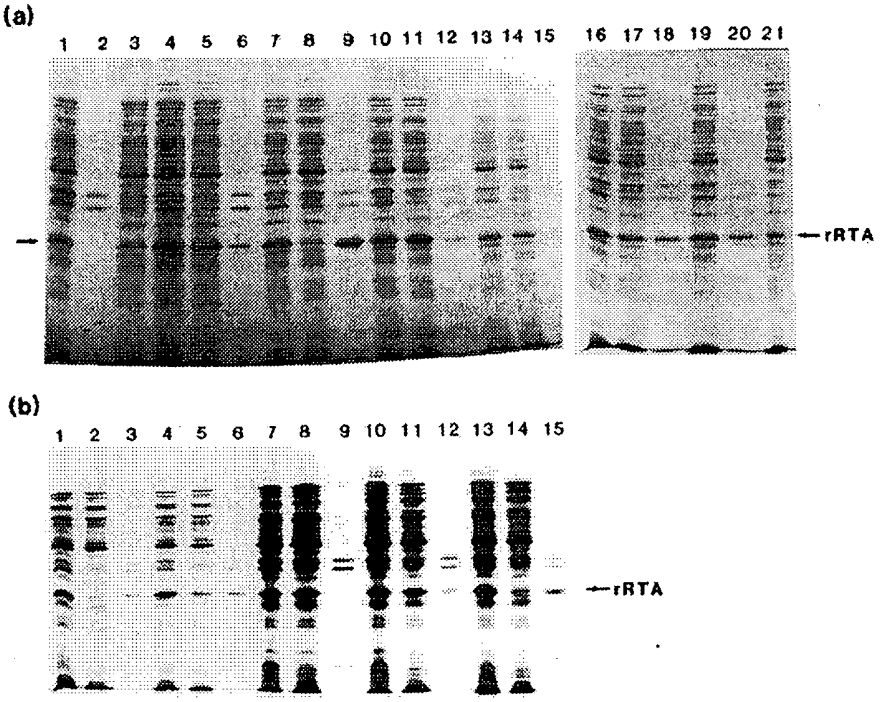

FIG. 5. **SDS-polyacrylamide gel electrophoresis analysis showing the effect of temperature on expression of rRA as a soluble *versus* insoluble product.** *a*, 500-ml culture of pRAL6/DG95λ was grown at 30 °C to an A_{550} of about 0.6. Aliquots (50 ml) were then removed and incubated under various conditions as noted below for a total of 3 h. Cells were harvested and disrupted by sonication and fractionated into 12,000 × *g* supernatant and pellet fractions. Aliquots (10 μl) adjusted to contain comparable amounts of material were loaded on a mini-gel (Hoeffer). *Lanes 1–3* show total sonicate, pellet, and supernatant, respectively, of cells incubated at 37 °C only. *Lanes 4–6* show total sonicate, supernatant, and pellet, respectively, of cells brought up to 42 °C and then immediately switched to 37 °C. *Lanes 7–9* show total sonicate, supernatant, and pellet, respectively, of cells brought up to 42 °C, then incubated at 37 °C for 2 h and 30 min, and then switched back to 42 °C for 30 min. *Lanes 10–12, 13–15, 16–18*, and *19–21*, respectively, are for cells incubated at 42 °C for 15 min, 30 min, 1 h, and 2 h followed by incubation at 37 °C for the remainder of the 3-h period. The loading order is total sonicate, supernatant, and pellet, respectively, for *lanes 10–12, 13–15*, and *16–18*; the loading order is total sonicate, pellet, and supernatant, respectively, for *lanes 19–21*. *b*, a 600-ml culture of pRAL6/DG95λ was grown at 30 °C to an A_{550} of about 0.6. The entire culture was quickly brought up to 42 °C and then incubated under the conditions given below. Cell fractions were prepared and aliquots were analyzed as noted above. The order of loading is the same in each set of samples, i.e. total sonicate, supernatant, and pellet, respectively. *Lanes 1–3* are for cells incubated at 42 °C for an additional 2 h. *Lanes 4–6* are for those cells incubated at 42 °C for 2 h and then incubated at 37 °C for 1 h. *Lanes 7–9* are for cells incubated at 37 °C for 5 h. *Lanes 10–12* are for those cells incubated at 37 °C for 5 h and then shifted to 42 °C for 1 min. *Lanes 13–15* are for the same as in the previous lanes, but shifted to 42 °C for 30 min. An *arrow* indicates the position of rRA.

12,000 × *g* for 10 min, and material pelleted in the same centrifugation were analyzed by SDS-polyacrylamide gel electrophoresis. The results from two series of experiments are shown in Fig. 5, *a* and *b*, respectively. First, it is clear that cells induced by incubation solely at 37 °C or by incubation at 42 °C for up to 30 min followed by continued incubation at 37 °C produced soluble rRA (Fig. 5*a*, *lanes 1–6* and *10–15*). The level of expression after 3 h at 37 °C was significantly lower than that achieved if the cells were briefly exposed to 42 °C (Fig. 5*a*, *lane 1 versus lane 4*). However, maximum levels of expression at 37 °C were attained if the length of the incubation was extended (data not shown). The small amount of insoluble rRA noted after even a brief exposure to 42 °C was reproducible. However, significant amounts of insoluble product were not observed until incubations at 42 °C were carried out for 1 h or longer (Fig. 5*a*, *lanes 16–21*; Fig. 5*b*, *lanes 1–6*). In the same cultures, though, continued incubations at 37 °C resulted in expression of soluble product. As is best shown in Fig. 5*b* (*lanes 1–6*) for cultures sampled before and after temperature shift, these results indicate that rRA produced at 42 °C is insoluble, whereas that produced at 37 °C is soluble. Also shown in Fig. 5*b* (*lanes 3* and *6*), the amount of insoluble rRA produced in 2 h at 42 °C remained fairly constant with incubation at 37 °C, suggesting that it is not easily converted, at least, to a soluble form. This is consistent with our earlier observations noted above.

We next tested if already produced soluble rRA could be converted to the insoluble form by shifting the incubation temperature from 37 to 42 °C. The results of such experiments are shown in Fig. 5*a* (*lanes 7–9*) and Fig. 5*b* (*lanes 7–15*). Cells were induced by briefly raising the temperature to 42 °C followed by incubation at 37 °C to establish production of soluble rRA. Samples were then shifted back to 42 °C for 1 and 30 min, respectively. The conversion of pre-expressed soluble rRA to insoluble rRA can clearly be followed in Fig. 5*b* (*lanes 7–15*). This conversion of soluble to insoluble product was also tested *in vitro*. Aliquots of the total sonicate fraction shown in Fig. 5*a* (*lane 4*) were incubated at 42 °C for 5, 10, 20, and 40 min, respectively, and analyzed as before. In each case, exactly the same profile as that shown in Fig. 5*a*

(*lanes 4–6*) resulted. In a complementary test, a fraction containing the insoluble material shown in Fig. 5*a* (*lane 7*) was incubated at 37 °C for 30 min and analyzed. As expected, no conversion of insoluble to soluble material was noted.

Taken together, these results suggest that production of insoluble rRA at 42 °C is not simply due to an inherent thermal instability of the protein. As one can obtain conversion of soluble to insoluble rRA *in vivo* but not *in vitro*, factors relating to the intracellular environment such as ionic conditions or local concentration or the active translation of rRA itself or another heat-induced protein might be important. Attempts to duplicate the *in vivo* phenomenon *in vitro* are still under study. It is clear from these data, however, that the temperature selected for production of heterologous proteins in *E. coli* can be a very important consideration. One of us has noted differences in the physical characteristics of other proteins expressed in *E. coli* at 37 °C or lower *versus* 42 °C.[5]

Activity and Characteristics of the Soluble rRA—For production of large amounts of rRA, pRAP229/MM294 was selected and scaled up in 10-liter fermentation. The rRA from this source was purified to greater than 95% homogeneity by sequential chromatography on phenyl-Sepharose and carboxymethylcellulose. As previously determined for the SDS-soluble rRA, we assessed the ability of the soluble rRA to inhibit reticulocyte translation *in vitro* and the activity of immunoconjugates prepared with it. In addition, the single-dose toxicity in mice for the recombinant and native proteins was compared. The results listed in Table II indicate that, within the parameters that we have set, rRA is equivalent in activity and toxicity to native RA. Others have reported on the use of this rRA in the preparation of selected immunoconjugates and have tested their effectiveness on target cells *in vitro* and *in vivo* (41, 42). The conjugates performed similar to expected for native RA conjugates but are still low in cytotoxic activity compared to that for the model compound, ricin.

Immunoconjugates prepared with whole ricin or with RA but assayed in the presence of RB display much higher cytotoxic activities and show greater potential to be effective for tumor therapy (48). However, the cell-binding properties of RB can significantly reduce the selectivity of the immunoconjugates and effectively eliminate any advantage that they may have in activity. There have been several attempts to eliminate this problem including the preparation of ricin immunoconjugates in which the RB galactose-binding sites are sterically (49) or chemically (50) blocked and by the delivery of RB to the target cell by a second antibody (7). Each approach, however, would present a new difficulty such as product purification and quality control in the former cases and complexity of therapeutic administration in the latter. The ability to produce active and fully functional rRA in *E. coli* reported here suggests that another approach is to extend the expressed rRA sequence to include a sequence for RB specifically modified to eliminate or diminish galactose-binding activity or to include only a portion of RB that could specifically enhance cell entry of rRA. However, the question of whether or not such a modified RB, or fragment thereof, is possible has yet to be resolved conclusively (50), and it is likely that genetic manipulation of a cloned sequence will be necessary to provide that information. The cloning and expression of active RB in a mammalian system has been reported recently (51), and residues important for galactose binding have been identified (44). Nonetheless, the design and expression of other types of "improved" hybrid rRA molecules containing membrane interaction or translocation domains such as, for example, those identified in diphtheria toxin (52) or *Pseudomonas* endotoxin A (34) might be possible. Robertus *et al.* (43) have obtained diffractable crystals of the rRA reported here, and a total structural determination should be useful in the design of such molecules. It will also be of interest to compare this structure to that of the native glycosylated RA as it exists in its heterodimer configuration with RB (44) and to address other structure/function relationships through changes in the expressed gene sequence.

As mentioned in the Introduction, the toxicity of native RA and its conjugates may be related to its sugar-selective uptake by the liver. The ultimate utility and/or any advantage that *E. coli*-expressed rRA may have over the native protein may be due to its lack of glycosylation. A final assessment of this molecule is dependent upon the results of pharmacokinetic studies as well as studies on the *in vivo* efficacy of rRA conjugate in relevant tumor model systems and patient therapy.

While this manuscript was in preparation, O'Hare *et al.* (45) reported on the expression of an RA fusion protein in *E. coli*. They indicated that product expressed at 37 °C is aggregated and substantially less active than if it is expressed at 30 °C. We have noted somewhat higher levels of rRA expression on a percent basis, *i.e.* about 10–11%, from pRAP229 if inductions are carried out at 30 °C but have not observed any differences in the physical or enzymatic characteristics of the protein. It is possible that this difference may be related to different culturing or extraction conditions, or more likely, to the additional 10 amino acids at the N terminus of their protein. Although the generation of a gene fusion can facilitate the expression of a desired sequence, one should be aware that important protein characteristics may be altered. In this case, the usefulness of their protein as a therapeutic agent may be limited.

Acknowledgments—We gratefully acknowledge the following contributions of our colleagues: K. Bauer and S. Clark, culture fermentation; S.-Y. Chang, D. Gelfand, L. Greenfield, and G. Horn, plasmids, helpful discussions, and computer assistance; L. Goda and D. Spasic, synthetic oligonucleotides; G. Groetsema, technical assistance; R. Bengelsdorf, K. Levenson, E. Ladner, and S. Nilson, manuscript preparation.

[5] W. Laird, unpublished results.

REFERENCES

1. Olsnes, S., and Pihl, A. (1982) *Pharmacol. Ther.* **15**, 355–381
2. Moller, G. (ed) (1982) *Immunol. Rev.* **62**
3. Vitetta, E. S., and Uhr, J. W. (1985) *Cell* **41**, 653–654
4. Olsnes, S., and Pihl, A. (1982) in *Molecular Action of Toxins and Viruses* (Cohen, P., and Van Heyningen, S., eds) pp. 51–105, Elsevier Scientific Publishing Co., Inc., New York
5. Endo, Y., Mitsui, K., Motizuki, M., and Tsurugi, K. (1987) *J. Biol. Chem.* **262**, 5908–5912
6. Endo, Y., and Tsurugi, K. (1987) *J. Biol. Chem.* **262**, 8128–8130
7. Vitetta, E., Cushley, W., and Uhr, J. (1983) *Proc. Natl. Acad. Sci. U. S. A.* **80**, 6332–6335
8. Morton, J. F. (1977) in *Forensic Medicine* (Tedeschi, C. G., Eckert, W., and Tedeschi, L. G., eds) pp. 1456–1567, W. B. Saunders Co., Philadelphia
9. Skilleter, D. N., Price, R. J., and Thorpe, P. E. (1985) *Biochim. Biophys. Acta* **842**, 12–21
10. Lamb, F. I., Roberts, L. M., and Lord, J. M. (1985) *Eur. J. Biochem.* **148**, 265–270
11. Halling, K. C., Halling, A. C., Murray, E. E., Ladin, B. F., Houston, L. L., and Weaver, R. F. (1985) *Nucleic Acids Res.* **13**, 8019–8033
12. Berger, S. L., and Birkenmeier, C. S. (1979) *Biochemistry* **18**, 5143–5149
13. Bjorn, M. J., Larrick, J., Piatak, M., and Wilson, K. J. (1984) *Biochim. Biophys. Acta* **790**, 154–163
14. Bjorn, M. J., Ring, D., and Frankel, A. (1985) *Cancer Res.* **45**, 1214–1221

16. Lord, J. M., and Roberts, L. M. (1982) *Planta (Berl.)* **152**, 420–427
16. Bellamy, A. R., and Ralph, R. K. (1968) *Methods Enzymol.* **12B**, 156–160
17. Pemberton, R. E., Liberti, P., and Baglioni, C. (1975) *Anal. Biochem.* **66**, 18–28
18. Maniatis, T., Fritsch, E. F., and Sambrook, J. (1982) *Molecular Cloning, A Laboratory Manual*, Cold Spring Harbor Laboratory, Cold Spring Harbor, NY
19. Maxam, A. M., and Gilbert, W. (1980) *Methods Enzymol.* **65**, 499–560
20. Sanger, F., Nicklen, S., and Coulson, A. R. (1979) *Proc. Natl. Acad. Sci. U. S. A.* **74**, 5463–5467
21. Messing, J., and Vieira, J. (1982) *Gene (Amst.)* **19**, 269–276
22. McCormick, F., and Innis, M. (1986) *Methods Enzymol.* **119**, 397–403
23. Greenfield, L., Dovey, H. F., Lawyer, F. C., and Gelfand, D. H. (1986) *Bio/Tech.* **4**, 1006–1011
24. Casadaban, M., and Cohen, S. N. (1980) *J. Mol. Biol.* **138**, 179–207
25. Meselson, M., and Yuan, R. (1968) *Nature* **217**, 1110–1114
26. Mark, D. F., Lu, S. D., Creasey, A. A., Yamamoto, R., and Lin, L. S. (1984) *Proc. Natl. Acad. Sci. U. S. A.* **81**, 5662–5666
27. Bolivar, R., Rodriguez, R. L., Greene, P. J., Betlach, M. C., Heynecker, H. L., Boyer, H. W., Crosa, J. H., and Falkow, S. (1977) *Gene (Amst.)* **2**, 95–113
28. Chang, A. C. Y., and Cohen, S. N. (1978) *J. Bacteriol.* **134**, 1141–1156
29. Wong, H. C., and Chang, S. (1986) *Proc. Natl. Acad. Sci. U. S. A.* **83**, 3233–3237
30. Michaelis, S., Guarante, L., and Beckwith, J. (1983) *J. Bacteriol.* **154**, 356–365
31. Nossal, N. G., and Heppel, L. A. (1966) *J. Biol. Chem.* **241**, 3055–3062
32. Laemmli, U. K. (1970) *Nature* **227**, 680–685
33. Nyari, L. J., Tan, Y. H., and Erlich, H. A. (1983) *Hybridoma* **2**, 79–86
34. Hwang, J., Fitzgerald, D. J., Adhya, S., and Pastan, I. (1987) *Cell* **48**, 129–136
35. Sanger, F., Coulson, A. R., Hong, G. F., Hill, D. F., and Petersen, G. B. (1982) *J. Mol. Biol.* **162**, 729–773
36. Ben-Bassat, A., Bauer, K., Chang, S.-Y., Myambo, K., Boosman, A., and Chang, S. (1987) *J. Bacteriol.* **169**, 751–757
37. Kikuchi, Y., Yoda, K., Yamasaki, M., and Tamura, G. (1981) *Nucleic Acids Res.* **9**, 5671–5678
38. Kozak, M. (1983) *Microbiol. Rev.* **47**, 1–45
39. Henning, U., and Yanofsky, C. (1962) *Proc. Natl. Acad. Sci. U. S. A.* **48**, 1497–1504
40. Ptashne, M. (1986) *A Genetic Switch, Gene Control and Phage L*, Cell Press and Blackwell Scientific Publications, Oxford and Palo Alto, CA
41. FitzGerald, D., Bjorn, M., Ferris, R., Winkelhake, J., Frankel, A., Hamilton, T., Ozols, R., Willingham, M., and Pastan, I. (1987) *Cancer Res.* **47**, 1407–1410
42. Bjorn, M. J., and Groetsema, G. (1987) *Cancer Res.* **47**, 6639–6645
43. Robertus, J. D., Piatak, M., Ferris, R., and Houston, L. L. (1987) *J. Biol. Chem.* **262**, 19–20
44. Montfort, W., Villafranca, J. E., Monzingo, A. F., Ernst, S. R., Katzin, B., Rutenber, E., Xuong, N. H., Hamlin, R., and Robertus, J. D. (1987) *J. Biol. Chem.* **262**, 5398–5403
45. O'Hare, M., Roberts, L. M., Thorpe, P. E., Watson, G. J., Prior, B., and Lord, J. M. (1987) *FEBS Lett.* **216**, 73–78
46. Foxwell, B. M. J., Donovan, T. A., Thorpe, P. E., and Wilson, G. (1985) *Biochim. Biophys. Acta* **840**, 193–203
47. Youle, R. J., Murray, G. J., and Neville, D. M., Jr. (1979) *Proc. Natl. Acad. Sci. U. S. A.* **76**, 5559–5562
48. Neville, D. M., Jr., and Youle, R. J. (1982) *Immunol. Rev.* **62**, 75–91
49. Thorpe, P. E., Ross, W. C. J., Brown, A. N. F., Myers, C. D., Cumber, A. J., Foxwell, B. M. J., and Forrester, J. T. (1984) *Eur. J. Biochem.* **140**, 63–71
50. Youle, R. J., Murray, G. J., and Neville, D. M., Jr. (1981) *Cell* **23**, 551–559
51. Chang, M. S., Russell, D. W., Uhr, J. W., and Vitetta, E. S. (1987) *Proc. Natl. Acad. Sci. U. S. A.* **84**, 5640–5644
52. Colombatti, M., Greenfield, L., and Youle, R. J. (1986) *J. Biol. Chem.* **261**, 3030–3035

Supplemental Material to:

Expression of Soluble and Fully Functional Ricin A-chain in *E. coli* is Temperature Sensitive

Michael Piatak, Julie A. Lane, Walter Laird, Michael J. Bjorn, Alice Wang and Mark Williams

EXPERIMENTAL PROCEDURES

Materials: Castor beans *Ricinus communis* var. *sanguineus* were purchased from G. Park Seed Co.; plant specimens were grown under greenhouse conditions. Chemicals and enzymes were obtained from various commercial sources and used in accordance with the manufacturer's recommendations. Oligonucleotides were synthesized by the DNA Synthesis Group at Cetus Corporation using the automated phosphite triester method. Vanadyl-ribonucleoside complex was prepared according to published methods (12) using $VoSO_4 \cdot 3H_2O$ (Aldrich). The *E. coli* host strains and plasmid vectors used were from various researchers at Cetus Corporation and are available from the Cetus Master Culture Collection. Native RA was prepared at Cetus Corporation or purchased from E-Y Laboratories, San Mateo, CA. Rabbit antisera to native RA was prepared by BABCO, Berkeley, CA. The monoclonal antibodies, 26OF9, 3L1, 2B2D11 and 9E4A12 have been described (13,14) and were prepared at Cetus Corporation. Balb/C mice (Charles River) were used for toxicity tests.

Isolation of mRNAs: The following protocol was developed to efficiently extract mRNA from castor beans. To minimize degradation after total nucleic acids were extracted from the beans, all solutions were treated with 0.1% diethylpyrocarbonate (DEPC) overnight and autoclaved. Only DEPC-treated and baked glassware or sterile-packaged plasticware was used. Immature castor beans were harvested at about the time of testa formation (the period of maximal mRNA synthesis) (13), and immediately frozen on dry ice. Plant materials were stored at -70°C until needed. For isolation of RNA, approximately 50 grams of frozen beans were placed in 100 ml of homogenizing buffer (150 mM NaCl, 50 mM TrisCl, pH 8.3, 5mM EDTA and 50 mM β-mercaptoethanol) to which was added 12 ml freshly prepared 0.2 M vanadium-ribonucleoside complex, 50 mg proteinase K, and 15 ml 20% SDS. This mixture was homogenized in a covered Waring blender at high speed for 4 min. The homogenate was left at room temperature for 2 h with occasional blending and then centrifuged at 8000 x g for 15 min to pellet insoluble debris. The supernatant was filtered through cheesecloth to remove lipids, extracted three times with phenol:chloroform:isoamyl alcohol (24:24:1) containing 1% hydroxyquinoline, and then extracted additionally with the same mixture but containing only 0.03% hydroxyquinoline until all vanadium and protein were removed. The aqueous layer was adjusted to 0.6 M NaCl and 10 mM EDTA, and nucleic acids were precipitated with ethanol.

Contaminating saccharides were removed from the preparation by the use of cetyltrimethylammonium bromide (CTAB) (16). Precipitated nucleic acids were converted to the sodium form by twice suspending the precipitate in cold 70% ethanol containing 0.1 M sodium acetate. Oxidized phenolic compounds and other undefined contaminants that interfere with cDNA synthesis were separated from RNA as follows. The RNA precipitate was dissolved in 2 ml of 20 mM TrisCl, pH 8, 1 mM EDTA, 0.3% SDS, 0.3 M NaCl and then passed over a Sephadex G-100 column equilibrated in the same buffer but lacking SDS. High-molecular weight RNA eluted at the void volume followed by smaller RNA species and contaminants. Fractions containing the higher-molecular weight RNA species were pooled to avoid contaminants and precipitated with ethanol.

The RNA sample was treated to dissociate complexes by dissolving it in a minimum volume of water and then adding nine volumes of deionized formamide containing 20 mM PIPES, pH 6.8. The mixture was warmed to 37°C for 5 min, and 10 volumes of 0.3 M NaCl, 10 mM TrisCl, pH 7.5, 1 mM EDTA were added. Polyadenylated RNA was then isolated by chromatography on oligo-dT cellulose (17).

cDNA Clones: Standard procedures for cDNA synthesis, cloning and manipulation of subclones were followed (18). The synthetic oligonucleotide 5'-GACCATTTCGACCT ACG-3' was used to prime cDNA synthesis to obtain a population of clones enriched for sequences encoding RA. This primer sequence is complementary to mRNA encoding the N-terminal region of RB and is located 3' to the RA sequences in prericin cDNA (10). Transformants were screened with a ^{32}P-labelled pool of all 4 isomers of the 33-mer 5'-GCATCTTCTTGGTTGTCNGGATGAAAGAAATAGGC-3' where N = A, G, C or T, derived from the sequence for RA. The sequences of cloned cDNAs were determined directly by chemical degradation methods (19) and by chain termination methods (20) after subcloning into M13 phage vectors (21).

Expression of cDNA Sequences: Cloned cDNA encoding RA was first modified to allow for subcloning and expression in suitable plasmid vectors. A BamHI fragment of pRA123 (Fig. 1) containing the entire coding sequence for mature RA was first cloned into M13mp18 (a derivative of the M13 vectors described in (21) containing additional cloning sites) in an antisense orientation relative to the *lac* coding sequence in the vector. Phage single-stranded DNA was then subjected to primer-directed mutagenesis following the method of McCormick and Innis (22) using as primers the synthetic oligonucleotides shown in Fig. 1. Mutant phage were detected by hybridization to the same oligonucleotides (^{32}P-labelled) at about 10°C below their respective melting temperatures (Tm), determined from the formula Tm = 7.2 ln(Na_+) + 0.41 (%G + C) + 81.2 - 500/(length in nucleotides). With reference to Fig. 1, the following plasmid/host expression systems were derived: The plasmids pRAL6 and pRAL7 are subclones of a HindIII-BamHI RA fragment in pPLOP (23), a temperature-sensitive runaway copy variant of ColE1 containing the phage λ major leftward promoter, P_L, and gene N ribosome binding site appropriately spaced upstream from a unique HindIII site. These plasmids were propagated in either MC1000A or DG93A at 30°C. MC1000A is MC1000 (24) lysogenized by the defective prophage $\lambda N_7 N_{53} c_{I857} Sus P_{80}$; DG93A is an Su^0 derivative of MM294 (25) lysogenized by the same prophage.

The plasmids pRAT1 and pRAT7 are subclones of the same HindIII-BamHI fragment noted above but in pTRP3 (26). These contain the *E. coli* trp promoter and ribosome binding site in similar placement, as noted above, to the HindIII site in pSR322 (27).

The plasmid pRAP218 is the product of a three-way ligation of (a) the large NarI (Klenow blunt repaired) - BamHI replicon-containing fragment from pSYC1089, (b) a modified MstII-ClaI fragment containing the N-terminal coding region of RA, and (c) the ClaI-BamHI fragment from pRAT1 containing the C-terminal coding region of RA. pSYC1089 is derived from pACYC184 (28) and contains, in order, a polylinker sequence, the *E. coli* phoA gene with a NarI site introduced at the C-end of the signal peptide coding sequence, and the *B. thuringiensis* positive retroregulator sequence (29) after a unique BamHI site.

The plasmid pRAP210 was derived similar to pRAP218 except that the NarI site in the vector was only partially repaired with dCTP to leave a 3' C overhang and the N-terminal coding region of RA was contained on a BglII (partially repaired with dTTP, dATP, and dGTP leaving a 3' G overhang) - ClaI fragment.

The plasmid pRAP229 is the product of a three-way ligation of (a) the large NarI-BamHI vector fragment of pSYC1089 and (b) the ClaI-ClaI and (c) the ClaI-BamHI fragments containing the N-terminal and the C-terminal coding regions, respectively, of RA taken from pRAT1.

pRAT1, pRAT7, pRAP218, pRAP2210 and pRAP229 were propagated in the *E. coli* host strain MM294. pRAT1 and pRAT7 were maintained under ampicillin selection; the pRAP series were maintained under chloramphenicol selection.

Expression of the RA sequences in the pRAL plasmids was normally achieved by shifting early to mid log-phase cultures from 30°C to 42°C or as described in the Results and Discussion. This temperature shift normally results in induction of the promoter, P_L, due to inactivation of the sensitive cI_{857} repressor with a concomitant increase in plasmid copy number. For the pRAT plasmids, protein expression was achieved by growing cultures in minimal medium lacking tryptophan; for the pRAP plasmids, expression was achieved by allowing for phosphate depletion in the cultures as described by Michaelis et al. (30).

Cell Fractionations: Cultures were concentrated by centrifugation, suspended at 1/20th to 1/6th the original volume in 0.03 x PBS, 30 mM mercaptoethylamine, 5 mM EDTA, or in 100 mM TrisCl, pH 8.5, 5 mM EDTA, and sonicated for 3-min intervals using a Heat Systems Model W-225R instrument with a 1/2" probe at power output 8 and 30% cycle. Insoluble material was pelleted by centrifugation at 12,000 x g. We found that prolonged sonication of cells in the Tris/EDTA, pH 8.5, system was most efficient for complete cell disruption and release of protein.

To release proteins secreted to the periplasm, osmotic shocks were performed as described by Nossal and Heppel (31).

Protein Analysis and Activity Assessments: Sodium dodecyl sulfate-polyacrylamide gel electrophoresis (SDS-PAGE) analyses were performed according to the methods of Laemmli (32). All running gels contained 12.5% acrylamide; proteins were stained with Coomassie. Western blot analyses were after Nyari et al. (33). The Fermentation Group at Cetus Corporation supplied us with large quantities of induced cells to facilitate protein purification. Essentially standard methods of chromatography were employed to purify rRA. Samples of originally insoluble rRA of greater than 90% purity as judged by SDS-PAGE analyses were easily obtained after differential centrifugation and chromatography on Sephacryl S-200 (Pharmacia). The originally soluble rRA from pRAP229 was

isolated to greater than 95% homogeneity as follows. Approximately forty grams, wet weight, of cells were suspended in 100 ml 0.1 M Tris·Cl, pH 8.3, 25 mM EDTA, 0.1% Sarkosyl (sodium salt of N-lauroylsarcosine), and 0.5 M NaCl. After 30 min of sonication, 1 mg of phenylmethylsulfonyl fluoride in 1 ml dimethylsulfoxide was added, and the mixture was centrifuged for 30 min at 12,000 × *g*. The supernatant was loaded onto a phenyl-Sepharose (Pharmacia) column having a bed volume of 200 ml that had been equilibrated with PBS. The column was washed with 1 bed volume PBS and then eluted with a 0–30% propylene glycol gradient in PBS. Fractions containing rRA were identified by SDS-PAGE. The rRA eluted at approximately 17% propylene glycol. The appropriate fractions were pooled and diluted 10-fold into 20 mM sodium acetate, pH 5.5, 1 mM EDTA, 0.1% β-mercaptoethanol. This was applied to a 250-ml carboxymethyl-Sepharose (Pharmacia) column equilibrated in the same buffer and then eluted with a 100–250 mM NaCl gradient in buffer. The rRA fractions eluted at approximately 150 mM NaCl and were approximately 95% pure.

Inhibition of protein synthesis in a cell-free system was determined by using commercially available rabbit reticulocyte systems. Test samples were diluted into 0.01 M PBS containing 50% γ-globulin bovine serum albumin and, where appropriate, 0.67% SDS. Antibody-rRA conjugates were prepared as described by Blythman et al. (19) except that 0.67% SDS was included in buffers where necessary. The human breast cancer reactive monoclonal antibodies, 260F9 and 260D11, and the human transferrin receptor monoclonal antibodies, BL1 and 454A12, have been described (13, 20) and were supplied by D. Ring, Centre Immune Corp. and by the Process and Development Group at Cetus Corporation. The cytotoxic activities of the conjugates were determined by their ability to inhibit protein synthesis in the human breast cancer cell line, MCF-7, as described previously (16).

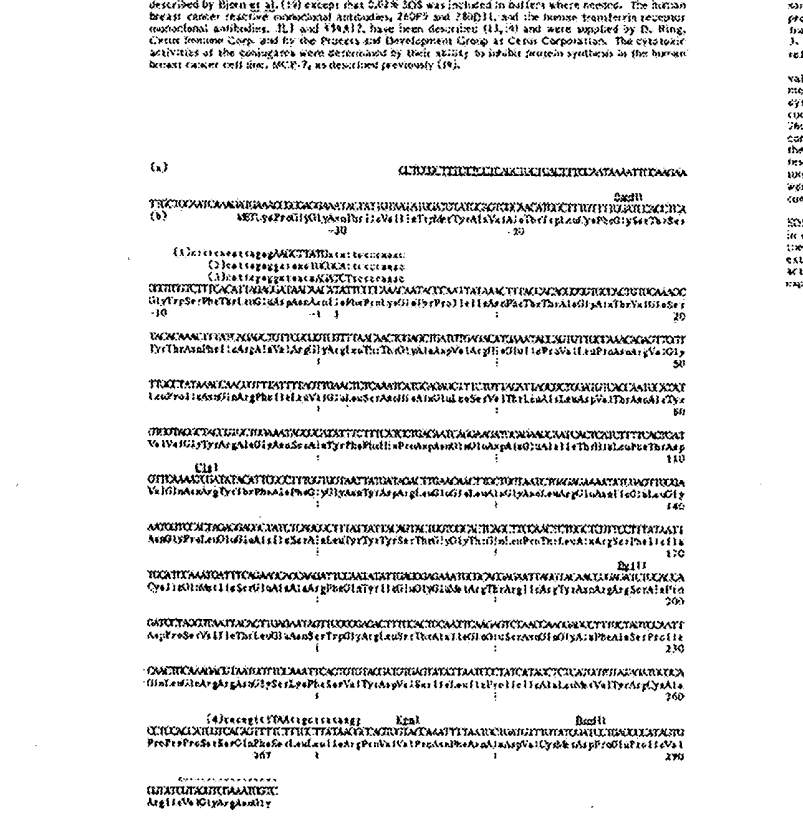

Figure 1. pRA123 cDNA Sequence and Encoded Protein. (a) The coding strand sequence of the cDNA insert of pRA123 is given with relevant restriction sites noted. (b) The encoded protein sequence, numbered for reference. Residues -30 through -1 specify a putative secretion signal peptide. Residues 1 through 267 specify the mature RA sequence. Residues 268 through 278 specify a sequence linking RA to RB in proricin (16). Residues 282 through 297 specify an N-terminal fragment of RB. Oligonucleotide primers employed for mutagenesis are included, with pertinent sequence changes in capital letters. As outlined in Experimental Procedures, (1) introduces a HindIII site (AAGCTT) and translation initiation codon for derivation of pRAL and pRAT plasmids; (2) introduces an MseI site (TGCGCA) for derivation of pRAP11A; (3) introduces a BglII site (AGATCT) for derivation of pRAP2210; (4) introduces a termination codon (TAA) at the end of the RA sequence. The underlined DNA sequence at the beginning indicates the major difference between this sequence and that of Halling et al. (11). ←——, indicates the sequence primed for cDNA synthesis.

RESULTS AND DISCUSSION

RA cDNAs. The cDNA sequence for RA is shown in Fig. 1. It agrees remarkably well with the cDNA (10) and the genomic DNA (11) sequences reported earlier, even though different castor bean variants were studied. This emphasizes the strong conservation of the protein sequence for RA. The differences noted in the 3′-untranslated region between this sequence and that of Halling et al. (11) is evidence that different genes are represented.

Early Expression Results. The cDNA sequence shown in Fig. 1 was modified by site-directed mutagenesis to allow for its appropriate placement in various expression vectors as described in the Experimental Procedures. In the first expression plasmids constructed, the pRAL and pRA1 series, translation of the RA sequence was initiated at an ATG start codon introduced adjacent upstream to the first codon of the mature protein sequence, ATA (Ile). As RA is normally processed at its C-end from a precursor, a termination codon, TAA, had been introduced adjacent downstream to the last codon of the mature sequence, TTT (Phe #267), to allow for independent expression of the rRA sequence in these and subsequent plasmid constructs.

In the pRAL plasmids, expression of the rRA sequence was regulated by the phage λ P_L promoter and gene N ribosome binding site. These plasmids are also temperature-sensitive for increased copy number. In the pRAT plasmids, the *E. coli* e_{10} promoter and ribosome binding site was utilized (Fig. 2a). Initially, two clones containing the P_L derivatives, pRAL6 and pRAL7, and two clones containing the P_{TRP} derivatives, pRAT1 and pRAT7, were appropriately induced and analyzed for expression of RA polypeptide. Fig. 2 shows the results of a Western blot analysis. Specific immunoreactive products were readily apparent in the cells carrying the pRAL and the pRAT plasmids (Fig. 2, lanes 6, 7 and 10, 11) but not in the cells carrying only the unmodified vectors, pHLC9 and pTRP3 (Fig. 2, lanes 1, 3, 8, and 9). The major product (rRA) migrated with an apparent M_r of 28–30k, slightly faster than the native RA marker. This size would be consistent for a nonglycosylated RA. The product migrating slightly slower than the native RA markers was probably an *E. coli*-specific protein since it was present in the cleared as well as the test samples. Background reactivity is also obvious but was associated only with the test samples, particularly the pRAL-carrying cells. Poor solubility of the pRAL expressed product (discussed below), even when boiled in 1.25% SDS gel loading buffer, may account for this as well as limited proteolysis.

In early experiments, we observed varying amounts of expressed product by SDS-PAGE analysis depending on the extraction treatment. Eventually, we determined that prolonged sonication in the absence of detergent and higher levels of SDS in the sample loading buffer greatly improved the release of rRA monomer and provided clearer lane backgrounds in Western blot analyses. Our final estimates of the amount of product expressed from the pRAL6 construct was 6–8% of total cell protein. Because this yield was substantially higher than what we had observed with the pRAT plasmids, i.e., approximately 2% of total cell protein, we initially selected this clone and system for scale-up and isolation of rRA.

Partial Purification and Activity of pRAL6 rRA. Because of the insoluble, aggregate properties of this expressed product, enriched preparations containing of about 30% cloned product were easily obtained by a combination of sonication and differential centrifugation (data not shown). Further purification required solubilization of this product. For this, we examined many conditions and reagents, including various nonionic and ionic detergents, urea, acidic conditions, basic conditions, and compatible combinations thereof at various temperatures, but met with limited success. Ultimately, we found that extreme denaturing conditions such as presented by 8M urea + 0.5% SDS at half-saturated guanidine hydrochloride efficiently solubilized rRA. Solubility was judged by the stability of the product in SDS-PAGE at room temperature with no additional pretreatment. Subsequently, rRA solubility could be maintained by low concentrations (0.01–0.02%) of SDS. Continued purification of rRA was then achieved by chromatography on Sephacryl S-200 resulting in preparations that were greater than 90% homogeneous (data not shown).

We compared the enzymatic activity of the cloned rRA to native RA in a rabbit reticulocyte translation system. To ensure solubility of the cloned product, we made dilutions in buffer containing 0.02% SDS. Samples of native RA were first adjusted to contain 0.02% SDS and then diluted in the same buffer. The presence of SDS at this level had minimal effects on the activity of the native protein (data not shown). Typically, 2–3 pg of native RA in a 50 μl reaction gave 50% inhibition of translation. The pRAL6 rRA was similarly active, although in repeated experiments it appeared to be 3- to 5-fold less active than the native protein on a per-weight basis. This lower specific activity may reflect improper or incomplete renaturation of the protein after solubilization.

Our primary objective in producing rRA is to use it in the production of conjugates of therapeutic value. Hence, we tested if this rRA could be used to make effective immunotoxins. The two monoclonal antibodies, BL1 and 260F9, were chosen for this study since they had made potent cytotoxins with native RA as the conjugate partner (13, 19). Due to the poor solubility of the rRA, the coupling of rRA to antibody was performed in the presence of 0.67% SDS. Conjugates of BL1 and 260F9 with native RA were also constructed in the presence of 0.67% SDS as controls. The conjugation efficiency in the presence of 0.02% SDS was reduced relative to the efficiency obtained in the absence of SDS. Still, sufficient quantities of conjugate were formed to allow for cytotoxicity testing. As shown in Table I, neither BL1-rRA nor 260F9-rRA were cytotoxic to the human breast tumor cell line at the highest doses tested. It was significant that BL1-native RA and 260F9-native RA were also inactive when they were constructed in 0.02% SDS, in contrast to their potent activity when constructed in the absence of SDS.

It was apparent from the above results that the usefulness of rRA solubilized in the presence of SDS was limited. Consequently, we screened many other detergents for their ability to maintain rRA in solution after its solubilization with guanidine hydrochloride as well as for their toxicity to cells and their effect on immunoconjugate synthesis and activity. None were completely satisfactory. Given its extreme, poor solubility and the harsh conditions required to manipulate it, it did not appear that full activity of this *E. coli*-expressed rRA could be obtained. Consequently, we explored the possibility of expressing rRA as a soluble protein in *E. coli*.

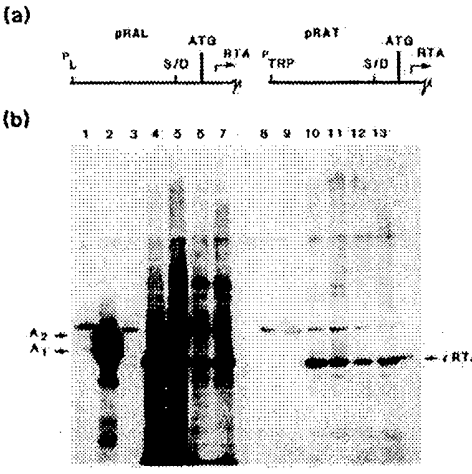

Figure 2. Western blot analysis of pRAL- and pRAT-expressed rRAs. (a) Schematics of regulatory regions of the pRAL and pRAT expression constructs. The figures are aligned for reference over the relevant lanes in (b). (b) Autoradiogram of a Western blot analysis of rRA expressed from pRAL and pRAT plasmids. Induced cells were collected by centrifugation, suspended in 20 μl 62 mM Tris·Cl, pH 6.8, 1.25% SDS, 1% β-mercaptoethanol, and heated to 100°C for 3 min. One-quarter volume of 25% glycerol, 0.1% bromophenol blue was mixed in, and the samples were run in an SDS-PAGE (12.5%). Lane 2 shows about 8 ng of native RA. In the following pairs of lanes, approximately 0.15 and 0.3 A_{550} units, respectively, of cells carrying the following plasmids were loaded: lanes 1 and 2, pHLC9 (no insert); lanes 3 and 5, pRAL6; lanes 6 and 7, pRAL7; lanes 8 and 9, pTRP3 (no insert); lanes 10 and 11, pRAT1; lanes 12 and 13, pRAT7. A_1 and A_2 indicate the two glycosylated forms of native RA (9k). rRA-expressed product is indicated.

Table I
Cytotoxicity of Immunotoxins Constructed With SDS-soluble rRA and Native RA

Immunotoxin	Constructed in the presence of 0.67% SDS	Cytotoxicity ID_{50} (nM)[a]
BL1-rRA	Yes	> 10
BL1-native RA	Yes	> 10
BL1-native RA	No	0.05
260F9-rRA	Yes	> 10
260F9-native RA	Yes	> 10
260F9-native RA	No	0.2

[a] Cytotoxicity was assessed by using the human breast tumor cell line MCF-7. ID_{50} is the concentration of immunotoxin causing a 50% decrease in the incorporation of ^{3}H-leucine into cellular proteins (16).

Table II
Representative Activities Determined for pRAP229-rRA and Native RA

	pRAP229-rRA	Native RA
Enzymatic Activity[a]	1.18 ng/ml	1.77 ng/ml
Toxicity[b]	300 pg	350 pg
Cytotoxicity of constructed immunotoxins against MCF-7[c]		
Mab 454A12	0.02 nM	0.01 nM
Mab 260F9	0.4 nM	0.1 nM

[a] Reported as the concentration of RA protein that inhibits translation 50% in a rabbit reticulocyte system. The average of two experiments is given.

[b] Reported as the single intravenous injected dose of protein that leads to 50% mortality in Balb/C mice.

[c] As indicated in Table I.

Nat. Gent. 1992 1:372-378
Science 1989 245:1234-1236

Eur. J Biochem. 1985 148:265-270

Mol. Immunol 1995 32:1057-1064

Science 1993 259:988-990

Nature 1988 336:348-352

J Clin. Invest. 1993 91:225-234

Mol. Cell. Biol. 1987 7:1576-1579

Gene 1982 19:33-42

Neuron 1992 8:507-520

Adv. Virus Res. 1989 37:35-83

1994 Cancer Res. 54:5258-5261

Cell 1987 50:435-443

Nucleic Acids Res. (1996) 24(10):1841-1848

J Biol. Chem. 1988 263 10 :4837-4843

Proc. Natl. Acad. Sci. USA 1992 89:2581-2584

1993 Nature 361:647-650

DNA Seq. 1993 4:185-196

Human Gene Ther. 1995 6:881-893

Science 1991 252:431-434

Cell 1992 68:143-155

Mol. Cell. Biol. 1990 10 6 :2738-2748

Nucleic Acids Res. 1996 24 15 :2966-2973

Human Gene Thera 1990 1:241-256

J Clin. Invest 1992 . 90:626-630

Curr. Topics in Micro. and Imm. 1995 199 part 3 :177-194

Lancet 1981 11:832-834

Cancer Res. 1996 56:1341-1345

J Virol. 1992 66 (6) :3633-3642

J Virol. 1996 70 (4) :2296-2306

Nature (1997) 389:239-242

J Virol. 1984 51 (3) : 822-831

Adv. Ex . Med. Biol. 1991 3098:61-66

Proc. Natl. Acad. Sci. 1983 80:5383-5386

Genomics 1990 8:492-500

Gastroenter. 1990 98:470-477 .

N. Vogel
Au 1636
12/9
10045116

Proc. Natl. Acad. Sci. USA
Vol. 89, pp. 2581–2584, April 1992
Medical Sciences

Adenovirus as an expression vector in muscle cells *in vivo*

BÉATRICE QUANTIN*, LESLIE D. PERRICAUDET†, SHAHRAGIM TAJBAKHSH‡, AND JEAN-LOUIS MANDEL*§

*Laboratoire de Génétique Moléculaire des Eucaryotes du Centre National de la Recherche Scientifique, Institut National de la Santé et de la Recherche Médicale, U184, Institut de Chimie Biologique, 11 rue Humann, 67085 Strasbourg Cedex, France; †Institut Gustave-Roussy, Laboratoire de Génétique des Virus Oncogènes, PR II, 39 rue Camille Desmoulins, 94805 Villejuif Cedex, France; and ‡Centre National de la Recherche Scientifique, U.A. 1148, Département de Biologie Moléculaire, Institut Pasteur, 25 rue du Docteur Roux, 75724 Paris Cedex 15, France

Communicated by Pierre Chambon, December 16, 1991

ABSTRACT **Attempting gene transfer in muscle raises difficult problems: the nuclei of mature muscle fibers do not undergo division, thus excluding strategies involving replicative integration of exogenous DNA. As adenovirus has been reported to be an efficient vector for the transfer of an enzyme encoding gene in mice, we decided to explore its potential for muscle cells. Advantages of adenovirus vectors are their independence of host cell replication, broad host range, and potential capacity for large foreign DNA inserts. We constructed a recombinant adenovirus containing the β-galactosidase reporter gene under the control of muscle-specific regulatory sequences. This recombinant virus was able to direct expression of the β-galactosidase in myotubes *in vitro*. We report its *in vivo* expression in mouse muscles up to 75 days after infection. The efficiency and stability of expression we obtained compare very favorably with other strategies proposed for gene or myoblast transfer in muscle *in vivo*.**

The eventual correction of muscle diseases, and especially Duchenne muscular dystrophy (DMD), raises very difficult problems. As much as 50% of DMD cases are sporadic (1) and thus cannot be prevented by current genetic counseling and prenatal diagnosis approaches; this frequency is even higher in mitochondrial myopathies (2). It is thus necessary to actively explore therapeutic strategies. The main problems to overcome are the large number of muscles to be treated and the nondividing nature of mature muscle cells. Moreover, the size of the sequences coding for dystrophin [11,056 base pairs (bp)] is incompatible with most vectors used for gene transfer; in addition, dystrophin is an intracellular protein thought to have a structural role in the muscle cells, whereas most of the current gene therapy approaches concern circulating proteins such as α_1-antitrypsin (3), or diseases due to an enzymatic defect, where a very partial restoration of the activity might be sufficient, such as adenosine deaminase (4).

Two strategies have been proposed to date: myoblast transplantation (5) and direct DNA injection (6). We decided to explore a third route using adenovirus as a vector for gene expression in muscle cells. Such a vector has already been used to correct postnatally an ornithine transcarbamoylase deficiency in mouse (7, 8) and more recently to direct the expression of α_1-antitrypsin in the rat lung epithelium (9).

The advantages of adenovirus include (*i*) a large host range, thus allowing the use of the animal models available for DMD (the *mdx* mouse and the *CXMD* dog), (*ii*) a low pathogenicity in man, (*iii*) a capacity for foreign DNA in principle compatible with the size of the dystrophin mRNA [the properties of adenovirus should allow the insertion of >30 kilobases (kb) of exogenous DNA, provided that a helper virus is used to propagate the recombinant virus], and (*iv*) the possibility to obtain high titers of virus, which is important for *in vivo* applications.

Our results suggest that adenovirus can be used to direct efficient gene expression in myotubes derived from rodent myogenic cell lines as well as in mouse muscle.

MATERIALS AND METHODS

Cell Lines, Cell Transfection, and Virus. Monolayer cultures of 293 cells (10) were propagated in minimum essential medium (MEM) supplemented with 10% fetal calf serum. The C2.7 (11) and the L6 myoblast cell lines were maintained in Dulbecco's modified Eagle medium (DMEM) with 20% fetal calf serum. Fusion of C2.7 myoblasts was induced when cells were confluent by lowering the serum to 2%. The induction medium used for the L6 cell line was DMEM with 1% FCS and 10 μg of insulin per ml.

Transfections were performed using the calcium phosphate method (12). Adenovirus stocks were prepared by infection of 293 cells. Cells and media were harvested 25–30 hr after infection, and virus was released by three cycles of freezing and thawing. The dl 324 mutant of adenovirus type 5 contains a deletion of E3 (78.5–84.7 map units) and of E1 (nucleotides 1334–3639).

Animals. Mice were F_1 individuals of the C57B6 × SJL strain. Injections (10–20 μl of the viral suspension) were performed in the thigh of the animals either newborn, 1 week old, or 4 weeks old, at a single site.

Construction of Plasmid pMβgal. Plasmid pMβgal is derived from plasmid pCH110 (13). It contains the first 454 nucleotides of adenovirus 5, followed by an enhancer fragment of the mouse myosin light chain 1/3 locus. This fragment was obtained by screening a plasmid containing the 3′ end of the mouse $MLC_{1/3F}$ gene with a rat probe (14). An 800-bp fragment that was isolated and sequenced was found to have >90% homology with the rat sequence and displayed at least a 30-fold enhancement, which was myotube specific, with the homologous promoter and a heterologous thymidine kinase promoter (S.T. and C. Biben, unpublished results). A fragment equivalent to nucleotides 387–680 of the rat sequence was amplified by PCR before cloning into the plasmid pMβgal. A mouse skeletal α-actin gene promoter, nucleotides −682 to +127 of the published sequence (15), was added between the enhancer and the β-galactosidase sequences. The poly(A) signal is from simian virus 40 (*Hpa* I–*Bam*HI fragment), and, finally, nucleotides 3328–6241 of adenovirus 5 (including sequences coding for peptide IX) were added downstream of the poly(A) signal.

Assay for β-Galactosidase Activity. β-Galactosidase activity in cell lines was assayed as described using histochemical methods (16) or a colorimetric assay (17). For the *in vivo*

The publication costs of this article were defrayed in part by page charge payment. This article must therefore be hereby marked "*advertisement*" in accordance with 18 U.S.C. §1734 solely to indicate this fact.

Abbreviations: DMD, Duchenne muscular dystrophy; ITR, inverted terminal repeat.

§To whom reprint requests should be addressed.

experiments, muscle samples were fixed and β-galactosidase activity was revealed as described (16).

RESULTS

Construction of a Recombinant Adenovirus. A recombinant adenovirus was designed to direct the muscle-specific expression of β-galactosidase. It was constructed via homologous recombination *in vivo* between the dl 324 mutant of adenovirus 5 and the plasmid pMβgal. The dl 324 mutant is deleted for two segments of the viral genome (≈5 kb total) that contain the E1 and the E3 regions. E3 is not necessary for viral growth, and the absence of E1 can be transcomplemented by the use of 293 cells, which harbor the E1 region of adenovirus 2. About 7 kb of exogenous DNA may be inserted without interfering with encapsidation of the recombinant genome.

Plasmid pMβgal contains sequentially the 5′ inverted terminal repeat (ITR), which is necessary for replication, and adjacent packaging sequences of adenovirus 5, the β-galactosidase gene of *Escherichia coli* under the control of a mouse α-actin gene promoter fragment reinforced by a muscle-specific enhancer sequence from the mouse $MLC_{1/3F}$ gene (myosin light chain), a poly(A) signal from simian virus 40, and sequences coding for polypeptide IX of adenovirus 5 with 3′ flanking sequences. The presence of polypeptide IX is necessary for encapsidation of a DNA with a size up to 104% that of the wild-type viral genome (18); it is absent from the dl 324 mutant. Initial experiments had shown that a recombinant adenovirus containing only the α-actin promoter fragment as a muscle-specific regulatory sequence was not able to direct efficient expression in myotubes in culture.

The linearized plasmid was cotransfected together with the large *Cla* I fragment of dl 324 DNA in 293 cells, which contains all of the viral genome except for 914 bp at the left end. Restriction analysis of the DNA content of the plaques obtained allowed us to isolate the recombinant adenovirus (Fig. 1); 8 of the first 10 plaques analyzed corresponded to the expected recombinant virus.

Expression of β-Galactosidase in Myogenic Cell Lines. We have tested the expression of β-galactosidase in two rodent myogenic cell lines infected with the recombinant virus. The mouse C2.7 myoblast line (11) can be induced to fuse into myotubes when confluent, by lowering the serum level in the culture medium. The cells were infected for 24 hr at various times before or after induction of fusion. Very little β-galactosidase activity was observed before fusion (however, occasional blue-stained mononuclear cells were observed by histochemical staining), whereas strong expression was detected when virus was added at the time of induction or up to 48 hr after it (further time points could not be obtained as the myotubes tend to detach from the plate, independent of virus infection) (Fig. 2). In similar experiments, high expression was also observed in the rat L6 myoblast line infected at 0, 24, or 48 hr after induction of fusion. As in both culture systems, a majority of myotubes is present 48 hr after the beginning of fusion, our experiments suggest that nondividing myotubes can be infected efficiently. In contrast, no β-galactosidase activity was detected in infected 3T3 mouse fibroblasts, confirming the muscle specificity of the regulatory sequences used.

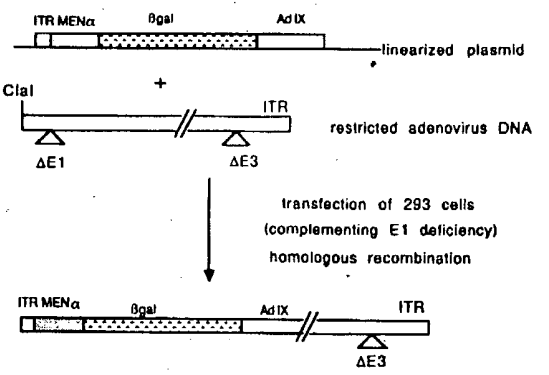

FIG. 1. Isolation of a recombinant adenovirus. MEN, enhancer of the mouse $MLC_{1/3F}$ gene; α, mouse skeletal α-actin promoter; βgal, β-galactosidase gene of *E. coli*; AdIX, sequences coding for peptide IX of adenovirus, with 3′ flanking region (nucleotides 3328–6241 of adenovirus 5); ITR, ITR and packaging sequence (nucleotides 1–454 of adenovirus 5).

Expression of β-Galactosidase in Muscle of Infected Mice. To test whether the adenovirus construct is able to direct β-galactosidase expression in muscle, we injected 10^8 plaque-forming units into the thigh of either newborn, 1-week-old, or

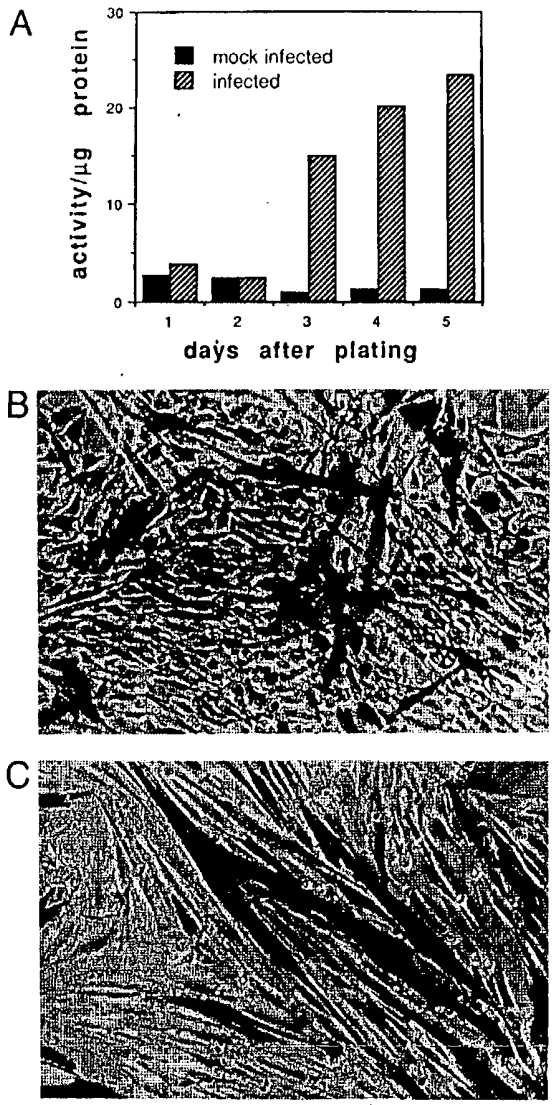

FIG. 2. Expression of β-galactosidase in myogenic cell lines. (*A*) Cells were infected at different stages and β-galactosidase was assayed by a colorimetric method. The fusion medium was added after day 2. (*B* and *C*) C2-7 myotubes (*B*) and L6 myotubes (*C*) infected 2 days after addition of the fusion medium.

Table 1. Expression of β-galactosidase in muscle of infected mice

Age at infection	Time of assay after injection, days	Number of mice			
		0	+	++	+++
1 day	5				3
	7		1		2
	10–15	1	1		5
	20–25	1	2		
	40	1			
	60–65	3	3	1	2
	75		3	2	4
1 week	25	1	1		
	48			1	
	53	2		2	
4 weeks	7				4
	14				4
	40	4			
	52	3		1	

+, 1–10 positive fibers; ++, 11–30 positive fibers; +++, >31 positive fibers.

4-week-old mice. Very strong histochemical staining (>30 positive fibers) was detected in the muscle around the injection site up to 2 weeks after infection, even in mice that were infected at 4 weeks (Table 1). In the latter case, staining was present over a distance of at least 8–9 mm, and most of the positive fibers appeared stained over a length of 1.5–2 mm (Fig. 3). Of the 37 injected muscles (35 mice) that were analyzed at >20 days after infection, 16 showed low (1–10 positive fibers) or moderate staining (11–30 positive fibers), and 6 showed strong staining at 60–75 days (Table 1, Fig. 3). No staining was observed in nonmuscle tissues surrounding the injection site. These data were obtained by staining the muscles as a whole. The internal fibers may not have been accessible to the reagents because of the tight structure of the muscle, thus leading to an underestimation of the number of stained fibers. This was confirmed by incising some infected muscles before staining: in addition to external fibers, some internal fibers appeared positive.

The status of viral DNA sequences was followed by Southern blotting of injected muscle DNA. Most or all of the viral DNA was nonintegrated, since we only detected the expected fragments containing the inverted terminal repeat sequences, up to the last tested time point of 33 days (data not shown). The amount of viral DNA detected appeared rather stable, if the increase in muscle mass is taken into account.

DISCUSSION

Correction of muscle diseases by gene transfer represents a very difficult problem because of the very large mass of tissue involved. Two approaches have recently been proposed toward this long-term goal: myoblast transplantation (5) and direct introduction of plasmid DNA into mature muscle, by injection or by particle bombardment (6, 19). Although retroviruses have been used for gene transfer in muscle cells in culture (20), they cannot be used on noncycling cells and thus on myofibers. Their use would thus also involve myoblast transplantation (for instance, for gene correction using autologous cells). We have decided to explore the potential of adenovirus vectors for gene transfer in muscle, as host cell proliferation is not required for expression of the viral proteins. Such vectors have been used previously for efficient transfer of the ornithine transcarbamoylase minigene into the liver of the *spf-ash* mice, leading to phenotypic correction (7, 8), and more recently to target expression of α_1-antitrypsin in the lung epithelium (9).

We constructed a recombinant adenovirus that allows muscle-specific expression of a reporter gene, β-galactosidase. It was tested successfully on two rodent myogenic cell lines and was then used *in vivo* by injection into muscle of mice.

Very efficient expression was observed in short-term experiments (up to 15 days), with intense staining in many fibers over distances of at least 8–9 mm. This appears much better than that observed for similar experiments carried out by direct injection of plasmid, where staining was reported over a depth of 1.2 mm at 7 days after injection (6), or by particle bombardment (19). Results were more variable in long-term experiments; however, moderate to high expression was

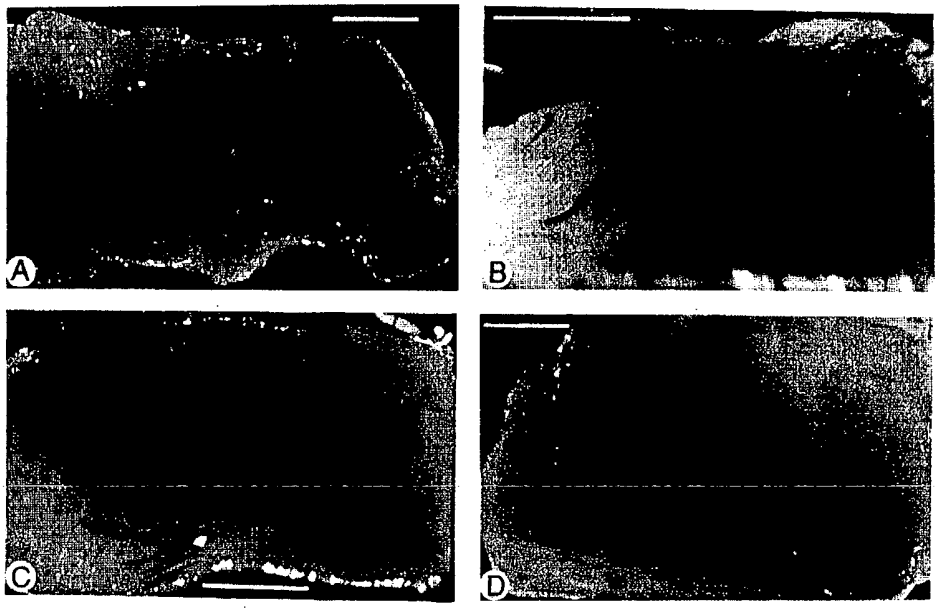

FIG. 3. Expression of β-galactosidase in muscle of infected mice. (*A* and *B*) Muscle of 4-week-old mice analyzed 14 days after injection. (*C* and *D*) Muscle of newborn mice analyzed 75 days after injection. (Bars = 2 mm.)

observed in 13 of 27 mice analyzed 48–75 days after injection, with positive fibers dispersed up to 1 cm. This can be related to the stable persistence of unintegrated adenovirus DNA, which was observed for at least 33 days in our experiments and for 3 months in various organs of rabbits injected intravenously with a different adenovirus recombinant (21). Stable muscle expression of reporter genes up to 60 days has also been reported by Wolff *et al.* (6) following direct injection of plasmid DNA. It is difficult to compare our results with myoblast transplantation, where the presence of donor proteins was ascertained up to 99 days in the *mdx* mouse (5) and 92 days in a single DMD patient (who was also under parallel cyclosporin treatment) (22). In the most successful experiments in *mdx* mouse, 10–30% of fibers were dystrophin positive. However, it was reported that the success rate was higher in nude mice, even when compared with major histocompatibility complex-compatible mice made tolerant at birth. In addition, the migratory power of injected myoblasts was reported not to exceed a few millimeters (ref. 5 and references therein).

One additional advantagous feature of such an adenovirus construct is the possibility to reach several muscles with a single injection. An intravenous route has previously been shown to be efficient for obtaining expression in liver (8) and has been tested for other organs (L.D.P., I. Makeh, M. Perricaudet, and P. Briand, unpublished). We have tested other routes of injection in preliminary experiments and obtained positive fibers in the thigh and abdominal wall of mice injected via an intraperitoneal route.

The performance of the adenovirus vector for obtaining muscle-specific expression appears superior to those reported for DNA injection or particle bombardment (with respect to the size of the area where expression occurs and/or time length of expression). Up to now, the myoblast transplantation strategy has been favored (5, 23), and some assays on Duchenne patients have even been attempted (22). However, this strategy would require a large number of closely spaced injections, each with several million myoblasts. Obtaining such amounts of cells for autologous transplantation (following transfer of a normal gene construct) would appear difficult for treatment of DMD, as it was reported that the replicative life-span of myoblasts already is much decreased early in the course of the disease (24). Heterologous transplantation would very likely require an immunosuppressive treatment. We feel that these problems justify the exploration of alternative strategies, although we recognize the very important issues raised by *in vivo* infection with live virus, even though the virus is replication incompetent and does not appear to have transforming potential. Moreover, recombination with a wild-type infecting adenovirus is very unlikely to generate a replication-competent recombinant. Meanwhile, it should be noted that such recombinant adenoviruses may be useful for gene expression studies in mature myotubes, which appear difficult to transfect, and in muscle *in vivo*.

We are presently constructing a recombinant adenovirus carrying the 6.3-kb sequences coding for a minimal dystrophin, corresponding to that described in a patient with a mild Becker muscular dystrophy (25) under the control of the same regulatory sequences. This dystrophin has a large portion of the spectrin-like domain deleted. Thanks to the wide host range of adenovirus, this construct may be tested in the two available animal models for DMD, the *mdx* mouse and the *CXMD* dog. Although the size of the complete dystrophin coding sequence is incompatible with the present adenovirus vector, it should be possible to integrate it into a recombinant virus using a helper virus, since the only cis-acting sequences necessary for replication and encapsidation are <1 kb (18).

We thank Dr. C. Pinset for the gift of the cell lines, Dr. M. Buckingham for providing the enhancer and promoter fragments, cloned by Dr. S. Tajbakhsh and Dr. S. Alonso, respectively, Dr. M. Perricaudet for very helpful discussions, and the Association Française contre les Myopathies for supporting this work.

1. Worton, R. G., Thompson, M. W. (1988) *Annu. Rev. Genet.* **22**, 601–629.
2. Harding, A. E. (1991) *Trends NeuroSci.* **14**, 132–138.
3. Garver, R. I., Chytol, A., Courtney, M. & Crystal, R. G. (1987) *Science* **237**, 762–764.
4. Wilson, J. M., Danos, O., Grossman, M., Raulet, D. H. & Mulligan, R. C. (1990) *Proc. Natl. Acad. Sci. USA* **87**, 439–443.
5. Partridge, T. A., Morgan, J. E., Coulton, G. R., Hoffman, E. P. & Kunkel, L. M. (1989) *Nature (London)* **337**, 176–179.
6. Wolff, J. A., Malone, R. W., Williams, P., Chong, W., Acsadi, G., Jani, A. & Felgner, P. L. (1990) *Science* **247**, 1465–1468.
7. Chasse, J. F., Levrero, M., Kamoun, P., Minet, M., Briand, P. & Perricaudet, M. (1989) *Médecine/Sciences* **5**, 331–337.
8. Stratford-Perricaudet, L. D., Levrero, M., Chasse, J. F., Perricaudet, M. & Briand, P. (1990) *Hum. Gene Therapy* **1**, 241–256.
9. Rosenfeld, M. A., Siegfried, W., Yoshimura, K., Yoneyama, K., Fukayama, M., Stier, L. E., Pääkkö, P., Gilardi, P., Stratford-Perricaudet, L. D., Perricaudet, M., Jallat, S., Pavirani, A., Lecocq, J. P. & Crystal, R. G. (1991) *Science* **252**, 431–434.
10. Graham, F. L., Smiley, J., Russel, W. C. & Nairn, R. (1977) *J. Gen. Virol.* **36**, 59–72.
11. Yaffe, D. & Saxel, O. (1977) *Nature (London)* **270**, 725–727.
12. Wigler, M., Sweet, R., Sim, G. K., Wold, B., Pellicer, A., Lacy, E., Maniatis, T., Siverstein, S. & Axel, R. (1979) *Cell* **46**, 777–785.
13. Lee, F., Hall, C. V., Ringold, G. M., Dobson, D. E., Luh, J. & Jacob, P. E. (1984) *Nucleic Acids Res.* **12**, 4191–4206.
14. Donoghe, M., Ernst, H., Wentworth, B., Nadal-Ginard, B. & Rosenthal, N. (1988) *Genes Dev.* **2**, 1779–1790.
15. Alonso, S., Garner, I., Vandekerckhove, J. & Buckingham, M. (1990) *J. Mol. Biol.* **211**, 727–738.
16. Sanes, J. R., Rubenstein, J. L. R. & Nicolas, J. F. (1986) *EMBO J.* **5**, 3133–3142.
17. Herbomel, P., Bourachot, B. & Yaniv, M. (1984) *Cell* **39**, 653–662.
18. Berkner, K. L. (1988) *BioTechniques* **6**, 616–631.
19. Yang, N.-S., Burkholder, J., Roberts, B., Martinell, B. & McCabe, D. (1990) *Proc. Natl. Acad. Sci. USA* **87**, 9568–9572.
20. Smith, B. F., Hoffman, R. K., Giger, U. & Wolfe, J. H. (1990) *Mol. Cell. Biol.* **10**, 3268–3271.
21. Ballay, A. (1986) Ph.D. thesis (Université Paris VI).
22. Law, P. K., Bertorini, T. E., Goodwin, T. G., Chen, M., Fang, Q., Li, H., Kirby, D. S., Florendo, J. A., Herrod, H. G. & Golden, G. S. (1990) *Lancet* **336**, 114–115.
23. Morgan, J. E., Hoffman, E. P. & Partridge, T. E. (1990) *J. Cell Biol.* **111**, 2437–2449.
24. Webster, C. & Blau, H. M. (1990) *Somatic Cell Mol. Genet.* **16**, 557–565.
25. England, S. B., Nicholson, L. V. B., Johnson, M. A., Forrest, S. M., Love, D. R., Zubrzycka-Gaarn, E. E., Bulman, D. E., Harris, J. B. & Davies, K. E. (1990) *Nature (London)* **343**, 180–182.

Nat. Gent. 1992 1:372-378
Science 1989 245:1234-1236

Eur. J Biochem. 1985 148:265-270

Mol. Immunol 1995 32:1057-1064

Science 1993 259:988-990

Nature 1988 336:348-352

J Clin. Invest. 1993 91:225-234

Mol. Cell. Biol. 1987 7:1576-1579

Gene 1982 19:33-42

Neuron 1992 8:507-520

Adv. Virus Res. 1989 37:35-83

1994 Cancer Res. 54:5258-5261

Cell 1987 50:435-443

Nucleic Acids Res. (1996) 24(10):1841-1848

J Biol. Chem. 1988 263 10 :4837-4843

Proc. Natl. Acad. Sci. USA 1992 89:2581-2584

1993 Nature 361:647-650

DNA Seq. 1993 4:185-196

Human Gene Ther. 1995 6:881-893

Science 1991 252:431-434

Cell 1992 68:143-155

Mol. Cell. Biol. 1990 10 6 :2738-2748

Nucleic Acids Res. 1996 24 15 :2966-2973

Human Gene Thera 1990 1:241-256

J Clin. Invest 1992 . 90:626-630

Curr. Topics in Micro. and Imm. 1995 199 part 3 :177-194

Lancet 1981 11:832-834

Cancer Res. 1996 56:1341-1345

J Virol. 1992 66 (6) :3633-3642

J Virol. 1996 70 (4) :2296-2306

Nature (1997) 389:239-242

J Virol. 1984 51 (3) : 822-831

Adv. Ex . Med. Biol. 1991 3098:61-66

Proc. Natl. Acad. Sci. 1983 80:5383-5386

Genomics 1990 8:492-500

Gastroenter. 1990 98:470-477 .

N. Vogel
Au 1636
12/9
10045116

REFERENCES AND NOTES

1. D. W. van Bekkum and B. Lowenberg, *Bone Marrow Transplantation: Biological Mechanisms and Clinical Practice* (Dekker, New York, 1985), pp. 311–350.
2. J. M. McCune *et al.*, *Science* **241**, 1632 (1988).
3. R. Namikawa, K. N. Weilbaecher, H. Kaneshima, E. J. Yee, J. M. McCune, *J. Exp. Med.* **172**, 1055 (1990).
4. S. Kamel-Reid and J. E. Dick, *Science* **242**, 1706 (1988).
5. R. Namikawa, H. Kaneshima, M. Lieberman, I. L. Weissman, J. M. McCune, *ibid.*, p. 1684.
6. Y. Reisner *et al.*, *Blood* **61**, 341 (1983).
7. C. A. Keever *et al.*, *ibid.* **73**, 1340 (1989).
8. W. Schuler *et al.*, *Cell* **46**, 963 (1986).
9. Y. Reisner *et al.*, *Lancet* ii, 327 (1981).
10. T. Lapidot, A. Terenzi, T. S. Singer, O. Salomon, Y. Reisner, *Blood* **73**, 2025 (1989).
11. R. Kiessling *et al.*, *Eur. J. Immunol.* **7**, 655 (1977).
12. W. J. Murphy, V. Kumar, M. Bennett, *J. Exp. Med.* **165**, 1212 (1987).
13. R. J. O'Reilly *et al.*, in *Preliminary Immunodeficiency Diseases*, M. M. Eibl and F. S. Rosen, Eds. (Elsevier, New York, 1986), pp. 301–307.
14. Y. Reisner, L. Itzicovitch, A. Meshorer, N. Sharon, *Proc. Natl. Acad. Sci. U.S.A.* **75**, 2933 (1978).
15. E. Schwartz, T. Lapidot, D. Gozes, T. S. Singer, Y. Reisner, *J. Immunol.* **138**, 460 (1987).
16. R. K. Saiki *et al.*, *Science* **239**, 487 (1988).
17. J. A. Todd, J. I. Bell, H. O. McDevitt, *Nature* **329**, 599 (1987).
18. K. S. Ronningen, T. Iwe, T. S. Halstensen, A. Spurkland, E. Thorsby, *Hum. Immunol.* **26**, 215 (1989).
19. We thank M. Martelli, F. Aversa, A. Terenzi, and W. Friedrich for the samples of human BM; B. Morgenstern, G. Black, and D. Ochert for editorial assistance; and R. O'Reilly for critical review of the manuscript. Supported in part by a grant from the Yeda Fund of the H. Levine Center for Applied Research, the Weizmann Institute of Science.

19 November 1990; accepted 7 February 1991

Adenovirus-Mediated Transfer of a Recombinant α1-Antitrypsin Gene to the Lung Epithelium in Vivo

MELISSA A. ROSENFELD, WOLFGANG SIEGFRIED, KUNIHIKO YOSHIMURA, KOICHI YONEYAMA, MASASHI FUKAYAMA, LARUE E. STIER, PAAVO K. PÄÄKKÖ, PASCALE GILARDI, LESLIE D. STRATFORD-PERRICAUDET, MICHEL PERRICAUDET, SOPHIE JALLAT, ANDREA PAVIRANI, JEAN-PIERRE LECOCQ, RONALD G. CRYSTAL*

The respiratory epithelium is a potential site for somatic gene therapy for the common hereditary disorders α1-antitrypsin (α1AT) deficiency and cystic fibrosis. A replication-deficient adenoviral vector (Ad-α1AT) containing an adenovirus major late promoter and a recombinant human α1AT gene was used to infect epithelial cells of the cotton rat respiratory tract in vitro and in vivo. Freshly isolated tracheobronchial epithelial cells infected with Ad-α1AT contained human α1AT messenger RNA transcripts and synthesized and secreted human α1AT. After in vivo intratracheal administration of Ad-α1AT to these rats, human α1AT messenger RNA was observed in the respiratory epithelium, human α1AT was synthesized and secreted by lung tissue, and human α1AT was detected in the epithelial lining fluid for at least 1 week.

ONE OF THE HURDLES TO OVERcome in most forms of somatic gene therapy is the specific delivery of the therapeutic gene to the organs manifesting the disease. The lung presents special advantages because a functional gene can be delivered directly to the respiratory epithelium by means of tracheal instillation. The disadvantage of such an approach is due to the normal biology of the respiratory epithelium; only a small proportion of alveolar and airway epithelial cells go through the proliferative cycle in 1 day, and a large proportion of the cells are terminally differentiated and are, therefore, incapable of proliferation (*1*). In this regard, it may be difficult to transfer functional genes to the respiratory epithelium by means of vectors (such as retroviruses) that require proliferation of the target cells for expression of the newly transferred gene (*2*).

To circumvent the slow target-cell proliferation, we have used a recombinant adenoviral vector to transfer a recombinant human gene to the respiratory epithelium in vivo. Host cell proliferation is not required for expression of adenoviral proteins (*3, 4*), and adenoviruses are normally trophic for the respiratory epithelium (*5*). Other advantages of adenoviruses as potential vectors for human gene therapy are as follows: (i) recombination is rare; (ii) there are no known associations of human malignancies with adenoviral infections despite common human infection with adenoviruses; (iii) the adenovirus genome (which is a linear, double-stranded piece of DNA) can be manipulated to accommodate foreign genes of up to 7.0 to 7.5 kb in length; and (iv) live adenovirus has been safely used as a human vaccine (*3–8*).

The adenovirus (Ad) major late promoter (MLP) was linked to a recombinant human α1AT gene (*9*) and was incorporated into a replication-deficient recombinant (Fig. 1) (*5, 10*). The vector has a deletion of a portion of the E3 region (that permits encapsidation of the recombinant genome containing the exogenous gene) and a portion of the viral E1a coding sequence (that impairs viral replication) but contains an insert of an α1AT expression cassette (Fig. 1) (*10, 11*). After packaging into an infectious, but replication-deficient virus, Ad-α1AT is capable of directing the synthesis of human α1AT in Chinese hamstery ovary (CHO) and human cervical carcinoma (HeLa) cell lines (*10*).

We obtained tracheobronchial epithelial cells by brushing the epithelial surface of the tracheobronchial tree from the lungs of the cotton rat [*Sigmodon hispidus*, an experimental animal used to evaluate the pathogenesis of respiratory tract infections caused by human adenoviruses (*12*)]. The freshly removed cells infected in vitro with Ad-α1AT expressed human α1AT mRNA transcripts, as demonstrated by in situ hybridization with a ^{35}S-labeled antisense human α1AT RNA probe (Fig. 2). In contrast, no human α1AT mRNA transcripts were observed in uninfected, freshly isolated tracheobronchial epithelial cells. Human α1AT mRNA transcripts in the infected cells were capable of directing the synthesis and secretion of human α1AT, as shown by biosynthetic labeling and immunoprecipitation with a specific antibody to human α1AT (Fig. 2E). The newly synthesized, secreted α1AT was human α1AT, as shown by the fact that human α1AT (Fig. 2E, lane 3), but not cotton rat serum, blocked the antibody to human α1AT.

Ad-α1AT transferred the recombinant α1AT gene to the cotton rat lung in vivo (Fig. 3). Human α1AT transcripts were observed in the lungs 2 days after intratracheal instillation of Ad-α1AT, but not in lungs of animals that received only phosphate-buffered saline (PBS) or in lungs of animals that received the Ad5 E1a-deletion mutant, Ad-dl312 (*13*). Biosynthetic labeling and immunoprecipitation of extracellular protein from lung fragments removed from infected animals demonstrated that de novo synthesis and secretion of human α1AT also occurred (Fig. 3B, lanes 11

M. A. Rosenfeld, W. Siegfried, K. Yoshimura, K. Yoneyama, M. Fukayama, L. E. Stier, P. K. Pääkkö, R. G. Crystal, Pulmonary Branch, National Heart, Lung, and Blood Institute, National Institutes of Health, Bethesda, MD 20892.
P. Gilardi, L. D. Stratford-Perricaudet, M. Perricaudet, Institut Gustave Roussy, Centre National de la Recherche Scientifique Unité Associée 1301, 94805 Villejuif Cedex, France.
S. Jallat, A. Pavirani, J.-P. Lecocq, Transgene SA, 67082 Strasbourg, France.

*To whom correspondence should be addressed.

through 15); this was not observed in uninfected animals (lane 10) or in animals infected with Ad-dl312. The de novo expression of the human α1AT protein lasted at least 1 week (lane 15), and the secreted human α1AT was functional, as shown by its ability to form a complex with its natural target, human neutrophil elastase (NE) (lanes 16 through 18).

Two lines of evidence demonstrated that the infection of the cotton rat lung with Ad-α1AT took place in vivo and was not the result of virus carried over into the in vitro biosynthetic analysis. First, immediate evaluation of lung tissue removed 2 and 3 days after in vivo infection with Ad-α1AT revealed human α1AT mRNA transcripts (Figs. 3A and 4). Second, evaluation of the respiratory epithelial lining fluid of cotton rats 3 days after infection with Ad-α1AT showed no evidence of infectious virus capable of directing the biosynthesis of human α1AT, as evidenced by exposure of the 293 cell line to epithelial lining fluid and ^{35}S-labeled methionine, followed by immunoprecipitation analysis in a manner identical to that used for the analysis of the α1AT biosynthesis by the lung fragments.

Evaluation of the cotton rat lung by in situ hybridization with antisense and sense α1AT RNA probes revealed human α1AT mRNA transcripts in lung cells of animals infected with Ad-α1AT, but not in those of uninfected animals (Fig. 4). The expression of human α1AT mRNA transcripts was patchy, as could be expected from the method of intratracheal administration of Ad-α1AT; more uniform expression should be achievable by modifications of vector delivery methods, such as by aerosol. Consistent with the observation that cotton rat respiratory epithelial cells were easily infected in vitro (Fig. 2), most of the transcripts were in epithelial cells; the available methodologies do not permit an accurate assessment of the distribution of expression among the multitude of epithelial cell types in the lung. Occasional grains were observed within interstitial cells.

Evaluation of the fluid lining the epithelial surface of the lungs with a human α1AT-specific enzyme-linked immunosorbent assay (ELISA) demonstrated the presence of human α1AT in animals infected with Ad-α1AT, but not in those infected with the deletion mutant virus Ad-dl312 or in uninfected animals (Fig. 5). Human α1AT could be detected at all the periods evaluated (days 1 to 7 after Ad-α1AT infection). No adverse effects were observed in the animals at any time after infection with either Ad-dl312 or Ad-α1AT. Because the methods available for administration of Ad-α1AT to the animals result in variable delivery and retention of the vector, it is difficult to make quantitative animal-to-animal comparisons. Thus, the time course for α1AT expression cannot be accurately determined at this time, although the de novo biosynthesis data demonstrate that the lung is still actively synthesizing human α1AT at day 7 (Fig. 3B, lane 15).

Our findings are relevant to gene therapy strategies for human diseases. The two most common lethal hereditary disorders of Caucasians, α1AT deficiency (allelic frequency

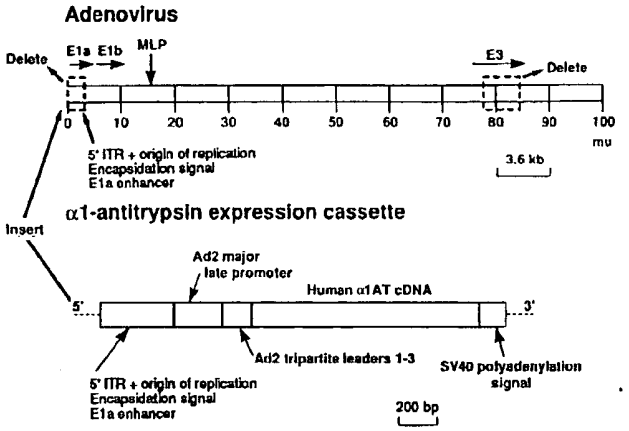

Fig. 1. Recombinant Ad vector. (**Top**) Wild-type Ad type 5 (Ad5) genome showing the E1a, E1b [map units (mu) 1.3 to 11.2; 100 mu = 36 kb], and E3 (mu 76.6 to 86.0) regions. The recombinant vector Ad-α1AT is constructed by deleting the majority of the E3 region and 2.6 mu from the left end of Ad5 and adding to the left end the α1AT expression cassette from the plasmid pMLP-α1AT, which contains regulatory sequences and a recombinant human α1AT gene (*10*). (**Bottom**) Details of the α1AT expression cassette. ITR, inverted terminal repeat. To construct the recombinant viral vector Ad-α1AT, we ligated the expression cassette with C1a I–precut Ad-dl327 DNA (*23*) (to remove a portion of the E1a region from Ad-dl327). The recombinant adenovirus DNA was transfected into the 293 cell line (*24, 25*), where it was replicated, encapsidated into an infectious virus, and isolated by plaque purification. Individual plaques were amplified by propagation in 293 cells, and the viral DNA was extracted (*26*). The intactness of the DNA of the recombinant virus was confirmed before use by restriction fragment analysis and Southern (DNA) blot. Stocks of Ad-α1AT and the Ad5 E1a deletion mutant Ad-dl312 were propagated and titered in 293 cells (*24*). The virus was released from infected cells 36 hours after infection by five cycles of freeze-thawing. For some in vivo experiments Ad-α1AT was further purified with CsCl (*25*).

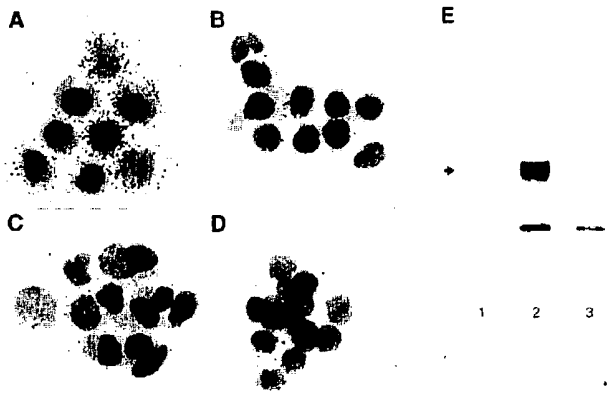

Fig. 2. Expression of human α1AT in respiratory epithelial cells freshly isolated from cotton rats infected with Ad-α1AT in vitro. (**A**) Ad-α1AT–infected cells, antisense probe. (**B**) As in (A) but for uninfected cells. (**C**) Ad-α1AT–infected cells, sense probe. (**D**) As in (C) but for uninfected cells. (**E**) Human α1AT biosynthesis and secretion. We anesthetized cotton rats (methoxyflurane inhalation), exposed the trachea and lungs through a midline thoracic incision, and perfused the pulmonary vasculature with LHC-8 medium (Biofluids) to remove blood. The trachea was transected, and the tracheobronchial epithelial cells (to the second order bronchi) were recovered with a cytologic brush. The epithelial cells were gently pelleted (300*g*, 8 min, 23°C), resuspended in LHC-8 medium, plated on fibronectin-collagen–coated plates (*27*), and infected with 2×10^7 plaque-forming units (PFU) of Ad-α1AT in LHC-8 medium or, as a control, exposed only to LHC-8 medium. After 1 day, we evaluated expression of α1AT mRNA transcripts in cytocentrifuge preparations by the technique of in situ hybridization (*28, 29*) with ^{35}S-labeled sense and antisense RNA probes (1.2×10^5 cpm/μl) prepared in pGEM-3Z (Promega). After hybridization, the cells were exposed to autoradiography film for 1 week and counterstained with hematoxylin and eosin (HE; all panels ×520). In (E), the cells were infected as in (A). After 1 day, the cells were labeled with [^{35}S]methionine (500 μCi/ml, 24 hours, 37°C), and the supernatant was evaluated by immunoprecipitation with goat antibodies to human α1AT (Cappel), SDS–polyacrylamide gel electrophoresis, and autoradiography (*30*). Lane 1, uninfected cells; lane 2, Ad-α1AT–infected cells; and lane 3, Ad-α1AT–infected cells with unlabeled human α1AT added to block the antibody. The position of migration of the 52-kD human α1AT is indicated by the arrow.

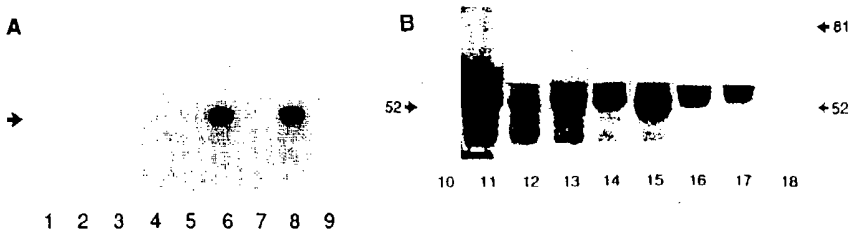

Fig. 3. Expression of human α1AT mRNA transcripts and synthesis and secretion of human α1AT by cotton rat lung after Ad-α1AT infection in vivo. Cotton rats were anesthetized, and Ad-α1AT was diluted in 300 μl of PBS to 10^8 PFU/ml and instilled into the trachea. Controls included 300 μl of PBS or 300 μl of PBS with Ad-dl312 at 10^8 PFU/ml. After 1 to 7 days, lungs were exposed and lavaged, and the pulmonary vasculature was perfused with methionine-free LHC-8 medium. (**A**) We extracted total RNA (*31*), treated the RNA with an excess of deoxyribonuclease (DNase) (RQ1 RNase-Free DNase, Promega), converted the RNA to cDNA by standard techniques, and amplified the cDNA by the polymerase chain reaction (PCR) for 25 cycles (*32*) with an adenoviral-specific primer in the tripartite leader sequences (Fig. 1) and a human α1AT exon III–specific antisense primer (*33*). PCR products were evaluated by agarose gel electrophoresis, followed by Southern hybridization with a human α1AT cDNA probe that was ^{32}P-labeled by random priming (*34*). The size of the expected fragment (1062 bp) is indicated by the arrow. Reverse transcriptase was present in lanes, 2, 4, 6, and 8. Lanes 1 and 2, uninfected lung RNA from the cotton rat (PBS control); lanes 3 and 4, 2 days after infection with Ad-dl312. Lanes 5 and 6, cotton rat 2 days after infection with Ad-α1AT; lanes 7 and 8, a different rat, treated as in 5 and 6; lane 9, PCR control without RNA or DNA template. (**B**) At various times after infection, the lungs were minced, incubated for 1 hour in methionine-free LHC-8 medium (37°C), and then incubated for 24 hours in medium with [^{35}S]-methionine (1 ml of medium/150 mg of tissue; 500 μCi/ml). The supernatant was then evaluated by immunoprecipitation with a rabbit antibody to human α1AT (Boehringer Mannheim), SDS–polyacrylamide gels, and autoradiography as in Fig. 2E. Trichloroacetic acid–precipitable radioactivity was evaluated by immunoprecipitation (for lanes 10 to 15, 2 × 10^6 cpm; for lanes 16 to 18, 1 × 10^6 cpm). Autoradiogram exposures for lanes 10 to 15 were identical; lanes 16 to 18 were evaluated at a different time, and the exposures adjusted such that the intensity of the α1AT band without NE was similar to that in lane 13. We evaluated the ability of the synthesized human α1AT to inhibit its natural substrate, NE, by incubating the supernatant with various dilutions of active NE (30 min, 23°C) before immunoprecipitation. Lane 10, uninfected control; lane 11, 1 day after infection with Ad-α1AT; lane 12, same as in 11 but with antibody exposed to unlabeled human α1AT before immunoprecipitation; lanes 13 through 15, 2, 3, and 7 days, respectively, after infection with Ad-α1AT; lanes 16 through 18, 2 days after infection with Ad-α1AT and with 3 nM, 30 nM, and 300 nM NE added to the supernatant before immunoprecipitation, respectively. The uninfected control evaluated in parallel to lanes 16 through 18 demonstrated no complexes. Indicated is the size of human α1AT (52 kD) and the human α1AT–human NE complex (81 kD).

0.01 to 0.02) and cystic fibrosis (CF; allelic frequency 0.022), have their major clinical manifestations in the lung (*9, 14*). In α1AT deficiency, mutations of coding exons of the 12.2-kb α1AT gene result in decreased serum and, hence, lung levels of α1AT, an antiprotease that normally protects the lung from destruction by the powerful proteolytic enzyme NE (*9*). Consequently, affected individuals develop emphysema by age 30 to 40, which results in a progressive respiratory impairment and a shortened life-span (*15*). Transfer of the normal α1AT gene to lung cells has the potential to protect the lung from NE by local production of the functional antiprotease.

In CF, mutations of coding exons of the 250-kb CF gene are associated with abnormalities in respiratory epithelial cell secretion of thick mucus, chronic colonization of the epithelium with pathogens such as *Pseudomonas aeruginosa*, and airway inflammation dominated by neutrophils (*14, 16*). Because the Cl^- secretory abnormalities of epithelial cells with the CF genotype can be corrected by the transfer of the normal CF gene in vitro (*17*), it should be possible to overcome the expression of the abnormal gene by transfer of the normal gene to airway epithelial cells in vivo.

A recombinant adenovirus–ornithine transcarbamylase (OTC) vector administered intravenously to *spf-ash* mice (OTC-deficient) corrected the enzyme deficiency for at least 1 year (*18*), which suggests that long-term expression is possible. In the lung, long-term expression would be aided by stable integration of the transferred gene into the appropriate stem cells (*1, 19, 20*). Production of human α1AT by lung cells continued for at least 1 week after in vivo infection with Ad-α1AT. If an inability of the virus to infect stem cells limits the length of the time of expression, repetitive administration of the recombinant virus could be used, as long as safety is ensured.

Respiratory epithelial lining fluid (ELF) levels of α1AT of 1.7 μM are sufficient to protect the human lung from its burden of NE (*21*). Because the lavage fluid used to obtain the ELF diluted the ELF 50- to 100-fold (*22*), we estimate that the actual ELF levels achieved in experimental animals with a single infection of Ad-α1AT were ~50-fold below threshold human protective level. Theoretically, it may be possible to achieve higher levels of α1AT by increasing the viral titer, delivering Ad-α1AT by aerosol (thus dispersing the vector over a broader surface area), and repeating the administrations of vector.

The safety aspects for human gene therapy of the recombinant adenoviral vectors, unlike retroviral vectors, have not been exam-

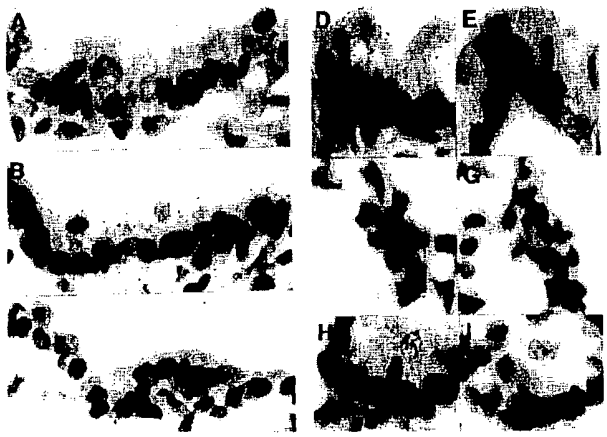

Fig. 4. In situ hybridization evaluation of lung from cotton rats infected in vivo with Ad-α1AT. (**A**) Uninfected lung (PBS control) with antisense probe. (**B** through **I**) Several examples of Ad-α1AT–infected lung. (B) Antisense probe. (C) As in (B) but with sense probe. (D) Antisense probe. (E) As in (D) but with sense probe. (F) Antisense probe. (G) As in (F) but with sense probe. (H) Antisense probe. (I) As in (H) but with sense probe. Cotton rats were infected in vivo as described in Fig. 3, with 300 μl of PBS alone or with 300 μl of Ad-α1AT diluted to between 10^8 and 10^{10} PFU/ml in PBS. After 3 days, the lungs were exposed, blood was removed by cardiac puncture, and the lungs were lavaged. The trachea and pulmonary vasculature were perfused with 4% paraformaldehyde (PFA; Fluka Chemical Corp.); the lungs were resected, fixed in 4% PFA, and frozen. Cryostat sections (7 to 10 μm) were serially treated with 0.2 M HCl and proteinase K (1 μg/ml) immediately before hybridization and evaluated with ^{35}S-labeled antisense and sense RNA probes as described in Fig. 2. As far as was possible, serial sections were used for the antisense and sense probes. All cryostat sections were stained with HE (all panels ×515).

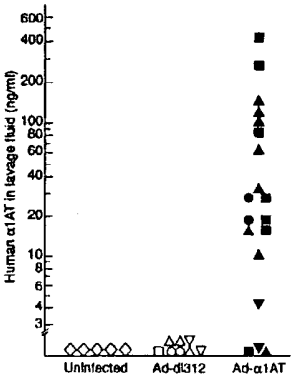

Fig. 5. The amount of human α1AT in the respiratory ELF of cotton rats after in vivo infection with Ad-α1AT. Animals were infected intratracheally with CsCl-purified Ad-α1AT (10^8 to 10^{10} PFU/ml) as described in Fig. 3; controls included uninfected animals and those infected with a similar titer of Ad-dl312. From 1 to 7 days after infection, ELF was obtained by lavage of the lungs with 2 ml of PBS. Lavage fluid was clarified (700*g*, 20 min), and the concentration of human α1AT was quantified (in quadruplicate) with a human α1AT–specific ELISA (*35*) with a sensitivity of ≥3 ng/ml. Each symbol represents the mean value of an individual animal. All uninfected animals, ◇; for infected animals, 1 (○, ●), 2 (△, ▲), 3 (□, ■), and 7 (▼, ▽) days after infection, respectively. No α1AT was detected by ELISA in the viral preparations used for infection.

ined in detail. Safety is particularly important in weighing risk and benefit in response to α1AT deficiency, in which augmentation therapy with human plasma α1AT is available (*21*). In contrast, no definitive therapy is available for CF. Most human adults have antibodies to one of the three serogroup C adenoviruses to which Ad5 belongs (*5*). This implies little risk to those working with these vectors but may have negative implications for the virus as a gene transfer vector in the human lung. If such problems are encountered, alterations in the vector construct may be helpful. The encouraging results obtained with the Ad-α1AT recombinant adenoviral vector in vivo suggest that similar recombinant vectors may be useful for in vivo experimental animal studies with genes such as the human CF gene.

REFERENCES AND NOTES

1. M. J. Evans and S. G. Shami, in *Lung Cell Biology*, C. Lenfant and D. Massaro, Eds. (Dekker, New York, 1989), pp. 1–36.
2. D. G. Miller, M. A. Adam, A. D. Miller, *Mol. Cell. Biol.* 10, 4239 (1990).
3. M. S. Horwitz, in *Virology*, B. N. Fields and D. M. Knipe, Eds. (Raven, New York, ed. 2, 1990), pp. 1679–1721.
4. K. L. Berkner, *BioTechniques* 6, 616 (1988).
5. S. E. Straus, in *The Adenoviruses*, H. S. Ginsberg, Ed. (Plenum, New York, 1984), pp. 451–496.
6. R. M. Chanock, W. Ludwig, R. J. Heubner, T. R. Cate, L.-W. Chu, *J. Am. Med. Assoc.* 195, 151 (1966).
7. Y. Haj-Ahmad and F. L. Graham, *J. Virol.* 57, 267 (1986).
8. A. Ballay, M. Levrero, M.-A. Buendia, P. Tiollais, M. Perricaudet, *EMBO J.* 4, 3861 (1985).
9. R. G. Crystal, *J. Clin. Invest.* 85, 1343 (1990).
10. P. Gilardi, M. Courtney, A. Pavirani, M. Perricaudet, *FEBS Lett.* 267, 60 (1990).
11. M. Courtney *et al.*, *Proc. Natl. Acad. Sci. U.S.A.* 81, 669 (1984).
12. H. S. Ginsberg *et al.*, *ibid.* 86, 3823 (1989).
13. N. Jones and T. Shenk, *Cell* 17, 683 (1979).
14. B.-S. Kerem *et al.*, *Science* 245, 1073 (1989); T. F. Boat, M. J. Welsh, A. L. Beaudet, in *The Metabolic Basis of Inherited Diseases*, C. R. Scriver, A. L. Beaudet, W. S. Sly, D. Valle, Eds. (McGraw-Hill, New York, ed. 6, 1989), pp. 2649–2680.
15. R. G. Crystal, *Trends Genet.* 5, 411 (1989).
16. J. M. Rommens *et al.*, *Science* 245, 1059 (1989); J. R. Riordan *et al.*, *ibid.*, p. 1066.
17. M. L. Drumm *et al.*, *Cell* 62, 1227 (1990); D. P. Rich *et al.*, *Nature* 347, 358 (1990); R. J. Gregory *et al.*, *ibid.* p. 382.
18. L. D. Stratford-Perricaudet, M. Levrero, J.-F. Chasse, M. Perricaudet, P. Briand, *Hum. Gene Ther.* 1, 241 (1990).
19. R. G. Breeze and E. B. Wheeldon, *Am. Rev. Respir. Dis.* 116, 705 (1977).
20. G. D. C. Massaro, in *Lung Cell Biology*, C. Lenfant and D. Massaro, Eds. (Dekker, New York, 1989), pp. 81–114.
21. R. C. Hubbard and R. G. Crystal, *Lung* 168 (suppl.), 565 (1990); M. D. Wewers *et al.*, *N. Engl. J. Med.* 316, 1055 (1987).
22. S. I. Rennard *et al.*, *J. Appl. Physiol.* 60, 532 (1986).
23. B. Thimmappaya, *Cell* 31, 543 (1982).
24. F. L. Graham, J. Smiley, W. C. Russell, R. Nairn, *J. Gen. Virol.* 36, 59 (1977).
25. F. L. Graham and A. J. Van Der Eb, *Virology* 52, 456 (1973).
26. B. Hirt, *J. Mol. Biol.* 26, 365 (1967).
27. J. F. Lechner, A. Haugen, I. A. McClendon, E. W. Pettis, *In Vitro* 18, 633 (1982).
28. M. E. Harper, L. M. Marselle, R. C. Gallo, F. Wong-Staal, *Proc. Natl. Acad. Sci. U.S.A.* 83, 772 (1986).
29. J.-F. Bernaudin *et al.*, *J. Immunol.* 140, 3822 (1988).
30. J.-F. Mornex *et al.*, *J. Clin. Invest.* 77, 1952 (1986).
31. J. M. Chirgwin, A. E. Przybyla, R. J. MacDonald, W. J. Rutter, *Biochemistry* 18, 5294 (1979).
32. R. K. Saiki *et al.*, *Science* 239, 487 (1988).
33. To eliminate the possibility of contaminating viral DNA amplification, we also used each DNase-treated sample of RNA as a PCR template without conversion to DNA.
34. G. M. Church and W. Gilbert, *Proc. Natl. Acad. Sci. U.S.A.* 81, 1991 (1984); A. P. Feinberg and B. Vogelstein, *Anal. Biochem.* 132, 6 (1983).
35. J. P. Michalski, C. C. McCombs, S. Sheth, M. McCarthy, R. deShazo, *J. Immunol. Methods* 83, 101 (1985).

36. We thank B. Trapnell and N. McElvaney (Pulmonary Branch, National Heart, Lung, and Blood Institute), M. Courtney (Research Department, Delta Biotechnology, Ltd.), B. Carter (Laboratory of Molecular and Cellular Biology, National Institute of Diabetes and Digestive and Kidney Diseases), and H. Ginsberg (Departments of Medicine and Microbiology, Columbia University) for helpful discussions; G. Prince and M. Redington (Laboratory of Infectious Diseases, National Institute of Allergy and Infectious Diseases) for making cotton rats available to us; and T. Raymer for assistance in preparing the manuscript.

16 November 1990; accepted 5 March 1991

Group I Intron Self-Splicing with Adenosine: Evidence for a Single Nucleoside-Binding Site

MICHAEL D. BEEN* AND ANNE T. PERROTTA

For self-splicing of *Tetrahymena* ribosomal RNA precursor, guanosine binding is required for 5′ splice-site cleavage and exon ligation. Whether these two reactions use the same or different guanosine-binding sites has been debated. A double mutation in a previously identified guanosine-binding site within the intron resulted in preference for adenosine (or adenosine triphosphate) as the substrate for cleavage at the 5′ splice site. However, splicing was blocked in the exon ligation step. Blockage was reversed by a change from guanine to adenine at the 3′ splice site. These results indicate that a single determinant specifies nucleoside binding for both steps of splicing. Furthermore, it suggests that RNA could form an active site specific for adenosine triphosphate.

GROUP I INTRONS SHARE CONserved sequence elements and a common core secondary structure (*1*). Consistent with these similarities, there is a common mechanism by which group I introns are excised and the exons ligated (*2, 3*). A significant feature of all group I introns is the requirement for G (*4*) to initiate the splicing reaction (*2, 5*). The first step is a G-dependent cleavage at the 5′ splice site. This step is a transesterification (phosphoester transfer) reaction in which the substrate G is covalently joined to the 5′ end of the intron. As a result, a free 3′ hydroxyl group is generated on the U at the end of the 5′ exon. In the second step of the splicing reaction, the exons are ligated by another transesterification reaction. In this case, attack occurs at the 3′ side of the conserved G at the 3′ end of the intron (G414) (*6*) (Fig. 1). This G is essential for completion of the splicing reaction (7). The 5′ splice-site cleavage can be viewed as the "forward" reaction, and the exon ligation can be viewed as the "reverse" of the same reaction (*8–10*). This idea was demonstrated

Department of Biochemistry, Duke University Medical Center, Durham, NC 27710.

*To whom correspondence should be addressed.

Nat. Gent. 1992 1:372-378
Science 1989 245:1234-1236

Eur. J Biochem. 1985 148:265-270

Mol. Immunol 1995 32:1057-1064

Science 1993 259:988-990

Nature 1988 336:348-352

J Clin. Invest. 1993 91:225-234

Mol. Cell. Biol. 1987 7:1576-1579

Gene 1982 19:33-42

Neuron 1992 8:507-520

Adv. Virus Res. 1989 37:35-83

1994 Cancer Res. 54:5258-5261

Cell 1987 50:435-443

Nucleic Acids Res. (1996) 24(10):1841-1848

J Biol. Chem. 1988 263 10 :4837-4843

Proc. Natl. Acad. Sci. USA 1992 89:2581-2584

1993 Nature 361:647-650

DNA Seq. 1993 4:185-196

Human Gene Ther. 1995 6:881-893

Science 1991 252:431-434

Cell 1992 68:143-155

Mol. Cell. Biol. 1990 10 6 :2738-2748

Nucleic Acids Res. 1996 24 15 :2966-2973

Human Gene Thera 1990 1:241-256

J Clin. Invest 1992 . 90:626-630

Curr. Topics in Micro. and Imm. 1995 199 part 3 :177-194

Lancet 1981 11:832-834

Cancer Res. 1996 56:1341-1345

J Virol. 1992 66 (6) :3633-3642

J Virol. 1996 70 (4) :2296-2306

Nature (1997) 389:239-242

J Virol. 1984 51 (3) : 822-831

Adv. Ex . Med. Biol. 1991 3098:61-66

Proc. Natl. Acad. Sci. 1983 80:5383-5386

Genomics 1990 8:492-500

Gastroenter. 1990 98:470-477 .

N. Vogel
Au 1636
12/9
10045116

2966–2973 Nucleic Acids Research, 1996, Vol. 24, No. 15

Oligo-2′-fluoro-2′-deoxynucleotide N3′→P5′ phosphoramidates: synthesis and properties

Ronald G. Schultz and Sergei M. Gryaznov*

Lynx Therapeutics Inc., 3832 Bay Center Place, Hayward, CA 94545, USA

Received April 25, 1996; Revised and Accepted June 7, 1996

ABSTRACT

Uniformly modified oligodeoxyribonucleotide N3′→P5′ phosphoramidates containing 2′-fluoro-2′-deoxypyrimidine nucleosides were synthesized using an efficient interphase amidite transfer reaction. The 3′-amino group of solid phase-supported 2′-fluoro-2′-deoxynucleoside was used as an acceptor and 5′-diisopropylamino phosphoramidite as a donor of a phosphoramidite group in the tetrazole-catalyzed exchange reaction. Subsequent oxidation with aqueous iodine resulted in formation of an internucleoside phosphoramidate diester. The prepared oligo-2′-fluoronucleotide N3′→P5′ phosphoramidates form extremely stable duplexes with complementary nucleic acids: relative to isosequential phosphodiester oligomers, the melting temperature T_m of their duplexes with DNA or RNA was increased ~4 or 5°C per modification respectively. Moreover, these compounds are highly resistant to enzymatic hydrolysis by snake venom phosphodiesterase and they are 4–5 times more stable in acidic media (pH 2.2–5.3) than the parent oligo-2′-deoxynucleotide N3′→P5′ phosphoramidates. The described properties of the oligo-2′-fluoronucleotide N3′→P5′ phosphoramidates suggest that they may have good potential for diagnostic and antisense therapeutic applications.

INTRODUCTION

Synthetic oligonucleotides have become powerful tools in modern molecular biology and nucleic acid-based diagnostics. They may become a new generation of rationally designed therapeutic agents based upon specific interference with gene expression via antisense or antigene modes of action (1,2). Additionally, use of natural and modified oligonucleotides as aptamers could offer an interesting approach to specific inactivation of proteins following high affinity binding (3,4). Several modifications have been introduced to improve binding properties of oligonucleotides and their resistance to enzymatic hydrolysis (5). Recently, we described a new class of oligonucleotide analogs, N3′→P5′ phosphoramidates, where the 3′-oxygen of each 2′-deoxyfuranose was substituted by nitrogen (6–8). These compounds form unusually stable duplexes with complementary DNA and, especially, RNA oligomers, as well as stable triplexes with polypurine–polypyrimidine double-stranded DNA targets. Thermal stabilization of the duplexes formed by phosphoramidates with single-stranded RNA was enhanced by up to 2.7°C per modification and with single-stranded DNA by up to 0.7°C per modification. Additionally, these compounds form very stable homoduplexes, whose melting temperatures T_m were 2.1–2.3°C per modification higher relative to their phosphodiester counterparts. The nature of the unusual stability of N3′→P5′ phosphoramidate hybrids is not yet completely clear. One of the factors contributing to the enhanced stability of the complex is a preference for N-sugar puckering of the 2′-deoxyfuranose of the phosphoramidates over the favored S-sugar puckering of phosphodiesters (7,9). Another contributing factor may be increased hydration and rigidity of the phosphoramidates relative to the parent phosphodiesters (8).

Oligonucleotide phosphoramidates are resistant to enzymatic hydrolysis by phosphodiesterases. Chemically, these compounds are stable under neutral and alkaline conditions and somewhat labile under acidic conditions. Acid-catalyzed hydrolysis of the phophoramidate presumably proceeds via protonation of 3′-nitrogen, followed by nucleophilic attack at phosphorus or by metaphosphate formation. This leads to cleavage of the internucleoside N–P bond and formation of nucleotidic fragments with terminal 3′-amino or 5′-phosphate groups (10). One of the possible approaches to increase acid stability of oligonucleotide phosphoramidates is to reduce the basicity of the 3′-nitrogen atom by placing a strong electron-withdrawing group nearby. An optimal candidate for this role could be fluorine, which is both strongly electron withdrawing and sterically undemanding. Phosphodiester and phosphorothioate oligonucleotides containing 2′-fluoro-2′-deoxynucleosides have been synthesized for antisense (11,12) and ribozyme (13) applications and they appear to adopt A-form duplexes determined by 3′-*endo* or N-sugar, puckering (14,15).

Here we report synthesis and some physico-chemical properties of pyrimidine-containing oligo-2′-fluoro-3′-aminonucleotide N3′→P5′ phosphoramidates. These oligo-2′-fluorophosphoramidates, as will be shown below, are more stable to acid-catalyzed hydrolysis of the phosphoramidate backbone and form exceptionally stable duplexes with complementary DNA and RNA. Two different approaches to the synthesis of these compounds were developed: one utilizing Atherton–Todd type oxidative phosphorylation coupling and another, more efficient method utilizing a phosphoramidite transfer reaction.

* To whom correspondence should be addressed

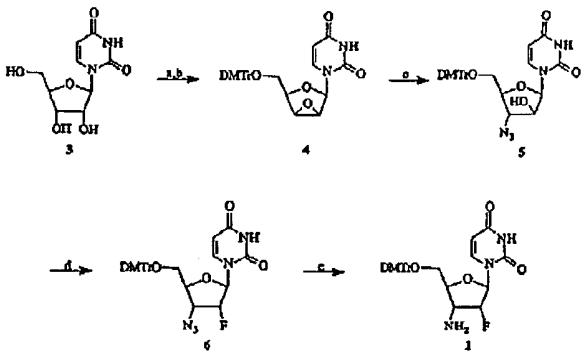

a) DMTrCl; MsCl
b) NaOH
c) NAN_3
d) DAST
e) H_2, Pd/C

Scheme 1.

RESULTS AND DISCUSSION

Preparation of monomers

Synthesis of the oligonucleotide N3′→P5′ phosphoramidates containing 2′-fluoro-2′-deoxynucleosides was conducted using two types of monomers, the structures of which are shown in Schemes 1–3.

Compound **1**, 5′-DMT-2′-fluoro-3′-aminouridine was prepared according to Scheme 1. This monomer was used for incorporation of 2′-fluoro-3′-aminouridine into oligonucleotide phosphoramidates via the oxidative phosphorylation method, which has been previously used for the synthesis of 2′-unmodified N3′→N5′ phosphoramidates (6). First, uridine **3** was transformed into the 5′-DMT-2′,3′-anhydrolyxouridine **4** by successive reaction with DMT-chloride, mesyl chloride and sodium hydroxide (16). The 2′,3′-epoxy ring was then opened by treatment with sodium azide (16), producing 5′-DMT-3′-azido-3′-deoxyarabinouridine **5** as the main product and isomeric 5′-DMT-2′-azido-2′-deoxy-xylouridine as a by-product, in an ~3:1 ratio. Compound **5** was isolated by silica gel chromatography and then fluorinated with diethylaminosulfur trifluoride (DAST) to give **6**. Finally, the azido group of **6** was reduced with hydrogen over palladium catalyst, giving 5′-DMT-2′-fluoro-3′-aminouridine **1** with a 5.3% total yield based on uridine **3**. The structure of nucleoside **1** was confirmed by ^1H and ^{19}F NMR analysis and by mass spectrometry (Materials and Methods).

A different synthetic strategy, as outlined in Scheme 2, was used to prepare phosphoramidite building block **2**. Uridine **3** was mesylated and then selectively benzoylated, with accompanying formation of the 2,2′-anhydrocycle by treatment with sodium benzoate, according to a literature procedure (17). These reactions resulted in compound **7** with 69–77% overall yields. By a second literature method (18), acid-catalyzed hydrolysis of **7** formed 3′-mesyl-5′-benzoylarabinouridine, which upon treatment with ammonium hydroxide closed to form the lyxo-2′,3′-epoxide **8** in 63–77% overall yields. Then, 2′,3′-anhydrolyxonucleoside **8** was heated with ammonium azide. Contrary to previous suggestion (19), this reaction was not completely stereoselective, but produced a chromatographically unresolvable mixture of the desired

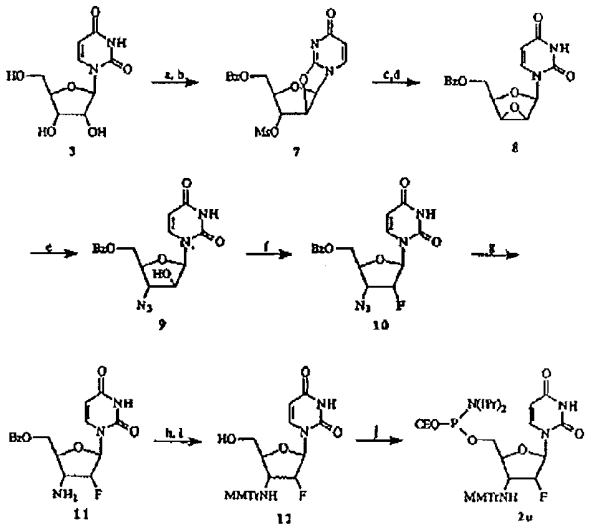

a) MsCl
b) NaOBz
c) HCl, H_2O
d) NH_4 OH
e) NH_4N_3
f) DAST
g) H_2, Pd/C
h) MMTrCl
i) NaOH, H_2O
j) CEOP(Cl)($NiPr_2$)

Scheme 2.

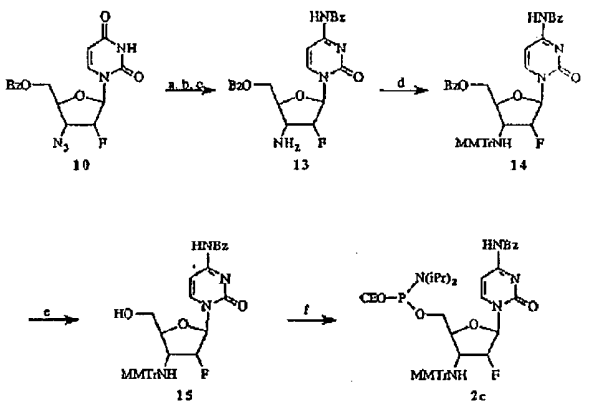

a) $POCl_3$, triazole, TEA; NH_4OH
b) BzCl
c) H_2, Pd/C
d) MMTrCl
e) NaOH, Pyr/MeOH/H_2O; H^+-Pyr dowex
f) CEOP(Cl)($NiPr_2$)

Scheme 3.

5′-benzoyl-3′-azidoarabinonucleoside **9** and its 2′-azido-2′-deoxy-regioisomer **9i** in an ~2.5:1 ratio. Crude arabinonucleoside **9** was fluorinated with DAST to give 2′-fluoro-3′-azidonucleoside **10**, then catalytically hydrogenated to give 2′-fluoro-3′-aminonucleoside **11**, which was separable from its regioisomer by silica gel chromatography. Protection of the 3′-amine with a monomethoxytrityl (MMT) group followed by 5′-debenzoylation produced intermediate **15**, with 5′-phosphitylation producing the desired phosphoramidite building block **2u** in a 28% overall yield from anhydronucleoside **8**.

Crude intermediate **10** was also used for preparation of the appropriately protected cytidine phosphoramidite **2c** (Scheme 3).

The uracil base of **10** was converted to cytosine by adaptation of the method of Reese (20). Subsequent *N*4-benzoylation and reduction of the 3′-azido to an amino group gave compound **13**, which was separable from its regioisomer by silica gel chromatography. Protection of the 3′-amine with an MMT group followed by selective 5′-*O*-debenzoylation produced intermediate **15**. Subsequent 5′-phosphitylation led to the desired phosphoramidite **2c** in an 18% overall yield based on anhydronucleoside **8**.

Additionally, intermediates **12** and **15** were 5′-succinylated and loaded upon a CPG solid support by standard procedures (21,22).

It has been reported that 2′-deoxy-2′-fluoro-substituted nucleosides prefer 3′-*endo* sugar ring puckering or the N-conformation (15). Phosphodiester and phosphorothioate oligonucleotides formed by these monomers are reported to adopt A-type duplexes in solution (11). In order to assess sugar ring conformations of 2′-fluoro-3′-aminonucleosides and compare them with those for 3′-amino-2′-deoxyribonucleosides as well as with parent ribonucleosides and 2′-deoxyribonucleosides, vicinal coupling constants for the anomeric and 2′-hydrogen atoms were derived from ^{1}H NMR spectra and are compared in Table 1. It is important to mention that small coupling constants are indicative of H1′–C1′–C2′–H2′ dihedral angles close to 90°, which is characteristic of the N-conformation. Vicinal coupling constants for 1′- and 2′-hydrogens summarized in Table 1 suggest, in good agreement with the literature, that replacement of the 3′-hydroxyl by a 3′-amino group favors N-conformation of the sugar rings (compare experiments 1 and 5, Table 1). Substitution of the 2′-hydroxyl by fluorine significantly increases the population of sugar N-conformation: H1′–H2′ coupling was greatly decreased, indicating a H1′-C1′–C2′-H2′ dihedral angle close to 90° (experiments 4 and 7, Table 1). For comparison, coupling constants determined for the ribonucleoside, 2′-methoxyribonucleoside and 2′-methoxy-3′-aminoribonucleoside are 2.4, 1.3 and 1.2 Hz respectively, also indicating a predominance of N-conformation (experiments 2, 3 and 6, Table 1). Interestingly, these nucleoside conformations are related to the thermal stability of duplexes formed by their corresponding oligonucleotides, which will be discussed later.

Synthesis of oligo-2′-fluoro-3′-aminonucleotide N3′→P5′ phosphoramidites

Two different approaches to the synthesis of the title compounds were developed. The first is analogous to the one being used for assembly of 2′-unmodified N3′→P5′ phosphoramidates and is based on carbon tetrachloride-driven oxidative phosphorylation of a nucleoside 3′-amine by a 5′-*H*-phosphonate of another nucleoside (6,10). In this scheme, 5′-DMT-2′-fluoro-3′-aminonucleoside **1** was substituted for 5′-DMT-3′-amino-2′-deoxynucleosides. Model dimer dU$^f_{np}$T was prepared using this scheme. The product was analyzed and isolated by reversed phase (RP) HPLC in 70% yield and the structure was confirmed by anion detection electrospray mass spectrometry (monoisotopic calculated and found mass was 548) and by acid-catalyzed hydrolysis, which gave 2′-fluoro-3′-amino-2′-deoxyuridine and 5′-thymidylic acid (see Materials and Methods).

Table 1. Chemical shifts and vicinal coupling constants for the H1′ and H2′ in 3′-aminonucleosides

Experiment	Nucleoside[a]	H1′ (δ, p.p.m.)	J^3 H1′–H2′ (Hz)	J^3 H1′–H2″ (Hz)
1	dU	6.30, dd	6.4	6.4
2	rU	5.87, d	2.4	
3	dU^m	6.00, d	1.3	
4	dU^f	6.10, dd[b]	1.4	
5	dU$_n$	6.17, dd	3.0	7.2
6	dU^m_n	5.92, d	1.2	
7	dU^f_n	6.00, dd[b]	<0.3	

[a]All nucleosides were 5′-*O*-DMT-protected and spectra were recorded in deuterochloroform; n, m and f represent 3′-amino, 2′-methoxy and 2′-fluoro groups respectively.
[b]J^3 H1′-F2′ were 16.3 and 16.2 Hz for experiments 4 and 7 respectively.

Table 2. Oligonucleotides and T_m values of their duplexes

Experiment	Oligonucleotide[a]	T_m (°C)[b]	
		DNA[c]	RNA[c]
1	UUUUUUUUUT, **18**	16.7; 24.6	17.9; 20.3
2	$U_{np}U_{np}U_{np}U_{np}U_{np}U_{np}U_{np}U_{np}U_{np}T$, **19**	18.5; 38.2	38.1; 47.2
3	$U_{np}U_{np}U_{np}U_{np}U^f_{np}U_{np}U_{np}U_{np}U_{np}T$, **20**	20.0; 41.0	40.1; 49.3
4	$U_{np}U_{np}U_{np}U^f_{np}U^f_{np}U_{np}U_{np}U_{np}U_{np}T$, **21**	23.4; 44.6	44.5; 52.7
5	$U^f_{np}U^f_{np}U^f_{np}U^f_{np}U^f_{np}U^f_{np}U^f_{np}U^f_{np}U^f_{np}U^f_{np}T$, **22**	37.4; 56.3	55.6; 61.9
6	$U^f_{np}U^f_{np}U^f_{np}U^f_{np}U^f_{np}U^f_{np}U^f_{np}U^f_{np}U^f_{np}U^f_{np}U^f_n$, **23**	39.4; 58.0	55.6; 61.7
7	$_pU^f_{np}U^f_{np}U^f_{np}U^f_{np}U^f_{np}U^f_{np}U^f_{np}U^f_{np}U^f_{np}U^f_{np}T$, **24**	34.6; 63.0	55.2; 64.6
8	$_pU^f_{np}U^f_{np}U^f_{np}U^f_{np}U^f_{np}U^f_{np}U^f_{np}U^f_{np}U^f_{np}U^f_n$, **25**	39.5; 63.2	56.4; 64.0
9	$C_{np}U_{np}U_{np}C_{np}U_{np}U_{np}C_{np}C_{np}U_{np}U_{np}A$, **26**	44.2	66.0
10	$C^f_{np}U^f_{np}U^f_{np}C^f_{np}U^f_{np}U^f_{np}C^f_{np}C^f_{np}U^f_{np}U^f_{np}A$, **27**	56.9	81.6

[a]All 2′-deoxy compounds; np, f, p and n represent 3′-NHP(O)(O$^-$)O-5′ internucleoside link, 2′-fluorine, 5′-phosphate and 3′-amine respectively.
[b]T_m was determined with 3 μM oligonucleotides; first values were determined in 10 mM sodium phosphate, 150 mM sodium chloride, pH 7.04; second values were determined in the same buffer containing an additional 10 mM magnesium chloride.
[c]Complementary target; poly(dA) or poly(rA) for experiments 1–6, d(ATAAGGAAGAAGC) or r(AUAAGGAAGAAGC) for experiments 9 and 10.

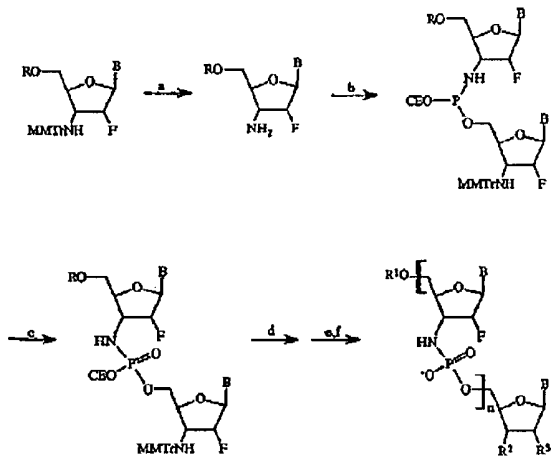

a) $CHCl_2OOH$ R = linker-CPG
b) 2, tetrazole $R^1 = H, PO_3^{2-}$
c) I_2, H_2O $R^2 = OH, NH_2$
d) $(CH_3CO)_2O$, NMI $R^3 = H, F$
e) repetition of steps a)–d) B = Ura, Cyt^{bz}, Cyt
f) NH_3

Scheme 4.

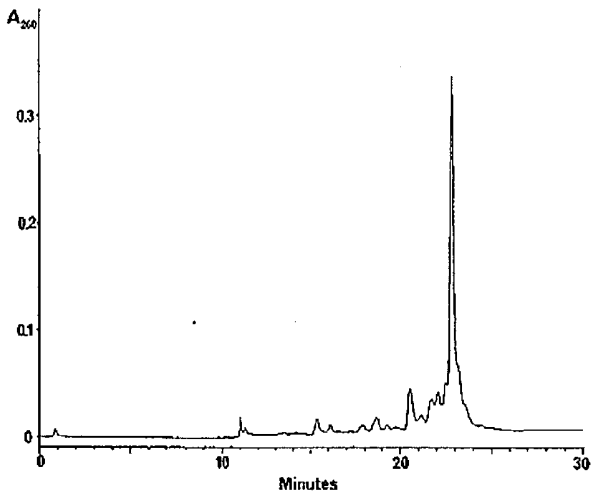

Figure 1. Ion exchange HPLC profile of the crude reaction mixture from synthesis of oligonucleotide **27** (Table 1). Pharmacia MonoQ 5/5 column was used for the analysis and gradient conditions are given in ref. 8.

The same synthetic strategy was used to introduce one or two 2′-fluoro-3′-aminonucleosides into longer oligonucleotide phosphoramidate chains. Compounds **20** and **21** (Table 2), containing one or two 2′-fluoronucleosides in the middle of the chain, were prepared and isolated by ion exchange (IE) HPLC. Coupling yields of the 2′-fluoronucleoside **1** did not exceed 70–75% (in contrast to 94–96% for the 2′-deoxynucleosides), as judged by step-wise measurement of released DMT cation and by IE HPLC analysis. Poor coupling efficiency of monomer **1** is probably due to a significantly diminished nucleophilicity of the 3′-amine by the nearby electronegative fluorine. Thus, incorporation of more than two 2′-fluoronucleosides by this method was difficult and impractical.

To overcome this problem, we developed another approach for the synthesis of uniformly modified oligo-2′-fluoronucleotide phosphoramidites. This is based on a phosphoramidite transfer reaction (for other applications of amidite transfer reactions in oligonucleotide chemistry see refs 23–25) between incoming 5′-diisopropylamino-2-cyanoethyl phosphoramidite **2** (Scheme 2) and the 3′-amino group of solid-phase supported 2′-fluoro-3′-aminonucleosides, according to the method outlined in Scheme 4.

Every synthetic cycle of oligonucleotide chain elongation consisted of the following chemical steps: (i) detritylation with acid of the 3′-amino group of nucleoside attached to a solid support through the 5′-terminus; (ii) a tetrazole-catalyzed amidite transfer reaction between 5′-diisopropylaminophosphoramidite **2** and the 3′-amino group of the nucleoside on a solid support, resulting in formation of an internucleoside phosphoramidite diester group, which may be repeated with intermediate washing with acetonitrile to achieve slightly higher efficiency of chain elongation; (iii) oxidation of the newly formed internucleoside phosphoramidite diester into a phosphoramidate diester group with aqueous iodine; (iv) capping of the unreacted 3′-amino groups with acetic anhydride.

This cycle can be repeated, resulting in oligo-2′-fluoronucleotide N3′→P5′ phosphoramidates after cleavage from the solid support and deprotection with ammonia. The average coupling efficiency as determined by released MMT cation assay was ~94–96% with single coupling per cycle and ~96% with double application of step (ii) per synthetic cycle. In this reaction, the strong electronegativity of the nearby fluorine appears to facilitate coupling, by lowering the basicity of the aminonucleoside 3′-nitrogen and pushing the equilibrium toward the more stable internucleoside phosphoramidite. Several oligo-2′-fluoronucleotide phosphoramidates were synthesized using the described procedures and their sequences and some physico-chemical characteristics are given in Table 2. A representative IE HPLC profile of a crude oligomer synthesis is shown in Figure 1. The hydrolytic stability and duplex forming properties of these oligonucleotides were studied and the results are presented below.

Hydrolytic stability of oligonucleotide N3′→P5′ phosphoramidites

The stability of the oligo-2′-fluoro- in comparison with the oligo-2′-deoxynucleotide N3′→P5′ phosphoramidates toward enzymatic hydrolysis was evaluated next. Thus, phosphoramidates **19** and **24** (Table 3) were treated with snake venom phosphodiesterase and alkaline phosphatase (for conditions see Materials and Methods) and analyzed at successive time points by IE HPLC. Under the conditions used, oligo-2′-deoxyphosphoramidate **19** and oligo-2′-fluorophosphoramidate **24** were hydrolyzed progressively and at similar rates, with calculated half-lives of the full-length strands equal to 4.9 and 5.4 h respectively. In comparison, decathymidylic acid with natural phosphodiester linkages was completely digested to thymidine within 10 min under the same conditions.

Table 3. Acid stability of the oligonucleotide N3′→P5′ phosphoramidates

Experiment	Oligonucleotide	$T_{1/2}$ (h)		
		pH 2.2	pH 4.7	pH 5.3
1	$U_{np}U_{np}U_{np}U_{np}U_{np}U_{np}U_{np}U_{np}U_{np}T$, **19**	0.34	12.3	68
2	$pU^{f}_{np}U^{f}_{np}U^{f}_{np}U^{f}_{np}U^{f}_{np}U^{f}_{np}U^{f}_{np}U^{f}_{np}U^{f}_{np}U^{f}_{np}T$, **24**	1.0	66	309

Additionally, the stability of the phosphoramidates toward acid-catalyzed hydrolysis was studied. Oligonucleotides **19** and **24** were incubated at room temperature in 10% acetic acid, pH 2.2, or in 20 mM sodium acetate buffers, pH 4.7 and 5.3. The hydrolysis reactions were monitored by IE HPLC and the data are summarized in Table 3. The observed half-lives of full-length oligonucleotide **19** at pH 2.2, 4.7 and 5.3 were 21.5 min and 12.3 and 68 h respectively. The oligo-2′-fluorophosphoramidate **24** was noticeably more stable under these conditions, with respective half-lives of this full-length oligomer of 61 min and 66 and 309 h. These results demonstrate a markedly reduced 3′-nitrogen basicity due to electron-withdrawing 2′-fluorine, with consequently greater acid stability of oligo-2′-fluorophosphoramidates relative to the parent oligo-2′-deoxyphosphoramidates.

Notably, oligo-2′-fluoro-3′-aminouridine phosphoramidate **22** is not stable to prolonged heating in concentrated aqueous ammonia, with by-products becoming detectable by IE HPLC after heating at 55°C for more than 1 h. After incubation for 8 h, nearly 50% of **22** was transformed into closely eluting products, which were isolated and analyzed by mass spectrometry. Two modifications were tentatively identified as arising from O2 uracil-mediated elimination of 2′-fluorine: full-length oligonucleotides containing one arabinonucleoside phosphoramidate or one 2,2′-anhydronucleoside phosphoramidate residue. Similar transformation to arabinouridine has been reported for an oligomer containing 3′-terminal 2′-fluorouridine (26). A third type of modification was detected but not identified (M+15 a.m.u.). In contrast, oligo-2′-deoxy-3′-aminouridine phosphoramidite **19** was stable to concentrated ammonia at 55°C even for 16 h.

Thermal stability of the phosphoramidite duplexes

We evaluated the ability of the oligo-2′-fluoronucleoside phosphoramidates to hybridize with complementary DNA and RNA. Melting temperatures were determined for duplexes formed under close to physiological salt concentrations and the results are summarized in Table 2. Substitution of one 2′-deoxynucleoside by one 2′-fluoronucleoside in a phosphoramidate decamer led to an increase in T_m by ~2°C for either DNA or RNA hybrids (experiments 2 and 3, Table 2). Accordingly, replacement of two 2′-deoxynucleosides with 2′-fluoronucleosides in the same phosphoramidate decamer led to an increase in duplex T_m of 3.5–6.4°C. In contrast, others have reported that substitution with two central 2′-fluoronucleosides destabilizes the duplexes of phosphodiester oligomers (27).

Substitution of all 2′-fluoronucleosides for 2′-deoxynucleosides in the decamer phosphoramidate resulted in significant enhancement of duplex thermal stability: T_m values were increased by 16–25°C (compare experiments 2 and 5, 6 and 7 Table 2). The data show that further increases in the proportion of N-sugar ring pucker in the N3′→P5′ phosphoramidates as well as additional negative polarization of 3′-amino groups (by 2′-fluorine) substantially stabilized oligonucleotide duplexes. It is noteworthy that T_m values of the duplexes formed by 2′-fluoroamidates were 38–44°C higher than those of isosequential phosphodiester compounds, with 4–5°C per modification increases in melting temperatures (compare experiments 1, 5 and 6, Table 2).

The mixing curves obtained for the oligonucleotides from experiment 6 (Table 2) in melting buffers containing 10 mM magnesium chloride demonstrate 1:1 stoichiometry of the complex formed by phosphoramidate **23** and the complementary polypurine strand. Moreover, thermal dissociation experiments conducted within the 15–80°C temperature range resulted in single transition melting curves with highest hypochromicity (~25%) for the 1:1 mixtures of purine and pyrimidine strands, but not for the 1:2 mixtures (15%). These data indicate that duplexes, not triplexes, are likely formed by the tested oligonucleotide phosphoramidates under the hybridization conditions used.

The same trend in duplex thermal stability was observed for mixed base 11mer **27** (Table 2), which formed more stable hybrids with complementary DNA and RNA than did the analogous oligo-2′-deoxynucleoside phosphoramidate **26** (compare experiments 9 and 10, Table 2).

In conclusion, the oligonucleotide N3′→P5′ phosphoramidates containing 2′-fluoro-3′-aminonucleosides were synthesized using two different approaches, with the phosphoramidite transfer reaction shown as an efficient method for assembly of uniformly modified oligomers. The 2′-fluoro-modified phosphoramidates form extremely stable duplexes with complementary DNA and RNA under close to physiological conditions, where T_m values were increased by 4–5°C per modification relative to natural phosphodiesters. In addition, these compounds were more stable in acidic media than 2′-deoxynucleoside phosphoramidates and are comparably resistant to enzymatic digestion by snake venom phosphodiesterase. The described properties of the oligo-2′-fluoro-3′-aminonucleotide phosphoramidates indicate that they have good potential as diagnostic and possible antisense agents.

MATERIALS AND METHODS

General methods

Phosphodiester oligodeoxyribonucleotides and oligoribonucleotides were prepared on an ABI 380B DNA synthesizer using standard protocol via the phosphoramidite method (28). Oligonucleotide N3′→P5′ phosphoramidates, containing 2′-deoxyribonucleosides and one or two 2′-fluoronucleosides were synthesized using the oxidative phosphorylation method on a ABI 394 synthesizer as previously described (6). Uniformly modified oligo-2′-fluoronucleotide N3′→P5′ phosphoramidates were prepared by the amidite transfer reaction on an ABI 380B synthesizer using the following protocol: (i) detritylation, 5% dichloroacetic acid in dichloromethane, 1 min; (ii) coupling, 0.1 M phosphoramidite **2** and 0.45 M tetrazole in acetonitrile, 3 min; (iii) oxidation, 0.1 M iodine in tetrahydrofuran/pyridine/water,

10/10/1 v/v/v, 1 min; (iv) capping, acetylation of unreacted 3′-amino groups by standard ABI capping solutions, 30 s.

Chemical steps within the cycle were followed by acetonitrile washing and flushing with dry argon for 0.2–0.4 min. After cleavage from the solid support and deprotection with concentrated aqueous ammonia (1–1.5 h, 55°C) oligonucleotides were analyzed and purified by IE HPLC. Oligonucleotides were desalted on Pharmacia NAP-5 or NAP-10 gel filtration columns immediately after purification and stored frozen or lyophilized at –18°C.

Preparation of the 5′-phosphorylated oligonucleotides was upon sulfone-derivatized CPG (29) and 5′-hydroxyl oligomers were synthesized upon oligonucleotide–succinyl CPG.

Oligonucleotide thermal dissociation experiments were carried out as previously described (7), with melting buffers as listed in Table 2.

Acid hydrolysis of 0.17 OD_{260} of the dimer $dU^{f}_{np}T$ was in 25 µl 64% acetic acid (2 h at 55°C) and the reaction mixture was analyzed by RP HPLC. Approximately 83% of the dimer, retention time (Rt) 15.0 min, was hydrolyzed to mainly 5′-thymidylic acid, Rt 10.6 min, and 2′-fluoro-3′-aminouridine, Rt 11.2 min, as identified by co-injection with authentic standards. Also, ~7.5% of thymidine, Rt 12.1 min, was found in the reaction mixture.

Acid hydrolysis of the oligonucleotide phosphoramidates (Table 3), 1–3 OD_{260} of each, was carried out at room temperature in 0.1–0.2 ml 10% acetic acid, pH 2.2, or in 20 mM sodium acetate buffers, pH 4.7 and 5.3. For enzymatic digestion, 0.2 OD_{260} of oligonucleotides **19** and **22** (Table 2) were treated with 0.02 U snake venom phosphodiesterase and 0.8 U alkaline phosphatase (Sigma, St Louis, MO) in 0.2 ml 10 mM Tris–HCl buffer, pH 8.9, at room temperature. Aliquots from the reaction mixtures were taken at multiple time points and analyzed by IE HPLC.

5′-*O*-DMT-2′,3′-anhydrolyxouridine (4)

This was prepared according to (16) in 64% yield after chromatography. Mass spectrometry, FAB^+, $M+H^+$, calculated, 529.1975; observed, 529.1963. ^1H NMR δ 7.58 (d, J = 8.2 Hz, 1H), 7.5–7.2 (mm, 10H), 6.86 (d, J = 8.2 Hz, 4H), 6.20 (s, 1 H), 5.68 (d, J = 8.1 Hz, 1H), 4.20 (dd, J = 5.8, 5.8 Hz, 1H), 3.96 (d, J = 2.9 Hz, 1H), 3.92 (d, J = 3.0 Hz, 1H), 3.82 (s, 6H), 3.47 (dd, J = 5.9, 9.7 Hz, 1H), 3.38 (dd, J = 5.7, 9.6 Hz, 1H).

5′-*O*-DMT-3′-azido-3′-deoxyarabinouridine (5)

To 13.8 g (26 mmol) **4** in 500 ml acetone was added 200 ml H_2O and 12.0 g (185 mmol) NaN_3. The mixture was refluxed overnight, then concentrated *in vacuo* to remove the acetone. The resultant slurry was extracted with 600 ml CH_2Cl_2, which in turn was washed with water (3 × 250 ml). Concentration of the CH_2Cl_2 layer and flash chromatography of the crude product provided 6.0 g (40%) of a pale yellow solid. Mass spectrometry, FAB^+, $M+H^+$, calculated, 572.2145; observed, 572.2147. ^1H NMR δ 9.4 (br s, 1H), 8.07 (d, J = 8.1 Hz, 1H), 7.4–7.3 (mm), 6.89 (d, J = 7.9 Hz, 4H), 6.10 (d, J = 5.5 Hz, 1H), 5.46 (d, J = 8.1 Hz, 1H), 4.55 (m, 1H), 4.19 (dd, J = 7.2, 7.7 Hz, 1H), 3.84 (m, 1H), 3.83 (s, 6H), 3.64 (dd J = 2.6, 11.3 Hz, 1H), 3.43 (dd, J = 2.6, 11.4 Hz, 1H).

5′-*O*-DMT-2′-fluoro-3′-azido-2′,3′-dideoxyuridine (6)

To 6.0 g (10.5 mmol) **5** in 120 ml anhydrous DMF was added 2.4 ml (18.2 mmol) diethylaminosulfur trifluoride. The mixture was stirred for 16 h, then poured into 300 ml cold saturated aqueous $NaHCO_3$. The product was extracted with 500 ml ethyl acetate, which in turn was washed with water (2 × 500 ml). Concentration of the organic layer and flash chromatography of the crude product provided 2.9 g (48%) of an off-white solid. Mass spectrometry, FAB^+, $M^{+\cdot}$, calculated, 573.2024; observed, 573.2011. ^1H NMR δ 8.95 (br s, 1H), 7.91 (d, J = 8.1 Hz, 1H), 7.2–7.4 (mm, 11H), 6.88 (d, J = 8.6 Hz, 4H), 6.02 (d, J = 17.2 Hz, 1H), 5.42 (d, J = 8.1 Hz, 1H), 5.27 (dd, J = 3.7, 55.0 Hz, 1H), 4.24 (m, 1H), ~4.21 (partially overlapping with signal 4.24 p.p.m., presumed ddd, J = 4, 4, ~25 Hz, 1H), 3.82 (s, 6H), 3.71 (d, J = 11.4 Hz, 1H), 3.49 (d, J = 11.3 Hz, 1H); ^{19}F NMR δ –196.7 (dddd, est. J = 3, 17, 25, 55 Hz).

5′-*O*-DMT-2′-fluoro-3′-amino-2′,3′-dideoxyuridine (1)

To 2.9 g (5.1 mmol) **6** in 75 ml 95% ethanol was added 0.5 g 10% palladium on carbon. The mixture was hydrogenated at 40 p.s.i. overnight and then the catalyst removed by filtration. The solvent was removed *in vacuo* and the resultant solid purified by flash chromatography to give 1.2 g (43%) of product as a white powder. Mass spectrometry, FAB^+, $M+H^+$, calculated, 548.2197; observed, 548.2206. ^1H NMR δ 8.04 (d, J = 8.0 Hz, 1H), 7.9 (br m, 1H), 7.2–7.4 (mm), 6.85 (d, J = 8.4 Hz, 4H), 6.00 (d, J = 16.2 Hz, 1H), 5.32 (d, J = 8.7 Hz, 1H), 4.83 (dd, J = 3.9, 52.2 Hz, 1H), 3.88 (br d, J = 11 Hz, 1H), 3.8 (s, 6H), 3.8–3.7 (mm, 2H), 3.52 (dd, J = 2.6, 11.1 Hz, 1H); ^{19}F NMR δ –200.1 (ddd, J = 16.4, 27.5, 52.1 Hz).

3′-*O*-Methanesulfonyl-5′-*O*-benzoyl-2,2′-anhydroarabinouridine (7)

This was prepared in two steps from **3** according to the procedure of Codington *et al.* (17) in 69–77% overall yields.

5′-*O*-benzoyl-2′,3′-anhydrolyxouridine (8)

This was prepared in two steps from **7** according to the procedure of Codington *et al.* (18) in 63–77% overall yields.

3′-Azido-5′-*O*-benzoyl-3′-deoxyarabinouridine (9)

This was prepared from **8** and anhydrous NH_4N_3 (30), according to the procedure of Reichman *et al.* (19), but without successful recrystallization. Mass yields were 98% or greater, but NMR suggested 25–35% of the regioisomer, 2′-azido-5′-*O*-benzoyl-2′-deoxyxylouridine **9i**, which co-eluted with the desired product on silica gel TLC. ^1H NMR, major component **9** δ 10.8 (br s, 1H), 8.11 (d, J = 7.5 Hz, 2H), 7.68 (d, J = 8.1 Hz, 1H), 7.62 (d, J = 7.3 Hz, 1H), 7.5 (m, 2H), 6.19 (d, J = 3.6 Hz, 1H), 5.40, (d, J = 8.0 Hz, 1H), 4.84 (m, 1H), 4.73 (d, J = 5.7 Hz, 1H), 4.63 (br d, J = 4.2 Hz, 1H), 4.2 (mm, 2H); minor component **9i** δ 10.6 (br s, 1H), 8.11 (d, J = 7.5 Hz, 2H), 7.81 (d, J = 8.1 Hz, 1H), 7.64 (d, J = 7.5 Hz, 1H), 7.5 (m, 2H), 5.85 (s, 1H), 5.47, (d, J = 8.1 Hz, 1H), 4.86 (m, 1H), 4.76 (d, J = 5.4 Hz, 1H), 4.62 (br d, J = 4.0 Hz, 1H), 4.3–4.2 (mm, 2H).

2′-Fluoro-3′-azido-5′-*O*-benzoyl-2′,3′-dideoxyuridine (10)

To 5.0 g (13.4 mmol) crude **9** (containing 25% **9i**) in 30 ml anhydrous CH_2Cl_2 was added 8.8 ml (66.6 mmol) diethylamino-

sulfur trifluoride. After stirring for 48 h, the mixture was diluted with 100 ml CH_2Cl_2 and poured into 200 ml saturated aqueous $NaHCO_3$. When evolution of gas ceased, the CH_2Cl_2 layer was washed with 100 ml fresh $NaHCO_3$ solution and then with water (2 × 100 ml). Concentration of the CH_2Cl_2 layer *in vacuo* and flash chromatography gave 3.5 g (70%) of product containing 20% of the largely chromatographically unresolvable isomeric impurity **10i**. ^{1}H NMR, major component **10** δ 8.7 (br s, 1H), 8.07 (d, J = 7.4 Hz, 2H), 7.62 (d, J = 7.5 Hz, 1H), 7.49 (dd, J = 7.6, 7.6 Hz, 2H), 7.39 (d, J = 8.1 Hz, 1H), 5.70 (d, J = 21.1 Hz, 1H), 5.65 (d, J = 8.2 Hz, 1H), 5.48 (dd, J = 4.7, 52.9 Hz, 1H), 4.7–4.4 (unresolved), 4.32 (dd, J = 4.7, 9.5 Hz, 1H), 4.27 (dd, J = 4.7, 9.5 Hz, 1H); minor component **10i** δ 8.7 (br s, 1H), 8.03 (d, J = 7.2 Hz, 2H), 7.64 (d, J = 7.6 Hz, 1H), 7.51 (dd, J = 7.4, 7.7 Hz, 2H), 7.33 (d, J = 8.2 Hz, 1H), 5.99 (d, J = 6.4 Hz, 1H), 5.67 (d, J = 9 Hz, 1H), 5.40 (ddd, J = 2.8, 5.0, 53.4 Hz, 1H), 4.8–4.4 (unresolved), 4.10 (mm, 2H); ^{19}F NMR, major component δ –193.1 (ddd, J = 21.8, 21.9, 52.8 Hz); minor component δ –197.3 (ddd, J = 17.2, 23.2, 53.4 Hz).

2′-Fluoro-3′-amino-5′-*O*-benzoyl-2′,3′-dideoxyuridine (11)

To 3.5 g (9.3 mmol) crude **10** (20% **10i**) in 200 ml 95% ethanol was added 600 mg 10% palladium on carbon. The suspension was hydrogenated at 40 p.s.i. overnight and then the catalyst removed by filtration. The solvent was removed *in vacuo*, giving 2.93 g (90%) of a light yellow solid consisting of two compounds which were resolvable by TLC. Flash chromatography provided 1.96 g (60% yield) of the desired product as a pure white solid. Mass spectrometry, FAB^+, $M+H^+$, calculated, 350.1152; observed, 350.1152. ^{1}H NMR δ 8.14 (br s, 1H), 8.06 (d, J = 7.1 Hz, 1H), 7.64 (dd, J = 7.4, 7.4 Hz, 1H), 7.57 (d, J = 8.2 Hz, 1H), 7.50 (dd 7.7, 7.8 Hz, 1H), 5.86 (d, J = 18.5 Hz, 1H), 5.51 (d, J = 8.2 Hz, 1H) 5.00 (dd, J = 4.3, 52.4 Hz, 1H), 4.81 (dd J = 2.2, 12.8 Hz, 1H), 4.73 (dd, J = 3.5, 12.7 Hz, 1H), 4.14 (ddd, J = 2, 3, 10.2 Hz, 1H), 3.57 (ddd, J = 4, 10.5, 26.6 Hz, 1H); ^{19}F NMR δ –198.3 (ddd, J = 18.5, 26.4, 52.2 Hz).

2′-Fluoro-3′-(4-methoxytrityl)amino-2′,3′-dideoxyuridine (12)

To 1.0 g (2.9 mmol) **11** in 50 ml anhydrous pyridine was added 1.0 g (3.2 mmol) 4-methoxytrityl chloride. The mixture was stirred overnight, 5 ml saturated aqueous $NaHCO_3$ was added and the mixture concentrated *in vacuo* to an oil. The oil was dissolved in 125 ml ethyl acetate, which was washed with water (3 × 100 ml) and reconcentrated *in vacuo* to 2.05 g of foam. The foam was dissolved in a mixture of 40 ml methanol, 40 ml dioxane and 10 ml water. NaOH (1 g, 25 mmol) was added and the mixture stirred overnight. The solution was concentrated *in vacuo* to a syrup, which was dissolved in 100 ml ethyl acetate and washed with water (3 × 100 ml). Concentration *in vacuo* of the organic layer gave 1.11 g of a foam, which upon flash chromatography gave 1.05 g (76%) of a white solid. Mass spectrometry, FAB^+, $M+H^+$, calculated, 518.2091; observed, 518.2076. ^{1}H NMR δ 8.64 (br d J = 4.2 Hz, 1H), 8.14 (br s, 1H), 7.57 (mm, 5H), 7.48 (d J = 8.7 Hz, 1H), 7.3 (mm, 8H), 6.83 (d J = 8.8 Hz, 2H), 5.67 (d, J = 17.7 Hz, 1H), 5.62 (d, J = 8.1 Hz, 1H), 4.23 (m, 2H), 4.03 (br d, J = 10.2 Hz, 1H), 3.80 (s, 3H), 3.31 (dddd, J = 3.6, 10.3, 10.9, 25.8 Hz, 1H), 2.80 (dd, J = 3.6, 50.9 Hz, 1H), 2.51 (dd, J = 3.0, 11.2 Hz, 1H); ^{19}F NMR δ –192.5 (dddd, J = 2.9, 17.7, 26.1, 50.9 Hz).

2′-Fluoro-3′-(4-methoxytrityl)amino-2′,3′-dideoxyuridine 5′-(2-cyanoethyl *N,N*-diisopropyl)phosphoramidite (2u)

Mass spectrometry, FAB^+, $M+H^+$, calculated, 718.3170; observed; 718.3194. ^{19}F NMR δ –190.9 (ddd, J = 21.7, 21.8, 51.3 Hz), –193.4 (ddd); ^{31}P NMR δ 150.5, 149.4.

N^4,5′-*O*-Dibenzoyl-2′-fluoro-3′-amino-2′,3′-dideoxycytidine (13)

To 6.9 g (18.4 mmol) crude **10** (containing 35% **10i**) in 50 ml anhydrous CH_3CN was added an ice-cold solution of 11.7 g (169 mmol) 1,2,4-triazole and 3.35 ml (36.1 mmol) $POCl_3$ in 90 ml anhydrous CH_3CN. The mixture was cooled in an ice bath and anhydrous triethylamine (23 ml, 165 mmol) was added, then the reaction allowed to warm to room temperature with stirring. After 90 min, 15 ml (108 mmol) triethylamine and 4 ml water were added and the mixture stirred for 10 min. The solvent was removed *in vacuo*, then 250 ml ethyl acetate was added and the solution was washed with saturated aqueous $NaHCO_3$ (2 × 250 ml) and with 250 ml water. TLC indicated a fluorescent intermediate with the same mobility as the starting material. The mixture was concentrated *in vacuo* to 6.7 g of a foam. Dioxane (100 ml) and 20 ml concentrated aqueous ammonia were added and, after 3 h, the mixture was concentrated *in vacuo* to a yellow gel. The gel was dissolved in 100 ml ethyl acetate and washed with water (3 × 200 ml). Concentration *in vacuo* and vacuum desiccation over P_2O_5 yielded 5.4 g of a solid which gave only one spot on silica gel TLC. Only two significant signals were observed by ^{19}F NMR, major component δ –192.8 (ddd, J = 22.8, 22.8, 53.1 Hz); minor component δ –200.7 (ddd, J = 13.6, 19.9, 53.4 Hz).

Anhydrous pyridine (100 ml) was added and the solution cooled to 4°C. Benzoyl chloride (11.7 ml 100 mmol) was added with stirring and the mixture allowed to warm to room temperature. After 2 h, 5 ml water was added and the solvent removed *in vacuo*, giving a brown oil, which was dissolved in 200 ml ethyl acetate, washed with water (3 × 200 ml) and then reconcentrated *in vacuo* to an oily foam. Ethanol (150 ml) and 2 g 10% palladium on activated carbon were added and the mixture was hydrogenated at 40 p.s.i. H_2 overnight. TLC indicated formation of two slower, closely migrating compounds. The catalyst was removed by filtration and the filtrate concentrated *in vacuo* to an oily yellow foam. Silica gel flash chromatography (500 ml silica, eluted with 0–3% CH_3OH in CH_2Cl_2) provided 1.85 g of semi-pure product, which was dissolved in 10 ml CH_2Cl_2. A solid quickly precipitated, which was collected by filtration and washed with fresh CH_2Cl_2. Vacuum desiccation yielded 1.5 g of product **13** (11% yield from **9** and **9i**) as fine white crystals. Mass spectrometry, FAB^+, $M+H^+$, calculated, 453.1574; observed, 453.1574. ^{1}H NMR δ 8.21 (d, J = 7.5 Hz, 1H), 8.08–8.13 (mm, 3H), 7.94 (d, J = 7.4 Hz, 2H), 7.46–7.7 (mm, 8H), 6.04 (d, J = 16.9 Hz, 1H), 5.08 (dd, J = 3.6, 51.5 Hz, 1H), 4.85 (dd, J = 3.3, 12.8 Hz, 1H), 4.80 (dd, J = 2.1, 12.8 Hz, 1H), 4.26 (m, 1H), 3.48 (dm, J = 27 Hz, 1H); ^{19}F NMR δ –200.1 (m).

N^4,5′-*O*-Dibenzoyl-2′-fluoro-3′-(4-methoxytrityl)amino-2′,3′-dideoxycytidine (14)

To 0.9 g (2.0 mmol) **13** in 25 ml anhydrous pyridine was added 0.86 g (2.8 mmol) 4-methoxytrityl chloride and the mixture stirred overnight. The reaction was quenched with 0.5 ml H_2O and concentrated *in vacuo*. CH_2Cl_2 (50 ml) was added and washed

with 50 ml saturated aqueous $NaHCO_3$ and with water (2 × 50 ml). The solvent was removed *in vacuo*, replaced with 10 ml CH_2Cl_2 and pipetted into 80 ml rapidly stirred 1/1 hexane/ether. After further stirring for 2 h, the product was collected by filtration and dried under vacuum, giving 1.3 g (88% yield) of product as a white powder. Mass spectrometry, FAB^+, $M+H^+$, calculated, 725.2775; observed, 725.2761. ^1H NMR δ 8.59 (br s, 1H), 8.07 (br d, J = 5.7 Hz, 1H), 7.89 (br d, J = 7 Hz, 2H), 7.83 (dd, J = 1.3, 6.7 Hz, 2H), 7.68 (dd, J = 7.4, 7.4 Hz, 2H), 7.5–7.6 (m, 8H), 7.43 (dd, J = 2.1, 6.9 Hz, 2H), 7.1–7.3 (mm, 7H), 6.71 (d, J = 8.9 Hz, 2H), 5.80 (d, J = 15.4 Hz, 1H), 5.03 (dd, J = 2.0, 13.0 Hz, 1H), 4.98 (dd, J = 2.3;, 13.1 Hz, 1H), 4.41 (br d, J = 10.5 Hz, 1H), 3.63 (s, 3H), 3.36 (dddd, J = 3.1, 11.1, 11.1, 25.7 Hz, 1H), 2.84 (dd, J = 3.1, 49.9 Hz, 1H), 2.52 (dd, J = 2.7, 11.5 Hz, 1H); ^{19}F NMR δ –196.3 (m).

N^4-Benzoyl-2′-fluoro-3′-(4-methoxytrityl)amino-2′,3′-dideoxycytidine (15)

To 1.3 g (1.75 mmol) **14** in 20 ml 65/30/5 pyridine/methanol/water, cooled in an ice bath, was added 10 ml cold 2 M NaOH in 65/30/5 pyridine/methanol/water. The mixture was stirred cold for 20 min, then neutralized with pyridinium-H^+ form BioRad AG 50W-X8 cation exchange resin. After 5 min, the resin was removed by filtration and washed with methanol. The combined filtrate and wash were concentrated *in vacuo* to an oil, which was dissolved in 100 ml ethyl acetate. The mixture was washed with 100 ml saturated aqueous $NaHCO_3$ and with water (2 × 100 ml). After concentration *in vacuo* to a foam, the product was dissolved in 10 ml CH_2Cl_2 and pipetted into 75 ml rapidly stirred hexane/ether, 2/1. The product was collected by filtration and dried under vacuum, giving 1.13 g (~100%) of product as a white powder. Mass spectrometry, FAB^+, $M+Cs^+$, calculated, 753.1489; observed, 753.1499. ^1H NMR δ 8.30 (br d, J = 6.8 Hz, 1H), 7.89 (br d, J = 6.7 Hz, 2H), 7.64 (dd, J = 7.4, 7.4 Hz, 1H), 7.44–7.56 (mm, 9H), 7.22–7.32 (mm, 9H), 6.82 (d, J = 8.8 Hz, 2H), 5.80 (d, J = 15.7 Hz, 1H), 4.26 (mm, 2H), 4.13 (d, J = 10.2 Hz, 1H), 3.81 (s, 3H), 3.26 (dddd, J = 3.4, 10.7, 10.8, 26.5 Hz, 1H), 2.93 (dd, J = 3.3, 50.5 Hz, 1H), 2.50 (dd, J = 2.8, 11.0 Hz, 1H); ^{19}F NMR δ –195.3 (m).

N^4-Benzoyl-2′-fluoro-3′-(4-methoxytrityl)amino-2′,3′-dideoxycytidine 5′-(2-cyanoethyl *N,N*-diisopropyl) phosphoramidite (2c)

Mass spectrometry, FAB^+, $M+Cs^+$, calculated, 953.2568; observed, 953.2531. ^{19}F NMR δ –193.6 (m); ^{31}P NMR δ 150.4, 149.4.

REFERENCES

1 Helene,C. and Toulme,J.-J. (1990) *Biochim. Biophys. Acta*, **1049**, 99–125.
2 Uhlman,E. and Peyman,A. (1990) *Chem. Rev.*, **90**, 544–584
3 Bielinska,A., Shivdasami,R.A., Zhang,L. and Nabel,G.J. (1990) *Science*, **250**, 997–101.
4 Wyatt,J.R., Vickers,T.A., Roberson,J.L., Buckheit,R.W.,Jr, Klimkait,T., DeBeats,E., Davis,P.W., Rayner,B., Imbach,J.-L. and Ecker,D.J. (1994) *Proc. Natl Acad. Sci. USA*, **91**, 1356–1360.
5 DeMesmacker,A., Altman,K.-H., Waldner,A. and Wendeborn,S. (1995) *Curr Opin. Struct. Biol.*, **5**, 343–355.
6 Gryaznov,S.M. and Chen,J.-K. (1994) *J. Am. Chem. Soc.*, **116**, 3143–3144.
7 Gryaznov,S.M., Lloyd,D.H., Chen,J.-K., Schultz,R.G., DeDionisio,L.A., Ratmeyer,L. and Wilson,W.D. (1995) *Proc. Natl Acad. Sci. USA*, **92**, 5798–5802.
8 Chen,J.-K., Schultz,R.G., Lloyd,D.H. and Gryaznov,S.M. (1995) *Nucleic Acids Res.*, **23**, 2661–2668.
9 Ding,D., Gryaznov,S.M., Lloyd,D.H., Chandrasekaran,S., Yao,S., Ratmeyer,L., Li Pan,Y. and Wilson,W.D. (1996) *Nucleic Acids Res.*, 24, 354–360.
10 Gryaznov,S. M. and Letsinger,R.L. (1992) *Nucleic Acids Res.*, 20, 3403–3409.
11 Kawasaki,A.M., Casper,M.D., Freier,S.M., Lesnik,E.A., Zounes,M.C., Cummins,L.L., Gonzalez,C. and Cook,P.D. (1993) *J. Med. Chem.*, **36**, 831–841.
12 Monia,B.P., Lesnik,E.A., Gonzalez,C., Lima,W.F., McGee,D., Guinosso,C.J., Kawasaki,A.M., Cook,P.D. and Freier,S.M. (1993) *J. Biol. Chem.*, **268**, 14514–14522.
13 Pieken,W.A., Olsen,D.B., Benseler,F., Aurup,K.H. and Eckstein,F. (1991) *Science*, **253**, 314–317.
14 Ikehara,M. (1984) *Heterocycles*, **21**, 75–90.
15 Guschlbauer,W. and Jankowski,K. (1980) *Nucleic Acids Res.*, **8**, 1421–1433.
16 Webb,T.R., Mitsuya,H. and Broder,S. (1988) *J. Med. Chem.*, **31**, 1475–1479.
17 Codington,J.F., Fecher,R. and Fox,J.J. (1960) *J. Am. Chem. Soc.*, **82**, 2794–2803.
18 Codington,J.F., Fecher,R. and Fox,J.J. (1962) *J. Org. Chem.*, **27**, 163–167.
19 Reichman,U., Hollenberg,D.H., Chu,C.K., Watanabe,K.A. and Fox,J.J. (1976) *J. Org. Chem.*, **41**, 2042–2043.
20 Divakar,K.J. and Reese,C.B. (1982) *J. Chem. Soc. Perkin Trans.*, **1**, 1171–1176.
21 Atkinson,T. and Smith,M. (1984) In Gait,M.J. (ed.), *Oligonucleotide Synthesis. A Practical Approach*. IRL Press, Oxford, UK, pp. 35–81.
22 Knorr,R., Trzeciak,A., Bannwarth,W. and Gillessen,D. (1989) *Tetrahedron Lett.*, **30**, 1927–1930.
23 Bannwarth,W. (1988) *Helv. Chem. Acta*, **71**, 1517–1527.
24 Gryaznov,S.M. and Letsinger,R.L. (1991) *J. Am. Chem. Soc.*, **113**, 5876–5877.
25 Gryaznov,S.M. and Letsinger,R.L. (1992) *Tetrahedron Lett.*, **33**, 4127–4128.
26 Krug,A., Oretskaya,T.S., Volkov,E.M., Cech,D., Shabarova,Z.A. and Rosenthal,A. (1989) *Nucleosides Nucleotides*, **8**, 1473–1483.
27 Williams,D.M., Beuseler,F. and Eckstein,F. (1991) *Biochemistry*, 30, 4001–4009.
28 Caruthers,M.H. (1991) *Acc. Chem. Res.*, **24**, 278–284.
29 Gryaznov,S.M. and Letsinger,R.L. (1993) *Nucleic Acids Res.*, **21**, 1403–1408.
30 Obenland,C.O., Mangold,D.J. and Marino,M.P. (1966) *Inorg. Synth.*, **8**, 53–56.

Nat. Gent. 1992 1:372-378
Science 1989 245:1234-1236

Eur. J Biochem. 1985 148:265-270

Mol. Immunol 1995 32:1057-1064

Science 1993 259:988-990

Nature 1988 336:348-352

J Clin. Invest. 1993 91:225-234

Mol. Cell. Biol. 1987 7:1576-1579

Gene 1982 19:33-42

Neuron 1992 8:507-520

Adv. Virus Res. 1989 37:35-83

1994 Cancer Res. 54:5258-5261

Cell 1987 50:435-443

Nucleic Acids Res. (1996) 24(10):1841-1848

J Biol. Chem. 1988 263 10 :4837-4843

Proc. Natl. Acad. Sci. USA 1992 89:2581-2584

1993 Nature 361:647-650

DNA Seq. 1993 4:185-196

Human Gene Ther. 1995 6:881-893

Science 1991 252:431-434

Cell 1992 68:143-155

Mol. Cell. Biol. 1990 10 6 :2738-2748

Nucleic Acids Res. 1996 24 15 :2966-2973

Human Gene Thera 1990 1:241-256

J Clin. Invest 1992 . 90:626-630

Curr. Topics in Micro. and Imm. 1995 199 part 3 :177-194

Lancet 1981 11:832-834

Cancer Res. 1996 56:1341-1345

J Virol. 1992 66 (6) :3633-3642

J Virol. 1996 70 (4) :2296-2306

Nature (1997) 389:239-242

J Virol. 1984 51 (3) : 822-831

Adv. Ex . Med. Biol. 1991 3098:61-66

Proc. Natl. Acad. Sci. 1983 80:5383-5386

Genomics 1990 8:492-500

Gastroenter. 1990 98:470-477 .

N. Vogel
Au 1636
12/9
10045116

Proc. Natl. Acad. Sci. USA
Vol. 80, pp. 5383–5386, September 1983
Genetics

A cell line that supports the growth of a defective early region 4 deletion mutant of human adenovirus type 2

(complementing cell line/*gpt* selection/mycophenolic acid)

DAVID H. WEINBERG AND GARY KETNER

Department of Biology, The Johns Hopkins University, Baltimore, Maryland 21218

Communicated by Daniel Nathans, June 6, 1983

ABSTRACT **Cell lines that produce viral gene products and that can support the growth of viral mutants lacking those products have been valuable in the genetic analysis of the transforming regions of several animal viruses. To extend the advantages of such complementing cell systems to regions of the adenoviral genome not directly involved in transformation, we have constructed a cell line that will support the growth of a defective adenoviral deletion mutant, H2*dl*808, that lacks most of early region 4 (E4). The right-hand terminal adenovirus 5 *Eco*RI restriction fragment, which contains all of E4, was first inserted into the vector pSV2*gpt*, and the recombinant plasmid was introduced into Vero cells by calcium phosphate precipitation. Clones containing the hybrid plasmid were selected by their resistance to mycophenolic acid. Five mycophenolic acid-resistant clones were then tested for the ability to support the growth of H2*dl*808. One of the five lines, W162, permits plaque formation by H2*dl*808 at an efficiency that is $>10^6$-fold higher than that of the parental Vero cells and allows the production of high-titer, helper-free H2*dl*808 stocks. Thus, W162 cells are permissive for at least one defective E4 mutant. The line carries, as expected, an intact E4, detected by hybridization. Using an H2*dl*808 lysate produced on W162 cells, we have accurately mapped the 808 deletion. It extends from between *Bcl* I and *Sma* I sites at positions 91.4 and 92.0, respectively, to just beyond a *Hin*dIII site at position 97.2 and, therefore, falls entirely within E4. H2*dl*808 and W162 should be of value in determining the physiological role of E4 in adenoviral infection.**

Studies that probe the functions of viral genes are frequently dependent upon the availability of viral mutants. Most of the mutants that have proved useful in studying viral gene function are conditionally defective; in animal virus systems, the majority of these are temperature sensitive (1, 2). An alternative approach to the isolation of conditionally lethal mutations exploits the fact that some virally transformed cells will support the growth of mutants with defects in transforming regions. For example, polyoma virus-transformed mouse cells support the growth of *hr-t* mutants which carry lesions in the polyoma early region (3); COS cells, a line of simian virus 40 (SV40)-transformed monkey cells, support the growth of SV40 early region mutants (4); and 293 cells, a line of human cells transformed by sheared adenoviral DNA (5), support the growth of mutants of adenoviral early region 1 (6–8). In each of these cases, mutant viruses can be propagated efficiently on the transformed cell line, and their phenotypes subsequently can be analyzed in normal, nonpermissive cell types. The value of a complementing cell line in the isolation and propagation of viral mutants is probably best illustrated by the last example; the examination of a wide variety of mutants of adenoviral early region 1 (E1) has provided a detailed picture of the functions of that region (6–13).

The publication costs of this article were defrayed in part by page charge payment. This article must therefore be hereby marked "*advertisement*" in accordance with 18 U.S.C. §1734 solely to indicate this fact.

In the examples cited above, the expression of integrated viral DNA is presumably responsible both for the cells' transformed phenotype and for their ability to complement the defective mutants. However, many segments of viral DNA do not transform cells, and there is no direct selection for cells that contain such DNA and that might support the growth of mutants in those regions of a viral genome. In an effort to extend the complementing cell approach to segments of viral DNA that do not transform cells and to make possible the analysis of mutants of adenoviral early region 4 (E4), we have used the *Escherichia coli gpt*-based selective system of Mulligan and Berg (14, 15) to introduce E4 DNA into cells that are permissive for human adenoviruses. E4 lies at the right end of the adenoviral genome, and although it is required for viral growth (see below), its role in the viral life cycle is not known. E4 is genetically ill-characterized, and so a cell line that would complement E4 mutants and simplify their isolation and analysis would be useful. One of the lines that we have obtained supports the growth of a defective adenoviral mutant, H2*dl*808 (16), which lacks most of E4. This paper describes the isolation of this line, its partial characterization, and the accurate mapping of the 808 deletion.

MATERIALS AND METHODS

Cells and Viruses. Vero cells were obtained from A. M. Lewis and 293 cells from F. Graham. Vero cells were grown in monolayers in Eagle's minimal essential medium containing 10% calf serum (medium A), and 293 cells were grown in Eagle's minimal essential medium containing 10% fetal calf serum (medium B). Mycophenolic acid-resistant Vero cell derivatives were grown in Dulbecco's modified Eagle's medium supplemented with 10% calf serum and selective drugs as described below.

Wild-type adenovirus type 2 (Ad2) was originally from A. Lewis. H2*dl*808 is an Ad2 deletion mutant lacking the viral DNA between about positions 92 and 97.1 on the standard map; its isolation was described by Challberg and Ketner (16).

Transformation and Mycophenolic Acid Selection. Derivatives of the pSV2*gpt* plasmid of Mulligan and Berg (14, 15) containing adenoviral DNA (see *Results*) were introduced into Vero cells by the calcium phosphate precipitation technique (17, 18). About 5×10^5 cells were plated in a 9-cm Petri dish on the day before they were to be transformed; 15–24 hr later, the medium was removed from the dishes, and 0.5 ml of a suspension of precipitated DNA (12.5 μg of plasmid DNA per 0.5-ml aliquot) was added to each dish. After 20 min at room temperature, the plates were filled with 9 ml of medium A and transferred to a 37°C incubator. Four hours later this medium was replaced with selective medium: Dulbecco's modified Eagle's medium containing calf serum (10%), mycophenolic acid (25 μg/ml), xanthine (250 μg/ml), hypoxanthine (15 μg/ml),

Abbreviations: Ad2, adenovirus type 2; Ad5, adenovirus type 5; E1 and E2, early regions 1 and 2 of adenoviral genome; SV40, simian virus 40.

amethopterin (2 μg/ml), and thymidine (10 μg/ml) (16). Mycophenolic acid was the generous gift of the Eli Lilly Research Laboratories. Mycophenolic acid-resistant colonies first became visible 7–9 days later and were picked after 14–20 days by using cloning cylinders cut from plastic Eppendorf centrifuge tubes. The transformants were grown up and are maintained in the selective medium. It is at present unclear whether continued selection is necessary if W162 cells are to retain their biological activity over long periods, although a brief period without selection does not affect complementing ability (see below).

Preparation of W162 Monolayers for Plaque Assays. To conserve mycophenolic acid, plaque assays on W162 monolayers were performed in the absence of selective drugs. When suddenly withdrawn from selective medium, however, W162 cells grew very poorly. This difficulty could be avoided by a single passage through Eagle's minimal essential medium containing hypoxanthine, xanthine, and thymidine without amethopterin and MPA (medium C). Therefore, W162 cells to be used for plaque assays were transferred first into medium C and, after 2 to 3 days, into 5-cm dishes containing Eagle's minimal essential medium. The resulting monolayers could be used without further special treatment.

Southern Transfers and Hybridization. Cellular DNAs, digested with the restriction endonucleases *Eco*RI or *Hin*dIII, were fractionated on 3-mm thick vertical slab gels and transferred to nitrocellulose filter sheets by the Southern procedure (19). Restriction fragments containing adenovirus type 5 (Ad5) sequences were detected by hybridization (20, 21) to adenoviral DNA labeled with ^{32}P by nick-translation (22) and subsequent autoradiography.

RESULTS

Construction of Cell Lines. The initial goal of these experiments was to introduce adenoviral early region 4 (E4) into a cell line permissive for human adenoviruses. To do so, we used the *gpt*-based selective system developed by Mulligan and Berg (14, 15). This system permits the selection of cells that take up one of a series of plasmid vectors containing the *E. coli gpt* gene linked to SV40 sequences that allow its expression in animal cells. The basis of the selection is the novel ability of such cells to utilize exogenous xanthine as a source of GMP, when *de novo* GMP synthesis is blocked by the drug mycophenolic acid: *gpt*-containing cells are resistant to mycophenolic acid in the presence of xanthine, whereas normal cells are not. Mycophenolic acid resistance is dominant, and the recipient cells need not possess any special properties. We constructed two derivatives of one of the *gpt* vectors, pSV2*gpt*. These plasmids (pE4*gpt*6 and pE4*gpt*16) both contain the Ad5 *Eco*RI B fragment inserted at the vector's single *Eco*RI cleavage site but differ in the orientation of the viral DNA segment. Ad5 *Eco*RI B covers the region 84–100 on the viral genome and contains all of E4, the fiber gene, and part of early region 3. The Ad5 *Eco*RI B fragment that we used has been modified by the addition to its right end of a synthetic *Eco*RI site and was kindly provided by K. Berkner. pE4*gpt*16 is diagrammed in Fig. 1.

The two E4-bearing plasmids were introduced into Vero cells by calcium phosphate precipitation, and mycophenolic acid-resistant clones were selected. On the average, two or three transformants were obtained from each plate exposed to plasmid DNA. A total of 13 clones were picked, 5 made with pE4*gpt*6 and 8 made with pE4*gpt*16. Four clones produced with pE4*gpt*16 (W162 through W165) and one clone produced with pE4*gpt*6 (W6B) were selected for further examination.

Assay for Complementing Activity. To determine whether any of the selected mycophenolic acid-resistant cell lines were capable of complementing an E4 defect, we tested each one for

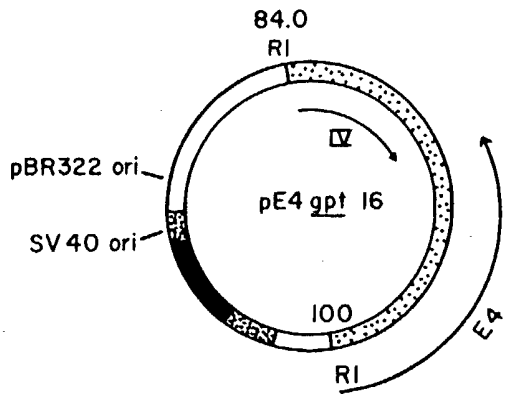

FIG. 1. Structure of pE4*gpt*16. pE4*gpt*16 consists of the Ad5 *Eco*RI B fragment (positions 84–100) inserted at the single *Eco*RI site of pSV2*gpt* (14). On the map, adenoviral sequences are indicated by light stippling, SV40 sequences by heavy stippling, and *E. coli gpt* sequences by the solid bar. The coordinates indicated are from the adenovirus physical map. Arrows indicate the direction of transcription and extent of adenoviral E4 and of the fiber gene (IV).

the ability to support growth of the defective E4 deletion mutant H2*dl*808 (16). The 808 deletion covers sequences from about 92 to about 97 map units on the Ad2 genome (see below) and, thus, is entirely within E4 (23, 24). A mixed stock containing both H2*dl*808 and its Ad5 *ts* helper, enriched for the deletion mutant by four cycles of CsCl equilibrium density gradient centrifugation, was titrated on each of the five mycophenolic acid-resistant lines listed above. The apparent titer of the stock on the five lines ranged from about 2×10^5 plaque-forming units/ml (W162, W163, W165, and W6B), to about 3×10^4 plaque-forming units/ml (W164). Five plaques produced on each of the lines W162–W165 and 10 plaques produced on W6B were picked and used to produce small lysates in cells of the same line. These lysates were then used to prepare small amounts of ^{32}P-labeled viral DNA, which were digested either with *Eco*RI or *Xba* I and analyzed by agarose gel electrophoresis. Judged by the restriction fragments produced, all of the plaques formed on four of the lines (W163–W165 and W6B) contained H2*dl*808 and its Ad5 helper, the helper alone, or Ad2/Ad5 recombinants lacking the 808 deletion. Therefore, none of these lines seems to support the growth of pure H2*dl*808. In contrast, three of the five plaques picked from lawns of W162 contained only H2*dl*808. No restriction fragments characteristic of the Ad5 helper were observed in digests of DNA from these plaques, and the Ad2 fragments affected by the 808 deletion (*Eco*RI C and *Xba* I C), were entirely replaced by the expected novel fragments. The remaining plaques contained both H2*dl*808 and Ad5. An *Eco*RI digest of DNA from descendants of one of the mutant plaques, subsequently replaqued and grown up on W162, is presented in Fig. 2.

Viral Growth on W162. To confirm that H2*dl*808 is defective on normally permissive cell lines and that it forms plaques efficiently on W162, we titrated Ad2 and H2*dl*808 stocks on W162 and on the parental Vero strain. The H2*dl*808 stock used was produced in W162 cells from virus purified by three successive rounds of plaque formation on W162 monolayers. As shown in Table 1, H2*dl*808 formed plaques more than 10^6-fold more efficiently on W162 cells than on Vero monolayers. We conclude that W162 complements a defect in H2*dl*808 that renders the mutant defective. That lesion is presumably the 808 deletion; thus, it seems certain that W162 will complement at least some defective E4 mutants.

Viral DNA in W162. Because we expected the complementing activity of W162 to be dependent upon the presence

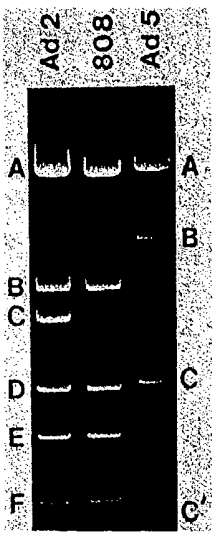

FIG. 2. *Eco*RI digest of H2*dl*808 DNA. DNAs obtained from purified H2*dl*808, Ad2, and Ad5 virions were digested with the *Eco*RI restriction endonuclease. The resulting fragments were fractionated by electrophoresis on a 1.4% agarose gel, stained, and photographed. In the digest of mutant DNA, the Ad2 C fragment is replaced by a shortened derivative (C'), which is slightly smaller than Ad2 *Eco*RI F.

of viral E4 DNA, we assayed W162 for viral DNA sequences by the Southern transfer procedure (19). W162, Vero, and 293 DNAs (10 μg each) were digested with either the *Hin*dIII or *Eco*RI restriction endonucleases, fractionated on a 1% agarose gel, transferred to nitrocellulose, and hybridized to ^{32}P-labeled Ad2 DNA. The *Hin*dIII digest of W162 DNA contained three bands that hybridized to viral DNA (Fig. 3). One of these comigrated with Ad5 *Hin*dIII F (89.5–98.2 map units), which contains most of E4. *Eco*RI digestion of W162 DNA produced one fragment containing viral sequences that had a slightly greater mobility than had Ad5 *Eco*RI B. Vero DNA contains no viral sequences, whereas 293 DNA digested with either enzyme yielded three fragments that hybridized with viral DNA. Because the fragment observed in the *Eco*RI digest of W162 DNA did not comigrate precisely with the Ad5 *Eco*RI B marker, the pE4*gpt*16 DNA present in these cells must have suffered some rearrangement during its incorporation. However, both the phenotype of the line and the presence of the *Hin*dIII F fragment suggest that W162 carries an intact, functional E4.

The 808 Deletion. The deletion in H2*dl*808 had previously been mapped by electron microscopy to coordinates 92.0–97.1 (14). To refine these measurements, we assayed DNA obtained from plaque-purified H2*dl*808 virions for the presence of several restriction sites near the ends of the deletion. The results of these mapping experiments (summarized also in Fig. 4) indicate that *Sma* I and *Hin*dIII cleavage sites at positions 92.0 and 97.2 (25), respectively, are missing from H2*dl*808 DNA, while *Bcl* I and *Sma* I sites at positions 91.4 and 98.4 (25), respectively, are present. Therefore, the left end point of the deletion falls in the roughly 200-base region between positions 91.4 and 92.0, and the right end point falls between positions 97.2 and 98.4. The size of the 808 deletion, measured by electron microscopy and estimated from the mobility of the novel restriction fragments produced in H2*dl*808 DNA by the deletion (Fig. 2) is just over 5%. It is likely, therefore, that the right end point lies quite close to the *Hin*dIII site at position 97.2 as shown in Fig. 4.

Table 1. Titration of Ad2 and H2*dl*808 on W162 and Vero cells

	Ad2	H2*dl*808
W162	4.0×10^7	7×10^7
Vero	1.5×10^7	$<1 \times 10^1$*

Ad2 and H2*dl*808 lysates were titrated on W162 and Vero cells. The titers of the two stocks on these cell lines appear above, expressed as plaque-forming units per ml.

* No plaques appeared on either of two dishes inoculated with 1.0 ml of the H2*dl*808 stock diluted 1:10.

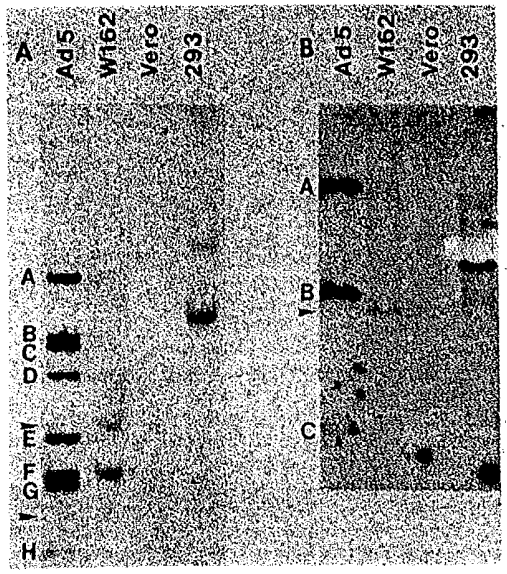

FIG. 3. Adenoviral DNA sequences in W162. W162, Vero, and 293 DNAs (10 μg each) were digested with *Hin*dIII or with *Eco*RI, transferred to nitrocellulose by the Southern procedure (19), and hybridized to ^{32}P-labeled Ad2 DNA. (*A*) *Hin*dIII digests. The eight largest Ad5 *Hin*dIII fragments are indicated by letters. The arrowheads mark the positions of two of the bands that contain viral sequences in the lane containing W162 DNA; the third band lies next to *Hin*dIII F. (*B*) *Eco*RI digests. The three Ad5 *Eco*RI bands are labeled, and an arrowhead marks the position of the band containing viral sequences in the digest of W162 DNA. The Ad5 standard contains viral DNA equivalent to about 10 copies per genome.

The 808 deletion, which does not cover the *Bcl* I site at position 91.4, cannot be any closer to the presumed polyadenylylation site for fiber mRNA (position 91.1; refs. 25 and 26) than about 100 bases. It is likely, therefore, that fiber mRNA is not directly affected by the 808 deletion. This is of particular interest in light of the observation that, even in W162 cells, H2*dl*808 substantially underproduced fiber protein (data not shown). Therefore, the 808 deletion may define a downstream site, outside of the sequences incorporated into stable mRNA,

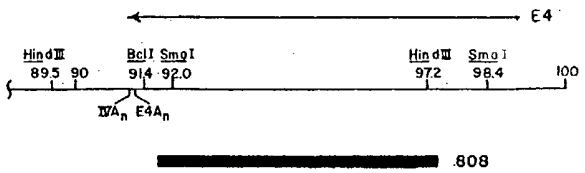

FIG. 4. Map of the H2*dl*808 deletion. The extent of the H2*dl*808 deletion, deduced from restriction digests and electron microscopy, is diagrammed. The end points of the deletion (black bar) fall between a *Bcl* I site at position 91.4 and a *Sma* I site at position 92.0 on the left and between a *Hin*dIII site at position 97.2 and a *Sma* I site at position 98.4 on the right. The positions of the presumed polyadenylylation signals for fiber (IVA$_n$) and E4 (E4 A$_n$) RNAs and the approximate extent of E4 transcription (arrow) are indicated (23, 24).

that is necessary for efficient expression of the fiber gene. More thorough analysis of H2*dl*808 will presumably shed light on this possibility and on the nature of the mutant's biochemical defect.

DISCUSSION

The genetic analysis of the transforming regions of several animal viruses has been facilitated by the fact that some transformed cell lines support the growth of otherwise defective viral mutants with lesions in those regions. Such transformed cell lines contain and express segments of viral DNA (3–5) and presumably are capable of supplying the essential products of those DNA segments to viral mutants that cannot produce them. The experiments described here were undertaken to extend the benefits of such complementing cell systems to a viral DNA segment not directly involved in transformation, early region 4 of human adenoviruses. In these experiments, a segment of adenoviral DNA containing early region 4 sequences derived from Ad5 was introduced into Vero cells as part of a plasmid containing the Ad5 *Eco*RI B fragment and the dominant, selectable *E. coli* gene *gpt* (14). Several of the resulting cell lines were then screened for biological activity and one, W162, was found to support the growth of the defective E4 deletion mutant H2*dl*808 (16). Thus, it is possible to construct complementing cell lines for at least some segments of viral DNA that do not transform cells, and a line that should be useful in the analysis of E4 was obtained. Recently, Shiroki *et al.* (27) and Babiss *et al.* (28) reported the use of the *gpt* selective system to construct KB cell derivatives containing adenoviral E1 sequences. Like 293 cells, some of these lines support the growth of E1 mutants.

Vero cells, which are of monkey origin but permissive for human adenoviruses, were chosen for these experiments rather than a human cell line partly for technical reasons: Vero cells grow well, form durable monolayers, and were easily transformed to mycophenolic acid resistance. Further, in Vero derivatives, resident E4 sequences should remain silent because Vero cells do not contain the adenoviral E1 sequences required for efficient E4 expression (9, 10). Thus, even if E4 expression is lethal, there ought to be no selection against E4-containing Vero transformants, as there might be against similar derivatives of, for example, 293 cells. We presumed that in E4-bearing Vero derivatives, infecting adenovirus would activate the resident E4 DNA by providing E1 products.

Five mycophenolic acid-resistant lines, all of which presumably carry the *gpt* gene and attached E4 DNA, were originally chosen for close examination. Of these, only one seems to complement the E4 mutant that we have used to test biological activity. The reason for the inactivity of the other four lines is not known. All of the lines examined, including W162, grow well and form long-lived monolayers.

E4 is one of the few segments of the adenoviral genome for which no function in the viral life cycle is known. This is due in part to the lack of E4 mutants: no conditionally defective mutants are available, and H2*dl*808, which until now has been propagated in the presence of a helper virus, carries a deletion too small to make its physical purification practical. One deletion mutant lacking E4 sequences (H2*dl*807; ref. 14) has been characterized, but the interpretation of its phenotype is complicated by the fact that it is missing a substantial amount of DNA outside of E4. The difficulties encountered in the genetic analysis of E4 should be considerably reduced by W162, which will make the analysis of H2*dl*808 possible immediately and should permit the eventual isolation of new E4 mutants.

Using lysates produced on W162 cells, we have begun the characterization of H2*dl*808, which lacks viral sequences from between positions 91.4 and 92.0 to just beyond position 97.2. This deletion falls entirely within E4 (ref. 24; see Fig. 4) and would disrupt all but the most promoter-proximal of the hypothetical protein-coding regions in E4 proposed on the basis of sequence data (25, 26). We are not yet certain of the level at which the growth of H2*dl*808 is blocked in nonpermissive cells. It is of interest that even in W162 cells, H2*dl*808 synthesizes little fiber protein. Because fiber mRNA ought not to be directly affected by the deletion, the missing DNA may contain a novel genetic element required for efficient expression of the fiber gene.

The W162 cell line should soon shed light on the functions of adenoviral early region 4. The method used in the construction of the line also should be of general utility in producing similar complementing cell lines for other regions of interest in animal virus genomes.

We thank Kathy Berkner for her gift of the cloned Ad5 *Eco*RI B fragment, Richard Mulligan and Paul Berg for pSV2*gpt*, and the Eli Lilly Research Laboratories for mycophenolic acid. Thomas Kelly, George Scangos, Janice Clements, and the members of this lab (Barry Falgout, Richard Rohan, and Ariane Fenton) all offered useful suggestions during the course of the work and critically reviewed the manuscript. George Scangos also provided valuable assistance with transformation experiments. Special thanks are due to Sherry Challberg, who participated in the early stages of this work, without whose enthusiasm it would not have been undertaken. This work was supported by National Institutes of Health Grant CA21309. This is contribution 1210 from the Department of Biology.

1. Ensinger, M. & Ginsberg, H. S. (1972) *J. Virol.* **10**, 328–339.
2. Williams, J. F., Gharpure, M., Ustacelebi, S. S. & McDonald, S. (1971) *J. Gen. Virol.* **11**, 95–101.
3. Benjamin, T. (1970) *Proc. Natl. Acad. Sci. USA* **67**, 394–399.
4. Gluzman, Y. (1981) *Cell* **23**, 175–183.
5. Graham, F. G., Abrahams, P. J., Mulder, C., Heijneker, H. L., Warnaar, S. O., deVries, F. A. J., Feirs, W. & van der Eb, A. J. (1975) *Cold Spring Harbor Symp. Quant. Biol.* **39**, 637–650.
6. Harrison, T. J., Graham, F. & Williams, J. F. (1977) *Virology* **77**, 319–329.
7. Jones, N. & Shenk, T. (1979) *Cell* **17**, 683–689.
8. Frost, E. A. & Williams, J. F. (1978) *Virology* **91**, 39–50.
9. Berk, A. J., Lee, F., Harrison, T., Williams, J. & Sharp, P. (1979) *Cell* **17**, 935–944.
10. Jones, N. & Shenk, T. (1979) *Proc. Natl. Acad. Sci. USA* **76**, 3665–3669.
11. Graham, F. G., Harrison, T. J. & Williams, J. F. (1979) *Virology* **86**, 10–21.
12. Carlock, L. R. & Jones, N. C. (1981) *J. Virol.* **40**, 657–664.
13. Montell, C., Fisher, E. F., Caruthers, M. H. & Berk, A. J. (1981) *Nature (London)* **295**, 380–384.
14. Mulligan, R. C. & Berg, P. (1980) *Science* **209**, 1422–1427.
15. Mulligan, R. C. & Berg, P. (1981) *Proc. Natl. Acad. Sci. USA* **72**, 2072–2076.
16. Challberg, S. S. & Ketner, G. (1981) *Virology* **114**, 196–209.
17. Graham, F. G. & van der Eb, A. J. (1973) *Virology* **52**, 456–467.
18. Huttner, K. M., Barbosa, J. A., Scangos, G., Prautcheva, D. & Ruddle, F. H. (1981) *J. Cell Biol.* **91**, 153–156.
19. Southern, E. M. (1975) *J. Mol. Biol.* **98**, 503–517.
20. Denhardt, D. (1966) *Biochem. Biophys. Res. Commun.* **23**, 641–646.
21. Ketner, G. & Kelly, T. J. (1980) *J. Mol. Biol.* **144**, 163–183.
22. Kelly, R. B., Cozzarelli, N. R., Deutscher, M. P., Lehman, I. R. & Kornberg, A. (1980) *J. Biol. Chem.* **245**, 39–45.
23. Pettersson, U., Tibbetts, C. & Philipson, L. (1976) *J. Mol. Biol.* **141**, 479–501.
24. Berk, A. J. & Sharp, P. A. (1978) *Cell* **14**, 695–711.
25. Gingeras, T. R., Sciaky, D., Gelinas, R. E., Bing-Dong, J., Yen, C. E., Kelly, M. M., Bullock, P. A., Parsons, B. L., O'Neill, K. E. & Roberts, R. J. (1982) *J. Biol. Chem.* **257**, 13475–13491.
26. Herisse, J., Rigolet, M., Dupont de Dinechin, S. & Galibert, F. (1981) *Nucleic Acids Res.* **9**, 4023–4042.
27. Shiroki, K., Saito, I., Maruyama, K., Fukui, Y., Imatani, Y., Oda, K. & Shimojo, H. (1983) *J. Virol.* **45**, 1074–1082.
28. Babiss, L. E., Young, C. S. H., Fisher, P. B. & Ginsberg, H. S. (1983) *J. Virol.* **46**, 454–465.